



UNIL | Université de Lausanne

Unicentre

CH-1015 Lausanne

<http://serval.unil.ch>

Year : 2016

Internal structure, dynamics and genesis of small debris-covered glacier systems located in alpine permafrost environments

Bosson Jean-Baptiste

Bosson Jean-Baptiste, 2016, Internal structure, dynamics and genesis of small debris-covered glacier systems located in alpine permafrost environments

Originally published at : Thesis, University of Lausanne

Posted at the University of Lausanne Open Archive <http://serval.unil.ch>

Document URN : urn:nbn:ch:serval-BIB_5295901FC4632

Droits d'auteur

L'Université de Lausanne attire expressément l'attention des utilisateurs sur le fait que tous les documents publiés dans l'Archive SERVAL sont protégés par le droit d'auteur, conformément à la loi fédérale sur le droit d'auteur et les droits voisins (LDA). A ce titre, il est indispensable d'obtenir le consentement préalable de l'auteur et/ou de l'éditeur avant toute utilisation d'une oeuvre ou d'une partie d'une oeuvre ne relevant pas d'une utilisation à des fins personnelles au sens de la LDA (art. 19, al. 1 lettre a). A défaut, tout contrevenant s'expose aux sanctions prévues par cette loi. Nous déclinons toute responsabilité en la matière.

Copyright

The University of Lausanne expressly draws the attention of users to the fact that all documents published in the SERVAL Archive are protected by copyright in accordance with federal law on copyright and similar rights (LDA). Accordingly it is indispensable to obtain prior consent from the author and/or publisher before any use of a work or part of a work for purposes other than personal use within the meaning of LDA (art. 19, para. 1 letter a). Failure to do so will expose offenders to the sanctions laid down by this law. We accept no liability in this respect.



UNIL | Université de Lausanne

Faculté des géosciences et de l'environnement
Institut des dynamiques de la surface terrestre

Internal structure, dynamics and genesis of small debris-covered glacier systems located in alpine permafrost environments

Thèse de doctorat

présentée à la faculté des géosciences et de l'environnement
de l'Université de Lausanne par

Jean-Baptiste Bosson

Diplômé en Science Politique (licence à l'Université de Lyon 3, France)
et Géographie (M.Sc. à l'Université de Lausanne, Suisse)

pour l'obtention du titre de Docteur en géosciences et environnement,
mention "géographie"

Jury:

Dr. Christophe Lambiel (Directeur de thèse)
Dr. Martin P. Kirkbride (Expert externe)
Prof. Etienne Cossart (Expert externe)
Prof. Emmanuel Reynard (Expert interne)
sous la présidence du Prof. Suren Erkman (colloque)
et du Prof. Grégoire Mariéthoz (défense publique)

LAUSANNE 2016



UNIL | Université de Lausanne
Décanat Géosciences et de l'Environnement
bâtiment Géopolis
CH-1015 Lausanne

IMPRIMATUR

Vu le rapport présenté par le jury d'examen, composé de

Président de la séance publique :	M. le Professeur Grégoire Mariéthoz
Président du colloque :	M. le Professeur Suren Erkman
Directeur de thèse :	M. le Docteur Christophe Lambiel
Expert interne:	M. le Professeur Emmanuel Reynard
Expert externe :	M. le Docteur Martin Kirkbride
Expert externe :	M. le Professeur Etienne Cossart

Le Doyen de la Faculté des géosciences et de l'environnement autorise l'impression de la thèse de

Monsieur Jean-Baptiste BOSSON

Titulaire d'une
Maîtrise ès Sciences en géographie
de l'Université de Lausanne

intitulée

Internal structure, dynamics and genesis of small debris-covered glacier systems located in alpine permafrost environments

Lausanne, le 1er juillet 2016

Pour le Doyen de la Faculté des géosciences et
de l'environnement

Professeur Grégoire Mariéthoz



A | The Entre la Reille glacier system (© S. Utz, July 2012)

Si ton œil était plus aigu, tu verrais tout en mouvement : comme le papier enflammé se déforme, toute chose se défait et se déforme.

Friedrich Nietzsche (Fragments posthumes)

...

Elle avait un visage aux traits si fins qu'on avait envie de la prendre au creux de la main et une vivacité harmonieuse dans chaque mouvement qui m'avait permis d'avoir une très bonne note à mon bac de philo. J'avais choisi l'esthétique à l'oral et l'examineur, excédé sans doute par une journée de travail, m'avait dit :

- Je ne vous poserai qu'une question et je vous demande de me répondre par un seul mot. **Qu'est-ce qui caractérise la grâce ?**

Je pensai à la petite Polonaise, à son cou, à ses bras, au vol de sa chevelure, et je répondis sans hésiter :

- **Le mouvement.**

J'eus un dix-neuf. Je dois mon bac à l'amour.

Romain Gary (Les cerfs volants)

JB. Bosson (2016). Internal structure, dynamics and genesis of small debris-covered glacier systems located in alpine permafrost environments

Originally published at: Thesis, University of Lausanne

Posted at the University of Lausanne Open Archive.
<http://serval.unil.ch>

Droits d'auteur

L'Université de Lausanne attire expressément l'attention des utilisateurs sur le fait que tous les documents publiés dans l'Archive SERVAL sont protégés par le droit d'auteur, conformément à la loi fédérale sur le droit d'auteur et les droits voisins (LDA). A ce titre, il est indispensable d'obtenir le consentement préalable de l'auteur et/ou de l'éditeur avant toute utilisation d'une oeuvre ou d'une partie d'une oeuvre ne relevant pas d'une utilisation à des fins personnelles au sens de la LDA (art. 19, al. 1 lettre a). A défaut, tout contrevenant s'expose aux sanctions prévues par cette loi. Nous déclinons toute responsabilité en la matière.

Copyright

The University of Lausanne expressly draws the attention of users to the fact that all documents published in the SERVAL Archive are protected by copyright in accordance with federal law on copyright and similar rights (LDA). Accordingly it is indispensable to obtain prior consent from the author and/or publisher before any use of a work or part of a work for purposes other than personal use within the meaning of LDA (art. 19, para. 1 letter a). Failure to do so will expose offenders to the sanctions laid down by this law. We accept no liability in this respect.

Summary

Small debris-covered glaciers are commonly associated with large and possibly frozen sediment accumulations in alpine permafrost environments. Tens of thousands of these complex systems, referred to herein as *small debris-covered glacier systems located in alpine permafrost environments* (SDCGSAPE), are present on Earth and similar landforms were observed on Mars. Their absolute number even increases around the world in the current climatic context. Glaciers become smaller and less dynamic with the recent intensification of glacier decline. Ice melt rate is especially rapid in temperate environments and ice masses are progressively confined within the coldest areas, subject to permafrost conditions. Finally, the debris layers on the glaciers surface extend in high relief environments, due to the deglaciation and permafrost degradation in the surrounding relief, and the decrease of glacier dynamics. Dynamics of small glaciers, glacier-permafrost interactions or the influence of the debris cover on glaciers behaviour remain however topics rather understudied by the scientific community. Thus, despite their very large and increasing numbers, and their importance as freshwater reservoirs and sediment accumulations in high relief environments, SDCGSAPE are still barely known.

This contribution synthesizes the results of five years of researches on these complex systems. Their internal structures, dynamics and genesis were investigated in seven sites, located in the northwest Alps. The results collected and the review of scattered literature allowed to lay the foundation of a comprehensive knowledge on these fascinating systems.

Ice and debris concentrations varied in time and space in these systems according to Holocene climatic fluctuations. The current highest ice concentration was found in the upper central zone of each study site, where a small glacier, inherited from past climate, subsisted. The glacier was the most dynamical components of these systems. Glacier flow and thinning were observed, reaching typically several decimetres per year and accelerating in summer. Compared with neighbouring debris-free glaciers, the decadal and recent responses of these glaciers to climatic variations appeared disturbed by the influence of the surrounding relief, the debris cover and permafrost conditions on accumulation and ablation rates. The occurrence of these mostly negative feedbacks delayed and attenuated the glacier response to climatic variations. The heavily debris-covered tongues still contained large amount of ice and the current extent of these glaciers is an anomaly at regional scale in the unfavourable climatic context. However, the upper snow accumulation was weak and the slow shrinking of these buried and less and less active sedimentary ice masses is expected in the next decades.

Ice concentration decreased toward the lower margins where Holocene glacier fluctuations accumulated lopsided sediment stores. No processes efficiently evacuated them in downward geomorphic system. Noticeable subglacial and postglacial water circulations hindered ground ice preservation in part of these debris accumulations. Up to several tens of meters of thickness of weakly active ice-free debris were thus observed in these systems. Conversely, ground ice was preserved in some margins weakly affected by water circulations and where the supraglacial debris cover thickness reached several meters that was close to the active layer thickness of permafrost. Slow and relatively constant creep was measured in these zones (typically few decimetres per year). The long-term viscous deformation of the ice-debris mixture allowed thus the formation of rock glaciers.

Ice concentration, supraglacial layer thickness and water circulations in these systems strongly control the current dynamics. Compared to other glacier systems, the influence of the surrounding relief on the snow, ice, and debris supply and the occurrence of permafrost conditions in the ablation areas induce particular glacial and postglacial dynamics in SDCGSAPE. The large debris concentration in these systems and the occurrence of negative feedbacks decrease their climatic sensitivity. In the future, the local importance of the amount of water sheltered in SDCGSAPE will further increase with the expected a rapid shrinking of debris-free glaciers.

Résumé

Les petits glaciers couverts sont communément associés dans les environnements périglaciaires alpins avec de grandes accumulations sédimentaires, possiblement gelées. Des dizaines de milliers de ces systèmes complexes, appelés ici *petits systèmes glaciaires couverts situés dans les environnements de permafrost* (SDCGSAPE), sont présents sur Terre et des formes similaires ont été observées sur Mars. Leur nombre est même en augmentation en raison des changements climatiques contemporains. Les glaciers deviennent plus petits et moins dynamiques avec l'intensification récente du retrait glaciaire. La vitesse de fonte est particulièrement rapide dans les environnements tempérés et les masses de glace sont progressivement confinées dans les zones les plus froides, soumises aux conditions de permafrost. Finalement, des sédiments s'accumulent à la surface des glaciers dans les environnements montagneux, en raison de la déglaciation et de la dégradation du permafrost dans le relief environnant et de la réduction de la dynamique des glaciers. La dynamique des petits glaciers, les interactions entre les glaciers et le permafrost ou l'influence des couvertures sédimentaires sur le comportement glaciaire demeurent toutefois des sujets relativement peu étudiés par la communauté scientifique. Ainsi, en dépit de leur grand nombre et de leur importance comme stock d'eau et de sédiments dans les environnements montagnards, les SDCGSAPE sont toujours très peu connus.

Cette contribution synthétise les résultats de cinq années de recherches sur ces systèmes complexes. Leur composition, leurs dynamiques et leur genèse ont été étudiées dans sept sites, localisés au nord-ouest des Alpes. Les résultats collectés et la synthèse de la littérature éparses ont permis d'établir les bases d'une connaissance approfondie de ces systèmes passionnants.

La concentration de la glace et des sédiments a varié dans le temps et l'espace dans ces systèmes en fonction des fluctuations climatiques holocènes. La plus grande concentration actuelle de glace a été retrouvée dans la zone amont et centrale de chaque site d'étude, où un petit glacier hérité du climat passé a subsisté. Ce glacier était le composant le plus dynamique de ces systèmes. Le fluage et l'amincissement glaciaire ont été observés, atteignant typiquement plusieurs décimètres par an et accélérant fortement au cours de l'été. En comparaison avec les glaciers blancs avoisinants, les réponses décennales et récentes de ces glaciers aux variations climatiques apparaissent perturbées par l'influence du relief, de la couverture sédimentaire et des conditions de permafrost sur les taux d'accumulation et d'ablation. L'occurrence de ces rétroactions essentiellement négatives retarde et atténue les réponses glaciaires aux variations climatiques. Les langues recouvertes d'une épaisse couche de débris contiennent toujours une quantité importante de glace et l'étendue actuelle de ces glaciers est une anomalie à l'échelle régionale dans le contexte climatique défavorable. Cependant, l'accumulation de neige en amont étant faible, la lente fonte de ces lambeaux de glace sédimentaire enterrés, de moins en moins actifs, est attendue dans les prochaines décennies.

La concentration de glace diminue vers les marges aval où les fluctuations glaciaires holocènes ont accumulé des stocks de sédiments disproportionnés. Aucun processus n'est parvenu à évacuer efficacement ces sédiments dans les systèmes géomorphologiques aval. D'importantes circulations d'eau sous-glaciaires et post-glaciaires ont empêché la préservation de la glace dans le sol dans une partie de ces accumulations sédimentaires. Jusqu'à plusieurs dizaines de mètres d'épaisseur de sédiments désenglacés et peu actifs ont ainsi été observés dans ces systèmes. À l'inverse, la glace dans le sol a été préservée dans certaines marges peu affectées par les circulations d'eau et où l'épaisseur de la couverture supraglaciaire s'apparente à celle du niveau actif du permafrost. Une lente et constante reptation a été mesurée dans ces zones (typiquement quelques décimètres par an). La déformation visqueuse à long-terme de la mixture de glace et de sédiments a ainsi permis la formation de glaciers rocheux.

Les dynamiques actuelles observées dans ces systèmes sont fortement contrôlées par la concentration en glace, l'épaisseur de la couverture supraglaciaire et les circulations d'eau. Par rapport aux autres systèmes glaciaires, l'influence du relief environnant sur l'approvisionnement en neige, en glace et en sédiments ainsi que l'existence des conditions de permafrost dans les zones d'ablations génèrent des dynamiques glaciaires et postglaciaires particulières dans les SDCGSAPE. La grande concentration de débris dans ces systèmes et l'influence de rétroactions négatives limitent leur sensibilité au climat. À l'avenir, l'importance locale du volume d'eau abritées dans les SDCGSAPE va encore augmenter, dans un contexte où une fonte rapide des glaciers blancs est attendue.

Acknowledgements and forewords

The writing of this section completes this PhD thesis and puts an end to an almost six-year long period of my life. This period was extremely rich and intense in both my intellectual and personal life. If my thirst for knowledge remains intact (it has even grown up) after this research, the intellectual stimulation and the valuable meetings that I had the chance to live during this period will now illuminate my personal path in future. Looking backward, it is hard for me to dissociate my scientific life from my personal life over the six last years. In this way, I would like to acknowledge all the people that directly or indirectly supported me throughout this challenging task.

This scientific work is above all the result of a sharing. As the tip of an iceberg, my sole name signs this PhD thesis. However, its scientific content arose from a large and continuous collective work, where ideas and results emerged from cooperation and were gathered. Because of my humanistic education, my atypical academic path from political sciences to geomorphology and glaciology and my *Nietzschean* aversion for all forms of spirit imprisonment, I deeply believe in the virtue of openness and blending in all aspects of life, including obviously the construction of the scientific knowledge. It is thus important for me to recognise that this PhD thesis reflects almost six years of rewarding discussions, collective field works and data processing. The questions, remarks and critics addressed to the scientific content indisputably improved its quality. Hence, I am deeply thankful for this decisive help and intellectual stimulation, and I sincerely acknowledge the numerous scientists and people from non-scientific domain who directly contributed to this PhD thesis. In addition, I received an unwavering support from all the people around me. I am fully aware of my chance and without this support, it would have been impossible to complete this long and ambitious work. For my part, I would like to apologize to those who suffered my stress, my impatience or my fatigue. Besides their support, I encountered a large understanding, patience and caring from the people around me.

I would like now to acknowledge the following people in particular. However, the fuzzy frontier between my personal and scientific life over the last years will probably make me forget some people that decisively help me along this way. I apologize in advance for this probable oblivion and I ask them to accept one more time my warm and sincere acknowledgements.

First and foremost, I would like to dedicate this PhD thesis to my parents, Monique and Pierre. As I have always lived close to them, they have strongly influenced my personality and my mind. In an always free manner, they share with me their sensitivity, their critical mind, their curiosity and their unfailing courage. Their support and trust, their presence close to me all along my life and in particular during this PhD thesis gave me strength, helping me to complete this work and to overcome the periods of doubt. As solid and exemplary large trees around a clearing, they inspired me, guided me and allowed me to develop myself freely between earth and sky.

I wish also to thank warmly Christophe Lambiel, the Director of this PhD thesis, for having offered me this challenging position of PhD student. Throughout our enriching collaboration, he offered

me two associated gifts that were very precious for a young scientist like me: a large degree of freedom in the choice of the subject and in the way to treat it and its confidence in my scientific skills. This situation is not that common in the scientific community, so I would like to thank my Director of research for being so open-minded. He helped me with encouragements and constructive critics along this work and was always open to my requests. He largely contributed to shape the researcher that I became and I learned a lot working with him in both scientific and human aspects. Finally, in an ominous time of increased competition and stress for productivity in the scientific community, he was a rare and useful example of how high-level in sciences can be conciliated with an intense personal life. I take the opportunity here to thank also Emmanuel Reynard for having opened the fascinating field of geomorphology and cryospheric sciences to a young student in political sciences in 2008. He also strongly influenced my scientific mind and my interest for a holistic naturalist approach.

During this PhD thesis, I had the chance to collaborate with brilliant young scientists with who I developed strong friendships. This ambitious work would have been hard to complete without the support, the contagious joy and the critical mind of my office partner Nicola Deluigi. His constructive critics on my work improved it noticeably. The moments we shared in University, after work or during the scientific meetings over Europe made me discover and appreciate this ticinese as a brother. I am sure now that he will complete successfully its PhD thesis on permafrost in the future months. Still heading South-East toward Ticino, I would like to acknowledge two others golden minds from this sunny land: my scientific big brother Cristian Scapozza and Natan Micheletti. Both were very important for me as reference scientists and friends. The study of alpine glaciers was an impossible dream I made years ago. I realized it with a lot of luck and the support of many people. However, the contribution of Mauro Fischer, my colleague PhD student at the University of Fribourg, was fundamental and our numerous discussions largely shaped the modest glaciologist that I became. It was an honour for me to collaborate with this talented scientist who already published many reference papers. Each time we met, I was impressed by its exceptional scientific skills and its precocious holistic knowledge. Our ambitious project of paper reviewing the knowledge and our findings on the very small alpine glaciers and its large contribution to Capt and al., 2016 strongly improved my knowledge and stimulated my scientific mind. Beyond this enriching sharing, I met one of the most beautiful human being I know. The meetings with this brilliant, sensitive, modest and honest man were always very special for me as he is the kind of particular light I research among men to illuminate my path. Finally, I thank the two master students (and great friends) with who I directly collaborated: Maxime Capt and Robin Darbellay. Partners in crimes, poetry and sciences, our collaboration was always a source intellectual stimulation, pride and laughs for me.

This PhD thesis is essentially based on field results. As scientific surveys require caution and a large energy in the harsh high mountain environments, I always had the chance to be accompanied by at least one person during data acquisitions. Although field campaigns were not always simple and even sometimes very dangerous, it was a great pleasure for me to share these moments of intense works, discussions and exchanges, hanged on some beautiful alpine mountains. Along

the successive summers of measurements, several field assistants were employed by the University of Lausanne to help me. It was a chance for me to be accompanied by good young researchers and mountaineers and it allowed me to deepen and/or strengthen my friendship with Lucien Grangier, Stephan Utz, Benoît Regamey, Maxime Capt, Thierry Nendaz, Robin Darbellay, César Vannay and Mathieu Henriod. Additionally, I sincerely acknowledge the 42 other fearless adventurers that accepted to follow me and helped me to collect data on the studied debris-covered glaciers (and especially those who did it for free :-): Nicola Deluigi, Marie Gardent, Philip Deline, Christophe Lambiel, Christian Scapozza, Mario Kummert, Mael Rossetti, Benoît Lovis, Valentin Zuchuat, Renaud Lay, Pauline Katz, Adrien Roy, Romain Bosson, Xavier Bodin, Emmanuel Malet, Hilary Dyer, Carole Barachet, Phillipe Schoeneich, Simone d’Aujourd’hui, Ludovic Raest, Christian David, Rafael, Tania Ferber, Natan Micheletti, Laetitia Laigre, Geoffrey Garcel, Adrien Dumas, Clément Gamin, Laurent Delomez, Romain Paras, Stefano Varricchio, Marilyne Dumas, Antoine Buisson, Thibault-Amaury De Kerchove D’Ousselghem, Patrick Perret, Mauro Fischer, Benjamin Lehman and Martin Calianno. My friends Alric Marchand, Déodat Bonneaux and Alexandre Breytrison are especially acknowledged for having been exceptional volunteer field scientists several times by my side.

Without getting into details, I would like to acknowledge all the people in the scientific community who made this research possible and improve its content: colleagues at the University of Lausanne (in particular Jean-Michel Fallot, Emmanuel Reynard, Simone d’Aujourd’hui, Marcia Curchod, Benjamin Lehman), at the University of Savoie and Grenoble (Marie Gardent, Florence Magnin, Philip Deline, Phillipe Schoeneich, Xavier Bodin, Ludovic Ravanel), all the researchers I met during scientific conferences (especially Ivar Berthling, Romain Perrier, Sébastien Monnier), all the readers, editors and reviewers of the scientific publications produced (especially Stuart Lane and Matthias Huss), friends of ASTERS (Geoffrey Garcel, Carole Birck, Aubrée Flammier, Laurent Delomez, Patrick Perret) and all the people and organisations that support this research financially and/or logistically : the University of Lausanne (State of Vaud), the State of Valais (Service des forêts et du paysage), the municipality of Evolène, ASTERS, the Swiss Geomorphological Society, the Swiss Snow, Ice and Permafrost society, the WSL Institute, Glacier 3000 (Gstaad 3000 AG), la Compagnie du Mont-Blanc, la Cabane des Diablerets (Sandrine Zweili), le refuge du Nid d’Aigle, Air Glacier, CMBH Hélicoptères, the Bosson, Dumas, Katz and Anzévui families.

I would like to acknowledge all the members of my thesis committee: Dr. Christophe Lambiel (Univ. Lausanne), Dr. Martin Kirkbride (Univ. Dundee), Prof. Etienne Cossart (Univ. Lyon III), Prof. Emmanuel Reynard (Univ. Lausanne), Prof. Suren Erkman (Univ. Lausanne) and Prof. Grégoire Mariéthoz (Univ. Lausanne). Our exiting discussion during the thesis evaluation and their respective comments on the manuscript noticeably improved the scientific content. Martin Kirkbride especially shared its bright ideas on the comprehensive view of glacier systems genesis and evolution in high relief environments.

I address a special thank to all the friends of the *team Geop* (especially Nicola Deluigi, Elisa Giaccone, Natan Micheletti, Nico Baetz, Chrystelle Gabbud, Stephan Utz, Lucien Grangier, Isaline

VonDaniken, Aline Burri, Martin Calianno, Benjamin Lehman). The permanent good mood of our group and the babyfoot games at Zelig were daily breath of fresh air. I have also a warm thought to all the former PhD students, PAT and researchers of IGUL and IDYST who have always been very kind with me.

To conclude, I would like to acknowledge all the people who embellish each day of my personal life. Throughout this PhD thesis, they were unwavering sources of support, energy and lightness. With my parents, my sisters and brothers Emilie, Romain, Marine De Lageneste and Daniel Herrera are the surest and most important landmarks of my life. To paraphrase William Shakespeare, they *are such stuff as dreams are made on*. My inspiration and personal balance strongly depend on their presence, love and intelligence. I also thank sincerely here my aunt Isabelle Bosson and my cousin Laurence Desbaillet for their infinite kindness. I shared my existence with Tania Ferber (and its lovely family) most of the time during this PhD. Her presence is drawn behind many lines of this thesis as she was the best source of support and constructive comments that I could have. We shared moments of grace that allowed me to become a better man and scientist. I also would like to acknowledge here my friends/brothers Déodat Bonneaux and Adrien Dumas who shaped and fed my original love for alpine mountains and shared with me their way to access these environments. My academic path toward high mountains was strongly influenced by these two freedom-loving mountaineers. Finally, in addition to thank my invaluable family and friends (Dim, Renaud, Alex, Nico, Audric, Romain, etc.) widespread across the world, I have a special thought to Olivia, my awesome roommate, for her amazing support during the laborious last writing months.

Je me permets d'écrire maintenant les dernières phrases de cette thèse en français. Elles concluent près de six années de recherches, d'exploration, de rêves et de réflexions dans les solitudes glaciales et paisibles de la haute montagne, aux marges de l'Humanité. Ces environnements, où l'Homme retrouve sa très modeste dimension géologique, vivent des changements rapides, majeurs, inquiétants. Comme chaque portion de la Nature, il convient donc de mieux connaître, partager et protéger ces lieux fascinants, fragiles héritages de l'Histoire de la Terre.

Ma main dessine ces derniers mots en français, la seule langue dont ma maîtrise relative me permet une humble et maladroite incursion dans le langage poétique, à la recherche du joli. À mon grand regret et au détriment de mon amour pour la littérature, ma connaissance superficielle de la langue anglaise et les contraintes du langage scientifique ont fortement réduit la place laissée à la créativité et la recherche de l'esthétique dans le texte de cette contribution scientifique. Avec du talent et du temps, j'aurais pu transformer ces contraintes en richesses mais je n'en ai pas été capable. Il était donc important pour moi de conclure ce travail rigoureux et encadré par ces quelques mots, dessinant avec, quelques battements d'ailes et cabrioles malicieuses vers le bleu, comme me l'ont appris les chocards lors des campagnes de terrain. Je profite de ce regard vers le ciel pour dédier ce doctorat et ces années de ma vie à mes deux grand-mamans, Edmée et Solange, parties rejoindre les étoiles au cours de cette période.

Jean-Baptiste
Lausanne, le 7 octobre 2016



B | Bivouac on the front of the Tsarmine glacier system during a field campaign. The Tsijjore Nouve Glacier and its Holocene morainic vallum can be observed in the background (August 2014)

Acronyms

AAR: accumulation-area ratio

AD: anno domini (year since the date of the birth of Jesus Christ)

BTS: bottom temperature of the snow cover

CC: climatically-controlled (glacier)

CW: Chaltwasser

DCG: debris-covered glacier

DEM: digital elevation model

dGPS: differential GPS

DInSAR: differential synthetic aperture radar interferometry

DoD: DEM of difference

DR: Drainage ratio

ELA: equilibrium line altitude

ELR: Entre la Reille

ERT: electrical resistivity tomography

GCP: ground control point

GFI: ground freezing index

GLOF: glacial lake outburst flood

GPR: ground penetrating radar

GST: ground surface temperature

HDCG: heavily debris-covered glacier

IGN: institut national de l'information géographique et forestière (France)

Ka BP: thousand years before present (ref. 1950)

LF: les Fours also referred to as RC: Rebanets Chassots

LGM: last glacial maximum

LIA: little ice age

Lidar: light detection and ranging

LoD: limit of detection

MAAT: mean annual air temperature

M(A)GST: mean (annual) ground surface temperature

MPA: mountain permafrost altitude

MRMV: model resolution matrix value

m w.e a⁻¹: meter water-equivalent per year

PC: Petit Combin

PDD: positive degree day

PR: Pierre Ronde

RG: rock glacier

RGI: Randolph Glacier Inventory

Ro: les Rognes

SDCGSAPE: small debris-covered glacier systems located in alpine permafrost environments

(this inelegant acronym is used in the following to ease the reading)

Tsa: Tsarmine

TC: topographically-controlled (glacier)

VCP: velocity cross-profile

WEqT: winter equilibrium temperature (pWEqT: presumed winter equilibrium temperature)

WGMS: World Glacier Monitoring Service

WPOF: water-pocket outburst flood

Structure

Five complementary parts compose this PhD thesis :

1. Introduction | p22

This part presents the context of research, the state of knowledge and the objectives of this study on small debris-covered glaciers located in alpine permafrost environments.

2. Publications | p74

The three scientific articles published during this PhD compose this part. A synthesis outlines the main findings of each article.

3. Compilation and synthesis of results by study sites | p147

Published and unpublished results are compiled and discussed by study sites.

4. Main outcomes and discussion | p244

The main findings are synthesised and put into a larger scientific context.

5. Conclusion and outlooks | p273

This contribution concludes with a general synthesis and some research perspectives.

Table of contents

Summary	vi
Résumé	vii
Acknowledgements and forewords	ix
Acronyms	xv
Structure	xvi

1. Introduction

1.1. Context of research	23
1.2. Definition and state of knowledge	31
1.2.1. A particular type of glacier	31
1.2.1.1. The influence of the supraglacial debris cover	33
1.2.1.2. The influence of the glacier size	43
1.2.1.3. The influence of the permafrost conditions	47
1.2.1.4. Synthesis	52
1.2.2. Glacigenic sediment accumulations in permafrost environments	52
1.2.2.1. The controversial consideration of ground ice and glacier-permafrost interactions	52
1.2.2.2. Possibly polygenic and multi-phased Holocene sediment accumulations	55
1.2.2.3. Type, composition and origin of the sediment acc. associated with SDCGSAPE	57
1.2.2.4. Synthesis	66
1.2.3. SDCGSAPE as a system	66
1.2.3.1. Organisation and components	66
1.2.3.2. The topographical basin	67
1.2.3.3. The proglacial area	68
1.2.4. General synthesis and definition of SDCGSAPE	69
1.3. Research objectives	70

2. Publications

2.1. Paper 1 (Bosson et al., ESPL, 2015)	75
2.1.1. Presentation	76
2.1.2. Content	77
2.1.2.1. Introduction	78
2.1.2.2. Study sites	79
2.1.2.3. Methods	81
2.1.2.4. Results and interpretation	86
2.1.2.5. Discussion	91
2.1.2.6. Conclusion	97
2.2. Paper 2 (Bosson and Lambiel, Frontiers, 2016)	100
2.2.1. Presentation	101
2.2.2. Content	102
2.2.2.1. Introduction	102
2.2.2.2. Study sites	104
2.2.2.3. Methods	107
2.2.2.4. Results	110

2.2.2.5. Interpretation and discussion	117
2.2.2.6. Conclusion	120
2.3. Paper 3 (Capt et al., J. of Glaciology, 2016)	122
2.3.1. Presentation	123
2.3.2. Content	124
2.3.2.1. Introduction	124
2.3.2.2. Study sites and climatic context	126
2.3.2.3. Methods	129
2.3.2.4. Results	133
2.3.2.5. Discussion	139
2.3.2.6. Conclusion	144

3. Compilation and synthesis of results by study site

3.1. Introduction	148
3.1.1. Study sites	148
3.1.2. Methods	149
3.1.2.1. Ground surface temperature measurements	150
3.1.2.2. Electrical resistivity tomography	151
3.1.2.3. Ground penetrating radar	154
3.1.2.4. Differential GPS	154
3.1.2.5. Photogrammetry and image comparison	155
3.1.2.6. LiDAR	155
3.2. Les Rognes and Pierre Ronde	156
3.2.1. Site description	156
3.2.2. Results	159
3.2.2.1. Ground surface temperature measurements	159
3.2.2.2. Electrical resistivity tomography	162
3.2.2.3. dGPS	162
3.2.3. Synthesis	167
3.2.3.1. The current relation between internal structure and surface dynamics	167
3.2.3.2. Genesis and evolution of les Rognes and Pierre Ronde glaciers	168
3.2.3.3. The current state of les Rognes glacier	171
3.3. Les Fours	172
3.3.1. Site description	172
3.3.2. Results and synthesis	174
3.3.2.1. Ground surface temperature measurements	174
3.3.2.2. Electrical resistivity tomography	174
3.3.2.3. dGPS	175
3.3.2.4. Result interpretation and synthesis	176
3.4. Entre la Reille	180
3.4.1. Site description	180
3.4.2. Results	184
3.4.2.1. Ground surface temperature measurements	184
3.4.2.2. Electrical resistivity tomography	187
3.4.2.3. Photogrammetry and image analysis	190
3.4.2.4. dGPS	191
3.4.2.5. LiDAR data	198
3.4.3. Synthesis	199

3.4.3.1. The glacier of Entre la Reille	199
3.4.3.2. Holocene glacier-permafrost interactions	201
3.4.3.3. Recent evolution and current internal structure	201
3.4.3.4. A particular glacier system	203
3.5. Tsarmine	205
3.5.1. Site description	205
3.5.2. Results	208
3.5.2.1. Ground surface temperature measurements	208
3.5.2.2. Electrical resistivity tomography	211
3.5.2.3. Ground penetrating radar	211
3.5.2.4. Photogrammetry and image analysis	212
3.5.2.5. dGPS	213
3.5.2.6. Webcam pictures analysis	218
3.5.3. Synthesis	220
3.5.3.1. The Tsarmine glacier	220
3.5.3.2. Recent glacier history and glacier-permafrost interactions	223
3.6. Chaltwasser	226
3.6.1. Site description	226
3.6.2. Results and synthesis	228
3.6.2.1. Electrical resistivity tomography	228
3.6.2.2. Photogrammetry	228
3.6.2.3. dGPS	230
3.6.2.4. Result interpretation and synthesis	230
3.7. Le Petit Combin	234
3.7.1. Site description	234
3.7.2. Results and synthesis	236
3.7.2.1. Electrical resistivity tomography	236
3.7.2.2. Photogrammetry and image analysis	237
3.7.2.3. Result interpretation and synthesis	238

4. Main outcomes and discussion

4.1. Introduction	245
4.2. Current Internal structure and dynamics	245
4.2.1. System components, organisation and size	245
4.2.1.1. Complex associations of ice, debris and water	246
4.2.1.2. Definition and size of SDCGSAPE	249
4.2.2. Main components and associated dynamics	251
4.2.2.1. Glaciers	251
4.2.2.2. Push-moraines - rock glacier complexes	256
4.2.2.3. Ice free debris accumulations	246
4.3. Genesis and evolution model of glacier systems in high relief environments	260
4.3.1. Debris concentration - ice preservation model and genetic sequence	260
4.3.1.1. Continuum in high relief and permafrost env. and associated glacialic landforms ...	260
4.3.1.2. Bare-ice glacier	263
4.3.1.3. Debris-covered glacier	265
4.3.1.4. Glacialic rock glacier	266
4.3.2. Paradoxical effects of atmospheric warming	269

5. Conclusion and outlook	
5.1. General synthesis	274
5.2. Research perspectives	276
References	280
List of personal publications and participations to conferences	295

1. Introduction



C | The Tsaamine glacier system from the Grande Dent de Veisisi ridge (© A. Dumas, Aug. 2013)

1.1. Context of research: A challenging study object in a changing cryosphere

L'inconvénient des mots, c'est d'avoir plus de contour que les idées. Toutes les idées se mêlent par les bords; les mots, non. Un certain côté diffus de l'âme leur échappe toujours. L'expression a des frontières, la pensée n'en a pas.

Victor Hugo (L'Homme qui rit, 1869)

Frontiers are social constructions. In science, the development of disciplines through distinct approaches, nomenclatures or communication systems erected relatively hermetic research frontiers although objects of study are parts of continuous spectrums and complex interconnected systems. The research objects situated at the artificial and fuzzy discipline boundaries receive therefore a lower attention. It is especially the case of the *small debris-covered glacier systems located in alpine permafrost environments* (SDCGSAPE), the object of study of this research.

This object does not exist hitherto under this appellation in the scientific literature. SDCGSAPE will be therefore discussed and defined in the section 1.2. They are composed by (1) a small sedimentary ice mass, moving under its own weight, partly or totally covered by a debris mantle and (2) its associated debris accumulations (Fig. 1.1). As systems, they constitute wholes of interacting

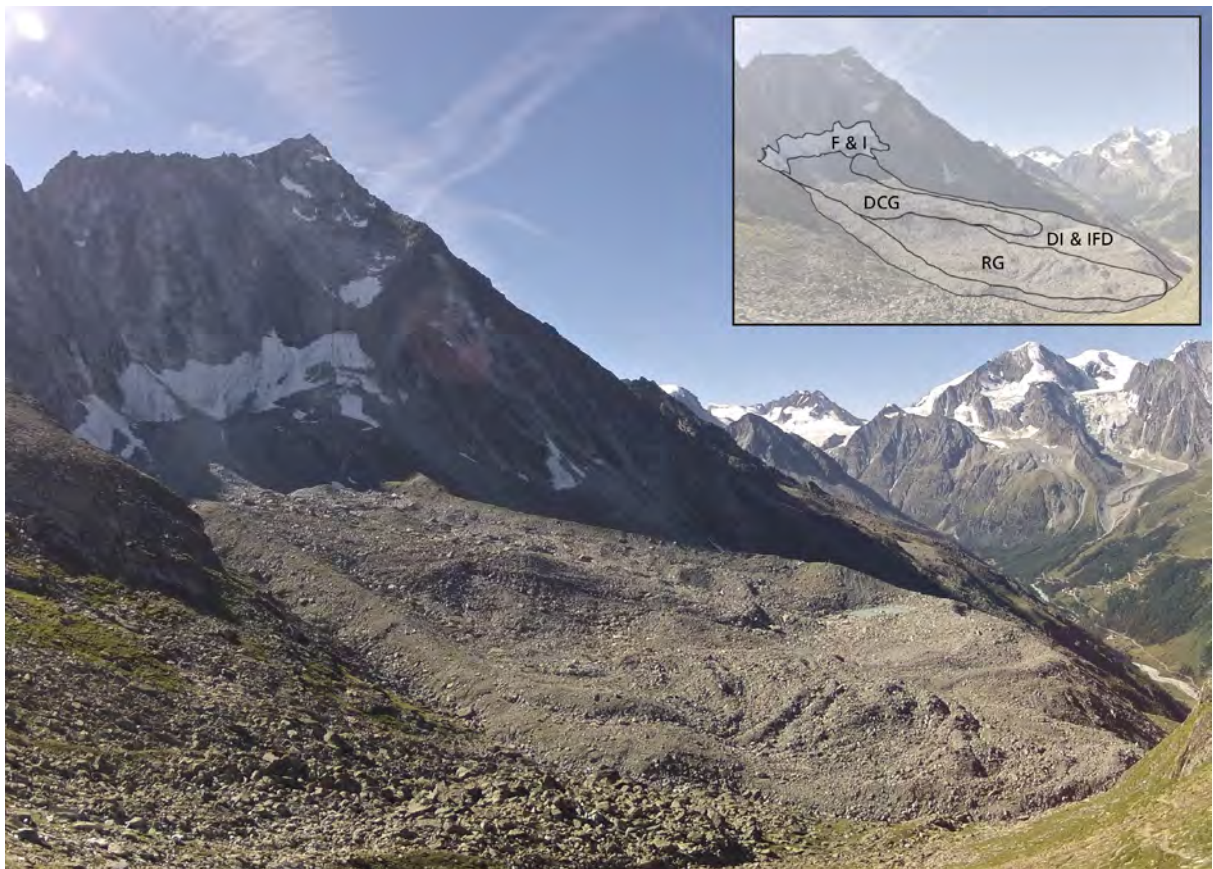


Fig. 1.1: The Tsarmine glacier system (46°03'N, 7°31'E; Switzerland). An upslope firn and bare-ice zone (F&I), a debris-covered glacier tongue (DCG), a marginal rock glacier (RG) and a zone of dead ice and ice-free debris (DI & IFD) compose this SDCGSAPE (© A. Dumas, Aug. 2013).

components, essentially constituted by ice and debris. Their dynamic is related to the fluxes in time and space of these two main constituents, which are mainly driven by gravity and secondarily by water. SDCGSAPE develop at the margin of the glacial domain and under permafrost conditions. They are common in cirques and valley floors of high relief environments, where the rockwalls erosion provides a high debris supply to the glacier system (Benn et al., 2003; Whalley, 2009). These systems are especially numerous in continental climates, where, the limited snow accumulation prevents the development of large glaciers, extending beyond the periglacial belt (Pfeffer et al., 2014).

Whereas glaciers are considered among the best climate indicators in nature (Haeberli et al., 2013; Vaughan et al., 2013), SDCGSAPE experience complex and nonlinear responses to the climate forcing. Several characteristics of these systems explain their atypical behaviour. First, particular processes or orders of magnitude in dynamic characterise the accumulation, the ablation and the motion of the smallest glaciers (Kuhn, 1995; Grunewald and Scheithauer, 2010; Carturan et al., 2013a). This is especially due to their geometry and the strong control that the surrounding topography can exercise on these restricted glaciated surfaces. On one hand, the snow accumulation is enhanced at the foot of rockwalls by wind drifting and avalanching (Rödder et al., 2008;

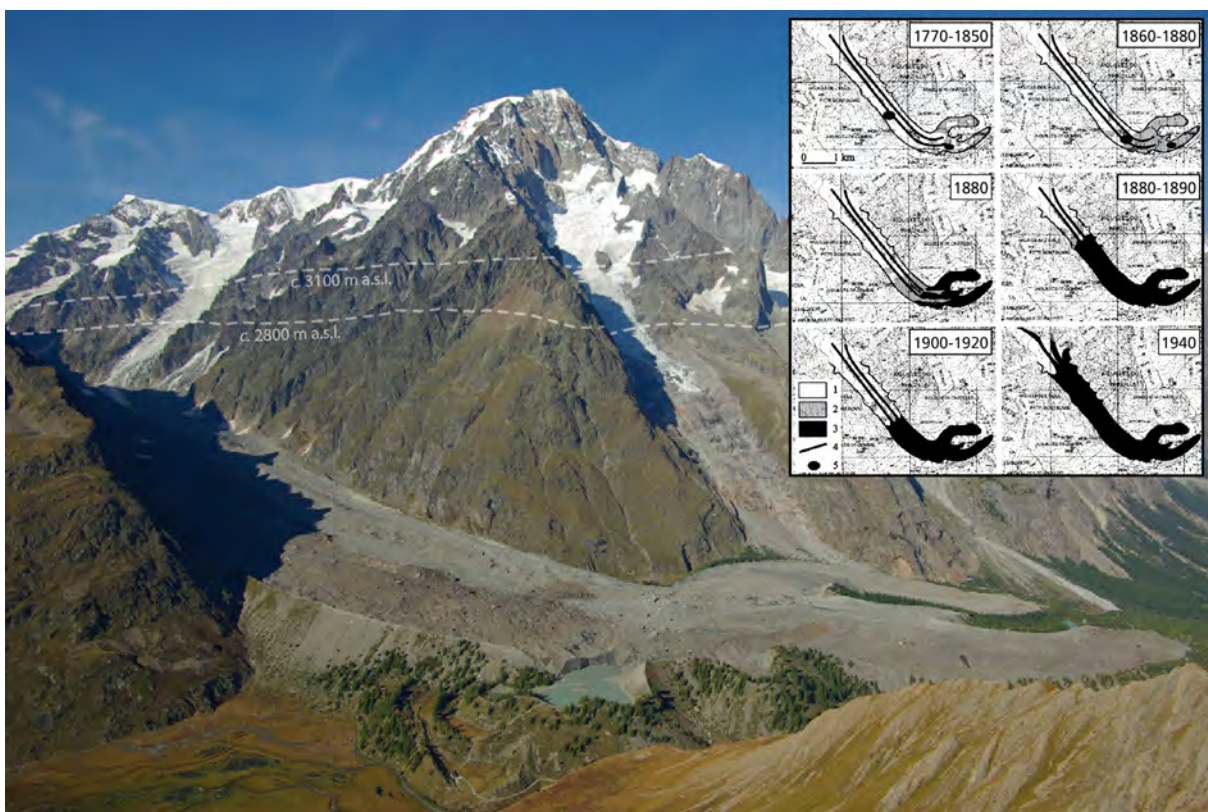


Fig. 1.2: The Miage debris-covered glacier (45°47'N, 06°52'E; Italy; © M. Le Roy, 2008; reproduced from Deline et al., 2012). The glacier area is c. 11 km². The lower part of the ablation area (c. 5 km²) is covered by debris, whose thickness increases from centimeters to >1m downglacier. The limits of 2800 and 3100 m a.s.l. are given respectively as very rough inferior limits of the local periglacial belt (Magnin, 2015) and equilibrium line altitude (according to elevation proposed in the massif by Deline et al., 2012; Gilbert et al., 2012; Godon et al., 2013 and Six and Vincent, 2014) in this area mainly oriented towards the SW. The top-right inset is modified from Deline (2005). It shows the variations of the discontinuous (grey) and continuous (black) debris cover extent since the Little Ice Age. Debris are mainly accumulated on the glacier by rockfalls and avalanches (Brock et al., 2010). The expansion of the debris mantle in time illustrates the transition from a transport dominant mode to an ablation dominant mode (Kirkbride, 2000).

Brown et al., 2010). On the other hand, shadow of steep relief limits direct solar radiation and thus ablation (DeBeer and Sharp, 2009; Gilbert et al., 2012; Scotti et al., 2014).

Moreover, erosion of rockwalls delivers large quantities of debris to the glacier. Their accumulation on the glacier surface strongly modifies their mass balance and motion (Nakawo et al., 2000; Benn et al., 2003 and 2012). Melt rate is enhanced or reduced if the debris cover thickness is respectively below or above a few centimetres threshold (Benn and Evans, 2010). Consequently, debris-covered glaciers have atypical dynamics in time (responses to climate variations) and space (ablation patterns) in comparison with bare-ice glaciers (Scherler et al., 2011; Deline et al., 2012; Shea et al., 2015). During the Holocene (11.7 ka BP – today; e.g. Wanner et al., 2011), this type of system commonly accreted large sediment accumulations (Kirkbride, 2000; Iturrizaga, 2013; Fig. 1.2). The disproportion between glacier size and sediment accumulation is particularly striking in the smallest debris-covered glacier systems, where the low magnitude of glacial and postglacial processes limited the transfer of coarse-grained sediments towards hydrosystem (Maisch et al., 1999; Otto et al., 2009; Matthews et al., 2014). These disproportionate sediment accumulations progressively constrained the ice flow and often contributed to the elevation of the debris-covered glaciers on their morainic bed during the Holocene (Hambrey et al., 2008; Iturrizaga, 2013).

Finally, the permafrost conditions allow the accumulation and preservation of ground ice in the marginal sediment accumulations (Etzelmüller and Hagen, 2005; Ribolini et al., 2010; Lilleøren et al., 2013). If the slope and the thickness of the frozen sediment accumulations are enough, the latter can deform downward and become glacigenic or glacier-derived rock glaciers (Ackert, 1998; Potter et al., 1998; Berthling, 2011; Monnier et al., 2014). Moreover, permafrost conditions also affect the glacier thermal regime (Etzelmüller and Hagen, 2005; Cuffey and Paterson, 2010). Cold or temperate ice can be present in these environments, strongly influencing ice deformation, basal slip, melt rates and glacier hydrology.

Cryosphere : portions of Earth's surface where water is in solid form

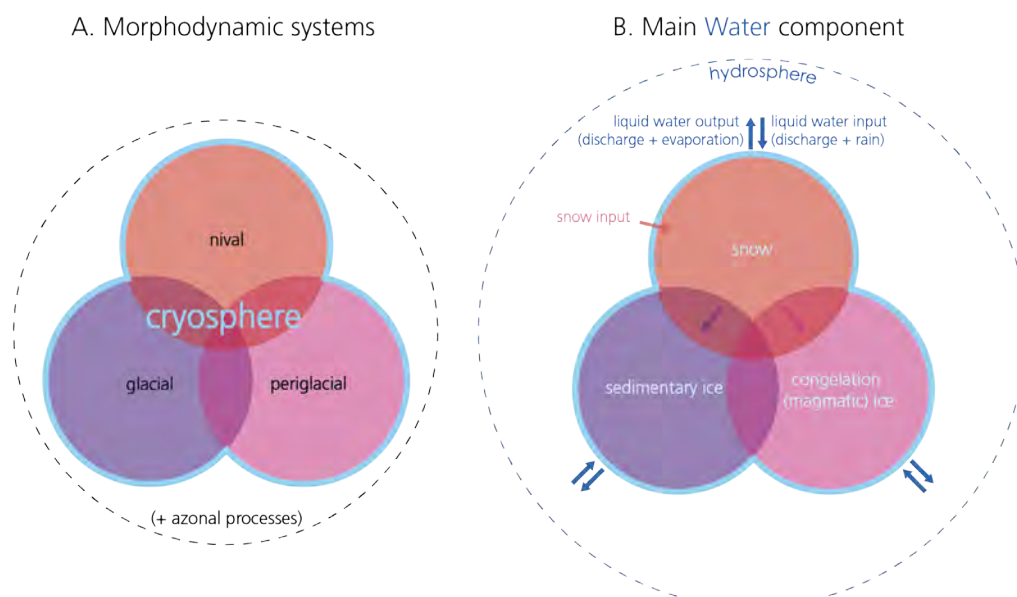


Fig. 1.3: Conceptual model of the morphodynamic systems (A) and the main water component (B) of the cryosphere.

As a consequence of all these characteristics, time lags, positive and negative feedbacks affect the responses of SDCGSAPE to climate forcing. Some of them can even become climatically decoupled (Benn et al., 2003). They appear therefore to be very complex glacier systems, especially in comparison with the majority bare-ice and commonly larger systems, on which most of the empirical knowledge of glaciology, monitoring programs and evolution models are based (e.g. WGMS, 2008; Huss and Hock, 2015; Zemp et al., 2015). The current knowledge on glaciers is still incomplete in time and space, and complex drivers of glaciers behaviours are still barely understood (Knight and Harrison, 2014). Hence, the collection of empirical field data and their integration in the very useful but simplistic large-scale modelling remain a challenging task in glaciology (Huss, 2012; Dohbal et al., 2013; Pellicciotti et al., 2015).

SDCGSAPE are not only complex glaciological objects, they are also complex transitional landforms between glacial and periglacial morphodynamics (Fig. 1.3). Indeed, the latter have coexisted, interacted or followed each other in these systems (Ackert, 1998; Shroder et al., 2000; Monnier et al., 2015; Seppi et al., 2015) as a function of Holocene climate fluctuations (e.g. Ivy-Ochs et al., 2009; Jomelli et al., 2009). Glaciers have thereby successively grown and declined in the

neighbouring of large, possibly frozen and flowing sediment accumulations. Consequently, SDCGSAPE have to be thought as polygenic and multi-phased legacy of Holocene climate history. In this way, they are objects situated between the glacial and periglacial researches. However, these two cryospheric sciences developed and evolved along separate lines in the last decades (Haeblerli, 2005; Knight, 2011; Berthling et al., 2013). Consequently, no integrative view exists today on SDCGSAPE to our knowledge. They are too rarely

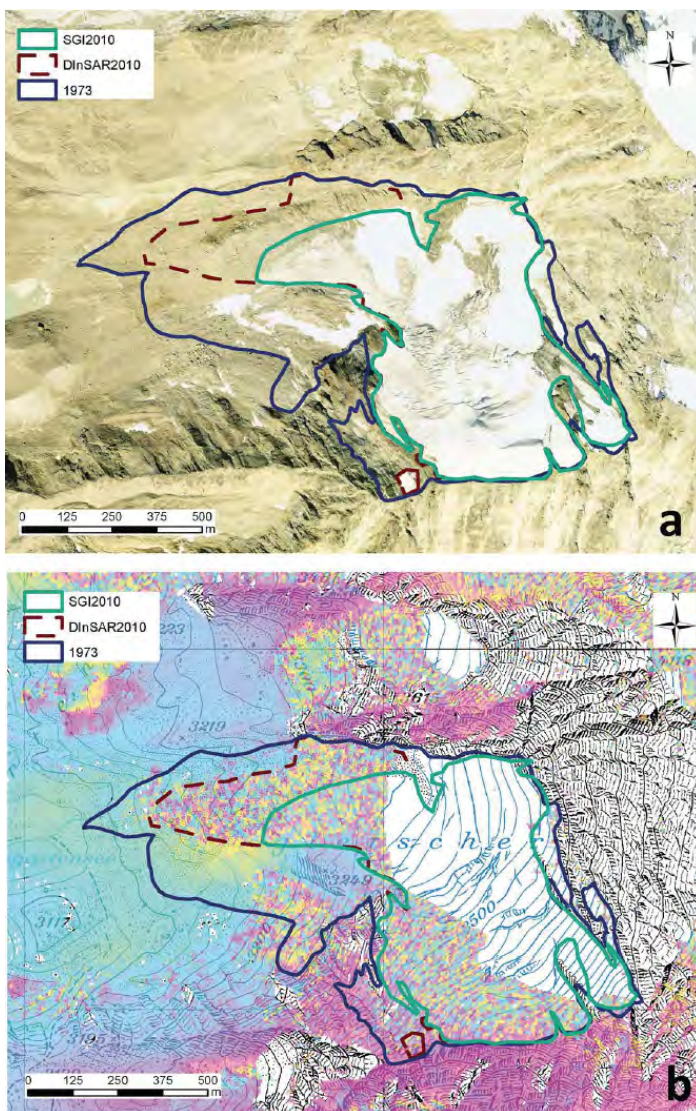


Fig. 1.4: Orthophoto of 2010 (a) and TSX 11 days DInSAR (Differential Synthetic Aperture Radar Interferometry) scenes from 9-20 September 2010 in combination with the topographic map (b) of the Weingartengletscher-S-II (46°04'N, 7°51'E; Switzerland). The debris accumulation in the lower zone hampers a clear distinction of the glacier outlines in 2010. In this way, the initial delineation of glacier boundary by photo interpretation (green limits) was corrected by the analysis of DInSAR data (purple limits). Clear patterns of pixel decorrelation in the debris area illustrate the movements and thus the extension of the debris-covered glacier zone. Reproduced from Fischer M et al. (2014).

thought as a whole entity, where glacial and periglacial dynamics are associated. On one hand, glaciological researches always neglected these complex assemblages of sedimentary ice and debris, especially because (1) the extensive debris cover hampers conventional measurements, (2) they are very complex climate indicators in comparison with bare-ice systems and (3) the distinction of the glacier area from debris accumulations and/or periglacial features remains problematic (Pfeffer et al., 2014; Fischer M et al., 2014; Janke et al., 2015; Fig. 1.4). On the other hand, periglacial researches mainly focused on the controversial origin of the landforms associating debris and ground ice, such as ice-cored moraines, push-moraines or rock glaciers (e.g. Berthling, 2011; Monnier et al., 2011; Janke et al., 2013; Lilleøren et al., 2013; Matthews et al., 2014). Rather led towards geomorphological objectives, these studies concentrated on the sedimentary margins, neglecting glaciological considerations on the upslope glacier. The fuzzy transition between glacial and periglacial dynamics in SDCGSAPE is therefore still poorly understood (Emmer et al., 2015). As a consequence, the consideration of these systems in glaciers or rock glaciers inventories or in regional studies is variable and never satisfactory. They can be voluntarily excluded in relation with their complexity or taken into account without having been clearly defined and distinguished from close landforms (e.g. Azócar and Brenning, 2010; Bockheim et al., 2013; Pfeffer et al., 2014; Fischer A et al., 2015).

According to the orders of magnitude proposed in regional or large-scale inventories (e.g. Delaloye et al., 2010; Krainer and Ribis, 2012; Pfeffer et al., 2014) and exploration of satellite imagery in *Google Earth*, there is likely tens of thousands of SDCGSAPE on Earth surface. Similar landforms can even be observed on Mars (Hubbard et al., 2014; Fig. 1.5). On Earth, their concentration is especially high in the tectonically young high relief located in continental climates (e.g. Hindukush–Karakorum–Himalaya, Andes or European Alps). Furthermore, SDCGSAPE are more and

more numerous in the context of worldwide glacier shrinkage (Zemp et al., 2015) and with the strong changes that affect the alpine cryosphere (Deline et al., 2012; Vaughan et al., 2013). The

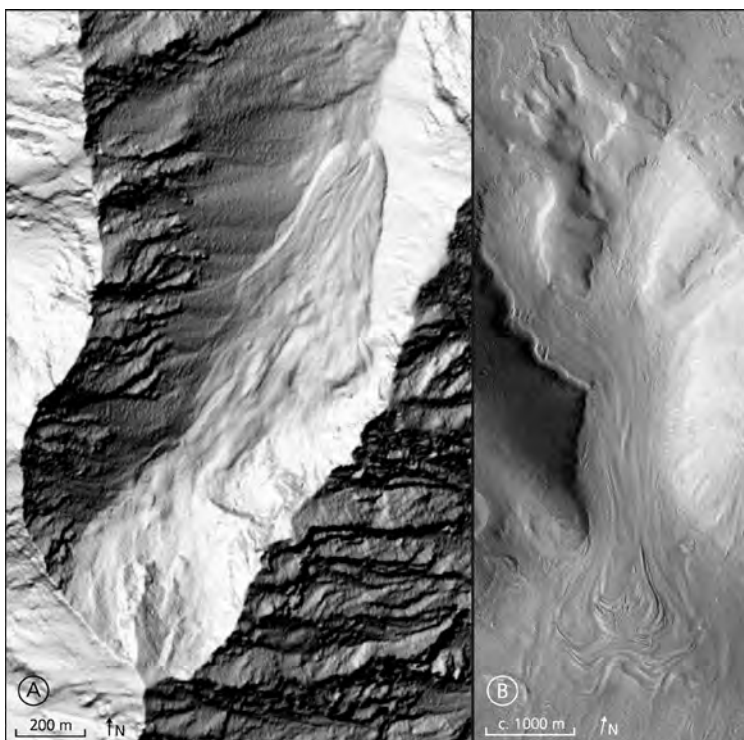


Fig. 1.5: Shaded relief of the Valetta glacier system (A; 46°38'N, 10°06'E; Switzerland; © SwissAlti3D, map.geo.admin.ch, 2015) and grayscale picture of an analogous landform on Mars (B; 45°14'N, 38°18'E; © Nasa/JPL/University of Arizona, picture of 2010, GoogleEarth 2015). The latter is discussed in Hubbard et al. (2014). Developed from a topographic niche, both landforms illustrate the viscous deformation –respectively towards the North in A and the South in B– of ice and debris under gravity. The formation of ice at the root of these systems is possible on Earth. Conversely, glacier-like forms on Mars are inherited from a past glaciation (Janke et al., 2013; Hubbard et al., 2014)

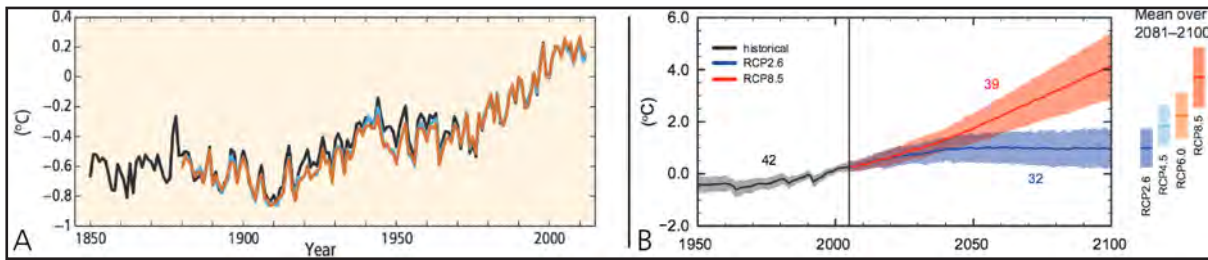


Fig. 1.6: Annually and globally Earth surface temperatures anomalies relative to the average over the period 1986 to 2005. **(A)** Observed anomalies since 1850, reproduced from IPCC (2014). **(B)** Modelled anomalies from 1950 to 2100. The numbers of models used to calculate the multi-model mean is indicated near the curves. RCP mean *Representative Concentration Pathways* used for simulations. Reproduced from Stocker et al. (2013).

atmospheric warming (Fig. 1.6) induces especially a rapid downwasting rate for glaciers that can lead to their fragmentation. Hence, glaciers become generally smaller and thinner (Paul et al., 2007; Scotti et al., 2014; Fig. 1.7). Their extent is progressively restricted within the periglacial belt, where the cold conditions limit the ice decay. Moreover, because glaciers driving stress is related to their thickness, thinning glaciers become less dynamic (Benn et al., 2012; Haeberli et al., 2013). The efficiency of sediment evacuation is then reduced and debris can accumulate on glacier surface (Kirkbride and Deline, 2013; Fig. 1.2). Simultaneously, the deglaciation of rockwalls and lateral sediment accumulation, and the permafrost degradation increase the sediment supply to glacier systems (Deline et al., 2015). The proportion of debris-covered ice is thus increasing in high relief regions (Carturan et al., 2013b; Kirkbride and Deline, 2013; Knight and Harrison, 2014).

As all the components of the cryosphere (Vaughan et al., 2013; Knight and Harrison, 2014), SD-CGSAPE are not simply passive indicators of the current climate changes. Located in the upper part of high relief regions, they are among the first main storage of freshwater and sediment of these environmental systems. Thus, their role is important at the local scale because they can possibly

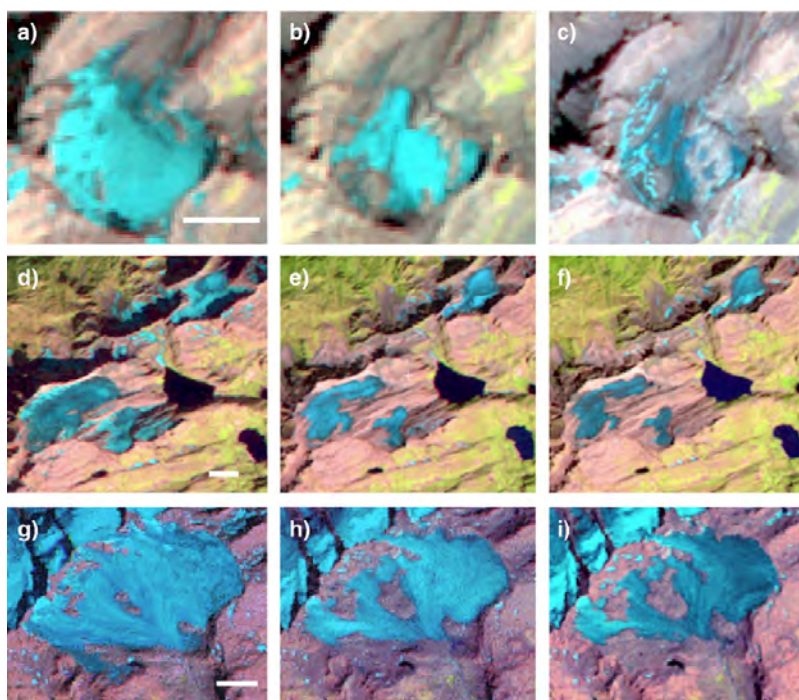


Fig. 1.7: Infrared satellite imagery showing the recent disintegration of glaciers in three areas located in the European Alps: Taelli Glacier which has currently disappeared (46°5'N, 7°6'E; **a**) in 1985, **b**) in 1998 and **c**) in 2004), Cavagnoli Glacier (46°5'N, 8°5'E; **d**) in 1985, **e**) in 1998 and **f**) in 2003) and Careser Glacier (46°5'N, 10°7'E; **g**) in 1985, **h**) in 1999 and **i**) in 2003). The white bare scale corresponds to 500 m. The rapid melt of the ice induces a fragmentation of the glaciers due to downwasting. At local scale, the individual response of glaciers to the same climate forcing can be very heterogeneous, as illustrated by comparison between the rapidly wasting Cavagnoli Glacier and the close and relatively stable the Valleggia Glacier in the upper right of d), e) and f). Reproduced from Paul et al. (2007).

influence physical, biological and social systems located up to tens of kilometres downslope. With their superficial insulating layer that limits the ice melt, debris-covered glaciers, rock glaciers and thus SDCGSAPE will constitute preserved freshwater reservoirs at local scale (Knight and Harrison, 2014; Janke et al., 2015; Rangecroft et al., 2015; Fig. 1.8), while a worrying reduction of water stores is announced in all the glacierized regions in the 21st century (IPCC; 2014). Their major role in environmental and social systems, as a component of hydrosystem will then further increase in the next decades. Moreover, as proglacial sediment accumulations, SDCGSAPE can act either as sinks or sources in sediment transfer systems (Owens and Slaymaker, 2004; Fig. 1.8). Influencing noticeably sediment fluxes, they are also sources of geohazards (Chiarle et al., 2007; Krainer et al., 2012; Deline et al., 2015).

SDCGSAPE are therefore complex, poorly known, very –and increasingly- numerous, and important water and sediment stores of cold high relief environments. Through the exploration of a discipline frontier, they offer fascinating and challenging perspectives of research. This PhD thesis will try to shed light on these objects and to lay the foundation of their comprehensive analysis. However, the construction of a holistic and exhaustive knowledge about these complex systems is an ambitious multidisciplinary challenge for the scientific community. This task is beyond the ambitions of this modest contribution. Its aim is rather to synthesize and to propose new insights on the internal structure, the dynamics and the genesis-evolution of these systems. This will be based on a review of the scattered existing literature and the exploration of new results obtained in a multi-sites, multi-methods and multi-temporal study, which has been carried out between 2010 and 2015 in the north-western European Alps.

In the following, a synthetic review of literature existing on SDCGSAPE is proposed, allowing to define these systems (1.2). The research objectives are the presented in 1.3. The second part compiles, in a chronological order, the scientific publications produced during this PhD thesis. As all the results were not presented in the publications, a compilation and a synthesis of the results obtained at each study site is proposed in the third part. The main outcomes on internal structure, dynamics and genesis of SDCGSAPE and their discussion with the scientific context compose the fourth part. This contribution finishes with a general conclusion and the identification of research perspectives.

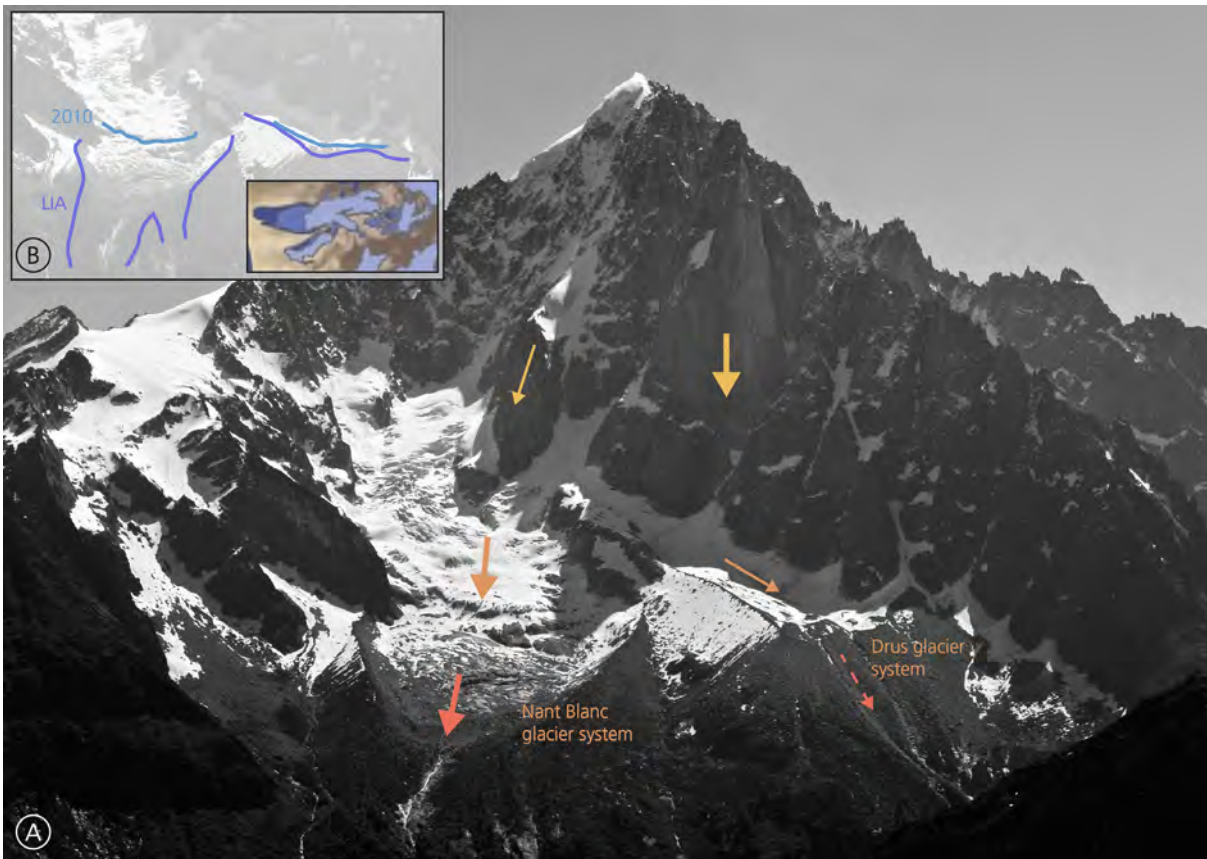


Fig. 1.8: Comparison between the Nant Blanc and Drus glacier systems (45°56'N, 6°57'E; France). **(A)** Photograph of June 2010 showing the different roles played by these glaciers in the sediment transfer system. First, the sediment production (yellow arrows) is higher in the Drus basin than in the Nant Blanc basin because the first one is less glacierized and subject to frequent and possibly large rockfall events (Ravanel and Deline, 2008). Second, the Nant Blanc glacier is thicker and larger than the Drus glacier and thus more efficient to transfer the sediment load (orange arrows). Third, the Nant Blanc glacier is better coupled with hydrosystem than the Drus glacier (red arrows). This is due to a higher meltwater production, the steeper topography and the absence of a distal moraine dam. The efficiency of Nant Blanc glacier to transfer sediment is evidenced by its deglaciated rocky bed and by the relatively limited size of Holocene's moraines. Conversely, the heavily debris-covered Drus glacier system can be considered as a sediment sink that accreted a large Holocene moraine dam. Sediment evacuation from this poorly coupled system only occurs with rare debris flow events. The consideration of the Drus glacier as a SDCGSAPE remains open because this system is located at the lower margin of the local periglacial belt. **(B)** The distinct glacier evolution since the LIA. Unlike the Nant Blanc glacier, the Drus glacier has weakly retreated since the LIA. This situation is due to the sheltering of the ice by the shadow effect and the presence of an extensive and thick debris-cover. In that way, the relative ice loss of heavily debris-covered glacier is largely inferior to the one of bare-ice systems and they will become fundamental water reservoir in the 21st century. The inset map is reproduced from Gardent (2014) and shows the local glacier extents in the LIA, late 1960s and 2008.

1.2. Definition and state of knowledge on small debris-covered glacier systems located in alpine permafrost environments

This section explores the consideration of SDCGSAPE in the scientific literature. However, these systems are rarely recognised and studied as a whole. Hence, most of this review relies on their partial or indirect investigation as debris-covered glaciers, small glaciers, or glaciers located in permafrost environments (1.2.1), or as glacialigenic sediment accumulations that possibly contain ground ice in permafrost environments (1.2.2). This literature analysis will allow us to highlight the characteristics and the possible peculiarity of SDCGSAPE in comparison with other glaciers systems and to define them as systems (1.2.3 and 1.2.4). Based on hundreds of peer-reviewed articles, book chapters and reports, this state of knowledge tries to give the most complete overview as possible of these systems. Nonetheless, because of the exponential growth in the number of the scientific publications (e.g. [Parolo et al., 2015](#)) and the position of SDCGSAPE at the frontier of disciplines covered by a multitude of scientific media, this review is in essence non-exhaustive.

1.2.1. A particular type of glacier

As their name implies, SDCGSAPE combine three fundamental characteristics of glacier systems: the presence of an extensive supraglacial debris cover, the small size and the location of the glacier within alpine permafrost environments. These characteristics differentiate these systems from larger and/or bare-ice glaciers that extend beyond permafrost areas. In the literature, these characteristics are rarely mentioned or investigated together and studies are commonly focused on one of them. Before, reviewing the implication of these characteristics on glacier behaviour, which were rapidly mentioned in the introduction, it is important to remind that the main component of SDCGSAPE is a **sedimentary ice mass, mainly formed by the recrystallization of compacted snow, which flows downhill under gravity**. This main component corresponds to the definition of a **glacier** ([WGMS, 2008](#); [Dobhal, 2011](#); [Fig. 1.9](#)).

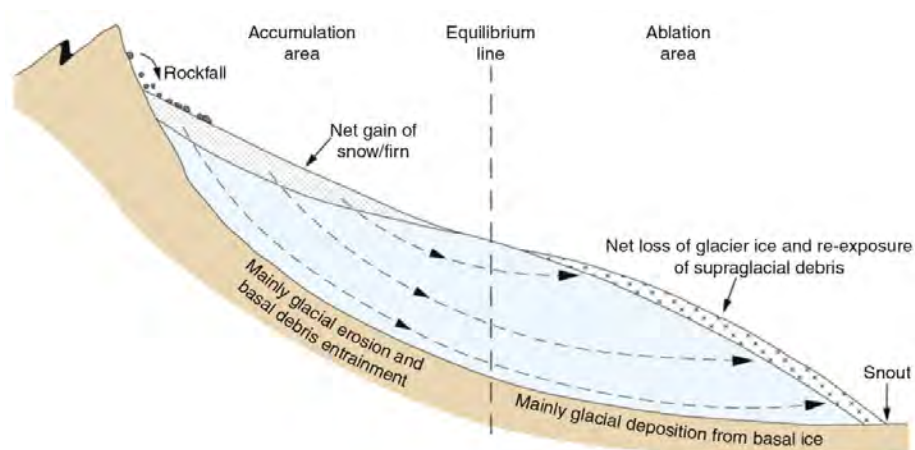


Fig. 1.9: Longitudinal profile of a glacier showing its main components and ice/sediment paths from accumulation to ablation areas. The ice flow is driven by gravity. According to the ratio between the net gain of snow/firn and the net loss of glacier ice, the mass balance is positive or negative. Reproduced from [Hambrey and Glasser \(2011\)](#).

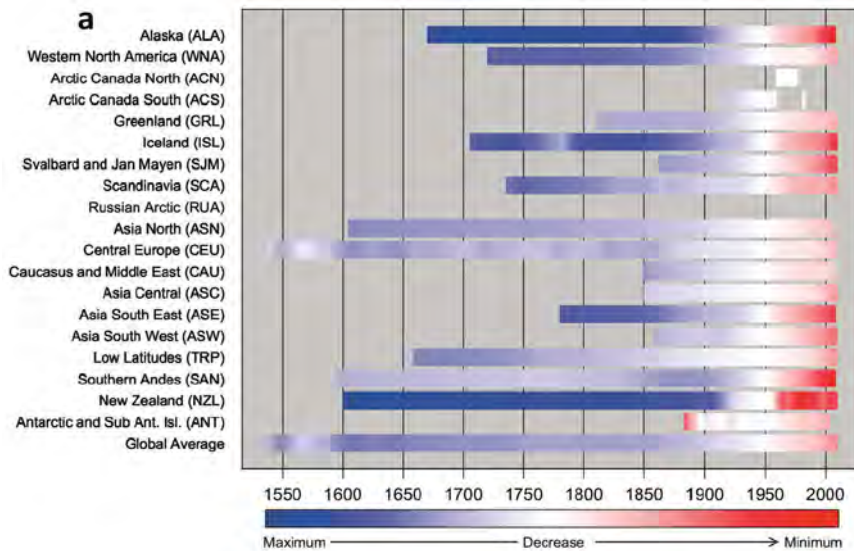


Fig. 1.10: Qualitative summary of cumulative glacier length variations on Earth. The white colour corresponds to the reference position of 1950, blue and red respectively illustrates glacier advances and retreats. All the observations and the reconstructions of the World Glacier Monitoring Network are taken into account in this figure, except the variations of calving and surging glaciers. Reproduced from Zemp et al. (2015).

As all glaciers, SDCGSAPE are climatically controlled natural systems. They develop on the coldest regions of the Earth surface where the snow accumulated over the years do not melt entirely during the ablation season and is progressively transformed into a moving ice mass. Their extent is related to the glacier mass balance that depends on the energy exchanges between the glacier and the atmosphere, hydrosphere, biosphere, and lithosphere (Benn and Evans, 2010). The formation of sedimentary ice in glacier systems can be active or inactive according to the net balance between snow accumulation and melt. This balance continuously changes in time, principally in relation with the variation of climatic conditions. The latter have become globally unfavourable on Earth since the end of the Little Ice Age (LIA: 1300-1850/60 AD in the European Alps; Ivy-Ochs et al., 2009). Indeed, glaciers have mainly experienced negative mass balances in relation with the significant atmospheric warming and its acceleration in the last decades (Vaughan et al., 2013; Zemp et al., 2015; Fig. 1.10). Ablation rates have been generally higher than accumulation rates since 1860, inducing a decrease in the glacier surface worldwide. Hence, accumulation

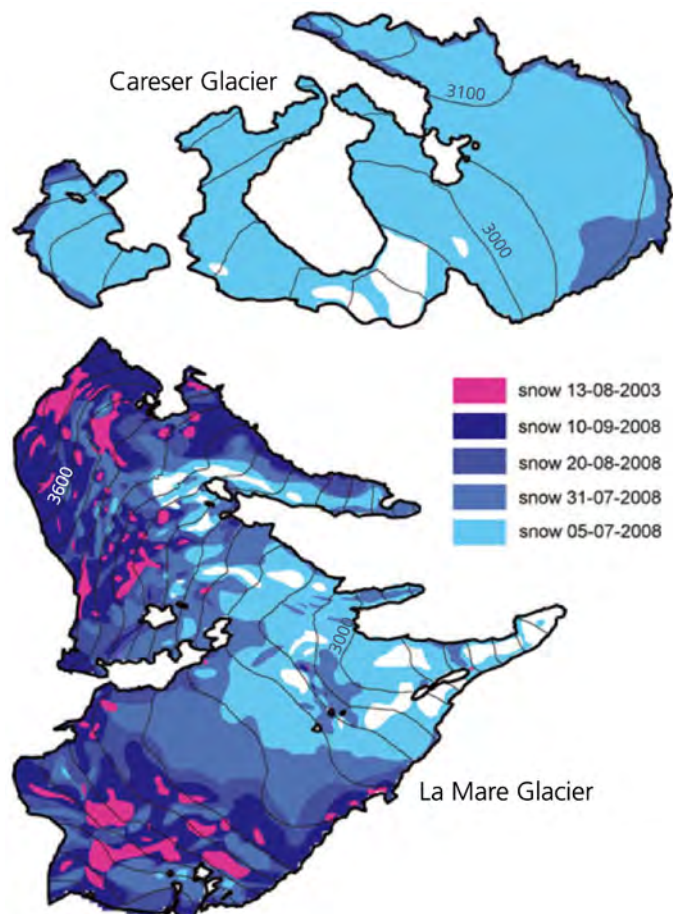


Fig. 1.11: Observations of snow cover during the melt season on two neighbouring Italian glaciers. The mass balance of both glaciers was strongly negative in the 2000s. Hence, no snow was accumulated at the end of the melt season on Careser glacier in 2003 and 2008 (this glacier is also used in the Fig. 1.6). Conversely, discontinuous patches of snow were accumulated at La Mare Glacier. Adapted from Carturan et al. (2012).

areas have reduced or even disappeared in some glacier systems (Fig. 1.11). However, numerous complex processes delay glacier responses to climate variations (e.g. upslope net balance diffusion downglacier, reduction of ablation rate by debris cover or shadow effect). The geometry of glaciers is thereby always partly inherited from the past and does not reflect solely the climatic conditions at a given time (Paul et al., 2007; Jouvét et al., 2011). Thus, current glaciers and SDCGSAPE have to be both considered as responsive indicators of climate variations and active legacies of recent colder and/or wetter climate. In this context, some glaciers have become *dead* ice bodies from a genetic point of view because cryogenesis is not active anymore in them (e.g. Ribolini et al., 2010). Nevertheless, they remain flowing sedimentary ice masses and correspond to the definition of glaciers. In this sense, they contrast from a dynamical point of view with *dead ice* (Schomaker, 2008; Dobhal, 2011), *ice patches* (Serrano et al., 2011) or *glacierets* (Nicholson et al., 2010; Kumar, 2011), which are defined as stagnant landforms.

The motion of glaciers can be due to basal sliding, internal deformation and/or bed deformation (Cuffey and Patterson, 2010; Fig. 1.12). Its intensity depends on the ratio between driving and resisting forces and is high when all these processes are involved and when the glacier is thick. In the current climatic context and especially because glaciers are thinning, the driving stress decreases. Thus, glaciers generally become less dynamic (e.g. Huss, 2010; Benn et al., 2012; Haeberli et al., 2013; Fig. 1.13). Glacier stagnation can even occur when the ice thickness and/or the topographic slope angle become too weak to allow their motion.

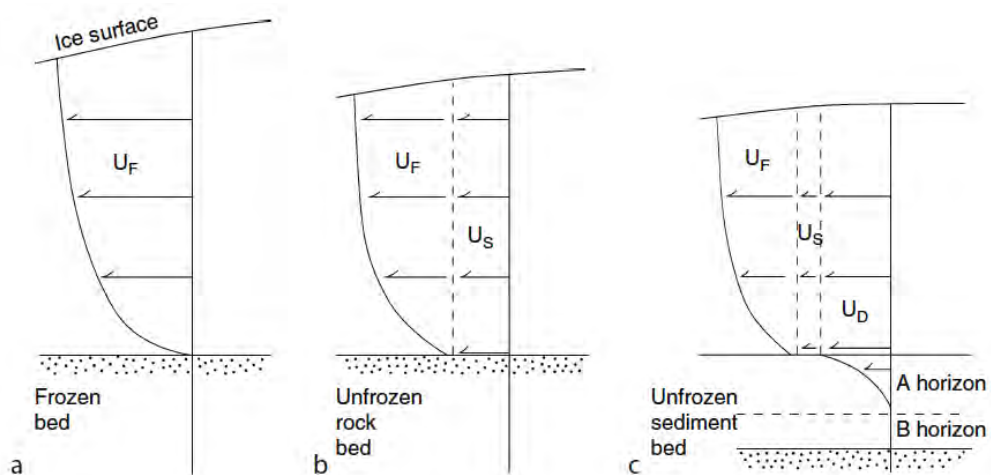


Fig. 1.12: Vertical velocity distributions in glaciers according to the thermal and mechanical conditions at its bed. Internal deformation (or creep or flow, U_F), basal slide (or slip, U_S) and bed deformation (U_D) can occur. Bed deformation is usually thought to be solely effective in unfrozen sediments of warm-bed glaciers. However, it can also occur within or below the frozen sediments of cold-based glaciers (e.g. Waller, 2001). Reproduced from Fitzsimons and Lorrain (2011), who redraw the diagram of Boulton (1996).

1.2.1.1. The influence of the supraglacial debris cover

Definition and research issues on debris-covered glaciers

SDCGSAPE are types of **debris-covered glaciers** (e.g. Fig. 1.1, 1.2 & 1.14A). They can be distinguished from bare-ice –also referred to as clean-ice or debris-free– glaciers by the presence on the ablation zone of “a continuous cover of supraglacial debris across its full width” (Kirkbride, 2011,

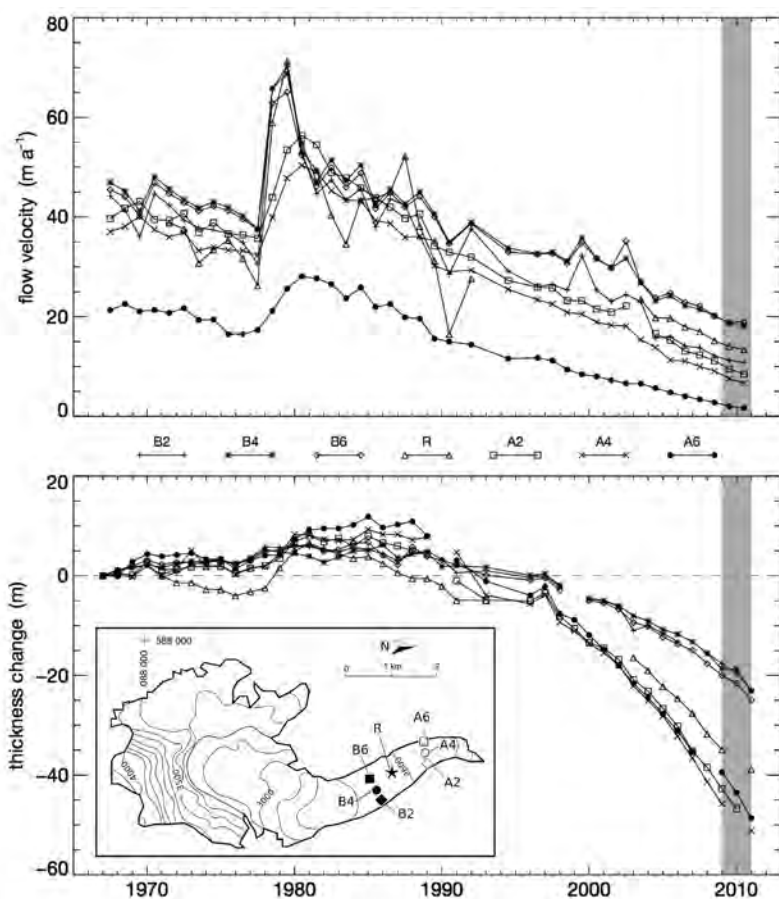


Fig. 1.13: Evolution of annual surface velocity and ice thickness at seven stakes of the glacier de Corbassière (46°N, 7°17'20E; Switzerland). The inset presents the glacier topography and the location of stakes. The relation between ice thickness and flow velocity is clear. Both have noticeably reduced since the 1990s. As a consequence, the debris cover is expanding on the Corbassière glacier. Modified from Bauder (2015).

p. 190). However, this definition remains relatively open and no absolute or proportional thresholds on the covered area are consensually used in the literature to distinguish this type of glacier. Some authors consider that more than the half of the ablation area must be covered (Kirkbride, 2011). Recently, Janke et al. (2015) classified respectively *semi*, *fully debris-covered glaciers* and

buried glaciers with the order of magnitudes of 25, 95 and 100% of coverage. The definition of debris-covered glaciers is also confronted to the problematic distinction between bare-ice and debris-covered ice. Indeed, the debris cover can be very thin (Zhang et al., 2011; Gabbi et al., 2015; Fig. 1.15), discontinuous and its distribution changes rapidly through time (Deline, 2005; Stokes et al., 2007). Thus, its transition with bare-ice is gradual and hard to clearly set. The thickening of the debris-cover in time and/or space is also challenging for the delineation of these glaciers. Supraglacial sediment layers can reach several meters of thickness, especially in the distal glacier areas (Mihalcea et al., 2008; Janke et al., 2015). This complicates noticeably the detection of the external glacier limits by *in situ* or by remote sensing measurements (Shukla et al., 2010; Fischer M et al., 2014; Pfeffer et al., 2014; Fig. 1.4).

Beyond these definition issues, debris-covered glaciers have received a reduced attention in glaciology for three other main reasons. First, although the proportion of the debris-covered ice can be relatively high in some high-mountain regions (e.g. up to 100% of some basins of the Semiarid Chilean Andes according to Azócar and Brenning, 2010; 25% of the Everest region according to Shea et al., 2015), only few percent of the glacier ice on the Earth is debris-covered. This weak proportion is especially related to the relatively small surfaces covered by debris on the glaciers of high latitudes, which correspond to more than 75% of the area occupied by glacier on Earth (Pfeffer et al., 2014). Second, the debris cover hinders conventional measurements and relatively few field data have been obtained on these glaciers (Nakawo and Rana, 1999; Kirkbride, 2011; Zhang et al., 2011). Third, the progresses of glaciology since the 20th century are, to a large extent,

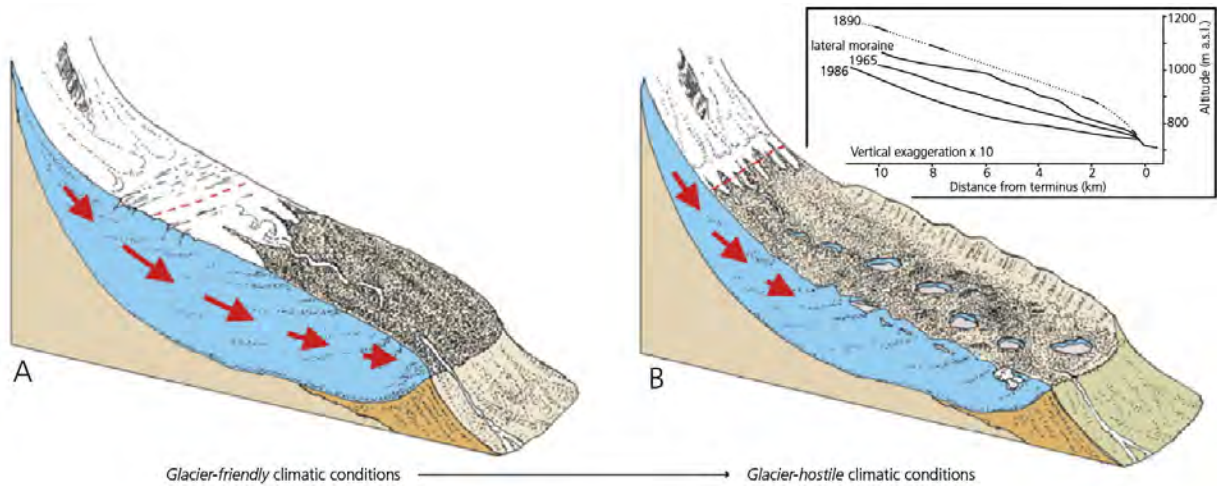


Fig. 1.14: (A) Schematic representation of a debris-covered glacier. The dotted red line corresponds to the equilibrium line altitude. (B) Possible evolution of this system under glacier-hostile climatic conditions. The glacier tongue becomes thinner, flatter and concave and the driving stress decreases as illustrated by the red arrows. The generalised downwasting dynamic induces the spread of the debris cover upglacier and the formation of supraglacial lakes. Reproduced from Benn et al. (2012). Inset: the recent longitudinal profile evolution of the surface of the Tasman glacier tongue (43°39'S, 170°12'E; New-Zealand). It illustrates the progressive transition from the A to B situations. Redrawn from Kirkbride and Warren (1999).

related to their consideration as excellent climatic barometers (Knight, 2011; Haeberli et al., 2013). Yet, as mentioned in the introduction and developed in the following, debris-covered glaciers react complexly to climatic variations. This contributes to limit the interest for these systems.

Debris-covered glaciers are therefore still relatively barely known and remain secondary objects of glaciology. Although debris-covered glacier zones are more and more numerous on Earth and recognized as preserved water reservoirs in a warming climate (Mayer et al., 2006; Pourrier et al., 2014; Janke et al., 2015), the complex effects of the debris-cover on glacier behaviour are for example still voluntarily ignored in large scale glaciers evolution models (e.g. Huss and Hock, 2015 and reference therein) and only integrated in few local scale modelling (Jouvet et al., 2011; Shea et al., 2015). Nonetheless, the knowledge about debris-covered glaciers has increased since the two last decades. Researches largely concentrated on medium and large-sized valley glaciers (c. 1-500 km²) and the smallest ones received significantly lower attention. However, most of knowledge can be transferred to all the debris-covered glaciers as they globally behave in the same way, regardless their size. Main findings are summarized in the next paragraphs. They precede reflexions on the influence of the small size and the confinement of the glacier in permafrost areas, the two characteristics that make SDCGSAPE a specific type of debris-covered glaciers.

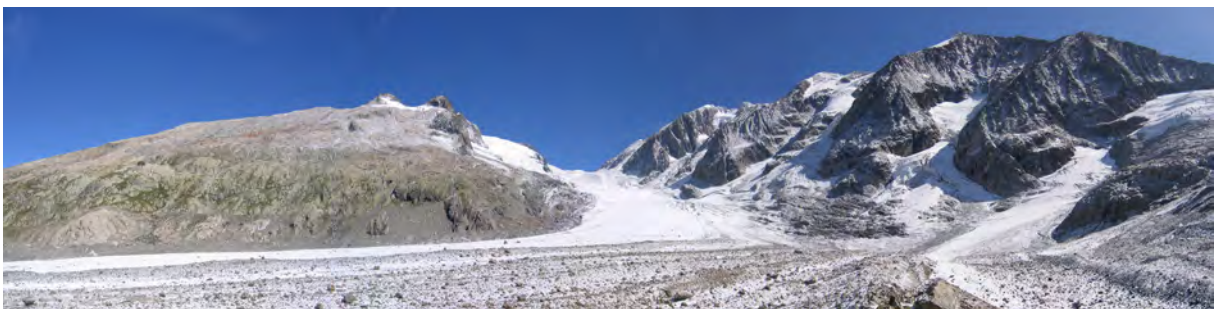


Fig. 1.15: View of the top part of the Tré la Tête glacier basin in the Mont-Blanc range (45°47'N, 6°47'E; France; July 2009). Bare-ice and debris-covered glacier zones are complexly imbricated. Their transition is rather gradational than sharp, which complicates their precise delineation.

Genesis of debris-covered glaciers

Debris-covered glaciers develop in all the glacierized and high relief regions of the Earth, where the effective erosion of ice-free steep slopes provides a major sediment supply to the glacier system. They are very common in the tectonically young mountain ranges (e.g. Hindukush–Karakorum–Himalaya, Andes or New-Zealand Alps) and less frequent in old relief regions because of a lower sediment production (e.g. Scandinavian Alps; [Benn et al., 2003](#)). Supraglacial debris layers mainly develop on low gradient glacier zones as cirque or valley floors. Indeed, the sediments cannot accumulate on ice surfaces too steep or frequently swept by snow and/or ice avalanches ([Fig. 1.15](#)).

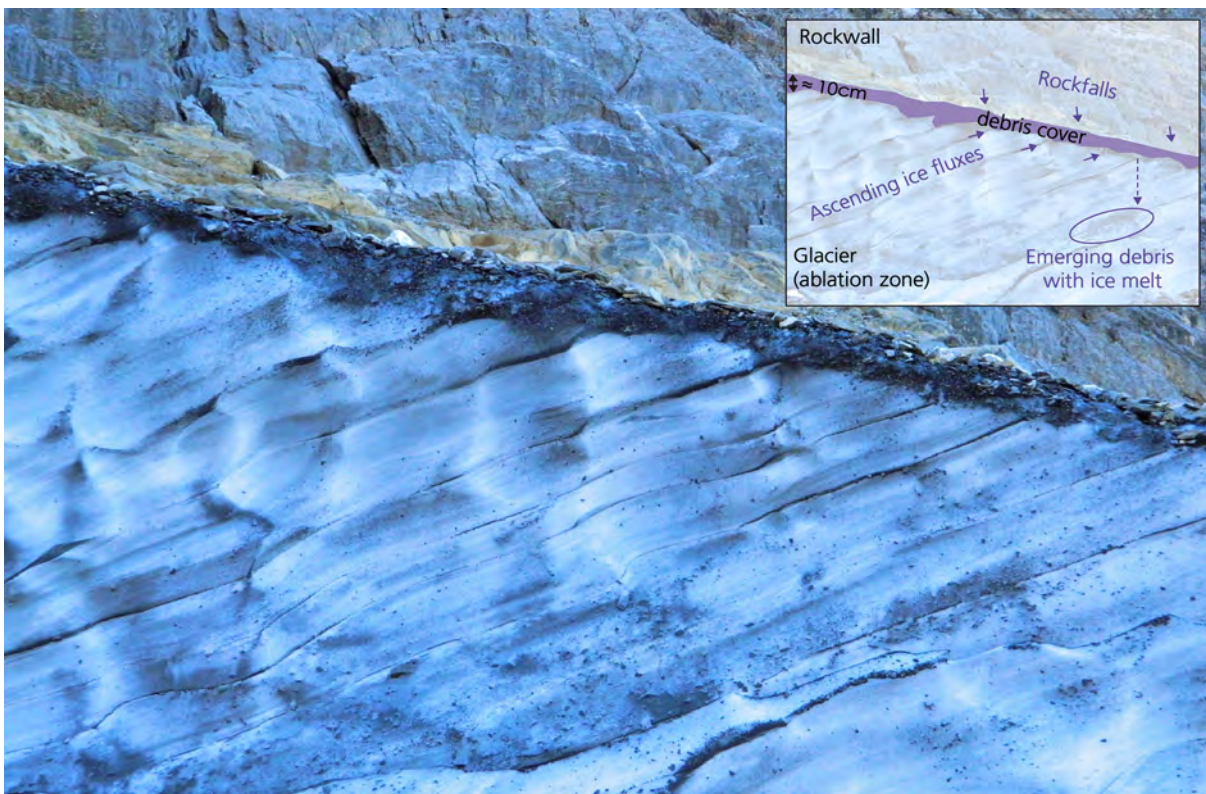


Fig. 1.16: Longitudinal cut in the distal zone of the remnant Pierredar glacier (46°19'07N, 7°11'45E; Switzerland; Sept. 2011). This cut is related to the collapse of a former ice cave. The three main processes inducing the accumulation of debris in the ablation area are described in the inset: rockfalls, the ascendance of ice fluxes and the emergence of debris with ice melt.

Three main processes, that can be active simultaneously, explain the accumulations of debris on the glacier surface ([Fig. 1.16](#)). First, the debris produced in the glacier basin can be directly deposited on the ablation area ([Ackert, 1998](#); [Kirkbride and Deline, 2013](#)). Numerous sediment transfer processes can generate this accumulation, the more common being rockfalls, rock avalanches and snow/ice avalanches ([Brock et al., 2010](#); [Benn et al., 2012](#); [Janke et al., 2015](#)). The angular debris accumulated in this manner mainly consist of coarse materials. They are usually transferred passively downward on the glacier surface ([Kirkbride, 1995](#); [Berger et al., 2004](#)). Conversely, the two other processes imply an englacial transfer that often reduces the size and the angular aspect of sediments ([Hambrey et al., 2008](#)). The debris deposited in the accumulation area are englacially transferred downward because they are covered by snow and ice ([Fig. 1.9, 1.14 & 1.17](#)). The englacial load can also originate from the accumulation of debris in crevasses or the

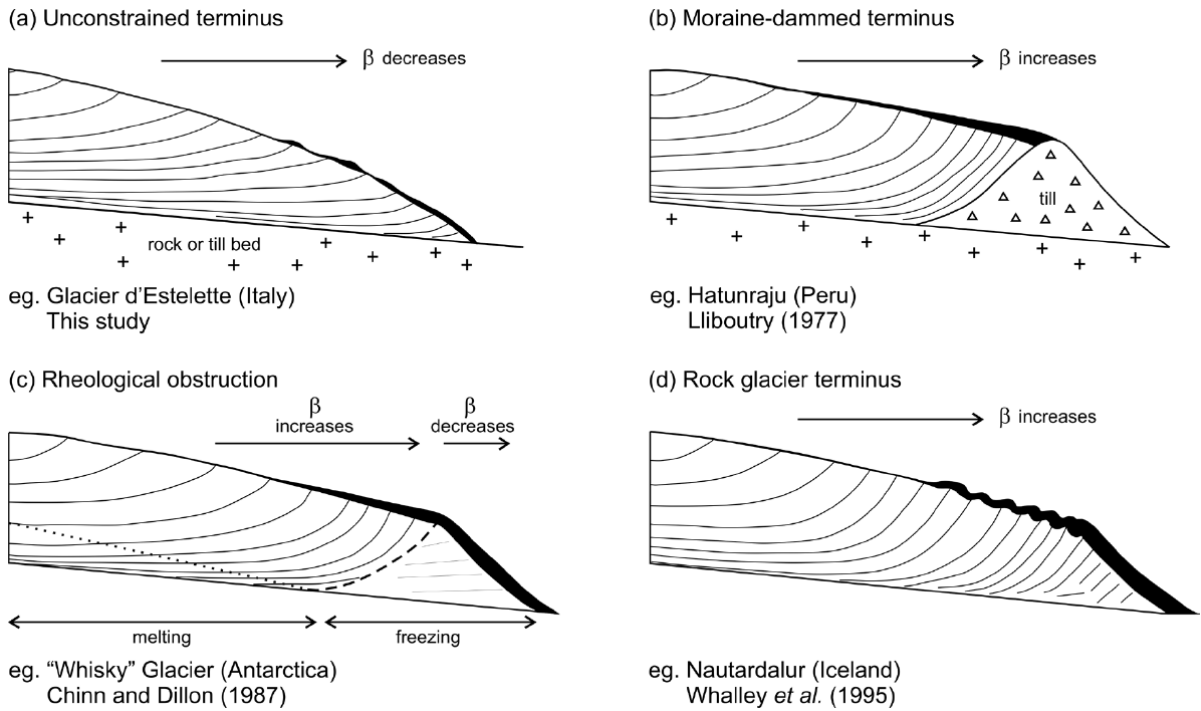


Fig. 1.17: Supraglacial accumulation of englacially-transported debris (black cover) associated with different mechanical and thermal situations at the glacier terminus. Lines within the glacier represent debris-rich layers (or septa). Their dip angle β increase with the terminus obstruction. Reproduced from Kirkbride and Deline (2013).

erosion of the bed (e.g. Godon *et al.*, 2013; Herman *et al.*, 2015). In the ablation area, a portion of englacial debris emerge and accumulate on the surface in relation with the progressive ice melt (Stokes *et al.*, 2007; Kirkbride and Deline, 2013). Finally, the ascending ice flux associated with the compressive flow in ablation area also contributes to accumulate supraglacial load (Fukui *et al.*, 2008; Bennett, 2011). The common increase of the compressive stress toward the terminal zone is related to the reduction of driving stress and/or to the presence of cold ice or possibly frozen sediment accumulations (Kirkbride and Deline, 2013; Fig. 1.17). Generally, because of the progressive accumulation of supraglacial debris and emergence of englacial load, the debris layer thickness increases downglacier (Kellerer-Pirklbauer *et al.*, 2008; Zhang *et al.*, 2011; Fig. 1.18 & 1.19).

According to the variation of glacier surface characteristics over time, two main types of debris-covered glaciers exist, although both dynamics can occur in a system: the *erosion-related* and the *ablation-related* systems. In the first group, the debris cover is always present on the glacier surface, regardless of climatic variations and their influence on glacier mass balance. For these glaciers, the sediment supply on the glacier is always high and ice-free rockwalls commonly

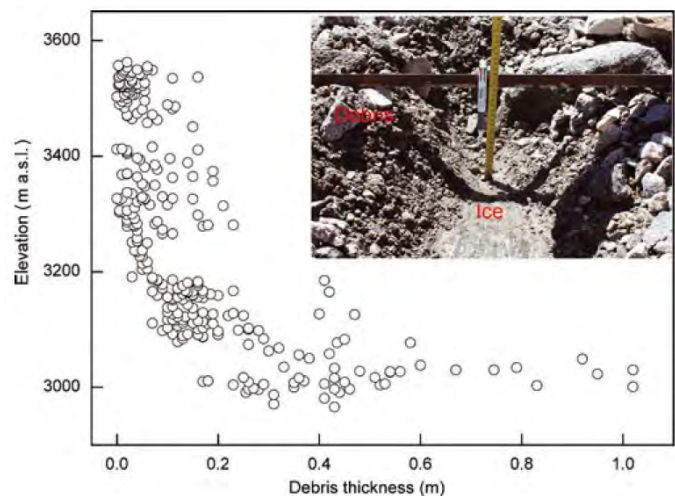


Fig. 1.18: Distribution of the debris cover thickness during the summer 2009 at different elevation in the ablation zone of Hailuogou glacier (29°34'N, 101°57'E; China). Reproduced from Zhang *et al.* (2011).

dominates the ablation area. Hence, several studies show that the tongues of this type of glacier were very likely debris-mantled during all the Holocene glacial periods (Ackert, 1998; Deline, 2005; Kirkbride and Winkler, 2012; Iturrizaga, 2013). Conversely, the development of the debris cover on the ablation-related type depends of the climatic variations. During glacier-favourable periods, several factors hamper the formation of a debris-cover on the glacier surface. On one hand, the debris supply is limited by the ice coverage of the relief and by the reductions of freeze/thaw cycles (Clark et al., 1994). On the other hand, glaciers are thicker and more dynamic. Their higher mass turnover allows an efficient evacuation of the sedimentary load. Thus, most of glaciers have a *transport-dominant* dynamic in favourable climatic conditions (Kirkbride, 2000; Fig. 1.19). When the latters become unfavourable, *ablation-dominant* dynamic induces the development of a debris mantle on mountain glaciers. Indeed, shrinking glaciers become less active and less efficient in sediment transfer (e.g. Paul et al., 2007; Benn et al., 2012; Fig. 1.13 & 1.14). The debris cover then spreads and thickens on the glacier surface by the emergence of englacial load or direct supraglacial deposition. In addition, the debris supply to the glacier can be noticeably intensified by the the so-called *para(periglacial erosive crisis* (Mercier, 2010). In fact, the deglaciation of surrounding relief and the degradation of permafrost increase the sediment production and transfer in ice loss context (Deline et al., 2015). With the current increase of atmospheric temperature, ablation-dominant conditions become the glacial norm worldwide (Vaughan et al., 2013; Zemp et al., 2015). It is not surprising therefore that the development of the debris cover has been documented in all the high relief regions (e.g. Paul et al., 2007; Stokes et al., 2007; Kirkbride and Deline, 2013).

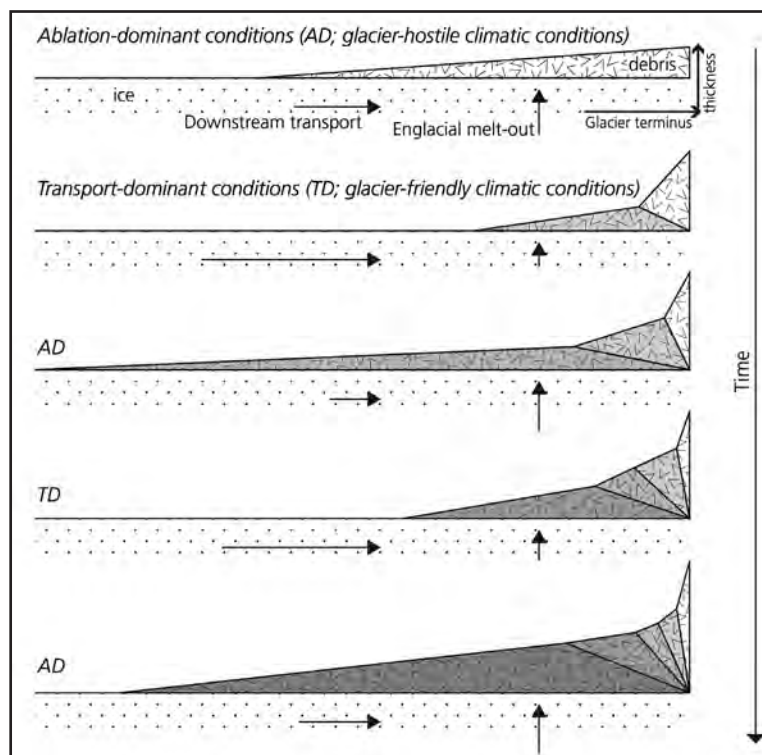


Fig. 1.19: Model of debris layer development and thinning on a glacier surface in relation with variations of climatic conditions. In ablation-dominant conditions, debris emerge on glacier surface by the ice melt-out. In transport-dominant conditions, the supraglacial layer is transferred towards the terminus. If the debris are not evacuated into the downstream hydrosystem, the debris cover progressively thickens downglacier. Modified from Kirkbride (2000).

Climate sensitivity and dynamics of debris-covered glaciers

According to its thickness, supraglacial debris layer can have a contradictory effect on the glacier surface energy fluxes (Bozhinskiy et al., 1986; Nicholson and Benn, 2006; Fig. 1.20). The

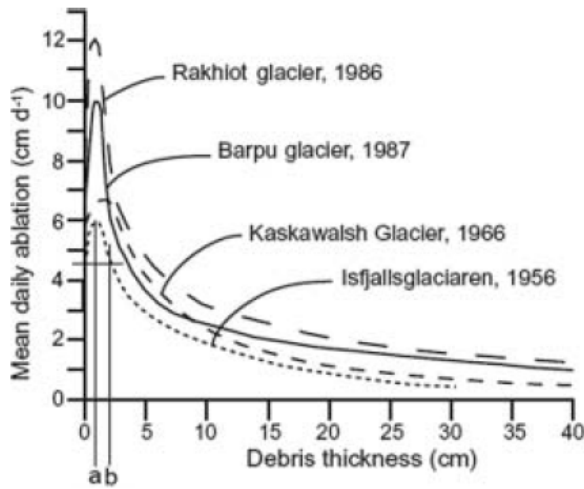


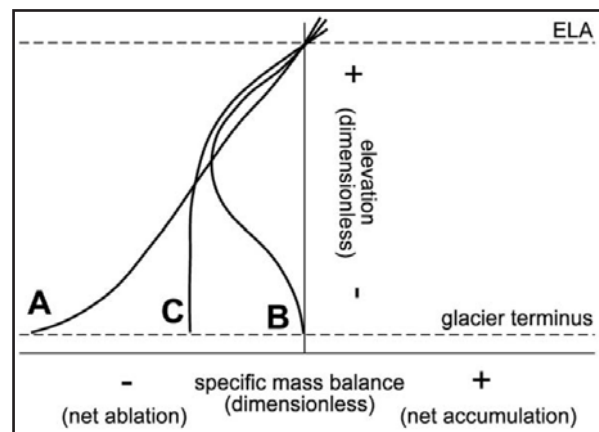
Fig. 1.20: Empirical measurement of the relation between the debris cover thickness and the mean daily ablation rate at several glaciers: Rakhiot and Barpu glaciers (Pakistan), Kaskawalsh (Canada) and Isfjällsglaciaren (Sweden). *a* corresponds where the melt rate is maximum and *b* illustrates the thickness where the melt rate under debris is at the same value than for clean ice. Reproduced from Nicholson and Benn (2006), who redraw the diagram of Mattson et al. (1993).

darkening of glacier surface by sediments, dust or black carbon decreases the albedo. It largely contributes to enhance the melt rate because much of the incoming shortwave radiation is absorbed (Kirkbride, 2011; Gabbi et al., 2015).

However, the poor thermal conductivity of debris can counter this effect and, beyond a debris thickness threshold of few centimetres, the insulation of ice by debris reduces the ablation rate (Nicholson and Benn, 2006; Brock et al., 2010; Lambrecht et al., 2011). The thickening of the debris layer decreases then the melt rate asymptotically. The glacier surface can then become strongly decoupled from the atmospheric temperature influence under several meters of debris. Hence, the debris cover is a major control of ice melt rate and thus glacier mass balance. As a function of its thickness, the debris layer enhances or limits the climate sensitivity of the glacier (e.g. Zhang et al., 2011).

In high relief regions, the effective erosion of relief generally allows the development of thick debris-cover and the insulating effect is thus prevailing (Scherler et al., 2011; Deline et al., 2012; Janke et al., 2015). At the glacier scale, the ice melt often decreases downglacier because the debris layer thickens in this zone on most of debris-covered glaciers. It induces particular ablation patterns (Kellerer-Pirklbauer et al., 2008; Fig. 1.21). The ablation gradient, which is normally increasing downglacier because of the air temperature control, can be reversed. Maximal melt rate is then experienced directly below the equilibrium line altitude (ELA), where the debris cover is absent or thin (Pellicciotti et al., 2015; Dobhal et al., 2013). Over time, the glacier can separate in two parts and abandon a sheltered dead ice body in its distal zone (Lilleøren et al., 2013; Shea et al., 2015). Before reaching this situation, this differential ablation dynamic usually leads to the decrease in the surface gradient and the glacier shifts from a convex to a concave longitudinal

Fig. 1.21: Schematic representation of variations of specific mass balance in ablation areas of glaciers. In the situation A, the ablation rate increases towards the terminus in relation with the increase of air temperature. This situation is typical for glaciers where the debris-cover is inexistent or relatively thin. In the situation B, the thickening of the debris-cover downglacier limits the sensitivity to air temperature, which can strongly reduce the melt rate. This situation is usual when the debris cover reaches several meters in the glacier distal zone. Between these two cases, the increase of the debris cover sometimes stabilizes the melt rate downglacier, as measured at Pasterze glacier in the last decades (47°05'N, 12°44'E; Austria; Kellerer-Pirklbauer et al., 2008). Reproduced from this publication.



profile (Kirkbride and Warren, 1999; Benn et al., 2012; Fig. 1.14). Associated with the glacier thinning in the negative mass balance context, its flattening induces a decrease in the glacier driving stress. Moreover, the presence of englacial debris, which can be high in the frontal zone of debris-covered glaciers (Kirkbride and Deline, 2013; Fig. 1.17), reduces the ice creep rate (Waller, 2001; Bolch, 2011). Finally, debris-covered glaciers build large moraines that can constrain the glacier flow (Shroder et al., 2000; Iturrizaga, 2013; Fig. 1.22). All of these factors explain that this type of glaciers often has a weak motion in the distal part and that downwasting dynamic predominates. Differential melt, related to the variation of debris-cover thickness, the presence of ice cliffs and thermokarst lakes, controls then the surface evolution (Kirkbride and Warren, 1999; Pellicciotti et al., 2015).

The sheltering of the ablation area confers therefore a particular behaviour to heavily debris-covered glaciers in comparison with bare-ice glaciers. However, these systems are not fully decoupled from the climate although its signal can be strongly filtered (Fig. 1.23). Few length variations are experienced over time, as ablation and driving stress are significantly reduced downglacier (Kirkbride, 2000; Schmidt and Nüsser, 2009; Fig. 1.7 & 1.24). In this way, climatic variations induce rather complex thickness variations (Benn et al., 2003; Mayer et al., 2006). In fact, the propagation downglacier of ice surplus or deficit experienced in the climate-sensitive accumulation area in responses to climatic variations produces delayed surface variations on debris-covered tongue (Thomson et al., 2000). Moreover, because ablation is limited in the distal zone, these glaciers are characterised by a lower accumulation-area ratio (AAR) than bare-ice glacier (typically 0.1-0.5 instead of 0.66; Clark et al., 1994; Kirkbride, 2011). They can thus behave phases of metastable equilibrium or even positive mass balance with very small accumulation area. Hence, in the current



Fig. 1.22: Google Earth view and simplified geomorphological map of the Jatunraju glacier (9°01'S, 77°40'W; Peru). The glacier flow was progressively canalised by the Holocene moraine. It induces this prominent 250-m high crooked landform. This glacier system is also discussed by Emmer et al. (2015), mentioned in this research. Reproduced from Iturrizaga (2013).

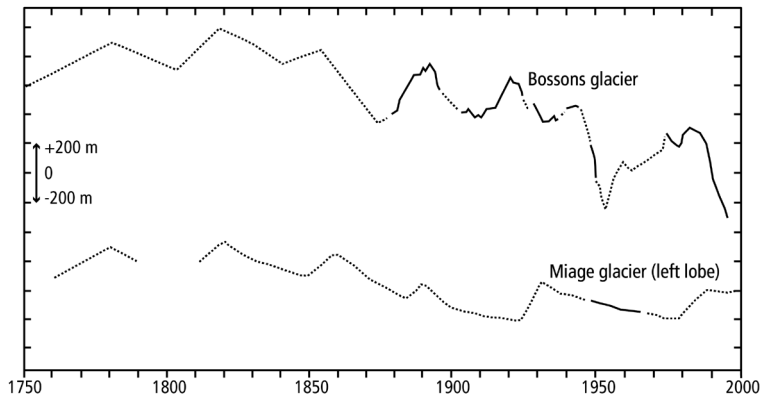


Fig. 1.23: Length variations of the mostly bare-ice Bossons glacier (45°52'N, 6°52'E; France) and of the debris-covered Miage glacier (45°47'N, 6°52'E; Italy). Solid lines and dashed lines indicate respectively documented and inferred length variations. These glaciers are in contact but they flow in distinct directions. In comparison with the Bossons glacier, Miage experience delayed and attenuated terminus fluctuations. Redrawn from Thomson (2000) and initially adapted from Deline (1999).

glacier unfavourable conditions, advancing, stable or slowly shrinking debris-covered glaciers usually coexists with rapidly vanishing bare-ice systems (e.g. D'Agata and Zanutta, 2007; Scherler et al., 2011; Carturan et al., 2013a). These glaciers are voluntarily excluded of worldwide monitoring programs because they are very complex and nonlinear climate indicators (WGMS, 2008; Haeberli et al., 2013; Zemp et al., 2015).

Finally, the motion of debris-covered glacier does not show specificity and ice deformation, basal slip and bed deformation can be active (e.g. Mayer et al., 2006). As bare-ice systems, they can be affected by surges (Copland et al., 2009) or calving dynamics (Kirkbride and Warren, 1999; Benn et al., 2012).

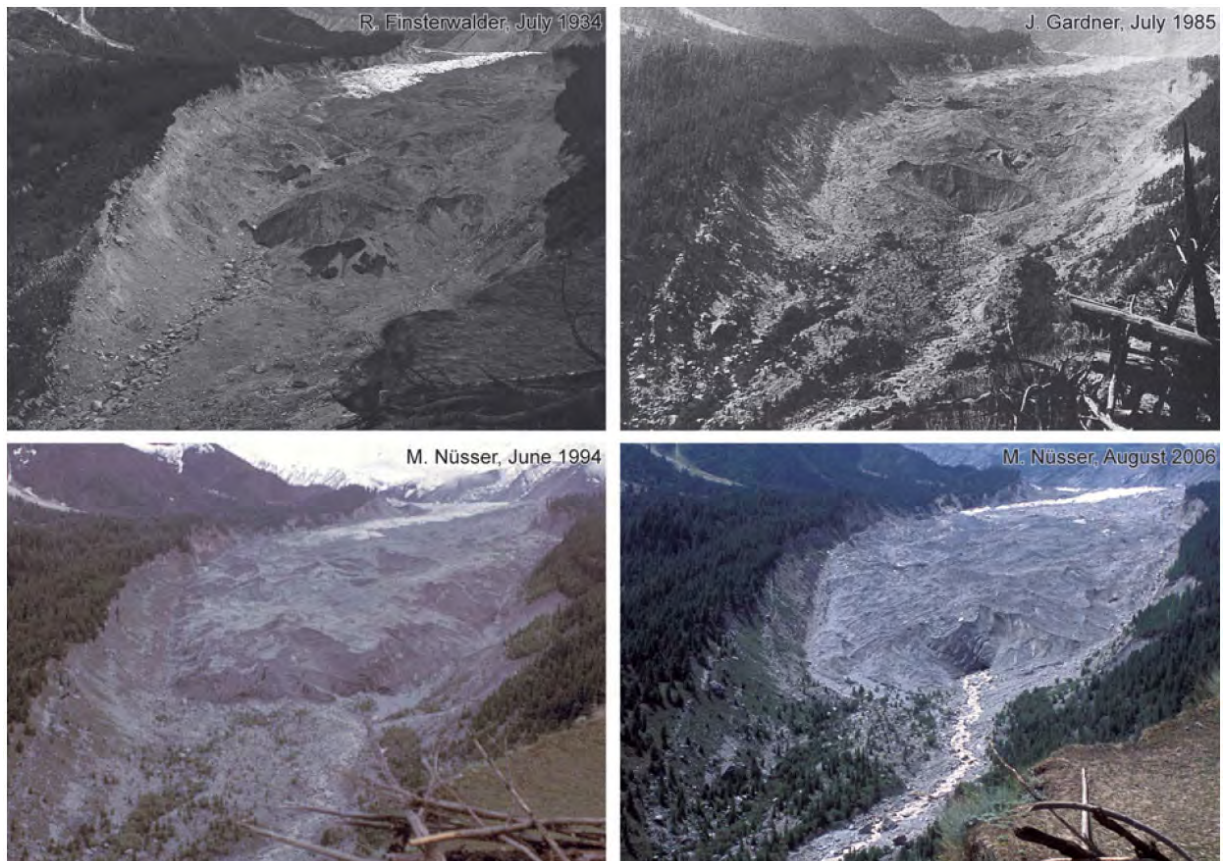


Fig. 1.24: Terrestrial photography showing the few fluctuations of the Raikot glacier front between 1934 and 2006 (32°20'N, 74°35'E; Pakistan). Reproduced from Schmidt and Nüsser (2009).

Debris-covered glaciers in hydrological and sediment transfer systems

In comparison with bare-ice glaciers, very few studies investigated the hydrology of debris-covered glaciers. However, they are important component of hydrosystems, especially in arid high mountain regions (e.g. Hagg et al., 2008; Janke et al., 2015). Due to the limitation of ice melt under a thick debris layer, the role of these preserved freshwater reservoir will be increasingly crucial at local scale in a warming atmosphere (Knight and Harrison, 2014; Rangecroft et al., 2015).

Directly related to ablation rate, the water production, can be increased or decreased in these systems according to the supraglacial layer thickness. Comparing a heavily debris-covered glacier with a neighbouring bare-ice one, Mattson (2000) showed that the weakly thermally conductive debris layer significantly influences glacier hydrology by reducing and delaying the water production, and limiting the variability of interannual runoff. Moreover, a part of the rainfall is directly evaporated on the debris or stored in them, reducing the water and the energy entering in the glacier (Brock et al., 2010). The frequent presence of supraglacial lakes is another particularity of this type of glacier (Benn et al., 2012; Fig. 1.14). Indeed, they develop relatively easily on the low gradient and concave debris-mantled tongue. Lakes can extend on large areas because the ablation is accelerated in contact with water (Kirkbride and Warren, 1999; Paul et al., 2007). Catastrophic glacial lake outburst floods (GLOFs) are a major concern in these systems, especially because the causes of possible distal ice and/or moraine dams' failure remain barely known (Iturrizaga, 2011; Benn et al., 2012; Iribarren Anaconda et al., 2015). Beyond these characteristics, debris-covered glaciers have generally the same hydrological behaviour than other glaciers (Pourrier et al., 2014). Efficient drainage networks can develop (e.g. Benn et al., 2012) allowing short-term diffusion of meltwater and rainwater in the ice (Mattson, 2000; Gudmundsson et al., 2000; Pourrier et al., 2014). As observed for other temperate-based glaciers, bed separation and speed-up events due to hydrological forcing can also occur in these glaciers (Gudmundsson et al., 2000).

Debris-covered glaciers are usually weakly efficient components of mountainous sediment transfer systems (Shroder et al., 2000; Benn et al., 2003). Indeed, most of them are characterised by an imbalance between the large debris load and the relative weak magnitude of the processes that transfer them (i.e. mainly glacial and fluvio-glacial processes). The presence of a large amount of coarse material, the gentle topography where these glaciers develop, the low glacier driving stress and the low production of meltwater especially contribute to this situation. As well, debris-covered glaciers are commonly *sediment sinks* and *transport-limited systems* that are unable to evacuate their sediment load towards downslope hydrosystem. They can build therefore very large basal and latero-frontal moraine complexes, which in turn, limit the efficiency of sediment transfer (Kirkbride, 2000; Hambrey et al., 2008; Iturrizaga, 2013; Fig. 1.8 & 1.22). Indeed, the progressive elevation of the glacier on the pedestal moraine further reduces the slope gradient and thus the magnitude of geomorphic process. Moreover, when the meltwater is not able to evacuate the sediment at the front, the distal moraines can completely encircle the glacier tongue and canalise and/or restrain its motion. These moraine *dams* are frequent and contribute to the decoupling of debris-covered glaciers from sediment transfer systems.

1.2.1.2. The influence of the glacier size

Definition and research issues on small glaciers

SDCGSAPE are types of **small and thin** debris-covered glaciers. Once again, the definition of small -and by extension very small- glaciers is fuzzy and no area thresholds are broadly recognised in the scientific community to classify the glaciers. Nevertheless, orders of magnitude between 0.1 and 1 km² and 1 and 10 km² are found respectively as upper limits for very small (e.g. DeBeer and Sharp, 2009; Huss, 2010; Bahr and Radić, 2012; Colucci and Guglielmin, 2014) and small glaciers (e.g. Anderson et al., 2004; Brown et al., 2010; Bælum and Benn, 2011). Likewise, no thickness thresholds are defined and the smallest glaciers are considered as the thinnest, exceeding rarely few tens of meters of mean thickness. However, the question of the relevance of this classification by size remains open. Indeed, the same main processes occur in all the glaciers. Moreover, they have continuous spectrum of geometrical settings and no natural breaks exist between them. Hence, glaciers are rather scaled than sharply classified by these size considerations, the smallest glaciers being rather affected by specific orders of magnitudes in processes than by specific processes (Kuhn, 1995; Tab. 1.1). The definition of small glaciers also faces their challenging distinctions with snow and ice patches (Serrano et al., 2011). Theoretically, this distinction relies on the dynamic of these masses: small glaciers have downward motion and snow/ice patches are static. The reality is more complex than this binary discrimination and researches have showed that snow patches or very small ice masses can slowly slide or deform (e.g. Shakesby, 1997; Grunewald and Scheithauer, 2010; Serrano et al., 2011). Conversely, glaciers can be stagnant in time and space, especially in their margins and/or in a strongly negative mass balance period (e.g. Fatland et al., 2003; Scherler et al., 2011; Evans, 2013).

Size	Ice thickness (H in m)	Glacier length (L in m)	H/L	Annual accumulation (AA in m a ⁻¹)	AA/H	Accumulation/precipitation	AA/ Annual horizontal flow
Polar ice sheets	1'000	1'000'000	10 ⁻³	0.1	10 ⁻⁴	1	<1
Outlet glaciers	1'000	100'000	10 ⁻²	0.1	10 ⁻⁴	↓	↓
Valley glaciers	100	10'000	10 ⁻²	1	10 ⁻²	10 (avalanche fed glaciers)	>1
Cirque glaciers	10	100	10 ⁻¹	10	1		

Tab. 1.1: Order of magnitude in geometry, process and ratios (in blue) associated with glacier size. According to these qualitative values, the smallest glaciers potentially react the fastest to climatic variations because they have the highest mass turnover. Synthetized from Kuhn (1995)

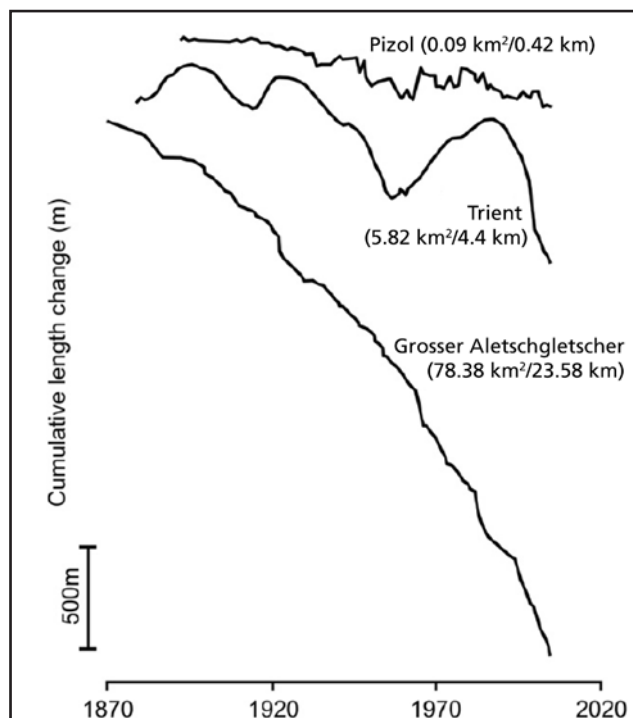
In comparison with medium and large-sized glaciers, small glaciers and especially the very small ones have been poorly studied (Kuhn, 1995; Huss, 2010; Carturan et al., 2013a). This situation is especially related to the fact that despite the very large numbers of small glaciers, they only correspond to a small fraction of the glacier ice on Earth and therefore freshwater stores. According to the latest version of the Randolph Glacier Inventory (RGI V4.0; Tab. 1.2) and although a large numbers of the smallest glaciers are still not inventoried (Pfeffer et al., 2014), 74.9% of the glaciers are smaller than 1 km². However, they only correspond to 5.6% of the surface and 0.7% of the volume of Earth glaciers (Huss and Hock, 2015). Moreover, as debris-covered glaciers, small glaciers are complex climate indicators. On one hand, they are considered as the glaciers responding

RGI 4.0 Region	All glaciers			Glaciers < 1 km ²					Glaciers < 0.5 km ²					Glaciers < 0.1 km ²				
	Count	Area	Slope	Count	%	Area	%	Slope	Count	%	Area	%	Slope	Count	%	Area	%	Slope
01_Alaska	27109	86722.727	24	21423	79.0	6371.881	7.3	25.4	17163	63.3	3371.271	3.9	26	5005	18.5	297.973	0.3	27.2
02_WesternCanadaUS	15215	14558.551	23.75	12469	82.0	3537.127	24.3	24.7	10208	67.1	1946.528	13.4	25.2	2887	19.0	198.105	1.4	25.7
03_ArcticCanadaNorth	4538	104873.108	15.2	1777	39.2	769.019	0.7	17.7	1068	23.5	291.659	0.3	18.3	106	2.3	3.946	0.0	16.7
04_ArcticCanadaSouth	7346	40882.573	17.6	4303	58.6	1501.107	3.7	18.8	3209	43.7	713.009	1.7	19	452	6.2	27.617	0.1	19.5
05_GreenlandPeriphery	20261	130071.082	20.4	13398	66.1	3716.726	2.9	22.6	11017	54.4	2021.657	1.6	22.9	3318	16.4	235.45	0.2	23.4
06_Iceland	568	11059.7	17.6	355	62.5	119.063	1.1	20.8	270	47.5	57.186	0.5	21.7	54	9.5	4.061	0.0	23.6
07_Svalbard	1615	33958.776	14.9	608	37.6	296.119	0.9	18.8	325	20.1	90.9	0.3	19.6	31	1.9	1.639	0.0	20.7
08_Scandinavia	2668	2851.015	20.4	2089	78.3	637.172	22.3	21.6	1675	62.8	353.615	12.4	22	148	5.5	10.521	0.4	19.8
09_RussianArctic	1069	51591.6	13.8	149	13.9	93.177	0.2	15.6	48	4.5	18.797	0.0	17.4					
10_NorthAsia	4403	3435.492		3632	82.5	1021.977	29.7		2945	66.9	551.081	16.0		567	12.9	27.631	0.8	
11_CentralEurope	3920	2063.261	26.54	3516	89.7	512.84	24.9	27.2	3242	82.7	325.65	15.8	27.5	2180	55.6	79.465	3.9	28.5
12_CaucasusMiddleEast	1725	1293.979	20.5	1445	83.8	377.492	29.2	20.7	1212	70.3	213.965	16.5	21.5	370	21.4	20.485	1.6	31.7
13_CentralAsia	46543	62605.848	26.2	35361	76.0	11710	18.7	27.3	27289	58.6	6031.061	9.6	27.8	4592	9.9	255.442	0.4	29.3
14_SouthAsiaWest	22822	33859.17	26.5	18014	78.9	4802.138	14.2	27.5	14755	64.7	2473.697	7.3	28	6340	27.8	324.17	1.0	29.2
15_SouthAsiaEast	14095	21799.378	27.6	10081	71.5	3422.835	15.7	28.5	7441	52.8	1536.157	7.0	29.2	2114	15.0	122.284	0.6	31.2
16_LowLatitudes	2941	2346.037	26.9	2312	78.6	535.361	22.8	27.3	1967	66.9	285.919	12.2	27.4	946	32.2	38.698	1.6	27.9
17_SouthernAndes	16046	29333.305	24.1	13274	82.7	2862.206	9.8	24.4	11483	71.6	1588.637	5.4	24.4	5851	36.5	260.621	0.9	24
18_NewZealand	3537	1161.801	31.3	3377	95.5	467.554	40.2	31.6	3173	89.7	327.401	28.2	31.8	2112	59.7	88.549	7.6	32.1
19_AntarcticSubantarctic	2753	132867.219		1660	60.3	358.782	0.3		1418	51.5	186.548	0.1		766	27.8	31.49	0.0	
Total / Prop. / Mean	199174	767335	22.2	149243	74.9	43113	5.6	23.6	119908	60.2	22385	2.9	24.1	37839	19.0	2028	0.3	25.7

Tab. 1.2: Glaciers numbers, areas and mean slope by size class according to the Randolph Glacier Inventory 4.0 (2014-12-01; available on www.glims.org/RGI)

the fastest to climatic variations (Jóhannesson et al., 1989; Haeberli, 1995; Kuhn, 1995; Ramírez et al., 2001; Tab. 1.2 & Fig. 1.25). On the other hand, many researches highlighted their poor or very complex coupling with the climate (DeBeer and Sharp, 2009; Carturan et al., 2013a; Scotti et al., 2014). Here again, this complexity as indicators of climate change can explain their relative negligence in glaciological researches. Still, the knowledge of small glaciers is important because with the temperature increase, glaciers are becoming smaller and thinner ice masses (Fig. 1.7 & 1.13). In this context, the relative influence of small-scale processes as downwasting or snow redistribution, that can be thoroughly studied on very small glaciers, increases (Huss, 2010). This partly explains why the number of studies on these glaciers increased in the last decade. A large number of them are however concentrated on the particular *topographically-controlled* systems located in the south of Europe (e.g. Grunewald and Scheithauer, 2010 and references therein) and a comprehensive analysis of small glaciers is still required.

Fig. 1.25: Cumulative length variations of the Pizol glacier (46°57'40N, 9°23'20E; Switzerland), the Trient glacier (46°N, 7°02'E; Switzerland) and Grosser Aletschgletscher (46°30'N, 8°02'E; Switzerland). Area and length in parenthesis originate from the Swiss Glacier Inventory 2010 (Fischer M et al., 2014; Bauder, 2015). These length variations illustrate how small glaciers can be very reactive to short-term climatic variations, in contrast to larger glaciers, where the latter are filtered. Modified from Kirkbride and Winkler (2012) and initially adapted from Haeberli (1995).



Types of small glaciers

Small glaciers develop (1) when the maximum altitude of the relief is little above the one of the climatic ELA or (2) when the topography allows snow accumulation anomaly at a lower altitude, by enhancing its redistribution or limiting its melt (Kuhn, 1995). Hence, small glaciers can be

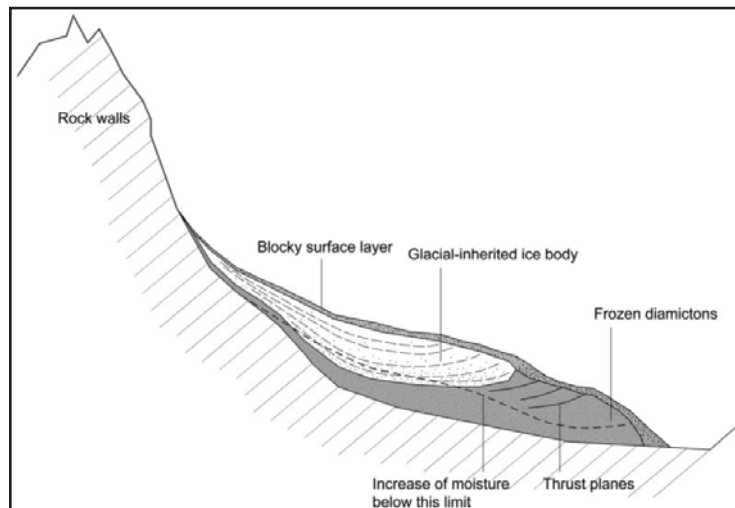
divided in two main groups according to their origin, the *climatically-* and the *topographically-controlled*, although both climate and topography influence every individual glacier. Two other distinctions can be superimposed to this first order classification. First, small glaciers that were always small during the Holocene glacier-friendly conditions (e.g. [Chueca et al., 2007](#); [Grunewald and Scheithauer, 2010](#)) can be opposed to those that become small with the ice shrinking or the possible disintegration of large glaciers during a negative mass balance period (e.g. [Paul et al., 2007](#); [DeBeer and Sharp, 2009](#); [Fischer M et al., 2014](#); [Fischer A et al., 2015](#); [Fig. 1.7](#)). Because of these processes, the relative number of small glacier on Earth is currently increasing ([Pfeffer et al., 2014](#)). Second, if the development of the glacier is related to a dominant process, the small glaciers can be divided into *accumulation-type* –also referred to as *avalanche-fed* or *drift-glaciers* ([Hoffman et al., 2007](#); [Carturan et al., 2013a](#); [Colucci and Guglielmin, 2014](#))- and *sheltered-type* glaciers. As the smallest glacier are commonly strongly controlled by the surrounding relief, which can be proportionally very high and extended (e.g. [Fig. 1.1 & 1.8](#)), this classification distinguishes the glaciers related to positive accumulation anomaly due to avalanching and snow drifting processes from those related to negative ablation anomaly associated to shadow or thick debris-cover influence.

Particularities of small glaciers

The same processes affect all glaciers, regardless their size. Amplitudes of processes, in absolute term, are nevertheless generally lower in small glaciers. Among others causes, the weak thickness and weight of these masses and the limited production of water explain their low driving stress and thus their relative reduced dynamic (e.g. [Paul et al., 2007](#); [Carturan et al., 2013a](#)). Moreover, the surrounding relief can be relatively very high and extended in comparison with the glacier size. Hence, small glacier systems can contain huge amounts of debris because of this geometric disproportion and in addition to their weak motion and capacity to evacuate the sedimentary load ([Maisch et al., 1999](#); [Grunewald and Scheithauer, 2010](#)). As a result, large areas on small glaciers can be debris-covered in high relief environments (e.g. [Brazier et al., 1998](#)). Furthermore, the weak water production and in general of proglacial geomorphic processes commonly hamper the evacuation of sediment toward the hydrosystems. Small glaciers can therefore become decoupled systems that build lopsided distal moraines, which in turn limit the glacier dynamic by obstructing the ice flux ([Shroder et al., 2000](#); [Benn et al., 2003](#); [Matthews et al., 2014](#); [Fig. 1.1; 1.8 & 1.26](#)).

The occurrence of rotational slipping is maybe the only particular process that can be found exclusively in small glaciers. This process is related to their particular geometry. Indeed, these glaciers have the largest thickness to length ratio ([Kuhn, 1995](#)). Their general lens shape (e.g. [Fig. 1.26](#)) contrasts with the relative elongated form of larger glaciers. Thus, paradoxically, if these glaciers are the thinnest in absolute value, they are also proportionally the thickest. Backward rotational movements can then affect these masses, the ice flux being respectively submerging and emerging in the proximal and distal zones ([Serrano et al., 2011](#)). This process is favoured by the weight exerted upglacier by snow accumulation and also by the common concave bed geometry ([Kuhn,](#)

Fig. 1.26: Schematic longitudinal profile of the 600 m long Sachette debris-covered glacier / rock glacier complex (45°29'N, 6°52'33E; France). The internal structure is inferred from *Ground Penetrating Radar* (GPR) profiles. It illustrates the lenticular shape of this very small cirque glacier (c. 300 m long and up to 40 m thick). The glacial zone has no accumulation area today and can be considered a heritage of a recent climatic conditions. Reproduced from Monnier et al. (2012).



1995). It contributes to bed abrasion. Sediments migrate towards the surface along shear planes that appear on the surface of ablation areas.

Theoretically, the smallest glaciers are the more reactive to climatic variations (Jóhannesson et al., 1989). Indeed, because of their limited surface and altitudinal gradient in comparison with larger glaciers, minor variations of the climatic ELA can induce important AAR and thus mass balance changes (Brown et al., 2010). As well, the relevance of the AAR or ELA as spatial notions is questioned for these glaciers where the notion of accumulation/ablation year may be more useful (Hughes, 2009; Whalley, 2009). Moreover, comparing accumulation rate and horizontal flow with the glacier area and thickness, small glaciers are supposed to have the highest mass turnover rates and therefore quick geometric adjustments to climatic variations (Kuhn, 1995; Tab. 1.1). However, many factors can slow or add complexity in the responses of small glaciers to the climate. Comparing their modelling results with observed geodetic mass balances, Huss and Hock (2015) showed that the responses of small glaciers to climate variations are the most difficult to predict. As mentioned before, it is mainly related to the common high control exerted by the topography on these restricted areas. This control is also active on larger glaciers but the zone potentially concerned is proportionally greater in small glaciers. Redistribution of the snow fallen in the glacier basin by avalanching or wind drifting can increase up to tens of times the accumulation rates (Hoffman et al., 2007; Rödder et al., 2008). The gentle glacier surface topography and the presence of marginal moraine ridges facilitate the supraglacial accumulation of snow (Kuhn, 1995; López-Moreno et al., 2006a; Fig. 1.27). Because of this enhanced mass input, some glaciers even become weakly sensitive to annual snow precipitation variations (Hoffman et al., 2007; DeBeer and Sharp, 2009; Scotti et al., 2014). The snow cover also influences the ablation rate. Its temporal presence on ablation area surface strongly limits the ice melt during the ablation season (Thibert et al., 2013). Indeed, snow acts as an isolating layer and because of its high albedo, a large amount of radiation is reflected. Otherwise, small glaciers often develop in niches surrounded by high relief. Thus, limiting the direct solar radiation at the glacier surface, the shadow effect also contributes to reduce the ice melt (Clark et al., 1994; López-Moreno et al., 2006b; DeBeer and Sharp, 2009; Gilbert et al., 2012). Finally, as mentioned in the 1.2.1.1, the presence of thick debris cover on small glaciers limits considerably ablation and also contributes to disconnect them from climatic variations (Grunewald and Scheithauer, 2010; Carturan et al., 2013a; Seppi et al., 2015).



Fig. 1.27: Snow accumulation in late summer (Sept. 4, 2013) in the Rebanets Chassots zone (45°44'33N, 6°43'47E; France). Winter snow is preserved directly at the foot of the backwalls where large quantities were redistributed by avalanching. In the centre of the picture, snow is also accumulated in the depression formed by the partial melt of a small glacier, behind its LIA moraines. This flattening and the damming effect induced by the moraine enhance the snow accumulation by avalanches.

1.2.1.3. The influence of the permafrost conditions

Elements of definition and research issues on the glaciers confined within the permafrost environments

SDCGSAPE are small debris-covered glaciers **confined within permafrost environments**. They form in locations where specific ranges of temperatures and precipitations only allow the development of relatively small glaciers (Whalley, 2009; Haeberli et al., 2013; Fig. 1.28). They are not present in the wettest maritime climates because they induce large accumulation of snow and, thereby, the development of glaciers below the periglacial belt (Pfeffer et al., 2014). At the opposite end of the spectrum, too dry conditions in continental climates hamper the formation of glaciers in cold environments (e.g. Azócar and Brenning, 2010).

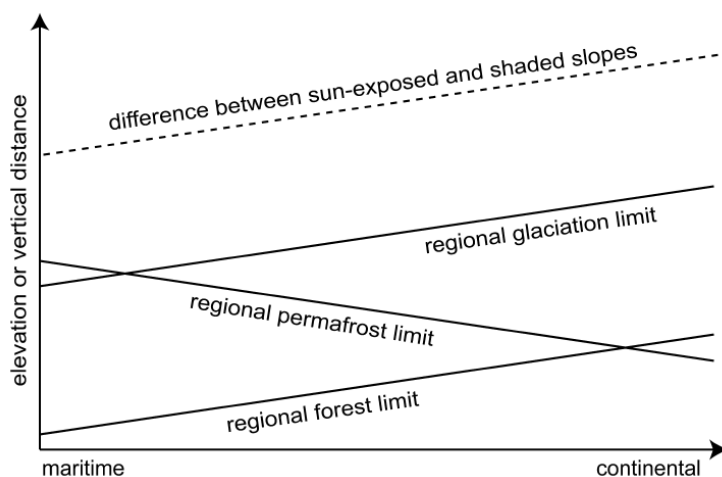


Fig. 1.28: Schematic influence of climatic characteristics on mountain environments. These lines are generalisation. Continental climates are characterised by weak total precipitation and cloudiness, high total solar radiation and annual/diurnal temperature amplitude. Under these climatic conditions, the treeline rises along with summer air temperature. The snowline and therefore glaciation limit rise in relation with the climate aridity. Conversely, the limit of discontinuous permafrost may rise in maritime regions because the thicker and longer snow cover shelters the ground from cold winter air temperature. However, this last generalisation is questioned in the scientific literature (Lambiel, personal communication). Reproduced from Gruber and Haeberli (2009) and initially adapted from King et al. (1992).

Relatively few glaciological investigations were led on the glaciers confined within the permafrost environments in mid-latitudes. Most of their knowledge relies on the results obtained in high latitudes and especially in the Arctic (e.g. [Etzelmüller and Hagen, 2005](#)). Despite the fact that this type of glacier can be affected by particular responses to the current climate variations (e.g. [Gilbert et al., 2012](#)) and that surface of shrinking glaciers on Earth will be more and more confined in the coldest areas ([Huss and Hock, 2015](#)), the knowledge on these glaciers remains extremely sparse and their comprehensive study is needed. Before detailing the main particularities of these glaciers, elements of definition of permafrost environments are required.

Permafrost depicts a thermal state of the sub-surface. It corresponds to lithosphere material (soil, rock and included ice and organic material) that is continuously at or below 0°C for at least two consecutive years ([Van Everdingen, 1998](#); [Shur et al., 2011](#); [Fig. 1.29](#)). The mean annual air temperature (MAAT) of -3°C serves usually as first order threshold to determine the lower limit of discontinuous permafrost and hence the permafrost environments ([Etzelmüller et al., 2003](#); [Gruber and Haeberli, 2009](#)). However, the spatial distribution of permafrost is very complex and discontinuous in reality. Indeed, spatial variability of ground temperature at the very local scale are marked and especially high in mountainous environments because of the complexity of the micro-relief and ground characteristics ([Scapozza et al., 2011](#); [Deluigi and Lambiel, 2012](#); [Otto et al., 2012](#); [Fig. 1.30](#)). Negative anomalies of ground temperature

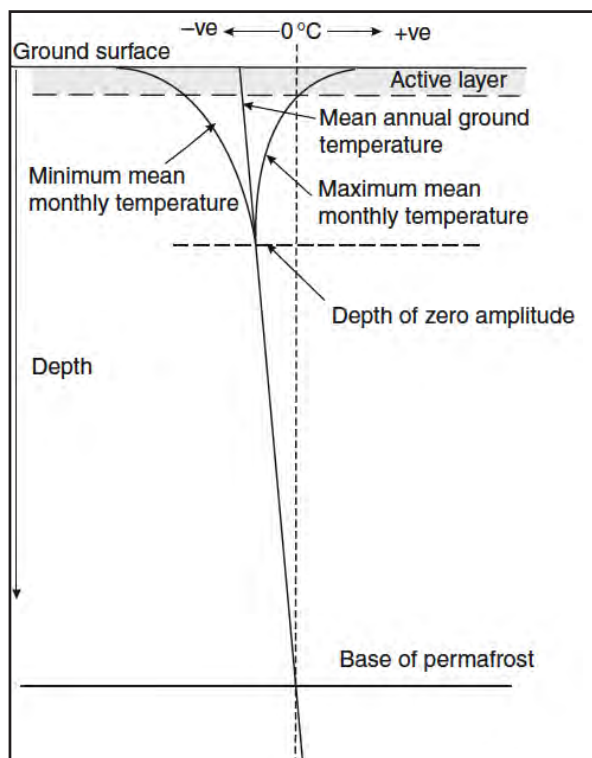


Fig. 1.29: Thermal profile of the subsurface in permafrost conditions. The active layer corresponds to the surface layer that temporarily thaws during the year. At depth, the ground temperature warms in relation with the geothermal gradient. Reproduced from [Harris \(2004\)](#).

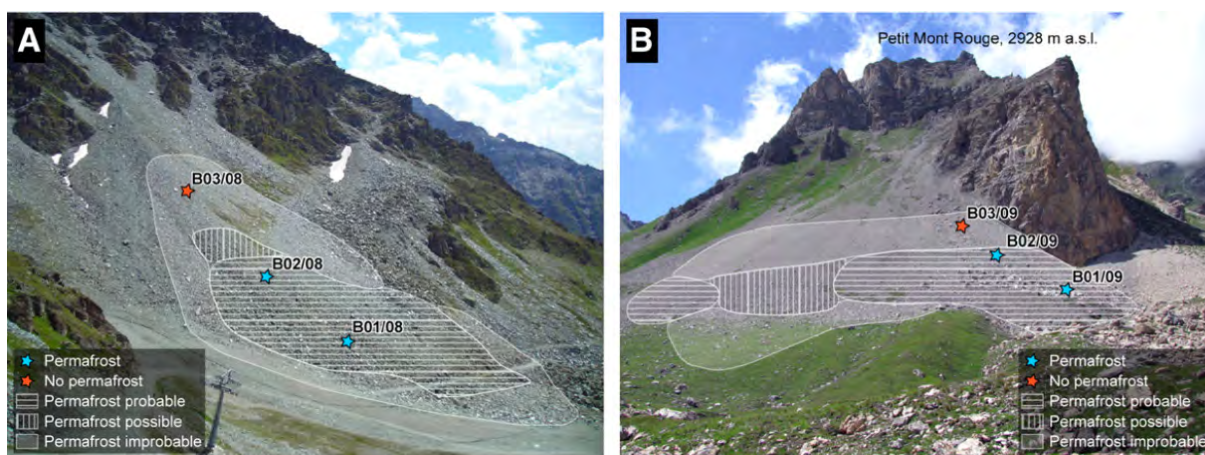


Fig. 1.30: Two examples showing the high discontinuity of permafrost distribution at local scale. The permafrost detection at Les Attelas (**A**; 46°06'N, 7°17'E; Switzerland) and Petit Mont Rouge (**B**; 46°01'N, 7°27'E; Switzerland) talus slopes relies on ground thermal and geophysical data. Reproduced from [Scapozza et al. \(2011\)](#).

exist at the local scale as a consequence of numerous processes (the balch effect, air advection in porous media, the sheltering of ground ice by a poorly thermally conductive debris layer, etc.; e.g. Lambiel, 2006). Permafrost can thereby exist in zones of MAAT warmer than -3°C . Conversely, positive temperature anomalies in the ground, due for example to its warming by meltwater circulation at the front of a glacier, explains the absence of permafrost in cold MAAT areas (e.g. Delaloye, 2004).

Particularities of glaciers confined within the permafrost environments

As the temperature of glacier ice depends on the energy exchanges with climate and Earth surface (Cuffey and Paterson, 2010), large amount of cold ice can be present in glaciers located in permafrost environments (Haeberli, 2005; Gilbert et al., 2012). Three main spatial configuration of thermal regime exist in these glaciers (Etzelmüller and Hagen, 2005). (1) If all the ice temperature is below the pressure melting point, the glacier is cold (Fig. 1.31a). The glacier can be polythermal when (2) a cold ice shell surround a temperate (at the pressure melting point) basal layer or ice core (Fig. 1.31b, c), or (3) the cold ice is only present in the maginal glacier zones (Fig. 1.31d, e), while all the central area is temperate. The thermal structure of a glacier is not static and can rapidly evolve in relation with climatic and hydrological variations (Pettersson et al., 2003; Bælum and Benn, 2011; Gilbert et al., 2012; Fig. 1.32). It mainly depends of the spatial, temporal and thickness variations of the snow cover, the glacier thickness, energy exchange processes related to phase transitions of water and water circulation. The release of latent heat due to the refreezing of percolating meltwater significantly warms the wet firn areas (Cuffey and Paterson, 2010). This

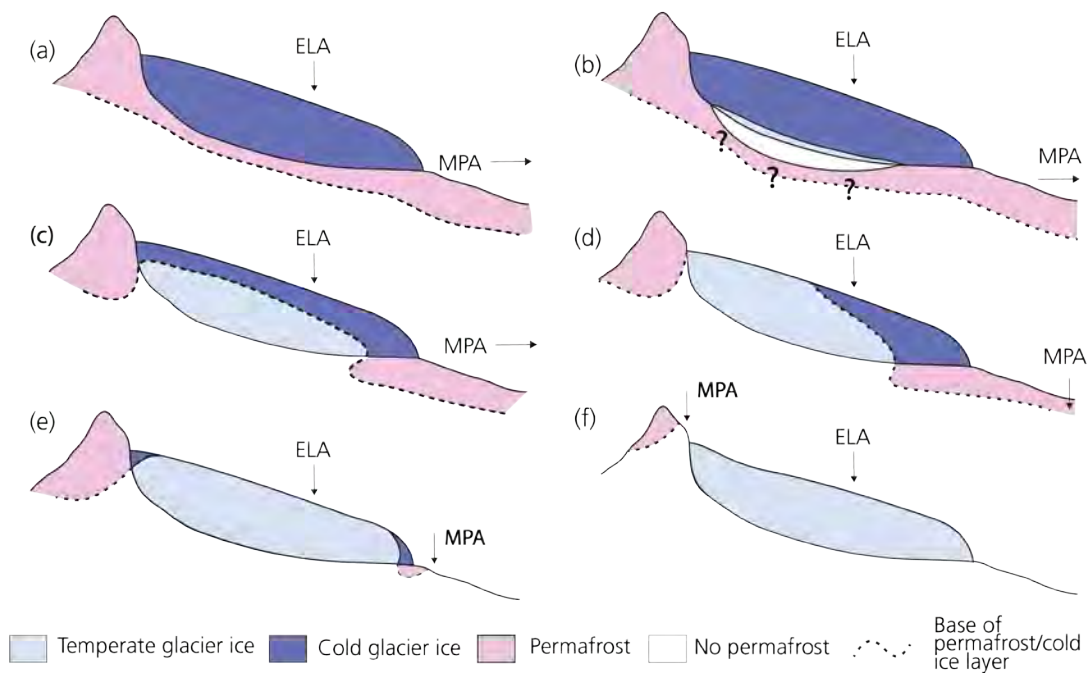


Fig. 1.31: Schematic longitudinal profiles of glaciers showing the distinct thermal regimes that possibly occur under permafrost conditions. ELA and MPA respectively refer to Equilibrium Line Altitude and Mountain Permafrost Altitude. In the (a) situation, the glacier is entirely cold, a common situation when MPA is far below the ELA. (b) to (e) situations refer to polythermal glacier structures that can be encountered when MPA and ELA are relatively close. Finally, (f) corresponds to completely temperate glaciers that develop below the MPA. Redrawn from Etzelmüller and Hagen (2005), where Norwegian examples for each regime are proposed.

common process explains why accumulation areas are usually temperate, even in cold environments. Conversely, the marginal glacier zones, especially in ablation areas, can be cold because they are cooled by air temperature during the winter period (the snow covers the ice latter in fall and the winter snow layer can be thinner than in the accumulation zone) and also because englacial or subglacial meltwater circulations that warm the ice are rare or absent in these zones, where the cold ice acts as an aquiclude (Gilbert et al., 2012).

The thermal regime has a strong influence on the motion of glaciers because it modifies their mechanical and hydrological properties (Cuffey and Paterson, 2010). As well, the viscosity increases significantly with the cooling of the ice (Cuffey and Paterson, 2010; Deline et al., 2015). Cold ice is therefore less subject to internal deformation than temperate ice. Moreover, the presence of water within the glacier and at its bed is a primary control of glacier dynamic. It allows basal slipping and, when sediments compose the bed, it also contributes to saturate them and enhances their potential of deformation (Waller, 2001; Fig. 1.12). The presence or absence of water strongly depends on the glacier thermal regime. By convention, wet temperate ice, which can contain up to 4% of water and have an efficient drainage network (Fountain et al., 2005; Bartholomew et al., 2010), is opposed to dry cold ice that is considered as an aquiclude (Hodgkins, 1997; Irvine-Fynn et al., 2006; Gilbert et al., 2012). In this way, because of the presence of water, bed processes are very efficient in warm-based glaciers, being commonly responsible to more than 75% of the glacier motion, while impermeable cold glaciers are theoretically stuck to the bed and are only affected by slow internal deformation (Waller, 2001). As a consequence, bed erosion is very limited in cold glacier zones (Waller, 2001; Bælum and Benn, 2011; Godon et al., 2013; Fig. 1.33) and very effective in rapidly sliding temperate glaciers (Herman et al., 2015). However, empirical field results have attenuated to some extent this theoretical hydro-dynamical dichotomy

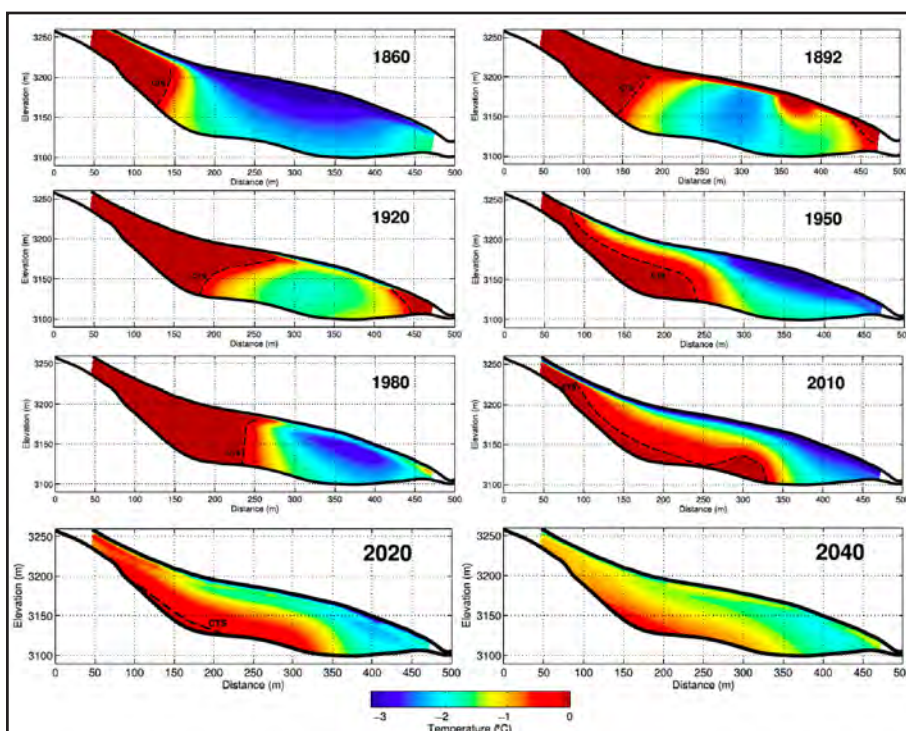


Fig. 1.32: Longitudinal profile of the Tête Rousse glacier (45°55'N, 6°57'E; France) with modelled englacial temperature between 1860 and 2040. CTS means Cold Temperate transition Surface. Adapted from Gilbert et al. (2012) where the origin of these complex and continuous thermal regime variations are discussed.

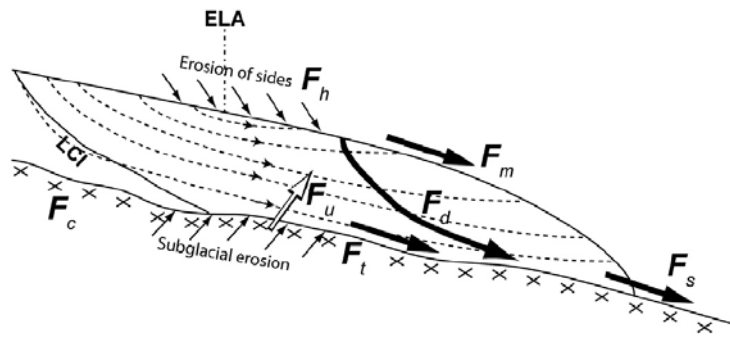


Fig. 1.33: Sketch of debris flux in a glacier system. LCI refers to lower Limit of Cold Ice. Supraglacial debris (F_h) supplied to the glacier can be englacially transported (F_d) or incorporated in the marginal moraines (F_m). In addition to englacial debris, the sediment produced at the bed of temperate glacier (F_r) can be mobilised by subglacial stream (F_s). Some sediment can also be produced under the cold glacier zone (F_c). However, this process, as the upward transport of sediment from base to surface (F_u), were found to be very low at the Bossons glacier (45°52'N, 6°52'E; France; Godon et al., 2013). Reproduced from this study.

between cold and temperate ice. Indeed, drainage networks, sometimes inherited, can allow water circulations in or below cold glaciers (Hodgkins, 1997; Moorman, 2005; Bælum and Benn, 2011). Speed-up events related to hydrological forcing in the cold-based or in the neighbouring warm-based zones were thus observed during the melt season in cold glacier zones (Bingham et al., 2003; Rippin et al., 2005). Moreover, deformation or sliding can also occur in or below the sedimentary bed of these glaciers (Waller, 2001). Nevertheless, cold ice zones remain significantly less mobile than temperate ice zones. In the frequent polythermal configuration found in permafrost environments, where the accumulation area is temperate and the ablation area is cold, the latter act as a thermomechanical dam and limit the motion of the upslope glacier zone (Rippin et al., 2005; Gilbert et al., 2012; Kirkbride and Deline, 2013; Fig. 1.17c).

Several other characteristics of permafrost environments also contribute to limit the driving stress of the glaciers that are confined within them. First, whereas they are fundamental for the glacier motion and melt, periods with positive air temperature and without supraglacial snow cover in the ablation area are shorter in these cold environments (Bingham et al., 2006; Gilbert et al., 2012). Fewer meltwater is then produced and enhance the glacier motion. During the long frozen period, glaciers become weakly active as melt and bed processes are frequently disrupted (Anderson et al., 2004; Bingham et al., 2008). Second, in continental or very cold climates, low accumulation rates limit the mass turnover (Etzelmüller and Hagen, 2005). Third, the debris production in surrounding rockwalls can be very high under permafrost conditions (Deline et al., 2015; Seppi et al., 2015). Glaciers can have high debris content and because of their poor coupling with downslope hydrosystem, they progressively build very large moraines (Matthews et al., 2014). These accumulations hinder then the glacial motion in the distal zone. The possible presence of ground ice that enhances the sediment cohesion strengthens this distal perturbation under permafrost conditions (Kirkbride and Deline, 2013; Fig. 1.17d). Finally, the ablation becomes close to zero in debris-covered zones when the supraglacial layer is thicker than the seasonally thawing layer (i.e. the active-layer; Humlum, 2000; Lilleøren et al., 2013; Fig. 1.29). It also explains the weak meltwater production in these environments. Because of the characteristics developed in this section, glaciers confined in permafrost environments are usually weakly active, as illustrated by their low crevasse density (Etzelmüller and Hagen, 2005).

1.2.1.4. Synthesis

According to the specific characteristics of debris-covered glaciers, small glaciers and glaciers confined within permafrost environments, SDCGSAPE are potentially **atypical and complex glaciers** in comparison with the bare-ice, medium-sized and extended in temperate areas glaciers, namely the *stereotype* that received most of the attention in the development of the glaciological knowledge. Local-scale environmental controls can noticeably modify the geometrical and dynamical responses of these glaciers to climatic variations. In addition to their common complex and nonlinear relation with the climate, this type of glacier is also usually **very weakly active** in comparison with other glaciers. Glacier motion and mass turnover processes can have very low magnitude while the **debris concentration can be huge**. As a consequence, they are commonly **poorly coupled with downslope hydrological and sediment transfer systems and they build large glacialic sediment accumulations that potentially contain ground ice in permafrost environments**.

1.2.2. Glacialic sediment accumulations that potentially contain ground ice in permafrost environments

1.2.2.1. Emergence of a knowledge around the controversial considerations of ground ice and glacier-permafrost interactions

As mentioned above, SDCGSAPE have been also partially studied as glacialic sediment accumulations that potentially contain ground ice in permafrost environments. Mainly led by geomorphologist, these studies focused on the genesis, the internal structure and the dynamic of the usually large sediment accumulation developed in the distal parts of SDCGSAPE (e.g. [Kneisel, 2003](#); [Ribolini et al., 2010](#); [Lilleøren et al., 2013](#)). Few considerations or direct investigations on the upslope glaciers can be found in these researches. Most of them aimed to improve the knowledge on the possible glacier-permafrost interactions in the marginal zones (e.g. [Delaloye, 2004](#)). More precisely, the influence of glacier fluctuations on the geometry and the thermal regime of former sediment accumulations, and on the formation of new landforms as push moraines, ice-cored moraines or rock glaciers were investigated. These researches focused thus on the detection, the characterisation and the interpretation on ground ice, trying to understand its role in landforms genesis. Conversely, few direct investigations and reflexions were carried out on the ice-free glacialic sediment accumulations of SDCGSAPE. Non-glacialic sediment accumulation, as talus slope deposits or former talus-derived rock glaciers, can also be present in the margin of SDCGSAPE. However, very few studies investigated them and here, we will focus on glacialic sediment accumulations. In the next sections, the ice-free, ice-cemented and ice-

cored sediment accumulations encountered in these systems will be presented. Nevertheless, a particular attention will be pay to the landforms containing ground ice because they concentrate most of the researches and debates.

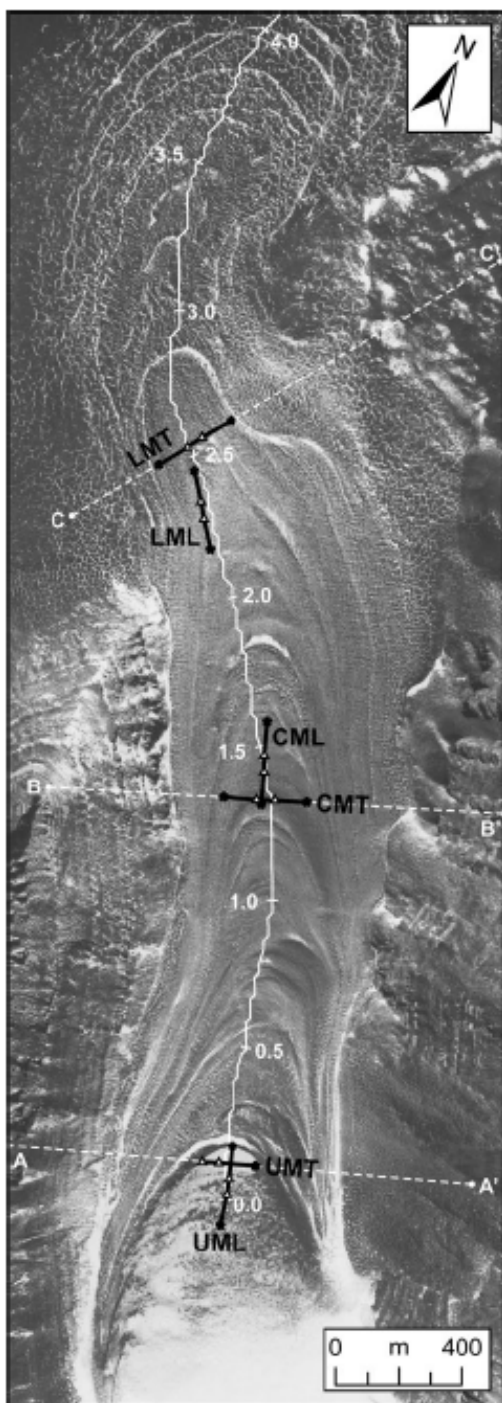
Through the study of glacier-permafrost interactions, a substantive debate emerged in the scientific community on the consideration of buried glacier ice as permafrost, and on the origin of rock glaciers (e.g. [Hamilton and Whalley, 1995](#); [Ackert, 1998](#); [Clark et al., 1998](#); [Haeberli, 2005](#); [Berthling, 2011](#)). Up to now, the controversies generated on these questions have never clearly ended. Open definitions are proposed (e.g. [Haeberli et al., 2006](#); [Janke et al., 2013](#)) to the detriment of a clear and definitive consensus. As a result, many confusions and inconsistencies, especially in terminology, are present in literature on these topics ([Berthling et al., 2013](#)).

The inconsistency mainly lies on the fact that, if a genetical and morphological continuum between glaciers and rock glaciers is recognized as possible (1), glacier ice remains strictly excluded from most of the permafrost definitions (2). Indeed, a glacier does not need permafrost conditions to develop. A considerable volume of glacier ice is able to form or flow in temperate environments ([Pfeffer et al., 2014](#)). However, large portion of the Earth glaciers occupies areas subjected to permafrost conditions and can be directly connected with sediment accumulations considered as permafrost indicators ([Etzelmüller and Hagen, 2005](#); [Janke et al., 2015](#)). At the same time, active rock glaciers are considered as reliable indicators of permafrost (3). The statements (1), (2) and (3) induce then an incoherent circular reasoning where the consideration of glacial rock glaciers or sedimentary ice within rock glaciers as permafrost indicator becomes problematic.

The fuzzy boundary between permafrost and glacier ice hindered the construction of a clear and consensual knowledge on glacier-permafrost interactions in the last decades ([Berthling et al., 2013](#)). Moreover, although landforms can seem similar despite distinct processes of formation (this principle has been defined as *equifinality*; e.g. [Slaymaker, 2004](#)), many researchers propose to base landforms classifications on morphological criteria (e.g. [Hamilton and Whalley, 1995](#); [Kraimer and Mostler, 2006](#); [Janke et al., 2013](#)). This considerably enhances the confusion in the glacier-permafrost research field. Consequently, the distinction between heavily debris-covered glaciers, glacial and non-glacial sediment accumulations containing ground ice is usually unclear in the literature. The same terminology can be found for genetically distinct landforms. The controversial discussions on the origin of *rock glaciers* especially well illustrate this confusion. Only based on a morphological definition, these landforms can be produced by glacial ([Ackert, 1998](#); [Potter et al., 1998](#); [Whalley and Palmer, 1998](#)), periglacial ([Haeberli, 1985](#); [Barsch, 1996](#)) processes and, for some authors, even by rock avalanches (e.g. [Ballantyne et al., 2009](#)). Their interpretation as permafrost indicators becomes therefore problematic because permafrost conditions are both fundamental for their periglacial morphogenesis and dispensable for the other morphogenesis. In this imprecise research context, different terminologies can also be used for the same landforms. For example, [Rignot et al. \(2002\)](#) and [Shean et al. \(2007\)](#) refer respectively to rock glacier and debris-covered glacier for the same feature in a dry valley of Antarctica ([Fig. 1.34](#)).

As mentioned above, because of the lack of clearness in the distinction of debris-covered glaciers and their associated sediment accumulations in permafrost environments, the inclusion of these landforms in glacial or periglacial inventories is still unsatisfactory (Azócar and Brenning, 2010; Benn et al., 2012; Pfeiffer et al., 2014).

Recent works, especially those of Ivar Berthling and its associated researchers (Berthling, 2011; Berthling and Etzelmüller, 2011; Berthling et al., 2013), propose interesting ways to go beyond these relatively disabling scientific debates on glacier-permafrost interactions. First of all, they recognise, as many others authors (e.g. Ackert, 1998; Benn et al., 2003; Haerberli et al., 2006; Whalley, 2009; Janke et al., 2015), that continuums in space, time and processes exist between the glacial



and periglacial domains (Fig. 1.3). Glacial, periglacial, nival and/or azonal processes participate to shape landforms in cold-climate regions. If these processes coexist, interact or follow each other in time and space, sub-zero thermal conditions exercise an overarching control in these environments. Hence, they propose the integrative concept of *cryo-conditioning* morphodynamics (also *cryo-conditioned* landforms; Fig. 1.35), which allows overtaking the traditional research boundaries. In cold regions, permafrost conditions have fundamental influence on bedrock, sediments, soils, water or glaciers present at the Earth surface. Moreover, to clarify the interpretation of ground ice, they propose to consider glacier ice covered by debris and subjected to permafrost conditions as permafrost. Finally, to prevent confusions on rock glaciers and related landforms, they strongly recommend the use of genetic definitions rather than morphological definitions. Permafrost becomes thereby a fundamental control of rock glacier development and existence.

Fig. 1.34: Aerial photo (USGS TMA3080-F32V-275) of the bare-ice / debris-covered glacier / rock glacier system located in the Mullins valley (77°51'S, 160°35'E; Antarctica). White numbers refer to longitudinal distance. Black lines represent the location of seismic profiles carried out by Shean et al. (2007). Note the progressive transition in surface morphology between the upslope bare-ice, central debris-covered and distal rock glacier zones. Reproduced from this study.

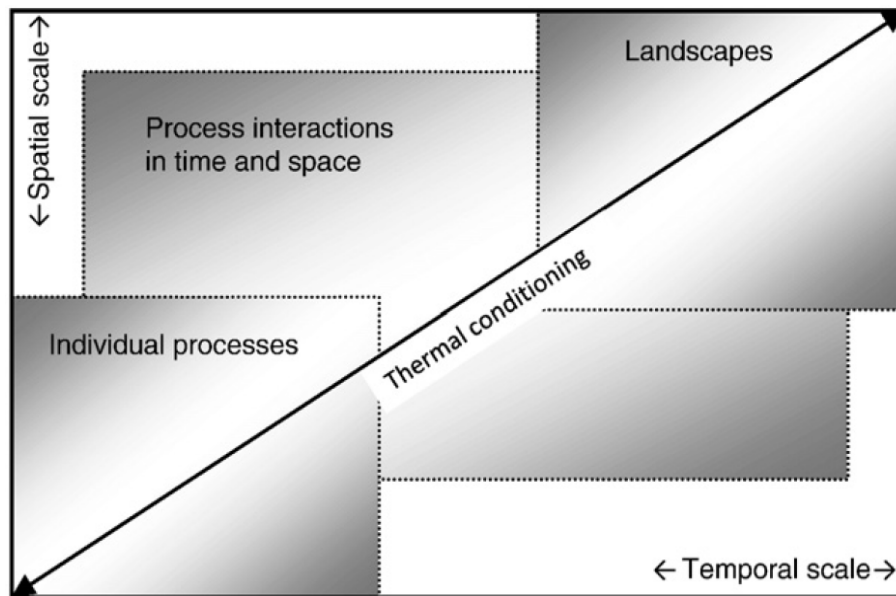


Fig. 1.35: Illustration of the cryo-conditioning concept. This concept encompasses all scales and influence single set of processes. The cold thermal condition exercises an overarching control on periglacial, glacial, nival and azonal processes and landforms. Reproduced from Berthling and Etzelmüller (2011).

1.2.2.2. Possibly polygenic and multi-phased Holocene sediment accumulations

As synthesized in 1.2.1.4, SDCGSAPE are characterized by their high debris content and weak coupling with downslope sediment transfer system. In such transport-limited systems, no processes efficiently evacuate the debris and bed or distal accumulations progressively grew by the accretion of the freshly produced material (Kirkbride, 2000; Benn et al., 2003; Iturrizaga, 2013; Fig. 1.22). However, the strictly *glacial origin* of these sediment accumulations remains questionable and the use of the term *glacigenic* is somewhat abusive. Indeed, the glaciers did not advance in *virgin* environments during their Holocene fluctuations. Former sediments can be present, deposited during the precedent glacial phase or ice-free period by non-glacial processes. At each new glacier advance, former sediments accumulations as talus slope deposits or talus-derived rock glaciers are “pushed, overridden and reworked” (Matthews et al., 2014, p. 544). Thus, if the most recent glacial and fluvio-glacial processes give the general appearance to these sediment accumulations, the origin of the material can be diverse.

Glaciers have fluctuated during the Holocene at a relatively similar amplitude than between the LIA maximum and their current extent (Maisch et al., 2003; Kirkbride and Winkler, 2012; Fig. 1.36). More extensive glacier advances could have existed, especially at the beginning of the Holocene but the associated moraines are rare and less developed than the late Holocene formations (e.g. Ivy-Ochs et al., 2009). Indeed, the frequency of glacier advances and thus of cycles of sediment production, accumulation and reworking, increased since the cold *Neoglacial* period in the last four millennia (Wanner et al., 2011; Fig. 1.36). Moreover, in numerous glacierized region and especially in the Northern Hemisphere, the last significant cold pulse -the LIA- corresponds to the largest glacier extent of the second half of the Holocene (Ivy-Ochs et al., 2009; Kirkbride and Winkler,

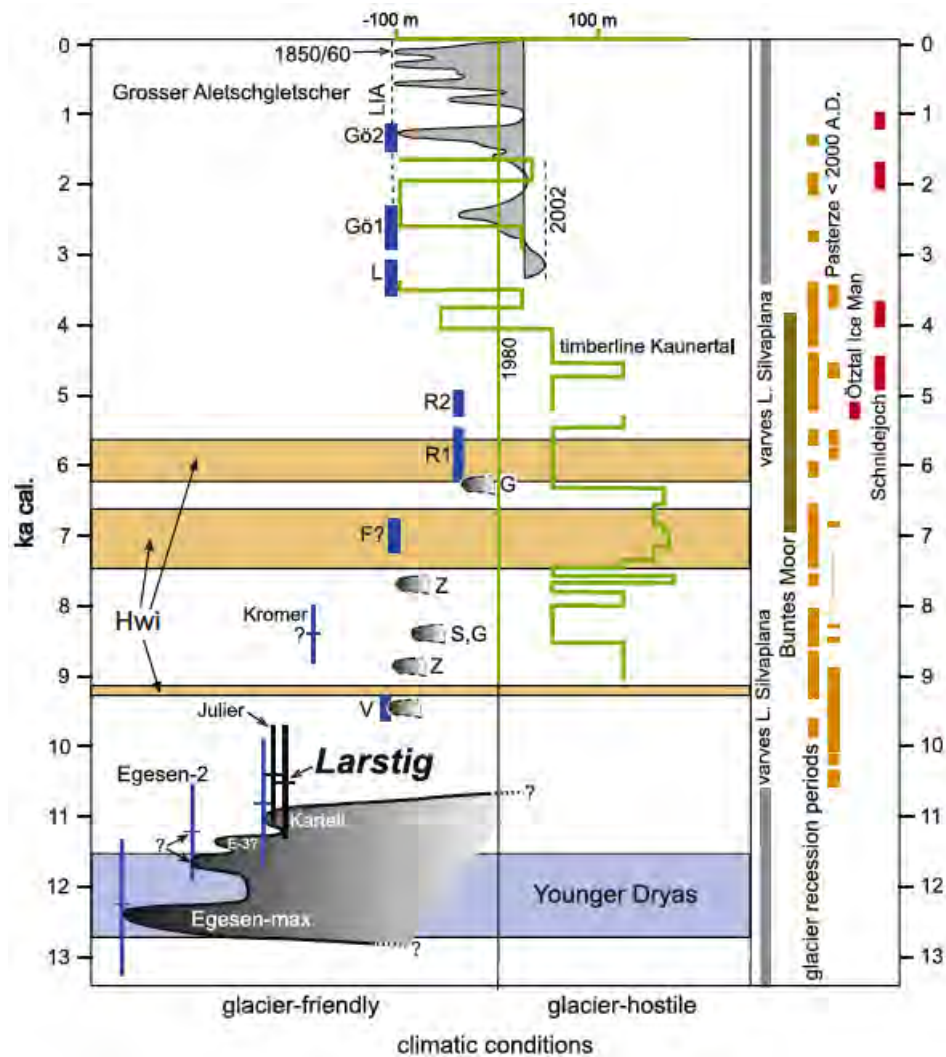


Fig. 1.36: Synthesis of Late Pleistocene and Holocene glacier fluctuations and climatic conditions in the European Alps. Reproduced from Ivy-Ochs et al. (2009). Because the figure is very complete and gathers references from diverse sources, we reproduce directly here its caption: "On the left-hand side of the figure: Interpreted time–distance glacier extent for Egesen and early Holocene glaciers from Maisch et al. (1999). ^{10}Be surface exposure ages for Egesen-max (12.2 \pm 1.0 ka), Egesen-2 (11.3 \pm 0.9 ka) and the Kartell (10.8 \pm 1.0 ka) moraines are shown as blue crosses. Julier (10.4 \pm 0.7 ka) and Larstig (10.5 \pm 0.8 ka) rock glacier ^{10}Be stabilization ages are shown as black crosses. Reported glacier advances to the LIA extents or less for the following glaciers are shown as dashed lines: G: Gepatschferner (Kaunertal); S: Simonykees and Z: Zettalunitzkees (Venediger Mountains, Nicolussi and Patzelt, 2001). Short blue bars indicate inferred cold oscillations V: Venediger; F?: Frosnitz; R1, R2: Rotmoos 1 and 2; L: Löbben oscillation; Gö1, Gö2: Göschener 1 and 2 oscillations (see text for references). Hwi: Holocene warm intervals (orange bands) based on data from Vadret da Tschierva (Engadin; Joerin et al., 2008). Green line indicates variations in timberline in Kaunertal (Nicolussi et al., 2005). Advances of Grosser Aletschgletscher from 3.5 ka to present are taken from Holzhauser et al. (2005). On the right-hand side of the figure: Varves present in Silvaplanaersee sediment (Engadin; Leemann and Niessen, 1994), as indicator of active glaciers in the catchment area. Buntes Moor, uninterrupted organic sedimentation (Nicolussi and Patzelt, 2001). Glacier recession periods (central and eastern Swiss Alps) from Joerin et al. (2006). Pasterze glacier smaller than at 2000 (Nicolussi and Patzelt, 2000, 2001). Ötztal Ice Man, glacier at Tisenjoch as small as in 1991 (Bonani et al., 1992, 1994; Baroni and Orombelli, 1996). Radiocarbon-dated archaeological materials found at Schnidejoch (Grosjean et al., 2007)" (p. 2143).

2012; e.g. Fig. 1.36). Therefore, in poorly coupled systems as SDCGSAPE, the current shape of sediment accumulations is largely due to this recent and major period of sediment accumulation and reworking (Matthews et al., 2014), although the post-LIA events (the general glacier decline and small glacier readvances; e.g. Fig. 1.10; 1.23 & 1.25) have also influenced the morphology. Nevertheless, the genesis of these landforms has to be thought at least at late-Holocene timescale. Indeed, glaciers fluctuations were multiple and the sediment production was continuous, even if

its intensity probably continuously varied (Humlum, 2000). Hence, although suggested in some researches (e.g. Whalley and Palmer, 1998; Krainer et al., 2012; Seppi et al., 2015), the consideration of the LIA and post-LIA periods alone for the formation of these sediment accumulations seems to be reductive and does not take into account their very likely repeated morphogenetic cycles. Moreover, the total volume of debris accumulated is usually disproportionate with what would have resulted from the erosion rates of the last centuries (Berthling, 2011; e.g. Fig. 1.1; 1.8 & 1.22). Sediment accumulations associated with SDCGSAPE are thus very likely rather a complex and multi-phased legacy of the sediment production and glacier fluctuations of the (at least late-) Holocene (Ackert, 1998; Maisch et al., 2003; Lambiel et al., 2004; Matthews et al., 2014; Monnier et al., 2014; Fig. 1.37).

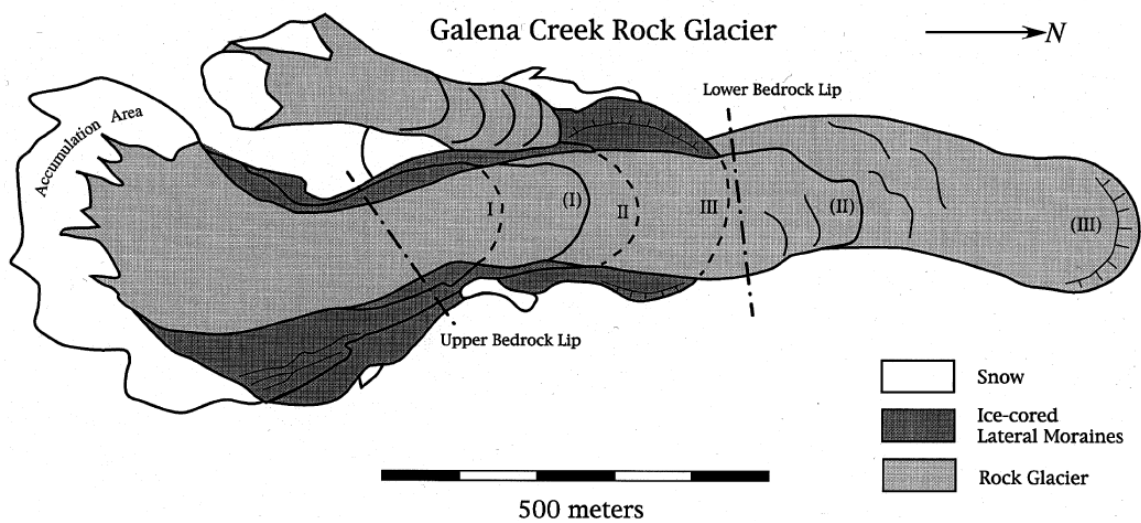


Fig. 1.37: Simplified map of the Galena Creek debris-covered / rock glacier system (44°38'30N, 109°47'30W; USA). According to Ackert (1998), I, II and III are considered as former neoglaciated debris covered glacier positions. Stage I is for instance attributed to late LIA. The debris-covered tongues have afterward evolved as rock glacier (I), (II) and (III) slowly creeping downstream. Reproduced from this study

1.2.2.3. Type, composition and origin of the sediment accumulations associated with SDCGSAPE

Subglacial sediment accumulations

As mentioned above, Holocene glaciers can have overridden pre-existent sediment accumulations. In addition, freshly eroded sediments can be deposited at the glacier bed by ice fluxes (Maisch et al., 1999; Kirkbride, 2000; Iturrizaga, 2013). Because of their weight, glaciers act as steamrollers on subglacial debris. The latter are hence generally dominated by fine material, because of the progressive crushing of debris by the stress exerted by the flowing glacier and by water circulations (e.g. Fu and Harbor, 2011). This also usually results in the induration of the overridden sediments. The presence of subglacial sediments can noticeably increase the glacier motion (Fig. 1.12). In temperate glaciers, high-pressurized water in the uppermost subglacial sediments induces their rapid deformation (Fitzsimons and Lorrain, 2011). In cold glaciers, deformations can occur within or at the base of the frozen sediments stuck to the glacier (Waller, 2001).

After the glacier retreat, subglacial sediment accumulations –also referred to as *ground moraines* or *basal till* when they are strictly glacigenic (Schomacker, 2011)- commonly have an undifferentiated and smoothed aspect. However, surface lineations parallel to the former ice-flow can be present (Evans, 2013). This is especially the case of the *fluted moraines* (Fig. 1.38). These longitudinal sediment ridges are rarely higher than few meters and form behind obstacles at the base of temperate glaciers (Benn, 1994; Etzelmüller and Hagen, 2005; Kneisel and Kääh, 2007).

The presence of permafrost and thus of ground ice in subglacial sediment accumulations is strongly dependant on the glacier thermal regime (Kneisel, 2003; Delaloye, 2004; Waller and Tuckwell, 2005; Ribolini et al., 2007). Indeed, basal water circulations in temperate glaciers degrade former permafrost while the *warm* thermal conditions prevent the formation of permafrost under the glacier. Conversely, former permafrost can be preserved under the cold glaciers zones (Reynard et al., 2003). Moreover, in cold environments, many glaciers tend to cool when they become thinner or when the winter snow cover decreases (Hodgkins, 1997; Bælum and Benn, 2011; Gilbert et al., 2012; Fig. 1.32). This process and the increase of the influence of cold atmospheric conditions on the ground can generate permafrost aggradation in the subglacial sediments (Etzelmüller and Hagen, 2005). Some patches of permafrost present in recently deglaciated areas have been interpreted as recently formed ground ice, and thus as an indicator of permafrost conditions (Kneisel, 2003; Etzelmüller and Hagen, 2005; Kneisel and Kääh, 2007; Ribolini et al., 2010). It could illustrate the thermal rebalancing of the ground with atmospheric conditions after the disappearance of the glacier, which acts as an insulator layer. Nevertheless, the high density of fine material in the ground can be factors that hinder the postglacial permafrost aggradation in subglacial sediment accumulations (Dusik et al., 2015). Indeed, permafrost conditions occur preferentially in porous and coarse-grained debris where cold air can accumulate (e.g. Haeberli and Gruber, 2008).

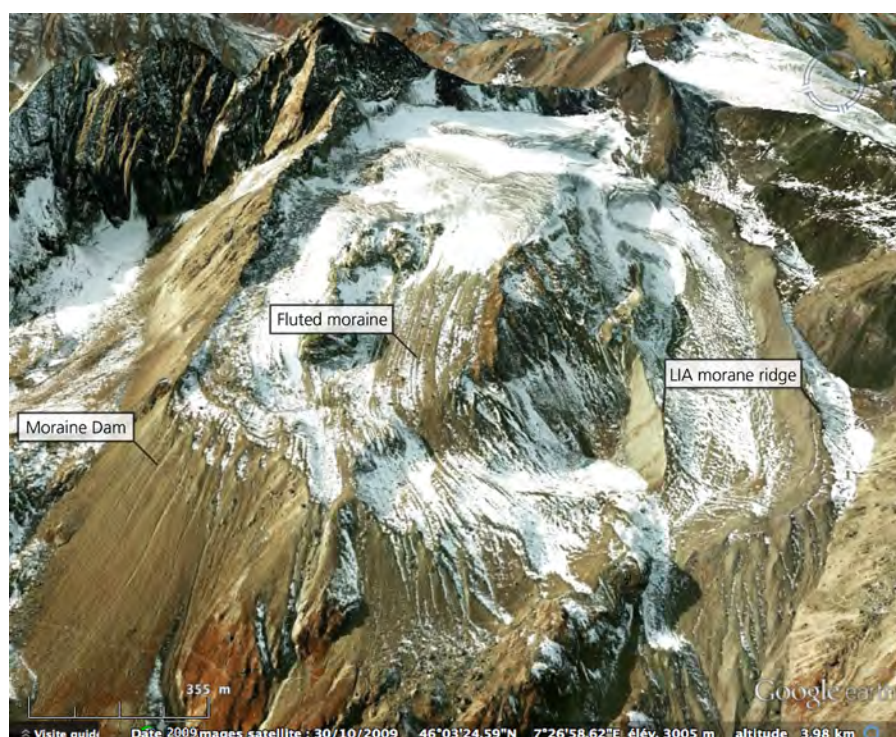


Fig. 1.38: Google Earth view of the Aiguilles-Rouges glacier system (46°03'30N, 7°27'E; Switzerland). This glacier is located above the regional lower limit of permafrost. However, the presence of fluted moraines in recently deglaciated zones illustrates the former temperate bed conditions. In the left-hand side of this figure, the 300 m high moraine dam highlights the poor coupling of this system with hydrosystem to evacuate the sedimentary load. This debris accumulation is only superficially reworked by debris flows.

Lateral and frontal sediment accumulations

In glacier systems, a large portion of the debris are transferred and deposited at the margins of the ablation areas. If the glacier geometry remains stable over time, the accretion of sediment leads to the formation of a lateral and/or frontal moraine ridge (Benn and Evans, 2010; e.g. Fig. 1.38). In some cases, disproportionate latero-frontal accumulation of debris can completely surround the glacier front (Fig. 1.22; 1.38). This occurs when the debris concentration is very high in the glacier and the fluvio-glacial processes have a too weak magnitude to evacuate sediments (Shroder et al., 2000; Benn et al., 2003). These *moraine dams* –also termed as *moraine dumps*, *bastions*, *ramparts* in literature- decouple the glacier from downslope sediment transfer system. Most of debris are then trapped in the glacier system but some of the smallest particles can be evacuated by meltwater runoffs (Berthling, 2011).

The bulldozing of old materials during a glacier advance is also an important shaping process of marginal moraine ridges (e.g. Evans, 2003; Winkler and Matthews, 2010). Even if these landforms are rightly referred to as *push-moraines*, the use of this term is sometimes restricted to such glaciotectonic disturbances in permafrost environments (Haeblerli, 1979; Reynard et al., 2003; Etzelmüller and Hagen, 2005; Waller and Tuckwell, 2005; Fig. 1.39). Indeed, this process is especially efficient when the pre-existent sediments are ice-cemented. The stress related to the glacier advance is effectively transmitted to this cohesive material, generating sometimes complexes of several concentric proglacial ridges (Monnier et al., 2011; Fig. 1.39).

Glacier ice can be integrated into the marginal sediment accumulations, forming *ice-cored moraines* (Lukas, 2011; Kirkbride and Deline, 2013; Matthews et al., 2014; Fig. 1.40). This type of moraine can be found in all the glacier systems containing debris (Schomaker, 2008). However, the lifetime of the ice core is relatively short in temperate environments because of the high temperatures and water circulations. Conversely, when the superficial sediment layer is thicker than the active layer (Fig. 1.29), the ice can be preserved for a long time in permafrost environments (Harris and Murton,



Fig. 1.39: Google Earth view of the Tabor debris-covered glacier/rock glacier system (45°07'N, 6°34'E; France). The Holocene advances of this glacier in very likely frozen sediments accumulations induced the numerous marginal arcuate ridges. In addition to these push-moraines, the distal active rock glacier also illustrates the glacier-permafrost relationships (Monnier et al., 2011).

2005). Differential ablation dynamics with nearby bare-ice glacier can lead to the disconnection of the ice-cored moraines with the active glacier during a retreat phase (Schomacker and Kjær, 2007; Lukas, 2011; Kirkbride and Deline, 2013; Fig. 1.40).

In the scientific literature, the use of the terms ice-cored and push-moraines is commonly narrowed to qualify the landforms of permafrost environments even if they can also exist under temperate conditions. Ice-cored and push-moraines are therefore considered as indicators of permafrost conditions because they contain perennial ground ice that would disappear without these cold conditions. Furthermore, in this narrow use, they also give an indication on the thermal regime of the glaciers that have shaped them. Indeed, the ice was very likely cold in the glacier margins where these moraines have developed, this thermal regime allowing the preservation and/or aggradation of permafrost and ground ice in contrast to temperate ice and associated water runoffs (Kneisel, 2003; Etzelmüller and Hagen, 2005; Lilleøren et al., 2013; Dusik et al., 2015). In this research, ice-cored and push-moraines will be used in this narrow sense, restricted to permafrost environments.

Regardless their origin or ice content, the marginal moraines described above are static landforms (Benn and Evans, 2010; Kirkbride and Deline, 2013; Emmer et al., 2015). Relict drainage network, which was formed under past climatic conditions, can be preserved for instance within ice-cored moraines (Moorman, 2005). Superficial mass wasting or fluvial processes may rework them (e.g. Cossart and Fort, 2008; Ravanel and Lambiel, 2012; Deline et al., 2015; Fig. 1.38). They can even be breached during high erosion events, which are mainly related to extreme hydrological forcing (Hambrey et al., 2008; Iturrizaga, 2011; Kääh, 2011; Huggel et al., 2012). When they contain ground ice, backwasting and downwasting processes control their evolution (Schomaker, 2008).

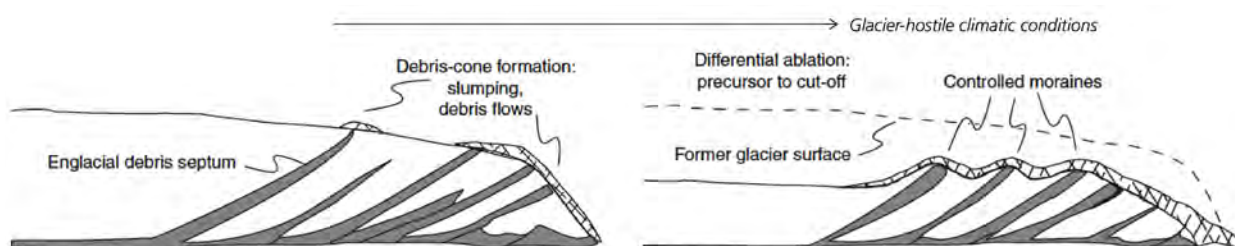


Fig. 1.40: Schematic diagram showing the formation of ice-cored moraines (controlled moraines) in a negative mass balance period. The marginal preservation of glacier ice is related to differential ablation associated with the presence of a debris cover. Adapted from Lukas (2011).

Ablation moraines

The sediment produced by the erosion of the glacier bed or the surrounding relief can be accumulated on the glacier surface or incorporated within the glacier (Fig. 1.33). The englacial and supraglacial sediment transfer and accumulation, and their influence on glacier dynamics are detailed in 1.2.1.1.

During the glacier retreat, these sediments are deposited as *ablation moraines* on the former glacier bed (Evans, 2013). Their aspect and thickness is commonly irregular and heterogeneous

at local scale. The differential ice-melt dynamics in debris-covered glaciers generates especially complex hummocky terrains (Schomacker, 2008 and 2011; Kirkbride and Winkler, 2012). Roughly, small size and rounded englacially-transported debris can be distinguished from the coarse angular debris, which are transferred passively on the glacier surface (Berger et al., 2004; Hambrey et al., 2008). These primary glacial deposits are often associated with material reworked during the glacier retreat by mass wasting and meltwater circulations. The thickness of ablation moraines exceeds rarely few meters. This layer can shelter glacier ice. Ground ice can also form in these sediments, especially in the coarse-grained zones. In permafrost environments, this ground ice can be considered as permafrost.

Glacigenic rock glaciers

All the static sediment accumulations described above can start to flow downward when the four following conditions are met: (1) the presence of ground ice, (2) the occurrence of permafrost conditions, a high enough (3) topographic slope angle and (4) thickness of sediment accumulation.

The first condition concerns the ice content within the sediment accumulation. Indeed, even in relatively steep slopes, dry sediments are static independent elements whose spatial organisation depends on the internal frictional threshold angles (Dikau, 2004). The presence of an internal massive ice body (ice core) or of interstitial ice (ice cement) changes their mechanical properties. The ice-debris mixture becomes thereby a cohesive material that can flow under gravity (Lambiel et al., 2011). Because of the reduced internal friction, ice-cored or ice-supersaturated sediments behave like pure ice bodies and have a potential unlimited deformation with non-zero stress (Haeberli, 2000). Conversely, saturated or non-saturated sediments retain their high internal friction and experience a limited creep. The ice content values proposed for flowing ice-debris mixture are typically ranging between 40 and 90% (Burger et al., 1999; Haeberli et al., 2006; Hausmann et al., 2007; Janke et al., 2015; Fig. 1.41). The relatively slow viscous deformation –magnitudes of movements are usually ranging from cm to m per year- generates a tongue-like landform, which is characterised by steep margins and commonly covered by superficial transversal and/or longitudinal ridges and furrows (Berthling, 2011; e.g. Fig. 1.34 & 39). However, the presence of ground ice in the sediment accumulation alone is not sufficient to allow its generalised deformation. In this way, no signs indicating such active viscous flow are visible in the marginal sediment accumulations of glaciers in temperate environments (Owen and England, 1998; Monnier and Kinnard, 2015; Fig. 1.2). Indeed, the rapid melt of ground ice under these *warm* climatic conditions prevents the development of these landforms. The creep process

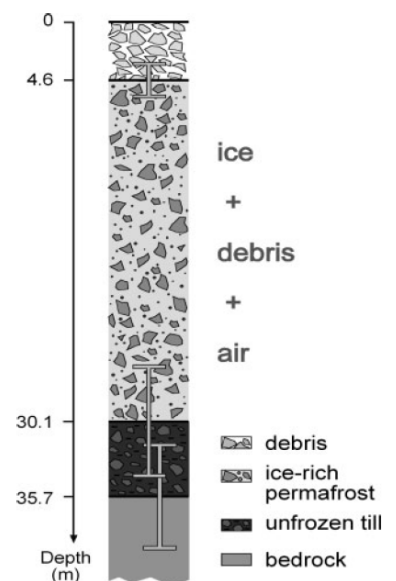


Fig. 1.41: Schematic vertical profile proposed by Hausmann et al. (2007) for the Reichenkar glacigenic rock glacier (47°02'50N, 11°02'E; Austria). According to these authors, the ice content is ranging from 45 to 60%. The rock glacier overrides possibly water-saturated unfrozen till where sliding seems occurring. Reproduced this study.

operates thus only under permafrost conditions, where the cold temperatures allow the long-term preservation and deformation of ground ice (Berthling, 2011). As showed before, the presence of ice can be related to the integration of sedimentary ice (glacial origin) in the distal sediment accumulations (Fig. 1.40). In permafrost environments, the refreezing of percolating water (congelation or magmatic ice; periglacial origin) or the metamorphosis of buried snow can also explain the occurrence of ground ice (Haeberli et al., 2006). Hence, ice from both glacial and periglacial origin may be found in marginal sediment accumulations of the glaciers located in permafrost environments (Kneisel, 2003; Whalley and Azizi, 2003; Ribolini et al., 2010). The two last conditions that allow the motion of ice-debris mixtures under gravity are minimum geometric thresholds. Below these slope and thickness conditions, landforms containing ground ice are stagnant. For instance, ice-cored moraines are non or little flowing landforms usually located in low relief terrains (Evans, 2013; Lilleøren et al., 2013; Matthews et al., 2014). These two geometric thresholds are interrelated: the slope angle has to be high to induce movements of thin frozen bodies while the thickest ones can flow with a relatively weak slope angle (Whalley and Martin, 1992). No minimum critical values are consensually recognised in the literature for these parameters, but flowing sediment accumulations containing ground ice are very often thicker than 10 m and override a slope steeper than 5 to 10° (e.g. Whalley and Martin, 1992; Barsch, 1996; Frauenfelder et al., 2003; Janke and Frauenfelder, 2008; Gärtner-Roer and Nyenhuis, 2010).

Because they result of the four conditions described above, flowing sediment accumulations located in glacier margins are in line with the genetic definition of an active *rock glacier* proposed by Berthling (2011, p. 103; Fig. 1.42): “the visible expression of cumulative deformation by long-term creep of ice/debris mixtures under permafrost conditions”. In the literature, these landforms are termed as *glacigenic* (Clark et al., 1998; Potter et al., 1998), *glacier-derived* (Humlum, 1988), *moraine-derived* (Lilleøren et al., 2013) or *debris rock glaciers* (Barsch, 1996). The term *Ice-cored rock glacier* (Potter, 1972; Berger et al., 2004), in opposition to *ice-cemented rock glacier*, is also sometimes used as a synonym of *glacigenic rock glacier*. In this dichotomy, the ice core is supposed to have a glacial origin (sedimentary ice), whereas the interstitial ice that cements the sediments is interpreted as magmatic

ice of periglacial origin. Nonetheless, the use of this descriptive

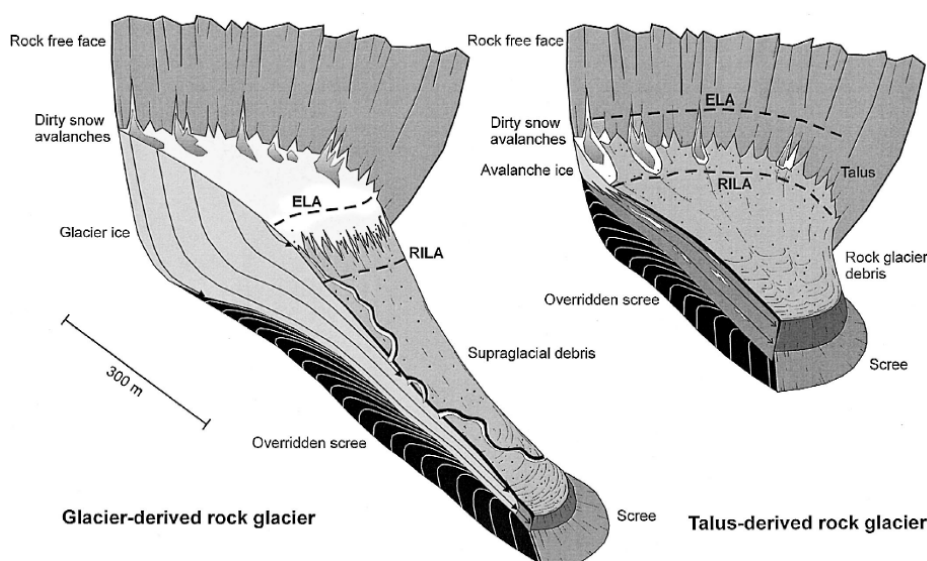


Fig. 1.42: Idealised models of glacier-derived and talus-derived rock glacier. SDCGSAPE can be composed by marginal glacier-derived rock glacier. RILA refers to Rock glacier Initiation Line Altitude. Note the progressive transition downglacier from bare ice, debris-covered ice to the rock glacier zone. Reproduced from Humlum (2000).

terminology as a genetic classification seems unsuitable. It adds confusion because the distinction between glacial and periglacial ice remains very challenging (Haeberli, 2000; Haeberli et al., 2006) and rock glaciers from both periglacial and glacial origins can have an ice-cored or ice-cemented structure. Indeed, the progressive integration of debris in melting massive sedimentary ice can generate an ice-cemented configuration (Clark et al., 1994). Conversely, ice cores (or massive ice) may be formed by the progressive segregation of refreezing groundwater or by the burying of snow avalanche deposits (Wayne, 1981; Haeberli, 2005; Haeberli et al., 2006).

Glacigenic rock glaciers illustrate the continuum existing between glacial and periglacial morphodynamics in cryo-conditioned environments (Benn et al., 2003; Haeberli et al., 2006; Whalley, 2009; Berthling, 2011; e.g. Fig. 1.26; 1.34; 1.37 & 1.42). A large number of scientific publications have investigated or discussed these landforms/processes continuum. However, except the qualitative recognition of the spatial and morphological continuity between debris-cover glaciers and rock glaciers (e.g. Janke et al., 2015; Seppi et al., 2015) and the detection of glacigenic ice within rock glaciers (e.g. Potter et al., 1998; Guglielmin et al., 2004; Fukui et al., 2008), clear and indisputable evidences of this continuum of processes in time are very sparse. To our knowledge, only Shroder et al. (2000) and Monnier and Kinnard (2015) have provided field evidences of the recent evolution of glacier tongues into rock glaciers. Analysis of the succession between glacial processes and periglacial processes is still lacking, especially in term of mass turnover and motion mechanisms. This is mainly due to the poor knowledge on the internal structure, the thermal conditions and the processes operating within and/or at the base of these landforms. Debris-covered glaciers and rock glaciers are recognised as end members of a continuous spectrum but their morphological and dynamical distinctions remain unclear (Azócar and Brenning, 2010; Berthling, 2011; Benn et al., 2012). For example, following Summerfield (1991), Emmer et al. (2015) recently used the thickening of the superficial debris layer and the decrease of surface velocities to interpret the transformation of a debris-covered glacier into a rock glacier (Fig. 1.22). These only two criteria seem unsubstantial because debris covered glacier tongues in temperate environments do not look or behave like rock glaciers, while they are also commonly characterised by a very thick debris cover and a significant decrease of velocity downglacier (e.g. Kirkbride, 1995; Fig. 1.2).

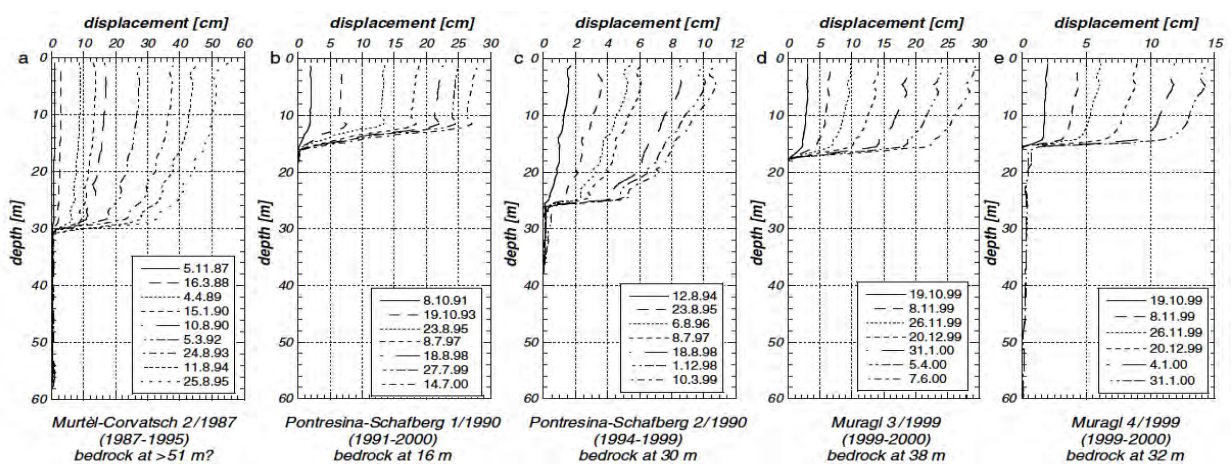


Fig. 1.43: Horizontal velocity recorded in boreholes at several rock glaciers in Switzerland. Horizontal movements are localised within thin shear horizons. The depth of the bedrock is indicated below each profile. Reproduced from Arenson (2002).

In a dynamical point of view, the same general flow law (Glen's law; Glen, 1955) is used for both glaciers (and hence debris-covered glaciers) and rock glaciers (e.g. Cuffey and Paterson, 2010; Lambiel et al., 2011). In addition to the internal deformation, rock glacier motion shows also similarities with glaciers (Fig. 1.12) because bed processes in water-saturated layers (Potter et al., 1998; Krainer and Mostler, 2006; Hausmann et al., 2007; Roer et al., 2008) and seasonal variations of velocities related to snow melt water infiltration and ground temperature (Perruchoud and Delaloye, 2007; Delaloye et al., 2008 & 2010) can also occur. Rock glaciers can also experience horizontal movements in shear zones located within the ice-debris mixtures (Arenson et al., 2002; Fig. 1.43). Except this last process, the same motion mechanisms can therefore be active in rock glaciers and debris-covered glaciers. Nevertheless, without being explained in the literature, the motions of these masses generate distinct surface morphologies (Janke et al., 2015). On the one hand, debris-covered glaciers zones can have hummocky or poorly differentiated surface patterns (Monnier et al., 2011; Monnier et al., 2014; Fig. 1.2). Most of them are confined between the static historic moraine ridges (Hambrey et al., 2008; Iturrizaga, 2013; Fig. 1.22 & 1.24). On the other hand, glacialigenic rock glaciers show generally superficial ridges and furrows that illustrate the viscous creep (Berthling, 2011; Monnier and Kinnard, 2015; Fig. 1.34, 1.42 & 1.42). Their fine-grained steep front slopes are usually extending beyond the LIA glacier limits (Owen and England, 1998; Berger et al., 2004; Fig. 1.26, 1.37 & 1.39). Some classification criteria have been recently suggested as the extent and the thickness of the debris cover, the ice/debris content, the presence of superficial patterns of viscous deformation or the intensity of ablation rate (e.g. Pourrier et al., 2014; Janke et al., 2015). However, most of them are qualitative and morphological criteria, and complementary quantitative data especially on the dynamical aspects are still required.

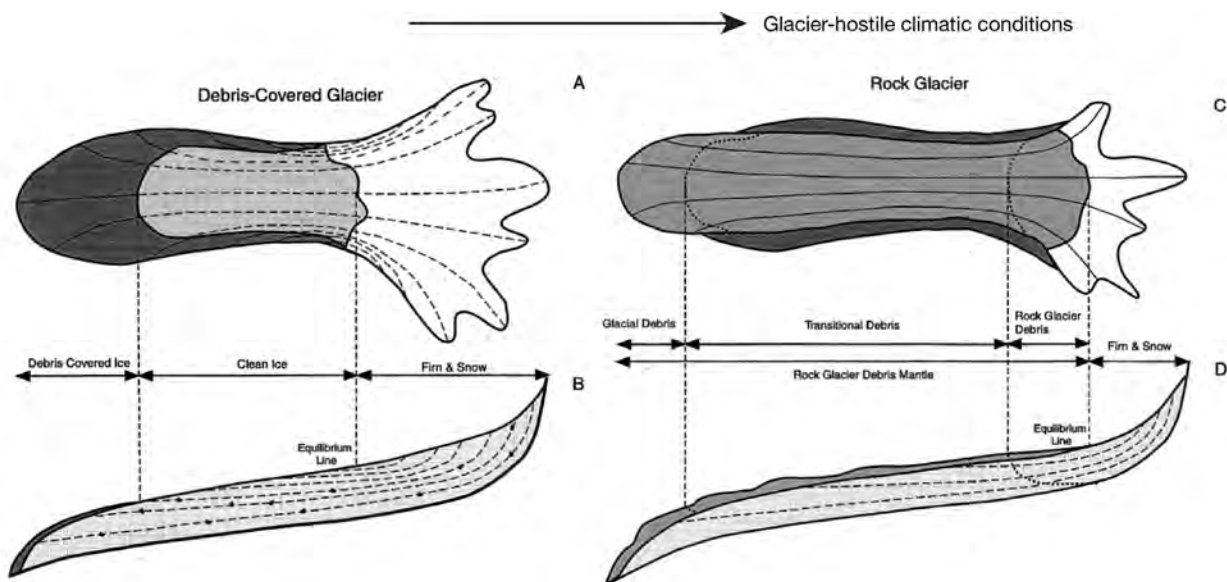


Fig. 1.44: Schematic evolution of the Galena Creek debris-covered / rock glacier system (44°38'30N, 109°47'30W; USA). In glacier-hostile climatic conditions, the snow accumulation is restricted and can even be disabled. The debris cover shelters ground ice, whose presence induces a generalised flow downstream. Ackert (1998) suggested that this transitional cycle occurred at least three times during the Neoglacial period to explain the current complex morphology of this system (Fig.1.37). Adapted from this study.

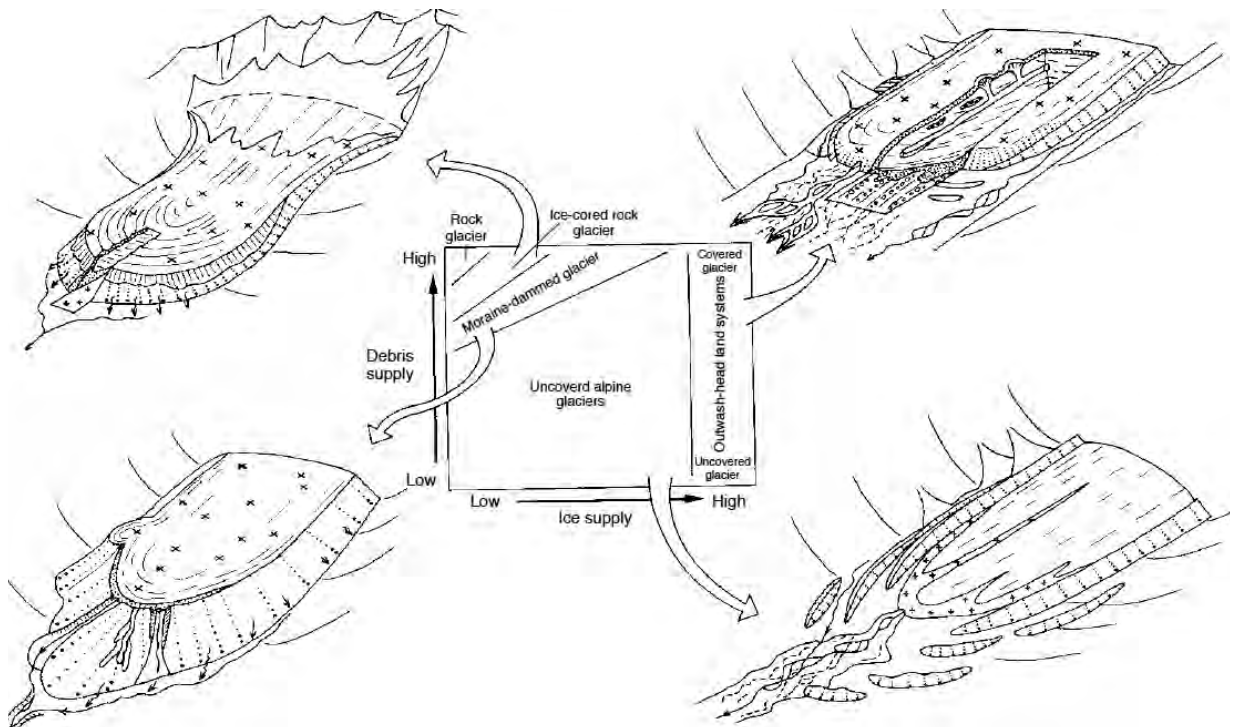


Fig. 1.45: Schematic illustration of ice-marginal environment associated with debris and ice supplies. As a function of their respective intensities, glaciers systems are coupled or decoupled with hydrosystem. Reproduced from Benn et al. (2003).

In spite of this relatively poor knowledge of operating processes, interesting general evolution models have been proposed for the transition between these landforms in permafrost environments (Clark et al., 1994; Ackert, 1998; Brazier et al., 1998; Shroder et al., 2000; Benn et al., 2003; Whalley, 2009; Fig. 1.44, 1.45 & 1.46). They consider the variations in time and space of the ice and debris supply, the glacier activity and the debris evacuation. In the glacier-favourable conditions, the ice supply is high and the ice-coverage of the surrounding relief limits the debris production. The glacier dynamic is high and sediments are efficiently evacuated, at least at the margin of the system. In the glacialigenic rock glacier-favourable conditions, the debris supply to the system is very high, while the ice supply is limited. The glacier has thereby a weak motion. The distal glacier zone or ice cores abandoned in the marginal sediments have limited ice melt because of the thick superficial debris layer (Fig. 1.40).

Moreover, magmatic ice can form in the sediment accumulations. If the slope angle is sufficient, the insulated ice-debris mixture can deform under gravity. It becomes thereby progressively disconnected from the upslope glacier accumulation area by the differential ablation dynamic and its downward flow (Ribolini et al., 2010; Monnier et al., 2011; Lilleøren et al., 2013; Seppi et al., 2015; Fig. 1.37).

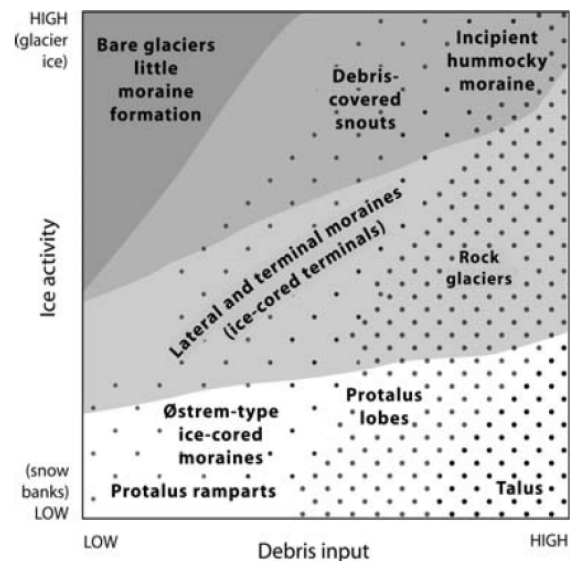


Fig. 1.46: Diagram illustrating the development of landforms in cold environments in relation with debris input and ice activity. Variations of these two parameters in time induce landforms evolutions. Reproduced from Whalley (2009).

1.2.2.4. Synthesis

Because of the high debris supply and their weak capacity to evacuate the sediment load in the hydrosystem, large sediment accumulations are usually present in SDCGSAPE. **They illustrate the role of Holocene glaciers in the production, the transfer, the deposition and the reworking of sediments.** They are thereby likely polygenic and multi-phased landforms inherited from the –at least recent- numerous climatic fluctuations of the Holocene. Located in permafrost environments, these sediment stores can be **ice-free, ice-cemented or ice-cored**, depending on the energy exchanges between the atmosphere, the glacier and the ground. **Ground ice gives cohesion to these sediment accumulations. They can then flow** in function of their thickness and of the topography, **becoming glacigenic rock glaciers.**

1.2.3. SDCGSAPE as a system

1.2.3.1. Organisation and components

Until now, SDCGSAPE have been considered from their two main components: (1) a small sedimentary ice mass, partly or completely covered by debris and flowing under permafrost conditions and, (2) their associated glacigenic sediment accumulations that possibly contain ground ice. However, this approach is incomplete from a systemic and spatial point of view. Indeed, if the fundamental and central component of SDCGSAPE is (1) the sedimentary ice mass, a holistic analysis has to take into account the two other principal components of these Earth surface landsystems (Fig. 1.47): (2) the topographical basin where they develop and (3) the proglacial areas where they exert a strong geomorphological and/or hydrological control. In this sense, the associated glacigenic sediment accumulations are only a part of the proglacial areas, which can also be composed by bedrock outcrops and non-glacigenic sediment accumulations (e.g. debris flow deposits, talus slopes). Nonetheless, the focus on the glaciers and their sediment accumulations so far is deliberate because this research concentrates on these components. The singularity of SDCGSAPE in comparison with other glacier systems strongly relies on these two components and their interactions. Both were presented and discussed previously. Conversely, the topographical basin and the other components of the proglacial areas have no fundamental specificities in SDCGSAPE and are therefore not studied thoroughly here. They will be rapidly presented in the next sections and can be indirectly discussed in the other sections of this research.

The distinction and the establishment of spatial limits between these components can be challenging. For example, temporal or permanent snow accumulations can be present on the accumulation basin and the upper delimitation of glacier in snow-covered area is commonly problematic (Pfeffer et al., 2014; Zemp et al., 2015). Similarly, the ice body and the glacigenic sediment accumulations can be complexly nested together (Berthling et al., 2013; Pfeffer et al., 2014; Janke et al., 2015; e.g. Fig. 1.39; 1.43 & 1.45). It often hinders their clear distinction. Other examples could be discussed here and these components have rather to be thought as spatially interconnected.

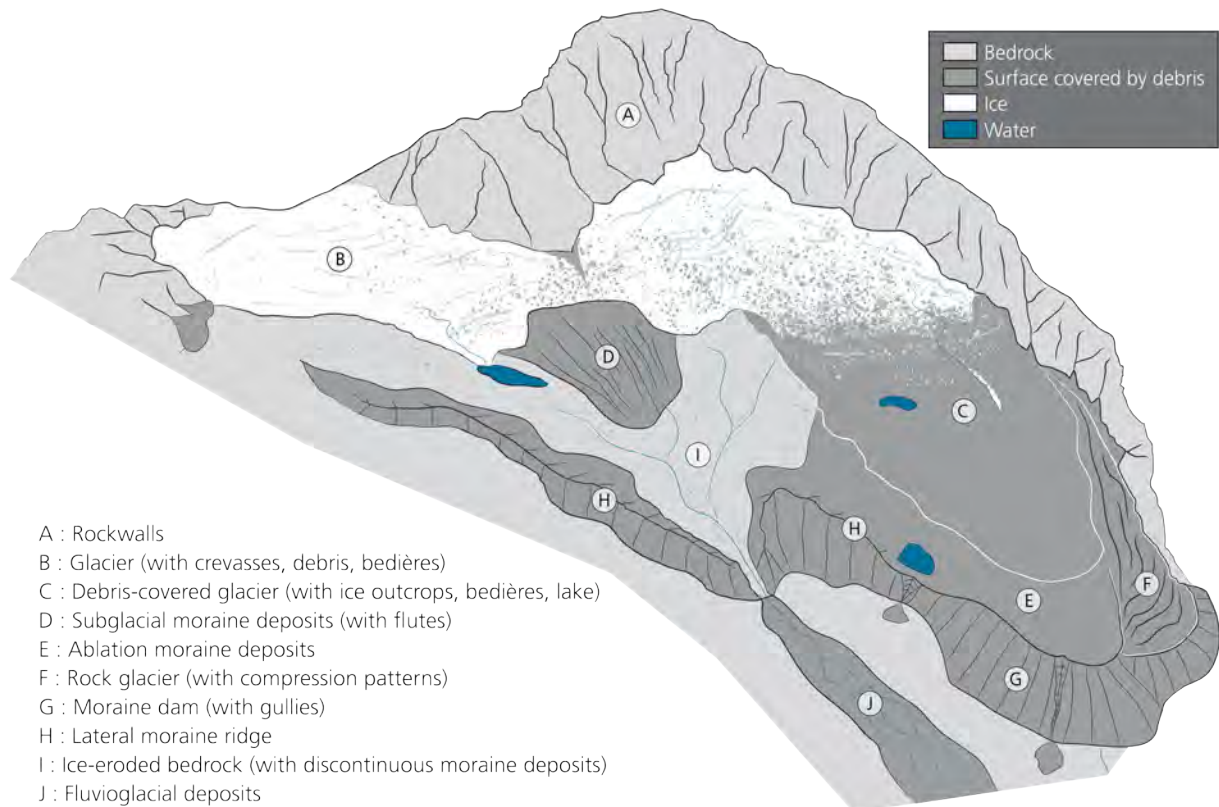


Fig. 1.47: Idealised model of a small debris-covered glacier system located in alpine permafrost environment. The rockwall height is lower in the right-hand part of the system. Hence, the glacier has been subjected to a weak topographical control (avalanching, shading, accumulation of debris cover) and experienced a large retreat since the last cold period. Marginal sediment accumulations are relatively small and the debris produced in this zone are evacuated towards the hydrosystem by fluvio-glacial processes. In contrast, the topographical control is more important on the left-hand side. The glacier is largely debris-covered and accumulated large amount of sediment at its margins. A portion of these sediments containing ground ice evolves as a rock glacier. This glacier zone is decoupled from downslope geomorphic system because of the damming effect and the weak production of meltwater by the debris-covered glacier. Supraglacial and proglacial lakes are also present in this system.

Ice is the fundamental material of glacier systems. In additions, snow, water and debris in various proportions can be present. In comparison with other glacier systems, the debris concentration is very high in SDCGSAPE because on the one hand, they develop in high relief environments where the sediment production is high and on the other hand, they are poorly coupled with hydrosystems to transfer the sediments downward. SDCGSAPE have thus large amount of ice and debris. They are dynamical systems where these two main constituents flux in time and space. Gravity and secondarily water are the main drivers of the fluxes. Secondary elements as soils, flora, fauna or even human infrastructures (e.g. [Hodkinson et al., 2003 and 2004](#); [Janke et al., 2015](#)) can also be found in these systems but their study is beyond the scope of this work.

1.2.3.2. The topographical basin

SDCGSAPE develop in high relief environments ([Fig. 1.1 & 1.47](#)). They usually occupy cirques or valley floors where the relief flattening allows ice and debris accumulation. The topographical basin is therefore an important component of these systems. It exercises a major control on their development and dynamic, influencing especially the accumulation and ablation rates of the ice mass. The redistribution of the snow fallen in the upslope topographical basin –also referred to

as *drainage area* or *avalanche area* when the sole slope $> 30^\circ$ is taken into account (DeBeer and Sharp, 2009; Hughes, 2009)- by wind drifting and avalanching can considerably increase the amount of snow accumulated on the glacier. In extreme cases, annual snow height can be multiplied by up to 10 or 20 times by these redistribution processes (Hoffman et al., 2007; Rödder et al., 2008). Ice avalanches from hanging glaciers also enhance the accumulation of some SDCGSAPE (e.g. Iturrizaga, 2013; Fig. 1.22). Besides, the topographical basin provides large quantities of debris in the systems. The freeze-thaw cycles are especially frequent and efficient in the erosion of the backwalls in the lower part of the periglacial belt (Davies et al., 2001). At Holocene timescale, typical denudation rates of rockwalls ranging between 0.5 and 5 mm/a are proposed in these environments (Humlum, 2000; Otto et al., 2009; Godon et al., 2013; Iturrizaga, 2013; Monnier and Kinnard, 2015). The sediments produced in the catchment are mainly accumulated on the glaciers by the numerous low-magnitude and high-frequency rockfall events. Rock avalanches and debris flows can also contribute to the transfer of debris towards the systems. Finally, avalanches and especially wet snow avalanches occurring during the melt season can also contain a debris load. Janke et al. (2015) showed for example that 15 m thick avalanches with about 2% of debris content deposit 30 cm of debris on glaciers. In addition to this aerial production of debris, erosion is also active in the bergschrund (Sanders et al., 2012) and at the base of small glaciers (Kuhn, 1995). The large influence of debris on the glacial dynamics has been discussed in the previous sections. The third major influence of the topographical basin on SDCGSAPE is the limitation of direct solar radiation by the shadow effect. It depends on the position and the height of the relief that surrounds the glacier. For example, the shading reduced the mean annual direct solar radiation by 16% on the Tête Rousse Glacier, a SDCGSAPE located in the Mont Blanc massif (Gilbert et al., 2012). As this variable is a fundamental component of the energy exchange at the glacier surface (Cuffey and Paterson, 2010), its reduction induces a noticeable decrease of ablation rate.

1.2.3.3. The proglacial area

Glacigenic sediment accumulations that possibly contain ground ice and/or a proglacial area compose the distal margins of SDCGSAPE. Both can be associated and the sediment accumulation can be considered as a surface feature of the proglacial area. However, the *proglacial area* –also referred as *glacier forefield*, *foreland*, *margin*, *outlet*, *recently deglaciated area* or *ice marginal environment* in the literature- can also comprise bedrock outcrops and non-glacigenic sediment accumulations. In this way, it can correspond to a space larger than the only glacigenic distal sediment accumulations. Nevertheless, the definition and the limits of proglacial areas remain unclear in literature. Indeed, spatiotemporal or dynamical criteria are both used to define these areas and no consensus is emerging. On the one hand, some authors limit this space to the zone deglaciated since the LIA, regardless the type of processes occurring and the degree of activity (e.g. Maisch et al., 1999; Kneisel, 2003; Reynard et al., 2003; Otto et al., 2009; Geilhausen et al., 2012; Dusik et al., 2015). However, numerous researches show that glaciers strongly influence the geomorphological and hydrological systems beyond the LIA limits, especially in high relief environments (e.g. Ballantyne, 2002; Benn et al., 2003; Chiarle et al., 2007; Pourrier et al., 2014).

For example, fluvioglacial fans or sandurs are proglacial landforms *sensu stricto*, although they can be developed outside the LIA limits. Therefore, from a dynamical point of view, the restriction of these spaces in the recently deglaciated areas is arbitrary. In this sense, [Slaymaker \(2011\)](#) proposes a wider and relatively open definition of proglacial areas. They are ice marginal environments affected by glaci-fluvial, glaci-lacustrine and glaci-marine processes where specific erosional or depositional landforms are shaped. The presence of marginal glacial sediment accumulations could be integrated to complete this definition. The latter were presented in 1.2.2. One of the particularities of SDCGSAPE in comparison with other glaciers systems is that, in extreme case, the lopsided sediment accumulations largely decouple these systems from downslope geomorphic and hydrological systems. In such cases, proglacial areas are only composed by these accumulations and their associated reworking landforms (e.g. right-hand side of the [Fig. 1.47](#)).

1.2.4. General synthesis and definition of SDCGSAPE

According to the fragmented elements of knowledge presented in this chapter, SDCGSAPE can be defined as **a system, whose fundamental component is a (very) small sedimentary ice mass, at least partially covered by debris and flowing under gravity in permafrost conditions**. A topographical basin and a proglacial area with which the glacier interacts also compose the system. In the ice marginal environment, very large glacial sediment stores can be accumulated in relation with the low energy and the high debris content of the glacier. Because of permafrost conditions, sedimentary ice can be preserved and magmatic ice can form in the marginal sediment accumulations. If the slope angle is sufficient, the ice-debris mixture can then start to flow, becoming glacial rock glacier that can be progressively disconnected from the upslope strictly glacial zone. The specific characteristics of these glacier systems potentially confer them a particular behaviour in response to climate variation in comparison with other glaciers.

1.3. Research objectives

The research objectives of this contribution are presented in the following and synthesized in the figure Fig. 1.48. As shown in the previous chapter, **the knowledge on SDCGSAPE** is already well developed. However, it **remains extremely sparse**. For instance, small glaciers, debris-covered glaciers and glaciers confined under permafrost conditions are now better known thanks to the intensification of researches on them in the last decades. Nonetheless, these types of glaciers are almost always considered independently in the literature. Furthermore, glaciological and geomorphological approaches usually investigate distinct parts of SDCGSAPE and the results obtained are rarely discussed together. The dispersion of the knowledge on these complex systems still generates **numerous confusions**. This concerns especially the definition of the distinct components of these systems and the distinction between glacial and periglacial dynamics. The few studies that consider SDCGSAPE as wholes mostly rely on qualitative and geomorphological approaches. Complementary data are particularly needed on the internal structure, glacier dynamics, glacier-permafrost interactions, operating processes and more largely on the main evolution controls of these systems. **An accurate and overarching approach is thereby still lacking** on these systems where glacial, periglacial, paraglacial and azonal morphodynamics can occur in responses to the current climate changes (Berthling, 2011; Berthling et al., 2013; Knight and Harrison, 2014).

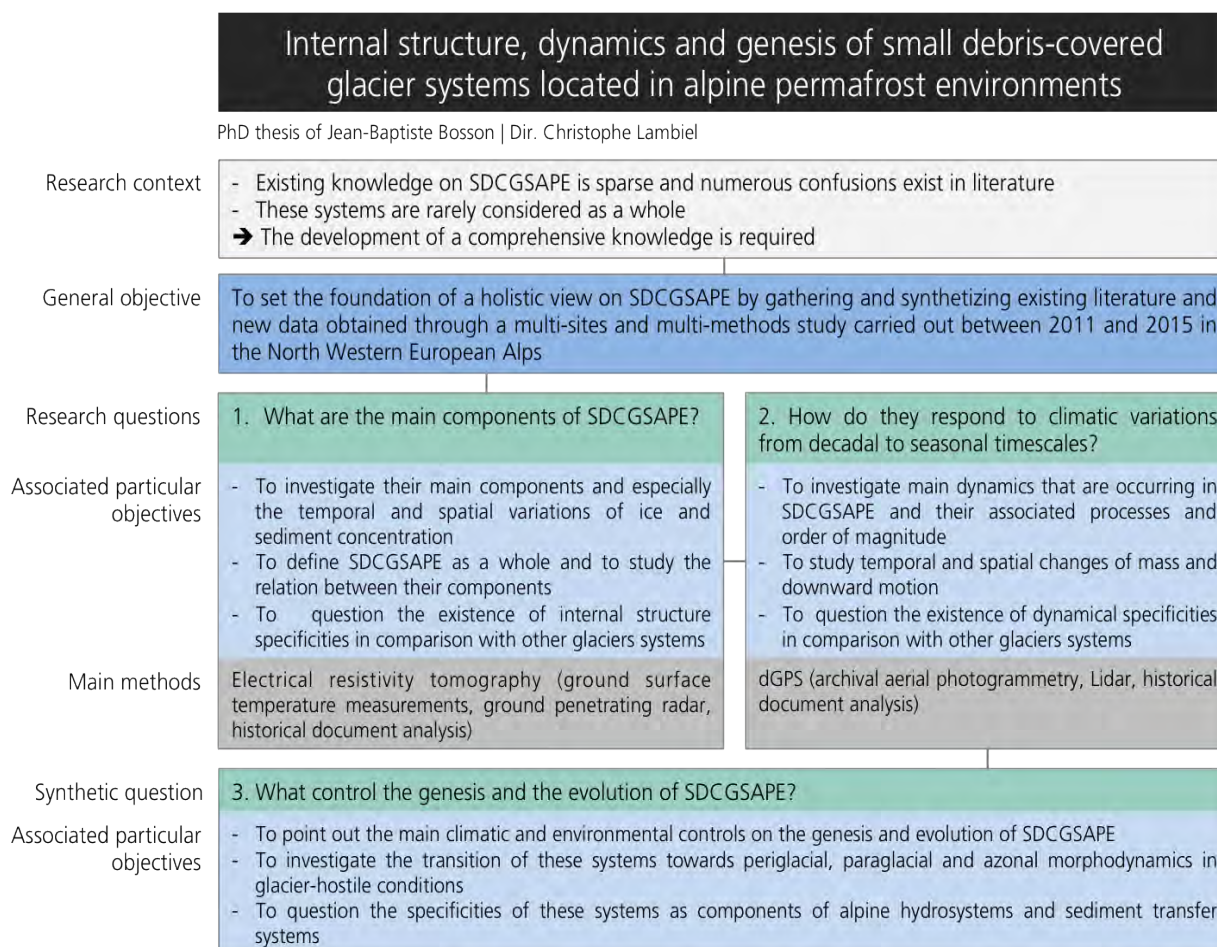


Fig. 1.48: Sketch of the research context, objectives and questions of this thesis on SDCGSAPE

This contribution modestly aims to set the foundation of such comprehensive view on SDCGSAPE. More precisely, **the internal structure of SDCGSAPE, their current dynamics and their genesis/evolution are investigated here by gathering and synthesizing (1) the fragmented existing literature and (2) new data obtained through a multi-sites and multi-methods study carried out between 2011 and 2015 in the North Western European Alps.** To avoid repetitions, the study sites and the methods used will be described in the *publications* (part 2) and *results compilation by study site* (part 3) parts.

According to the objective of this contribution, **the previous *Definition and state of knowledge* chapter (1.2) is somehow already an original result of this contribution.** To our knowledge, no similar broad review of literature and definition of SDCGSAPE has been proposed so far. Later and especially in the *discussion and general synthesis* part (part 4), our field results and our reflections will be discussed with this literature synthesis.

Field investigations have been led according to three main research questions, each including the definition of particular objectives (Fig. 1.48):

1. What are the main components of SDCGSAPE? A clear definition of SDCGSAPE and of their components is required. The **current internal structure**, and especially the concentration of ice and debris in the ground, the thickness of the structures and the presence of water is discussed with field observations and mapping, analysis of historical sources (e.g. maps, photographs) and especially with the results of geophysical prospections (mainly *Electrical Resistivity Tomography –ERT–* and secondarily with *Ground Penetrating Radar –GPR*). The analysis of surface movements and elevation changes at different timescales also provides indications on the ground composition. The spatial and temporal variations of the system components and their interrelations are also questioned.

2. How do these systems respond to climatic variations from decadal to seasonal timescales? The current dynamics of these systems in a changing climate context is studied. We try to figure out what are the processes involved and at which order of magnitude through the analysis of surface movements at timescales ranging from decades to seasons. We also try to distinguish the surface changes related to the gravity-flow from those related to mass changes and especially ice volume variations. This analysis of surface movements allows us to see if the same general dynamics can be pointed out at the system-scale or if dynamics are heterogeneous within them. In this way, the drivers of dynamics are investigated. In addition to field observations and analysis of historical sources, *differential GPS* (dGPS) monitoring, *archival aerial photogrammetry* and secondarily *Light detection and ranging* (Lidar) and ERT monitoring are used to reach these objectives.

3. What control their genesis and evolution? Results on the current internal structure and on

the dynamics occurring in SDCGSAPE finally allow us to consider their genesis and evolution. From sites specificities to general models of evolution, these synthesis reflexions question the **main controls and stages of evolution of SDCGSAPE in time**. It allows highlighting the possible specificities of these systems in comparison with the other glacier systems as climatic barometers and components of alpine hydrosystems and sediment transfer systems. A special focus is put on the evolution of these systems in the extremely negative mass balance periods, as the current one, to evaluate how these systems confined in permafrost environments pass from glacial to periglacial, paraglacial or azonal dynamics. These more global reflections based on our set of results are discussed and completed with the existing literature.

The three scientific articles produced during this thesis (part 2) present some answers to these large research questions. The first article (2.1) investigates the current ground ice distribution, glacial and geomorphic dynamics and their respective evolution since LIA in two neighbouring SDCGSAPE. The second article (2.2) details the composition of three SDCGSAPE and the distinct responses of their components to short-term (annual to seasonal) climatic variations. The third article (2.3) studies the current geometry of a small heavily debris-covered glacier located in Alpine permafrost environments and analyses its decadal evolution, especially in comparison with local larger glaciers. Detailed scope, content and outcomes of each article are presented before them in the part 2. These articles were produced in distinct research contexts (contribution to special issue for article 1, collaboration with other researchers or research team for article 1 and 3, etc.) and do not present all the results collected for this thesis. The compilation of all the results obtained (part 3) completes thereby these publications and precedes the general discussion part (part 4), where detailed responses to the three main research questions are proposed.

2. Publications



D | Ice cave and debris-covered glacier terminus in the Rognes system (© S. Utz, Aug. 2012)

2.1. Paper 1:

The influence of ground ice distribution on geomorphic dynamics since the Little Ice Age in proglacial areas of two cirque glacier systems

Earth Surface Processes and Landforms, 2015

EARTH SURFACE PROCESSES AND LANDFORMS
Earth Surf. Process. Landforms 40, 666–680 (2015)
 Copyright © 2014 John Wiley & Sons, Ltd.
 Published online 24 November 2014 in Wiley Online Library
 (wileyonlinelibrary.com) DOI: 10.1002/esp.3666

The influence of ground ice distribution on geomorphic dynamics since the Little Ice Age in proglacial areas of two cirque glacier systems

Jean-Baptiste Bosson,^{1*} Philip Deline,² Xavier Bodin,² Philippe Schoeneich,³ Ludovic Baron,⁴ Marie Gardent² and Christophe Lambiel¹

¹ Institut des dynamiques de la surface terrestre, Université de Lausanne, Lausanne, Switzerland

² Laboratoire EDYTEM, Université de Savoie, CNRS, Le Bourget-du-Lac, France

³ Institut de Géographie Alpine, PACTE/Territoire, Université Joseph Fourier, Grenoble, France

⁴ Institut des sciences de la Terre, Université de Lausanne, Lausanne, Switzerland

Received 15 August 2013; Revised 13 October 2014; Accepted 14 October 2014

*Correspondence to: Jean-Baptiste Bosson, Institut des dynamiques de la surface terrestre, Université de Lausanne, Lausanne, Switzerland.
 E-mail: jean-baptiste.bosson@unil.ch

ESPL
 Earth Surface Processes and Landforms

ABSTRACT: Holocene glaciers have contributed to an abundance of unstable sediments in mountainous environments. In permafrost environments, these sediments can contain ground ice and are subject to rapid geomorphic activity and evolution under condition of a warming climate. To understand the influence of ground ice distribution on this activity since the Little Ice Age (LIA), we have investigated the Pierre Ronde and Rognes proglacial areas, two cirque glacier systems located in the periglacial belt of the Mont Blanc massif. For the first time, electrical resistivity tomography, temperature data loggers and differential global positioning systems (dGPS) are combined with historical documents and glaciological data analysis to produce a complete study of evolution in time and space of these small landsystems since the LIA. This approach allows to explain spatial heterogeneity of current internal structure and dynamics. The studied sites are a complex assemblage of debris-covered glacier, ice-rich frozen debris and unfrozen debris. Ground ice distribution is related to former glacier thermal regime, isolating effect of debris cover, water supply to specific zones, and topography. In relation with this internal structure, present dynamics are dominated by rapid ice melt in the debris-covered upper slopes, slow creep processes in marginal glacial rock glaciers, and weak, superficial reworking in deglaciated moraines. Since the LIA, geomorphic activity is mainly spatially restricted within the proglacial areas. Sediment exportation has occurred in a limited part of the former Rognes Glacier and through water pocket outburst flood and debris flows in Pierre Ronde. Both sites contributed little sediment supply to the downslope geomorphic system, rather by episodic events than by constant supply. In that way, during Holocene and even in a paraglacial context as the recent deglaciation, proglacial areas of cirque glaciers act mostly as sediment sinks, when active geomorphic processes are unable to evacuate sediment downslope, especially because of the slope angle weakness. Copyright © 2014 John Wiley & Sons, Ltd.

KEYWORDS: proglacial area; permafrost; glacier–permafrost interaction; debris-covered glacier; ground ice; sediment transfer system

Introduction

Glacier shrinkage, initiated at the end of the Little Ice Age (LIA: AD 1300–1850/60 in the Alps; Ivy-Ochs *et al.*, 2009) and accelerated since the mid 1980s, has led to the rapid growth of many proglacial areas worldwide (Vaughan *et al.*, 2013). These recently deglaciated areas are incredibly dynamic and rapidly changing as a result of intensive paraglacial readjustment and high sediment flux (Ballantyne, 2002; Meigs *et al.*, 2006; Otto *et al.*, 2009; Carrivick *et al.*, 2013). Proglacial areas have a key role in the sediment cascade systems in mountainous environments (Geilhausen *et al.*, 2012). As a function of their ability to transfer sediment load downslope, they can act 'either as a sink or as a source of sediment' (Owens and Slaymaker, 2004, p. 15).

In high relief and permafrost environments, proglacial areas may have one or both of two characteristics in relation with

sediment flux. First, there may be thick moraine accumulations. Repeated Holocene fluctuations of heavily debris-covered glaciers can result in the formation of moraine ramparts (also called dams, dumps or bastions; Shroder *et al.*, 2000; Benn *et al.*, 2003; Hambrey *et al.*, 2008). These landforms are especially common in flatter terrain dominated by high rock walls, such as cirques or valley floors inherited from the last Pleistocene glaciation, where the linkage between the glacial and the hydrological transport systems is inefficient (Benn *et al.*, 2003). Second, there may be strong glacier–permafrost interactions. As a consequence of development of polythermal glacier systems within the periglacial belt (Cuffey and Paterson, 2010) and of ice recession, massive ice, ice-cemented and ice-free sediments may coexist in proglacial areas (Reynard *et al.*, 2003; Haeberli, 2005; Kneisel and Käab, 2007; Ribolini *et al.*, 2010). As shown by examples in mountainous and polar regions, glacier

2.1.1.Presentation:

The influence of ground ice distribution on geomorphic dynamics since the Little Ice Age in proglacial areas of two cirque glacier systems

Citation

Bosson JB, Deline P, Bodin X, Schoeneich P, Baron L, Gardent M and Lambiel C (2015). The influence of ground ice distribution on geomorphic dynamics since the Little Ice Age in proglacial areas of two cirque glacier systems. *Earth Surface Processes and Landforms* 40, 666-680. Doi: 10.1002/esp.3666

Scope and research questions

- Proglacial areas are considered among the most active geomorphic systems in the current climate change context. *Is that also true in small debris covered glacier systems located in alpine permafrost environments (SDCGSAPE)? What are the main processes involved?* Proglacial areas can act as sediment sinks or sources in geomorphic systems. *Which one of these two roles dominates in SDCGSAPE and why?*
- In comparison with other glacier systems, ground ice can be preserved in distal sediment accumulations of SDCGSAPE. *What control this preservation and what is its influence on glacier and sediment fluxes? Does the occurrence of ground ice generate a continuum between glacial and periglacial morphodynamics?*
- Climate changes affect strongly glacier systems. *What are the main responses of SDCGSAPE since the LIA?*

Approach and content

The distribution of ground ice and its influence on geomorphic dynamics since the LIA is investigated in two neighbouring SDCGSAPE located in the Mont-Blanc massif. The current composition and dynamic of these systems is mainly assessed with field observations and measurements (Electrical resistivity tomography, ground surface temperature and dGPS monitoring). Both glaciological and geomorphic evolution since the LIA, leading to the present situation, are discussed by comparing field results, historical documents, glaciological data on the neighbouring Tête Rousse glacier and examples found in the scientific literature.

Main outcomes

- The investigation of very small neighbouring sites in an area relatively well documented since the LIA allowed a **comprehensive analysis in time and space**.
- The field results highlight **coherent and marked spatial contrasts between relatively homogeneous zones**. Debris-covered glaciers, marginal ice-debris mixtures and ice-free debris compose these systems. The spatial distribution of these components seems mainly related to the glacier thermal regime, water circulations, differential ablation in the glacier due to the debris-cover influence and the deformation of former frozen sediments.
- *SDCGSAPE* and associated proglacial areas are **active geomorphic systems**. Their dynamics are mainly related to the presence of ground ice. Ice melt, ice and ice-debris mixtures deformation, postglacial superficial mass wasting are the main occurring processes. Their magnitude does not exceed decimeters to few meters per year. The debris are mostly supplied by rockfalls but debris flows can also deposit sediments. These systems are mainly **sediment sinks**. This is especially due to the gentle bedrock topography, the weak magnitude of sediment transfer processes and the distal damming of the systems by large and sometimes frozen sediment accumulations. However, as in Pierre Ronde, *SDCGSAPE* can act as **sedimentary sources during extreme hydrological events** (water pocket outburst flood, debris flows).
- The **debris volume was estimated** in each system. The amount accumulated depends especially on the coverage or not of the backwalls by ice during the cold periods of the Holocene. Hence, half of the debris amount estimated at Pierre Ronde ($2.6 \times 10^6 \text{ m}^3$) seems accumulated in the Rognes system ($1.3 \times 10^6 \text{ m}^3$), where the backwalls were temporarily covered by ice during the Holocene.
- The **two glaciers have strongly changed since the LIA**. They become remnant debris-covered ice masses that have a talus slope appearance in the upper zone. Downwasting dynamic is dominating. In the distal zone of the Rognes, buried glacier ice is connected to the distal flowing ice-debris mixture, illustrating the **morphological and dynamical continuum that exists in SDCGSAPE between debris-covered glaciers and rock glaciers**.

Personal contribution

I designed this research with my supervisor C. Lambiel. We also collaborated with P. Deline and M. Gardent who were interested in the Pierre Ronde area for the *GlaRiskAlp* project. I organised and conducted field investigations and gathered additional data. I made data analysis, prepared figures and wrote the manuscript, which was noticeably improved by the constructive comments and corrections of the co-authors.

2.1.2.Content:

The influence of ground ice distribution on geomorphic dynamics since the Little Ice Age in proglacial areas of two cirque glacier systems**Jean-Baptiste Bosson¹, Philip Deline², Xavier Bodin², Philippe Schoeneich³, Ludovic Baron⁴, Marie Gardent² and Christophe Lambiel¹**¹ Institut des dynamiques de la surface terrestre - Université de Lausanne, LAUSANNE, SWITZERLAND ;² Laboratoire EDYTEM, Université de Savoie, CNRS, LE BOURGET-DU-LAC, FRANCE ;³ Institut de Géographie Alpine, PACTE/Territoire, Université Joseph Fourier, GRENOBLE, FRANCE ;⁴ Institut des sciences de la Terre - Université de Lausanne, LAUSANNE, SWITZERLAND

Abstract

Holocene glaciers have contributed to an abundance of unstable sediments in mountainous environments. In permafrost environments, these sediments can contain ground ice and are subject to rapid geomorphic activity and evolution under condition of a warming climate. To understand the influence of ground ice distribution on this activity since the Little Ice Age (LIA), we have investigated the Pierre Ronde and Rognes proglacial areas, two cirque glacier systems located in the periglacial belt of the Mont Blanc massif. For the first time, electrical resistivity tomography, temperature data loggers and DGPS are combined with historical documents and glaciological data analysis to produce a complete study of evolution in time and space of these small landsystems since LIA. This approach allows to explain spatial heterogeneity of current internal structure and dynamics. The studied sites are a complex assemblage of debris-covered glacier, ice-rich frozen debris and unfrozen debris. Ground ice distribution is related to former glacier thermal regime, isolating effect of debris cover, water supply to specific zones, and topography. In relation with this internal structure, present dynamics are dominated by rapid ice melt in the debris-covered upper slopes, slow creep processes in marginal glacial rock glaciers, and weak, superficial reworking in deglaciated moraines. Since LIA, geomorphic activity is mainly spatially restricted within the proglacial areas. Sediment exportation has occurred in a limited part of the former Rognes Glacier and through water pocket outburst flood and debris flows in Pierre Ronde. Both sites contributed little sediment supply to the downslope geomorphic system, rather by episodic events than by constant supply. In that way, during Holocene and even in a paraglacial context as the recent deglaciation, proglacial areas of cirque glaciers act mostly as sediment sinks, when active geomorphic processes are unable to evacuate sediment downslope, especially because of the slope angle weakness.

Keywords

Proglacial area, permafrost, glacier-permafrost interaction, debris-covered glacier, ground ice, sediment transfer system

2.1.2.1. Introduction

Glacier shrinkage, initiated at the end of the Little Ice Age (LIA: 1300-1850/60 AD in the Alps; [Ivy Ochs et al., 2009](#)) and accelerated since the mid 1980s, has led to the rapid growth of many proglacial areas worldwide ([Vaughan et al., 2013](#)). These recently deglaciated areas are incredibly dynamic and rapidly changing as a result of intensive paraglacial readjustment and high sediment flux ([Ballantyne, 2002](#); [Meigs et al., 2006](#); [Otto et al., 2009](#); [Carrivick et al., 2013](#)). Proglacial areas have a key role in the sediment cascade systems in mountainous environments ([Geilhausen et al., 2012](#)). As a function of their ability to transfer sediment load downslope, they can act “either as a sink or as a source of sediment” ([Owens and Slaymaker, 2004](#): p15).

In high relief and permafrost environments, proglacial areas may have one or both of two characteristics in relation with sediment flux. First, there may be thick moraine accumulations. Repeated Holocene fluctuations of heavily debris-covered glaciers can result in the formation of moraine ramparts (also called *dams*, *dumps* or *bastions*: [Shroder et al., 2000](#); [Benn et al., 2003](#); [Hambrey et al., 2008](#)). These landforms are especially common in flatter terrain dominated by high rock walls, such as cirques or valley floors inherited from the last Pleistocene glaciation, where the linkage between the glacial and the hydrological transport systems is inefficient ([Benn et al., 2003](#)). Second, there may be strong glacier-permafrost interactions. As a consequence of development of polythermal glacier systems within the periglacial belt ([Cuffey and Paterson, 2010](#)) and of ice recession, massive ice, ice-cemented and ice-free sediments may coexist in proglacial areas ([Reynard et al., 2003](#); [Haeberli, 2005](#); [Kneisel and Käab, 2007](#); [Ribolini et al., 2010](#)). As shown by examples in mountainous and polar regions, glacier oscillations in permafrost environments may form complex marginal sediment accumulations that contain ice, such as rock glaciers, push moraines, and ice cored moraines ([Brazier et al., 1998](#); [Owen and England, 1998](#); [Serrano and López-Martí nez, 2000](#); [Kraimer and Mostler, 2006](#); [Lilleøren et al., 2013](#)). The distribution of ground ice in these environments appears to be ambivalent in relation to sediment flux ([Gomez et al., 2003](#); [Etzelmüller and Hagen, 2005](#); [Käab et al., 2005](#); [Chiarle et al., 2007](#); [Huggel et al., 2011](#)). It can both increase flux, by encouraging the sliding, deformation and/or melting of the frozen zone, and by acting as an aquiclude layer or a sliding plane; but also limit, by sediment cementation, the transfer process.

In addition to the difficulties of field investigations in high mountain environments, the development of appropriate methods to study the internal structure (e.g. boreholes, geophysical prospecting) and surface dynamics (e.g. differential Global Positioning System (dGPS), photogrammetry, terrestrial laser scanning) of proglacial areas is only quite recent. Although research in this area has developed rapidly over the last fifteen years (see e.g. [Kneisel, 1999](#); [Delaloye, 2004](#)), knowledge remains sparse. Existing studies have mainly focused on the current distribution of ground ice and/or geomorphic activity. Detailed analyses of post-LIA evolution are few, and characterisation of the internal structure, using geophysics or boreholes, has been restricted to small parts of former glacier systems. Deglaciation and its influence on current ground ice distribution, ice/sediment

volumes, active geomorphic processes, and sediment flux rates are topics that are still largely unknown. Complete temporal and spatial geomorphic analysis of proglacial areas in mountainous permafrost environments remains a challenging task. Such complete study would also allow identifying the specificities of these complex landforms in sediment transfer systems in comparison with other proglacial areas.

This paper aims to quantify for two small neighbouring Alpine sites in the periglacial belt of the Mont Blanc massif how the ground ice that remains following deglaciation has impacted upon geomorphic processes since the LIA. Our study combines several methods for internal structural characterisation (electrical resistivity tomography, ground surface temperature measurements) and surface evolution analysis over various time scales (dGPS survey, geomorphological mapping, historical documentation).

2.1.2.2. Study sites

The Rognes and Pierre Ronde areas ($45^{\circ}51'38''\text{N}$, $6^{\circ}48'40''\text{E}$; 2600-3100 m a.s.l.) are two cirque glacier systems located north of the Bionnassay Glacier basin, in the French part of the Mont Blanc massif (Fig. 2.1 & 2.2). The lithology comprises micaschists and mylonitised gneiss of the Mont-Blanc external units (Mennessier *et al.*, 1976). Intense rockfalls affect the surrounding rockwalls,

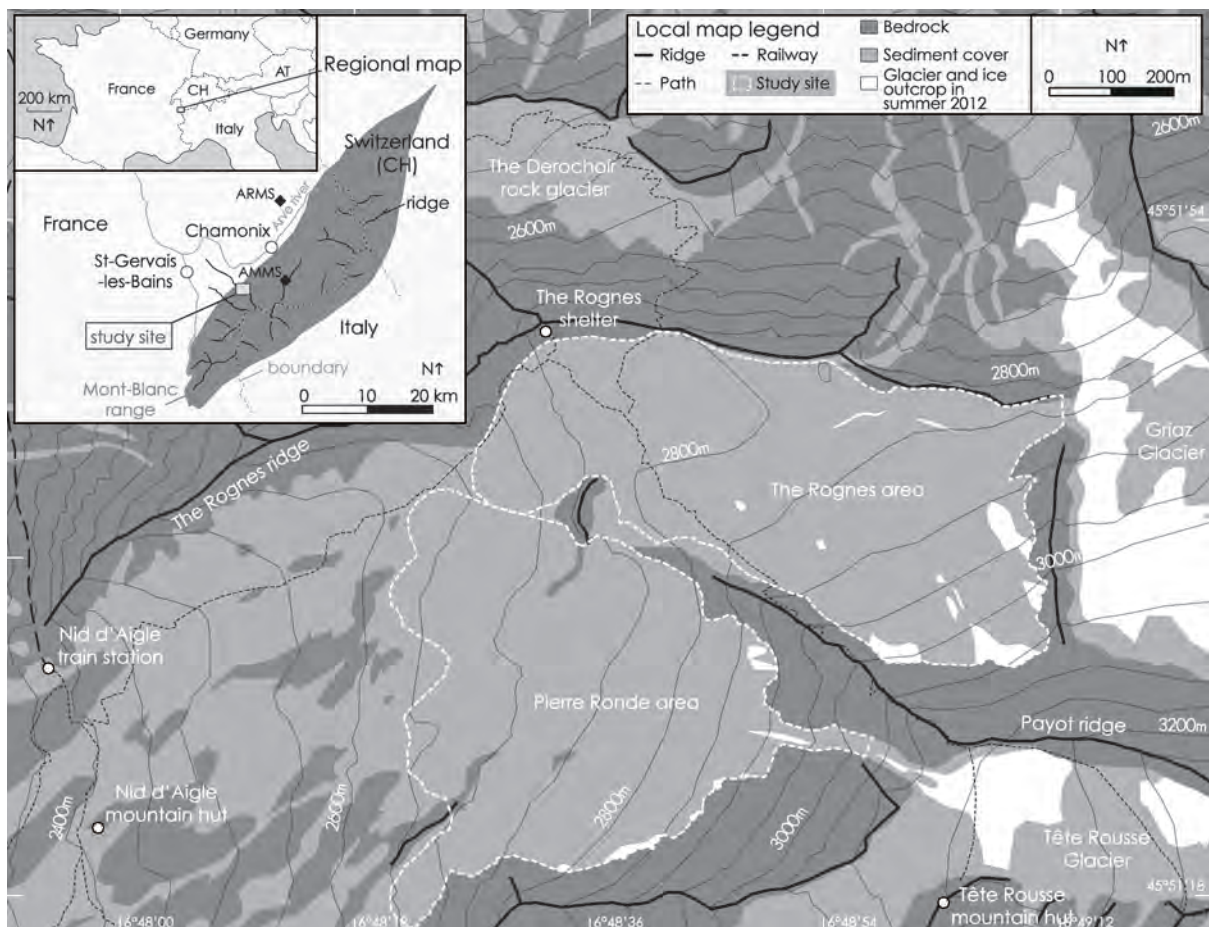


Fig. 2.1. Location and topography of the Rognes and Pierre Ronde areas. AMMS and ARMS: Aiguille du Midi and Aiguilles Rouges weather stations.

explaining the frequent extended debris cover on local glaciers (Deline, 2005). The NW part of the Mont Blanc massif acts as a topographic barrier for the dominant westerly humid air masses. This partly explains why the local glaciers have experienced slower recession than others in the French Alps (Gardent *et al.*, 2014). Because of this humidity, Holocene glacial morphodynamics prevails in the massif, and periglacial landforms such as rock glaciers are relatively uncommon (Bosson, 2012). Extrapolated from Krysiecki *et al.* (in prep.) and Gilbert *et al.* (2012), the current mean annual air temperature (MAAT) at the Rognes shelter (2768 m a.s.l., Fig. 2.1 & 2.2) is - 0.9°C and the average annual precipitation is c. 2000 mm. Since the 1990s, the local mean glacier equilibrium-line altitude (ELA) has fluctuated around 3200 m a.s.l. (Gilbert *et al.*, 2012), c. 100 m above the studied sites. The local lower limit of the periglacial belt is close to 2450 m a.s.l. as indicated by the nearby active Dérochoir rock glacier (Krysiecki *et al.*, in prep.).

Whereas many glaciological data exist for the local glaciers (e.g. Bossons, Tête Rousse, Taconnaz), the Pierre Ronde and Rognes areas have never been studied. Historical documents, such as post-1860s maps, give imprecise and contradictory information on glacier extents at these sites. Today, the Rognes and Pierre Ronde are two small vanishing debris-covered cirque glaciers. They dominate a sediment area bounded downstream by a steep 25- to 40-m-high talus. The steepness of the foreslope and the absence of a noticeable vegetation cover suggest recent glacier recessions and active post-glacial dynamics.

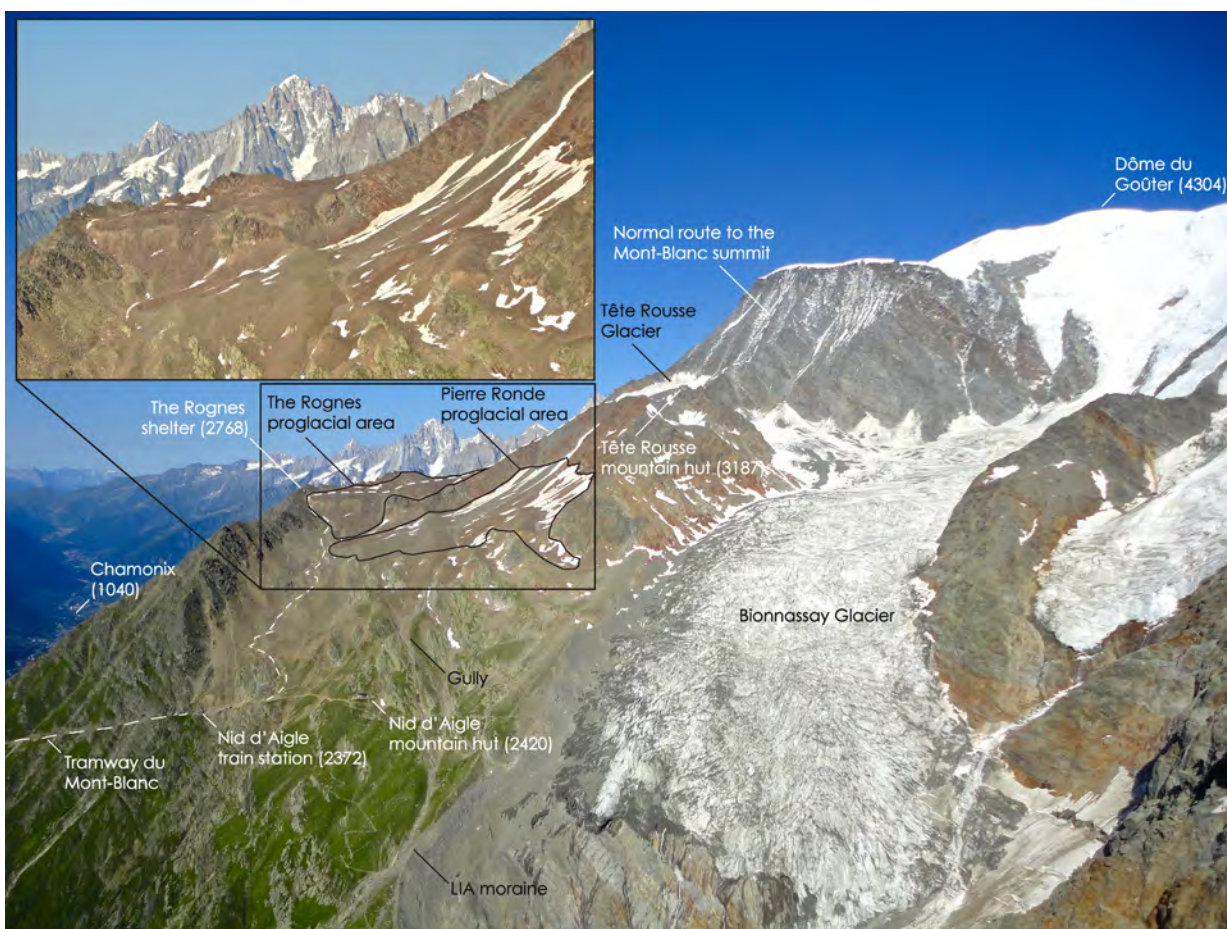


Fig. 2.2. Upper Bionnassay Glacier basin seen from the Tricot ridge (photo D. Bonneaux, July 2012)

The Rognes system (0.29 km², 2650–3100 m a.s.l.) lies in a small cirque floor oriented N-NW, that appears filled by sediments (Fig. 2.2 & 2.3). A debris-covered slope with few ice outcrops dominates a depressed area with marginal, rounded sediment ridges. The glacier front is hidden, except on the north side, where a 0.5–1-m-high vertical rim and an ice cave expose glacier limits (Fig. 2.3c). During the LIA, the north branch of the Rognes Glacier was connected to the Griez Glacier and flowed into the Chamonix valley, whereas the main NW branch is located in the Bionnassay basin.

The Pierre Ronde system (0.28 km², 2600–3000 m a.s.l.) occupies a small NW-facing cirque floor below the Tête Rousse trough (Fig. 2.1 & 2.3). A talus slope with some ice outcrops overlooks a depression in which the limits of the glacier are invisible. Gullies and fresh deposits illustrate debris flow activity in the last few years; the last major event mobilized c. 10,000 m³ of sediments in September 2009 (B. Demolis, Service Restauration des terrains en montagne de Haute-Savoie, personal communication). In the distal part, the smoothed fine sediments on the west contrast with the coarse accumulation with ridges and furrows on the north. The Pierre Ronde Glacier was connected to the Tête Rousse Glacier by an ice couloir during the LIA. In 1892, a major water-pocket outburst flood (WPOF) occurred; 200,000 m³ of water and ice hurtled down this couloir and travelled across Pierre Ronde, where a part of the till cover was mobilized. The debris flow of 800,000 m³ covered a distance of 14 km and devastated the village of Saint-Gervais-les-Bains, causing 175 fatalities (Vincent *et al.*, 2010). Because of the development of cold ice at the base of Tête Rousse Glacier snout since 1980s, a new subglacial lake has formed (Gilbert *et al.*, 2012; Vincent *et al.*, 2012). To prevent further WPOFs, water has been pumped each summer since 2010. As well, the important amount of unconsolidated sediment in Pierre Ronde could be mobilized with a new WPOF.

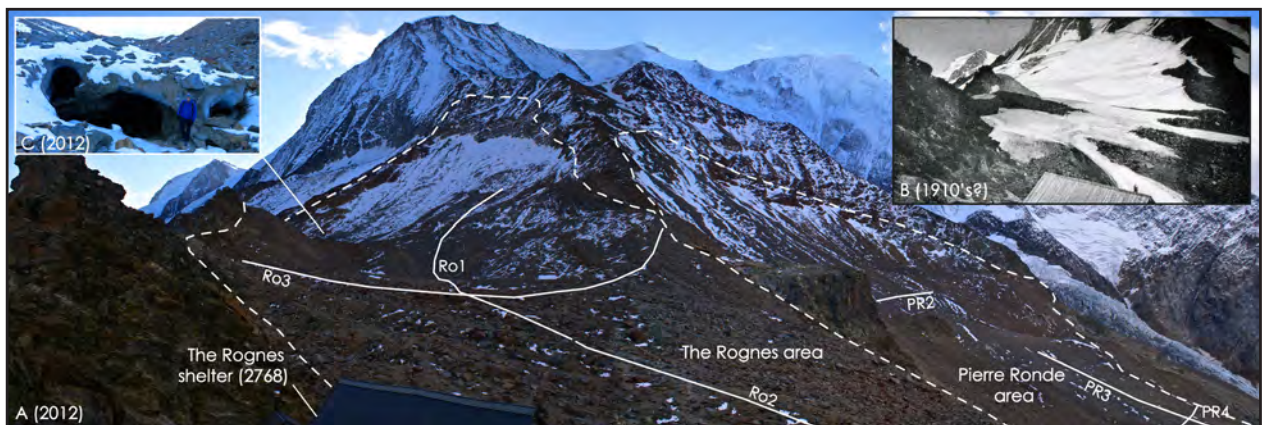


Fig. 2.3. View of the upper area of Rognes taken from the same location on October 2012 (A, photo S. Utz) and probably in the 1910s (B, CNM collection). Dotted lines: studied area limits; solid lines: ERT profiles. C: ice cave in the N distal part of Rognes area (location on Fig. 2.8).

2.1.2.3. Methods

Field data were collected in 2011 and 2012 to detect the current distribution of ground ice and to understand its origin and influence on geomorphic dynamics.

Geoelectrical survey

Because of the contrast between ice (resistive) and water (conductive, Fig. 2.4), electrical resistivity tomography (ERT) is a commonly used method in permafrost and ground ice investigation (e.g. Hambrey *et al.*, 2008; Hauck and Kneisel, 2008; Ribolini *et al.*, 2010; Scapozza, 2012). Apparent resistivity is measured along transects between n pairs of electrodes installed at the ground surface. A plausible image of the specific resistivity of subsurface layers is modelled through an inversion process and repeated iterations.

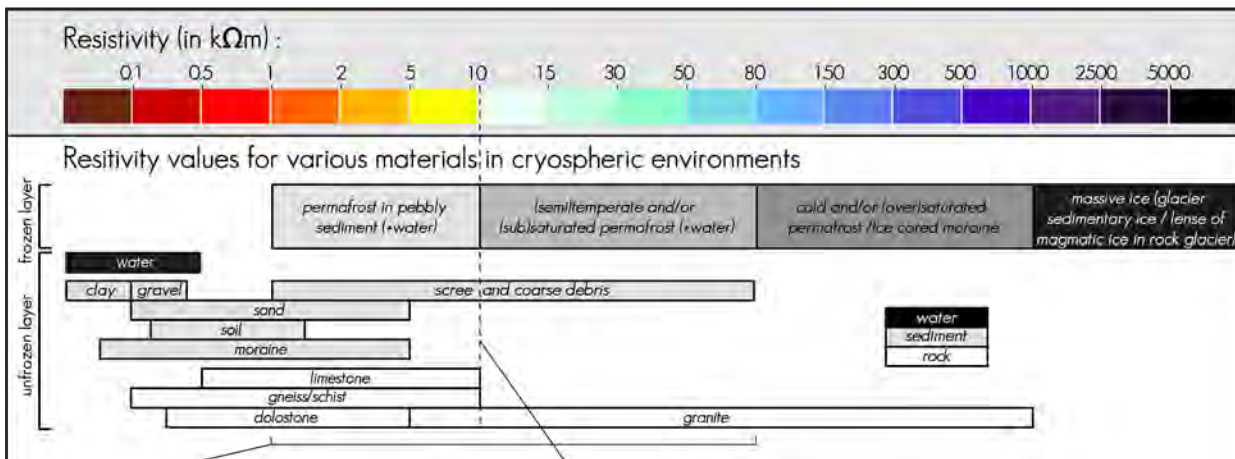


Fig. 2.4. Resistivity scale used in this study and typical values of various materials. Adapted from Hauck and Kneisel (2008) and Scapozza (2012).

In Summer 2012, 5 m inter-electrode spacing ERT profiles were measured at Rognes and Pierre Ronde, leading to two 24e (i.e. electrodes), three 48e, one 60e and one 120e profiles (Fig. 2.3 & 2.5). Apparent resistivities were measured with a Syscal Pro Switch 96 with a Wenner-Schlumberger configuration, the latter being chosen because it represents a good compromise between horizontal resolution and depth of investigation. We improved the electrodes-sediments contact with salt-water saturated sponges. Results were treated with Prosys II (Iris Instruments), taking into account the surface topography measured with dGPS. The inversion was processed with Res2DInv, based on least-squares inversion and robust parameters (which allow a good visualisation of high resistivity contrasts) with the following parameters: initial damping factor = 0.15; minimum damping factor = 0.02; vertical to horizontal flatness filter ratio = 1; (robust) cutoff factor for data constrain = 0.05; (robust) cutoff factor for model constrain = 0.005. Final tomograms express the plausible ground resistivities with absolute error corresponding to the difference in % between inverted model and measured data. To evaluate the reliability of the inverted model and distinguish regions that are well constrained by measured data to those that could correspond to inversion artefacts, we produced a model resolution matrix analysis (see details in Stummer *et al.*, 2004; Hilbich *et al.*, 2009). The model resolution matrix value (MRMV) compares modelled values with measured values: the better modelled and measured values fit, the closer to 1 the MRMV. MRMV is a function of ground conductivity, and decreases rapidly with depth and in highly resistive zones (Fig. 2.5; Hilbich *et al.*, 2009). We have displayed the thresholds of 0.05 and 0.005 MRMV in our tomograms and considered regions with $\text{MRMV} > 0.05$ as reliable, regions with $\text{MRMV} > 0.005$ as moderately to weakly reliable, and regions with $\text{MRMV} < 0.005$ as only very weakly reliable.

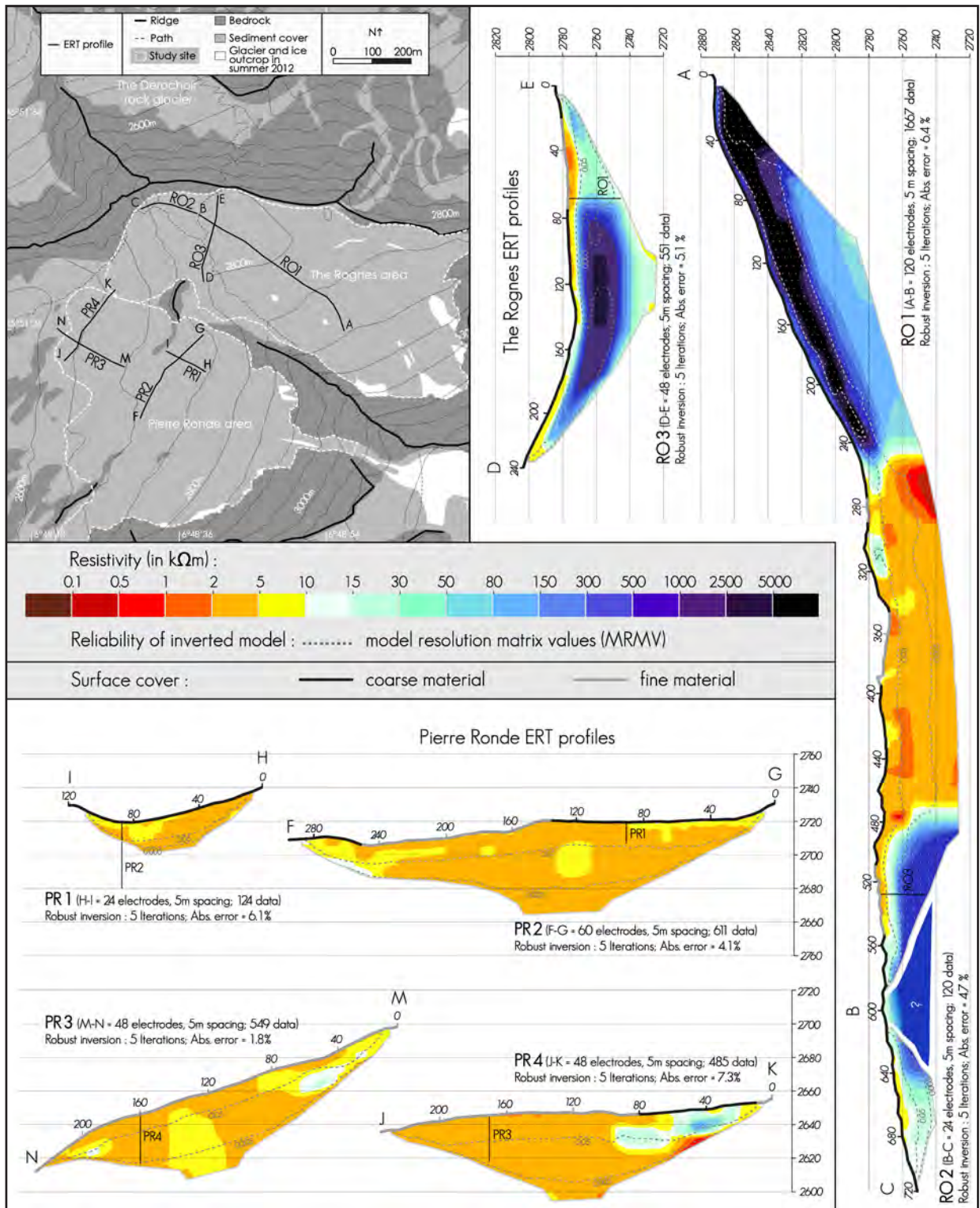


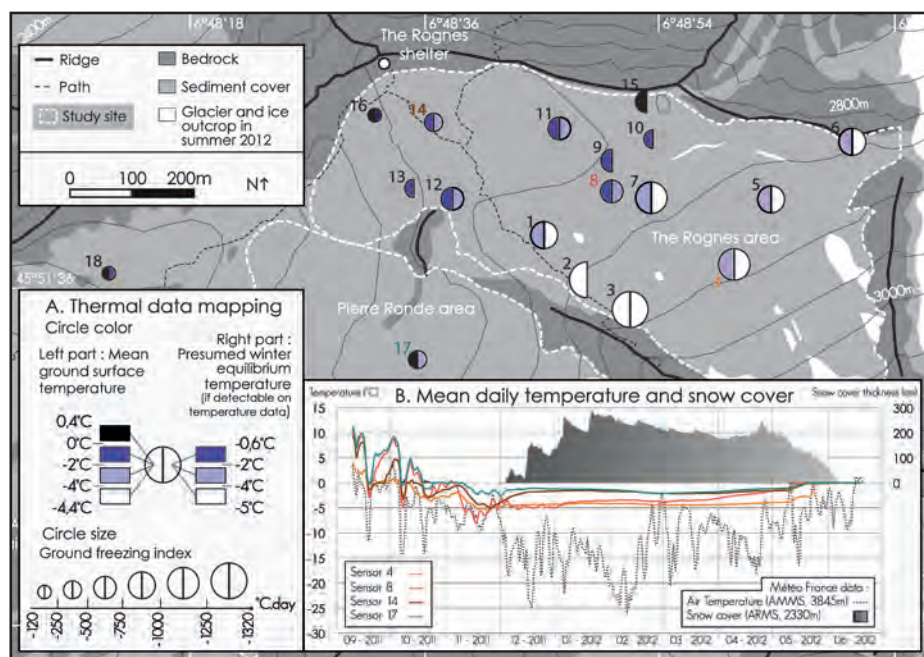
Fig. 2.5. Transversal and longitudinal electrical resistivity tomograms obtained in Rognes and Pierre Ronde areas on 28th and 29th August 2012

Ground surface temperature (GST) measurements

In order to obtain quantitative indicators of the thermal state of the ground surface and of the possible presence of ground ice close to the surface, a network of 18 miniature temperature sensors (IButton DS1922L, accuracy of 0.065°C) was set up at the near ground surface, shielded from

direct solar radiation (see Fig. 2.6 for location). Temperature was sampled at a 2 hour frequency for all sensors between the 10th September 2011 and the 20th June 2012. Mean ground surface temperature (MGST) for the measurement period, ground freezing index (GFI, i.e. sum of negative mean daily temperatures) and winter equilibrium temperature (WEqT; Delaloye, 2004) were calculated. As ground surface is an interface layer, influenced by the ground and the atmosphere, these climatic parameters (calculated for the nine coldest months of a year in this study) give interesting and complementary information on the ground thermal state and on the possible occurrence of ice near the surface. Negative MGST values may indicate an influence of cold ground thermal regime (related to ice occurrence and/or cold air trapping in the interstices) and/or cold topoclimatic conditions. In this way, ground ice is more likely to exist and to persist under the coldest negative GST means. GFI estimates the “amount of cold” stored in the ground during the frozen days. Finally, WEqT is reached when a significant snow cover isolates the ground from atmospheric influence and temperature tends to an equilibrium controlled by the heat transfer from the upper ground layers. Cold WEqT values (some degree below 0°C) possibly indicate an influence of ground ice or permafrost conditions in the ground.

Fig. 2.6. A: Mean Ground Surface Temperature, presumed Winter Equilibrium Temperature, and Ground Freezing Index obtained at 18 locations with ground surface temperature measurements between 10th September 2011 and 20th June 2012 at Rognes and Pierre Ronde. For sensors 2, 9, 10, 13 and 15, the important variability of winter temperatures (probably due to a thin snow cover) did not allow to determine the winter equilibrium temperature. B: Mean daily temperature of sensors 4, 8, 14, 17 and air at the Aiguille du Midi weather station, and snow cover thickness at Aiguilles Rouges weather station between 10th September 2011 and 20th June 2012 (Météo France data).



In addition, mean daily temperature curves were displayed for each sensor to characterise the ground surface thermal regime and its relation to air temperature and snow cover. We present the daily temperature curves of four sensors (three sensors along a longitudinal profile in Rognes and the sensor located in Pierre Ronde, see Fig. 2.6B) in parallel with air temperature at Aiguille du Midi weather station (AMMS in Fig. 2.1; at 3845 m a.s.l. and 6 km distant of study sites, Météo France data) and the snow cover thickness at the Aiguilles Rouges weather station (ARMS in Fig. 2.1; at 2330 m a.s.l. and 15 km distant of study sites, Météo France data).

Results from ground temperature measurements have to be considered carefully. They vary strongly in time and space and rarely allow the definitive identification of permafrost and/or ground ice

occurrence (Delaloye, 2004). They are qualitative indicators (thermal state of the ground during a specific period, possibility of permafrost and/or ground ice occurrence, local cold/warm area repartition) rather than quantitative in order to characterize the ground.

dGPS measurements

The position of 63 boulders in Rognes and 24 boulders in Pierre Ronde were measured with a *Leica SR500* in September 2011 and 2012, respectively in July and October 2012. Both vertical (V_m) and horizontal (H_m) movements were computed, with a precision of ± 5 cm.

Following Lambiel and Delaloye (2004), we assume that in ground ice sedimentary environments, the measured vertical component of the movement corresponds to a possible combination of 3 main processes: (1) loss in elevation consecutive to the downslope movement along inclined bed, which depends directly on the horizontal component and the slope angle; (2) change in elevation relative to extending and compressing flow; and (3) change in elevation relative to variation of ice volume (local gain or loss of ice). Compressing and extending flows are difficult to point out in our field sites and are assumed to be secondary in the time study window (3 months for Pierre Ronde, 1 year for Rognes). In this way, we calculated the difference (Δv) between the measured vertical component and the expected downslope vertical component (calculated for each point from the measured horizontal component and topographical slope obtained with a 4 m resolution DEM). Thus, we assume that Δv can be interpreted as a marker of ice volume variation.

Geomorphological analysis

Finally, a critical and comparative analysis of field measurement results, field observations and historical documents (Tab. 2.1 and Fig. 2.3B) was used to provide a global insight on current internal structure and geomorphic dynamics and their evolution since the LIA.

To go beyond the controversy over rock glacier origins, and because high altitude cryospheric landforms can generally be thought as a complex continuum where massive and interstitial ice can coexist, we grouped glacial and periglacial landforms together in our map legend. We term rock glacier a complex, deformed, sediment accumulation with ground ice, steep front with fine material, and ridges and furrows in coarse sediment surface like the Rognes frozen marginal zone or the upper south side of Pierre Ronde. Types of rock glaciers have been discerned according to sediment origin (debris vs. talus rock glacier; Barsch, 1996).

Based on the literature, field observations (front thickness of sediment accumulation, surface topography and morphology, bedrock outcrops) and ERT results, sediment volume was approximated. The sediment/ice ratio in the frozen coarse blocky zone was extrapolated from existing literature (Barsch, 1996; Burger *et al.*, 1999; Haeberli *et al.*, 2006; Hausmann *et al.*, 2007; Otto *et al.*, 2009; Scapozza, 2012) and ERT results: we used the value of 30% of sediment content for

complex landforms derived from the glacier system (debris rock glaciers) and 60% of sediment content for the almost inactive talus rock glacier of Pierre Ronde. The rough estimation of sediment volume was simply calculated with:

$$\text{For unfrozen sediment accumulation: } V_s = A \cdot T \quad (1)$$

$$\text{For frozen sediment accumulation: } V_s = A \cdot t + A \cdot (T-t) \cdot C \quad (2)$$

where V_s is the estimated sediment volume, A is the area of sediment accumulation, T is the mean estimated sediment thickness, t is the mean estimated unfrozen surface layer thickness of frozen accumulation and C the estimated sediment content in frozen accumulation.

Date	Title	Type	Author	Scale	Source
1865	Massif du Mont Blanc	Map	J.J. Mieulet	1:40 000	www.savoie-archives.fr
1876	Le Massif du Mont Blanc	Map	E. Viollet-le-Duc	1:40 000	Frey (1988)
1892 (?)	Limites de la zone affectée par la vidange de la poche d'eau du glacier de Tête Rousse	Map	P. Mougin (?)	?	-
1896	La chaîne du Mont Blanc	Map	A. Barbey, X. Imfeld and L. Kurz	1:50 000	http://imagebase.uvbu.vu.nl/cdm/ref/collection/krt/id/2837
1900's (?)	Les Rognes – Chalet Forestier	Photograph (postcard)	N. Allantaz	-	-
1910's (?)	Le glacier des Rognes (fig.4)	Photograph	Anonymous	-	Centre de la Nature Montagnarde (Sallanches) collection
1920's (?)	Chemin de fer du Mont-Blanc conduisant au Glacier de Bionnassay (2800m). N°655	Photograph (postcard)	L. Morand	-	-
1939	Massif du Mont-Blanc. Région du Sud-Ouest	Map	C. Vallot and E. de Larminat	1:50 000	-
1949	IGNF_PVA_1-0_1949-09-04_C3 630-0121_1949_F3630-3631_0044	Aerial photograph	IGN	1:23 430	http://www.geoportail.gouv.fr/accueil (click on Remonter le temps and Les prises de vues aériennes)
1951	Les Houches. St-Gervais-les Bains N°4 Nord	Map	IGN	1:10 000	-
1959	IGNF_PVA_1-0_1959-09-09_C3 530-0081_1959_FR166_0036	Aerial photograph	IGN	1:31 889	http://www.geoportail.gouv.fr/accueil (click on Remonter le temps and Les prises de vues aériennes)
1960	St-Gervais-les-Bains. Serie M 731. Feuille XXXV-31	Map	IGN	1:50 000	-
1977	St-Gervais-les-Bains. Serie M 731. Feuille 31-35	Map	IGN	1:50 000	-

Tab. 2.1. Main historical documents used in this study

2.1.2.4. Results and interpretation

ERT profiles

Two sectors were investigated in Pierre Ronde (Fig. 2.3 and 2.5). In the upper area (2740-2710 m a.s.l.), a short 24e longitudinal profile (PR1: H-I) extends from the distal part of the talus slope to a small topographical hump probably related to bedrock. PR1 cuts PR2 (F-G), a 60e (a 48e profile partially overlaid with a 24e profile) transverse profile which crosses the central depression and the fresh debris flow deposits. In the lower area (2700-2610 m a.s.l.), PR3 (M-N, 48e) is a longitudinal profile in the west smooth fine sediments, whereas PR4 (J-K, 48e) is a transverse profile that crosses the whole sediment area from the coarse and wrinkled NE to the fine SW.

With resistivity mostly in the range 2-5 k Ω m (with patches of material in the range 5-10 k Ω m), conductive materials dominate all tomograms in the whole depth of investigation (up to 40 m for PR2, PR3 and PR4). The good penetration of electric current in this conductive ground is expressed by the MRMV >0.05 in the first 10 m deep. In PR2 and PR3, zones with resistivity in the range of 10-30 k Ω m are visible at 10-15 m depth. In PR4, a 60 m large and 20 m deep sector with resistivities comprised between 10 and 150 k Ω m is located under the coarse and wrinkled surface on the NE side. Except for this zone, there is no specific link between variation of ground resistivity and grain size at the surface. Intersections of PR1-PR2 and PR3-PR4 show a good correspondence between tomograms.

Three profiles were carried out in Rognes area (Fig. 2.3 and 2.5). RO1 is a 600 m longitudinal profile of 120e (A-B, superposition of four 48e profiles), which starts in the upper slope. RO2 (B-C, 24e) extends the previous profile up to few meters above the steep front. RO3 (D-E, 48e) cuts the whole distal part of Rognes area.

More contrasting electrical resistivities were measured than at Pierre Ronde. The upper slope (c. 250 m of length on RO1) displays resistivities >1000 k Ω m directly under the coarse debris cover. The thickness of this resistive zone is hard to estimate because of the weak correlation between modelled and measured values in depth (very low MRMV). Below this 20 m deep zone, the resistivity decreases to 50 k Ω m, possibly due to an inversion artefact in this poorly resolved model region. The central topographic depression consists of conductive materials (0.5-10 k Ω m on RO1) in the whole investigated thickness (c. 40 m), except for a more resistive lens (10-50 k Ω m, 10 m thick, 25 m long) located just before 320 m. In comparison with the top slope and the distal part, the better penetration of electric current in this conductive zone is expressed by the deepest location of MRMV thresholds. The distal part, visible on RO1, RO2 and RO3, shows a strong increase of resistivities in comparison with the central depression. Buried under 1 to 5 m thick conductive surface layer (<15 k Ω m), a highly resistive body roughly 100 m wide and 30 m thick appears with values in the range 15-5000 k Ω m. The weak correspondence of resistivity values at the crossing between RO1 and RO3 is probably due to inversion artefacts, expressed by very low MRMV (especially on RO1). Generally, but not systematically as shown by RO1, fine surface sediments are located above lower resistivity values.

GST measurements

Calculation of thermal indexes (*MGST*, *WEqT* and *GFI*) at 18 locations results in three main types of ground surface thermal behaviour (Fig. 2.6A & Appendix A). The first one concerns all the sensors (1 to 7) located in the Rognes upper area. It is characterized by the coldest values obtained for the three indexes: *MGST* is between -2 and -4.4°C, *WEqT* is between -4 and -5°C, and *GFI* is <-750°C.day. The second type of thermal behaviour characterizes sensors 8 to 14, located downslope in the central and distal areas of Rognes, with intermediate values: *MGST* is between 0 and -2°C, *WEqT* between -2 and -4°C, and *GFI* between -250 and -750°C.day. Finally, the third type of

behaviour is detectable for the sensors located in the Rognes marginal areas (sensors 15 and 16), in the upslope depression of Pierre Ronde (sensor 17) and in the southern side of the Rognes Ridge (sensor 18): *MGST* is positive, *WEqT* is between -0.6 and -2.1°C , and *GFI* is $>-600^{\circ}\text{C}\cdot\text{day}$. The spatial distribution of these three types of behaviour outlines different thermal characteristics in the Rognes upper slopes, the Rognes central area, and the marginal and downslope sectors. Moreover, the vicinity of sensors 7, 8, 9, 10 and 15 suggests clear spatial limits between index values instead of progressive changes. It might indicate an important control of ground ice content and depth on ground surface temperatures.

Mean daily temperatures for four sensors are displayed in parallel with air temperature and snow cover from Météo France data (Fig. 2.6B). Three different periods can be identified. First, there are daily temperature fluctuations, noticeably in the autumn, related to air temperature. The warm summer ground is freshened by cold air during this period, which can be trapped in the ground interstices. November corresponds to a frozen period for all sensors. This whole phase is attenuated for sensor 4, probably because of an early snow cover related to its elevation and slope aspect. The second period corresponds to the stabilisation of ground surface temperature in winter under snow cover. The insulation of the ground from atmosphere by the thickening of snow mantle between late November and early January (earlier than in ARMS data because the studied sites are located higher) is expressed by the slight rise in ground temperature curves (the heat transfer from the upper ground layers takes over the cold autumn air temperature influence) and its stabilisation between January and mid April. Sensors 4 and 8 have the coldest *WEqT* (around -4°C) and sensors 14 and 17 have a similar behaviour with a *WEqT* at -2.1°C . Finally, the temperature rises rapidly to 0°C for all sensors in May, in relation to the rise of air temperature and the moistening of snow cover; it occurs later for sensor 4 because of its elevation and aspect. This phase lasts during the whole melting of the snow mantle, which is not achieved in late June for all sensors. These temperature curves indicate that the ground surface experiences warmer conditions toward the distal part of Rognes. Sensor 17 at Pierre Ronde has higher values in autumn (a few days below 0°C before mid November) than in the low part of Rognes (sensor 14), but a similar *WEqT*.

dGPS measurements

Only a few small movements have been picked-up at Pierre Ronde (Fig. 2.7). 18 boulders moved less than 5 cm (i.e. the precision threshold) in all calculated fields. Displacements up to 10 cm (*Hm* and *Vm*) only affected 2 boulders in the upper area and 4 boulders in the distal one. Movements have heterogeneous directions and most of them do not correspond with the slope direction.

Movements in Rognes are significant in both vertical and horizontal components (Fig. 2.7). Δv is <-25 cm for two-thirds of the 63 points, expressing an important generalized surface lowering. Four heterogeneous kinematic behaviours affecting specific sectors can be roughly distinguished. First, the upper area (10 points in the upper slope and associated footslope) is characterized by the highest values: *Hm* >50 cm, *Vm* and Δv <-50 cm. The movement direction is well correlated

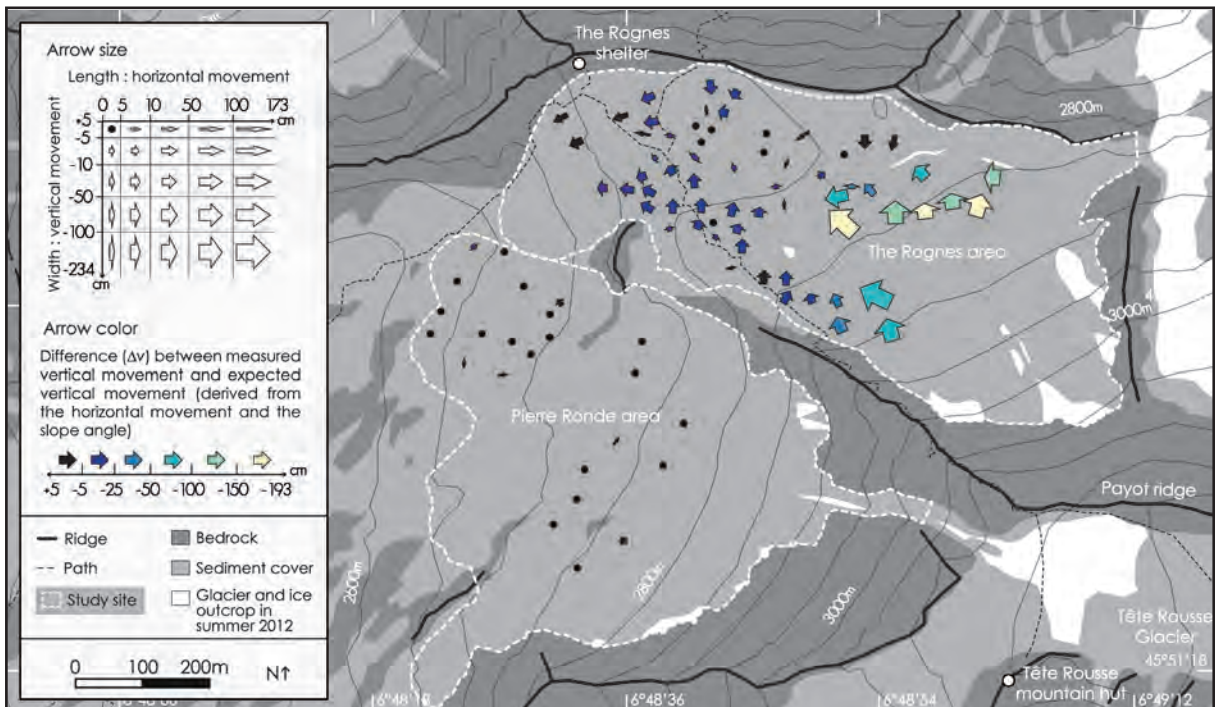


Fig. 2.7. Movements measured with DGPS in Rognes between 9th September 2011 and 28th August 2012 and in Pierre Ronde between 19th July and 3rd October 2012. The slope angle used for the Δv calculation was determined with a 4m-resolution DEM (Source: RGD 73-74).

with the slope aspect. Significant surface kinematics particularly affects the terrain near 2850 m a.s.l., with displacements (H_m , V_m , ΔV) > 1 m. Second, the SW margin up to the left area of the front (25 points) mostly displays homogeneous displacements: H_m between 10 and 50 cm, V_m between -10 and -50 cm, and Δv between -5 and -25 cm. The movement direction is to the north (direction of the central depression) for most of the boulders except for the 5 boulders of the front, which are oriented to the west (i.e. the slope aspect). Third, the N margin and the central depression (22 points) display contrasted direction and movements (H_m from 0 to 50 cm, V_m from -50 to 5 cm); 6 boulders moved < 5 cm and Δv is always > -25 cm. Finally, in the right part of the front, W-SW movements are mostly homogeneous (H_m between 10 and 50 cm, V_m between -5 and -50 cm, and Δv between +5 and -25 cm).

Interpretation of current ground ice distribution

The main landforms and the probable distribution of ground ice were mapped according to our observations and field measurements (Fig. 2.8). Those results, which are all rather coherent, outline a different situation between Pierre Ronde and Rognes, whose origin and influence on sediment transfer are examined and discussed in the following section.

In the Pierre Ronde upper depression and SW side of the distal slope, ground resistivity values are homogeneous, mostly in the range 2-10 k Ω m in the total investigated depth (Fig. 2.5: PR1, PR2, PR3 and the west side of PR4). Thermal measurements of sensor 17 reveal relatively warm conditions that appear weakly favourable to ground ice occurrence (MGST= 0.1 $^{\circ}$ C, WEqT= -2.1 $^{\circ}$ C and GFI= -289 $^{\circ}$ C.day; Fig. 2.6). In comparison with Rognes thermal data, the positive MGST and

the limited number of frozen days in autumn in the central area of Pierre Ronde (Fig. 2.6B) may be related to a lower elevation and to the westerly slope aspect. Surface kinematics is almost inactive in this area except some very weak subhorizontal movements with heterogeneous direction (Fig. 2.7). Morainic material is colonized by small pioneer plant species. It contrasts with recent debris flow deposits located in the south of this area (Fig. 2.8), which illustrate the local supply of water in the sediment store. These characteristics all express a very likely absence of ground ice in this area ($122,000 \text{ m}^2 = 44\%$ of Pierre Ronde area; Tab. 2.2 and Fig. 2.8). Although based on few field data, we can assume that three other sectors of Pierre Ronde potentially contain ground ice (Fig. 2.8). The upper slopes (one third of the total surface area; Tab. 2.2) still probably contain an important amount of glacier ice. Even if no significant movements can be attributed to ice deformation or melt-out in this area during the Summer 2012 (Fig. 2.7), our hypothesis is based on small ice outcrops and on the glacier evolution since the LIA (see below). The upper SW side probably contains a frozen sediment zone, as suggested by some ground deformation patterns and a steep front with fine material. An important volume of massive ice might be present, as in the Rognes marginal frozen zone (see later and Fig. 2.5). Finally, the NE part of the distal zone shows typical features of a slightly active talus rock glacier: resistivity of 10-150 k Ω m illustrating frozen sediments (PR4 on Fig. 2.5), few deformation patterns (Fig. 2.7), and a steep front with fine material. This area was probably not occupied by the glacier during the LIA and has probably evolved independently from glacial history in the last millennia.

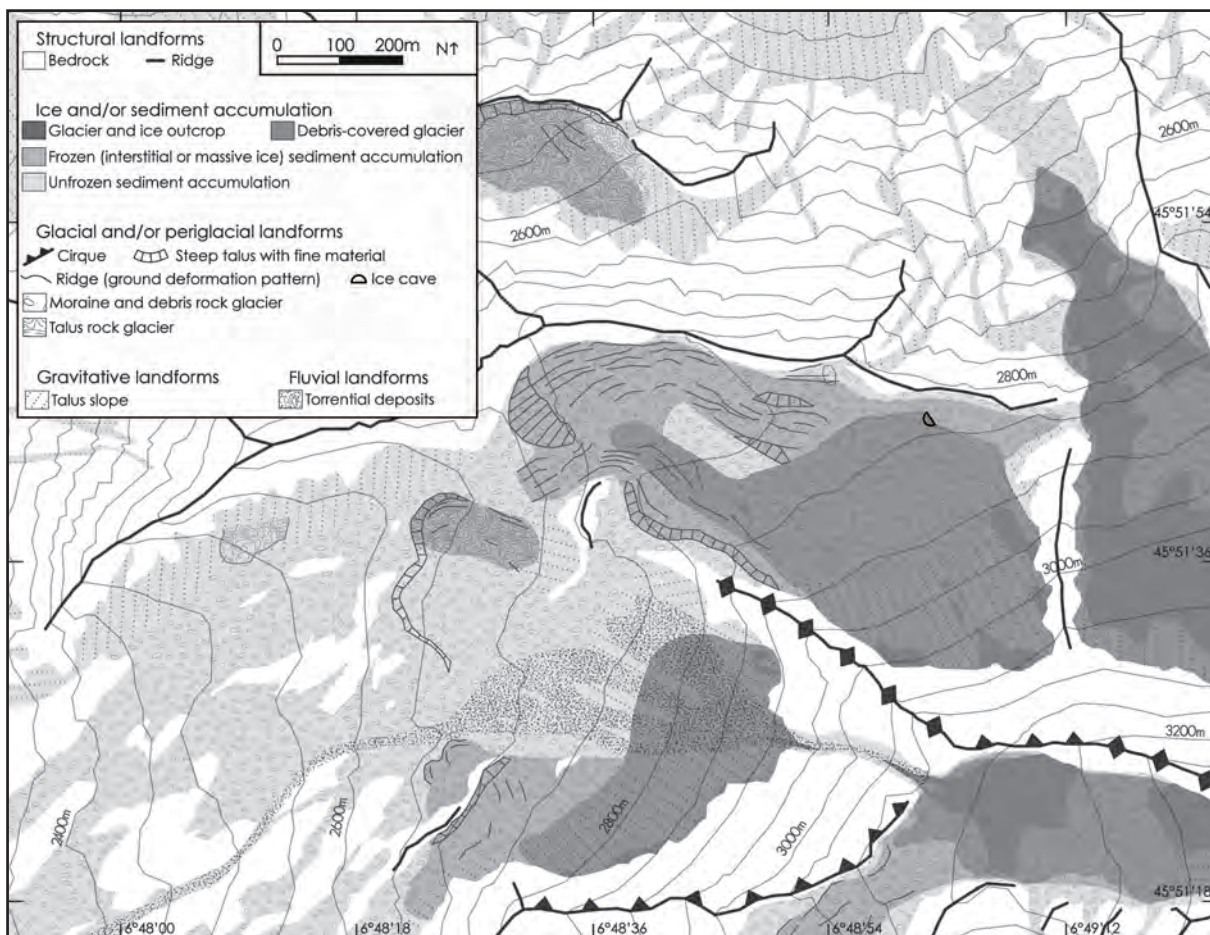


Fig. 2.8. Simplified geomorphological map of Rognes and Pierre Ronde areas and ground ice distribution inferred from field observations and measured data (ERT, GST, dGPS)

The internal structure of Rognes differs noticeably from Pierre Ronde (Fig. 2.8). Only the confined central depression ($10,000 \text{ m}^2 = 3\%$ of the area; Tab. 2.2) does not contain ground ice. The resistivity of this 200-m-long sector is mainly in the range 2-5 $\text{k}\Omega\text{m}$. Movements are limited at this smooth depressed surface partially covered by pioneer plant species (Fig. 2.7). Thus, this sector can be considered as an unfrozen moraine. The upper slopes and a narrow tongue on the left side of Rognes entirely correspond to a debris-covered glacier occupying 57% of the total area ($165,000 \text{ m}^2$; Tab. 2.2). Massive ice is visible in many locations below the coarse-grained debris mantle. ERT, GST and DGPS data agree on glacier extent (resistivity $> 1000 \text{ k}\Omega\text{m}$; $MGST < -2^\circ\text{C}$; $pWEqT < -4^\circ\text{C}$ and $GFI < -750^\circ\text{C}\cdot\text{day}$; $Hm > 50 \text{ cm}$, Vm and $\Delta v < -50 \text{ cm}$). The maximal Δv values, reaching almost -2 m in the central and top slopes, suggest a rapid melt-out of the buried massive ice. By contrast, slower movements of the narrow NW tongue (Fig. 2.7 & 2.8) could result from the insulating effect of a few meter thick debris cover, as evidenced by the conductive top layer on RO3 (Fig. 2.5). In the distal part, a frozen sediment zone surrounds the glacier and the central depression (Fig. 2.8). Its surface, mostly convex, is dominated by coarse material; the many ridges, furrows and steep slopes with fine material give a chaotic topographical aspect to the sector. Resistivities of 10-500 $\text{k}\Omega\text{m}$ suggest an ice-rich internal structure buried under a mean 3 m thick active layer. Ground surface temperatures are higher than on the glacier ($MGST > -2.3^\circ\text{C}$; $pWEqT > -4.5^\circ\text{C}$ and $GFI > -750^\circ\text{C}\cdot\text{day}$; Fig. 2.6 & Appendix A). Surface kinematics is contrasted in term of values and direction, except for the boulders located in the NW distal part where homogeneous westerly subhorizontal displacements have been pointed out (Hm in the range 10-50 cm; Fig. 2.7).

	Sector	Area (m^2)	Area (%)	Estimated mean sediment thickness (m)	Estimated mean active layer thickness on frozen body (m)	Estimated sediment content in frozen body (%)	Estimated sediment volume (m^3)	Estimated volume (%)	Sediment volume/area ratio (m^3/m^2)
The Rognes area	Glacier and debris-covered glacier	165 000	57	1	-	-	165 000	12	1
	Marginal frozen body (debris rock glacier)	115 000	40	20	3	30	931 000 (345 000+586 000)	69	8.1
	Unfrozen central depression	10 000	3	25	-	-	250 000	19	25
	Total	290 000	100				1 346 000 ($\pm 336 000$)	100	4.6
Pierre Ronde area	Glacier and debris-covered glacier	85 000	30	2	-	-	170 000	6	2
	Upslope marginal frozen body (debris rock glacier)	49 000	17	15	3	30	323 000 (147 000+176 000)	12	6.6
	Downslope marginal frozen body (talus rock glacier)	24 000	9	20	2	60	307 000 (48 000+259 000)	12	12.8
	Unfrozen central slopes	122 000	44	15	-	-	1 830 000	70	15
Total	280 000	100				2 630 000 ($\pm 657 000$)	100	9.4	

Tab. 2.2. Geometrical characteristics of sediment accumulation in Rognes and Pierre Ronde. Mean sediment thickness and active layer thickness are inferred from field and measured data (ERT, GST, dGPS). The volume is roughly estimated with Equations 1 and 2 (see Methods) and given with a global error margin of 25% for the total volume of Rognes and Pierre Ronde areas.

2.1.2.5. Discussion

Glacier and ground ice evolution since the LIA

Based on (i) the hypothesized current ground ice distribution (Fig. 2.8), (ii) the historical document analysis, and (iii) recent published data for the near Tête Rousse Glacier (cumulative mean specific

net balance in [Vincent et al., 2010](#); cold ice proportion in glacier volume in [Gilbert et al., 2012](#)), we have reconstructed the evolution of both glacier and ground ice of the Pierre Ronde and Rognes since the last LIA maximum with 30-year steps ([Fig. 2.9](#)). We describe and discuss here the main probable stages of this evolution.

First, at the LIA last maximum (locally ca. 1820s; [Vincent et al., 2010](#)), the Pierre Ronde Glacier was connected to the Tête Rousse Glacier ([Fig. 2.9a](#)). Because of the deglaciated rockwall above it, Pierre Ronde Glacier was possibly partly debris-covered ([Fig. 2.9b](#)), which could explain its absence in many historical sources. In contrast, the Rognes Glacier was most probably a bare-ice glacier connected to the Griaz Glacier. According to the many marginal deformation patterns of the NW part ([Fig. 2.8](#)), it was likely obstructed by pre-existing frozen sediments, and formed push moraines (western part of RO2 in [Fig. 2.5](#); [Fig. 2.9c](#)). These glaciotectonically-deformed patterns result generally from glacier advances in permafrost environments (e.g. [Etzelmüller and Hagen, 2005](#);

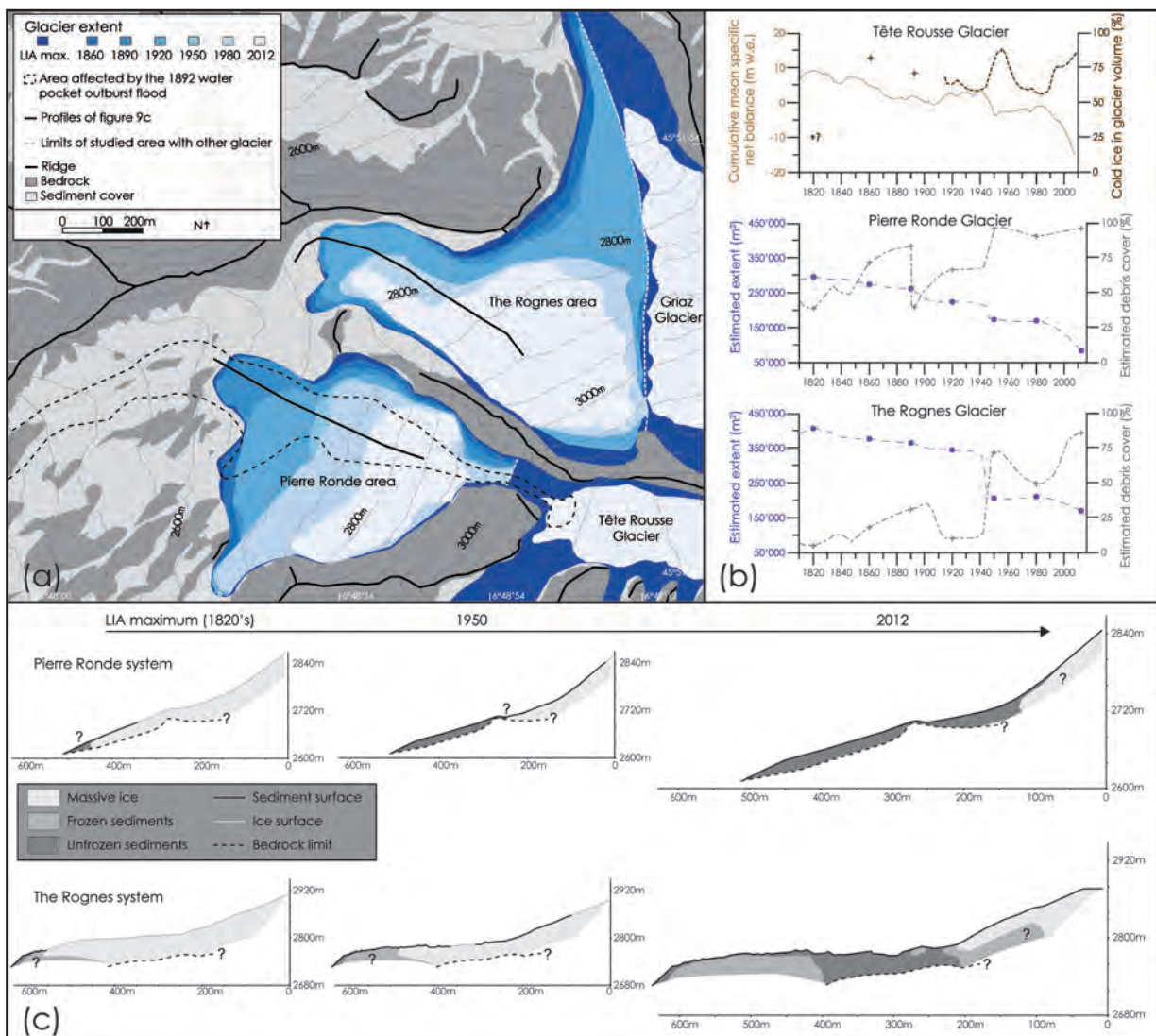


Fig. 2.9. Evolution of Rognes and Pierre Ronde Glacier systems since the LIA maximum. **(a)** Successive (30-year periods) extents of the studied glaciers. **(b)** Upper graph: recent cumulative mean specific net balance (synthesized from [Vincent et al., 2010](#)) and ratio of cold ice in glacier volume (from [Gilbert et al., 2012](#)) proposed for Tête Rousse Glacier. Combining these data with historical document analyses and proposed glacier extent in (a), we reconstructed the evolution of surface area (dots) and the ratio of debris cover (crosses) for Pierre Ronde and Rognes since 1820 (b: middle and lower graphs). Finally, **(c)** exposes longitudinal profiles of the studied areas for three different stages, following [Fig. 2.5](#), [2.9a](#) and [2.9b](#) data.

Kneisel and Kääh, 2007). The elevation and aspect of the Rognes lower area are more favourable than at Pierre Ronde for the preservation of permafrost between Holocene glacier readvances (Tab. 2.3). According to the maximal LIA extent of local glaciers, the ELA should have been around 2800 m. Therefore, without taking into account secondary ice supply by adjacent glaciers, the accumulation zone would have corresponded to the upper two-thirds of Rognes Glacier, but only to the upper one-third of Pierre Ronde Glacier (Fig. 2.9a). Hence, the ratio between accumulation and ablation areas for the Pierre Ronde Glacier was lower than for bare-ice glaciers, as is typically the case for debris-covered glaciers (Ackert, 1998; Benn *et al.*, 2003).

Second, from the late LIA to about 1890, ice volume and extent likely remained large in both glaciers, reflecting the strong influence of LIA glacio-climatic conditions. The increase of debris cover on local glaciers during this period of dominant negative mass balance (Deline, 2005) was probably reduced on Rognes Glacier as rockfall activity was low due to a rockwall still noticeably ice-covered.

Third, for the period 1890 – 1950, we can assume that the Pierre Ronde supraglacial debris cover was in part mobilized by the 1892 Tête Rousse WPOF (path in Fig. 2.9a). An impervious ice layer under supraglacial moraine facilitated their mobilization: water was maintained at the surface, saturating the debris cover and ice played the role of failure plane, as shown in recent events in the Italian Alps (Chiarle *et al.*, 2007). Thus, with the probable loss of the insulating debris cover (Fig. 2.9b) and ice warming by water, negative mass balance in the decade would have accelerated Pierre Ronde Glacier shrinkage. After a period with positive or zero mass balance (1910-1930) and almost no debris cover on the Rognes Glacier (Fig. 2.3B), significant negative mass balance in the 1940s, related to enhanced solar radiation and positive Atlantic Multidecadal Oscillation (Huss *et al.*, 2009 and 2010), led to rapid glacier wasting, as experienced by other glaciers in the Mont Blanc massif (Vincent *et al.*, 2010; Nussbaumer and Zumbühl, 2012). The thinning of ice has probably restricted Pierre Ronde Glacier in the upper depression (Fig. 2.9c), whereas Rognes Glacier separated from the Griez Glacier and became confined in its cirque. Like many glaciers unable to evacuate sediment load (Shroder *et al.*, 2000), both glaciers became mostly debris-covered. For this kind of glacier, the ablation gradient (i.e. the increase of melt rate toward glacier terminus in relation with rising of air temperature) can be inverted by an improved insulation of ice under a thickening debris layer in the distal area (Benn *et al.*, 2003; Hambrey *et al.*, 2008; Kellerer-Pirklbauer *et al.*, 2008). Maximal melt rate is experienced just below the ELA and the most distal and sheltered part is progressively disconnected from accumulation area (Benn *et al.*, 2012). This process can explain the situation in the Rognes area, where ice, protected by a thicker debris layer, has subsisted in the marginal parts and not in the central depression. In addition, a thinner snow cover in winter and meltwater surface runoff during summer could have increased the proportion of cold ice in the ablation area, whereas the ice in accumulation area is isolated from winter cold by the thick snow cover and warmed to the melting point by the release of latent heat when the meltwater refreezes in summer, as proposed for Tête Rousse Glacier (Gilbert *et al.*, 2012; Fig. 2.9b). This process might explain the preservation and the progressive integration

of cold glacier ice in the distal part of Rognes area, in addition to pre-existent frozen sediments (Fig. 2.9c). As well, polythermal glaciers are common in alpine or arctic permafrost environments (Etzelmüller and Hagen, 2005); their thermal regime explains the frequent glacier-permafrost interactions in the former lower and marginal areas whereas former central upper areas remain commonly unfrozen (Reynard *et al.*, 2003; Berger *et al.*, 2004; Kneisel and Kääh, 2007; Avian *et al.*, 2009; Ribolini *et al.*, 2010; Lilleøren *et al.*, 2013).

Mass balance roughly stabilized between 1950s and mid-1980s (Fig. 2.9b). We presume that the regional ELA was around 3000 - 3100 m, as it is located around 3200 m since the 1990s (Gilbert *et al.*, 2012). Thereby, the Rognes and Pierre Ronde Glaciers were almost completely below ELA and continued to shrink. However, glacier surface areas were nearly stable during these decades (Fig. 2.9), probably due to the rapid and direct melt of glacier surface (downwasting) that contrasts with the delayed and complex variation of glacier length (Haeberli *et al.*, 2013). In this way, many glaciers have passed in the last decades from an active retreat dynamics to a progressive stationary thinning mode (Paul *et al.*, 2007; Hambrey *et al.*, 2008). It is especially the case for debris-covered glaciers (Scherler *et al.*, 2011; Deline *et al.*, 2012), where the glacier driving stress is weakened by the ice mass thinning and by the reduction of surface gradient that results from the inversion of the ablation gradient by the debris cover (Benn *et al.*, 2012). With this stationary thinning mode, ice caves development, due to sub- or intraglacial water discharge and/or warm air circulation in summer, are common in ablation area (Haeberli *et al.*, 2013), as in the distal NE limit of the Rognes area (Fig. 2.3 & Fig. 2.8). With warm air penetration, the glacier melt-out is accelerated and can generate collapse structures.

Since the mid-1980s, mass balance has become extremely negative for local glaciers (Vincent *et al.*, 2010; Fig. 2.9b). Despite extensive debris cover, warming climate led to rapid ice melt-out and current contrasted ground ice extent between Rognes and Pierre Ronde (Fig. 2.8 and Fig. 2.9). This contrast most probably results from: (i) differences in elevation and aspect (Tab. 2.3); (ii) the effect of the 1892 WPOF on Pierre Ronde debris cover; and (iii) repeated water supply by debris flows after 1892 in Pierre Ronde that led to a temperate thermal regime and hindering the formation of frozen sediment (Fig. 2.5, 2.8 & 2.9), as it is commonly the case in areas covered by temperate glacier ice and affected by water circulation (Delaloye, 2004; Kneisel and Kääh, 2007; Ribolini *et al.*, 2010). In contrast, marginal areas seem to still contain ground ice (Tab. 2.2 and Fig. 2.8). Finally, a vanishing dead ice zone inherited from LIA conditions occupies the upper slope of Pierre Ronde, where the shadow created by the rockwall and debris layer has limited ice melt. With a high rockfall activity, this sector can be interpreted as the first immature stage of talus slope development in a context of deglaciation (Gomez *et al.*, 2003). Rognes still contains a large amount of ground ice as pointed out by our field measurements (Fig. 2.5, 2.6 & 2.7). The marginal frozen sediment zone is related to deformed pre-existent permafrost where cold massive ice of a polythermal glacier has been incorporated, a common situation in proglacial areas located in permafrost environments (Ackert, 1998; Reynard *et al.*, 2003; Etzelmüller and Hagen, 2005; Kneisel and Kääh, 2007). The relatively lower resistivity values (<5000 kΩm) in the NW narrow glacier snout in comparison to the upslope debris-covered glacier (>5000 kΩm, fig.5) and the

moderate movements (Fig. 2.7) suggest such transition from glacier ice to ice/debris mixture. The debris-covered glacier occupies an important surface area in the upper slopes. It can be also interpreted as a dead ice downwasting zone in transition to talus slope (Gomez *et al.*, 2003). The measured loss in elevation (Fig. 2.7) between the GPS campaigns and the current meltwater circulation at the front of Rognes Glacier suggest a probable domination of temperate ice.

Little Ice Age extent of:	Mean elevation (m a.s.l.)	Mean slope (°)	Aspect (N/E/S/W in %)	Mean direct solar radiation (Wh/m ²)
the Rognes glacier	2820	29.5	66.5 / 3 / 11.5 / 19	291 000
Pierre Ronde glacier	2760	27.5	9.5 / 1 / 8 / 81.5	289 000

Tab. 2.3. Topographical characteristics of the LIA maximal extent of Rognes and Pierre Ronde Glaciers derived from a 4 m resolution DEM (from RGD 73-74)

Sediment transfer systems

According to our rough estimation of sediment volume (Tab. 2.2), the store in Pierre Ronde (c. 2.6 Mm³) appears to be twice that of Rognes one (c. 1.3 Mm³). This contrast might result from the intense frost weathering that affected non-glaciated Pierre Ronde rockwalls during the Holocene cold periods. Sediment volume/area ratio is 4.6 and 9.4 at Rognes and Pierre Ronde, respectively (Tab. 2.2). The ratio of 11.8 for glacier forefield and 12-17 for hanging valley subsystems proposed by Otto *et al.* (2009) in the 75 km distant Turtmantal (Switzerland) suggests that our estimation is realistic and might be slightly underestimated (especially in relation to our mean sediment thickness values).

The major sediment supply in the studied systems is the rockfall activity from the dominant fractured rockwalls (Fig. 2.10). Permafrost degradation and/or intensification of freeze-thaw cycles might have led to an increasing activity of this process since the LIA (Deline *et al.*, 2012). With a negative mass balance, glaciers have been quite rapidly buried under debris (Fig. 2.9b) as in other high relief contexts. 1949 and 1959 aerial photographs (Tab. 2.1) and field observations show that debris flow deposits filled the upper depression in Pierre Ronde (Fig. 2.8). Their frequency is difficult to evaluate, although it appears low with some events per century, and some thousands of m³ per debris flow (J. Lievois, Service Restauration des terrains en montagne of Haute-Savoie, personal communication). Since the recent formation of a new water pocket in Tête Rousse Glacier (Vincent *et al.*, 2012), a major local issue concerns the potential mobilization of Pierre Ronde sediments by an outburst flood: as revealed by ERT profiles (Fig. 2.5), the central part of Pierre Ronde is composed of several meters of unconsolidated glacial sediments.

The reworking of the current sediment store within the studied area is the consequence of three main dynamics and is clearly related to ground ice occurrence (Fig. 2.10). First, the debris-covered glacier sectors are the most active. The dynamics typical of almost stationary vanishing debris-covered glacier are occurring (Paul *et al.*, 2007; Schomacker, 2008; Benn *et al.*, 2012): massive ice melt-out, ice deformations, landslides on ice layer, ice cave formation. Movements can exceed one

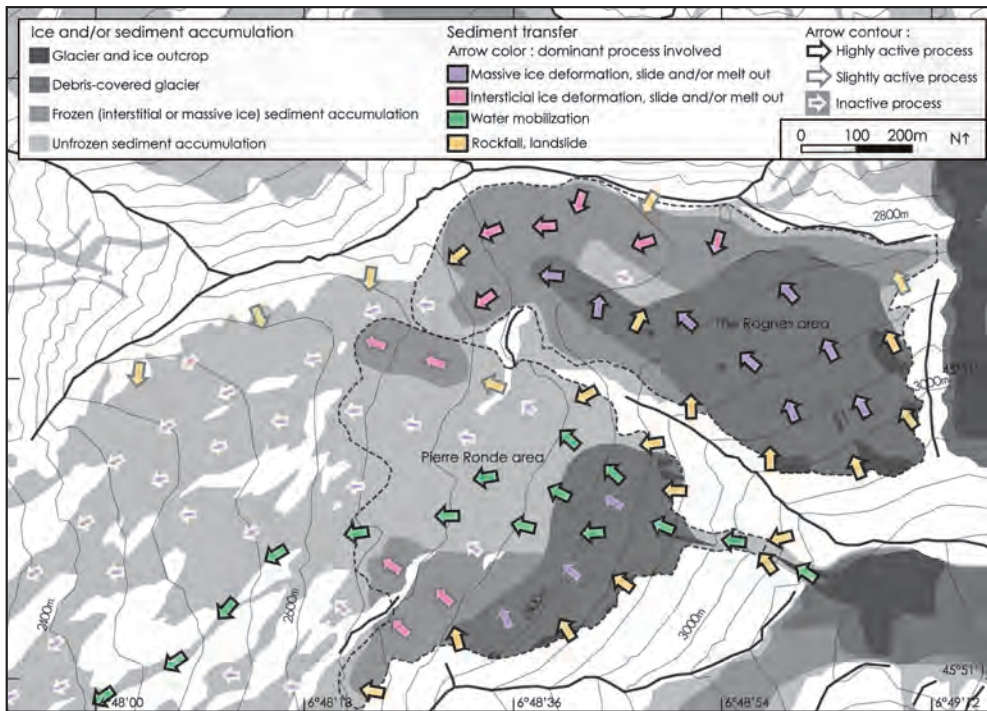


Fig. 2.10. Schematic map on current sediment transfer in Rognes and Pierre Ronde areas. The main geomorphic processes involved and their degree of activity are figured.

metre per year (Fig. 2.7). Second, the weaker movements in frozen sediment areas are related to downslope creeping of ice/debris mixture. A thicker debris layer better insulates ground ice than in the upper slopes, as illustrated by lower Δv values. In addition to compressive patterns related to glacier advance, ice/debris mixture creeping generates the successive ridges and furrows and the steep front that are not visible in debris-covered glacier sectors. In this way, the active margins of Rognes and Pierre Ronde correspond to rock glaciers, defined as “the visible expression of cumulative deformation by long-term creep of ice/debris mixtures under permafrost conditions” (Berthling, 2011: p103). Our results support the numerous studies on the glacier-rock glacier continuum that occurs in a negative mass balance context in permafrost environments (e.g. Ackert, 1998; Brazier *et al.*, 1998; Benn *et al.*, 2003; Krainer and Mostler, 2006; Avian *et al.*, 2009; Lilleøren *et al.*, 2013). Third, movements on the sides of the Rognes central depression can be interpreted as post-glacial re-equilibration as shown in other central areas of proglacial margins (Reynard *et al.*, 2003). The weak displacements in unfrozen sectors illustrate the limited mass wasting of sediments (Fig. 2.10).

Fig. 2.10 shows a conceptual map of sediment transfers in the studied areas and on the nearby slopes. Activity is mainly limited to Rognes and Pierre Ronde areas. Thus, we agree with other studies (e.g. Otto *et al.*, 2009; Carrivick *et al.*, 2013) that areas affected by glacial recession (even those with inherited ground ice) should be considered as some of the most dynamic parts of cold region geomorphic systems. However, as Pierre-Ronde and Rognes are not connected to downslope hydrosystems (any permanent surface runoff connects the studied sites downstream), this activity is mainly restricted to sediment store reworking within LIA glacier extents, and these sites can be considered as transport-limited systems and sediment sinks. Several complementary reasons, common in hanging valleys and glacier cirques, explain the decoupling of the studied areas from the sediment transfer system (Shroder *et al.*, 2000; Benn *et al.*, 2003). First, the

bedrock topography inherited from the last glaciation has a relatively gentle slope (cirque floor) that has been progressively filled by sediments. Contributing to the reduction of relief energy, the current geometry of sediment accumulation (see the weakness of the slope angle on the ERT profiles on Fig. 2.5) also contributes to the sediment trapping. Second, associated with this low relief energy, Holocene glacier and post-glacial processes had limited capacity to transfer sediment. Downstream sediment transport only occurred when the NE tongue of Rognes Glacier was coalescent with the Griez Glacier, during the Tête Rousse WPOF, and with debris flows in the Pierre Ronde area. Finally, the moraine dam and/or marginal ice/debris mixture have contributed to the confinement of glaciers (the west tongue of Rognes Glacier), enhancing sediment stores. Therefore massive sediment stores have accumulated during the Holocene by successive glacier and post-glacial dynamics as in other decoupled glacier systems (Benn *et al.*, 2012). As well, even if proglacial areas are particularly active in a paraglacial context, their contribution to sediment flux can be episodic rather than constant, in function of the capacity of geomorphic process to evacuate the sediment load downstream. This capacity can be strongly (sometimes completely) limited by the topography: glacier erosion and/or sediment accumulation geometry can generate sediment sinks. Its is particularly frequent in the very numerous low active and small glacier systems (Brazier *et al.*, 1998; Shroder *et al.*, 2000; Benn *et al.*, 2003) and typically like the two study cirque glacier systems, where conjugate effects of low energy relief and limited capacity of Holocene geomorphic processes (even glacial transfer) have contributed to the formation of hypertrophic sediment stores. This situation is exacerbated in permafrost environment, when a distal ice/debris mixture (as in the Rognes area) obstructs the sediment transfer (Ackert, 1998; Brazier *et al.*, 1998; Berger *et al.*, 2004; Etzelmüller and Hagen, 2005; Krainer and Mostler, 2006). In contrast, this situation is scarcer in proglacial areas of large valley glaciers where the coupling between glacier system and hydrosystem heighten the efficiency of sediment transfer (e.g. Meigs *et al.*, 2006). Nevertheless, major sediment sinks, as proglacial lakes and the marginal zones (lateral moraines and slopes) disconnected from the valley floor hydrosystem, can exist even in these highly active landsystems (Cossart and Fort, 2008; Geilhausen *et al.*, 2012; Carrivick *et al.*, 2013).

2.1.2.6. Conclusion

According to our field observations and data, historical documentary analysis and published glaciological data on a small neighbouring glacier, a novel integrated geomorphological study has been provided for two small cirque glacier systems located in the periglacial belt of the Mont Blanc Massif. Pierre Ronde Glacier was probably debris-covered at the end of the LIA, whereas Rognes Glacier has been progressively buried due to the rockwall deglaciation that intensified during the 20th century. Our results outline three main contrasted situations in terms of glacier system evolution since the LIA, current ground ice distribution, and geomorphological dynamics.

First, in the upslope debris-covered glacier areas, significant surface downwasting occurs currently, indicating the rapid melt-out of an ice body close to the melting point. The global negative mass balance that has followed LIA has led to the confinement of glacier in the top slopes, where a decimeter thick debris mantle covers now the inherited ice.

Second, surface deformation patterns (ridges and furrows, steep front) and measured movements illustrate the creep of the marginal ice/debris mixtures. These accumulations have probably crept continuously since LIA, decoupled from the upslope shrinking glacier. The probable integration of glacier ice in these landforms may be related to the existence of cold ice in the distal part of polythermal glaciers in permafrost environments. In addition, the inversion of ablation gradient due to the debris cover preserves ground ice better than in the central and upper slopes, as revealed by a convex topography and lower Δv values. As well, it expresses the glacier-permafrost interactions and the morphogenetic continuum between a debris-covered glacier and a rock glacier in a context of negative mass balance in permafrost environment.

Third, the lower half of Pierre Ronde surface and the central zone of the Rognes, characterized by concave topography, patches of fine material, and pioneer vegetation, correspond to deglaciated, unconsolidated moraine accumulations. In Pierre Ronde, post-LIA torrential dynamics has contributed to the recovery of the moraines by debris flow deposits. Absence of ground ice in these areas is mainly related to the former temperate thermal regime of glaciers and to the local frequent water supply. The current very weak surface activity reflects the slow rebalancing of sediment mass that affects these areas recently deglaciated.

At the Holocene time scale, Pierre Ronde and Rognes areas can be considered as sediment sinks and transport-limited systems. Sediment transfer occurred rarely, for instance on the occasion of events like the 1892 WPOF. In this way, Holocene geomorphic activity, in spite of repeated glacier advance and recession cycles, is largely restricted to sediment production and deposition within the glacier systems. The decoupling of these landforms with downslope geomorphic systems is common in small low active glacier systems (as the numerous cirque glaciers systems): geomorphic processes are unable to evacuate sediment especially because of the flat topography. In permafrost environments as in the Rognes area, this situation can be enhanced because marginal ice/debris mixtures obstruct sediment transfer. In that way, these small, decoupled landsystems act as sediment traps, as well as potential sediment source (especially in Pierre Ronde with a potential new WPOF from Tête-Rousse) and water reservoirs at catchment scale; their global understanding is important in a context of intensified changing climate.

Acknowledgements

We would like to thank the following people and institutions for their precious help during field measurements and documentary research: S. Utz, B. Regamey, L. Grangier, N. Deluigi, V. Zuchuat, R. Bosson, E. Malet, H. Dyer, J.-M. Krysiecki, C. Barachet; J.-F. Couix (*Refuge du Nid d'Aigle*); *Météo France* for data from Aiguilles Rouges and Aiguille du Midi stations; the *Tramway du Mont-Blanc* crew (in particular E. Adami); *Remontées Mécaniques des Houches* (in particular K. Gafanesh); *ONF-RTM74* (in particular B. Demolis, J. Lievois and A. Evans); *LGGE* (in particular C. Vincent); *the Municipality of Saint-Gervais-les-Bains*; F. Amelot (*Centre de la Nature Montagnarde*,

Sallanches). This manuscript has been improved thanks to the precious critics and comments of S. Lane and N. Deluigi (*IDYST, UNIL*), D. Morche, S. McColl and T. Heckmann (special issue editing team) and two anonymous reviewers.

Appendix


Sensor number (location on Figure 6A)	Mean ground surface temperature (MGST, °C)	Presumed winter equilibrium temperature (WEqT, °C)	Ground freezing index (GFI, °C day)
1	-2.6	-4.2	-815
2	-4	—	-1320
3	-4.4	-5	-1308
4	-3.1	-4.4	-911
5	-3	-5	-907
6	-2.3	-4.5	-744
7	-2.9	-5	-1025
8	-1.9	-3.5	-720
9	-1.8	—	-684
10	-0.3	—	-351
11	-1.1	-2.8	-547
12	-1.1	-3.5	-557
13	-0.9	—	-439
14	-1.2	-2.1	-437
15	0	—	-600
16	0.1	-1.6	-230
17	0.2	-2.1	-289
18	0.4	-0.6	-120

Appendix A. Mean Ground Surface Temperature, presumed Winter Equilibrium Temperature, and Ground Freezing Index obtained at 18 locations with ground surface temperature measurements between 10th September 2011 and 20th June 2012 in Rognes and Pierre Ronde areas. Background colours correspond to classification in Fig. 2.6a.


2.2. Paper 2:

Internal structure and current evolution of very small debris-covered glacier systems located in alpine permafrost environments

Frontiers in Earth Science (Cryospheric Sciences), 2016



ORIGINAL RESEARCH
published: 13 April 2016
doi: 10.3389/feart.2016.00039



Internal Structure and Current Evolution of Very Small Debris-Covered Glacier Systems Located in Alpine Permafrost Environments

Jean-Baptiste Bosson* and Christophe Lambiel

Faculty of Geosciences and Environment, Institute of Earth Surface Dynamics, University of Lausanne, Lausanne, Switzerland

This contribution explores the internal structure of very small debris-covered glacier systems located in permafrost environments and their current dynamical responses to short-term climatic variations. Three systems were investigated with electrical resistivity tomography and dGPS monitoring over a 3-year period. Five distinct sectors are highlighted in each system: firm and bare-ice glacier, debris-covered glacier, heavily debris-covered glacier of low activity, rock glacier and ice-free debris. Decimetric to metric movements, related to ice ablation, internal deformation and basal sliding affect the glacial zones, which are mainly active in summer. Conversely, surface lowering is close to zero (-0.04 m yr^{-1}) in the rock glaciers. Here, a constant and slow internal deformation was observed (c. 0.2 m yr^{-1}). Thus, these systems are affected by both direct and high magnitude responses and delayed and attenuated responses to climatic variations. This differential evolution appears mainly controlled by (1) the proportion of ice, debris and the presence of water in the ground, and (2) the thickness of the superficial debris layer.

Keywords: debris-covered glaciers, rock glaciers, permafrost, ground ice, electrical resistivity tomography, dGPS

OPEN ACCESS

Edited by:
Matthias Huss,
ETH Zurich, Switzerland

Reviewed by:
Sebastien Morner,
Pontifical Catholic University of
Valparaíso, Chile
Roberto Steppi,
University of Pavia, Italy

***Correspondence:**
Jean-Baptiste Bosson
jeanbaptiste.bosson@gmail.com

Specialty section:
This article was submitted to
Cryospheric Sciences,
a section of the journal
Frontiers in Earth Science

Received: 05 January 2016
Accepted: 29 March 2016
Published: 13 April 2016

Citation:
Bosson JB and Lambiel C (2016)
Internal Structure and Current
Evolution of Very Small
Debris-Covered Glacier Systems
Located in Alpine Permafrost
Environments. *Front. Earth Sci.* 4:39.
doi: 10.3389/feart.2016.00039

INTRODUCTION

Numerous positive and negative feedbacks characterize the current adaptation of glacier systems to climatic changes (WGMS, 2008; Haeberli et al., 2013). Among them, the accumulation of debris at the glacier surface by the emergence of englacial load and/or direct supraglacial deposition in high relief environments significantly impacts glacial dynamics (Benn et al., 2003). Indeed, depending on its thickness, the debris cover enhances or limits the ice ablation (Nicholson and Benn, 2006; Lambrecht et al., 2011). The melt rate increases below a few centimeters of thickness threshold (2–8 cm, e.g., Hagg et al., 2008) because more incoming shortwave radiation is absorbed in relation to the albedo reduction. This effect is canceled out by the thickening of the debris layer beyond this threshold: its low thermal conductivity induces an exponential reduction of the ablation rate. Thus, the development of decimeters to meters thick debris cover constitutes one of the most efficient negative feedback to current climatic changes, while worldwide glacier shrinkage is expected over the next decades (e.g., Huss and Hock, 2015).

Frontiers in Earth Science | www.frontiersin.org 1 April 2016 | Volume 4 | Article 39

F | First page of the article 2

2.2.1. Presentation:

Internal structure and current evolution of very small debris-covered glacier systems located in alpine permafrost environments*Citation*

Bosson JB and Lambiel C (2016). Internal structure and current evolution of very small debris-covered glacier systems located in alpine permafrost environments. *Frontiers in Earth Science: Cryospheric sciences*. 4:39. Doi: 10.3389/feart.2016.00039

Scope and research questions

- Debris-covered glacier systems are more and more numerous in high relief and permafrost environments. *What are the main components of these systems? How do they respond to short term climatic variations? What processes are involved? What are their main evolution controls?*
- Numerous confusions exist on glacier-permafrost relationships and especially on the distinction between heavily debris-covered glaciers and rock glaciers. *Which characteristics differentiate them? Are they affected by the same responses to short-term climatic variations? Does a continuum between these landforms can exist in SDCGSAPE?*

Approach and content

The internal structure and the current evolution of three SDCGSAPE (les Rognes, Entre la Reille and Tsarmine) are investigated and discussed with field measurements (Electrical resistivity tomography and a dGPS monitoring), observations and historical documents. The spatial homogeneities in ground composition and surface dynamics allows a transversal analysis and the generalisation of the results. The same main components are characterised, mapped and defined in each studied system. The data of the three-year dGPS monitoring are explored to point out the zonal responses to short-term climatic variations and especially the operating processes.

Main outcomes

- The characterisation of internal structure and surface movements are in line with the existing literature. The amount of data, their collection at the system-scale and their coherence between sites allow to propose **a comprehensive model of the composition and the current dynamics occurring in SDCGSAPE**.
- **Five distinct homogeneous sectors are present in each studied system:** firm and bare-ice glacier, debris-covered glacier, heavily debris-covered glacier of low activity, rock glacier and ice-free debris. **Ice concentration and the thickness of the superficial debris layer are the two main ground characteristics that vary in space and explains the different zonal responses to short-term climatic variations.**
- No measurements were carried out on the bare-ice zones. **The debris-covered zones are the most active. They experience direct and high magnitude** (up to few meters per years) **to short-term climatic variations.** Debris-covered glaciers zones seem to behave the same way than temperate bare-ice glaciers, although the magnitude of processes is likely lower due to the insulation effect. Basal sliding, ice deformation and ice melt are active, mostly in summer. It illustrates the strong influence of the seasonal climatic forcing and also of the very likely hydraulic forcing. **The thickening of the superficial debris layer and the decrease in ice concentration towards the distal zones attenuate and delay the responses to climatic variations. The current evolution of distal rock glaciers is mainly driven by a slow and constant internal deformation.** Rock glaciers were deformed during past glacier advances and glacier ice can have been integrated in them. They progressively disconnect from the upslope glacier because of their flow and differential ablation dynamics. **These rock glaciers illustrate the continuum that can occur between glacial and periglacial processes under permafrost conditions.** Periglacial dynamics succeed to glacial dynamics in ice-debris mixtures with the progressive reduction of ground sensitivity to climatic and hydraulic forcing. Finally, only slow surface movements were measured in ice-free debris zones.
- **The wasting stage of Entre la Reille and the Rognes glaciers is more advanced than the one of Tsarmine glacier.** Indeed, they are almost completely buried and downwasting dynamics dominates.

Personal contribution

I designed this research with my supervisor C. Lambiel. I organised and conducted field investigations, and gathered additional data. I made data analysis, prepared figures and wrote the manuscript, which was noticeably improved by the constructive comments and corrections of C. Lambiel.

2.2.2. Content:

Internal structure and current evolution of very small debris-covered glacier systems located in alpine permafrost environments

Jean-Baptiste and Christophe Lambiel

Institut des dynamiques de la surface terrestre - Université de Lausanne, LAUSANNE, SWITZERLAND

Abstract

This contribution explores the internal structure of very small debris-covered glacier systems located in permafrost environments and their current dynamical responses to short-term climatic variations. Three systems were investigated with electrical resistivity tomography and dGPS monitoring over a 3-year period. Five distinct sectors are highlighted in each system: firn and bare-ice glacier, debris-covered glacier, heavily debris-covered glacier of low activity, rock glacier and ice-free debris. Decimetric to metric movements, related to ice ablation, internal deformation and basal sliding affect the glacial zones, which are mainly active in summer. Conversely, surface lowering is close to zero (-0.04 m yr^{-1}) in the rock glaciers. Here, a constant and slow internal deformation was observed (c. 0.2 m yr^{-1}). Thus, these systems are affected by both direct and high magnitude responses and delayed and attenuated responses to climatic variations. This differential evolution appears mainly controlled by (1) the proportion of ice, debris and the presence of water in the ground, and (2) the thickness of the superficial debris layer.

Keywords

Debris-covered glaciers, rock glaciers, permafrost, ground ice, electrical resistivity tomography, dGPS

2.2.2.1. Introduction

Numerous positive and negative feedbacks characterize the current adaptation of glacier systems to climatic changes (WGMS, 2008; Haeberli et al., 2013). Among them, the accumulation of debris at the glacier surface by the emergence of englacial load and/or direct supraglacial deposition in high relief environments significantly impacts glacial dynamics (Benn et al., 2003). Indeed, depending on its thickness, the debris cover enhances or limits the ice ablation (Nicholson and Benn, 2006; Lambrecht et al., 2011). The melt rate increases below a few centimeters of thickness threshold (2 to 8 cm, e.g. Hagg et al., 2008) because more incoming shortwave radiation is absorbed in relation to the albedo reduction. This effect is cancelled out by the thickening of the debris layer beyond this threshold: its low thermal conductivity induces an exponential reduction of the ablation rate. Thus, the development of decimeters to meters thick debris cover constitutes one of the most efficient negative feedback to current climatic changes, while worldwide glacier shrinkage is expected over the next decades (e.g. Huss and Hock, 2015).

This insulating layer confers specific behavior to heavily debris-covered glaciers. Because ice melt is limited in the ablation area, they have smaller accumulation area ratios than other glaciers (typically 0.1 - 0.4 instead of 0.6 – 0.7; Clark et al., 1994). They can thus have a positive mass balance with a restricted accumulation area, reach lower elevation and advance when neighboring bare-ice glaciers are retreating (Scherler et al., 2011; Deline et al., 2012; Carturan et al., 2013). The increase of debris thickness toward the glacier front can also reverse the ablation gradient, which usually induces a glacier surface flattening and limits the driving stress (Kirkbride and Warren, 1999; Benn et al., 2012). Thickness variations then become more pronounced than length variations for debris-covered tongues (Benn et al., 2003; Mayer et al., 2006). Finally, glacial hydrology and especially the concentration and the temporal variation of water release are also atypical in these systems (Mattson, 2000; Hagg et al., 2008). In this way, from a consequence of glacial dynamics, the covering of a glacier by a thick debris layer can become its main control (Deline et al., 2012).

Two main causes, enhanced by the acceleration of ice melt since the mid-1980s (e.g. Zemp et al., 2015), explain the current extent and thickening of supraglacial debris cover observed in mountainous regions (Kirkbride and Deline, 2013). Firstly, the deglaciation of rockwalls and permafrost degradation increase the debris supply to glacier systems (Bosson et al., 2015; Deline et al., 2015). Secondly, because the driving stress is positively related to ice thickness, thinning glaciers have weaker flow and, therefore, less ability to evacuate the sediment load to the hydrosystem (Benn et al., 2003; Paul et al., 2007). These two dynamics are particularly effective in the very small cirque glacier systems located in permafrost environments (Brazier et al., 1998; Seppi et al., 2015). Indeed, large amounts of debris are usually associated with these systems because of the rapid weathering of the surrounding rockwalls. Moreover, the height and surface of the latter can be lopsided in comparison with the restricted glacier surface (Maisch et al., 1999; Grunewald and Scheithauer, 2010). Finally, the debris evacuation can be limited because the weak driving stress of these thin ice masses is commonly reduced by the presence of cold ice (Gilbert et al., 2012) and/or large and possibly frozen sediment accumulations in the distal zone, such as moraine dam (*sensu* Benn et al., 2003), ice-cored moraines or rock glaciers (Shroder et al., 2000; Kirkbride and Deline, 2013; Bosson et al., 2015).

This contribution focuses on very small cirque debris-covered glacier systems located in permafrost environments. These particular systems are composed of a flowing ice mass mainly formed by the metamorphosis of snow (WGMS, 2008; Cogley et al., 2011; Dobhal, 2011), and associated, possibly frozen, debris accumulations. The existence of this type of glacier is especially related to the influence of the surrounding relief upon snow accumulation and shadow effects (Paasche, 2011; Capt et al., 2016). The size class of glaciers remains an open question in glaciology but 0.01 to 0.5 km² appear suitable thresholds to define very small glaciers (e.g. Kuhn, 1995; Fischer M et al., 2014; Pfeffer et al., 2014). The ablation areas of the glaciers present in these systems are partly, or totally, debris-covered (Kirkbride, 2011). In the system margins, rock glaciers can be present. They are related to the long-term slow viscous creep of ice/debris mixtures under permafrost conditions, which generates particular surface patterns like ridges and furrows and a fine-grained steep front (Benn et al., 2003; Berthling, 2011; Monnier and Kinnard, 2015). In contrast to the debris-covered

glaciers, they do not have accumulation areas from a glaciological point of view. The ice present below the block surface can have glacial (sedimentary ice) and/or non-glacial (e.g. magmatic ice) origin and its concentration is typically lower than within upslope glacier zones (usually < 70%, e.g. [Haeberli et al., 2006](#); [Janke et al., 2015](#)).

The landsystems investigated here remain poorly known in comparison with other glacier systems despite their large number and the fact that they can constitute considerable water reservoirs at a local scale ([Azócar and Brenning, 2010](#); [Knight and Harrison, 2014](#); [Rangecroft et al., 2015](#)). The complexity of these associations of ice and debris, their position at the frontier between glaciological and periglacial research and the confusion between debris-covered glaciers and rock glaciers mainly explain their limited consideration in cryospheric sciences ([Haeberli, 2005](#); [Berthling et al., 2013](#); [Janke et al., 2015](#)). Consequently, very small debris-covered glaciers associated with rock glaciers are commonly ignored in regional glacier inventories ([Pfeffer et al., 2014](#)). To our knowledge, no modelling considers their evolution. Furthermore, recent contributions investigated the transition from very small debris-covered glaciers to rock glaciers at the site-specific scale (e.g. [Bosson et al., 2015](#); [Emmer et al., 2015](#); [Monnier and Kinnard, 2015](#); [Seppi et al., 2015](#)), but quantitative data on internal structure and on the operating processes are still lacking. In particular, the definition of the distinct components of these systems, the understanding of their origin and the identification of their responses to climatic variations is needed. This is the overall aim of this paper, which we achieve through the comprehensive study of three very small debris-covered glacier systems. The following research questions were addressed: what is the internal structure of these systems? How do their different components react to annual and seasonal climatic variations? What are the main processes involved in these responses?

2.2.2.2. Study sites

Les Rognes, Tsarmine and Entre la Reille, the three sites investigated, are very small cirque glacier systems located in the north-western European Alps ([Fig. 2.11](#) and [Fig. 2.12](#)). In the three sites, the general concave topography between perched historic moraine accumulations show the glaciers shrinkage since the Little Ice Age (LIA). Ice outcrops are rare and the extensive debris cover masks the glacier limits. Meltwater streams are absent at the glacier outlet. Although water fluxes are visible and/or audible in summer, they disappear into the distal sediment bodies, emerging in temporary springs several hundred meters downslope. At the Holocene timescale, the high amount of sediment in the three systems contributed to the construction of imposing marginal sediment accumulations, part of which present typical rock glacier morphology. Because of these debris accumulations, the low slope angle, the weak glacial dynamics and the reduced meltwater streams, sediment evacuation is negligible. These systems are thus sediment sinks, decoupled from downslope sediment transfer systems ([Shroder et al., 2000](#); [Benn et al., 2003](#); [Bosson et al., 2015](#)). The investigated sites are located within permafrost areas, as shown by regional permafrost maps ([BAFU, 2005](#); [Bodin et al., 2008](#); [Lambiel et al., 2009](#); [Boeckli et al., 2012](#)). The local occurrence of permafrost conditions was also shown in talus rock glaciers near les Rognes ([Bosson et al., 2015](#); [Fig. 2.12](#)) and Tsarmine ([Lambiel et al., 2004](#); [Micheletti et al., 2015a](#)), or in frozen talus slopes near Entre la Reille ([Reynard et al., 1999](#)).

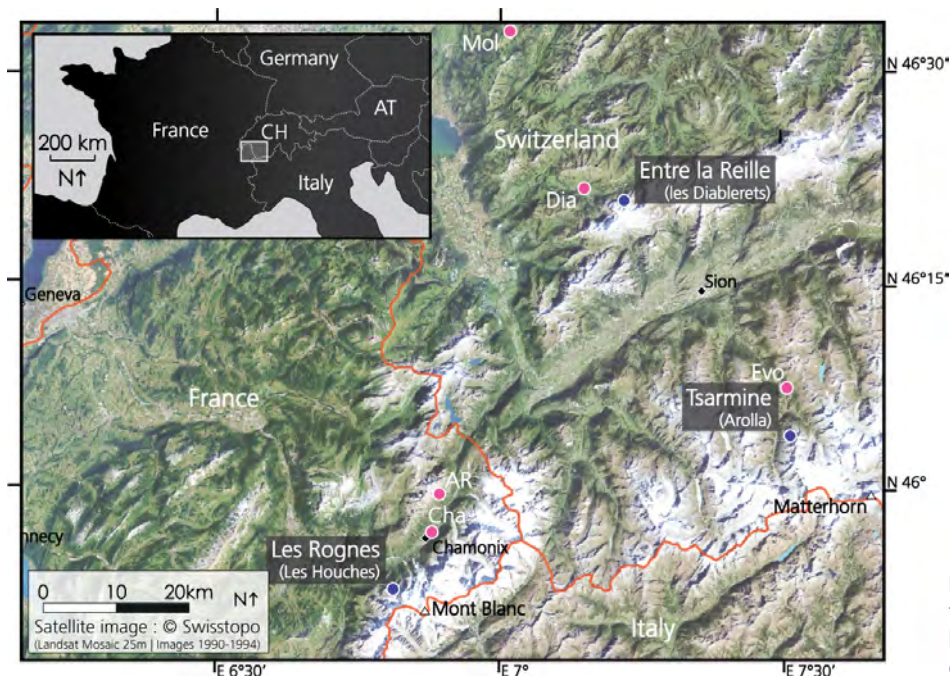


Fig. 2.11. Satellite image of the NW Alps showing the location of the three studied glacier systems

Les Rognes glacier system

Les Rognes ($45^{\circ}51'40''\text{N}$, $6^{\circ}48'50''\text{E}$; 0.29 km^2 ; 2650-3100 m a.s.l.) occupies a small cirque oriented N-NW in the Mont-Blanc massif. The lithology is dominated by micaschists and gneiss (Menessier et al., 1976). Mean annual air temperature is -1°C at 2800 m a.s.l. and annual precipitation is c. 2000 mm, according to Météo-France data (Chamonix and les Aiguilles-Rouges weather stations, respectively at 1042 and 2330 m a.s.l., Fig. 2.11). The local equilibrium line altitude (ELA) has fluctuated above the glacier, at around 3200 m a.s.l. since the 1990s (Gilbert et al., 2012). This glacier is identified in the French glacier inventory and inherited from the disintegration of the LIA Tête-Rousse-Griaz-Rognes glacier complex (Gardent et al., 2014; Bosson et al., 2015). Today, under a 100 m high backwall, a debris-covered slope with few ice outcrops dominates a depressed area with marginal, rounded sediment ridges, which is terminated by a 30 m high steep slope in the northwestern part (Fig. 2.12).

Tsarmine glacier system

Tsarmine ($46^{\circ}03'\text{N}$, $7^{\circ}31'\text{E}$; 0.49 km^2 ; 2600-3070 m a.s.l.) is located in the Pennine Alps. The bedrock is composed of granitic gneiss. Mean annual air temperature and precipitation are around -1°C and 1200 mm/yr at 2800 m a.s.l. respectively, according to MeteoSwiss data (Evolène weather station, 1825 m a.s.l., Fig. 2.11). The Tsarmine glacier is identified in the Swiss glacier inventory (Fischer M. et al., 2014). The decadal mass balance variations and current geometry of this $4 \times 10^6 \text{ m}^3$ ice mass are presented in Capt et al. (2016). These results exhibit its atypical behavior over time (mass balance divergence since the 2000s) and space (reversed ablation pattern) in comparison with other local glaciers, due to the combined influence of the decimeters thick debris cover, permafrost conditions, avalanching and solar shading on this very small glacier. Until the early 1980s, the upper part of Tsarmine glacier occupied the steep 600 m high north face of the Blanche de

Perroc (Delaloye, 2008). The rockwalls are now deglaciated, providing an important sediment supply to the glacier. Shaded and crevassed debris-free glacier occupies the backwall foot. Arcuate rounded ridges are visible on the central part of the debris-covered glacier (Fig. 2.12). The distal southern part, confined by the 100 m high moraine dam, is composed of glacier ice and ice-free debris (Lambiel et al., 2004). A lake of fluctuating level is also present since the 1980s. In the narrow northern distal part of the system, a rock glacier with a 15 m high steep front is present.

Entre la Reille glacier system

Entre la Reille (46°20'20"N, 7°13'12"E; 0.04 km²; 2380-2550 m a.s.l.) lies in the Diablerets massif

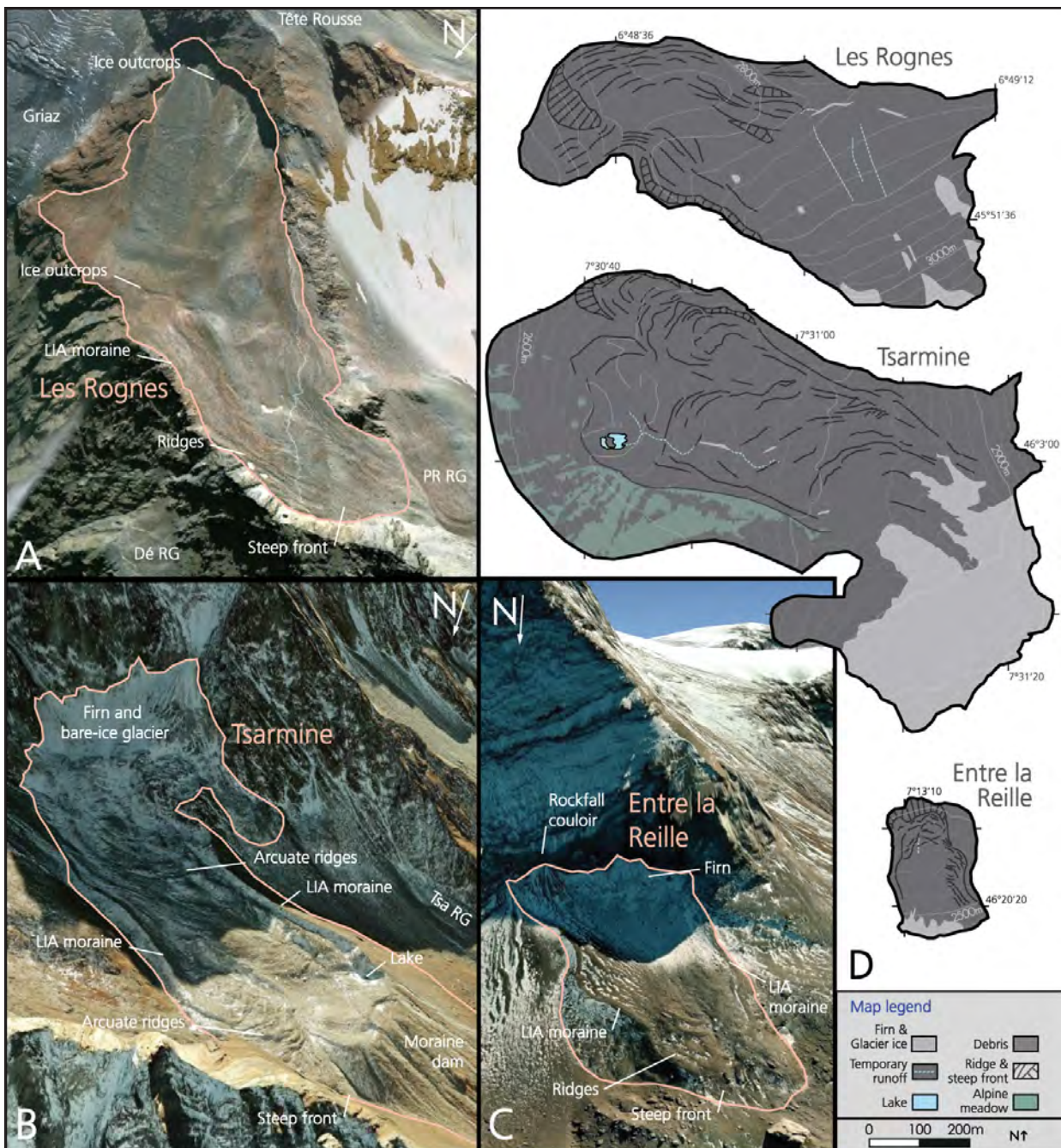


Fig. 2.12. 3d view of the study sites (A, B, & C; © Google Earth 2015) and simplified maps (D). As the extension of glacier ice outcrops varies each year, its representation on map is an indication, derived from field observations and recent aerial images. RG refers to rock glacier in A and B.

where the lithology alternates limestone and marl (Badoux and Gabus, 1991). Mean annual air temperature and precipitation are respectively close to 0.3°C and 2000 mm/yr at 2450 m a.s.l., according to MeteoSwiss data (les Diablerets, and le Moléson weather stations, respectively at 1162 and 1972 m a.s.l., Fig. 2.11). This ice mass has developed below the 300 m high north face of the Oldenhorn. Previous geoelectrical surveys interpreted Entre la Reille as a body of sedimentary ice with locally high debris concentration, illustrating the burying of a very small glacier after the LIA (Reynard et al., 1999). In the upper zone, the concave west side contrasts with the convex east side, which is actively fed by a rockfall couloir (Fig. 2.12). Ice outcrops are very rare and a small permanent snowfield occupies the top part. A gully where water can be heard in summer is present in the center. Ridges and furrows cover the distal part, which is delimited by a 20 m high steep fine-grained slope.

2.2.2.3. Methods

General approach

The internal structure and the current dynamical responses to short-term climatic variations were respectively assessed in the three study sites with Electrical Resistivity Tomography (ERT) and dGPS. In addition, current and recent surface morphology was analyzed with field observations, old oblique photographs that we collected, and numerous maps and aerial photographs available from the websites of national topographic institutes (map.geo.admin.ch and geoportail.gouv.fr; e.g. Fig. 2.13). However, we considered surface morphology with care because confusion and controversy emerged from morphology-centered approaches and relatively hampered the knowledge construction on the complex landsystems study here (Berthling, 2011; Janke et al., 2015). To simplify the analysis, we tried to identify homogeneous sectors that share the same general ground electrical resistivities, surface dynamics and morphology in each study site. We manually delineated them and concentrated on sectors where a large proportion of ice and debris are associated. Indeed, no direct measurements were possible on firn and bare ice zones because of rockfall hazards, and the weak surface activity of ice-free debris prevents to clearly distinguish movements from measure uncertainty.



Fig. 2.13. Aerial images of the study sites. The Rognes picture was taken the 04/09/1949 (© IGN; n°IGNF_PVA_1-0__1949-09-04__C3630-0121_1949_F3630-3631_0045, available on geoportail.gouv.fr). The Entre la Reille picture (white inset) was taken the 29/09/1969 (© Swisstopo; n°19690475128861, available on map.lubis.admin.ch). The Tsarmine picture was taken the 10/08/1988 (© Swisstopo; n°19880990037583, available on map.lubis.admin.ch).

Electrical resistivity tomography (ERT)

ERT was used because of its efficiency for ground ice characterization (Hauck and Kneisel, 2008). Indeed, the contrast between resistive ice and conductive unfrozen terrain allows the distinction between deglaciated debris (resistivity $r < 80 \text{ k}\Omega\text{m}$), ice-debris mixtures ($5 < r < 1000 \text{ k}\Omega\text{m}$) and massive sedimentary ice ($r > 500 \text{ k}\Omega\text{m}$). These rough thresholds have to be considered carefully. They give an order of resistivity magnitudes, which also vary as a function of several factors (air/water content, temperature, etc.; Hauck and Kneisel, 2008). A scale of typical resistivities of material existing in permafrost environments is available in Bosson et al. (2015).

Profiles with 24 or 48 electrodes, sometimes overlapping, were measured at each site between summers 2011 and 2014. Ground apparent resistivity was measured with a Syscal Pro Swich 96 and a Junior Swich 48 (Iris Instruments, France). We used the Wenner-Schlumberger configuration because it constitutes a compromise between horizontal resolution and depth of investigation. The inter-electrode spacing was 5m in the largest sites (les Rognes and Tsarmine) and 4m in Entre la Reille. Following Hauck et al. (2003), salt-water saturated sponges were used to improve the electrical contact between electrodes and the porous surface material. Results were processed with Prosys II. To create a plausible image of the ground specific resistivities, data were inverted in Res2DInv with Least Square Inversions and Robust parameters (see details in Bosson et al., 2015). It allowed a good visualization of the high resistivity contrasts expected in these environments. The absolute error of the final tomograms is the difference between the inverted model and the measured data. The reliability of the inverted model was also evaluated by the model resolution matrix value (Hilbich et al., 2009). This method allows the areas near the surface where the model is well constrained by data (highest model resolution matrix values) to be distinguished from inversion artefacts (lowest values). 0.05 and 0.005 model resolution matrix values thresholds are displayed.

Differential GPS (dGPS)

The position of numerous blocks (87 in les Rognes, 78 in Tsarmine and 44 in Entre la Reille) was measured with a Leica SR500 or a Trimble R10 eight times between late September 2011 and 2014 (Tab. 2.4). These dGPS have respectively a theoretical maximum 3D accuracy of 0.05 and 0.02 m. The systematic measurement of control points showed that the accuracy was lower than 0.02-0.03 m. We considered movement values higher than this threshold as significative. Field surveys were carried out in mid-July and late September to distinguish movements of the winter period with snow cover from those of the short snow-free period. Measurements were also performed in late August 2012 (les Rognes) and 2014 (Entre la Reille and Tsarmine) to compare the dynamics of early and late summer. However, the ablation period starts with the melt of the snow cover in spring. It can induce a glacier acceleration (e.g. Anderson et al., 2004). Unfortunately, because of the extensive thick snow mantle, it was not possible to measure the block positions in spring and the likely acceleration of velocities in the early ablation season is concealed in winter values.

Study site	Early-summer surveys	Mid-summer surveys	Late-summer survey
Les Rognes	19.07.2012; 22.07.2013; 18.07.2014	28.08.2012	05.09.2011; 03.10.2012; 26.09.2013; 26.09.2014
Tsarmine	10.07.2012; 08.07.2013; 24.07.2014	18.08.2014	13.09.2011; 25.09.2012; 08.10.2013; 23.09.2014
Entre la Reille	24.07.2012; 25.07.2013; 17.07.2014	22.08.2014	25.09.2011; 21.09.2012; 23.09.2013; 03.10.2014

Tab. 2.4. Date of dGPS surveys in each study site

As the mean slope angle around each block was not measured on site, it was derived from high-resolution digital elevation models (DEMs): 4 m resolution at les Rognes (source: RGD 73-74) and 2 m resolution at Entre la Reille and Tsarmine (source: Swisstopo). The mean standard deviation of the slope angle calculated in a 12 m square around each block was lower than 3° . Assuming no change in surface gradient between surveys, we computed the values of expected vertical movements ($dZ_{exp.}$) and downslope movements (M_d) from horizontal movements (dX) and the slope angle for each block (Fig. 2.14). dH , namely the difference between $dZ_{exp.}$ and dZ , was then derived (see Isaksen et al., 2000 for similar methodology). This value provided useful indication of local topographical variations, related to ice volume variation and/or compressing/extending flow. We assess the uncertainty of dH by calculating the means of dX , dZ and slope angle for all the blocks of each site. Then we recomputed dH taking into account these means and their respective uncertainty values. The standard deviation of the dH obtained was around 0.05 m.

Indices were computed by homogeneous sector in each system to characterize the intensity, the temporal variation and the type of the occurring dynamics. We used the blocks whose positions were measured in every field survey for this calculation. Here, we only present the mean of the values obtained in the three systems. Indeed, the same contrasted dynamical behaviors between the system components appeared clearly in each study site. The calculated mean indices provide, therefore, indications of the dynamical behaviors that can be found in these landsystems. To assess the sensitivity to short-term and medium-term climatic variations, we calculated the standard deviation of seasonal and annual velocities of every individual year for each sector. In addition, the proportions of movement for each season and each part of summer were computed to highlight the main periods of activity. We also calculated the downslope movement / surface lowering (M_d/dH) ratio to determine which dynamic is dominant: the downslope movement value is higher than the surface lowering one when $M_d/dH > 0$, equal when $M_d/dH = 0$ and smaller when $M_d/dH < 0$. Finally, following Copland et al. (2009) and using the mean horizontal velocities between 2011 and 2014, three Velocity Cross-Profiles (VCP) for each study site were used to highlight the

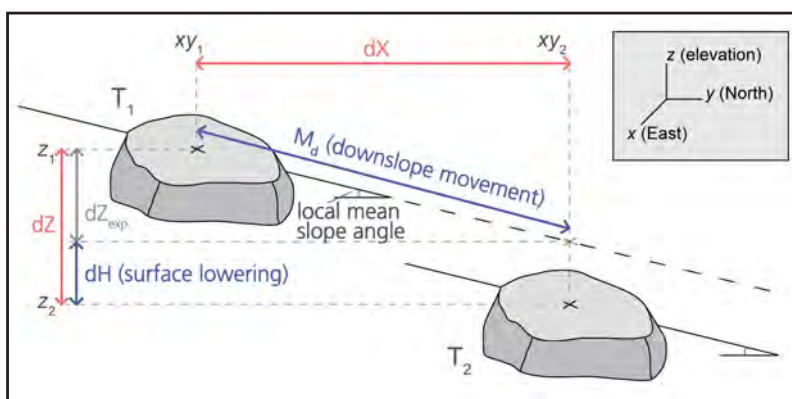


Fig. 2.14. Sketch showing the principle of a dGPS measurement and the parameters that can be calculated with a moving block: dX (horizontal movement), dZ (vertical movement) and, if the slope angle has not significantly varied during the two measurements, M_d (downslope movement, derived from dX and the local mean slope angle), $dZ_{exp.}$ (expected vertical movement derived from dX and the local mean slope angle) and dH (the difference between expected movement and the measured vertical movement; this parameter is an expression of surface lowering).

dominant motion mechanism. Cubic-shaped velocity cross-profiles suggest an en masse movement related to the basal sliding. Conversely, a parabolic shape indicates the internal deformation of viscous fluid, related to the friction increase toward the margins (Cuffey and Paterson, 2010). This method was used for larger glaciers and has to be considered with caution here because the horizontal velocities taken in account have weak magnitude. However, the results obtained here and at the decadal timescale (see Capt, 2015) illustrate that analysis of velocity cross-profiles also provides valuable information on the motion mechanisms in very small glacier systems.

2.2.2.4. Results

ERT results

In the Rognes glacier system, resistivity values are very high (>1000 k Ω m) directly under the surface of the 250 m long upper slopes of Ro-2 (Fig. 2.15). The thickness of this structure is hard to define, because the inversion is poorly constrained by the data at depth (very low model resolution matrix values). A 200 m long conductive zone showing resistivities mostly lower than 10 k Ω m, occupies the flatter downslope area. The end of Ro-2 and Ro-1 cross ridges and furrows in a 250 m long convex zone toward the NW, contrasting with the previous concave zone. Resistivities reach 500 k Ω m under 3 to 5 m of conductive material (< 30 k Ω m), in a structure where model resolution matrix values are very low. The values decrease to 5-50 k Ω m in the 80 m located above the north steep fine-grained front (Ro-1). Finally, the south part of the cross-profile that cuts the distal zone (Ro-A) shows a 100 m large and approximately 25 m thick highly resistive structure (>500 k Ω m) under several meters of conductive material. This contrasts with moderate resistivities in the north (<150 k Ω m).

In Tsarmine, resistivities exceed 5000 k Ω m at a depth of 4-6 m over the whole width of the upper zone (Tsa-C). The prolongation of this structure is observable downslope (120 m long in the SE of Tsa-4 and 250 m long in Tsa-2 and in the SE of Tsa-1) but the resistivity values drop locally to 150 k Ω m. A 150 m long more conductive zone with patchy resistive structures ($2 < r < 300$ k Ω m, 15m thick, center of Tsa-4) occupies the slope located above the distal 300 m long rock glacier-like sector. In this zone (NW of Tsa-4 and Tsa-3), resistivities can exceed 1000 k Ω m under several meters of material with higher conductivity (<30 k Ω m). Tsa-B shows contrasted resistivities and Tsa-A illustrates the presence of a resistive structure (>150 k Ω m) a few meters below the surface of the flakt distal area. Finally, a conductive zone (< 30 k Ω m; NW of Tsa-1 and SW of Tsa-A) composes the southwestern margin near the lake.

The upper part of Entre la Reille contains a very resistive layer located close to the surface in the west concave part (>1000 k Ω m on Elr-1 and Elr-C). A 50 m long resistive layer (> 150 k Ω m; Elr-2 and SE of Elr-B) composes the east convex side, where surface deformation patterns are visible. Its thickness is around 20 m, but here the model resolution matrix values are low. The resistivities progressively drop toward the distal part and values become lower than 10k Ω m in the steep fine-grained front (Elr-1). Finally, a layer of moderate to high resistivities (<1000 k Ω m; Elr-A and Elr-B) is visible in the central zone below several meters of material with high conductivity.

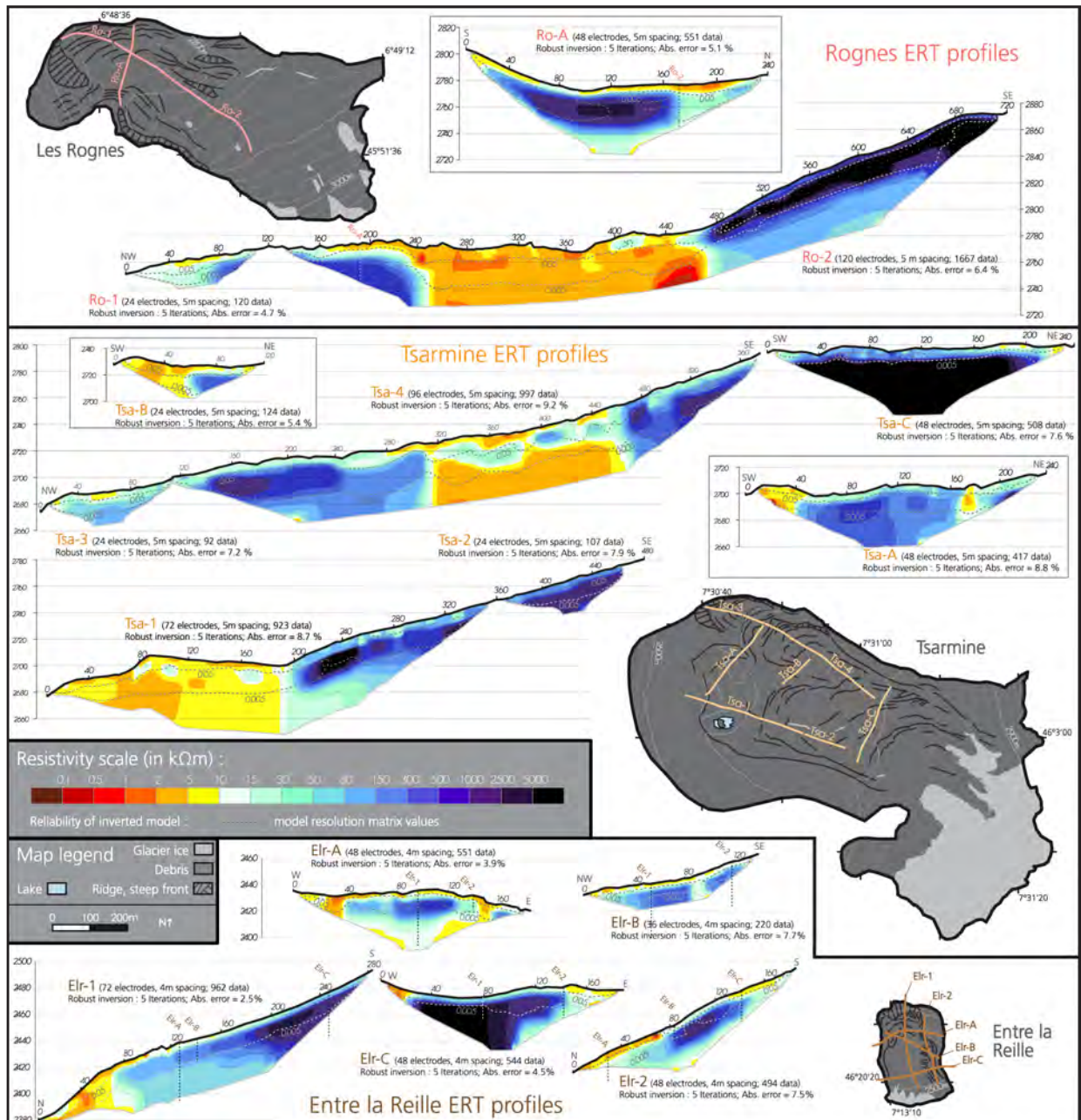


Fig. 2.15. Longitudinal (1 & 2) and transversal (A, B & C) electrical resistivity tomograms (ERT) profiles obtained in August 2012 in Rognes, in August 2014 in Tsarmine and between 2011 and 2013 in Entre la Reille

dGPS results

For each block, we calculated the total, yearly, seasonal and early/late summer horizontal (v_x), vertical (v_z) and surface lowering (v_h) velocities. Only the mean velocities (v) for the whole period are presented here to give an overview (Fig. 2.16A).

All the blocks in the Rognes system moved more than 0.02 m yr^{-1} between 2011 and 2014. The most significant velocities occur in the upper slope, with all component values being higher than $|0.25| \text{ m yr}^{-1}$. Here, surface lowering is smaller than -0.5 m yr^{-1} for many blocks. Downslope, most of the blocks are moving toward the central depression with moderate velocities ($v < |0.25| \text{ m yr}^{-1}$). The distal part is generally flowing toward the west and SW. v_x values sometimes exceed 0.5 m yr^{-1} whereas the v_z and v_h values are smaller (-0.05 to -0.25 m yr^{-1}) on the south part of the front than on the north.

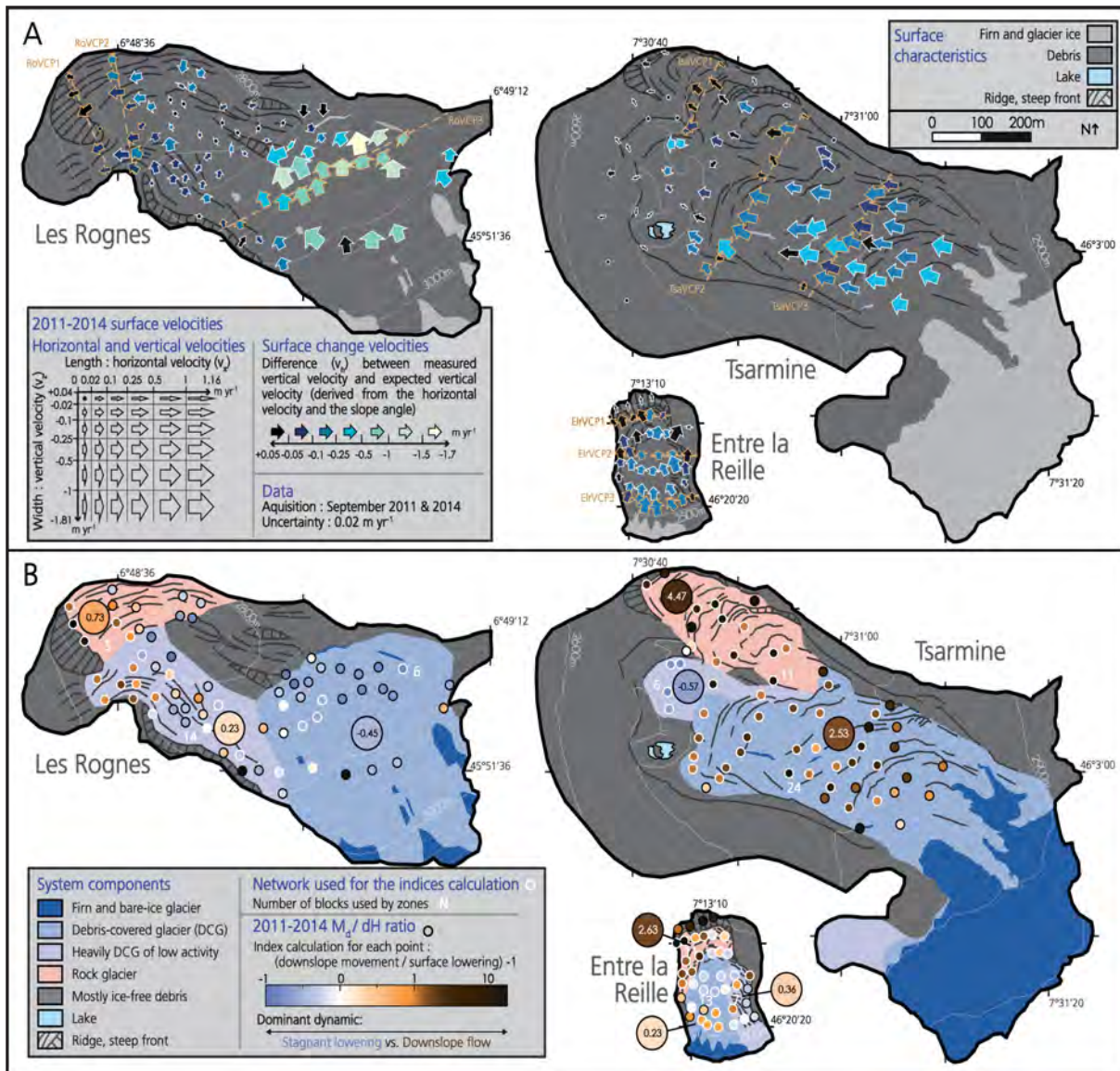


Fig. 2.16. A. Velocities measured with dGPS in the study sites between September 2011 and 2014. Orange lines correspond to the velocity cross-profiles of Figure 8 where the horizontal velocity of the points in orange is depicted. **B.** Components of the glacier systems and downslope movement / surface lowering (M_s/dH) ratio results based on the movements measured between September 2011 and 2014 (Figure 2.16A). The large circles correspond to the mean M_s / mean dH value by zone in each site. White circles correspond to the position of the dGPS network used for the calculation of the dynamical index in Figure 2.17.

In Tsarmine, the most striking behavior concerns the blocks situated in the upper zone, corresponding roughly to half of the blocks. Movements are homogeneous: v_x values toward the NW are faster than 0.5 m yr⁻¹, whereas v_z values range between -0.25 and -1 m yr⁻¹. The highest surface lowering ($v_h < -0.25$ m yr⁻¹) is observed here and in a small zone in the center of the distal part. Elsewhere, velocities are more variable. On the rock glacier, velocities are mainly significant in the horizontal component ($v_x > 0.1$ m yr⁻¹) and surface lowering is weak. The south frontal part experiences very slow multidirectional movements.

Entre la Reille is a completely active system, although velocities never exceed $|0.5|$ m yr⁻¹. v_x , v_z and v_h values range mostly between $|0.1|$ and $|0.25|$ m yr⁻¹ in the top and central part, corresponding to almost two thirds of the blocks. The margins show similar to smaller v_x and v_z values, but the surface lowering rate is weaker. The four blocks located on the steep fine-grained front reflect a slow horizontal north oriented flow ($v_x < 0.1$ m yr⁻¹).

System composition

ERT and dGPS results, field observations and historical documents provide coherent information on the system components. For example, the net changes in homogeneous surface kinematic behaviors between the top slopes and the distal flat zones in les Rognes or Tsarminé (Fig. 2.16A) precisely correspond to large contrasts of ground resistivity (Ro-2 and Tsa-1 in Fig. 2.15). The differences of resistivities also match spatially with differences in surface characteristics, such as the presence of ridges and ice outcrops, visible during the field campaign or on historical images. Another example is the upper zone of Entre la Reille. The concave left-hand side and the convex right-hand side, where superficial deformation patterns are numerous, clearly exhibit distinct ground resistivities. With all these consistent elements, five main homogeneous sectors can be defined, characterized (Tab. 2.5 and Tab. 2.6) and mapped (Fig. 2.16B) in each site.

Firn and bare-ice glacier zones occupy variable parts of the top of the glacier systems, changing each year in relation to the snow accumulation at the end of the melt season and the spread of the debris mantle. A thin (millimeters to decimeters) and discontinuous debris layer can cover the snow and ice. Buried ice is also exposed locally by supraglacial landslides and by incision related to water runoffs in the debris-covered zones. Currently, this sector is continuous and occupies a large area (0.11 km²; Tab. 2.6) at Tsarminé. Here, avalanches enhance the snow accumulation. Its metamorphosis in ice and downward flow is illustrated by the presence of crevasses (Fig. 2.12 and Fig. 2.13). In les Rognes, the size of this zone, where crevasses and bergschrund were visible in last decades (Fig. 2.13), is now very restricted. Conversely, the upper zone of Entre la Reille has been occupied only by a firn area whose extension has changed continuously over the last decades.

Debris-covered glacier zones are present in large portions of the systems (Tab. 2.6), generally in the top and central concave parts (Fig. 2.16B). They illustrate the progressive covering of the glaciers since the LIA. Crevasses are observable in these sectors on aerial images of les Rognes and Tsarminé until the early 2000's (Fig. 2.13). These zones may also have been temporarily covered by snow at the end of the ablation seasons over the last decades but this situation has become rare since the 1980's. The high measured resistivities (>500 kΩm, with extended zones >5000 kΩm) reveal

Part of the glacier system	Surface characteristics	Surface curvature	Massive ice outcrop	Water runoff in summer	Soil and vegetation	Debris cover (active layer) thickness	Ground resistivity	Surface velocity
Firn and bare-ice glacier	- Ice/snow surface varying between years - Locally covered by dust or debris - Crevasses (Tsa)	Concave (except avalanche cones in Tsa)	Everywhere	Visible and/or audible	Absent	Absent to few centimeters	Probably > 1000 kΩm	Probably several decimeters to meters per year
Debris-covered glacier	- Mainly coarse debris - Relatively undifferentiated topography (except in Tsa) - Arcuate rounded ridges (on Tsa, ELR) - Angular crest on the side (Tsa and ELR) - Rare gullies	Mainly concave	Rare	Visible and/or audible	Absent	Decimeters to meters	> 500 kΩm	Several decimeters to meters per year
Heavily debris-covered glacier of low activity	- Mainly coarse debris - Relatively differentiated topography - Angular crest on the side (Tsa and ELR) - Arcuate rounded ridges	Concave (Tsa) and convex (Ro, ELR)	Very rare	Rarely visible and/or audible	Absent	Several meters	> 100 kΩm	Centimeters to decimeters per year
Rock glacier	- Mainly coarse debris - Organized viscous topography - Arcuate ridges and furrows - Distal steep fine-grained front	Mainly convex	Absent	Absent	Absent (except rare developments in Ro)	Several meters	> 10 kΩm	Centimeters to decimeters per year
Mostly ice-free debris	- Coarse and fine debris - Angular crests on the side and arcuate rounded ridges	Mainly concave	Absent	Absent	Absent (ELR) to various stage of development	Meters to several tens meters of deglaciatiated debris	< 30 kΩm	Null to few centimeters per year

Tab. 2.5. Characteristics of the main components of these glacier systems

that these sectors are composed of massive sedimentary ice with probably low debris content. The current thickness of the glaciers is unknown, except in Tsarmine where a GPR survey in 2015 revealed respectively mean and maximum thickness of 15 and 35 m (Capt et al., 2016). According to its dimension and the height of the surrounding moraines, this glacier is likely the thickest of the three studied here. Supraglacial debris thickness can vary locally but generally increases downglacier (decimeters to meters according to ERT results and field observations). The surface topography is undifferentiated, except in Tsarmine, where many arcuate rounded ridges are present. They were generated by the compressive stress induced during the downward migration of the snow and ice accumulated in the 1960s to mid-1980s period (Capt et al., 2016). Water runoff is observable or audible in summer especially in gullies (Fig. 2.12). In each site, the fastest surface velocities were measured in these zones.

Heavily debris-covered glacier zones of low activity are present in some marginal areas. It starts at the foot of the backwall on the east of Entre la Reille and prolong downslope from the debris covered glacier parts in les Rognes and Tsarmine. The transition between these two sectors is gradational, even though several characteristics allow their distinction. Heavily debris-covered zones are also composed of buried massive ice but the concentration of englacial debris is probably higher, as revealed by lower resistivities (80-2500 kΩm). Moreover, the surface layer where the resistivity decreases is thicker, suggesting that the supraglacial debris layer here reaches several meters. It explains the rare observations of ice outcrops and runoff. Surface velocities are weak, exceeding rarely $[0.25]$ m yr⁻¹. The rounded ridges present in les Rognes and Entre la Reille probably result from the slow local viscous deformation. No crevasses or ice outcrops have been visible in these sectors over the last decades, illustrating the weak dynamic of these completely buried glacier zones (Fig. 2.13).

Rock glaciers occupy some frontal and lateral parts of the systems investigated. Again, the transition with the neighboring zones is gradational. ERT profiles exhibit generally lower resistivities than in the previous glacier zones. The moderate resistivities (10 - 150 kΩm) show the probable overall higher debris-concentration in the ground and the domination of ice-cemented structures. However, resistivities reach 2500 kΩm in some locations, illustrating the presence of massive ice lenses. No ice outcrops or evidence of water runoff were visible in these sectors during field investigations or in historical sources. The surface morphology, composed of arcuate ridges and furrows bounded by a steep fine-grained front, has not shown remarkable changes over the last decades (Fig. 2.12

and Fig. 2.13). It illustrates the long term slow viscous deformation of frozen debris. Currently, slow sub-horizontal movements dominate and surface lowering is very low.

	Les Rognes (area in km ² ; mean slope in °)	Tsarmine	Entre la Reille	Mean
Firn and bare-ice glacier	0.01; 39	0.11; 29	0.003; 33	0.04; 34
Debris-covered glacier	0.13; 24	0.15; 18	0.013; 23	0.10; 22
Heavily debris-covered glacier of low activity	0.05; 20	0.03; 17	0.009; 29	0.03; 22
Rock glacier	0.03; 12	0.04; 18	0.007; 28	0.03; 19
Mostly ice-free debris	0.09; 24	0.17; 28	0.010; 33	0.12; 28
All	0.29; 24	0.49; 25	0.042; 28	0.27; 26

Tab. 2.6. Area (in km²) and mean slope angle (in degree) of the main components of these glacier systems

Ice-free debris zones are essentially present in the steep distal areas (Tab. 2.6). The low resistivity values (0.5-30 k Ω m) show the generalized absence of ground ice. The debris thickness can reach several tens of meters. Patches of vegetation are present locally (Fig. 2). In Tsarmine, a small lake developed in this sector in the 1980's (Fig. 3). Surface movements are mainly lower than 0.1 m yr⁻¹.

Current dynamics

The *intensity of dynamics* was investigated by the calculation of annual, summer and winter v_x , v_z and v_h means (Fig. 2.17). Debris-covered parts of the glaciers have the highest velocities in all periods. The annual v_x , v_z and v_h means (< |0.5| m) are relatively homogeneous. In summer, v_x values are four times and v_z and v_h values more than thirteen times faster than during winter. Mean velocities exceed 1 m yr⁻¹ in summer and vertical and surface lowering values are especially high (< -1.6 m yr⁻¹). The latter are low in winter (> -0.14 m yr⁻¹), while v_x values remains relatively high at 0.28 m yr⁻¹. Seasonal variations are similar in heavily debris-covered glacier zones, although the overall velocity values are about three times lower. Annual velocities do not exceed |0.2| m yr⁻¹, summer velocities are limited to |0.67| m yr⁻¹ and winter values are minor (especially v_h). The situation is different in rock glaciers, where maximal velocities reach |0.25| m yr⁻¹. The v_x values are relatively constant during summer and winter. The main change concerns the summer acceleration and winter deceleration of v_z and v_h . On the annual timescale, the surface lowering is very weak (-0.04 m yr⁻¹).

The *temporal variation of dynamics* was assessed by computing the standard deviation of annual and seasonal velocities of all the individual years and quantifying the proportion of movement

Dynamical indexes		Debris-covered glaciers	Heavily debris-covered glaciers of low activity	Rock glaciers	Legend
Intensity of dynamics	Annual velocity				Horizontal velocity v_x (m yr ⁻¹) Vertical velocity v_z (m yr ⁻¹) Surface lowering v_h (m yr ⁻¹) Color scale for each index Min Max
	Summer velocity				
	Winter velocity				
Temporality of dynamics	Annual and seasonal variability of velocity				Standard deviation of annual velocities of seasonal velocities
	Proportion of summer activity on annual activity				Horizontal movement (%) Vertical movement (%) Surface lowering (%)
	Proportion of early summer activity on summer activity				
Main dynamics	Downslope movement vs. surface lowering				

Fig. 2.17. Mean values of dynamical indexes calculated by zones where ice and debris are associated in the three study sites with dGPS data. The dGPS network used for this calculation appears in Figure 2.16B

realized each season and each part of summer (Fig. 2.17). Debris-covered glacier zones have the highest Standard deviation values, indicating a high temporal variability of velocities. Most of the annual movements occur in summer (almost the whole surface lowering), whereas early and late summer activity is balanced. On the other hand, marginal rock glaciers experience low temporal velocity variability (standard deviation < 0.08) and generally winter dominant dynamics. Summer activity is mainly concentrated in late summer, especially in vertical and surface lowering components. Between these two opposing behaviors, heavily debris-covered glacier zones have moderate standard deviation values, summer and late summer dominant dynamics.

The *dominant dynamic* was evaluated by comparing downslope movement and surface lowering values (Fig. 2.16B and Fig. 2.17). Debris-covered glacier zones show the most heterogeneous M_d/dH values (Fig. 2.16B). Indeed, values were negative here in les Rognes and in the lower part of Entre la Reille and positive in the upper part of the latter and in Tsarmine. The mean value of 0.77 in these three zones reflects the slight domination of downslope flow (Fig. 2.17). M_d/dH values are also heterogeneous in heavily debris-covered glacier zones but the global mean suggests that downslope movement and surface lowering have similar magnitudes here. Finally, rather homogeneous values are found in rock glaciers, where M_d/dH is commonly above 1. The mean of 2.61 between these zones in the three sites illustrates the predominance of downslope flow.

The *motion mechanism* was inferred from 9 horizontal velocity cross-profiles (Fig. 2.18). Appearances of the velocity cross-profiles do not reveal undisputable cubic or parabolic patterns, showing the probable multiple origin of motion. For example, TsaVCP3 gathers cubic and parabolic aspects: at least 0.5 m yr^{-1} can be attributed to an en masse movement that adds up to the central velocity increase related to internal deformation. On the left hand side of RoVCP1, RoVCP2, RoVCP3, TsaVCP2, ElrVCP3, on TsaVCP3 and on the right hand side of ElrVCP2, the rapid increase of velocity from the margin and/or the main tabular-shape of velocity profiles indicate the likely occurrence of basal sliding. Conversely, the profiles are arcuate and velocity progressively increases

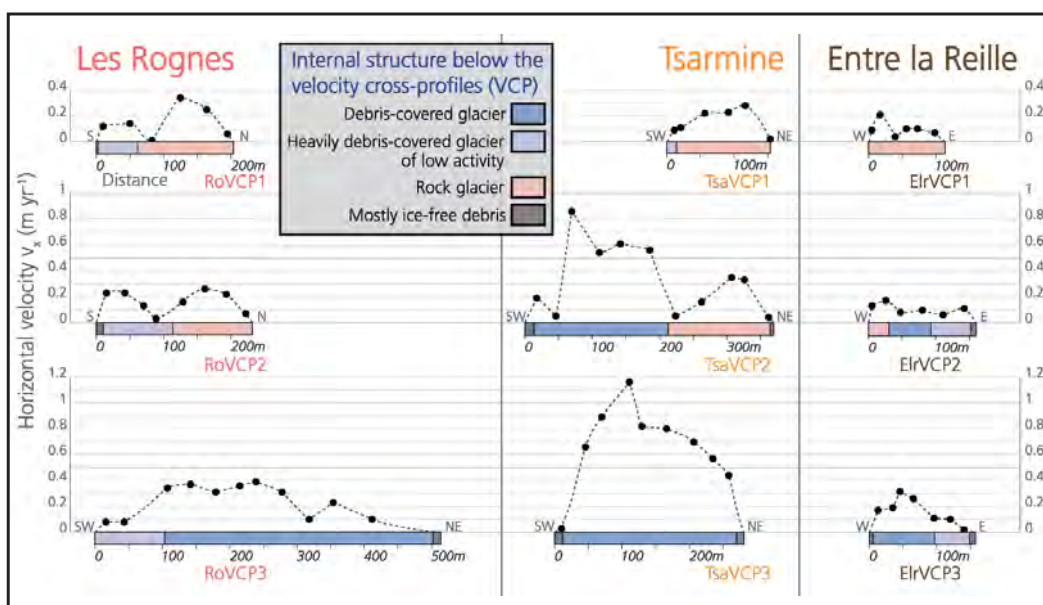


Fig. 2.18. Velocity cross-profiles (VCP) obtained from horizontal velocities between September 2011 and 2014 and internal structure below each profile. The 9 cross-profiles and the data used are depicted in Figure 2.16A.

toward the central flowline in the northern side of RoVCP1, RoVCP2, TsaVCP2 and on TsaVCP1 and ElrVCP1, reflecting the effect of internal deformation. Thus, basal sliding seems important in (heavily) debris-covered zones whereas the rock glaciers appear mainly affected by internal deformation.

2.2.2.5. Interpretation and discussion

Internal structure

Fig. 2.19 synthesizes our interpretation of the internal structure of the main components encountered in the study sites. The comprehensive results obtained are in line with the internal structure characteristics proposed in this type of landsystem by individual site studies (e.g. Kneisel, 2003; Reynard et al., 2003; Kneisel and Kääh, 2007; Ribolini et al., 2010; Monnier et al., 2014). At the system scale, atypical characteristics differentiate the study sites from the larger and bare-ice glacier stereotype: the small size of the upslope firn and bare-ice zones and the associated large relative area of debris-covered glacier zones, the existence of marginal rock glaciers and the overall very high amount of debris in comparison with the glacier size. The glacier zones are extensively covered by a coarse-grained debris layer that thickens downglacier due to flux emergence, compressive stress and ice melt (Kirkbride and Deline, 2013). This also explains the debris concentration increase in the glacier margins. These very small glaciers have, therefore, typical characteristics of buried glaciers (Ackert, 1998; Janke et al., 2015). In rock glaciers, large ranges of ground electrical resistivities were measured (Fig. 2.15), outlining the coexistence of ice-cored and ice-cemented structures under the several meters thick unfrozen surface layer. The decrease of ice concentration and increase of surface debris layer thickness distinguish rock glaciers from debris-covered glaciers here, as proposed by Janke et al. (2015). Finally, ice-free debris areas are present in the frontal and some lateral zones of the studied systems.

Surface movements and associated processes

Fig. 2.19 also synthesizes the current responses to short-term climatic variations detected in the studied systems. Two main dynamics are active: (1) surface lowering, which can be related to ice melt and extending flows (Lambiel and Delaloye, 2004); and (2) downslope movement, which can result from internal deformation, basal sliding and bed deformation (Haeberli et al., 2006; Benn and Evans, 2010). Only ice melt, basal sliding and internal deformation are considered here, since we have no data on the possible bed deformation. Moreover, extending flows that occurs locally (Fig. 2.16A) were not quantified as the thickness of the deforming bodies is largely unknown. However, ridges and furrows and surface velocities suggest the large domination of compression. We interpret, therefore, surface lowering (v_n) mainly as an expression of ice melt rather than extending flow. Its high value in stagnant zones or where compressive stress would compensate surface lowering (e.g. the footslope of the debris-covered zone of les Rognes) supports this interpretation. The dynamical behaviors of debris-covered glacier zones, heavily debris-covered glacier zones of low activity and rock glaciers are respectively discussed in the following paragraphs.

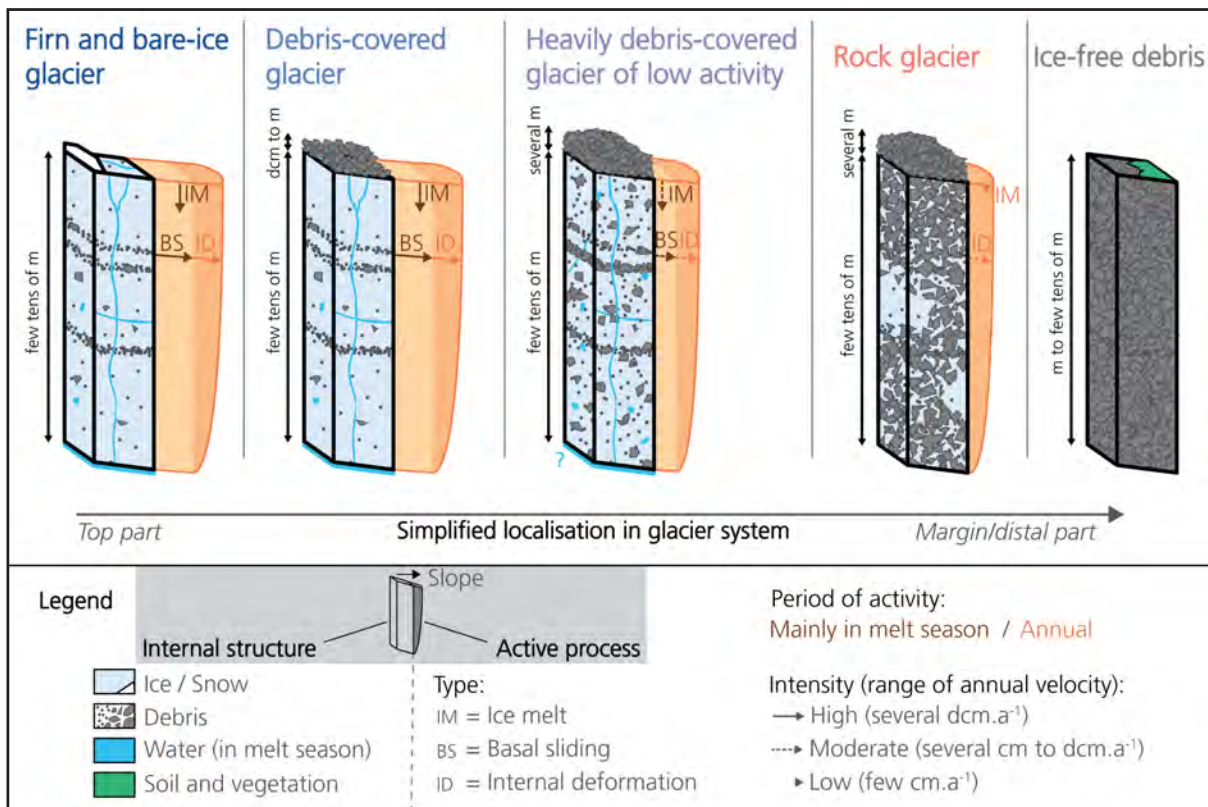


Fig. 2.19. Schematic diagrams showing the internal structure characteristics and the main dynamics occurring in the five main zones of les Rognes, Tsarmine and Entre la Reille systems

Polythermal glaciers are common in permafrost environments (Etzelmüller and Hagen, 2005; Gilbert et al., 2012). This situation may characterize the studied glaciers (Bosson et al., 2015). However, the proportion of cold ice seems low at the base of the debris-covered glacier zones if we consider, as other authors, basal sliding signature as an indicator of temperate ice (Mayer et al., 2006; Bingham et al., 2008; Fig. 2.18). The basal sliding pattern also clearly appears at the decadal timescale at Tsarmine glacier (Capt et al., 2016). The influence of water here is likewise supported by the marked seasonal variation of surface velocities, the recording of maximum horizontal velocities in early summer when the water production is very high and field observations and audition of water circulation. Hence, these sectors, where an efficient drainage network can be present (Pourrier et al., 2014), show rapid responses to climatic and hydraulic forcing during the melt season. Our results suggest the following annual behavior. The snow cover strongly decouples the glacier from the atmosphere between October and June. Surface lowering is slight and horizontal movements produce half of the annual total (Fig. 2.17). Winter motion is mainly attributed to internal deformation because basal sliding often deactivates (Anderson et al., 2004; Bingham et al., 2006). During summer, the ablation rate is very high and induces most of the annual surface lowering (91%). The water supply increases the flow. Mean v_x decreases in late summer, probably because of the drainage network development at the glacier bed (Anderson et al., 2004; Rippin et al., 2005; Bingham et al., 2006). The maximum movements are then observed in the zones where water runoffs are concentrated, as in the SW of Tsarmine (Fig. 2.12 and TsavCP3 and TsavCP2 of Fig. 2.18).

The presence and influence of water is also possible in heavily debris-covered glacier zones, considering its summer observation and audition, the cubic shape of velocity cross-profiles (Fig. 2.18) and the summer dominant activity (Fig. 2.17). However, Evans (2013) suggested that viscous surface patterns, as observed in these sectors in les Rognes and Entre la Reille, illustrate a cold thermal regime and therefore low water content. Ice melt, basal sliding and ice deformation seem active here but with a weaker intensity than in debris-covered glacier zones (Fig. 2.17). The period of activity is brought forward to late summer and winter because of the filtering of short-term climatic variations by the weakly thermally conductive thick debris cover.

The motion of rock glaciers appears mostly due to internal deformation. Water content and influence seem low: no water runoff was heard during field campaigns, velocity cross-profiles have a parabolic aspect, dynamics occur mainly in winter and mean v_x is relatively stable over the year (Fig. 2.17). However, water can be temporarily present in rock glaciers and influence their dynamics (Haeberli et al., 2006; Hausmann et al., 2007; Delaloye et al., 2008). It could explain the slight increase in velocities observed in summer. Surface lowering is almost ineffective at the annual timescale, illustrating the low ice melt. Thus, only internal deformation seems noticeably effective here and short-term climatic variations induce attenuated and shifted responses. This behavior contrasts, therefore, with the one observed in the upper glacier zones. Its origin is mainly related to the filtering and slow propagation of summer temperatures in the poorly conductive thick superficial debris layer (Delaloye et al., 2008), the limited ice concentration, and if water is present, its probable slow and diffuse circulation (Pourrier et al., 2014).

In the studied systems, direct and high-magnitude responses contrast with delayed and attenuated responses to short-term climatic variations. This different climate sensitivity appears mainly related to the proportion of ice, debris and water (and associated hydrological network properties) in the ground and the thickness of the superficial debris layers (Fig. 2.19). This is in accordance with previous studies, which illustrated the influence of these factors individually: climate sensitivity in ice-debris associations decreases when the ice concentration reduces (Kääb et al., 1997), when the superficial debris layer thickness increases (Benn et al., 2003; Kirkbride and Deline, 2013), when the water content decreases (Schomacker and Kjær, 2007) and when the water circulations are null or rare and diffuse (Pourrier et al., 2014). Finally, null to very slow movements were measured in the ice-free debris zones, illustrating the strong control of ice content on surface dynamics (Fig. 2.16A).

Genesis and evolution

The genesis of the studied systems has to be considered in light of the numerous Holocene climatic oscillations, although their current structures are mainly related to the last glacial pulse (LIA and subsequent decay; Ackert, 1998; Matthews et al., 2014; Monnier et al., 2014). Indeed, the extent of both glacier and debris-covered zones probably continuously oscillated over the last millennia in relation to climatic variations (e.g. Ivy-Ochs et al., 2009). During positive mass balance periods, glaciers were larger than today and progressively accumulated lopsided amounts of sed-

iments at their bed and margins. Their accumulation areas shrank and even disappeared under warmer and/or drier conditions, as it has occurred since the end of the LIA. Unable to evacuate the debris provided by the bed erosion and weathering of the backwalls, these very small rag glaciers progressively became stagnant, downwasting and buried ice bodies (Bosson et al., 2015; Carrivick et al., 2015; Capt et al., 2016). With their regular concave topography and dominating stagnant lowering dynamic, les Rognes and Entre la Reille glaciers will likely transform into buried ice patches (Serrano et al., 2011), then talus slopes (Gomez et al., 2003) with the projected future deglaciation context (e.g. Huss and Hock, 2015). Conversely, Tsarmine glacier still retains a flow-dominant dynamic (Fig. 2.16B), due to its larger thickness and the presence of a small accumulation area upslope. The studied glaciers thus illustrate distinct stages of debris-covered glacier decay in the negative mass balance periods.

The studied rock glaciers have numerous ridges at their roots, illustrating their probable deformation by glacier advances during positive mass balance periods such as the LIA. These so-called push moraines are very common at the cold glacier margins in permafrost environments (Etzelmüller and Hagen, 2005; Matthews et al., 2014; Dusik et al., 2015). As it currently occurs in the study sites (Fig. 2.16B and Fig. 2.17), differential flow and ablation induce the progressive disconnection between rock glaciers and the upslope glacier zones in negative mass balance periods (Ackert, 1998; Ribolini et al., 2010; Lilleøren et al., 2013). The internal structure to the North of Tsarmine illustrates this situation: a lens of sedimentary ice (distal zone of Tsa-4; Fig. 2.15) may have been recently integrated into the distal former frozen sediments (Tsa-3). Conversely, ice rapidly melts in the concave rooting zone, disconnecting the flowing rock glaciers from the upslope vanishing glacier zones. The long-term individual flow of ice-debris mixtures, weakly sensitive to climatic variations, explains, therefore, the development of rock glaciers at the system margins (Ackert, 1998; Berthling, 2011). This illustrates the morphodynamical continuum that can exist between glacial and periglacial processes, which coexist or follow each other according to climatic variations in these permafrost environments (Benn et al., 2003; Whalley, 2009; Berthling et al., 2013).

2.2.2.6. Conclusion

This study proposes a comprehensive analysis of the relationship between the structure and the current evolution of small debris-covered glaciers located in permafrost environments. The systems studied are complex assemblages of heterogeneous dynamical components, comprised of five sectors associating ice and/or debris in various proportions. Their genesis and organization is related to Holocene climatic fluctuations and illustrate the morphodynamical continuum between glacial and periglacial processes that can exist locally in high mountain environments.

Overall, the same components and dynamics were found in the three sites. The top slopes are almost entirely composed of sedimentary ice, which outcrops or is covered by snow or debris. They experience the most intense and direct responses to climatic variations. The magnitude of surface lowering and downslope motion, a consequence of ice melt, internal deformation and

basal sliding, are at least three times higher than in the other sectors. The summer dominant activity shows the noticeable control of warm temperatures and water circulation. In neighboring heavily debris-covered glacier zones of low activity, englacial debris proportion is higher and the supraglacial debris layer is thicker. Consequently, these sectors are less sensitive to the climate and dynamical responses are delayed and attenuated. Active rock glaciers are present in some marginal areas. Their internal structure consists of ice-cored or ice-cemented debris. They experience very low ice melt. The slow flow mainly occurs in winter and progressively detaches them from upslope glaciers. Finally, weakly active ice-free debris are also present.

These results show that direct and high-magnitude responses contrast with delayed and attenuated responses to climate forcing. The variation of ice, debris and water concentration and of the superficial debris layer thickness mainly control this differential evolution. The extended debris cover slows down the ice melt here compared to the rapid decline currently observed in bare-ice glaciers. Their role as local freshwater reservoirs will, therefore, become increasingly important in the next decades. In future research, the results obtained here need to be completed, especially by combining glaciological and geomorphological approaches. In particular, quantification of ice and debris content, hydrological processes and ice origin are avenues worth exploring.

Acknowledgements

The repeated field investigations would have been impossible to carry out without the help of numerous people. In addition to the authors, during the 38 days of field investigations performed between September 2011 and 2014, 32 other people have contributed to collecting the data synthesized in this article. We sincerely thank them for their indispensable and generous help. We also acknowledge the teams of *Glacier 3000*, *Compagnie du Mont-Blanc*, *Remontées Mécaniques des Houches*, *Refuge du Nid d'Aigle*, *Cabane des Diablerets*, the *municipality of Evolène* and the *Service des forêts et du paysage du Canton du Valais* for logistical support and the Dumas, Katz and Anzévi families for lending local accommodation. This manuscript has been improved thanks to the precious critics and comments of N. Deluigi, A. Tahir, T. Ferber, M. Huss and the two anonymous reviewers. M. Blake is acknowledged for proofreading the English text.

2.3. Paper 3:

Decadal evolution of a very small heavily debris-covered glacier in an Alpine permafrost environment

Journal of Glaciology, 2016

Journal of Glaciology (2016), Page 1 of 17

doi: 10.1017/jog.2016.56

© The Author(s) 2016. This is an Open Access article, distributed under the terms of the Creative Commons Attribution licence (<http://creativecommons.org/licenses/by/4.0/>), which permits unrestricted re-use, distribution, and reproduction in any medium, provided the original work is properly cited.

Decadal evolution of a very small heavily debris-covered glacier in an Alpine permafrost environment

M. CAPT,¹ J.-B. BOSSON,¹ M. FISCHER,² N. MICHELETTI,¹ C. LAMBIEL¹

¹Institute of Earth Surface Dynamics, University of Lausanne, Lausanne, Switzerland

²Department of Geosciences, University of Fribourg, Fribourg, Switzerland

Correspondence: J.-B. Bosson <jeanbaptiste.bosson@gmail.com>

ABSTRACT. Glacier response to climate forcing can be heterogeneous and complex, depending on glacier system characteristics. This article presents the decadal evolution of the Tsarmin Glacier (Swiss Alps), a very small and heavily debris-covered cirque glacier located in the Alpine periglacial belt. Archival aerial photogrammetry and autocorrelation of orthophotos were used to compute surface elevation, volume and geodetic mass changes, as well as horizontal displacement rates for several periods between 1967 and 2012. A GPR survey allowed us to investigate glacier thickness (15 m mean) and volume ($4 \times 10^6 \text{ m}^3$) in 2015 and to anticipate its future evolution. Different dynamics occurred in recent decades because of the heterogeneous surface characteristics. The climate-sensitive upper debris-free zone contrasts with the progressively stagnant heavily debris-covered glacier tongue. Between 1967 and 2012, the glacier lost 1/3 of its initial volume ($2 \times 10^6 \text{ m}^3$). The average mass balance stabilised at $\sim -0.3 \text{ m w.e. a}^{-1}$ since 1999. Compared with other local glaciers, the Tsarmin Glacier shows a particular decadal behaviour both in time (divergence of mass balance since the 2000s) and space (inverted ablation pattern). This might be explained by the combined influence of debris cover, shadow, snow redistribution and permafrost conditions on this very small glacier.

KEYWORDS: climate change, debris-covered glaciers, glacier mass balance, mountain glaciers, permafrost

1. INTRODUCTION

Knowledge about the global response of the >200 000 glaciers on Earth to climate change has considerably improved in recent years (Vaughan and others, 2013; Pfeffer and others, 2014), especially through large-scale modelling (e.g. Gardner and others, 2013; Radić and others, 2014; Huss and Hock, 2015). On a local scale, however, large uncertainties remain for individual glaciers because processes and glacial dynamics are implemented in a simplified manner in the models. Indeed, each glacier shows specific behaviour to some extent, influenced by local topoclimatic factors, glacier hypsometry or surface characteristics (Carturan and others, 2013a; Fischer and others, 2015). These particularities may generate non-linearities that complicate the response of glaciers to climate change (Paul and others, 2007; Scherler and others, 2011; Carrivick and others, 2015). Understanding of this local complexity and its integration in global approaches remain a major task (Huss, 2012; Huss and Fischer, 2016; Pellicciotti and others, 2015).

In high-relief environments, three characteristics can strongly influence the individual response of glaciers to climatic variations: (1) small glacier size, (2) debris cover on the ice and (3) permafrost conditions. These characteristics affect an increasing number of mountain glaciers with the current rise in the ELA (Benn and others, 2003; Vaughan and others, 2013). Indeed, shrinking glaciers are becoming smaller and thinner. Glacier melt is especially rapid in temperate environments and glaciers tend to be confined within the coldest areas of the Earth's surface (e.g. Huss, 2012; Huss and Hock, 2015). Moreover, because ice deformation is related to ice thickness, the dynamics of

shrinking glaciers is decreasing (Paul and others, 2007) and their capacity to evacuate their sediment load is thus reducing. At the same time, deglaciation and permafrost degradation in the surrounding relief increase the debris supply. As a result, supraglacial debris covers are expanding on mountain glaciers (Carturan and others, 2013a; Kirkbride and Deline, 2013).

Very small glaciers (<0.5 km²) have a reduced motion (Haeberli, 1985; Benn and others, 2003; Paasche, 2012). Usually too thin to allow noticeable ice deformation, they are also weakly affected by basal processes. The production of meltwater and the shear stress acting on the glacier bed are both limited. In general, these glaciers react more rapidly to climatic variations (Jóhannesson and others, 1989; Kuhn, 1995; Colucci and Guglielmin, 2014). Due to the small altitudinal range, variations in the ELA of these glaciers rapidly change the proportion of accumulation and ablation areas, and strongly impact on glacier mass balance. On the other hand, the influence of the surrounding topography on small cirque glaciers can significantly attenuate their climate sensitivity (DeBeer and Sharp, 2009; Carturan and others, 2013b; Scotti and others, 2014). Accumulation and ablation anomalies occur in relation to the snow redistribution by avalanches, shadow effects or the presence of a debris cover. They can decouple the climatic control on mass-balance variations. Debris covers exceeding several decimetres in thickness are especially efficient thermal insulator layers and significantly reduce the ablation rate (Benn and others, 2003; Deline and others, 2012). Finally, permafrost conditions can strongly influence glacier dynamics. The thermal regime of the glacier can be cold or polythermal because of the surface and basal energy balance (Etzelmüller and

[G](#) | First page of the article 3

2.3.1. Presentation:

Decadal evolution of a very small heavily debris-covered glacier in an Alpine permafrost environment*Citation*

Capt M, Bosson JB, Fischer M, Micheletti N and Lambiel C (2016). Decadal evolution of a small heavily debris-covered glacier located in Alpine permafrost environment. *Journal of Glaciology* 62(233), 535-551. Doi: 10.1017/jog.2016.56

Scope and research questions

- The small glacier size, the presence of an extensive and thick debris cover, as well as permafrost conditions can strongly control glacier behaviour. Empirical data are needed to analyse the influence of these characteristics on glacier dynamics. *Do they generate atypical glacier behaviours at decadal timescale? What are the main responses of SDCGSAPE at this timescale? Are they affected by the same general dynamics than those observed in alpine glaciers (rapid mass loss and decrease of driving stress)?*
- Geometry (area, thickness and volume) of small debris-covered glaciers is barely known. *What is the current geometry of Tsarmine glacier?*

Approach and content

The decadal variations of surface elevation and horizontal surface displacements, as well as the current geometry of the Tsarmine glacier are investigated. Height digital elevations models are produced from archival aerial photogrammetry between 1967 and 2012 and compared to obtain surface elevations changes. The decadal geodetic mass balance and spatial patterns of surface elevation changes of the Tsarmine glacier are compared with those of other local glaciers. Horizontal surface displacements are studied with autocorrelation of orthophotos and feature tracking. Ground penetrating radar data allows us to investigate the current glacier geometry and anticipate its future evolution.

Main outcomes

- **Differential elevation changes were observed in the last decades. The upper bare-ice zone was especially highly sensitive to summer temperature variations** and exhibited up to 30 m of surface lowering between 1967 and 2012. Conversely, **the weaker dependence to climatic variations of the heavily debris covered tongue results in lower surface elevation changes**. Up to 10 m of uplift related to the transfer of the ice accumulated upslope and to the associated increase of compressive stress are even observable locally at the 45 years' scale. The propagation of this mass induced local acceleration of velocities. **The glacier motion decreased in the last decades**, in relation with the reduction of ice thickness, surface gradient and mass turnover. The glacier shows an *en masse* flow, probably due to its basal sliding.
- **The mean and maximum thickness and volume of the Tsarmine glacier in 2015 are respectively 15 m, 35 m and $4 \times 10^6 \text{ m}^3$. The glacier lost one third of its volume between 1967 and 2012** (average mass balance of $-0.15 \text{ m w.e.yr}^{-1}$). The mass balance was positive between 1967 and 1983. Significant negative mass balance was then experienced until 1999, mostly due to the melt of snow and ice accumulated in the previous decades. The mass balance finally stabilised around $-0.3 \text{ m w.e.yr}^{-1}$ since 1999. This value is less negative than the one measured in other local glaciers or at the alpine scale. Maximum melt occurred in the upper half of the Tsarmine glacier, highlighting the inversion of the ablation pattern observed on local glaciers. **The Tsarmine glacier exhibited thus an atypical temporal and spatial behaviour at decadal timescale. The influence of topography, debris cover and permafrost conditions upon accumulation and ablation of this very small glacier explains its relative limited decline during the period of analysis.**
- The decadal behaviour of the Tsarmine glacier illustrates that **consequences of glacier-hostile conditions as thinning or front retreat are less experienced by debris-covered glaciers because the debris layer limits the climatic control in the ablation area**. Conversely, **consequence of favourable conditions, as the transfer of mass gain down-glacier are more visible at their surface**. The **distal damming** of heavily debris-covered glaciers by sediment accumulation probably also participate to the **increase of compressive stress** that can generate uplifts or limit downwasting.

Personal contribution

We designed this research with C. Lambiel as a master thesis proposition to get complementary data and analysis at decadal timescale for my PhD thesis. M. Capt led this research under our supervision, mainly by using the photogrammetric data produced by N. Micheletti. I collected additional GPR, climatic and glaciological data, especially with M. Fischer. who processed the GPR data and designed the figures 2.26 & 2.28. M. Capt wrote the basis for this paper and prepared some of the figures. I produced the final figures and wrote the final version of the manuscript which was noticeably improved by the constructive comments and corrections of co-authors.

2.3.2. Content:

Decadal evolution of a very small heavily debris-covered glacier located in an permafrost environment

M. Capt¹, J.-B. Bosson¹, M. Fischer², N. Micheletti¹ & C. Lambiel¹

¹ Institut des dynamiques de la surface terrestre - Université de Lausanne, LAUSANNE, SWITZERLAND ;

² Department of Geosciences – University of Fribourg, FRIBOURG, SWITZERLAND

Abstract

Glacier response to climate forcing can be heterogeneous and complex, depending on glacier system characteristics. This article presents the decadal evolution of the Tsarmine Glacier (Swiss Alps), a very small and heavily debris-covered cirque glacier located in the Alpine periglacial belt. Archival aerial photogrammetry and autocorrelation of orthophotos were used to compute surface elevation, volume and geodetic mass changes, as well as horizontal displacement rates for several periods between 1967 and 2012. A GPR survey allowed us to investigate glacier thickness (15 m mean) and volume ($4 \times 10^6 \text{ m}^3$) in 2015 and to anticipate its future evolution. Different dynamics occurred in recent decades because of the heterogeneous surface characteristics. The climate-sensitive upper debris-free zone contrasts with the progressively stagnant heavily debris-covered glacier tongue. Between 1967 and 2012, the glacier lost one third of its initial volume ($2 \times 10^6 \text{ m}^3$). The average mass balance stabilised at around $-0.3 \text{ m w.e. a}^{-1}$ since 1999. Compared with other local glaciers, the Tsarmine Glacier shows a particular decadal behaviour both in time (divergence of mass balance since the 2000s) and space (inverted ablation pattern). This might be explained by the combined influence of debris cover, shadow, snow redistribution and permafrost conditions on this very small glacier.

Keywords

Debris-covered glacier, very small glacier, permafrost environments, geodetic mass balance, glacier geometry

2.3.2.1. Introduction

Knowledge about the global response of the $> 200,000$ glaciers on Earth to climate change has considerably improved in recent years (Vaughan et al., 2013; Pfeffer et al., 2014), especially through large-scale modelling (e.g. Gardner et al., 2013, Radić et al., 2014; Huss and Hock, 2015). On a local scale, however, large uncertainties remain for individual glaciers because processes and glacial dynamics are implemented in a simplified manner in the models. Indeed, each glacier shows specific behaviour to some extent, influenced by local topoclimatic factors, glacier hypsometry or surface characteristics (Carturan et al., 2013a; Fischer M. et al., 2015). These particularities may generate non-linearities that complicate the response of glaciers to climatic variations (Paul et al. 2007; Scherler et al., 2011; Carrivick et al., 2015). Understanding of this local complexity and its integration in global approaches remain a major task (Huss, 2012; Pellicciotti et al., 2015; Huss and Fischer, 2016).

In high relief environments, three characteristics can strongly influence the individual response of glaciers to climatic variations: (1) small glacier size, (2) debris cover on the ice and (3) permafrost conditions. These characteristics affect an increasing number of mountain glaciers with the current rise in the ELA (Benn et al., 2003; Vaughan et al., 2013). Indeed, shrinking glaciers are becoming smaller and thinner. Glacier melt is especially rapid in temperate environments and glaciers tend to be confined within the coldest areas of the Earth's surface (e.g. Huss, 2012; Huss and Hock, 2015). Moreover, because ice deformation is related to ice thickness, the dynamics of shrinking glaciers is decreasing (Paul et al., 2007) and their capacity to evacuate their sediment load is thus reducing. At the same time, deglaciation and permafrost degradation in the surrounding relief increase the debris supply. As a result, supraglacial debris covers are expanding on mountain glaciers (Carturan et al., 2013a; Kirkbride and Deline, 2013).

Very small glaciers (< 0.5 km²) have a reduced motion (Haeberli, 1985; Benn et al., 2003; Paasche, 2012). Usually too thin to allow noticeable ice deformation, they are also weakly affected by basal processes. The production of melt water and the shear stress acting on the glacier bed are both limited. In general, these glaciers react more rapidly to climatic variations (Jóhannesson et al., 1989; Kuhn, 1995; Colucci and Guglielmin, 2014). Due to the small altitudinal range, variations in the ELA of these glaciers rapidly change the proportion of accumulation and ablation areas, and strongly impact on glacier mass balance. On the other hand, the influence of the surrounding topography on small cirque glaciers can significantly attenuate their climate sensitivity (DeBeer and Sharp, 2009; Carturan et al., 2013b; Scotti et al., 2014). Accumulation and ablation anomalies occur in relation to the snow redistribution by avalanches, shadow effects or the presence of a debris cover. They can decouple the climatic control on mass balance variations. Debris covers exceeding several decimetres in thickness are especially efficient thermal insulator layers and significantly reduce the ablation rate (Benn et al., 2003; Deline et al., 2012). Finally, permafrost conditions can strongly influence glacier dynamics. The thermal regime of the glacier can be cold or polythermal because of the surface and basal energy balance (Etzelmüller and Hagen, 2005; Cuffey and Paterson, 2010). Otherwise, repeated freeze/thaw cycles increase the sediment production in the surrounding relief (Deline et al., 2015) and the amount of debris deposited on the glacier surface. Ablation rate is then significantly reduced in these environments when the thickness of the debris cover is close to that of the permafrost active layer (i.e. seasonally thawing layer; Lilleøren et al., 2013). At the glacier margins, the deposition of the large amount of debris may induce the build-up of moraine dams (Benn et al., 2003; Iturrizaga, 2013). Complex glacier/permafrost interactions can also occur around the glacier (Ackert, 1998; Berthling et al., 2013). Thereby, the presence of cold ice, a moraine dam and/or a rock glacier commonly restrain the glacier's downward flow under permafrost conditions (Kirkbride and Deline, 2013). Consequently, very small heavily debris-covered glaciers located in permafrost environments often react with thickness variations rather than length changes.

Studies focusing on this type of glacier are relatively few and are led by geomorphological rather than glaciological questions. Mainly focused on glacier-permafrost interactions, research has characterised the internal structure (e.g. Reynard et al., 2003; Ribolini et al., 2010) and its relation

to glacier dynamics or hydrology (e.g. [Kneisel and Käab, 2007](#); [Pourrier et al., 2014](#); [Seppi et al., 2015](#); [Bosson and Lambiel, 2016](#)). There have been fewer studies on the decadal behaviour of these glaciers and, at this timescale, their past and future evolution still remains largely unknown. This paper combines remote sensing and geophysical surveys to determine the response of a very small mountain glacier in the Swiss Alps to climate variations over the past five decades. Changes in surface elevation and ice dynamics were assessed for successive observation periods by comparing high-precision DEMs with aerial images. Geodetic glacier mass balance was computed for each period. In addition, a GPR survey was carried out to determine the current ice thickness distribution and glacier volume. Finally, we compare the decadal evolution of the Tsarmine Glacier with other local glaciers to uncover potential particularities in the behaviour of very small and heavily debris-covered cirque glaciers located in permafrost environments.

2.3.2.2. Study site and climatic context

The Tsarmine glacier system

The Tsarmine Glacier system is located in the Arolla valley in Switzerland (46°03'N, 7°31'E; 0.49 km²; 2600-3070 m a.s.l.; [Fig. 2.20](#)). Detailed geomorphological analysis and mapping of this complex assemblage of interacting landforms can be found in [Lambiel et al. \(2004\)](#), [Micheletti et al. \(2015a\)](#) and [Bosson and Lambiel \(2016\)](#). This very small cirque glacier (0.25 km² in 2015) occupies the foot of the 400-600 m high rock walls of the Grande Dent de Veisivi and Blanche de Perroc. Until the 1980s, a north-facing ice apron covered the latter ([Delaloye, 2008](#)). Nowadays, the rock walls are affected by strong rockfall activity. For instance, a major rockfall occurred in near the top of the west face of the Grande Dent de Veisivi in September 2015, following an extraordinarily warm summer. The presence of water in the scarp coming from ice melt indicated the existence of permafrost conditions in the area.

Situated at the shade-dominated base of Blanche de Perroc between 3070 and 2920 m a.s.l., the uppermost debris-free part of the glacier receives little solar radiation (zone 1; [Fig. 2.20c](#)). Avalanching enhances snow accumulation, leading to a cone-like surface morphology. Below, down to ~ 2830 m a.s.l., a discontinuous and relatively thin (millimetres to decimetres) layer of debris covers the glacier today (zone 2a; [Fig. 2.20c](#)). This zone showed continuous variation in surface conditions (debris-free vs. debris-covered) in recent decades, but overall the debris cover progressively extended upward through time. Down-slope, a thick (decimetres to few metres) and continuous debris mantle has been present since at least 1967 (zone 2b; [Fig. 2.20c](#)). The supraglacial layer is made up of coarse-grained angular deposits of rockfalls, indicating their passive transfer on the glacier. Ice outcrops become very rare and are related to thermokarstic erosion. Arcuate round ridges are visible on the surface ([Fig. 2.20c](#)). The debris layer, which thickens down-slope, masks the lower limits of the glacier. It was detected with electrical resistivity tomography (ERT) near 2715 m a.s.l. ([Bosson and Lambiel, 2016](#)). These results also allowed distinguishing debris-covered dead ice (zone 3; [Fig. 2.20c](#)) from ice-free debris located around a proglacial lake (zone 5 and 6). Down-slope, a large gullied moraine dam delimits the Tsarmine system. Accumulated during the

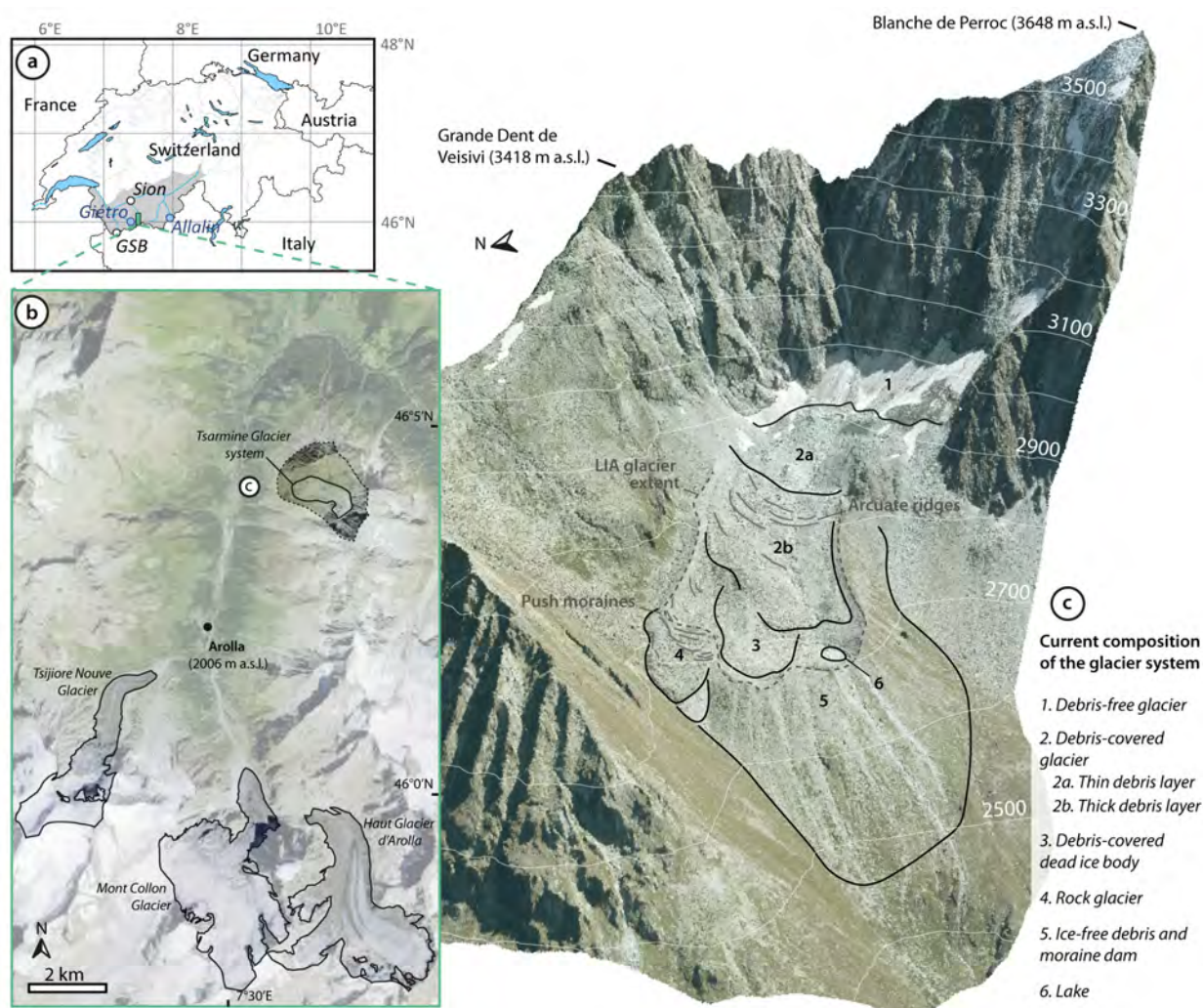


Fig. 2.20. Geographic setting and main components of the Tсарmine Glacier system: **(a)** Location of the Arolla valley. **(b)** Location of the Tсарmine Glacier system and of the three larger valley glaciers referred to in this study (aerial image: Landsat 25 1990-1994; Swisstopo). **(c)** Main components of the Tсарmine Glacier system (aerial image: orthophoto 2012).

Holocene glacial pulses (Ivy-Ochs et al., 2009), it illustrates that this fluctuating glacier probably always contained large amounts of debris, produced by the erosion of the surrounding rock walls composed of fractured gneiss. The presence of an active rock glacier at the northern margin of the Tсарmine system points to the local occurrence of permafrost conditions (zone 4; Fig. 2.20c). The presence of push moraines indicates a deformation by the readvance of Tсарmine Glacier during the Little Ice Age (LIA; Lambiel et al., 2004). Like other similar systems (Bosson et al., 2015; Micheletti et al., 2015a), Tсарmine is disconnected from down-slope sediment transfer systems because of the presence of the moraine dam and the rock glacier, the relatively weak slope angle (17° of mean slope for the longitudinal profile between the top of the glacier and the top of the moraine dam), the reduced magnitude of sediment transfer processes and the absence of a proglacial meltwater stream.

Bosson and Lambiel (2016) quantified the surface kinematics of the Tсарmine system between 2011 and 2014 with repeated dGPS measurements. The results highlighted the existence of different dynamic behaviours at annual and seasonal timescales between zones 2b, 3, 4 and 5. The mean horizontal surface displacement was 60 cm a^{-1} and the mean vertical change rate -17 cm

a⁻¹ in the debris-covered glacier zone (zone 2b). Surface dynamics were weaker elsewhere: ~ 20 cm a⁻¹ of down-slope creep in the marginal rock glacier (zone 4), ~ 15 cm a⁻¹ of surface lowering in the proglacial dead ice body (zone 3) and discontinuous, very slow movements in ice-free debris (zone 5).

Climatic context

The Tsarmine Glacier system is located in a dry intra-Alpine valley. Topography acts as a barrier for wet air masses and reduces annual precipitation rates considerably. Combining meteorological data collected by *Hydro-exploitation SA* between 2001 and 2013 at 2000 m a.s.l. on the valley floor with monthly lapse rates estimated locally (between 0.54 and 0.63 °C (100 m)⁻¹ with an annual mean of 0.59 °C (100 m)⁻¹ at these elevations, Bouët, 1985), the mean annual air temperature at 2800 m a.s.l. is currently ~ -0.8°C. Mean annual precipitation measured on the valley floor between 2001 and 2013 is ~ 900 mm.

Figure 2.21 shows the evolution of the regional climate (south-western Valais) between 1930 and 2015. Homogenised monthly data for Sion (482 m a.s.l.; 24 km distance from Tsarmine, Fig. 2.20a), and Col du Grand St Bernard (GSB) (2472 m a.s.l.; 34 km distance from Tsarmine, Fig. 2.20a) weather stations were used (MeteoSwiss). To highlight the variations of the most important climatic parameters on the glacier, the mean deviation of annual and summer (July to September in this high-mountain environment) air temperatures and annual and winter precipitation (Octo-

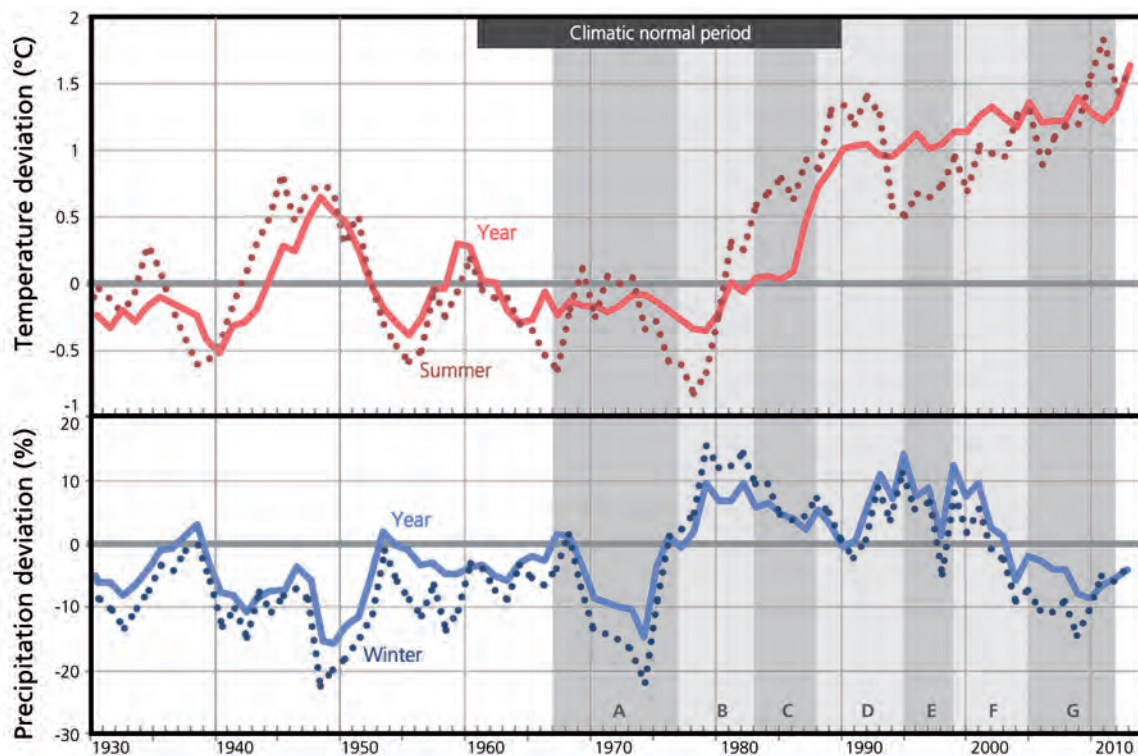


Fig. 2.21. Evolution of annual (solid curve) and summer (dotted curve; means of monthly values from July to September) air temperature and annual (solid curve) and winter (dotted curve; sums of monthly values from October to May) precipitation in the south-western Valais between 1950 and 2014. Based on homogenised monthly series of MeteoSwiss, the mean deviations of data from Sion and Grand St Bernard (GSB) stations (location in Fig. 2.20a) from the 1961-1990 climatic normal period have been computed. Only the 5-year running means are represented.

ber to May) relating to the 1961-1990 normal climate period were calculated for both stations. Between the 1950s and the mid-1980s, annual temperatures fluctuated around or slightly below the climatic norm. Subsequently, a clear warming trend set in: temperatures exceeded the norm by at least 1°C and continued to progressively increase until 2012. Summer temperatures behaved similarly, but the rapid increase had already started some years before, around 1980. Annual and winter precipitation showed larger fluctuations. Both were generally below the climatic norm before 1980 and after 2000 while the twenty years in between were wetter.

2.3.2.3. Methods

The methodology of this study was based upon: (1) the creation of DEMs using archival digital photogrammetry; (2) use of these DEMs to derive surface elevation changes and orthorectified imagery; (3) calculation of mass balance from the surface elevation changes; (4) analysis of surface displacement rates through image correlation applied to the orthorectified images; (5) application of GPR to quantify the spatial ice thickness distribution and volume.

Creation of DEMs using archival digital photogrammetry

DEMs were created by applying archival digital photogrammetry (Walstra et al., 2004; Chandler et al., 2007) to historical aerial photographs held by the Swiss Federal Office of Topography (Swiss-topo) for the period 1967 to 2005. Additionally, we used aerial images acquired in 2012 by the commercial company Flotron AG (Table 2.7). DEM creation from aerial orthoimagery is described in detail by Micheletti et al. (2015b), and therefore only a summary is presented here. Digital aerial photogrammetry requires a number of Ground Control Points (GCPs) for the photogrammetric restitution. A network of GCPs was established using a Leica System 500 dGPS during a field campaign in 2012. These points must be stable through the whole observation period, well distributed over the area of interest and easy to identify on the images. Given varying image quality and contrast, it was not always possible to retrace all GCPs locations with high accuracy and confidence. It was therefore crucial to obtain as many GCPs as possible, to always have adequate observations well distributed over the (varying) extent covered by the photographs. Consequently, GCPs employed (and unused) varied between pairs of images. Survey data were post-processed and corrected using data from an automated GNSS Network for Switzerland (AGNES) to a vertical and horizontal precision better than ± 0.05 m. Image processing for DEM creation was performed using ERDAS IMAGINE Leica Photogrammetry Suite (LPS). It involved three main steps: (1) definition of the internal orientation of the camera using camera calibration certificates available for each image pair; (2) after manually identifying the GCPs, estimating the exterior orientation using a conventional bundle adjustment; (3) application of automatic stereomatching algorithms to identify homologous points on image pairs and so to compute ground coordinates. The resulting point clouds were used to compute 1 m resolution DEMs for each period by applying a kriging interpolation in ArcGIS 10. DEMs were derived for eight dates between 1967 and 2012 (Table 2.7).

Date of aerial imagery	Scale	Emulsion	DEM mean error	Standard deviation of errors	Mean snowline altitude	Accumulation area ratio (AAR)
			m	m	m a.s.l.	
28 Sept 1967	1:15 700	BW	0.315	0.765	2900	0.40
08 Sept 1977	1:20 900	BW	0.504	0.82	2870	0.47
07 Sept 1983	1:20 900	BW	0.281	0.953	2885	0.41
10 Aug 1988	1:20 900	BW	0.296	0.644	2920	0.22
07 Oct 1995	1:26 800	BW	0.551	0.751	(2855)	(0.52)
02 Sept 1999	1:28 000	RGB	0.493	0.827	2930	0.12
17 Aug 2005	1:24 800	RGB	0.453	0.998	2900	0.31
20 Sept 2012	1:5200	RGB-NIR	0.356	0.462	2910	0.21

Tab. 2.7. Characteristics of the aerial imagery, DEM accuracy and precision estimates using dGPS survey data (Micheletti et al., 2015b), mean snowline altitude and accumulation area ratio at each date. These two values in brackets have to be considered carefully because fresh snow hampered the identification of the real snowline in 1995. BW: black and white; RGB: red, green, blue (colour); NIR: near infrared.

Calculation of surface elevation changes

To obtain surface elevation changes, DEMs of different years were differenced to obtain DEMs of Difference (DoDs). At this stage, areas of ineffective photogrammetric restitution became visible; these corresponded to zones where, because of low image texture, shadow effects, excessive steepness or occlusion, stereomatching algorithms failed and only a few low quality points were used to represent the topography. As a consequence, unrealistic elevation differences were found, especially in the upper part of the glacier. To avoid unreliable estimates, these areas were identified and removed from the analysis.

To distinguish real topographical changes from noise associated with random error in the derived surface elevation changes, a standard error propagation procedure was employed (Lane et al., 2003). First, the quality of each DEM was assessed with dGPS data from unused GCPs by computing the difference in elevation with DEM values in the respective locations (Table 2.7). The precision of each DEM, estimated as the standard deviation of these errors, was used to quantify limits of detection for each DoD, following Lane et al. (2003). The significance level was set to 90% in order to obtain a greater confidence that values in the DoD actually corresponded to real topographical changes. The limits of detection for each pair of DEMs are given in Table 2.8. Only differences larger than these values were employed to compute elevation changes. Real topographical changes were also employed to compute surface elevation and volumetric changes (ΔV) for individual observation periods.

Calculation of average mass balance

Area-averaged specific geodetic mass balance rates \dot{B} (m w.e a⁻¹) were computed for each observation period with:

$$\dot{B} = \frac{\Delta V \cdot f \Delta v}{A \cdot \Delta t}, \quad (1)$$

Tab. 2.8. Limits of detection of elevation changes for each pair of images (both absolute values and normalized per year) with a confidence level of 90% computed following the approach by Lane et al. (2003). See Micheletti et al. (2015b) for details

Pair of images	Limits of detection	Limits of detection
	90% $\pm m$	90% $\pm m a^{-1}$
1967-1977	1.839	0.18
1977-1983	2.04	0.34
1983-1988	1.862	0.37
1988-1995	1.623	0.23
1995-1999	1.833	0.45
1999-2005	2.126	0.35
2005-2012	1.804	0.25
1967-2012	1.466	

where A is the glacier area (m^2), and Δt the length of each observation period. Equation (1) includes a conversion factor $f\Delta v$, set to 0.85, which corresponds to a density of volume change of $850 \pm 60 \text{ kg m}^{-3}$. Such a value is commonly used (e.g.

Fischer M. et al., 2015) and is recommended for periods > 5 years, for a study site composed by a firm area and for volume changes significantly different from zero (Huss, 2013). ERT (Bosson and Lambiel, 2016) and GPR results allow us to quantify the current glacier area to $252\,000 \text{ m}^2$ (zones 1, 2a, 2b; Fig. 2.20c). This value was always used to calculate the glacier's average mass balance because the presence of extensive debris cover has hampered a clear determination of down-slope glacier boundaries in recent decades. Weak variations of debris-covered glacier areas observed elsewhere at a decadal timescale support this approach (e.g. Deline, 2005; Schmidt and Nüsser, 2009; Benn et al., 2012). The evolution of the specific geodetic mass balance rates between 1967 and 2012 were compared with the mean glaciological mass balances from Huss et al. (2015) for two nearby glaciers (Giétro and Allalin, 5.5 and 9.7 km^2 , at 12 and 30 km distance from Tsarmine; Fig. 2.20a) and to the decadal extrapolated mass balance means of glaciers in the European Alps (Huss, 2012). In addition, we compared the surface elevation and mass changes of the Tsarmine Glacier since the 1980s with those of the neighbouring Tsijiore Nouve Glacier, Mont Collon Glacier (also known as Bas Glacier d'Arolla) and Haut Glacier d'Arolla (Fig. 2.20b) using the data provided by Fischer M. et al. (2015).

Quantification of horizontal surface displacement rates and aerial imagery analysis

Archival aerial photogrammetry also allowed orthorectification of the aerial photographs, which were then used to quantify horizontal surface displacement rates within the observation periods. For this purpose, we used the 7D software (Vacher et al., 1999). Based on image autocorrelation, this software identifies the same features on images of two different dates based upon correlation of image grey-scale values. The comparison of images generates vectors illustrating the value of the pixel displacement, which, by using image resolution, can be expressed in $m a^{-1}$. The quality and the quantity of identified vectors depended on quality and characteristics of the source images themselves and was impaired considerably by the presence of shadow or fresh snow, and by poor image contrast. Thus, it was not always possible to quantify horizontal surface displacements for some areas (especially the upper half of the glacier) or during some periods. We only present results obtained within the Tsarmine Glacier system. Horizontal surface displacement rates detected in neighboring stable areas were below the limit of detection ($<0.1 \text{ m a}^{-1}$). Otherwise, movements of some large boulders were manually tracked on the photographs. The horizontal velocity values

obtained with image autocorrelation and feature tracking for the most recent period are close to those measured between 2011 and 2014 by dGPS (Bosson and Lambiel, 2016).

Mean snowline altitude and accumulation area ratio (AAR) were calculated for each period based on the orthorectified aerial photographs to investigate the evolution of the accumulation area of the Tsarmine Glacier over the past few decades (Table 2.7). These values provide interesting information on the recent evolution of the Tsarmine Glacier. Nevertheless, their interpretation requires care because the identification of annual accumulation of snow and ice is challenging on aerial images. Moreover, snow accumulation on very small glaciers can be very patchy and variable from year to year (Huss, 2010). Aerial photographs were taken a bit too late (7 October) in 1995 and a fresh snow cover hinders the identification of the end of ablation season snowline.

Measuring glacier thickness and volume

GPR data for Tsarmine Glacier were acquired on 10 March 2015 with a Malå Geoscience ProEx System consisting of a control unit mounted in a backpack, a portable monitor and a 100 MHz rough terrain antenna with a constant offset of 2.2 m. Taking 4 measurements s^{-1} , the antenna was pulled across the glacier at walking speed. For each measurement, 728 samples were recorded within a time window of 550 ns. The measurement (trace) positions were acquired with a conventional GPS receiver connected to the monitor. Horizontal accuracy in the position of the GPR-derived glacier thickness data is ± 5 m. Individual radar profiles were collected along a total length of ~ 3500 m and covered the entire debris-free and debris-covered parts of the glacier (1, 2a, 2b; Fig. 2.20c), at high spatial resolution.

A series of standard processing steps (e.g. Sold et al., 2013) were applied to the GPR raw data using Reflexw 2D data analysis (Sandmeier Scientific Software). These included a spatial interpolation to a constant 1 m spacing of traces to account for variations in the walking speed, a frequency bandpass filtering to reduce noise, a background removal, a gain function to compensate for radar wave power loss with depth and a fk (Stolt) migration to account for omnidirectional reflections of the signal and correct geometrical irregularities. Only unambiguous reflection horizons of the glacier bed were picked and stored as x-, y-, thickness data. For time/depth conversion, a constant radar propagation velocity in ice of 0.167 m ns^{-1} was assumed (Hubbard and Glasser, 2005). Following Fischer A (2009), we expect the accuracy of measured glacier thicknesses to be in the order of 5–10% of the measured values. Uncertainty may be caused by the measurement system itself, but is primarily attributed to changes of the signal velocity below the glacier surface, e.g. within the debris-cover layer. The measured glacier thickness data were imported in ArcGIS to derive the spatial distribution of ice thickness and glacier volume. To avoid and/or reduce linear interpolation artefacts, the measured point density was reduced to 1% of the originally recorded data by only considering every hundredth measurements (dots of measured glacier thickness in Fig. 2.26). Zero glacier thickness was assigned to the glacier outline prior to the spatial interpolation of point thickness data. Because different algorithms have been shown to produce significantly varying results (Fischer A. and Kuhn, 2013), topo to raster, kriging and inverse distance weighting (IDW)

techniques were applied to create 10 m x 10 m grids of the 2015 glacier thickness, and their results were subsequently compared with each other.

2.3.2.4. Results

Movements and elevation changes in the proglacial zones

The marginal zones of the Tsarmine system (3, 4, 5, 6; Fig. 2.20c) are not analysed in detail here. Their comprehensive analyses at both decadal and annual/seasonal timescales were carried out by Micheletti et al. (2015a) and Bosson and Lambiel (2016). Elevation changes of the proglacial zones between 1967 and 2012 revealed a surface lowering of up to 20 m that can be attributed to three main processes: (1) ice melt in the debris-covered dead ice body and the rooting zone of the rock glacier (zones 3 and 4; Fig. 2.22h), (2) thermokarstic erosion of the ice by lake formation near the glacier front (zone 6; Fig. 2.22h) and (3) gullying of the outer side of the moraine dam (zone 5; Fig. 2.22h). Except for the development of a proglacial lake between 1983 and 1999 (Fig. 2.22c-e), the magnitude of these processes was generally too weak to be systematically observable over the short term. Horizontal surface displacement rates (Fig. 2.23) showed a recent acceleration of the rock glacier, where velocities reached 70 cm a⁻¹ in the rooting zone between 1999-2005 (Fig. 2.23). Discontinuous, slow movements were reconstructed for the proglacial area (zones 3 and 5; Fig. 2.23). They show that the delineation of glacier boundaries in debris-covered environments can be challenging. For instance, the dead ice zone was almost completely stagnant between the 1967-1988 and 1995-1999 periods and was flowing during the 1999-2005 period. Still, the distinction of this zone from the up-slope glacier (zone 1, 2a, 2b) relies on their different dynamic behaviour on both decadal (Fig. 2.23) and seasonal timescales (Bosson and Lambiel, 2016). The few movements reconstructed at these timescales for the area surrounding the lake indicate that most of the remnant ice present in this zone melted during recent decades (Fig. 2.22).

Elevation changes and geodetic mass balances of the Tsarmine Glacier

There were clear differences in the elevation changes between the upper part of the glacier, composed of the debris-free zone, the middle part covered by a thin debris mantle (zones 1, 2a; Fig. 2.22), and the down-slope heavily debris-covered one (zone 2b). From 1967 to 1977, a lowering of ~ 0.18-0.4 m a⁻¹ was found in the heavily debris-covered part and contrasted with elevation gain up-glacier (Fig. 2.22a). Between 1977 and 1983, changes were more homogeneous over the whole glacier and a significant positive elevation change up to 1 m a⁻¹ affected its central part (Fig. 2.22a). Between 1983 and 1995 (Fig. 2.22c-d), surface lowering was observed in the upper half, but a discontinuous elevation increase affected the heavily debris-covered zone and migrated progressively down-slope. This is clearly noticeable between 1983 and 1988 for instance (Fig. 2.22c), when a significant volume loss of 820,000 m³ in the upper part contrasts with a positive volume change of 140,000 m³ in the lower part. Since 1995, elevation loss has been dominant, but the lowering rate decreased after 1999 in zone 1 (Fig. 2.22e-g).

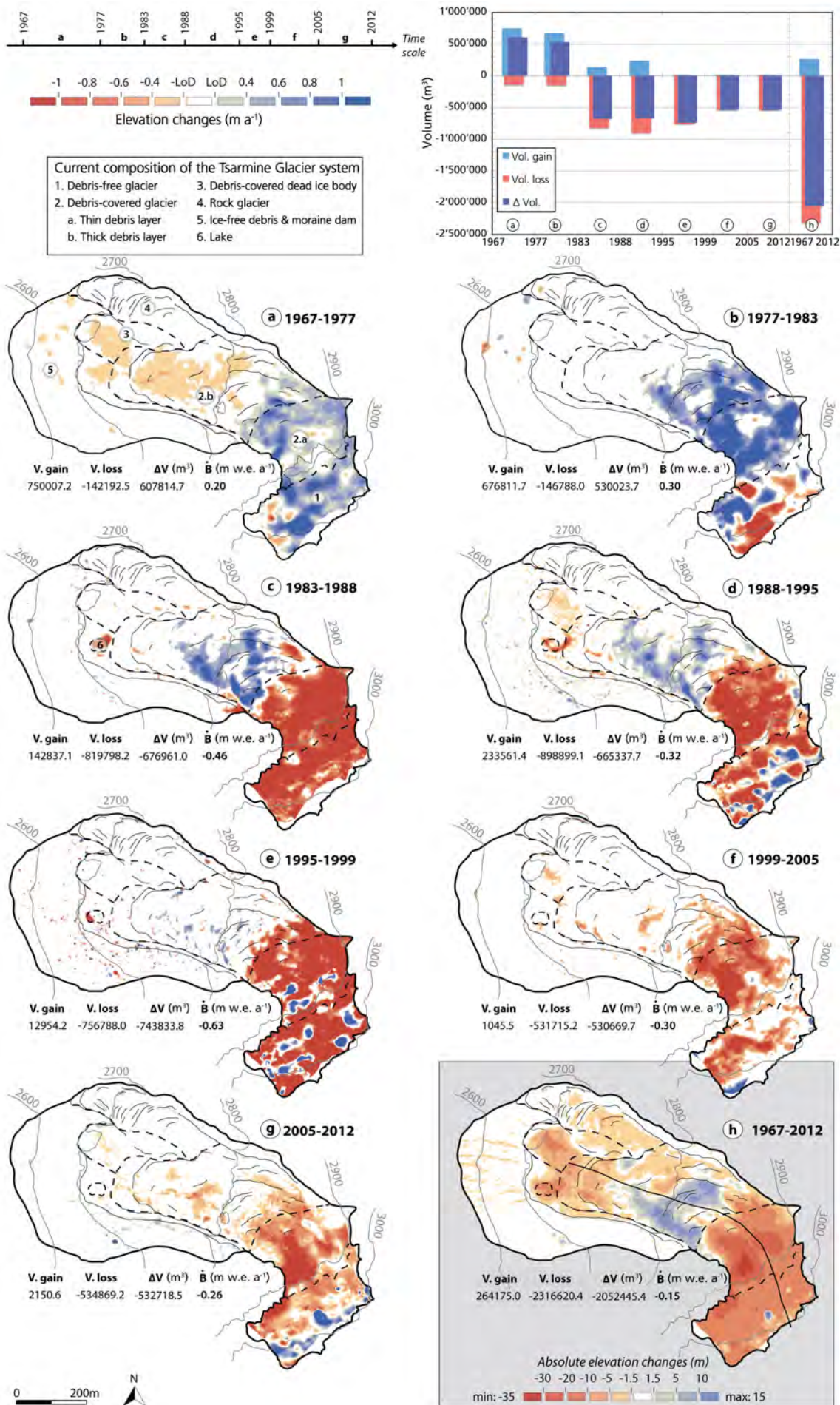


Fig. 2.22. (left page) Surface elevation, volume and average geodetic mass balance changes of Tсарmine Glacier for seven different periods between 1967 and 2012, derived from archival aerial photogrammetry. The longitudinal transect in the synthesis map (h) is referred to in Figures 2.24 and 2.29. The limit of detection (LoD) values are listed in Table 2.7.

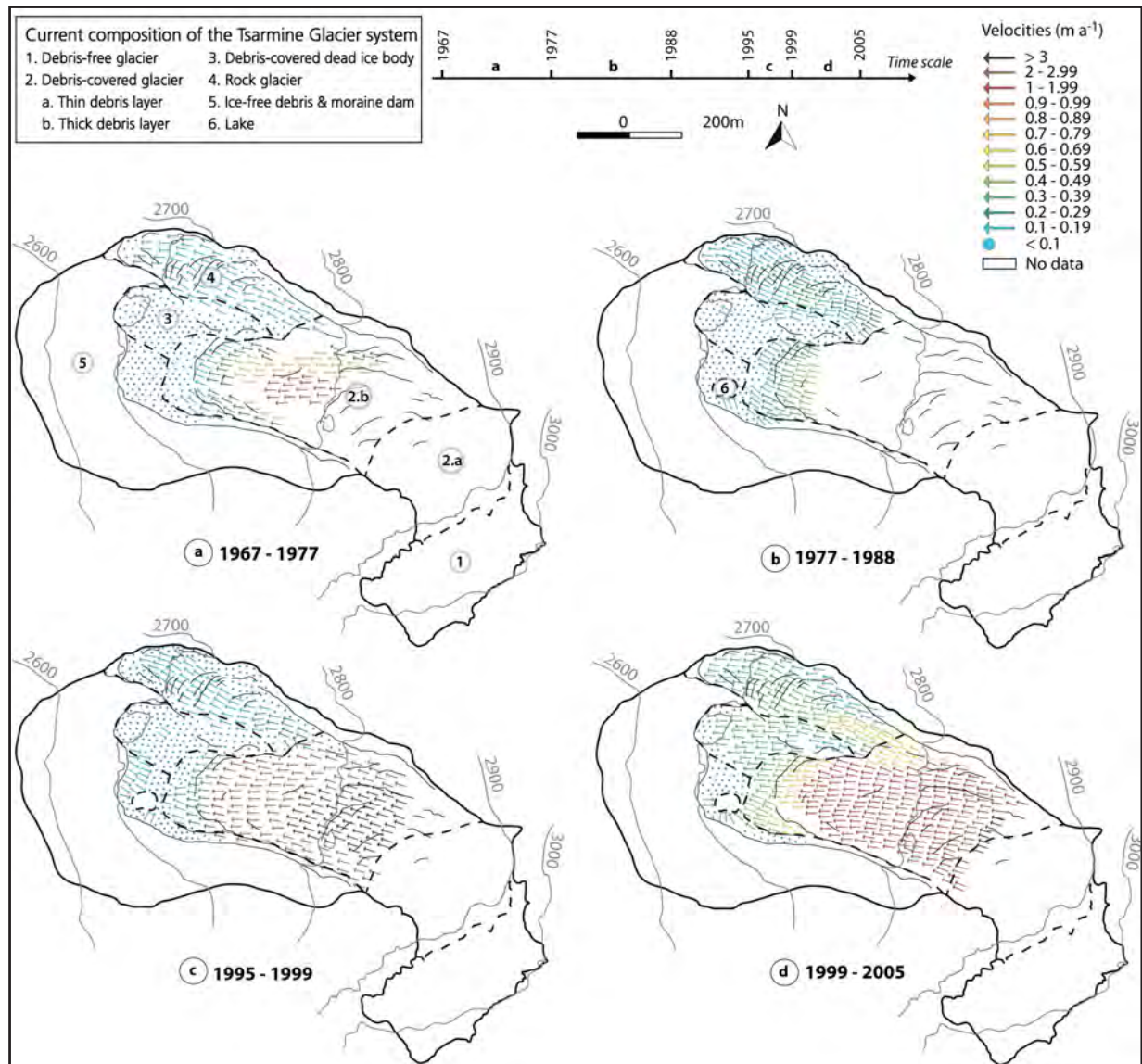


Fig. 2.23. Horizontal surface displacement rates for different parts of the Tсарmine Glacier system between 1967 and 2005, obtained with 7D software

For the entire period (1967 to 2012) (Fig. 2.22h), the volume change was negative, with a loss of $2 \times 10^6 \text{ m}^3$ over 45 years. Whereas the volume losses mainly affected the up-slope part (with up to 30 m of elevation loss in zone 2a) and secondarily the glacier front, the middle part, covered by a thick layer of debris, actually gained in volume ($\sim 260,000 \text{ m}^3$). This corresponds to a maximum positive elevation change of 15 m. These clear heterogeneous spatial patterns are also observable on a central longitudinal flowline transect (Fig. 2.24a) and have changed the glacier surface topography: whereas in 1967 the surface was convex for the debris-free zone and slightly concave for the heavily debris-covered part, the surface of the glacier was generally convex in the debris-covered portion and slightly concave in the debris-free zone by 2012 (Fig. 2.24b).

Between 1967 and 2012, two stages of resulting mass changes were recorded for the Tсарmine Glacier. It went from a positive mass balance context, with rates of $0.20 \text{ m w.e. a}^{-1}$ for the period

1967-1977 (Fig. 2.22a), and 0.30 m w.e. a⁻¹ between 1977 and 1983 (Fig. 2.22b), to a negative mass balance context with most negative values between 1995 and 1999 (-0.62 m w.e. a⁻¹, Fig. 2.22e). However, mass balances for the 2000s were less negative again (-0.26 m w.e. a⁻¹ between 1999 and 2005 and -0.30 m w.e. a⁻¹ between 2005 and 2012, respectively Fig. 2.22f, g). Over the entire period 1967 to 2012, there was a negative average mass balance of -0.15 m w.e. a⁻¹.

Horizontal surface displacements rates of the Tsarmin Glacier and aerial imagery analysis

The horizontal surface displacements shown in Figures 2.23 and 2.24b illustrate significant spatial

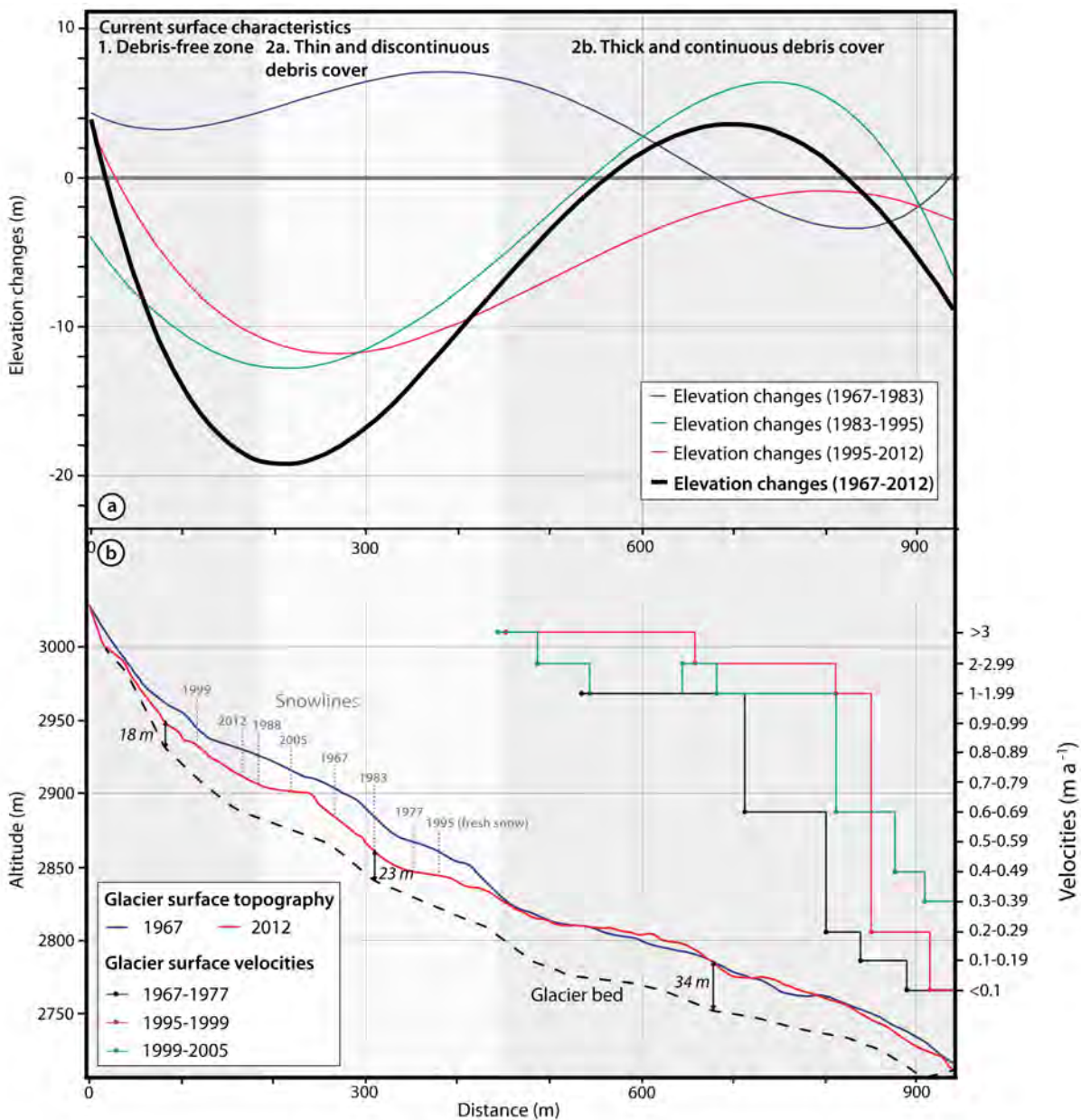


Fig. 2.24. (a) Surface elevation changes between 1967-1983 (blue), 1983-1995 (green), 1995-2012 (red) and 1967-2012 (bold black) along a longitudinal transect of Tsarmin Glacier, visible in Figure 2.22h. The graphs were computed with the 'interpolate line' tool in ArcGIS 10. (b) Longitudinal elevation profiles in 1967 (blue) and 2012 (red). The dashed black curve shows the glacier bed derived from ground penetrating radar data. The snowline altitude along the longitudinal transect, detected from aerial imagery, is reported at each date. On the right-hand side, the horizontal displacement rates along the longitudinal transect are derived from the image autocorrelation (Fig. 2.23).

and temporal variations. The period 1967-1977 revealed horizontal surface displacements of $\sim 1\text{-}2\text{ m a}^{-1}$, which decreased down-glacier to ~ 0.1 to 0.2 m a^{-1} (Fig. 2.23a). For the following decade, values between 0.1 and 0.5 m a^{-1} were obtained over the debris-covered glacier snout (Fig. 2.23b). In the late 1990s, horizontal surface displacements increased to up to 1 m a^{-1} for this area (Fig. 2.23c). Meanwhile, displacement rates exceeded 3 m a^{-1} in the central up-glacier zone and decreased towards the margins. Except for the glacier terminus, a velocity decrease affected all the debris-covered part in the early 2000s (Fig. 2.23d; 2.24b).

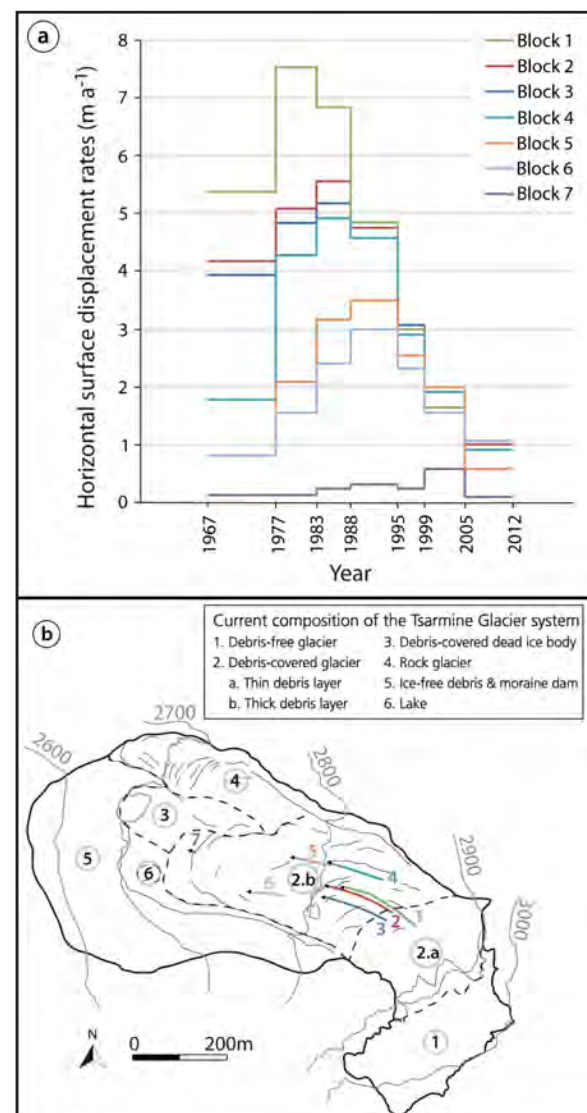
Two main outcomes were obtained from tracking large boulders (Fig. 2.25): (1) horizontal surface displacements decreased down-glacier and (2) the periods with highest displacement rates varied spatially. Glacier surface motion in the central up-slope zone reached its maximum between 1977 and 1983, with values $> 7\text{ m a}^{-1}$ (block n°1). At the glacier snout (block n°7) the displacements were much lower and highest velocities were reached between 1999 and 2005 (0.7 m a^{-1}). Thus, from up-slope to down-slope, there was an apparent attenuation of the maximum surface displacement rates and a temporal delay of the maximum values over time. This shows the progressive translation down-glacier of a wave of maximum superficial displacement rates. Between 2005 and 2012, the motion of Tsarmine Glacier decreased, as shown by the displacement rates of all boulders.

Reconstructions of estimated mean snowline altitudes and AARs from aerial photographs showed that the relative proportion of the accumulation area of the Tsarmine Glacier generally decreased in recent decades (Table 2.7; Fig. 2.24b). More than the upper third of the glacier was snow covered in 1967, 1977 and 1983. Without considering the unrepresentative values of 1995, the accumulation area was above 2900 m a.s.l. and corresponded to $< 30\%$ of the glacier surface in 1988, 1999, 2005 and 2012.

Current ice thickness and volume of Tsarmine Glacier

The 2015 GPR survey (Fig. 2.24b; 2.26) revealed a maximum ice thickness of 36 m , recorded in the lower heavily debris-covered part. There, cross-section profiles showed a U-shaped glacier bed with the steeper thickness gradients towards

Fig. 2.25. (a) Horizontal surface displacement rates obtained by tracking some large boulders on the debris-covered glacier and (b) their successive position on the glacier



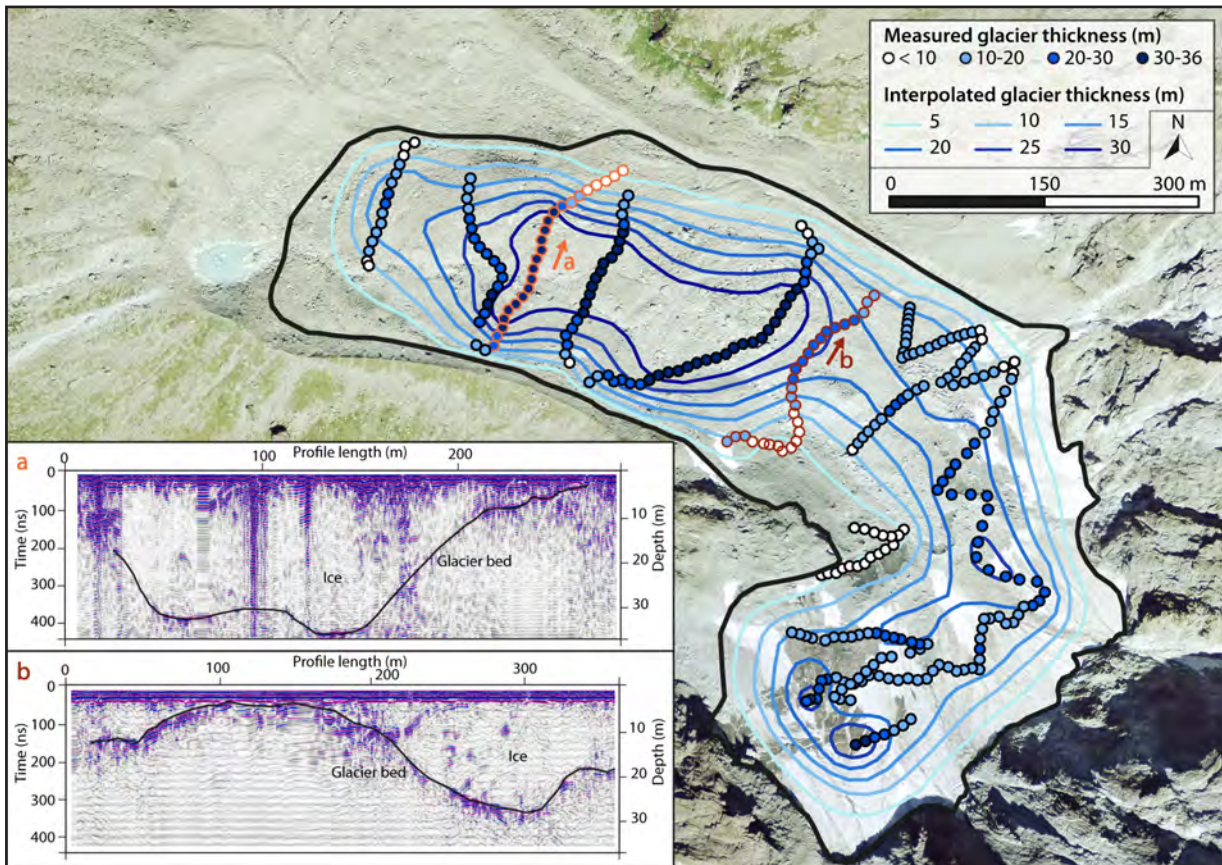


Fig. 2.26. Measured ice thickness and interpolated ice thickness contours obtained from March 2015 GPR data, as well as two examples of radargrams showing the glacier bed with black lines (aerial image: Swiss image level 2 2013; Swisstopo).

the left LIA moraine (Fig. 2.26a). Up-slope, in the middle part covered by a thinner debris layer, the glacier thickness decreased and was particularly shallower towards the lateral margins. The glacier bed here has a gentle V-shaped profile along a cross-section, with thickest measured values of slightly > 20 m for a very narrow central part (Fig. 2.26b). Up-glacier a trough-like bed was found, with glacier thicknesses > 15 m in its centre.

The mean interpolated glacier thickness was ~ 15 m (Table 2.9). Due to the comparatively high relative spatial density and the complete coverage of measured GPR profiles, the different interpolation algorithms applied to the measured point data returned very similar results, both for the spatial glacier thickness distribution and mean glacier thickness. The present (2015) bed topography and volume of Tarmine Glacier, which amounted to $4.05 \pm 0.4 \times 10^6 \text{ m}^3$, can be derived if the interpolated glacier thickness grids are subtracted from the latest high-resolution DEM of 2012 and the 2012-2015 surface elevation changes are considered in the calculation. The volume change exceeded $2 \times 10^6 \text{ m}^3$ between 1967 and 2012. The glacier thereby lost one third of its initial volume in the past 45 years.

	h_{mean}	h_{max}	std
	m	m	m
GPR point measurements	19.5	35.8	8.6
Topo to raster	15.1	39.2	9.6
Kriging	15.2	36	10.7
IDW	15.5	36	10.7

Tab. 2.9. Mean (h_{mean}) and maximum (h_{max}) glacier thickness derived from GPR point measurements and different interpolation algorithms. Std refers to as standard deviation.

2.3.2.5. Discussion

Main controls on decadal elevation changes of Tsarmin Glacier

From the spatial distribution of the surface elevation changes (Fig. 2.22), it is possible to infer that the most dynamic part of the glacier is the upper half, including the debris-free zone (1) and the zone covered by a relatively thin and discontinuous debris layer (2a). Volume changes were marked here and related to snow and ice accumulation and ablation, ice fluxes and, to a lesser extent, debris deposition. They were likely to be strongly controlled by air temperature, especially during summer, as reported in other studies (Arendt et al., 2009; Diolaiuti et al., 2012; Thibert et al., 2013). The periods of mass gain correspond to the coldest years (Fig. 2.21; 2.22a-b). Significantly higher summer temperatures resulted in rapid surface lowering (Fig. 2.22c-g). Thus, the temperature-driven summer mass balance is a primary control on the annual mass balance in debris-free zones as observed for other glaciers (e.g. Huss et al., 2015). Because of the consistency of air temperature on the regional scale (Begert et al., 2005), the decadal evolution of surface elevation changes in the upper part of Tsarmin is very representative for the behaviour of Alpine glaciers during this period (Deline et al., 2012; Huss, 2012; Vaughan et al., 2013; Huss, et al., 2015). However, winter snow can modify and enhance these effects. The greatest mass gain (Fig. 2.22b) occurred during a period when winter precipitation generally exceeded the long-term average (Fig. 2.21). Since the 2000s, lower winter precipitation may have reduced snow cover at the start of summer, leading to an earlier transition to ice exposure, lower albedo and enhanced melt (e.g. DeBeer and Sharp, 2009). The most rapid and spatially homogeneous volume loss occurred between 1983 and 1999 ($> -650\,000\text{ m}^3$; Fig. 2.22c-d). Three main reasons, visible on aerial photographs, can explain the deceleration of lowering rates since 1999 whilst air temperature continued to increase: (1) the snow and ice accumulated from the 1960s to the mid-1980s has largely and rapidly melted in subsequent warmer years, as observed elsewhere in the Alps (Paul et al., 2007); (2) the increasing emergence and deposition of debris in this zone has reduced the ablation rate; (3), the concomitant confinement of the accumulation area at the shaded and avalanche-fed backwalls' foot has limited the sensitivity to climate (Table 2.7; Fig. 2.24b).

The influence of climatic variations on the elevation changes of the debris-covered glacier tongue (zone 2b) is not so obvious. Elevation changes were slightly negative on the tongue between 1967-1977, while they were positive up-slope (Fig. 2.22a). Conversely, they were positive or close to zero between 1983 and 1999 in zone 2b, when elevation in the upper zone decreased rapidly (Fig. 2.22c-e). From 1967 to 2012, the centre of the down-glacier parts presented positive surface elevation changes, whereas the frontal zone was lowered by up to 10 m (Fig. 2.22h). Two processes may interact to explain this effect. First, the increased thickness of the debris layer down-glacier will slow down melt rates because ablation rate and the superficial debris thickness are negatively correlated (e.g. Benn et al., 2012). It induces an inversion of the ablation pattern down-glacier, as revealed by the surface elevation changes along the longitudinal profile since 1967 (Fig. 2.24a). The maximum melt rate then occurs at the transition between debris-covered and debris-free,

just below the ELA (Kellerer-Pirklbauer et al., 2008; Shea et al., 2015), where ice loss generally exceeded 20 m between 1967 and 2012 (zone 2a; Fig. 2.22h). Second, there was probably a progressive down-glacier migration of the mass accumulated up-slope between the 1960s and the mid-1980s (Fig. 2.22a-e; e.g. Carrivick et al., 2015). The downward propagation of a wave of maximum but decreasing surface displacement over time supports this assumption (Fig. 2.25a). Similar observations were reported by Thomson et al. (2000) for a larger debris-covered glacier over the 20th century (Miage Glacier; area of 11 km²). They illustrate the delayed and attenuated effects of climatic variations on mass changes of heavily debris-covered tongues: up-slope surface elevation changes are dynamically transferred but attenuated towards the glacier front. Because of their reduced ablation rates, heavily debris-covered glacier tongues are less affected than debris-free glaciers by negative mass balance perturbations, such as downwasting or frontal retreat (Thomson et al., 2000; Scherler et al., 2011; Haeberli et al., 2013). Conversely and as observed for Tsarmine, significant positive mass balance perturbations can lead to an increase in surface elevation of the debris-covered glacier snouts.

Surface displacement rates and associated dynamics

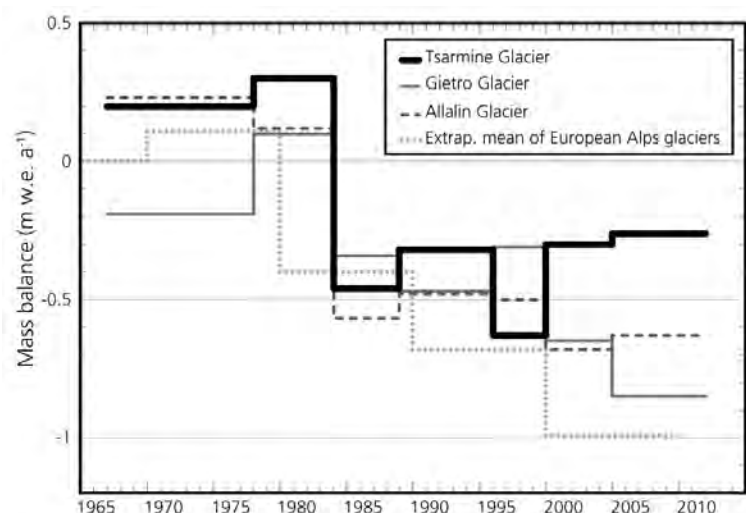
The analysis of surface displacement rates (; Fig. 2.23; 2.25) highlights four main characteristics of the decadal dynamics of Tsarmine Glacier. (1) Due to the propagation of the snow and ice accumulated from the 1960s to the mid-1980s, a kinematic wave of maximum displacement rates with progressively decreasing intensity migrated down-glacier (Fig. 2.25; Thomson et al., 2000; Cuffey and Paterson, 2010). (2) Surface displacement rates decrease significantly towards the glacier terminus (Fig. 2.24b; 2.25), which can be explained by the reduced driving stress in this area (Cuffey and Paterson, 2010). This effect may be enhanced by the downstream accumulation of sediments. Increasing the compressive flow, it often contributes to restraining the glacier motion (Kirkbride and Deline, 2013). Hence the uplift of the central part of the glacier is probably both due to an advective mass transfer and associated compression (Gudmundsson et al., 2000; Kellerer-Pirklbauer et al., 2008). The formation of arcuate superficial ridges around the uplift zone in recent decades is very likely related to this compressive stress increase (Fig. 2.22h). (3) The glacier motion generally tends to decelerate over time, as observed elsewhere in the Alps since the 1980s in the context of negative mass balances (Paul et al., 2007). There are multiple causes of this reduction in dynamics. Several metres of ice have been lost in the upper half and frontal glacier zone of Tsarmine since 1967 and, except for the central zone of the heavily debris-covered part, it is now mostly thinner than 25 m (Fig. 2.26). Moreover, the glacier surface is flattening, as revealed by its current linear or even concave profile (Fig. 2.24b). Both processes lead to a decrease in driving stress (Benn et al., 2012; Carrivick et al., 2015). Finally, snow and ice accumulation on Tsarmine Glacier have been limited and discontinuous since 1983, reducing the mass turnover and thus glacier dynamics (Paul et al., 2007). The overall decrease of the glacier motion contrasts with the acceleration of the rock glacier and dead ice zones between 1999 and 2005 (Fig. 2.23). Accelerations of similar landforms were also observed in the Alps (e.g. Delaloye and other, 2008). They were especially related to the increase of the permafrost temperature, the melt of ground ice and the increased presence of ground water induced by the 2003 heatwave. (4) The spatially

rather homogeneous motion between 1995 and 2005 (Fig. 2.23c-d) points to the domination of an *en masse* flow. Even if ice and maybe bed deformation can also be active, it indicates the occurrence of basal sliding (Mayer et al., 2006; Copland et al., 2009). Hence, even though this glacier may be polythermal because of the surrounding permafrost conditions, a large portion of the basal ice likely has a temperate thermal regime, as indicated by its basal slip (Bingham et al., 2008). Similar results and interpretations were proposed from dGPS monitoring data (Bosson and Lambiel, 2016).

A particular behaviour?

Before 2000, the average geodetic mass balance of Tsaamine Glacier was consistent with the average glaciological mass balance of Giétro and Allalin glaciers (Huss et al., 2015) and with the extrapolated decadal mean of glaciers in the European Alps (Huss, 2012; Fig. 2.27). Except in comparison with the negative 1967-1977 anomaly for Giétro Glacier, the mass balance of Tsaamine Glacier shows both magnitude and temporal variations comparable with the other larger glaciers. It illustrates the homogenous control of regional climate on glaciers during this period. The computed mass balance of Tsaamine between 1988 and 1999 has to be considered with care. Indeed, fresh autumnal snow is observable in the upper zone on the aerial image of 1995 and integrated in the calculation. Thus, the mass balances between 1988-1995 ($-0.32 \text{ m w.e. a}^{-1}$) and 1995-1999 ($-0.63 \text{ m w.e. a}^{-1}$) are likely under- and overestimated and the real values are probably closer to those obtained for Giétro and Allalin glaciers. The period 2003-2012 appears to be the one with strongest mass losses for the Swiss glaciers for at least the last century (Huss, et al., 2015). However, this remarkably negative trend does not affect the Tsaamine mass balance, which stabilised at around $-0.3 \text{ m w.e. a}^{-1}$ after 1999 (Fig. 2.27). This particular behaviour is not observable on other (very) small debris-free Alpine glaciers. For instance, the mass balances of Pizol (Huss, 2010) and Sarennes (Thibert et al., 2013) glaciers were three times more negative ($< -1 \text{ m w.e. a}^{-1}$) in recent years compared with Tsaamine. On a larger timescale, while Tsaamine lost one third of its initial volume between 1967 and 2012; this value exceeded 68% at Pizol between 1973 and 2006 (Huss, 2010). The progressive shrinking of the accumulation area in a north-facing shaded and avalanche-fed niche and the concomitant extension of the debris cover explain this peculiar variation in the Tsaamine Glacier mass balance since 1999. It highlights the recent decrease of the control of regional climate on this glacier once most of the snow/ice accumulated during the 1960s to mid-1980s had melted. This consequence of the

Fig. 2.27. Average geodetic mass balance of Tsaamine Glacier, average glaciological mass balance of Giétro and Allalin glaciers (location on Figure 2.20a, Huss et al. 2015) and extrapolated decadal mean of the glaciers of the European Alps (Huss, 2012).



increasing influence of topography and debris cover supports results found in other studies that analysed the behaviour of some small cirque glaciers in the final stage of glaciers vanishing (e.g. López-Moreno et al., 2006; DeBeer and Sharp, 2009; Carturan et al., 2013b; Carrivick et al., 2015). It contrasts with the dynamics recently undergone by climatically-driven (very) small bare-ice mountain glaciers (e.g. Huss, 2010; Thibert et al., 2013; López-Moreno et al., 2015).

Comparing glacier surface elevation changes of Tsarmine since the 1980s with those of the nearby larger valley glaciers also reveals a particular spatial pattern for Tsarmine (Fig. 2.28). While

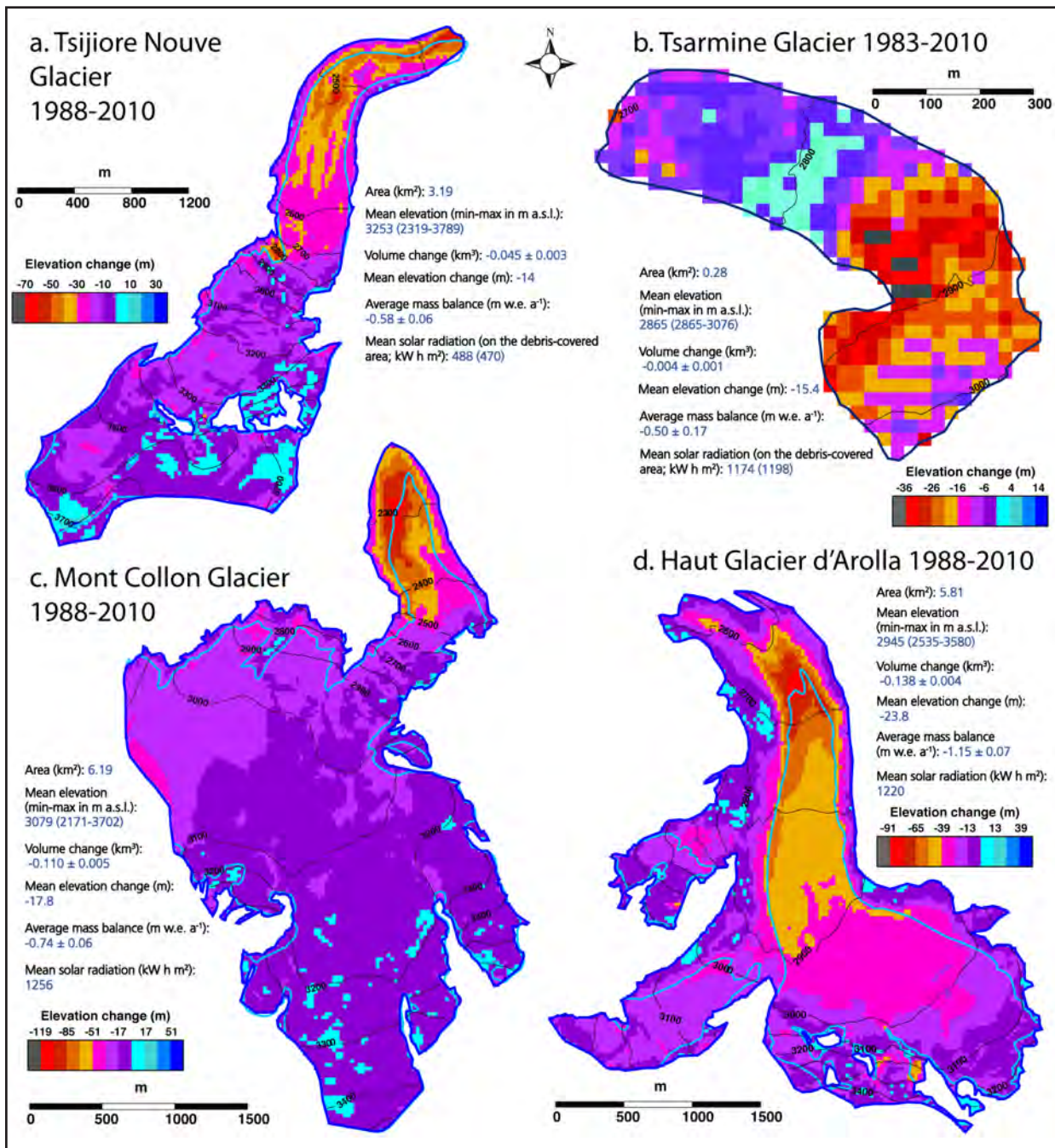


Fig. 2.28. Spatial distribution of elevation changes within the digital glacier outlines from the 1973 (dark blue) and the 2010 (light blue) Swiss Glacier Inventories (Müller et al., 1976; Fischer M. et al., 2014), derived by Fischer M. et al. (2015) through a comparison of the DHM25 Level 1 DEMs from the 1980s with the 2010 swissALTI^{3D} DEMs for (a) Tsijiore Nouve Glacier, (b) Tsarmine Glacier (location on Fig.1a), (c) Mont Collon Glacier and (d) Haut Glacier d'Arolla. Mean area solar radiation was computed with ArcGIS Spatial Analyst tool on the 2010 swissALTI^{3D} DEMs and according to the 2010 glacier extents (Fischer M. et al., 2014).

the three large glaciers showed strongest lowering towards their terminus, Tsarmine Glacier lost most within its upper third. This highlights the importance of air temperature and thus altitudinal gradients for large glaciers. As very small cirque glaciers have a limited altitudinal gradient, other processes can superimpose on the effects of altitudinal temperature gradients. The decadal elevation changes of Tsarmine Glacier rather illustrate the influence of the delayed and attenuated mass transfer from the upper debris-free part to the debris-covered part and the debris cover thickening down-glacier. Interestingly, the snout of Tsijiore Nouve Glacier was also covered by a several decimetre thick debris layer in recent decades (e.g. [Small, 1983](#)) and is significantly less exposed to solar radiation than the Tsarmine snout (2.5 times smaller mean solar radiation; [Fig. 2.28](#)). However, up to 50 m of surface lowering occurred at the Tsijiore Nouve tongue since 1988. There, the presence of a thick debris cover and a weak exposure to solar radiation are thereby not sufficient to prevent rapid ice melt. The Tsarmine Glacier snout is located 300 m above the one of Tsijiore Nouve and within the discontinuous permafrost belt. The neighbouring rock glaciers show that ground ice can be preserved from noticeable melt under a several metre thick superficial debris layer ([Lambiel et al., 2004](#); [Bosson and Lambiel, 2016](#)). Therefore, (1) the sheltering of a large portion of the glacier under a heavy debris mantle and (2) its confinement in a zone where air and ground temperatures are lower than for the other glaciers explain why the average mass balance since the 1980s is up to two times less negative for Tsarmine Glacier ($-0.5 \text{ m w.e. a}^{-1}$) compared with the three larger systems (-0.58 to $-1.15 \text{ m w.e. a}^{-1}$; [Fig. 2.28](#)). On a larger scale, it is also less negative than the average of glaciers in the European Alps from 1980 to 2000 ($-0.69 \text{ m w.e. a}^{-1}$; computed from decadal means of [Huss, 2012](#); [Fig. 2.27](#)).

Projections of climate change for the next few decades suggest continued increase of air temperature ([Collins et al., 2013](#)). The observed varying patterns of elevation changes since 1983 are expected to sustain and govern the future evolution of Tsarmine Glacier. Negative mass balance stabilised between 1999 and 2012 and the mean lowering rates of -0.5 , -0.7 and -0.2 m a^{-1} were computed for the zones 1, 2a and 2b. In [Fig. 2.29](#), we extrapolate these rates, taking into account the known ice thickness. In the upper half of the glacier, the lowering exceeded 10 m in the past 30 years, roughly corresponding to the remaining glacier thickness in 2015 ([Fig. 2.24b](#); [2.26](#)). This rapid thinning particularly affects the transition zone between debris-free and heavily debris-covered zones and could cause the disintegration of the Tsarmine Glacier into two entities, as evoked for other heavily debris-covered systems ([Benn et al., 2012](#); [Shea et al., 2015](#)). In contrast, the uppermost debris-free part appears a bit less sensitive to the air temperature increase because of the influence of topography on snow accumulation and solar radiation. The control of air temperature tends to decrease in this shaded avalanche-fed area, as observed since 1999 ([Fig. 2.22](#)). Conversely, the control of winter precipitation can increase here in the next few decades ([Carturan, 2013b](#); [Scotti et al., 2014](#)). Sheltered in its proximal niche, this thinning glacier zone may progressively become an inactive and debris-covered ice patch ([Serrano et al., 2011](#)), as the input of debris on the glacier surface is likely to increase in the next few decades ([Deline et al., 2015](#)). Finally, this zone could evolve toward a talus slope ([Gomez and al., 2003](#)). In the lower half, the glacier thickness exceeds 30 m ([Fig. 2.26](#)). Here, the ice melt could take more than a hundred years if the mean lowering rates of 0.2 m a^{-1} observed over the past decade remain constant in

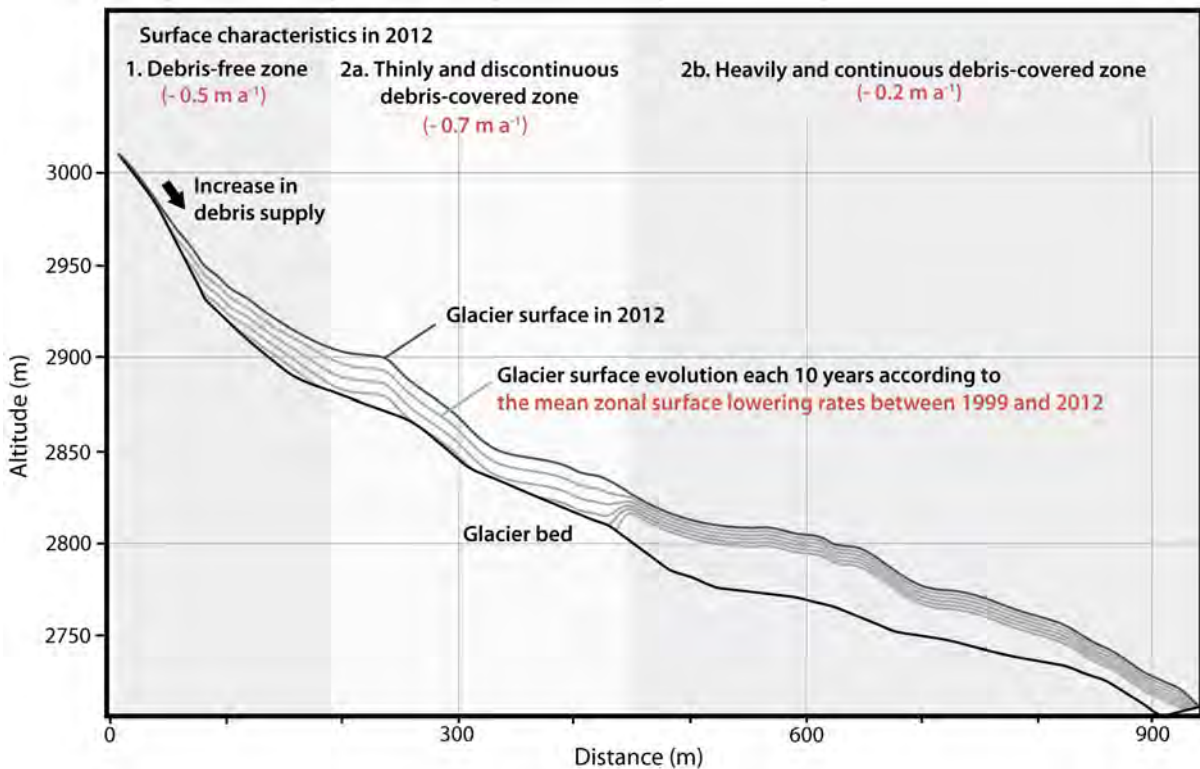


Fig. 2.29. Evolution model of Tsarmine Glacier for the next few decades. The potential future surface elevation changes have been simply generated using the mean zonal lowering rates between 1999 and 2012.

the future. Several studies mention the recent transformation of similar heavily debris-covered glacier tongues into rock glaciers under permafrost conditions (e.g. [Shroder et al., 2000](#); [Monnier and Kinnard, 2015](#); [Seppi et al., 2015](#)). [Bosson and Lambiel \(2016\)](#) discuss this possible evolution, which seems unlikely, given the probable domination of temperate thermal conditions in the glacier ([Kneisel, 2003](#)). However, the integration of glacier ice in the rock glacier during or after the LIA is probable on the northern margin of the Tsarmine Glacier system ([Bosson and Lambiel, 2016](#)).

2.3.2.6. Conclusion

Archival aerial photogrammetry, autocorrelation of orthophotos and GPR have been used to study the decadal behaviour of Tsarmine Glacier, a very small heavily debris-covered glacier located in an Alpine permafrost environment.

Spatial and temporal heterogeneity has characterised the glacier dynamics in recent decades. The upper half of the glacier presents the largest elevation changes, which are mainly related to (summer) air temperature variations. The accumulation of snow/ice in the period 1967-1983 and its rapid, almost complete, melt between 1983 and 1999 have induced related significant volume gains and losses. Volume loss has particularly affected the upper central part, where the surface lowering exceeded 30 m between 1967 and 2012. The consequences of climatic variations have been attenuated on the lower half of the glacier because of its covering under a thick debris layer. Whilst the frontal zone showed several metres of lowering between 1967 and 2012, the

lower central zone surface rose by up to 10 m. This was related to the downward transfer of the ice accumulated before 1983 and associated compressive stress. The surface displacement rates have slowed down in recent decades in relation with the glacier thinning. In 2015, the glacier volume was $4.05 \pm 0.4 \times 10^6 \text{ m}^3$, corresponding to two thirds of the volume in 1967. The mean interpolated 2015 glacier thickness was 15 m. In the next few decades, the differential ablation observed at the glacier scale could lead to its separation in two entities: an uppermost shrinking glacier and a lowermost heavily debris-covered dead ice body.

The decadal behaviour of Tsarmine Glacier exhibits particularities in time and space compared with other local larger glaciers. Until the late 1990s, average geodetic mass balances ranged between 0.30 and $-0.63 \text{ m w.e. a}^{-1}$. The temporal variation and magnitude of these values were consistent with those measured for other local glaciers, illustrating the dominant control of regional climate. However, Tsarmine has had less negative mass balances than neighbouring glaciers (stabilised above $-0.30 \text{ m w.e. a}^{-1}$) since 1999. The spatial pattern of elevation changes also contrasts with neighbouring glaciers. Whereas Tsarmine was mainly affected by lowering in its upper half, the larger valley glaciers lost most of their mass at their tongues. Both temporal and spatial particularities highlight the limitation of the regional climate control on Tsarmine Glacier. The recent occurrence of this negative feedback is mostly related to the retreat of the debris-free area into a shaded and avalanche-fed north-facing niche, whereas the thick debris cover and cold air/ground conditions limit the ablation rate in this permafrost environment.

These results show that the evolution model of larger valley glaciers cannot be transferred 1:1 to very small debris-covered glaciers. Glacier system characteristics may complicate glacier responses to the climate forcing in time and space, and local additional controls generate heterogeneities and non-linearities in dynamics. In that way, studies focusing on complex glacial behaviours have to be thorough and backed up by field surveys. This study also highlights the potential of archival aerial photogrammetry to improve the knowledge on complex glacial dynamics on a decadal timescale.

Acknowledgements

The first two authors contributed equally to this work. We acknowledge those people who helped during field measurements (especially D. Bonneaux). Hydro-exploitation SA, Alpiq SA and Grande Dixence SA kindly provided the Arolla climate data. This manuscript was improved thanks to the valuable advice and comments of J-M Fallot and N. Deluigi (Uni. Lausanne) and M. Huss (Uni. Fribourg & ETH Zürich). B. Scott is acknowledged for proofreading the English text.

3. Compilation and synthesis of results by study site



H | dGPS campaign in the Chaltwasser system with B. Lehmann (© M. Calianno, 2015)

3.1. Introduction

The three articles published during this PhD work only present and discuss a part of the results obtained. Complementary information on study sites and methods and non-published results are synthetically presented in the following.

3.1.1. Study sites

As stated in the research objectives (1.3), this contribution studies the internal structure, the current dynamics and the genesis of SDCGSAPE. To reach this goal, seven study sites, located in the NW part of the European Alps (Fig. 3.1), were investigated between 2011 and 2015. Their main topographical and environmental characteristics are summarised in the Tab. 3.1.

Three main study sites were selected during the first year of research: Les Rognes, Entre la Reille and Tsarmine. Their choice relied mainly on their complementarity (Tab. 3.1). These SDCGSAPE are located in heterogeneous lithological (sedimentary vs. crystalline rocks) and climatic (humid vs. dry conditions) contexts. They also have different areas, the Tsarmine system being respectively ten and two times larger than Entre la Reille and Les Rognes. Hence, even during the LIA, the Entre la Reille glacier was thin and very small whereas the Tsarmine glacier had larger dimensions and theoretical driving stress. Moreover, while a bare-ice zone is still present at the top of Tsarmine, Les Rognes and Entre la Reille glaciers are almost completely buried. Hence, they illustrate a distinct stage of evolution of SDCGSAPE in the current negative mass balance period. The study of these complementary sites allowed thus outlining the existence of common and/or particular characteristics in SDCGSAPE. In addition, these research sites were selected because of the existence of

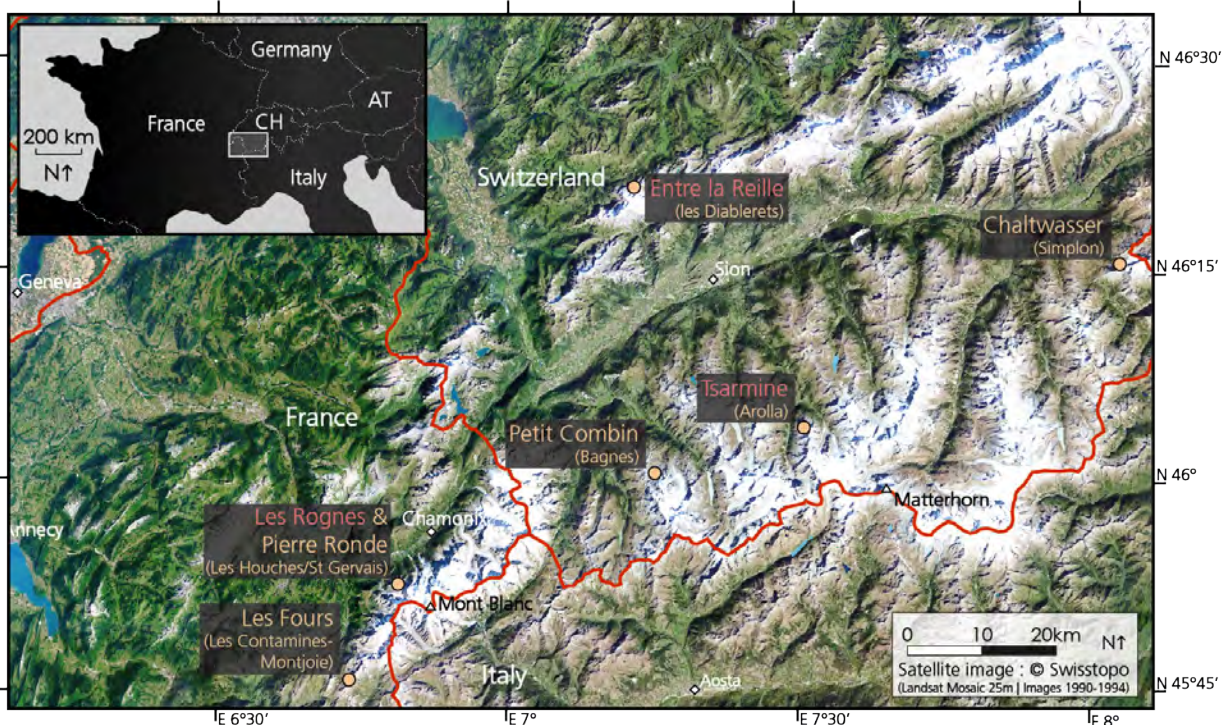


Fig. 3.1. Location of the seven study sites

geolectrical data (at Entre la Reille and Tsarmine; respectively published by [Reynard et al., 1999](#); [Lambiel et al., 2004](#)), the presence of a cable car and a mountain railway to ease their access (respectively at Entre la Reille and Les Rognes) and the interest and support of local public authorities (Etat du Valais for Tsarmine). Most of the investigations concentrated thus on these three systems.

To complete the data set on SDCGSAPE and deepen their analysis, four other study sites were investigated: Pierre Ronde, les Fours, le Petit Combin and the Chaltwasser systems. The two firsts are very small systems located in the Mont-Blanc massif. Pierre Ronde was especially studied because it was affected by the Tête Rousse water pocket outburst flood (WPOF) in 1892 and could be exposed to a similar event, since the detection of a new water pocket in Tête Rousse in 2010 ([Vincent et al., 2012 & 2015](#)). The past and potential effect of such event could be thus analysed in this site and its vicinity with Les Rognes allowed comparisons. The study of Les Fours system was mandated by the conservatory of the Haute-Savoie Natural Reserves (ASTERS) to question by field measurements the existence of very small remnant glaciers under the debris in this zone, proposed by [Bosson \(2010 & 2012\)](#). Finally, the results of the master thesis of [D’Aujourd’hui \(2013\)](#) and [Darbellay \(2015\)](#) were used and completed here. In these works, I collaborated in the research project design, the data collection and/or interpretation. Both investigated the current internal structure and the decadal elevation changes of larger glacier systems ([Tab. 3.1](#)). Their study allowed comparison with the characteristics obtained for the five other sites and to question the control of the site size in the development and evolution of glacier systems in high relief and permafrost environments.

	Location	Area (glacier + associated sediment accumulations in km ²)	Elevation (min-max, mean in m)	Maximum backwalls height in m	Aspect (N / E / S / W in %)	Main lithology	Estimated climatic parameters (MAAT in °C; MAP in mm)
Les Rognes	Massif du Mont Blanc; Les Houches (Haute-Savoie, France); 45°51'40"N, 6°48'50"E	0.29	2650-3100; 2820	100	66 / 3 / 12 / 19	Micaschists and mylonitised gneiss	-1; 2000
Entre la Reille	Hautes-Alpes calcaires; Ormont dessus (Valais, Switzerland); 46°20'20"N, 7°13'12"E	0.04	2380-2550; 2455	300	90 / 2 / 0 / 8	Limestone and marl	0; 1800
Tsarmine	Alpes penniques; Evolène (Valais, Switzerland); 46°03'N, 7°31'E	0.49	2600-3070; 2775	600	35 / 2 / 10 / 53	Granitic gneiss	-1; 1200
Pierre Ronde	Massif du Mont Blanc; St-Gervais-les-bains (Haute-Savoie, France); 45°51'30"N, 6°48'40"E	0.28	2600-3000; 2760	200	10 / 1 / 8 / 81	Micaschists and mylonitised gneiss	-1; 2000
Les Fours	Massif du Mont Blanc; Les Contamines-Montjoie (Haute-Savoie, France); 45°44'33"N, 6°43'47"E	0.21	2320-2640; 2450	100	54 / 1 / 0 / 45	Micaschists and mylonitised gneiss	-0.5; 2000
Chaltwasser	Monte Léone Massif; Ried-Brig (Valais, Switzerland); 46°14'35"N, 8°04'E	4.4	2350-3380; 2800	500	34 / 1 / 6 / 59	Gneiss and calcschists	-0.5; 1650
Petit Combin	Massif des Combins; Bagnes (Valais, Switzerland); 46°N, 7°15'40"E	4.3	2330-3660; 2890	500	61 / 18 / 2 / 19	Albitic gneiss and prasinite	-1; 1100

Tab. 3.1. Main characteristics of the seven study sites. The three main sites are presented first. Topographical data are derived from high-resolution DEMs (respectively the 4 m-resolution DEM of RGD 73-74 for the sites in France and the 2 m-resolution swissALTI3D of Swisstopo for the Swiss sites). Climatic parameters are roughly estimated near the mean altitude according to Météo-France and MeteoSwiss data. They are respectively derived from [Darbellay \(2015\)](#) and [D’Aujourd’hui \(2013\)](#) for the Petit Combin and Chaltwasser systems.

3.1.2. Methods

The main methods used in this work to study the SDCGSAPE are synthetically presented in the publications (Part 2). In order to avoid repetitions, only complementary information and the description of the other methods used are presented here. Ground characteristics of the SD-

CGSAPE were investigated with *ground surface temperature measurements, electrical resistivity tomography and ground penetrating radar*. Their recent dynamics, at timescales ranging from decades to months, were assessed with *differential GPS, photogrammetry and image comparison, and LiDAR*. Beyond this simple dichotomy, all the results obtained provided information on both ground characteristics and recent evolution of the SDCGSAPE: the current ground characteristics help to understand the recent evolution of these systems and the analysis of surface dynamics allows inferring ground compositions. This empirical dataset was completed by field observations and analysis of the historical documents collected (maps, photographs, draws, reports, etc.).

3.1.2.1. Ground surface temperature measurements

Ground surface temperature (GST) measurements are presented in the section 2.1.2.3 and complete overview can be found in [Delaloye \(2004\)](#) or [Lambiel \(2006\)](#). Miniature temperature sensors (IButton DS1922L, accuracy of 0.065°C) were installed at the subsurface in Les Rognes, Tsarmines, Entre la Reille, Pierre Ronde, les Fours. The sensors were placed between blocks, at depth of 5 to 50 cm, to insulate them from direct solar radiation and precipitations. However, because of the occurrence of local surface movements (related to the ground flow/slide, variation of ice content or avalanches), some of them were found directly at the surface during field investigations or disappeared. Moreover, several sensors broke down during the measurement periods without evident cause (in relation with ground humidity, a problem in the programming software or in the connector?). The GST dataset is therefore extremely discontinuous and few data are available for the most recent measurement period. For this reason and also because subsurface thermal data provide qualitative and debatable information on ground characteristics in sediment accumulations (see below), the results of this method were not analysed in detail in the articles.

The sensors were programmed to measure the temperature each two hours. Several variables were calculated from the GST data: mean (annual) ground surface temperature (M(A)GST), ground freezing index (GFI), winter equilibrium temperature (WEqT) and the duration of the zero-curtain period (second part of *état de fonte* on [Fig. 3.2](#)). GFI and WEqT are presented in the section 2.1.2.3. MAGST was computed when the thermal data covered a complete year. In the last decades, negative MAGST value was commonly used to infer the distribution of permafrost and ground ice in sedimentary environments (e.g. [Kneisel, 2003](#)). However, because of the complexity of energy transfer in a porous ground, negative and positive thermal anomalies are numerous and permafrost can be balanced or even aggrading with a positive MAGST ([Burn and Smith, 1988](#)). This variable appears to be also a fundamental control of ice-debris mixture flow velocity. Indeed, a correlation between the variation of MAGST and surface velocities measured several months to one year later was highlighted in rock glaciers ([Perruchoud and Delaloye, 2007](#); [Delaloye et al., 2008](#)). Finally, the zero-curtain period, where ground surface temperature stabilise at 0°C, illustrates the moistening of the snow layer during the melt period, until its disappearance ([Lambiel, 2006](#)). The variation of the zero-curtain length in a study site shows the heterogeneity of snow cover thickness and of microclimatic conditions and the date of snow disappearance.

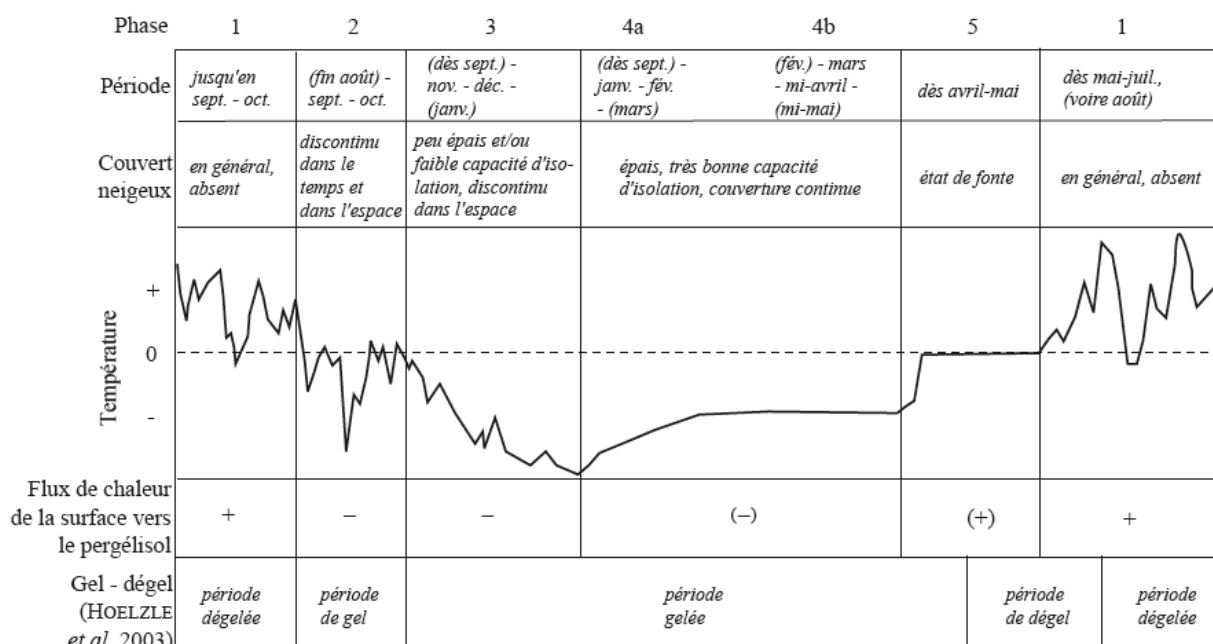


Fig. 3.2. Typical annual thermal behaviour of ground surface under permafrost conditions. The temperature curve is fictive. Reproduced from Delaloye (2004).

In addition to the installation of thermal sensors, the bottom temperature of the snow cover (BTS, [Haeberli, 1973](#); [Delaloye, 2004](#)) was measured in March 2011 at Entre la Reille. As for the calculation of WEqT, the measurement of the temperature with a resistivity sensor aims to know the ground surface temperature in winter, when the ground is efficiently insulated from atmospheric conditions by the snow cover. The ground surface temperatures are then mainly controlled by subsurface conditions and temperature few degree Celsius below 0 indicate the potential presence of permafrost conditions or ground ice at depth.

The thermal data collected here provided quantitative data on the ground thermal regime ([Fig. 3.2](#)) and indications on the presence of ground ice and permafrost conditions at depth. However, GST is controlled by numerous complex processes and for instance, the inter-annual variation of MAGST, BTS or WEqT can reach 2-3°C ([Lambiel, 2006](#)). Therefore, these results need to be discussed and completed by other data although they give interesting information on the spatial distribution of cold/warm zones within a study site ([Delaloye, 2004](#)).

3.1.2.2. Electrical resistivity tomography

The data acquisition and processing of Electrical resistivity tomography (ERT) are briefly presented in 2.1.2.3 and 2.2.2.3. We complete here these sections by elements on the method principle, on our approach and on result uncertainty. [Hauck and Kneisel \(2008\)](#) or [Scapozza \(2012\)](#) review for example in detail this method that relies on the measurement and interpretation of subsurface contrast of electrical resistivity. The latter are especially marked between frozen and unfrozen terrains because ice and cold temperature hinder considerably the circulation of the electric field in the subsurface ([Fig. 2.4](#)). ERT is thereby frequently used and considered as one of the most (if

not the most) reliable geophysical methods to detect ground ice in sedimentary accumulations located in permafrost conditions (Ribolini et al., 2010; Dusik et al., 2015).

In a first step, ERT requires to measure the difference of potential (Δv) between two electrodes (M and N on Fig. 3.3A) by injecting an electric current between two other electrodes (A and B on Fig. 3.3A). Electrodes are stuck to the ground and the electrical connectivity can be improved in porous terrains by the use of sponges wetted by salted water. Δv allows then calculating the apparent resistivity ($\rho_{app.}$) of the crossed subsurface by:

$$\rho_{app.} = G * (\Delta v / I)$$

where $\rho_{app.}$ is in Ωm , G is a geometrical factor depending of the electrode configuration on the field in m (e.g. inset in Fig. 3.3A), Δv is measured in mV and I is the injected current in mA.

The measure is then repeated several times in an automated process, where deeper zones are theoretically investigated by increasing the electrode spacing (e.g. measure 1, 17 and 30 in Fig. 3.3A). The Wenner-Schlumberger electrode array (inset in Fig. 3.3A) was used for all the ERT profiles carried out in this study because the dataset obtained with this configuration has a good compromise between the depth of investigation and the horizontal resolution (Scapozza, 2012). Once the 2d data have been collected (pseudo section of $\rho_{app.}$), the specific resistivity ($\rho_{spec.}$) of all the subsurface layers crossed by the electric field below the device is inferred through an inversion process with the creation of a model of the inverted resistivities (Fig. 3.3B). The inversion process was constrained by the use of robust parameters (2.1.2.3; Scapozza, 2012). Indeed, normal (or smooth) inversion parameters are less efficient to evidence the large and localised contrasts of resistivity expected in the environments containing massive buried ice and ice-free debris. Non-robust inversions can thus provide a simplified and filtered picture of internal structure in the investigated sites. In contrast, robust inversion parameters generate tomograms that better take into account small-scale resistivity contrasts in the data and gives, thereby, a more realistic overview of local internal structure heterogeneity. However, this inversion method has the disadvantage to generate cubic patches of resistivity (e.g. Fig. 2.15). Hence, the different ground components evidenced by these resistivity contrasts have probably a more rounded and lenticular shape in reality.

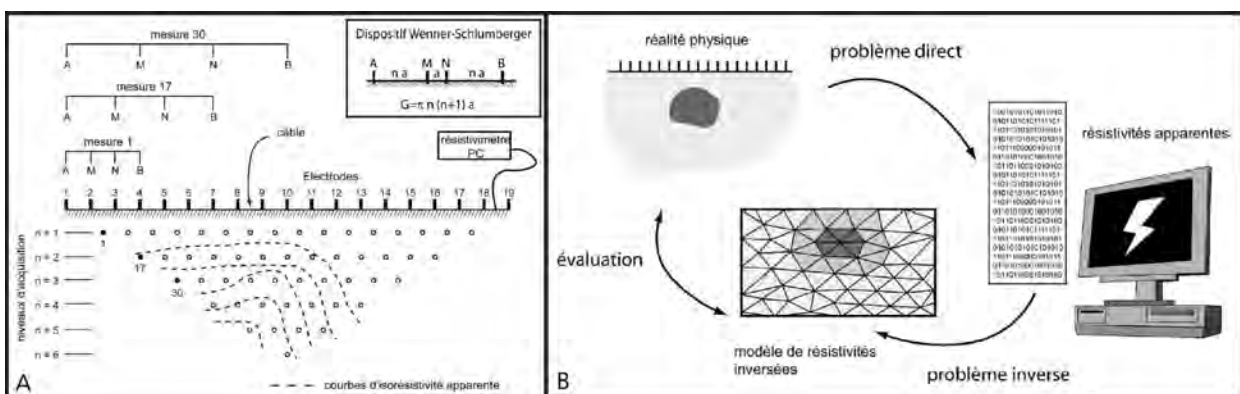


Fig. 3.3. A. Sketch illustrating the resistivity data acquisition with a Wenner-Schlumberger configuration. B. Sketch showing the data inversion principle. Adapted from Marescot (2006).

All the models produced in this research are displayed with the same resistivity thresholds and colour scale to ease their comparison. This scale is presented in [Fig. 2.4](#). Typical values gathered in the literature are associated to provide a key of data interpretation. However, the resistivity ranges boundaries proposed are open and the values proposed have to be considered rather as indications and orders of magnitude than indisputable thresholds.

The reliability of ERT data was assessed in different ways. During field measurements, automatic test between neighbouring electrodes allowed to check (and to improve if necessary) the quality of the electrical contact between the electrodes and the ground. During the data processing, in the first time, we controlled manually the quality of each raw dataset and filtered the measurement errors (e.g. negative resistivity values, measure with unrealistic 2d coordinates). At the end of the inversion process, the quality of the final tomograms was automatically quantified after the 5 iterations of data inversion, by comparing the measured and inverted data (absolute error in %). Following [Hilbich et al. \(2009\)](#), we also computed the model resolution matrix value (e.g. [Fig. 2.15](#)) to highlight the areas where the inverted model is well constrained by the measured data from possible inversion artefacts in poorly documented areas. This value shows that the uncertainty of inverted structures increases at depth, especially below the highly resistive layers. This situation was also observed by [Hilbich et al. \(2009\)](#) and related to the limitation of electric field penetration by ground resistive layers. Hence, ERT data at depth have to be interpreted with caution, especially below highly resistive layers as glacier ice. The estimation of glacier thickness with ERT is thus strongly uncertain and we voluntarily made few considerations on structure thickness from ERT data along this research. Nevertheless, the comparison of ERT data and direct observations in boreholes in talus slopes located in permafrost environments showed the very high consistency between the contrast of resistivity and the real distribution of ground ice, and thus, the potential of ERT to predict ice occurrence in the first tens of meters below the ground surface ([Scapozza et al., 2011](#)). However, the results of the model resolution matrix obtained here support those of [Hilbich et al. \(2009\)](#) and suggest prudence in the consideration of ERT data below ice-cored structures. The comparison of the spatial limits of internal structure components evidenced by ERT data with those obtained with other methods (e.g. GPR, dGPS, photogrammetry) showed a very high consistency. Therefore, if the trustworthiness of ERT data at depth can be questioned, this method provided very reliable data in the first meters below the ground surface and allowed to characterise and map precisely the different components of the studied systems.

An extensive investigation of the ground resistivities in a study site is a challenging task in high mountain, especially because of the weight and amount of the material required, the difficulty to have a good electrical connectivity between highly porous surface and electrodes, and the relative time required for material installation and measurement (e.g. [Hilbich et al., 2009](#)). The numerous geoelectrical data collected recently in SDCGSAPE (e.g. [Kneisel, 2003](#); [Reynard et al., 2003](#); [Kneisel and Kääh, 2007](#); [Ribolini et al., 2010](#); [Dusik et al., 2015](#); [Seppi et al., 2015](#)) remain thus extremely discontinuous and concern small parts of the systems. To our knowledge, ERT profiles that cross completely longitudinally or transversally SDCGSAPE are very rare (two complete profiles can be observed in [Reynard et al., 2003](#)). We have thus tried here to collect the most

complete possible ground resistivity dataset in each study site. Moreover, because Entre la Reille is relatively easily accessible by cable car, a longitudinal ERT profile was measured each mid-July at the same location between 2011 and 2014. These repeated surveys aimed at studying the annual variation of ground resistivities and assessing the potential of ERT monitoring in such landsystem.

3.1.2.3. Ground penetrating radar

A ground penetrating radar (GPR) campaign was carried out in March 2015 at Tsarmine. M. Fischer (University of Fribourg) led the field campaign and processed the data. This method is succinctly presented in the section 2.3.2.3. A broad presentation of its application in glacial environment can be found in [Nobes \(2011\)](#). This geophysical technique “uses the propagation of a shaped pulse or wavelet of radio-frequency electromagnetic energy (radar) into the subsurface and measures the radar echoes returned to yield radargrams or profiles of the physical property variations in the subsurface” ([Nobes, 2011](#), p 490). GPR is frequently used to study the geometry and internal structure of glaciers or ice-rich environments, because it allows highlighting the dielectric permittivity contrast between water, ice and air ($\kappa = 80$, $\kappa = 3$, $\kappa = 1$, respectively; e.g. [Irvine-Fynn et al., 2006](#); [Fukui et al., 2007](#); [Florentine et al., 2014](#); [Monnier et al., 2014](#)).

3.1.2.4. Differential GPS

Surface displacements were investigated in all the study sites (except the Petit Combin system) by the repeated measurements of the spatial coordinates of blocks with a differential GPS (dGPS). [Fig. 2.14](#) presents the principle and the variable that can be calculated with two dGPS measurements. This tool is also presented in 2.1.2.3 and 2.2.2.3 and is thoroughly discussed in [Lambiel and Delaloye \(2004\)](#). This time-consuming in situ collection of punctual measurements can appear somehow outdated in a period where the progress of remote sensing methods allows rapid, accurate and site-scale dynamical analysis of SDCGSAPE (e.g. [Avian et al., 2009](#); [Fischer M et al., 2014](#); [Monnier et al., 2014](#); [Seppi et al., 2015](#); [Fischer M et al., 2016](#)). However, dGPS data provide very precise three-dimensional information on individual blocks movements. Operating dynamics and associated processes can be inferred from dGPS monitoring (see the publication 2, part 2.2).

According to the frequency of the block position measurement, surface dynamics of the study sites were analysed from multi-annual to infra-seasonal timescales. Measurements were carried out with a Leica SR500 or a Trimble R10. Both have respectively a theoretical maximum 3D accuracy of 5 and 2 cm. The systematic measurement of control points showed that the accuracy was lower than 2-3 cm. Relatively small movements between surveys were thus detected. However, the relative uncertainty increases exponentially when the movement magnitude decreases. To reduce the uncertainty level, we compared the movements detected at the shortest timescales with those more reliable obtained at the largest timescales for each block. Hence, we manually corrected the small movements that presented significant inconsistency of magnitude and/or 3D direction. This process only concerned few small movements and generally, this block-to-block control showed the consistency and reliability of the surface movements dataset. In addition to

the horizontal and vertical movements, elevation changes (which were mainly negative and thus usually mentioned to as surface lowering) and downslope movements were inferred from the measured movements and the slope angle derived from high-resolution DEMs (Fig. 2.14, see the section dGPS in 2.2.2.3). As the slope angle around each block was an estimation of the reality, which was considered as stable over the investigated years, the calculated elevation changes and downslope movements have to be considered as orders of magnitudes whose measurements are relatively reliable but, in any case, as definitive and undisputable results.

3.1.2.5. Photogrammetry and image comparison

The decadal surface elevation changes at Tsarmine, Entre la Reille, Chaltwasser, and the Petit Combin systems were investigated with archival aerial photogrammetry. N. Micheletti and M. Capt, M. Capt, S. D’Aujourd’hui and R. Darbellay respectively produced these analyses for each site. Three-dimensional information was derived from pairs of areal photographs according to the principle of stereoscopic viewing. The comparison between the digital elevation models (DEMs) created allowed then to study elevation changes between two periods. The successive steps of the procedure are described in the section 2.3.2.3. Complete reviews of the use and potential of photogrammetry in glacial and high mountain environments are presented in Kappas (2011) and Micheletti et al. (2015b). As describe in 2.3.2.3, the ortho-rectification of aerial images for photogrammetry also permitted to study the horizontal surface displacement rates by producing manually feature tracking or using a software of image autocorrelation (7D; Vacher et al., 1999).

3.1.2.6. LiDAR

Two terrestrial laser scan surveys were carried out in summer 2013 and 2014 in Entre la Reille. The LiDAR (Light Detection And Ranging) technique allows measuring the distance of a target by calculating the “time of flight” of a laser signal emitted and reflected by the target. High-resolution DEMs are thus generated with this remote sensing technique. The procedure and potential of this method in cold environments are detailed for example in Demuth (2011), Kummert and Delaloye (2015) or Fischer M et al., (2016). The laser scan surveys were performed the 13.08.2013 and the 22.09.2014 with a Riegl VZ-6000 by N. Micheletti, M. Fischer and M. Capt. The data were then processed by M. Capt, who investigated surface elevation changes and horizontal velocities from DEMs and hillshades comparison (Capt, 2015).

3.2. Les Rognes and Pierre Ronde

3.2.1. Site description

Les Rognes and Pierre Ronde are two neighbouring SDCGSAPE located in the Mont-Blanc massif (Fig. 3.4). The two sites were presented in the sections 2.1.2.2 and 2.2.2.2 and only complementary observations are given here. Both systems have the same area but compared to Les Rognes, Pierre Ronde is extended slightly lower and its backwall is two times higher (Tab. 3.1). Pierre Ronde occupies a slope facing West whereas les Rognes is mainly oriented toward the North.

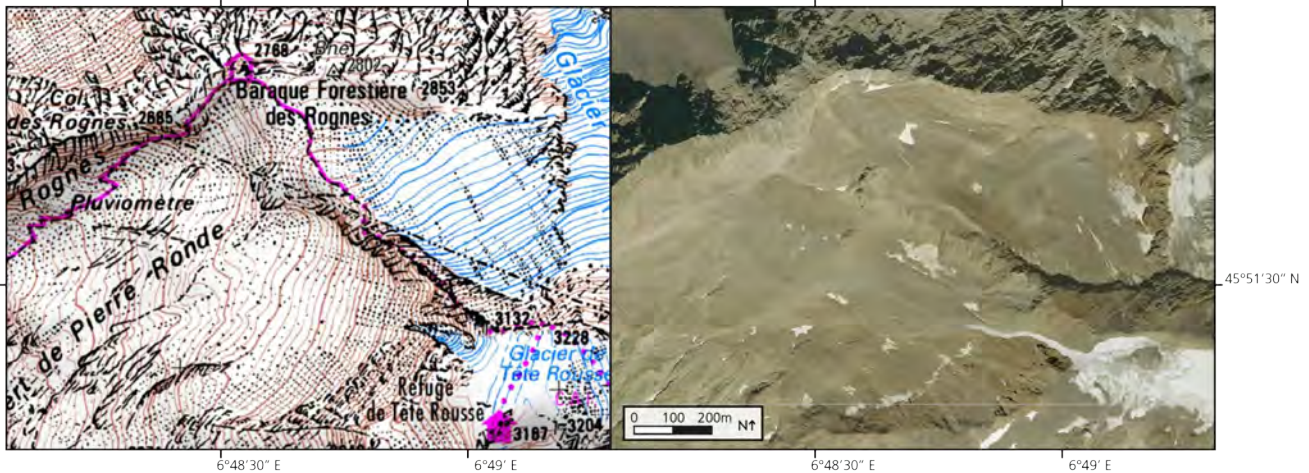


Fig. 3.4. Map (Top25, leave 3531 ET, 2008) and aerial photograph (2008) of Les Rognes and Pierre Ronde (© IGN, available on geoportail.gouv.fr). The glacier extent in the map did not change since the 1980s.

The lithology is mainly composed by highly fractured gneiss and micaschists (Fig. 3.5), where glacial erosion efficiently shaped cirques. Les Rognes and Pierre Ronde are two remnant cirques glaciers that belonged to the same glacier complex during the LIA maximum. Indeed, Les Rognes was connected to the neighbouring Griez glacier. Moreover, an ice apron was covering its backwall and linked this glacier to the Tête Rousse glacier, which probably overflowed its hollow bed toward Les Rognes. Tête Rousse was also connected to Pierre Ronde glacier by the Bossonnet couloir, which is still covered by snow (Fig. 3.4). Unfavourable climatic conditions for glaciers and especially the warming of air temperature (e.g. Fig. 3.6) contributed to the fragmentation of this glacier complex. As observed on the 1949 areal photograph, this fragmentation was probably already effective during the 1940s negative mass balance period (Vincent et al., 2010; Deline et al., 2012) and the

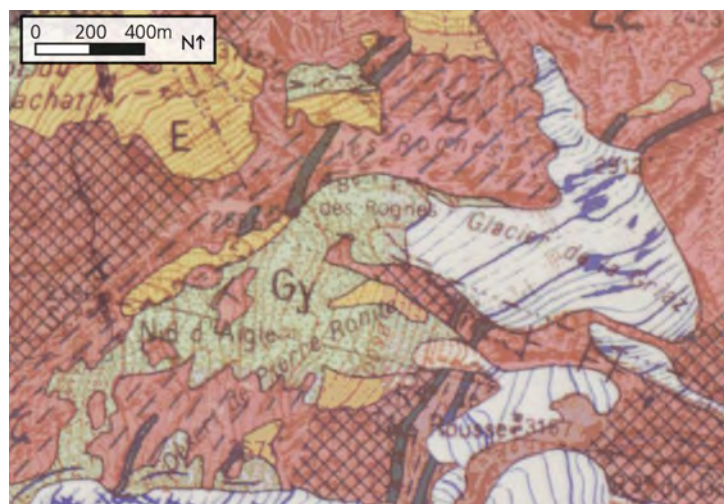


Fig. 3.5. Extract of the leave 703 (St-Gervais les Bains) of the 1: 50'000 French geological Atlas (Available on geoportail.gouv.fr; Mennessier et al., 1976). White areas correspond to glaciers. The Rognes glacier is integrated in the Griez glacier here. Green and yellow areas are respectively moraine deposits and talus slopes. The pink background corresponds to the gneiss and micaschists of the Mont-Blanc massif.

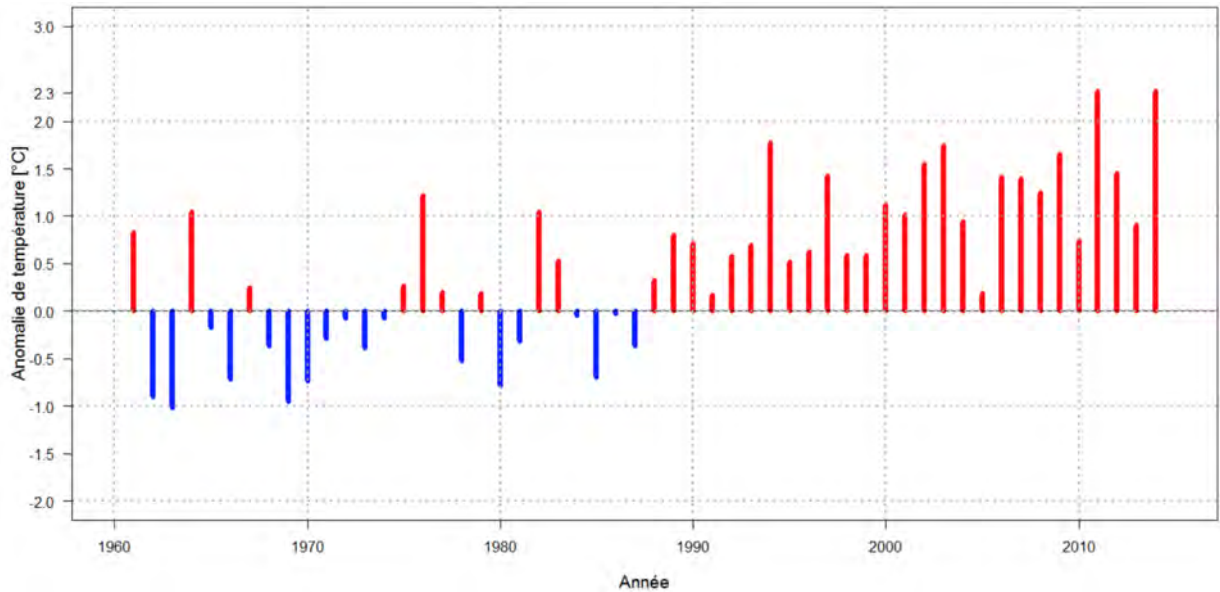


Fig. 3.6. Anomaly of mean annual air temperature compared to the 1961-1990 climatic norm measured at Chamonix weather station (1042 m a.s.l.; 45°55'40"N, 6°52'40"E; 9 km distant from Les Rognes). Reproduced from Magnin (2015; data: © Météo France).

local glaciers were strongly debris-covered (Fig. 3.7). Conversely, large snow accumulation and rapid reconnection between the individual glaciers can have occurred locally during positive mass balance periods, as the one experienced between the 1960s and the mid-1980s (Fig. 3.7). The

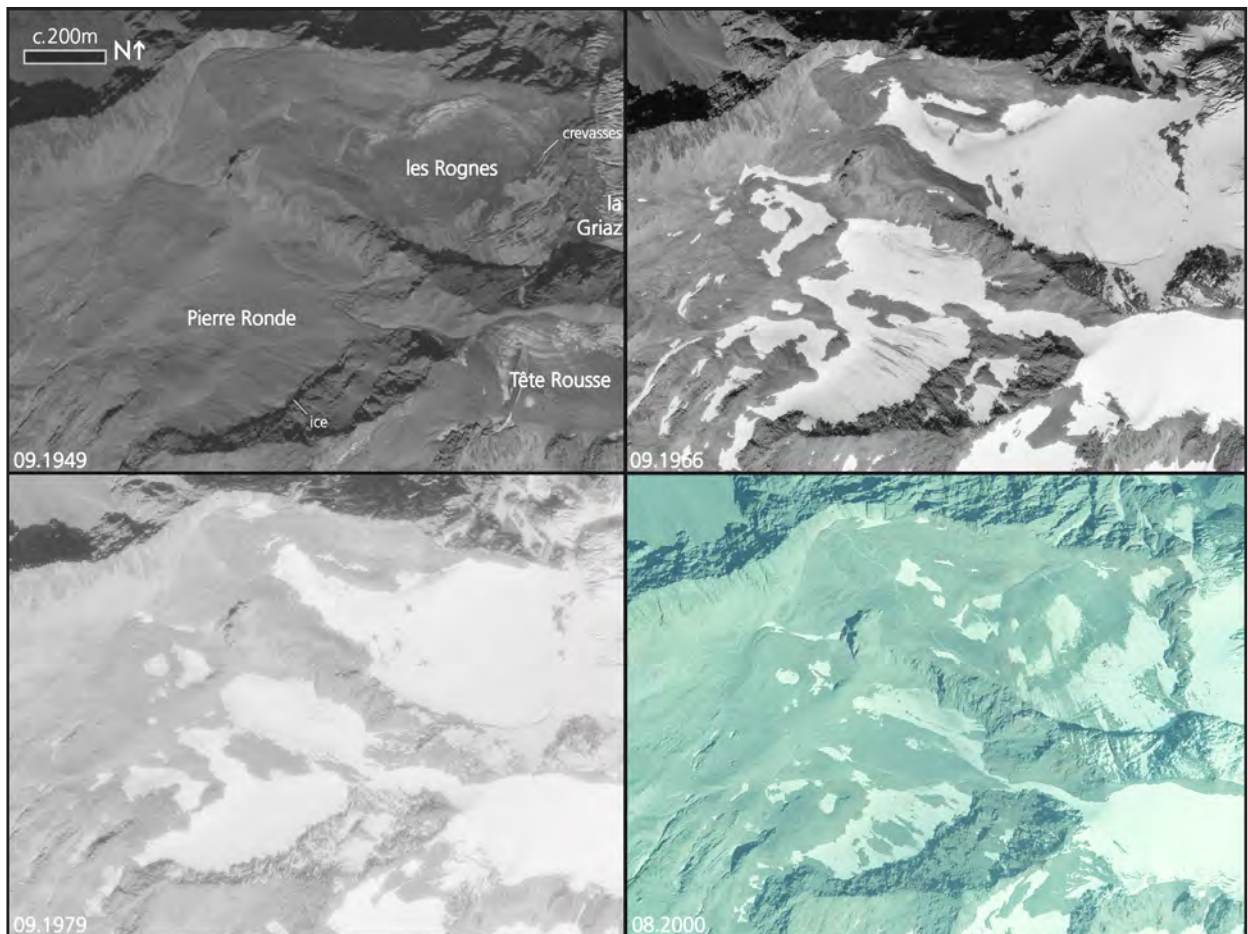


Fig. 3.7. Aerial images of Les Rognes and Pierre Ronde over the last decades (© IGN, photographs respectively C3630-0121_1949_F3630-3631_0044, C3531-0061_1966_F3531_0008, C3531-0031_1979_F3531-3631_0105 & CA00S00932_2000_fd0174_250_1254, available on geoportail.gouv.fr).



Fig. 3.8. Photographs of Les Rognes. The old photograph originates from the “centre de la Nature Montagnarde” collection. The recent ones were taken by T. Ferber, S. Utz and JB. Bosson.

local conditions have become strongly unfavourable for glaciers since the mid-1980s. Hence, ice outcrops and crevasses rapidly disappeared on local glacier surface (compare the 2000 and the 2008 pictures of the Fig. 3.7 and 3.4). In addition to the recent weak dynamic of these cirque glaciers, their burying under the debris is also very likely accelerated by the permafrost degradation in the fractured backwalls (Magnin, 2015). Indeed, numerous rockfall events were observed during the field investigations in summer.

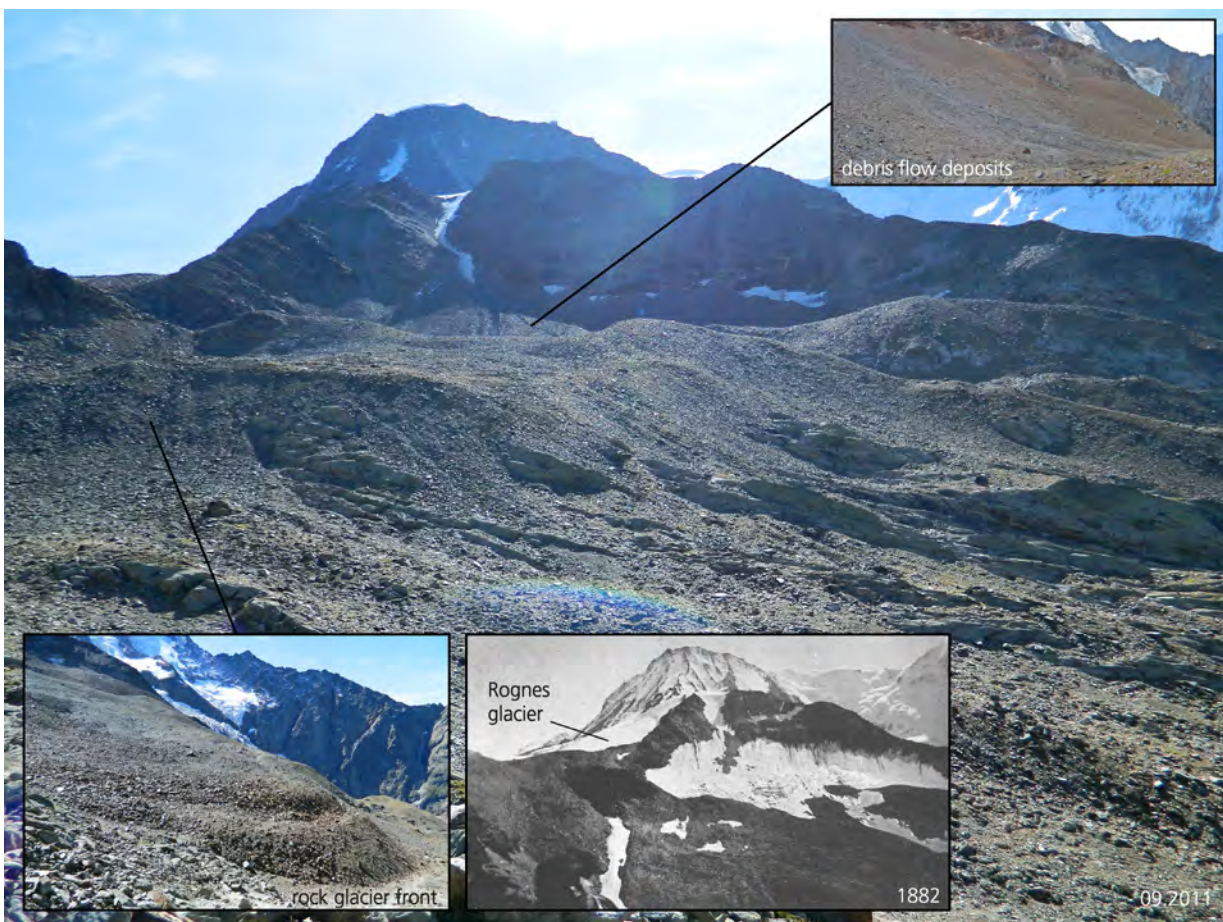


Fig. 3.9. Photographs of Pierre Ronde. The old photograph originates from the RTM collection. The recent ones were taken by S. Utz and JB. Bosson.

The surface morphology of Les Rognes and Pierre Ronde systems showed differences (Fig. 3.8 and 3.9). Whereas snow, ice, crevasses or bergschrunds were visible on several old photographs of Les Rognes, only snow and rare ice outcrops were observed in the last decades in Pierre Ronde. Moreover, the current glacier limits are locally outcropping in Les Rognes whereas they are invisible in Pierre Ronde. A complex of numerous arcuate ridges is present in the distal part of Les Rognes and only a rock glacier located at the lower and northern margin has superficial deformation patterns in Pierre Ronde (Fig. 3.9). Finally, debris-flow deposits fill the upper depression of Pierre Ronde and no sign of such torrential activity was observed in Les Rognes.

3.2.2. Results

3.2.2.1. Ground surface temperature measurements

The ground surface temperature was measured each two hours at 20 locations in Les Rognes and Pierre Ronde system. 2011-2012 data were already presented in the publication 1 (section 2.1). Several thermal indices were computed from the results obtained between 2011 and 2014 (Fig. 3.10 and Tab. 3.2). Unfortunately, these data have several gaps and the indices were not computed at annual timescale but during approximately three 10-month periods. Nevertheless, this incomplete dataset provides large amount of information on the local ground thermal regime.

The coldest conditions were observed in the upper half of Les Rognes for all the indices computed (Ro_1 to Ro_8). The winter equilibrium temperatures were especially cold here ($< -4^{\circ}\text{C}$ for most sensors and periods) and illustrates the probable presence of ground ice at shallow depth.

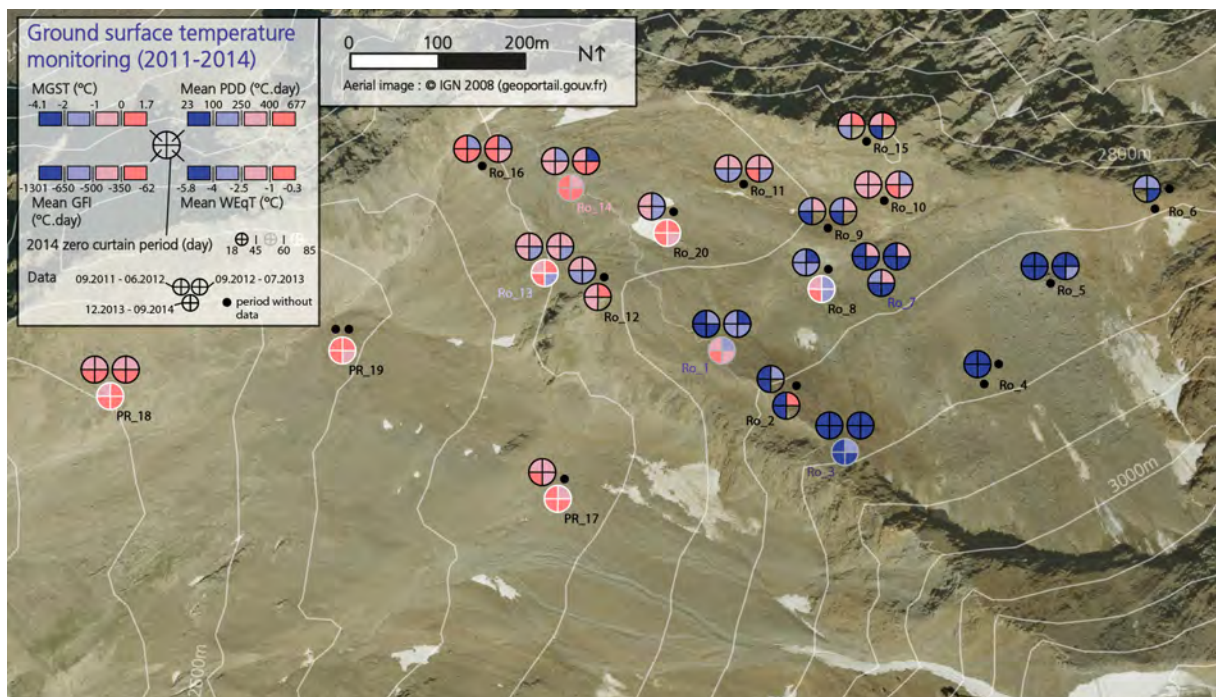


Fig. 3.10. Indices measured with the thermal sensors in Les Rognes and Pierre Ronde. The data are detailed in Tab. 3.2. The dataset comprised some gaps at the 3-year scale and only the three most complete periods between September 2011 and 2014 are presented here. PDD, GFI and WEqT correspond respectively to positive degree day, ground freezing index and winter equilibrium temperature.

Thermal sensor	Elevation (m a.s.l.)	Location	Mean ground surface temperature (MGST, °C)			Mean summer GST (°C)	Positive degree day (PDD, °C.day)			Winter equilibrium temperature (WEqT, °C)			Ground freezing index (GFI, °C.day)				Zero Curtain period (day)		
			2012	2013	2014		Mean	2012	2013	2014	Mean	2012	2013	2014	Mean	2012		2013	2014
Ro_1	2820	Centre of the western zone	-2.3	-1.4	-0.2	-1.3	100	78	218	132	-4.2	-3.6	-2	-3.3	-787	-533	-279	-533	53
Ro_2	2855	Centre of the western zone	-3.6	-1.4	-2.5	4.2	248		457	352					-1301		-873	-1087	18
Ro_3	2880	Top of the western zone	-4.1	-3	-2.6	1.8	84	49	175	103	-5.3	-5.7	-5	-5.3	-1297	-1036	-942	-1297	53
Ro_4	2890	Upper central zone	-3.1				31				-4.5			-957					
Ro_5	2845	Eastern footslope of the top zone	-2.8	-2.1	-2.4		78	51	64	64	-4.8	-3.9	-4.4	-4.4	-895	-725			
Ro_6	2845	Rognes-Griaz transition	-1.9				159							-733					
Ro_7	2800	Western footslope of the top zone	-2.5	-2	-2.2	3.3	271	269	290	276	-5.5	-5.2	-5.7	-5.5	-1001	-937	-879	-939	42
Ro_8	2775	Western footslope of the top zone	-1.6	-0.1	-0.9	2.5	78		228	153	-3.3	-2.9	-2.9	-3.1	-550		-272	-411	79
Ro_9	2800	Central bulge	-1.4	-1.3	-1.4		251	320	285	285	-3	-2.9		-3	-674	-744		-709	
Ro_10	2810	South-facing slope of the North zone	0	-0.3	-0.2		309	249	279	279	-2.3	-1.9		-2.1	-322	-361		-341	
Ro_11	2775	Northern distal zone	-0.7	-0.2	-0.4		319	282	301	301	-3	-2.9		-3	-534	-336		-435	
Ro_12	2785	Southern distal zone	-0.7		-0.4	4.8	335		439	383	-3.5				-540		-451	-495	34
Ro_13	2745	Southern frontal part	-0.6	-0.5	-0.3	4.5	250	280	314	314	-3.3	-3.5	-2.5	-3.1	-429	-448	-315	-397	62
Ro_14	2770	Northern distal zone	-0.9	0	0.7	3.8	128	93	188	188	-1.9	-0.8	-0.8	-1.2	396	-103	-134	-211	56
Ro_15	2845	Northern LIA moraine	0.4	-0.8	-0.2		677	587	632	632					-545	-850		-698	
Ro_16	2750	Northern frontal part	0.3	0.3	0.3		246	234	240	240	-0.8	-1.2		-1	-143	-124		-134	
Ro_20	2790	Distal central depression	-0.9		1.7	6.1	104		349	349	-2.5		-1.4	-1.9	-381		-91	-236	76
PR_17	2720	Upper Pierre Ronde depression	0		0.7	3	258		263	263	-1.3		-0.5	-0.9	-266		-62	-164	71
PR_18	2570	South-facing talus slope	0.9	0.7	1.7	1.1	362	319	442	442	-0.5	-0.3	-1.2	-0.7	-100	-86	-135	-107	85
PR_19	2650	Rock glacier front in Pierre Ronde			1.2	5.6			519				-1.6				-158		
Interpol. Air T°	2850		-2.6	-3	-0.8	-2.1	427	516	503	503					-1184	-1513	-807	-1168	

Tab. 3.2. Synthesis of the indices computed from the thermal sensor data between September 2011 and 2014. Air temperature at 2850 m. a.s.l. is extrapolated using the daily data of les Aiguilles Rouges weather station (2365 m a.s.l.; 45°59'06"N, 6°53'48"E; 15 km distant from the study sites, © MétéoFrance) with a thermal gradient of 0.65°C.100m, obtained comparing the 4-year daily data of les Aiguilles Rouges with those of the Aiguille du Midi weather station (3845 m a.s.l.; 45°52'43"N, 6°53'15"E; 6 km distant from the study sites, © MétéoFrance).

Ground conditions were clearly warmer in the lower half of Les Rognes (Ro_9 to Ro_20) and the highest temperatures were measured in the rock glacier zone (Ro_14 and Ro_16). This marked thermal contrast between the upper half and the distal zone was observed on the three periods. In addition to the influence of subsurface (presence of ground ice, permafrost conditions), this heterogeneous situation is very likely enhanced by the topographical influence. Indeed, the upper steep zone faces the North and is efficiently shadowed by the backwalls. Small amount of energy is received in the upper zone (for instance, PDD was lower than 200°C.days for the sensors Ro_3 to Ro_5). In contrast, the distal zone is flatter, locally oriented towards the SW and less shadowed by the relief. Consequently, direct solar radiation is higher here and less cold can be trapped in the porous ground. The sensors deposited in the Pierre Ronde SDCGSAPE (PR_17 and PR_19) and in the lower talus slope (PR_18) measured even warmer temperature than in the distal zone of Les Rognes. The ground surface conditions are thus less favourable for permafrost and ground ice occurrence in Pierre Ronde compared to Les Rognes.

The 3-year temperature curves of the sensors that have the most complete dataset is showed in the Fig. 3.11. Ground and air temperatures presented similar values during the snow-free period (typically July to October). As a consequence, the ground temperatures were significantly lower during the summer 2014 than during the previous one. The insulation of the ground by the snow resulted in the stabilisation of ground temperature from January. The coldest values were then measured by the highest sensor (Ro_3) and the one located in the footslope of the upper zone (Ro_7). Conversely, winter equilibrium temperatures were warmer downward and relatively close to -1°C in the rock glacier zone (Ro_14). The influence of the debris-cover thickness on ground

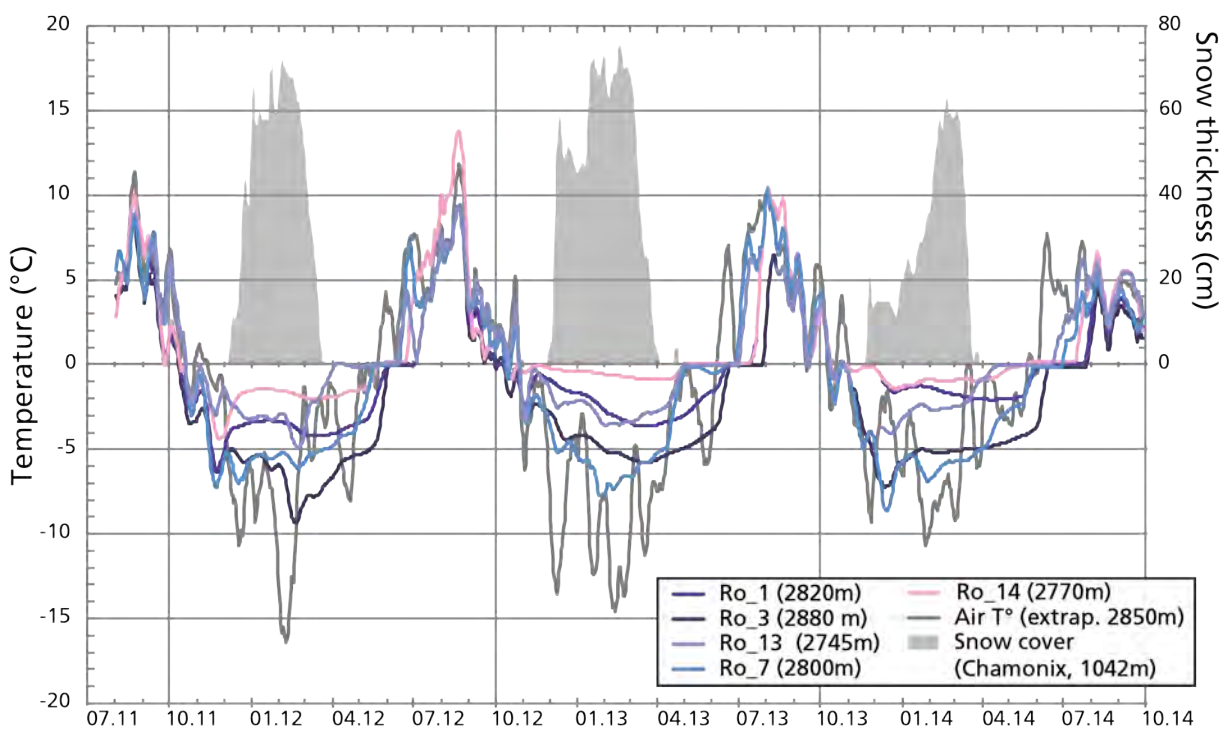


Fig. 3.11. 11-day running means of ground and air temperature in Les Rognes. The position of these thermal sensors is shown on Fig. 3.10. See the caption of the Tab. 3.2 for the description of the extrapolation of air temperature at 2850 m a.s.l. The 5-day running mean of the snow cover height at Chamonix (1042 m a.s.l.; 45°55'42"N, 6°52'36"E; 9 km distant from Les Rognes, © MétéoFrance) indicates temporal and thickness variations of snow mantle at regional timescale although the snow typically covers the study site with a thick layer from October to early-July.

temperature was investigated in Ro_7, where two sensors were respectively placed at depth of 5 and 25 cm (Fig. 3.12). Few data were measured in summer but they clearly showed lower temperatures and variations at depth. Less temperature variations were also evidenced at depth in winter but the temperature was slightly higher (0.5 to 1.5°C) than directly below the surface. This situation was probably due to the larger influence exerted by cold autumn temperature near the surface. Ground thermal regime during both snow-free and snow-covered periods showed thus the relatively poor thermal conductivity of the debris layer. A difference of ~ 20 cm of thickness induced a noticeable insulation of the ground from air temperature variations.

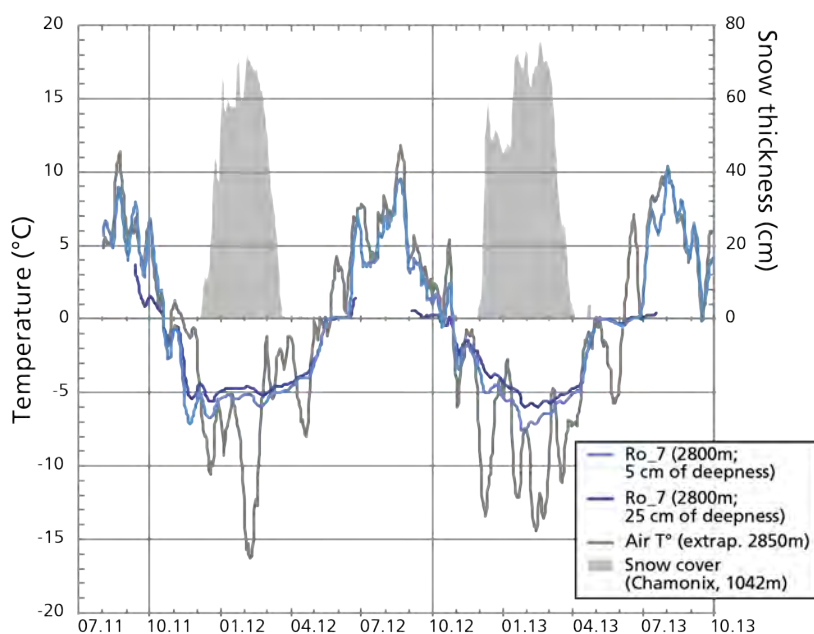


Fig. 3.12. 11-day running means of air and ground temperature at 5 cm and 25 cm of thickness in Les Rognes. Ro_7 position is shown in Fig. 3.10. See the caption of the Tab. 3.2 and Fig. 3.11 for the description of the air temperature and snow cover thickness.

3.2.2.2. Electrical resistivity tomography

The ERT results obtained in Les Rognes and Pierre Ronde were presented and discussed in the publications 1 and 2 (respectively sections 2.1 and 2.2; see especially the Fig. 2.5). The ground resistivities were very high (> 500 kΩm) directly below the surface in the upper slope of Les Rognes and from a few meters of deepness in the distal zone. Resistivities between 15 and 300 kΩm were found below 5 m of more conductive material in the rock glacier zones of Les Rognes and Pierre Ronde. Finally, the central depression of Les Rognes and all the other zones investigated in Pierre Ronde had a ground resistivities lower than 10 kΩm.

3.2.2.3. dGPS

The position of respectively 96 and 59 blocks was measured up to height times between 2011 and 2014 in Les Rognes and up to four times between 2012 and 2013 in Pierre Ronde with a dGPS. Some of the results were already presented in the publications 1 and 2 (respectively sections 2.1 and 2.2). Les Rognes was significantly more active than Pierre Ronde at both annual and seasonal timescales (Fig. 3.13). Maximum movements over the three years reached here respectively 305, -554 and 521 cm in horizontal, vertical and surface lowering components in Les Rognes (see Fig. 2.14 for details on the calculation). All these maximum movements were measured at the foot-

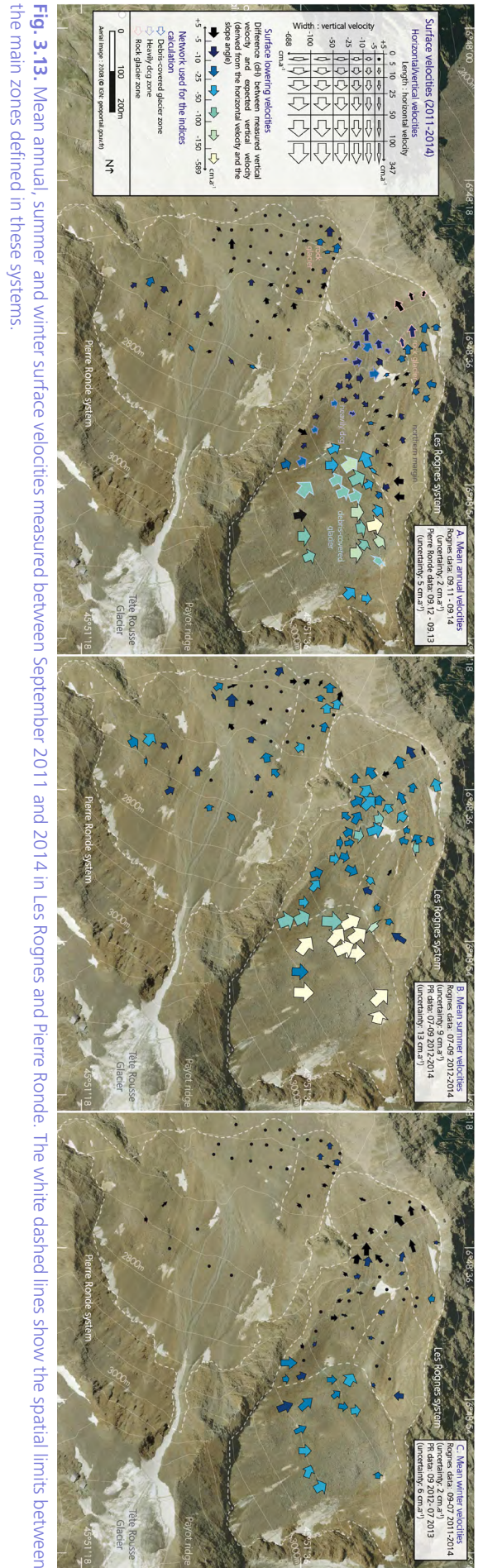


Fig. 3.13. Mean annual, summer and winter surface velocities measured between September 2011 and 2014 in Les Rognes and Pierre Ronde. The white dashed lines show the spatial limits between the main zones defined in these systems.

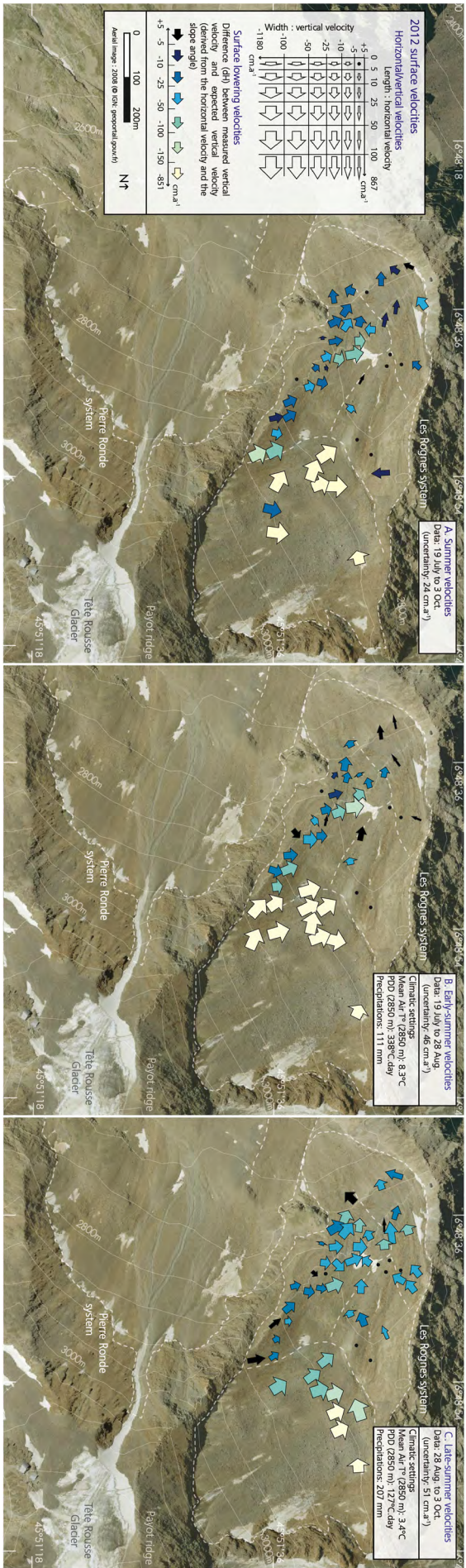


Fig. 3.15. Summer, early-summer and late-summer surface velocities measured in 2012 in Les Rognes. The climatic settings are derived from the extrapolated air temperature at 2850 m.a.s.l and precipitation at Chamonix weather station (see caption of Tab. 3.2 for details).

slope of the upper sector and surface lowering was especially high above the ice cave zone (Fig. 3.8). The results in Les Rognes at annual timescale are not detailed here since they were presented in the section 2.2.2.4. Except one block located in the middle of the front, all the blocks monitored in Les Rognes (85) moved faster than 2 cm.a^{-1} between 2011 and 2014 (Fig. 3.13A). In contrast, half of the blocks monitored in Pierre Ronde were stagnant or very weakly active. The most significant movements were slower than 25 cm.a^{-1} and were measured in the upper slope, the central zone and the rock glacier. Surface lowering was also limited in Pierre Ronde ($< 25 \text{ cm.a}^{-1}$). We compared the downslope movement with the surface lowering at annual timescale to highlight which dynamic was the most important (Fig. 3.14). Downwasting mode dominated in Les Rognes and a negative M_d/dH value was computed for two halves of the blocks, whose location especially concentrated in the upper and central zones. Conversely, downslope movements prevailed in the lateral and frontal margins of the glacier system. Few data were exploitable in Pierre Ronde because of the weak dynamic of this site. Surface lowering dominated in the centre of the rock glacier and in the upper slope whereas mostly downslope movements were measured elsewhere.

In both sites, surface velocities strongly increase in summer and reach several meters per year in the upper slope in Les Rognes (Fig. 3.13B). Surface lowering was especially high here ($> 100 \text{ cm.a}^{-1}$ for 19 blocks). Conversely, all the lower half of Les Rognes was less active. Horizontal and vertical velocities typically ranged between $[25]$ and $[50]$ cm.a^{-1} whereas the surface lowering was slower than 50 cm.a^{-1} . More blocks appeared active in Pierre Ronde compared to annual

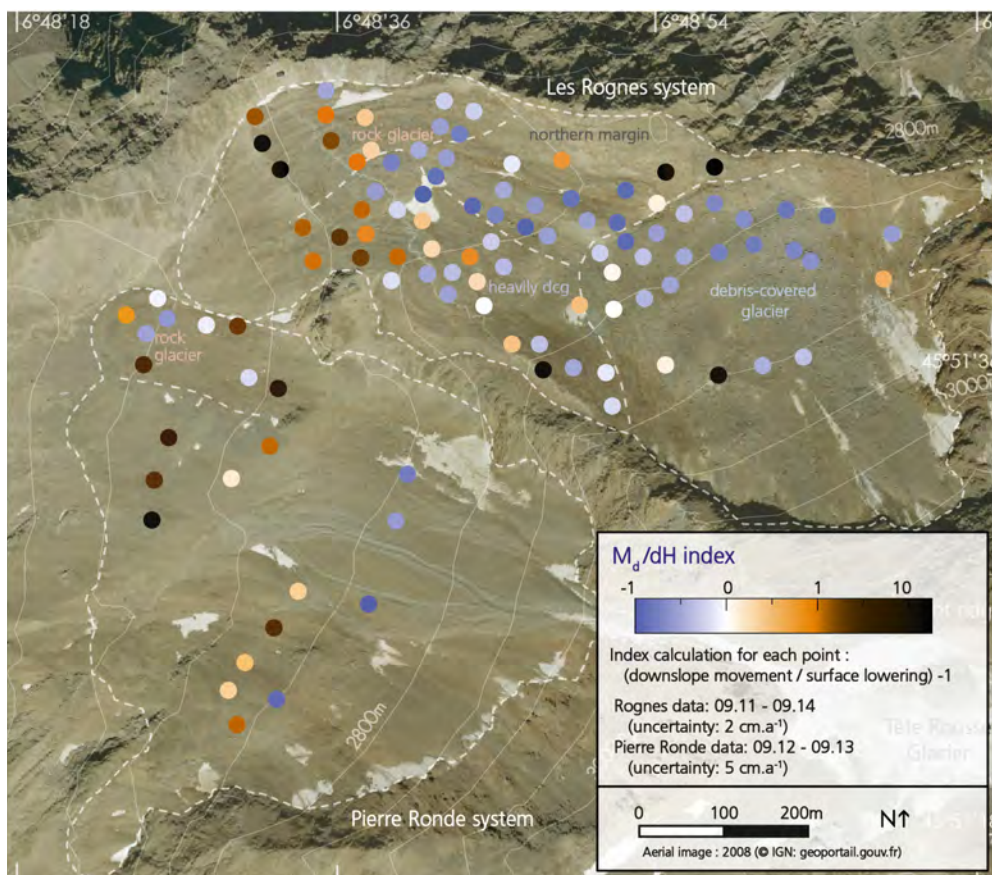


Fig. 3.14. Downslope movement / surface lowering index computed respectively with the 3-year and 1-year surface velocities measured in Les Rognes and Pierre Ronde. Only the most significant movements ($> 5 \text{ cm}$ in a year) were considered in Pierre Ronde. See Fig. 2.14 for representation of surface lowering and downslope movement.

timescale but they had small velocities that must be considered with caution according to the relatively high measurement uncertainty. Nevertheless, movement directions were consistent with the slope angles. The most active zones were the same than at annual timescale. Surface lowering was the highest in the rock glacier and the upper slopes ($> 10 \text{ cm.a}^{-1}$). During the winter period, surface velocities significantly decreased in both sites (Fig. 3.13C). Blocks are then most of the time covered by a thick snow layer and surface velocities were generally slower than 25 cm.a^{-1} . The most active zone was again the upper slope of Les Rognes. Surface lowering was also mainly effective here. In contrast, the movements measured in the distal zones were mostly subhorizontal and downwasting was weak or null. The rock glacier was the main active zone in Pierre Ronde but movements were slower than 10 cm.a^{-1} .

We performed three dGPS surveys during the summer 2012 in Les Rognes to investigate the variations of surface velocities (Fig. 3.15). The summer 2012 velocities were roughly similar to those measured during the three summer (Fig. 3.15A and Fig. 3.13B). In early summer, velocities were especially high in the upper slope and maximum values, including surface lowering, were around 10 m.a^{-1} during this hot and dry period (Fig. 3.15B). In contrast, the lower half was less active and velocities were slower than 1 m.a^{-1} . Only subhorizontal flow was observed on the rock glacier. Temperature strongly decreased in late summer and precipitations doubled (Fig. 3.15C). During this period, the surface velocities became more homogeneous at the system scale because they noticeably decreased in the upper slope and increased in the lower half. The faster velocities were again measured upslope but the maximum magnitude was generally below 1 m.a^{-1} . In the distal area, surface lowering was slower than 50 cm.a^{-1} .

As explained in the section 2.2.2.3, we divided Les Rognes in four main homogeneous zones according to surface characteristics, ground electrical resistivities and surface dynamics (Fig. 3.13). We used the blocks whose position was the most often measured (Fig. 3.13) to compute zonal dynamical indices (Fig. 3.16 and Fig. 3.17). Very few dGPS and ERT data were collected in the northern margin. As a consequence, we voluntarily excluded this zone from this analysis. Annual and seasonal velocities were the highest in the debris-covered glacier zone that correspond to the upper slope. Most of the movements occurred in summer here (velocities accelerated up to ten times compared to winter) and especially in early summer (Fig. 3.17). Mean surface lowering was especially very high (76 cm.a^{-1} over the three years) and explained the downwasting dominant dynamic highlighted by the M_d/dH index. Interannual and seasonal variations of velocities were the largest here, showing the high sensitivity of this zone to short-term climatic variations. Maximum velocities occur in summer when the snow is absent and the air and ground surface temperature are the warmest. Summer velocities and consequently annual velocities decreased in 2013 and 2014 in comparison with 2012. According to climatic parameters (Fig. 3.16), this could be related to colder summer air temperature. Secondly, several climatic parameters as the decrease of the winter snow cover height or spring precipitations could also explain this velocity decrease. Less energy and amount of water could thus limit the surface velocities of the debris-covered glacier. The shape of the velocity cross profile over this zone can show the associated influence of internal deformation and basal sliding on the downward motion (Fig. 2.18). The heavily debris-covered

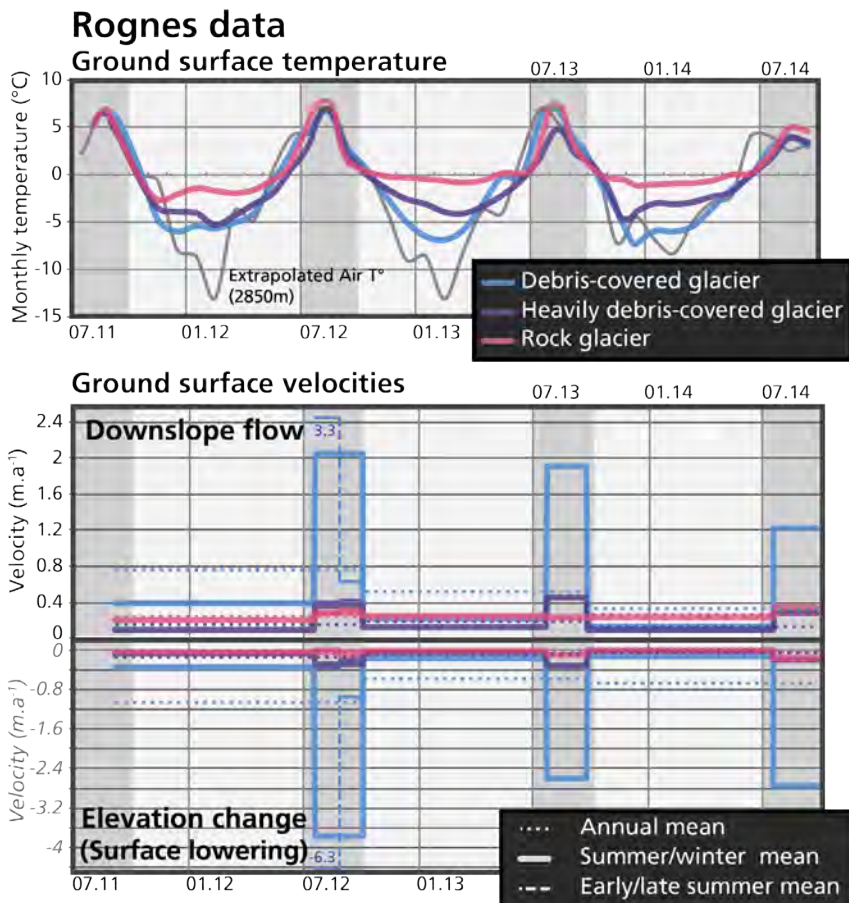
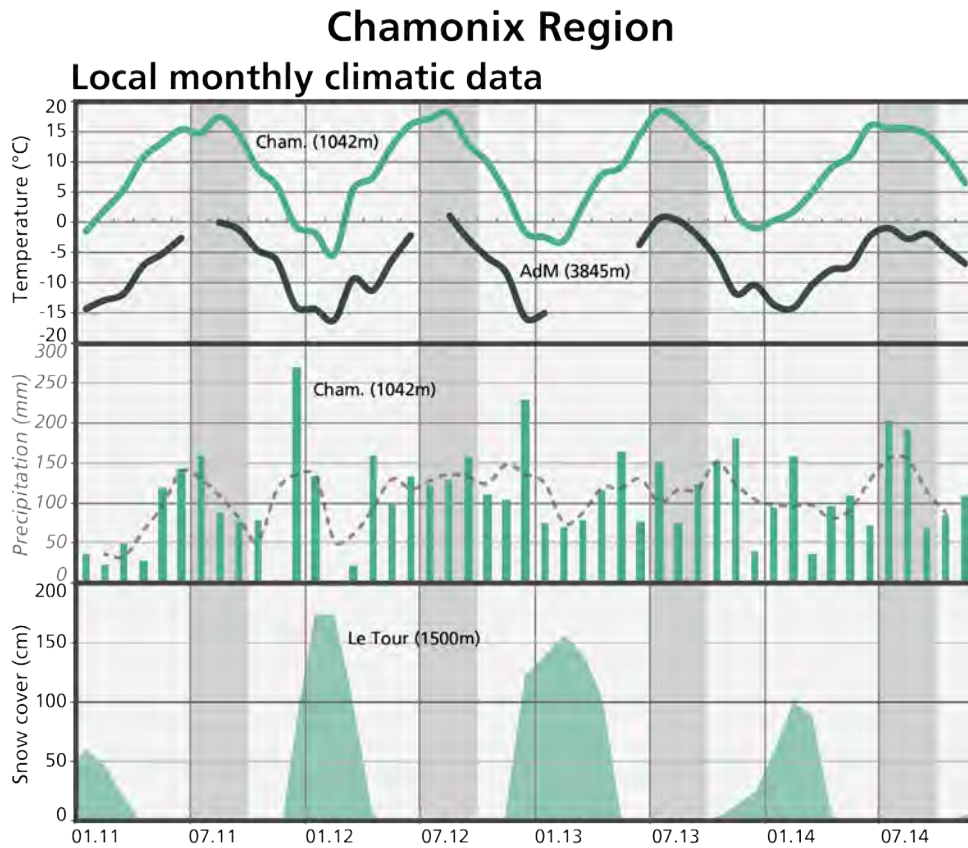


Fig. 3.16. Annual, seasonal and early/late-summer mean downslope flow and surface lowering velocities measured in the three main zones containing ground ice in Les Rognes between September 2011 and 2014. Monthly means of ground surface temperatures and regional climatic data are represented above. The used weather stations were presented previously except Le Tour (1500 m a.s.l.; 46°00'12"N, 6°56'54"E; 19 km distant from the study site, © MétéoFrance).

glacier has generally the same dynamical behaviour than the previous zone but all the measured mean velocities were significantly slower (Fig. 3.16 and Fig. 3.17). Velocities in summer were up to five time faster than in winter. The winter/summer and early/late summer proportions on annual and summer velocities were balanced. M_v/dH index value was close to zero indicating the similar magnitudes of the two movements. Annual and seasonal velocities remained generally stable over the three years and a slight decrease of downslope flow and surface lowering were observed in 2014, probably in relation with this relatively cool summer. Finally, the rock glacier zone presented a different dynamical behaviour in comparison with these two zones (Fig. 3.16 and Fig. 3.17). All the measured mean surface velocities were slower than 27 cm.a^{-1} and their values were relatively stable over the year. Summer accelerations were lower than three orders of magnitude (for surface lowering) and horizontal velocities especially remained relatively high in winter (22 cm.a^{-1}). Consequently, most of the movement occurred in winter. Late summer velocities were faster than early summer velocities. At annual timescale, surface lowering was 4 cm.a^{-1} and explains the domination of downward movement in this zone (M_v/dH index of 0.73). In contrast with the DCG and HDCG zones, annual and summer velocities increased in 2014. The parabolic shape of VCP could indicate the prevalence of internal deformation here (Fig. 2.18).

Dynamical indexes		Debris-covered glacier	Heavily debris-covered glacier	Rock glacier	Legend
Intensity of dynamics	Annual velocity				
	Summer velocity				
	Winter velocity				
Temporality of dynamics	Annual and seasonal variability of velocity				
	Proportion of summer activity on annual activity				
	Proportion of early summer activity on summer activity				
Main dynamics	Downslope movement vs. surface lowering				

Fig. 3.17. Mean dynamical index computed in the three main zones containing ground ice in Les Rognes between September 2011 and 2014

3.2.3. Synthesis

3.2.3.1. The current relation between internal structure and surface dynamics

The synthesis of dGPS and ERT results illustrates the strong relation existing between surface velocities and ground electrical resistivities in Les Rognes and Pierre Ronde (Fig. 3.18). The spatial

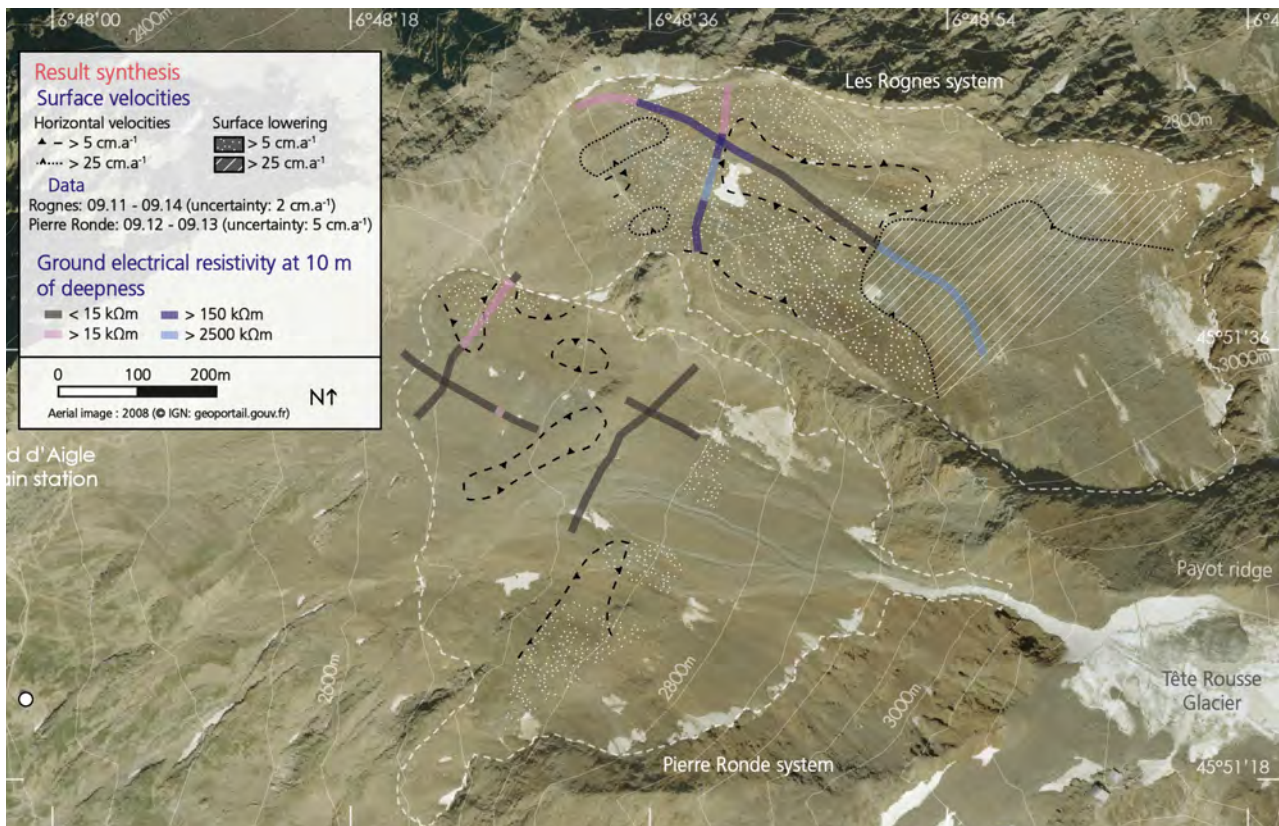


Fig. 3.18. Synthesis of the results obtained on the surface velocity and ground electrical resistivity at Les Rognes and Pierre Ronde

limits between the zones that have different ground resistivities and surface dynamics show a good consistency. It highlights **the strong influence of the concentration and depth of ground ice on the distribution of surface movements** in these systems. Indeed, the fastest horizontal and surface lowering velocities ($> |25| \text{ cm.a}^{-1}$) were mainly measured in the upper slope of Les Rognes, where a layer of very high resistivity ($> 2500 \text{ k}\Omega\text{m}$) directly below the surface indicated the presence of a debris-covered glacier. In both sites, surface velocities were faster than 5 cm.a^{-1} in all the areas where ground resistivities at 10 m depth were higher than $15 \text{ k}\Omega\text{m}$. Conversely, surface dynamics were slower than this value in the zones where ground resistivities were lower than $15 \text{ k}\Omega\text{m}$ and indicated the likely generalised absence of ground ice.

3.2.3.2. Genesis and evolution of les Rognes and Pierre Ronde glaciers

The morphogenesis and evolution of Les Rognes and Pierre Ronde since the LIA were already discussed and detailed in the sections 2.1.2.5 and 2.2.2.5 and in the associated figures. **Very small cirque glaciers**, connected respectively to Tête Rousse and la Griez and Tête Rousse glaciers, occupied Les Rognes and Pierre Ronde during the coldest and/or wettest Holocene periods, like the LIA (Fig. 3.19A and Fig. 3.20). These glaciers advanced in area occupied by **former sediments accumulations** (moraines, talus slope, rock glaciers), possibly frozen in this permafrost environment, overlying them and/or pushing them away. The ridges and steep fronts present in the lower half of Les Rognes especially illustrate their reworking process and a former rock glacier was likely pushed in the northern part of the glacier terminus. In contrast, the rock glacier located in the lower zone of Pierre Ronde probably evolved independently from glacier history over the



Fig. 3.19A. Mapping of local LIA glacier extent, the area affected by the 1892 WPOF event, recent debris flow deposits and current ridges and steep front in Les Rognes and Pierre Ronde. **B.** Main current components of the two SDCGSAPE

last millennia (see 2.1.2.5). The debris mobilised by its slow creep originate from small rockwalls in its rooting zone.

The **elevation and aspect at Pierre Ronde is less favourable for glacier development compared to Les Rognes**. Nevertheless, the presence of a 0.11 km² and up to 200 m high **ice-free backwall probably fostered the glacier development** in this site during the cold Holocene periods. On one hand, snow accumulation was enhanced by avalanching and wind drifting. Pierre Ronde had a drainage ratio (= basin area/glacier area; equal to avalanche ratio here because all the slopes of the basin are steeper than 30°; e.g. [Hughes, 2009](#)) of 0.41, illustrating that **snow redistribution processes** can significantly increase the snow accumulated by precipitations on this glacier. On the other hand, as mentioned in the 2.1.2.5, the **debris produced in the backwalls probably always covered the distal part** of the glacier and limited the ablation rate. Conversely, the relief that dominates Les Rognes is smaller and was largely covered by an ice apron in the Holocene positive mass balance periods. As a consequence, it is probable that **the Rognes glacier was mostly a bare-ice glacier** during the climatic periods favourable to glaciers, as illustrated by the early 20th century photograph ([Fig. 3.8](#)). The drainage and avalanche ratios were 0.12 for this glacier, showing that snow redistribution has a lesser potential in Les Rognes.

Currently, **Les Rognes and Pierre Ronde are two inherited SDCGSAPE without any accumulation area**. Large snowfields, crevasses and a bergschrund were visible in Les Rognes between the 1960s and the 1980s, whereas only snow accumulation areas were observed during this period in Pierre Ronde (e.g. [Fig. 3.7](#)). Since the late-1980s, the climatic conditions have been unfavourable locally for snow accumulation ([Fig. 3.6](#)) and the formation of sedimentary ice was locally deactivated. However, according to ground thermal conditions ([Fig. 3.10](#) and [Tab. 3.2](#)), the formation of magmatic ice below the sedimentary surface still appears possible in Les Rognes, especially in its shaded upper half (see the 3.2.2.1), while the warmer conditions seem less favourable for this process in the Pierre Ronde area.

The current ground ice distribution and surface dynamics are very different in the two neighbouring systems ([Fig. 3.18](#)). Large amount of ice is still present in the Rognes system and



Fig. 3.20. Reconstitution of the LIA glacier extent in the Bionnassay basin (photograph by D. Bonneaux, July 2012)

most of the blocks monitored showed movements between 2011 and 2014. In contrast, Pierre Ronde is poorly active and excepted the talus-derived rock glacier, its lower half seems mostly ice-free (Fig. 3.19B). As explained in the publication 1, we mainly attribute the origin of these distinct situations to **the influence of topography and water circulation on glacier evolution after the LIA**. Indeed, elevation and aspect are less favourable for ice preservation in Pierre Ronde compared to Les Rognes. Consequently, ground thermal conditions are significantly warmer here (Fig. 3.10 and Tab. 3.2). Moreover, Pierre Ronde was affected by a water pocket outburst flood (WPOF) in 1892 and several debris flow events occurred in the last decades. These repeated hydrological events probably warmed the ground and accelerated the ice melt. Ground ice seems now mainly localised in the distal talus rock glaciers and in the upper heavily debris-covered glacier zones. All these zones were weakly active according to the dGPS monitoring and the maximum movements measured in Pierre Ronde were around $15 \text{ cm}\cdot\text{a}^{-1}$. The elevation changes obtained between 2003 and 2013 by Berthier et al. (2014; Fig. 3.21) also show the weak activity of this system. Surface lowering can have occurred in the right-hand side of the upper depression.

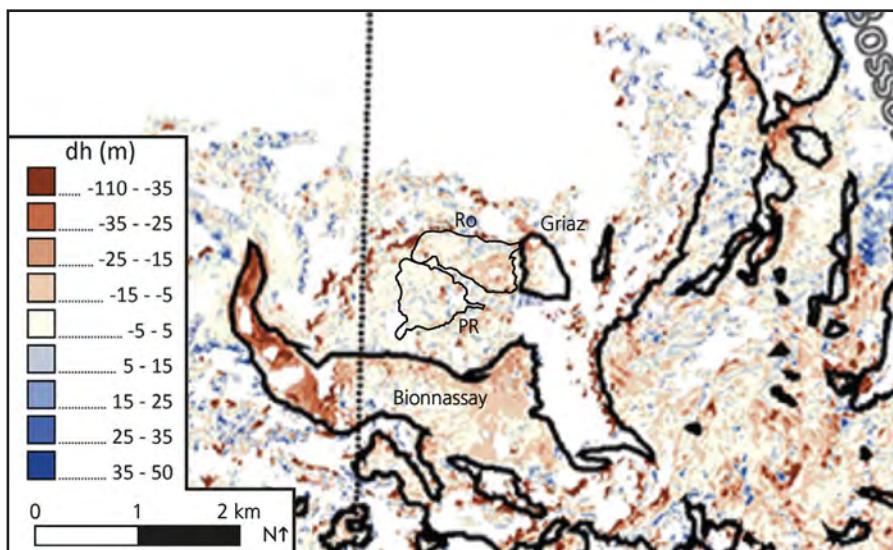


Fig. 3.21. Elevation differences between the SPOT 5 DEM from 19 to 23 August 2003 and Pléiades DEM from the 19 August 2012 in the Mont-Blanc massif. The 2003 outlines of the glaciers are represented by black lines. We added the limits of the Rognes and Pierre Ronde systems. Adapted from Berthier et al. (2014).

3.2.3.3. The current state of les Rognes glacier

The upper slope of Les Rognes is composed by a **debris-covered glacier** (0.15 km²; Fig. 3.19B). Its thickness is unknown but according to the empirical relationship proposed by Chen and Ohmura (1990; mean glacier thickness = 28.5 x area (in km²)^{0.357}), mean glacier thickness could be around 15 m. The fastest surface dynamics were measured over this zone, the downward movements and the surface lowering exceeded several decimetres per year and even reached two meters per year at some points (Fig. 3.13). Downward movements and surface lowering were mainly active in summer and especially in early summer, illustrating **the strong influence of air temperature and also probably of hydrological forcing in this zone**. Ice outcropped locally but was generally covered by a decimetre thick debris layer that limited significantly the influence of air temperature variations (Fig. 3.12). However, despite the existence of this insulating layer and the fact that the coldest thermal conditions were measured here (Fig. 3.10 and Tab. 3.2), **ice melt appeared very rapid** and affected especially the footslope. A rapid downwasting dynamic was also observed in this zone between 2003 and 2013 by Berthier et al. (2014; Fig. 3.21). The magnitude of lowering at this 10-year timescale (0.5 to 2.5 m.a⁻¹) is consistent with the one found between 2011 and 2014 during the dGPS monitoring, illustrating the relative regularity of this dynamic during this warm climatic period (Fig. 3.6). Surface lowering movements were larger than downward motion movements, highlighting the evolution of this debris-covered glacier towards a **stagnant lowering mode**. Large amount of glacier ice is probably still also present in the left distal margin of Les Rognes. However, the lower ground resistivities and slower surface velocities indicate that the concentration of debris within the ice body and the supraglacial debris cover thickness increase in this heavily debris-covered glacier zone. The burying of massive ice by a 2 to 5 meter thick debris layer limited the ice melt here and only decimetric movements towards the central depression and the glacier front were observed. This zone has a lateral steep front and surface ridges. However, the frontal zone differs from the adjacent steep rock glacier front. On the **rock glacier**, ground resistivities and surface movements decreased. Here, the ice-debris mixture, where glacier ice could have been integrated, creeps at a relatively stable velocity over the year and surface lowering in the frontal zone is very slow at annual timescale (< 5 cm.a⁻¹). Finally, the presence of ground ice in the northern central part of Les Rognes seems limited. Surface movements are slow and ground thermal conditions are relatively warm here. The low resistivities measured in the central depression highlight the very probable absence of ground ice. According to the internal structure and surface dynamics encountered in Les Rognes, the differential evolution is expected to continue within the next decades. The debris-covered glacier, and especially its distal zone where ice caves are developed, will probably disappear rapidly, if we consider the rapid lowering rate observed here (> 1 m.a⁻¹). Conversely, the shadow effect in the upper slope and the presence of a several meter thick debris cover in the distal area will probably induce a better preservation of ground ice.

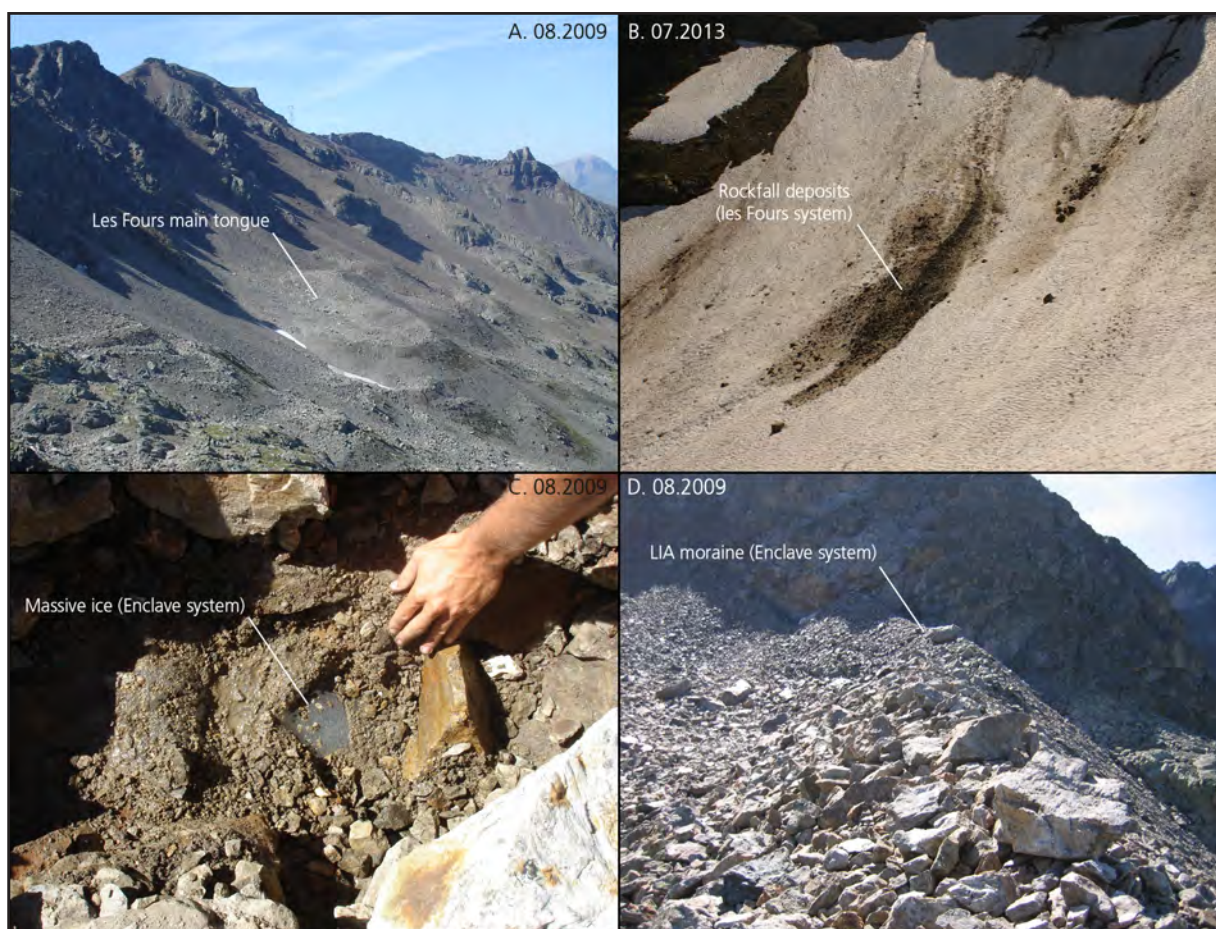


Fig. 3.24. Assemblage of photographs taken in les Fours and Enclave system. S. Utz took the one in the top-left corner.

no maps, drawings or pictures indicated the existence of these very small buried glaciers (Bosson, 2012). These landforms are nested with rock glaciers and other periglacial creeping landforms are present locally (e.g. les Tufs system 1; Fig. 3.22). As a consequence, they were previously also considered as rock glaciers. However, the relatively regular morphology of the main tongues of les Fours, les Tufs 2 and Enclave systems and the presence of morainic ridges around their current depressed central zones (Fig. 3.24) evidence the development of very small glaciers during the LIA. Moreover, the dimension of these tongues in les Fours and Enclave system (300 m long, surrounded by a 40 m high moraine dam) contrasts with the lower size of local periglacial landforms.

Neither ice outcrops nor crevasses were visible on the glacier surface over the last decades (Fig. 3.25). Only permanent snowpatches occupied the surface during the cool and wet conditions that occurred between the 1960s and 1980s. The subsequent noticeable warm of air temperature (e.g. Fig. 3.6) induced the rapid melt of these snowpatches and currently, the presence of snow at the end of summer is rare in these systems. A continuous debris layer covers the surface and only one ice outcrop was observed in the Enclave system at 60 cm depth during manual excavations, carried out during summers 2009 and 2010 (Fig. 3.24).

Detailed presentation of these systems can be found in Bosson (2010; 2012; 2013 & 2014). In the following, we only synthesize the field results obtained in les Fours system between 2013 and 2014 and their interpretations.

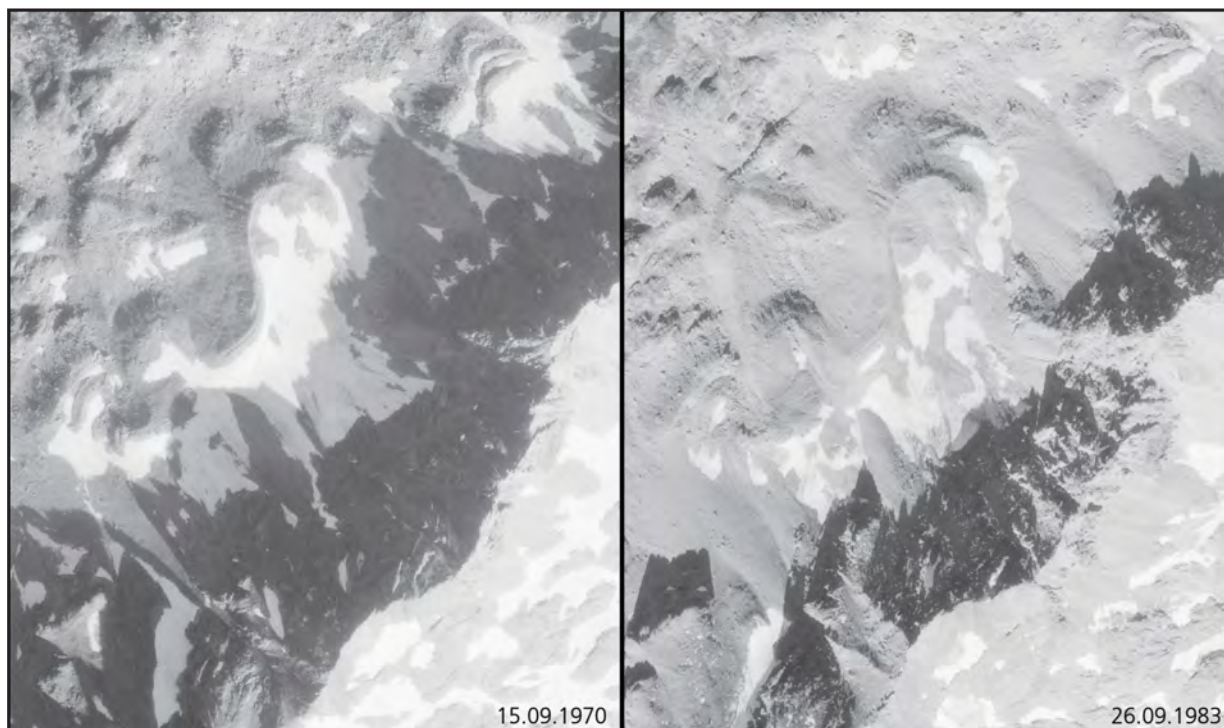


Fig. 3.25. Aerial images of les Fours system in 1970 and 1983 (© IGN, photographs respectively IGNF_PVA_1-0__1970-09-15__C3531-0041_1970_F3531_0027 & IGNF_PVA_1-0__1983-09-26__C3531-0021_1982_F3531_0066, available on geoportail.gouv.fr)

3.3.2. Results and synthesis

3.3.2.1. Ground surface temperature measurements

Measurements of ground temperatures (Fig. 3.26 and 3.27), resistivities (Fig. 3.28) and surface displacements (Fig. 3.26) were carried out during summers 2013 and 2014 in les Fours system. The ground thermal conditions were relatively mild: mean annual ground surface temperature were all positive, WEqT were $> -3^{\circ}\text{C}$, PDD were $> 450^{\circ}\text{C}\cdot\text{day}$ and GF were $> -350^{\circ}\text{C}\cdot\text{day}$. The three lower sensors showed the warmest temperatures and had winter temperature $> -1.5^{\circ}\text{C}$ (Fig. 3.27). The positive values measured during winter by the sensors LF_1 and LF_5 were even somewhat surprising and could indicate a measurement problem. However, the summer values of these sensors fit with the one of other sensors and air temperature. Hence, it could highlight the existence of a positive thermal anomaly that we do not explain. Cooler conditions were measured upward in the system and the thermal regime of the LF_2 sensor is typical of the one found in permafrost environment, especially with a WEqT close to -3°C .

3.3.2.2. Electrical resistivity tomography

Ground electrical resistivity was generally $> 10\text{ k}\Omega\text{m}$ in les Fours (Fig. 3.28). Highly resistive patches ($> 500\text{ k}\Omega\text{m}$) were detected 5 m below the surface in the main tongue of les Fours (RC6 and RC7), in its rooting zone (RC5 and RC6) and in the depression located at its left (RC5). In the main tongue, a conductive zone, located below the central gully where water runoff was heard during the measurement campaign, cut the highly resistive layer in two parts (RC7). Two conductive

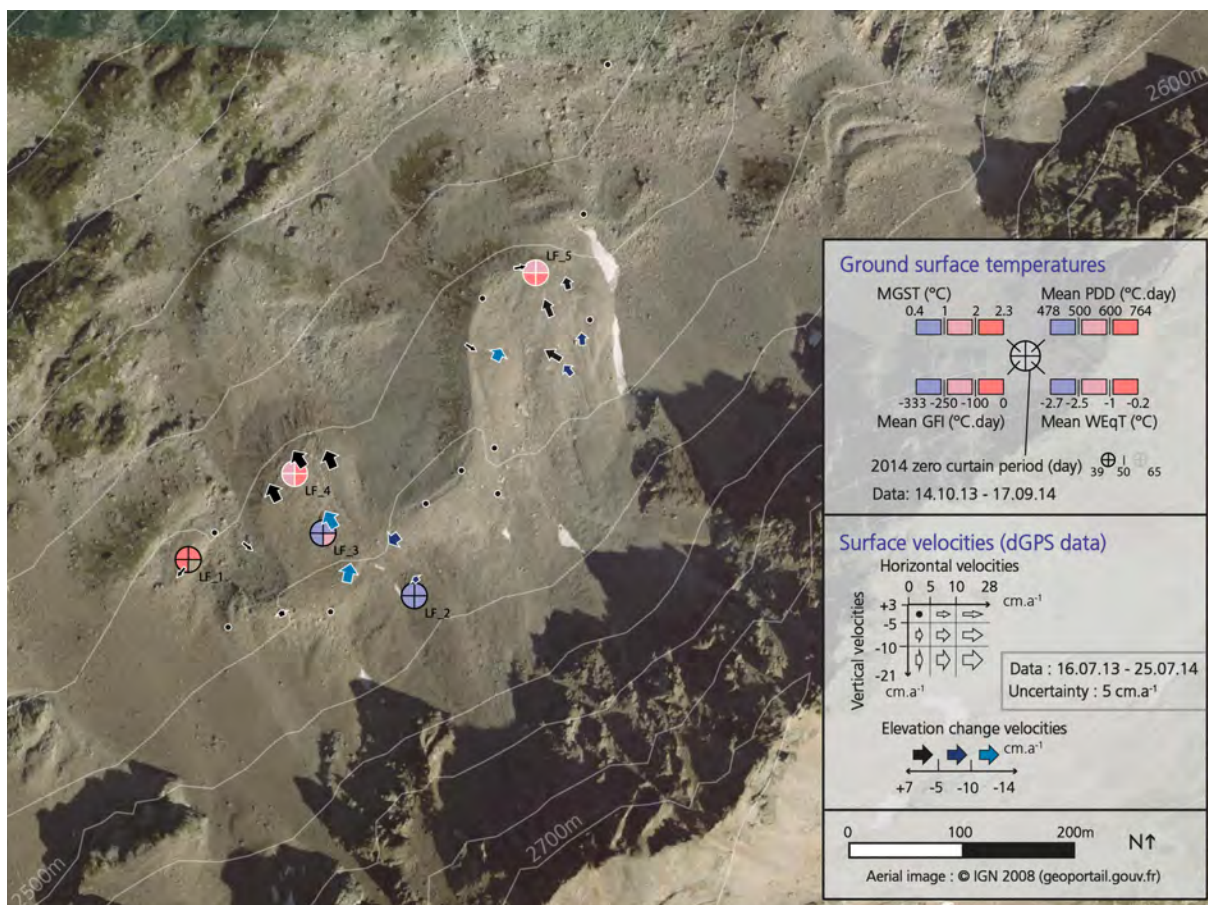


Fig. 3.26. Thermal conditions and surface velocities measured in les Fours between summer 2013 and 2014. PDD, GFI and WEqT correspond respectively to positive degree day, ground freezing index and winter equilibrium temperature.

zones (<10 kΩm) were highlighted in the top of the main tongue (RC5 and RC6). The resistivities ranged between 10 and 150 kΩm in the small tongues located in the western part of the system (RC1 to RC7).

3.3.2.3. dGPS

Surface velocities were relatively slow in les Fours and most of the movements detected at the

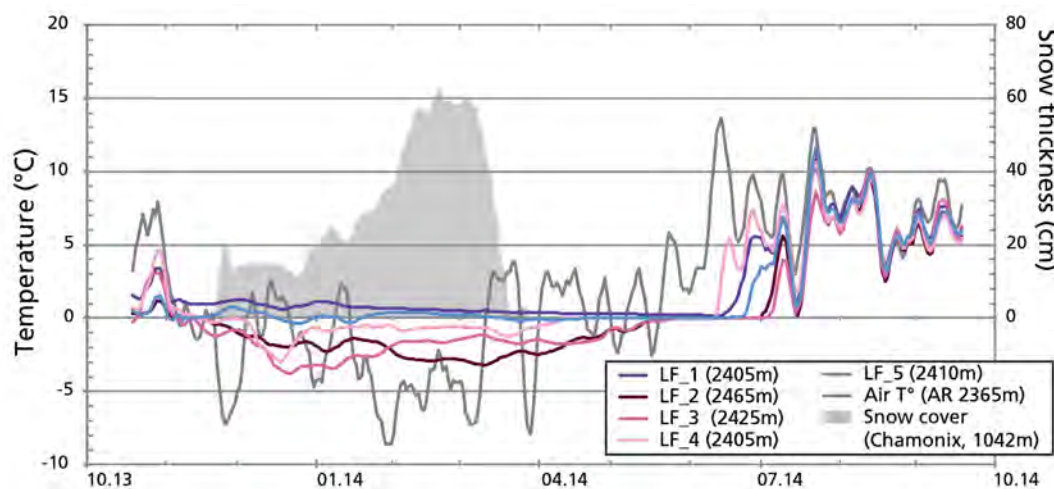


Fig. 3.27. 5-day running means of ground temperature in les Fours. The position of the thermal sensors is shown on Fig. 3.26. The air temperature at 2365 m a.s.l. was measured at the Aiguille Rouge weather station (45°59'06"N, 6°53'48"E; 30 km distant from the study sites, © MétéoFrance) and the snow cover height at the Chamonix weather station (1042 m a.s.l.; 45°55'42"N, 6°52'36"E; 23 km distant from les Fours, © MétéoFrance).

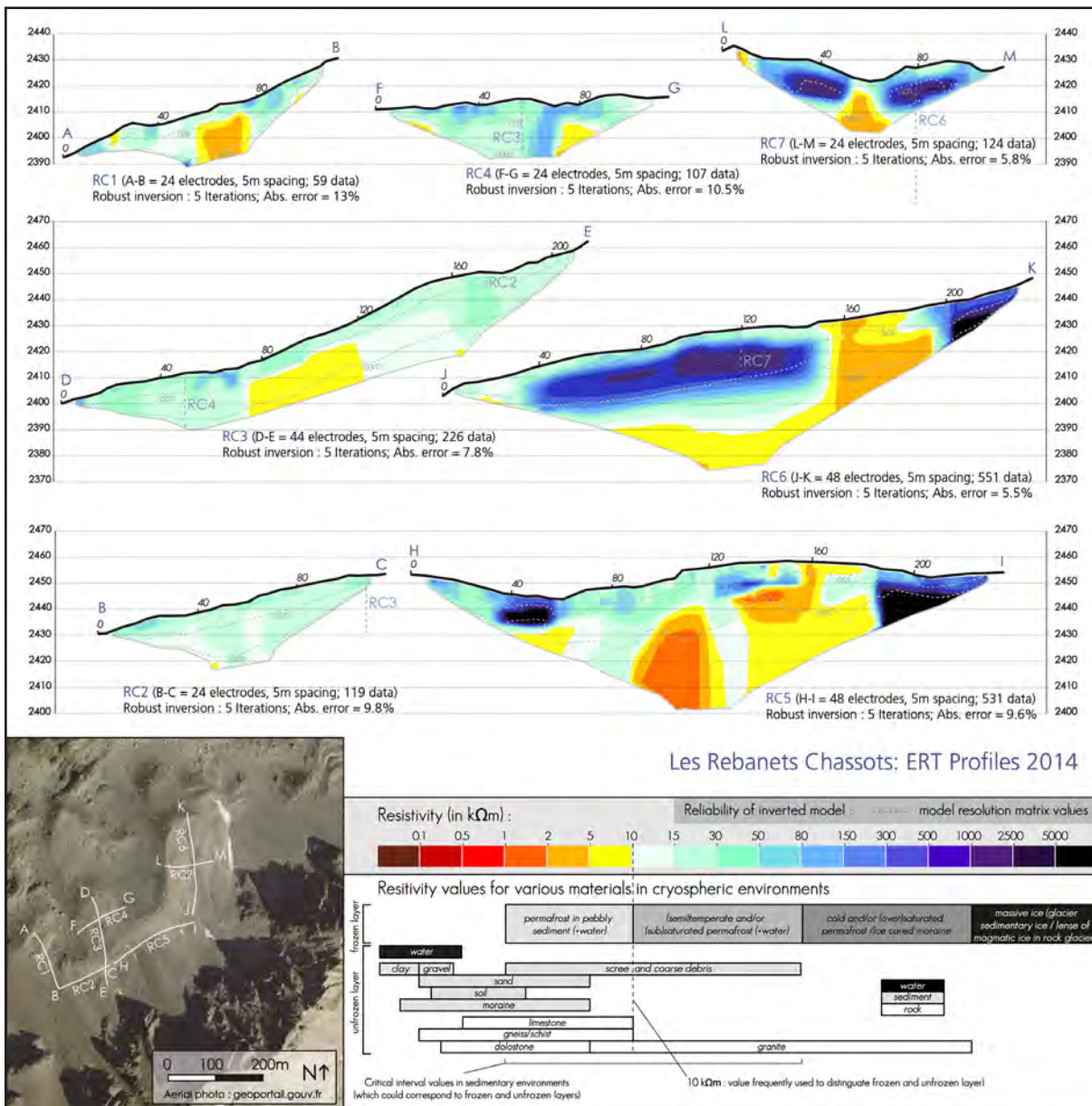


Fig. 3.28. Electrical resistivity tomograms measured in les Fours in September 2014

summer timescale were too small to be reliably distinguished from measurement uncertainty. Hence, only the velocities measured at annual timescale are presented here. The fastest horizontal, vertical and surface lowering velocities were detected in the central small tongue. Maximum velocities reached few decimetres. The distal zone of this tongue showed especially subhorizontal movements whereas surface lowering also occurred in the central zone. The areas located directly at the West and the East of this tongue were mostly inactive at this timescale. Finally, the distal part of the main tongue, at the East of the system, had dynamics slower than $20 \text{ cm} \cdot \text{a}^{-1}$ and was dominated by downward movements.

3.3.2.4. Result interpretation and synthesis

According to these results and field observations, an interpretation of the current internal structure and the main components in les Fours system, and of local LIA glacier extents are proposed (Fig. 3.29 and Fig. 3.30). The very high resistivity values ($> 500 \text{ k}\Omega\text{m}$) measured in 2013 and 2014

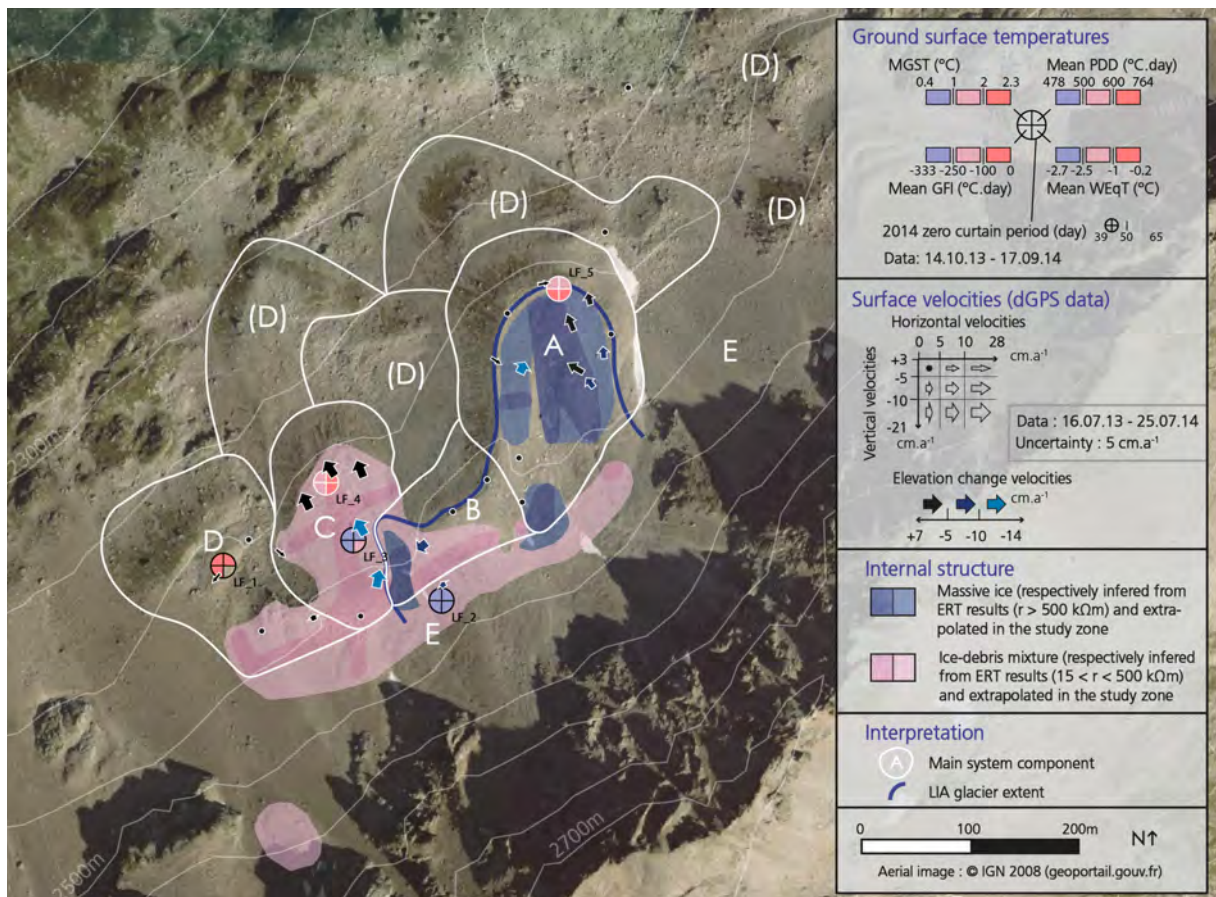


Fig. 3.29. Synthesis and interpretation of the field results obtained in les Fours

few meters below the debris surface in the main tongue of les Fours system highlighted **the existence of massive ice bodies** (Fig. 3.29). It supports thus the hypothesis considering **the local existence of buried glaciers, inherited from the LIA**. According to the moraine ridges, three very small cirque glaciers developed during the LIA and had an area < 0.08 km² (Fig. 3.30).

The regional ELA was around 2700 m a.s.l. during the LIA (e.g. Bret, 2011). **The formation of these very small glaciers between 2675 m and 2410 m a.s.l. was thus an anomaly, related to the local enhancement of snow accumulation and limitation of snow and ice melt.** The influence of the topography was fundamental on these glaciers: they developed in the **local shaded cirques**, where the relatively flat footslope located above 2500 m a.s.l. allowed the accumulation of snow and the formation of sedimentary ice. The drainage (and avalanche) ratios of the LIA glaciers were around 1, indicating that **snow redistribution processes** potentially strongly increase accumulation in the cirque floor (Fig. 3.30). The development of these cirque glaciers during the cold periods of the Holocene also induced two positive feedbacks that further increased the snow accumulation in comparison with neighbouring unglaciated steep areas. First, glacier erosion overdeepened the cirque howls and shaped a relief more favourable for snow redistribution and accumulation, and shadow effect. Second, the relatively flat glacier surface and the building of marginal morainic dam also favoured snow accumulation (Fig. 1.27; Kuhn, 1995). Conversely, Holocene talus slopes and/or talus rock glaciers formed in the local steep slopes, where less snow can be accumulated (e.g. western part of les Fours system, Les Tufts system 1). The presence of talus rock glaciers points out the occurrence of permafrost conditions, although

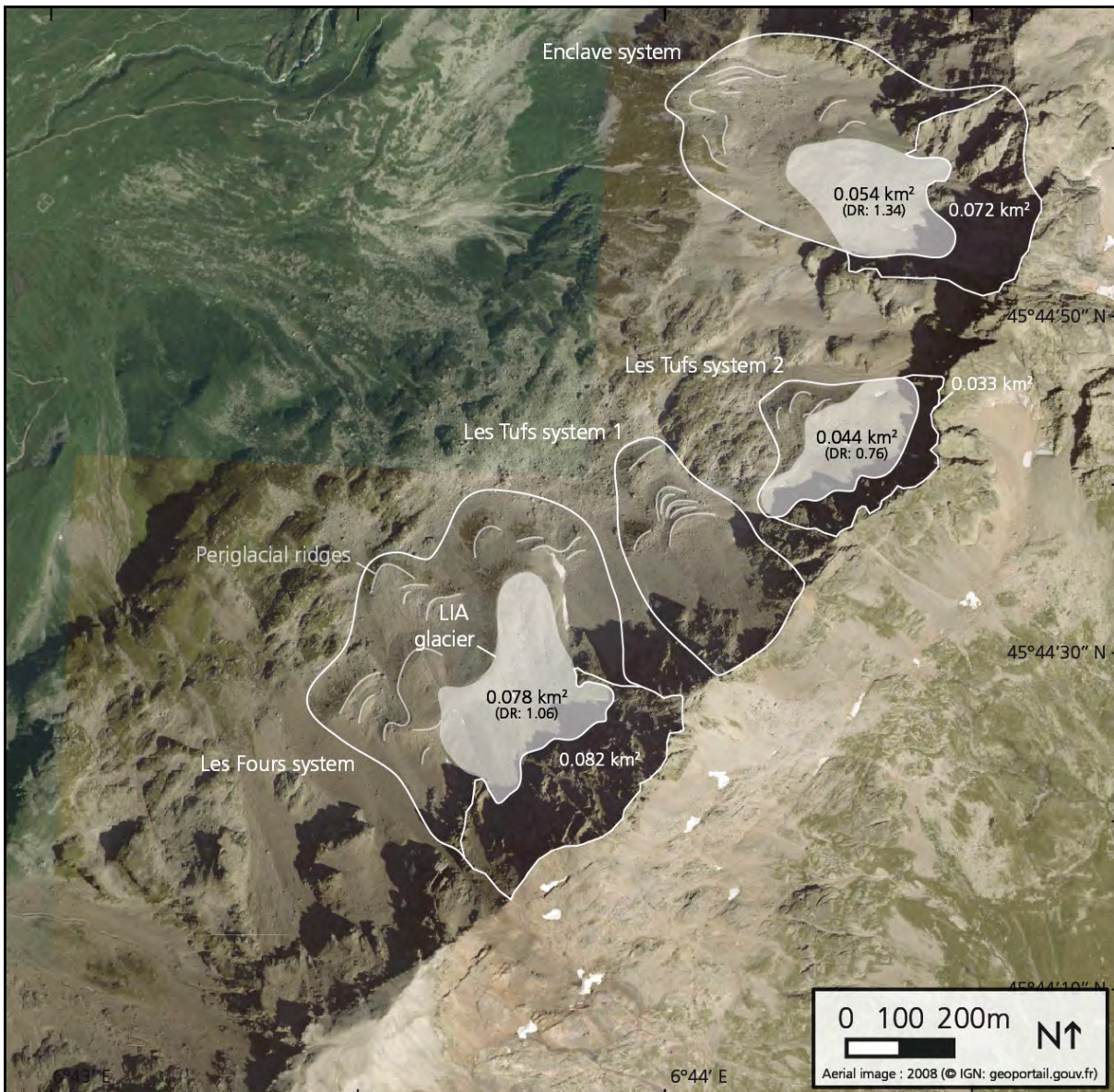


Fig. 3.30. LIA glacier extent in the South end of the Mont-Blanc massif. The areas of the LIA glacier and backwalls are indicated, as well as the local periglacial ridges. In the glacier areas, DR refers to the respective drainage ratio (i.e. backwall area/ glacier area).

ground surface temperature were relatively mild during the year of measure (Fig. 3.26 and 3.27). Finally, because of the rapid erosion of the fractured relief and taking into account the high amount of sediment accumulated by these glaciers, it is also very likely that **these glaciers were already partly debris-covered during the LIA**. The domination of snow and debris on the surface of these very-small glaciers could explain their absence on historical sources. The debris cover also contributes to explain the development of these glaciers because it limited the ablation rate in the tongues. The presence of snow in the glacier roots at the end of the ablation season is very rare since the 1980s. These buried glaciers are thus inherited from past climate. The depressed surface between LIA moraines (e.g. Fig. 3.24D) indicates that ice loss could have exceeded 15 m in some sectors.

Surface velocities measured in **les Fours glacier showed mainly a downward flow between 2013 and 2014**. Surface lowering was relatively slow ($< 11 \text{ cm.a}^{-1}$), which could illustrate that

the glacier is relatively efficiently insulated from air temperature by the several meter thick debris cover in this permafrost environment. Nevertheless, water circulation in the central gully probably induced locally the complete melt of ice (Fig. 3.28). According to the 2013 and 2014 ERT results, the glacier tongue (A in Fig. 3.29) seems now disconnected from its roots where ice free debris, massive ice and ice-debris mixture could coexist. The backwalls are affected by an active erosion (e.g. Fig. 3.24B) and talus slope have formed at their feet (E in Fig. 3.29). The western glacier zone probably partly covered an **active rock glacier** during the LIA (respectively B and C in Fig. 3.29). Currently, ground ice seems largely present in this zone and the ice-debris mixture creep reaches up to 30 cm.a⁻¹. Finally, several poorly active to inactive rock glaciers are present in the lower part of les Fours system (D in Fig. 3.29). The thermokarstic depressions, the warm thermal conditions (sensor LF_1) and the vegetation development on some fronts indicate the lower concentration or even absence of ground ice in these old periglacial landforms. Their formation could have occurred during the first millennia of the Holocene, that were cold and induced the development of others currently inactive rock glaciers in the European Alps (e.g. Ivy Ochs and al., 2009).

3.4. Entre la Reille

3.4.1. Site description

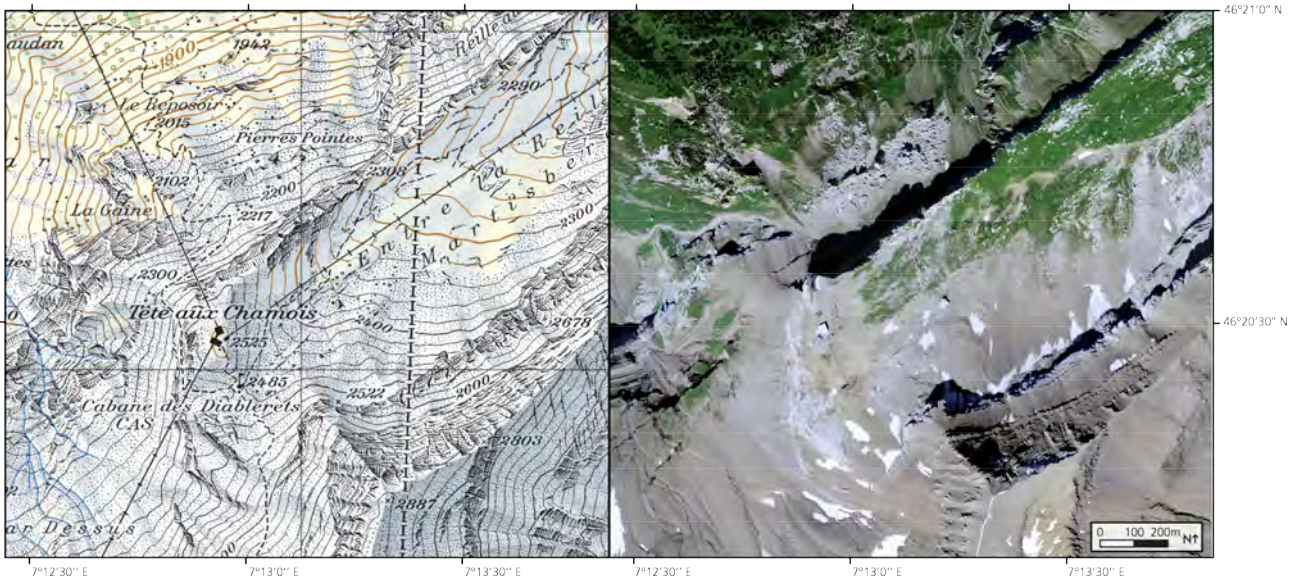


Fig. 3.31. Map (CN25, leave 1285, 2008) and aerial photograph (SWISSIMAGE Level 2, 2010) of Entre la Reille (© Swisstopo). The studied SDCGSAPE is located at the centre of the map and photograph, between the elevation point 2522 m a.s.l. and the contour lines 2400 m a.s.l. on the map.

Entre la Reille is briefly presented in the section 2.2.2.2. (Fig. 2.12 shows a 3d view and a simplified map) and some of its physical and environmental characteristics are displayed in the Tab. 3.1. This SDCGSAPE is located in les Diablerets (Vaud, Switzerland; Fig. 3.31), within the ski area of *Glacier 3000*. Despite its vicinity with the Cabane des Diablerets (2485 m a.s.l.), very few people know its existence. This is especially due to the almost complete burying of the ice mass under the debris and firn. Consequently, as other very small debris-covered ice masses, this glacier is neither represented on topographical map nor considered in the Swiss Glacier Inventory (Fischer M et al., 2014).

This SDCGSAPE is located in the Entre la Reille (or Martisberg) valley which corresponds to a perched syncline of the Wildhorn tectonic unit (Badoux et Gabus., 1991; Fig. 3.32). Alternation of marl and limestone composes the local bedrock. Erosion is especially active in the marl and siliceous limestone in the rockwalls of the Oldenhorn-Nägelihorn massif. Coalescent talus slopes occupy hence their footslopes. Climatically, Entre la Reille is situated in the relatively cool and humid northern side of the western Alps region. The Fig. 3.33 shows the regional evolution of air temperature and precipitation in the last decades. A clear temperature warming is observable since the 1980s and accelerated since the 2010s, exceeding 1.5°C the 1961-1990 climatic norm. Annual and winter precipitations also decreased since the late 1980s. Hence, climatic conditions have recently become very unfavourable for glaciers. Compared to other alpine regions, the north-western Alps receive abundant precipitations especially because they act as a barrier for the humid air masses originating from the Atlantic. According to MeteoSwiss data, annual precipitations are > 2000 mm above 2000 m a.s.l.. The local limit of discontinuous permafrost is relatively low. Models simulate the possible occurrence of permafrost conditions above 2400 m a.s.l. (BAFU, 2005; Lambiel et al., 2009; Boeckli et al., 2012). Reynard et al. (1999) also inferred the likely occurrence of perma-

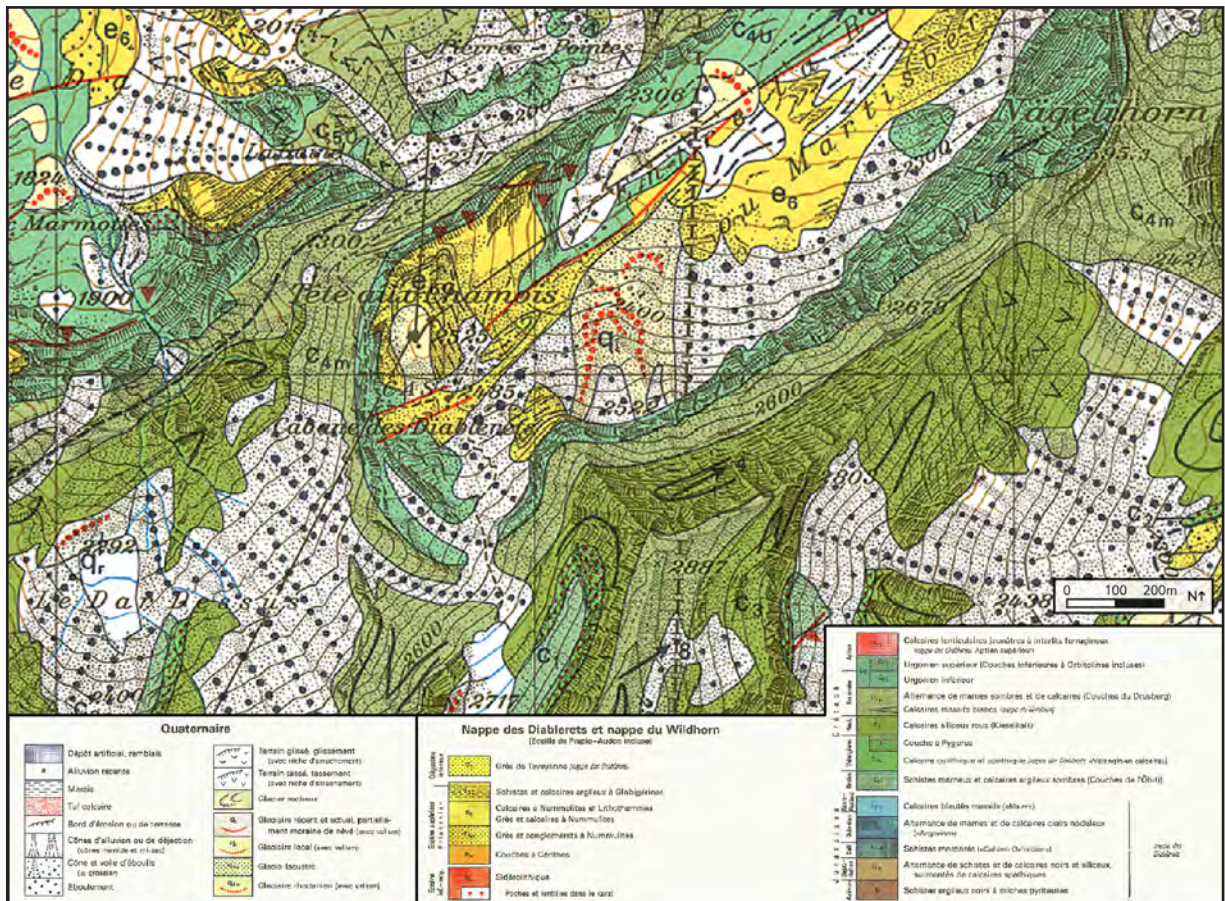


Fig. 3.32. Extract of the leaf 88 (Les Diablerets) of the 1: 25'000 Swiss geological Atlas and associated caption (Available on map.geo.admin.ch; Badoux and Gabus, 1991). Entre la Reille system is located at the center, outlined by the red lines of Holocene moraines.

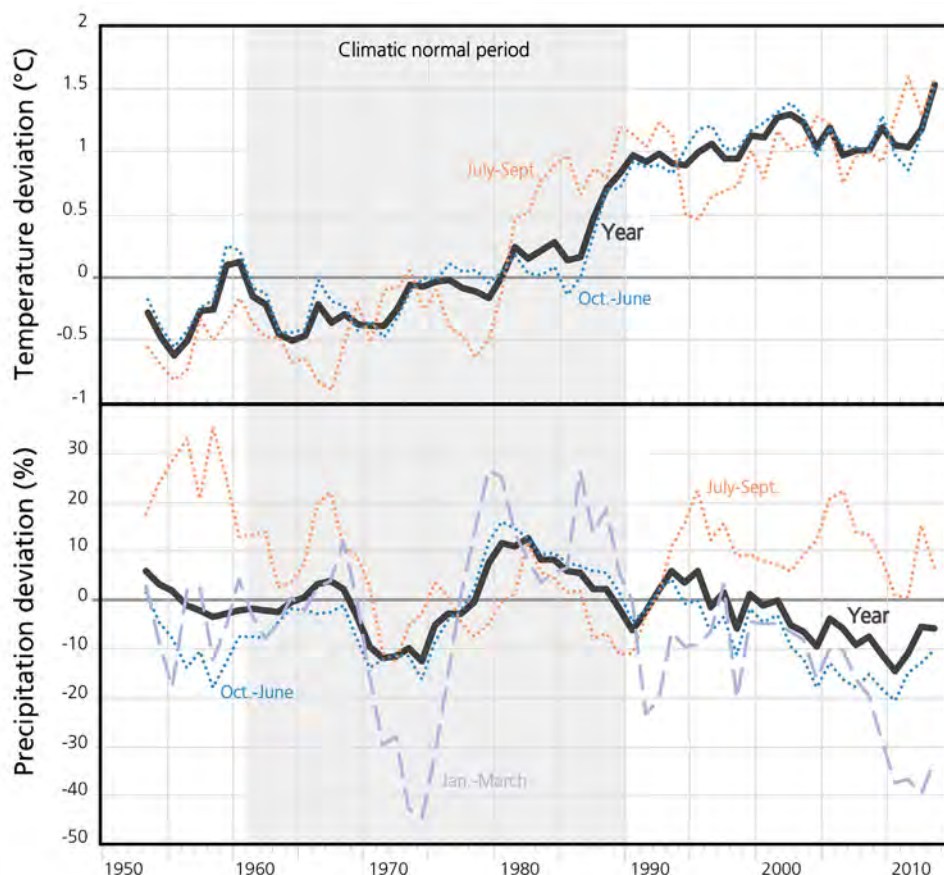


Fig. 3.33. Evolution of air temperature and precipitation in Château-d'Oex (985 m a.s.l.; 46°28'8"N, 7°8'4"E; 17 km distant from Entre la Reille, © MeteoSwiss) between 1950 and 2015. Based on homogenized monthly series of MeteoSwiss, the mean deviations of hydrological years, July to September, October to June and January to March periods from the 1961-1990 climatic normal period have been computed. Only the 5-years running means are represented.

Fig. 3.34. Photograph of Entre la Reille system (18.08.2014). A moraine, older than this glacier system is located in the left corner of the photograph, in the large boulders zone (indicated by the white arrow).



frost conditions at this altitude in the talus slope near the Entre la Reille glacier from geoelectrical and BTS measurements. Despite these favourable thermal conditions, rock glaciers are extremely rare in the

region. This is mainly due to the wet climatic conditions that have allowed the development of glaciers a low altitude during the Holocene, as in Entre la Reille (Lambiel et al., 2009). The overall steep topography and domination of fine sediments, which are less favourable for the rock glacier development (e.g. Haerberli et al., 2006) also explain this situation.

Today, the Entre la Reille glacier is almost completely covered by debris (Fig. 3.34). A very small firn zone (~ 3000 m² in 2014) is present at the backwall foot. Its area strongly varied over the last decades (Fig. 3.35) and during the last years, as observed during field surveys. Crevasses were observed in the 1990s in this zone (Fig. 3.36), illustrating the tensile stress exerted by the ice downward motion. The firn zone was/is mainly located in the upper western concave zone and less snow was/is accumulated in the convex eastern zone (Fig. 3.37). Here, a rockfall couloir actively supplies sediments. Small surface deformation ridges and lobes are present in this zone and contrast with the regular aspect of the central slope (Fig. 3.37). Ice outcrops are very rare in Entre la Reille but ice was observed below the debris during manual excavation in the upper central zone (Fig. 3.36). The upper half of this system is bounded by the lateral LIA moraines. In the distal zone, surface morphology shows typical characteristics of rock glacier: succession of ridges and furrows

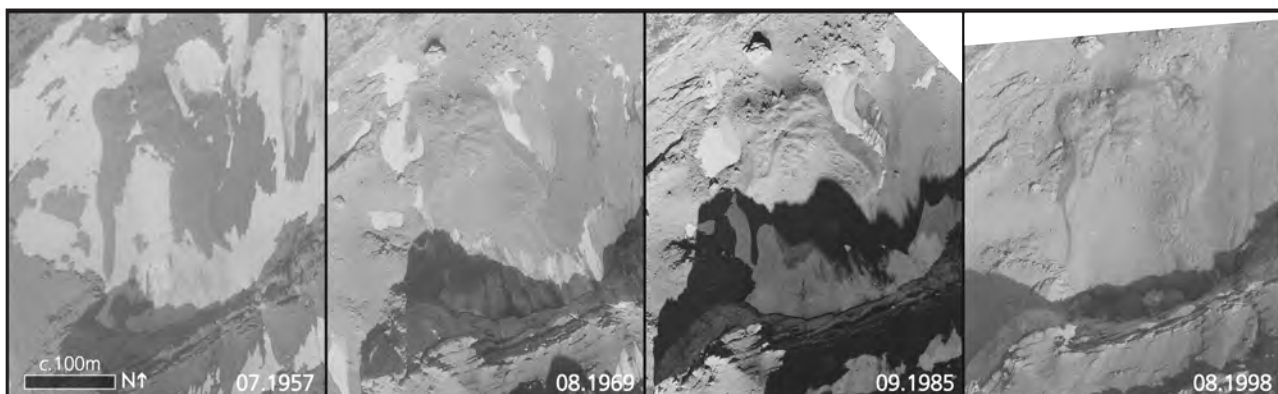


Fig. 3.35. Aerial images of Entre la Reille over the last decades (© Swisstopo, photographs respectively n°19571330012461, 19691320010703, 19850680195431 & 19981320027517, available on map.lubis.admin.ch).

Fig. 3.36. Side photographs of Entre la Reille in the 1990s and in 2011. The two 2011 photographs (side view and ice exposure inset) were taken by S. Utz.

and a steep fine-grained front. A gully, where water circulation concentrates in summer is present in the transitional zone between the glacier and the rock glacier. A former frontal ridge is located directly below the rock glacier front (Fig. 3.32 and 3.34). The large depression present in its inner side suggests the melt of former ground ice.

The glacier system of Entre la Reille was investigated by Reynard et al. (1999). The general high resistivity measured with vertical soundings and resistivity mapping lines was interpreted as an evidence of the alternation of ice-rich (from sedimentary origin) and debris-rich layers below the debris surface. In the upper central depression, the ice body was observed at 15 cm depth. Its thickness was comprised

between 5 and 10m according to resistivity values. The ice concentration decreased toward the eastern convex and distal zones. For the authors, this buried glacier – rock glacier system and its multi-layered structure illustrated the local complexity of Holocene climate history: cold and humid periods favourable to ice accumulation (as the LIA) have alternated with temperate and dry periods favourable to the debris accumulation (as the post-LIA period).

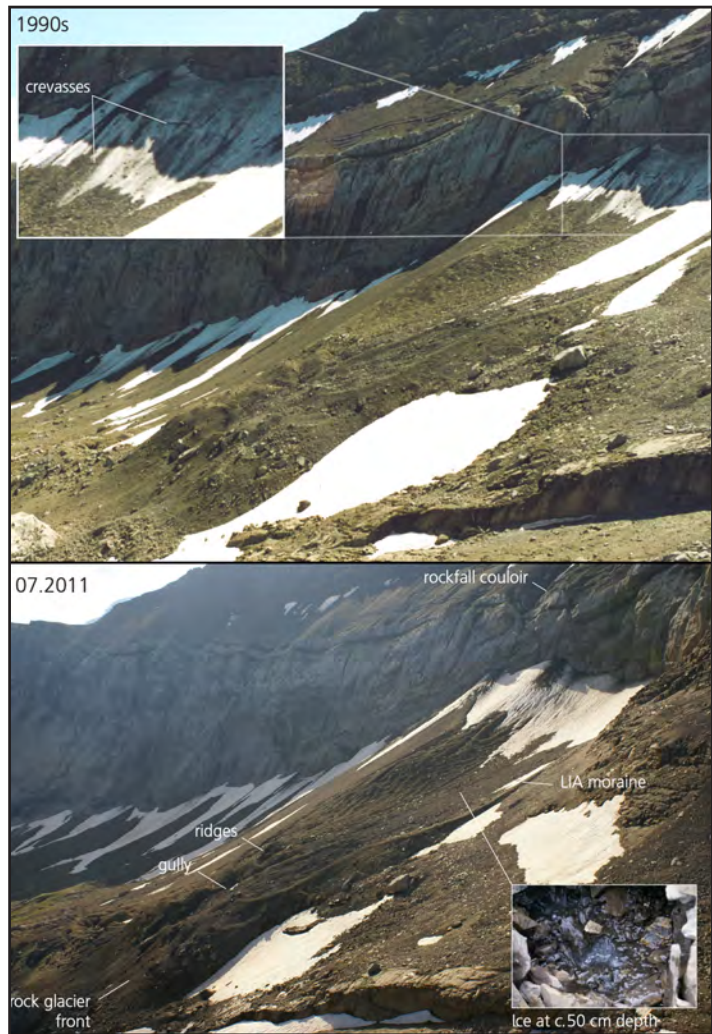


Fig. 3.37. View from the center of Entre la Reille toward the upper part. The upper convex East side (left part of the picture) contrast with the concave West side (center of the picture). Photograph: S. Utz, 24.07.2012.

3.4.2. Results

3.4.2.1. Ground surface temperature measurements

Base temperature of the winter snow cover

BTS were measured in March 2011. The snow layer was generally thick enough to insulate the ground from air temperature (Fig. 3.38). However, some BTS values have to be considered with caution because the snow layer was thinner than 90 cm for 15 measurements. BTS values can thus reflect here the influence of air temperature. Nevertheless, the large range of BTS measured whereas air temperature was relatively stable during the survey shows that ground conditions probably control at least partly this parameter. The results obtained point out the existence of a cold zone in the upper central and East part (BTS < -3°C) and the downslope warming of ground temperatures toward the NE (BTS > -2). The coldest values (BTS < -4°C) were measured on the convex upper eastern site but the snow mantle was relatively thin in this shadowed area.

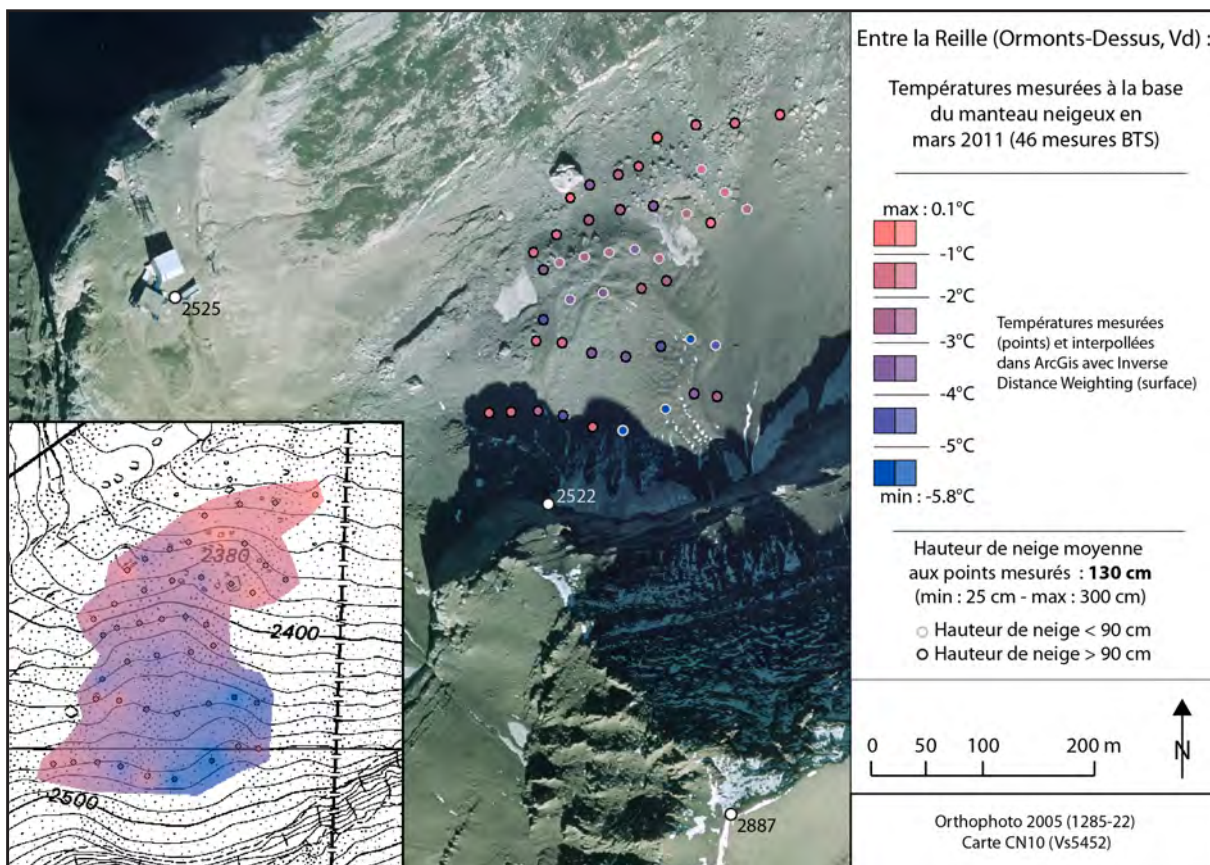
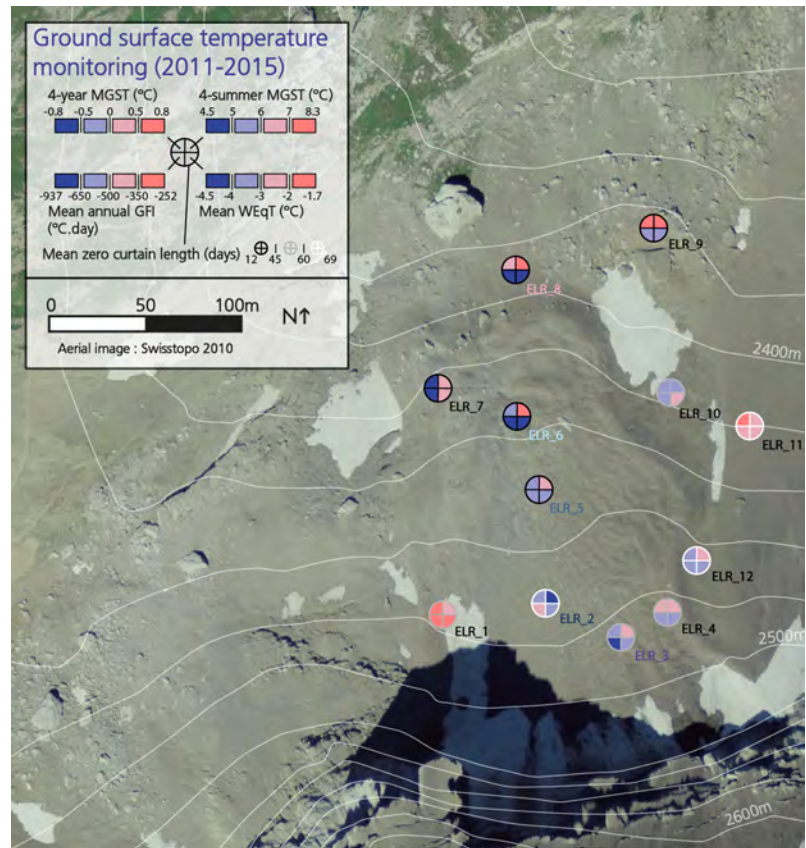


Fig. 3.38. Results of BTS measurements in Entre la Reille. The inset in the lower left corner corresponds to the data interpolation in ArcGIS with the Inverse Distance Weighting tool.

Ground surface temperature monitoring

Ground surface temperature was measured with 12 thermal sensors in Entre la Reille and the neighbouring slopes between July 2011 and September 2015 (Fig. 3.39; 3.40 and Tab. 3.3). We only present here the main information provided by these data. Several indices for each sensor

Fig. 3.39. Indices measured with the thermal sensors deposited in Entre la Reille. The data are detailed in Tab. 3.3 and only the 4-year means (bold in the table) are presented here. Although the dataset is almost full at the 4-year scale, some gaps exist between the data and mean ground surface temperature (MGST) are not equal to mean annual ground surface temperature (MAGST). GFI and WEqT correspond respectively to ground freezing index and winter equilibrium temperature.



were computed at the 4-year scale (Fig. 3.39 and Tab. 3.3). The values obtained showed the local spatial and temporal heterogeneity of ground thermal conditions. Because of the inter-annual variability of air temperature and snow cover thickness, mean annual and summer GST and GFI largely

varied over the 4 years. WEqT showed less variations (typically < 1°C), illustrating the control of ground thermal conditions on this parameter.

At the 4-year timescale, the warmest values were obtained in the SW and NE margins of the system (sensors ELR_1, ELR_9 and ELR_11) and the others sensors located between these two zones showed colder conditions (Fig. 3.39 and Tab. 3.3). The same general spatial distribution of cold/warm zones was highlighted by BTS measurements (Fig. 3.38). The coldest mean ground surface temperature was measured by the sensors located in the central zone (ELR_2, ELR_3, ELR_5, ELR_6 and ELR_7). Conversely, marginal sensors showed generally positive MGST. In summer, the coldest zone corresponded to the highest zone (MsummerGST < 7°C for ELR_1 to ELR_6 and ELR_10 to ELR_12). This situation is very likely due to the effect of elevation and the reduction of direct solar radiation by shading. Generally, ground temperature between July and September showed similar temporal and magnitude variations compared to air temperature (Tab. 3.3 and Fig. 3.40). Consequently, ground surface temperatures in summer 2014 and 2015 were respectively significantly colder and warmer compared to the situation of previous summers.

According to the thermal sensor data and to the direct measurements performed during the BTS survey, the snow cover thickness was very heterogeneous in Entre la Reille during winters. For instance, only one stabilisation of winter temperature (WEqT) and very short zero curtain periods were observed in ELR_7 data (Tab. 3.3), illustrating the winter snow cover thinness at this location. Furthermore, the early-February cold air wave of 2012 influenced similarly the ground temperature measured at ELR_3, ELR_6 and ELR_8 (Fig. 3.40). In contrast, ELR_2 and ELR_5 were efficiently decoupled from atmosphere by the snow mantle during this period. As a consequence,

Thermal sensor	Elevation (m a.s.l.)	Location	Mean ground surface temperature (MGST; °C)					Mean summer (July to September) GST (°C)					Winter equilibrium temperature (WEqt; °C)					Ground freezing index (GFI; °C.day)					Zero Curtain period (day)							
			2012	2013	2014	2015	Mean	2011	2012	2013	2014	2015	Mean	2012	2013	2014	2015	Mean	2012	2013	2014	2015	Mean	2012	2013	2014	2015	Mean		
ELR_1	2475	Inner side of the west LIA moraine	0.3	0.8	1.2	0.8	0.8	5.2	6	7.8	6.5	6.5	-2	-1.3	-1.7	-1.7	-365	-163	-229	-252									58	58
ELR_2	2466	Upper zone of the central depression	-0.5	-0.4	0	-0.3	5.1			3.9	4.5	4.5	-2.9	-2	-2.4	-2.4	-530	-210	-347	-362									69	69
ELR_3	2483	West of upper convex zone	-1.5	-0.2	-0.3	0.1	-0.5	5.8	6.4	4.7	6.1	6.1		-3.6	-4.4	-4	-1034	-548	-589	-712	60	64	34	43					50	50
ELR_4	2483	East of upper convex zone	-1.2	0.6	-0.1	0.7	0	5.9	6.7	5.2	6.8	6.8		-2.4	-3.9	-3.5	-927	-300	-535	-581	62	59	43	52					54	54
ELR_5	2447	Lower zone of the central depression	-0.8	0.5	0.2	-0.2	-0.1	5.8	7.2	5.3	6.2	6.2	-3.7	-2.7	-3	-3.2	-792	-403	-449	-564	15	51	38	72					44	44
ELR_6	2435	Glacier-rock glacier transitional zone	-0.8	0.2	-0.4	0.6	-0.1	6.9	7.8	5.2	7.2	7.2	-5	-3.8	-4.5	-4.5	-911	-553	-671	-706	32	61	27	40					40	40
ELR_7	2423	West of rock glacier	-1.3	-1	-0.7	-0.1	-0.8	5.8	7.1	5.5	6.5	6.5		-3	-3	-3	-1066	-984	-857	-937	5	10	21	12					12	12
ELR_8	2390	Rock glacier front	-1.2	0.2	0.2	1.1	0.1	6.9	7.6	6	7.6	7.6		-4.2	-3.8	-4.3	-1015	-492	-513	-658	26	51	48	37					41	41
ELR_9	2385	Old moraine	0.4	0.8	0.6	1	0.7	7.9	8.5	6.6	9	9		-2.7	-3.5	-3.1	-618	-380	-492	-527	21	54	44	39					40	40
ELR_10	2418	Outer side of East moraine	-0.3		0.3		0	6.9		4.1	5.5	-3		-2	-2.5	-2.5	-704		-301									59	59	
ELR_11	2422	East talus slope central zone		0.7	0.6	0.3	0.5	7.3	7.2	6.6	6.7		-2.2	-2.5	-2.4		-314	-492	-383	-396									65	65
ELR_12	2468	East talus slope upper zone	-0.4	0.1	0		-0.1	6.3	7.3	5.1	6.2	6.2	-3.8	-2.9	-2.9	-3.2	-711	-530	-462	-568									61	61
Interpol. Air T°	2450		0.9	-0.1	0.7	1.4	0.7	7.8	7.6	5.8	7.5						-905	-1138	-745	-894										

Tab. 3.3. Synthesis of the indices computed from the thermal sensor data between July 2011 and September 2015. Air temperature at 2450 m. a.s.l. is extrapolated using the daily data of the Moléson weather station (1972 m a.s.l.; 46°32'5"N, 7°01'05"E; 28 km distant from Entre la Reille, © MeteoSwiss) with a thermal gradient of 0.57°C/100m, obtained comparing the 5-year daily data of le Moléson and les Diablerets weather station (2966 m a.s.l.; 46°19'37"N, 7°12'14"E; 2 km distant from Entre la Reille, © MeteoSwiss).

WEqT, GFI and MGST have to be considered with caution because the cold values observed can be both due to the influence of air temperature on a poorly insulated ground and ground conditions. The relatively cold values obtained in the lower half of Entre la Reille glacier system (sensors ELR_6, ELR_7 and ELR_8; Tab. 3.3) illustrate thus probably the conjugate influence of winter air temperature and ground conditions. Conversely, the temperatures measured in the highest and/or concave zones (e.g. ELR_2, ELR_5), where large snow accumulation and avalanche deposits efficiently insulated the ground in winter, give more reliable indications on subsurface thermal conditions. The WEqT observed in the sensors ELR_2, ELR_3, ELR_5 and ELR_6 data show that the values decrease from -2 to -5°C toward the front of Entre la Reille system (Fig. 3.40 and Tab. 3.3). This is probably related to the earlier accumulation of a snow layer in the upper part, which partly insulates the ground from cold autumn air temperatures. The moistening and the complete melt of the snow cover (zero curtain period) lasts typically one to two month and ends in early-July (Fig. 3.40). From a general point of view, the annual temperature curves and the value of indices computed for the thermal sensors located on the Entre la Reille glacier system (ELR_2 to ELR_7) illustrate the local cold ground conditions and are typical of those obtained in permafrost environments, where ground ice is present (e.g., Lambiel, 2006).

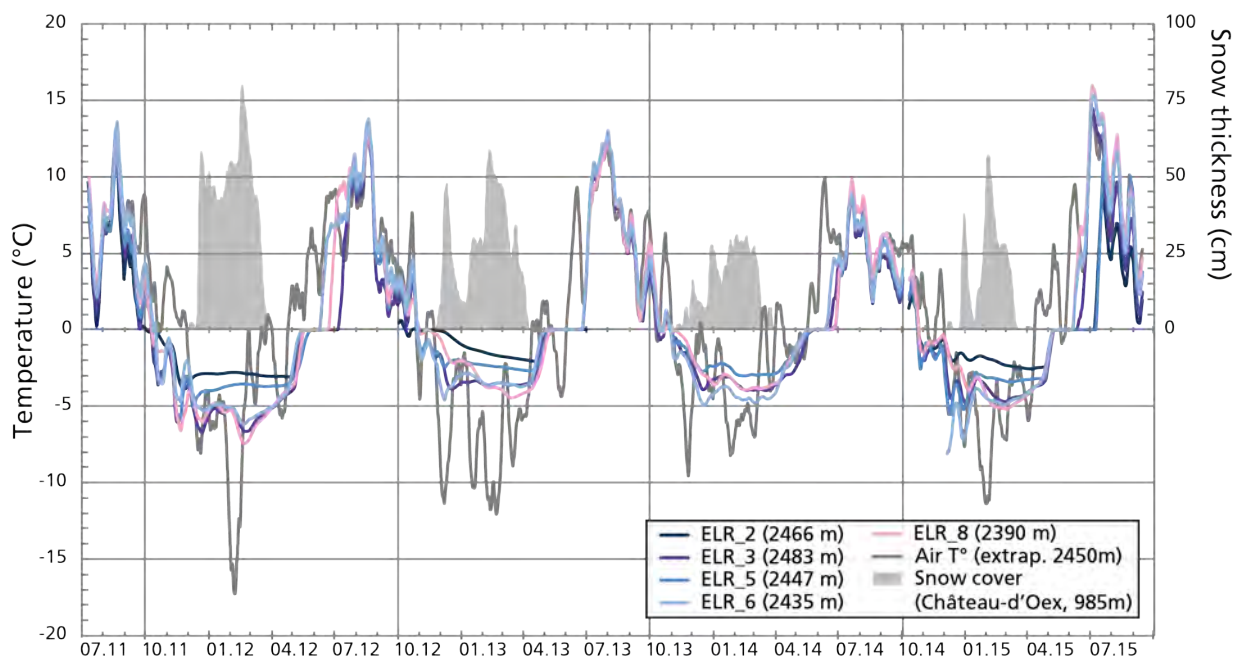


Fig. 3.40. 11-day running means of ground and air temperature in Entre la Reille. The position of the thermal sensors is shown on Fig. 3.39. See the caption of the Tab. 3.3 for the description of the extrapolation of air temperature at 2450 m a.s.l. The 5-day running mean of the snow cover height at Château-d'Oex (985 m a.s.l.; $46^{\circ}28'8''\text{N}$, $7^{\circ}8'4''\text{E}$; 17 km distant from Entre la Reille, © MeteoSwiss) indicates temporal and thickness variations of snow mantle at regional timescale although the snow typically covers Entre la Reille with a thick layer from October to early-July.

3.4.2.2. Electrical resistivity tomography

Because of its relative small size and proximity with the *Glacier 3000* cable car station, Entre la Reille is the site where the most complete ERT investigation was carried out in this study (Fig. 3.41). Moreover, compared to the very high surface porosity encountered in the other study sites, the presence of relatively fine marl and limestone debris in Entre la Reille allowed the collection of highly reliable electrical resistivity data. The main ERT results were presented in 2.2.2.4 section.

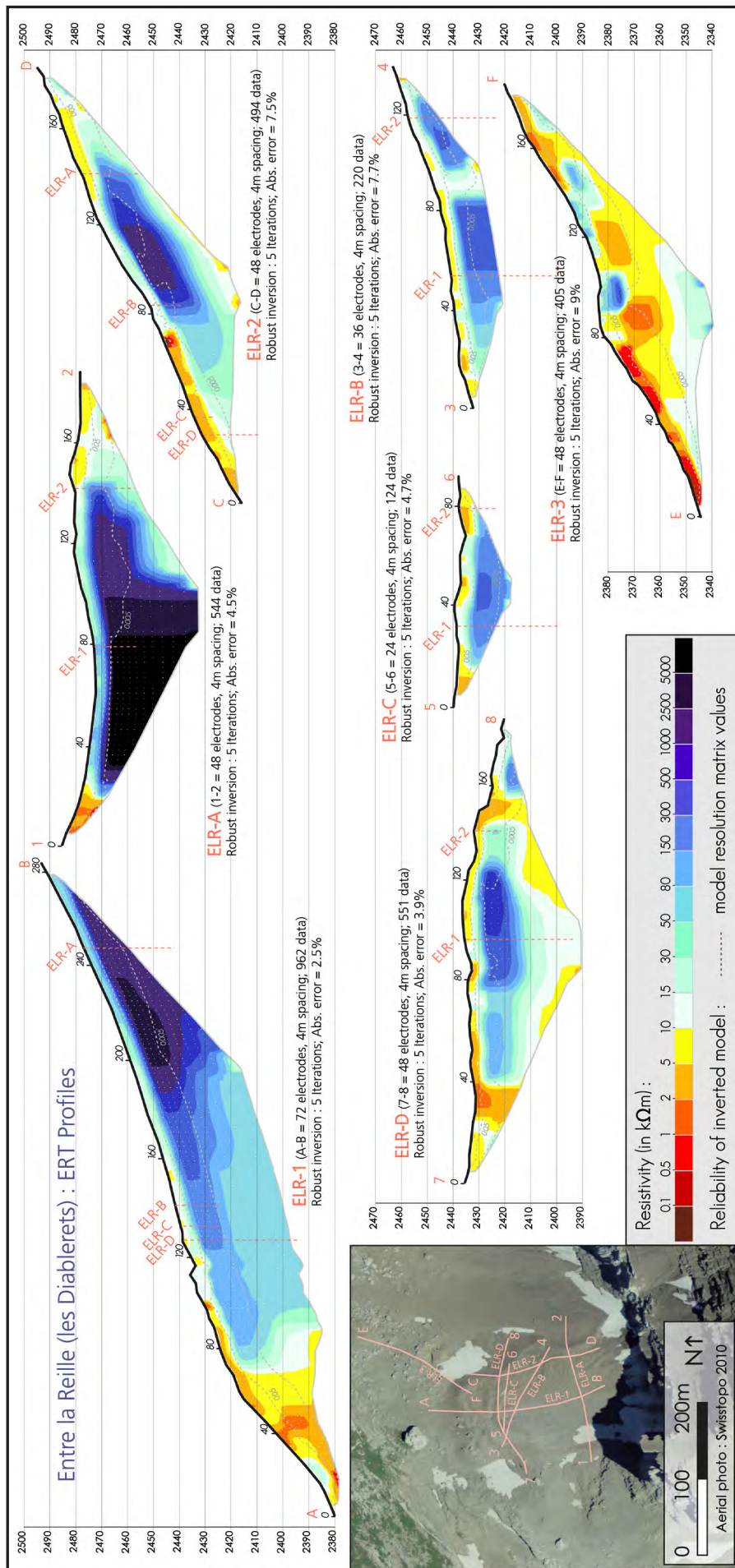


Fig. 3.41. Electrical resistivity tomograms measured in Entre la Reille. ELR-1, ELR-A and ELR-D were measured in July 2011, ELR-2 and ELR-3 in July 2012, ELR-B in July 2013 and ELR-C in July 2014

They are very coherent with the one-dimensional results obtained by Reynard et al. (1999): a layer of very high resistivity ($> 1000 \text{ k}\Omega\text{m}$) is present close to the surface in the upper concave zone. Towards the East and North margins, ground resistivity decreases and the conductive surface layer thickens. The profiles ELR-C and ELR-3 were not presented in the 2.2.2.4. ELR-C is located between ELR-B and ELR-D profiles and present similar results: a resistive layer ($> 80 \text{ k}\Omega\text{m}$) is present below a $\sim 5 \text{ m}$ thick conductive surface layer in this transitional zone between the upslope convex and concave zones and the distal rock glacier zone. ELR-3 crosses the old ridges located beyond the NE limit of Entre la Reille system. This tomogram has to be considered with caution because a snow layer was present during field survey in the upper depression of this profile and some electrodes were directly installed in the snow. 25% of inconsistent data were thus removed during the inversion procedure. The ground resistivity is largely lower than $30 \text{ k}\Omega\text{m}$ in this sector and contrasts with the significantly higher values measured upslope in the SDCGSAPE.

The longitudinal profile ELR-1 was measured each July between 2011 and 2014 (Fig. 3.42; 3.43). Results show a general good consistency and for example, the 2011 and 2012 profiles present relatively similar patterns of resistivity contrasts in the ground. However, a detailed analysis reveals the constant changes of ground resistivities over time (see especially the vertical variations of all resistivity layers displayed in the inset of the Fig. 3.42). Time-lapse comparison between the 2011 and 2012 profiles (Fig. 3.43) shows a decrease of resistivities ($< -10\%$) in almost all the upper two third of Entre la Reille. A decrease exceeding -30% also appeared in the steep front. Conversely, resistivity increased in the 4 m thick surface layer between the positions 160 and 230 m ($> 70\%$), below the rock glacier front ($> 60\%$) and in the lower part. We tried to understand the origin of these changes gathering information on ground thermal conditions and water content during the

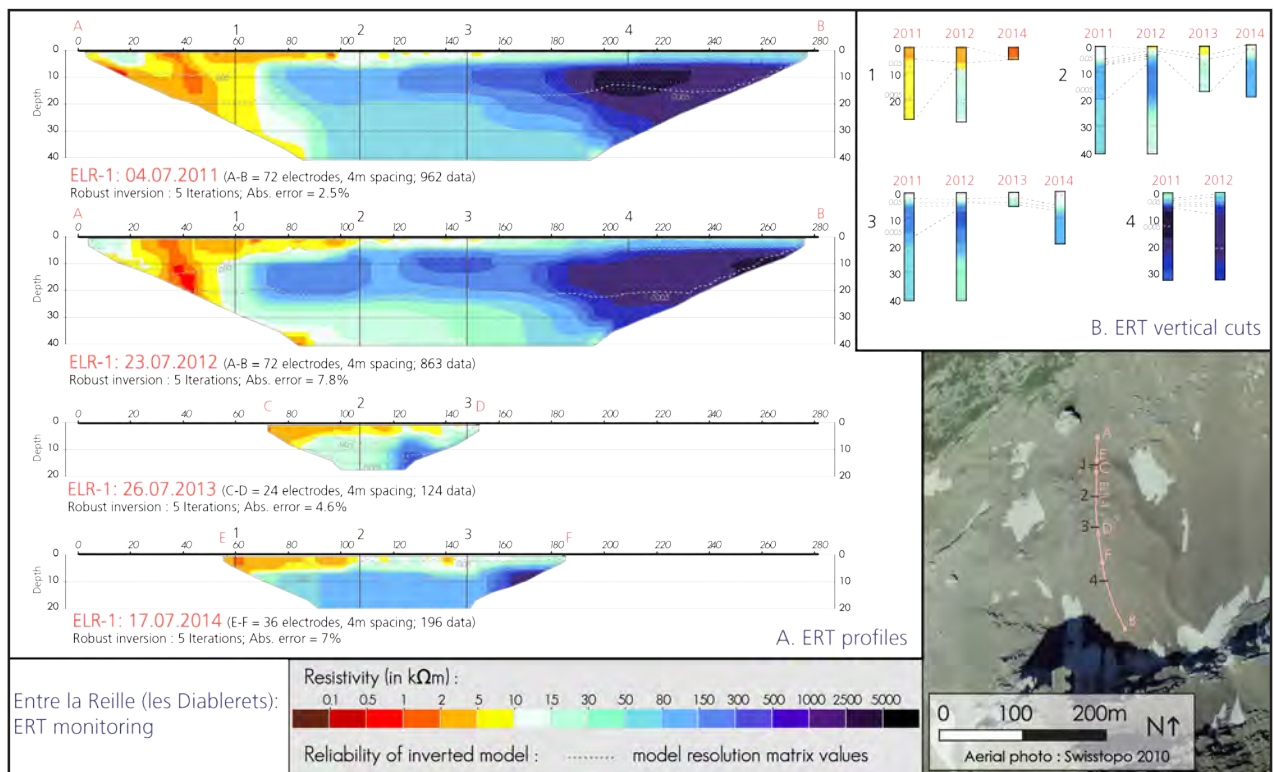


Fig. 3.42. Results of the ERT monitoring carried out in July between 2011 and 2014 in the central longitudinal profile of Entre la Reille

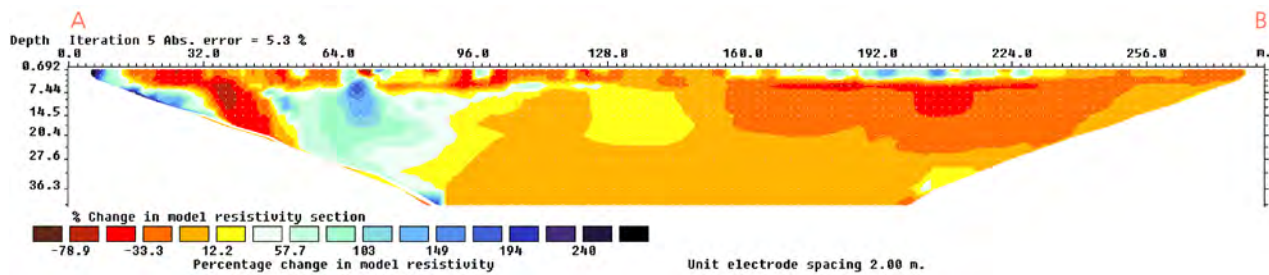


Fig. 3.43. Comparison between the ERT data of ELR-1 in 2011 and 2012. The difference is expressed as a percentage of resistivity.

ERT surveys (Tab. 3.4). However, no clear relation appeared between electrical resistivity variations and climatic parameters and only supposition can be made. For instance, the general decrease of resistivities in more than 80% of the profile in 2012 (Fig. 3.43) could be related to a larger water content due to the melt of the thicker snow layer and/or to higher June-July air temperatures (see the regional monthly temperature in the top of the Fig. 3.48). Compared to other years, the thickening of the conductive surface layer and the relative lower values inverted between 7 and 20 m of deepness ($< 150 \text{ k}\Omega\text{m}$) in 2014 could be related to the presence of ground water following the very heavy rainfall that occurred few days before the survey. The general decrease of resistivity observed over time could also be related to the progressive melt and/or warming of ground ice in the unfavourable climatic context (Fig. 3.33). Results of this ERT monitoring are very difficult to interpret and speculative considerations can not be prevented. Hilbich et al. (2009) also showed the large inter-annual variability of the ERT monitoring values measured on a rock glacier. The quality of the electrical contact between the electrodes and the ground and the thermal/hydrological conditions in the surface layer during each individual survey are key parameters to understand the subsurface resistivities. These authors recognized therefore the limit of the ERT monitoring and recommended to focus on the changes observed in the first investigated meters. In Entre la Reille a thickening of the surface conductive layer could be inferred in some sectors (e.g. vertical cuts 1 and 3 in the inset of Fig. 3.42). This process could show a thickening of the active layer. In addition, the decrease of ground resistivities below the rock glacier front (80 first investigated meters in Fig. 3.42 & 3.43) could evidence a permafrost degradation in this zone. However, additional data are required to evaluate these assumptions.

	04.07.2011	23.07.2012	26.07.2013	17.07.2014	data
Mean daily GST during the ERT survey (°C)	10.3	8.2	13.8	12.1	ELR_5 and ELR_6
Mean daily GST 7 days before the ERT survey (°C)		10	11.5	4.9	ELR_5 and ELR_6
Daily air T at 2450 m a.s.l. during the ERT survey (°C)	8.3	6.7	14.8	12.8	Air temp. extrap. From le Moléson
Mean daily air T at 2450 m a.s.l. 7 days before the ERT survey (°C)	7.4	5.4	10.8	5.2	Air temp. extrap. From le Moléson
Sum of daily precipitations 7 days before the ERT survey (mm)	17.4	12.6	10.6	132.1	Le Moléson weather station
Sum of winter snowfalls (cm)	121	266	332	218	Château-d'Oex weather station

Tab. 3.4. Climatic parameters measured during and before the ERT surveys carried out in July 2011 to 2014. See caption of Fig. 3.40 and Tab. 3.3 for details on the air temperature extrapolation and weather stations.

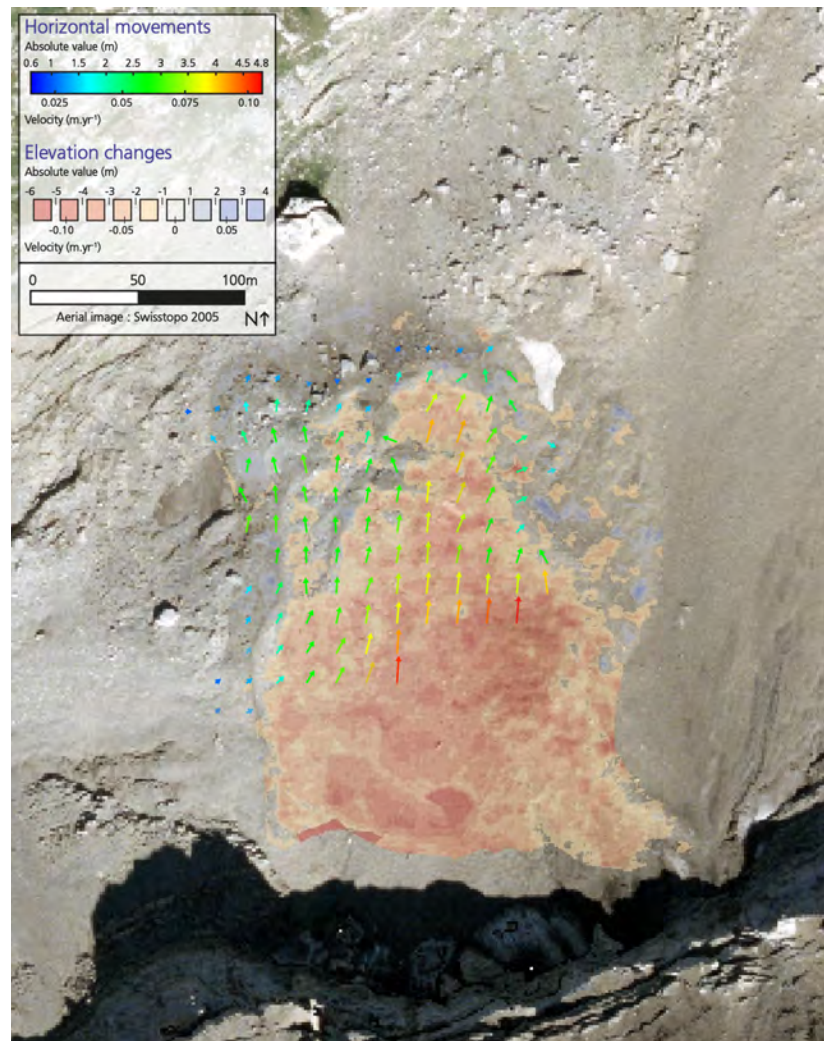
3.4.2.3. Photogrammetry and image analysis

M. Capt tried to study the decadal behaviour of Entre la Reille system during his master thesis. However, because of the noticeable shadow induced by the Oldenhorn rockwall on this very small site and its weak dynamic, very few usable data were produced and no results were pre-

Fig. 3.44. Horizontal movements and surface elevation changes between 1959 and 2005 in Entre la Reille extracted respectively from the comparison of ortho-rectified aerial images and DEMs. These data were produced by M. Capt.

sented in the final document. We only show here the most complete results, the decadal elevation changes and horizontal movements obtained comparing DEMs and aerial images of 1959 and 2005 (Fig. 3.44).

At this 46-year timescale, almost the whole surface of Entre la Reille lowered of few meters, corresponding to a volume of $\sim 0.06 \text{ km}^3$. Cumulative mass balance was thus negative during this period characterised by an increase of 1°C of the regional



air temperature and a decrease of annual and winter precipitations (Fig. 3.33). Surface lowering affected mainly the upslope central depression and the lower zone of the convex East side. In these two zones, losses exceeded generally 3 m. Conversely, no significant changes were observed in the NW part of the rock glacier and in the distal part of the system. Patches of mass gain are even locally present here. However, they remained spatially limited and corresponded to a weak volume in comparison with the mass loss.

Horizontal movements exceeded 3.5 m in the upper and in the central zones and decreased towards the system lateral and frontal margins. Over the last decades, movements were relatively slow and did not exceed 10 cm.a^{-1} in the lower half of Entre la Reille. Nevertheless, all this zone was active at this timescale.

3.4.2.4. dGPS

The position of 66 blocks were measured up to ten times (depending on snow cover extent during the survey) in Entre la Reille and neighbouring slopes between July 2011 and September 2015. Some results were already presented in the section 2.2.2.4 and we only synthetize here the main outcomes of this dGPS monitoring.

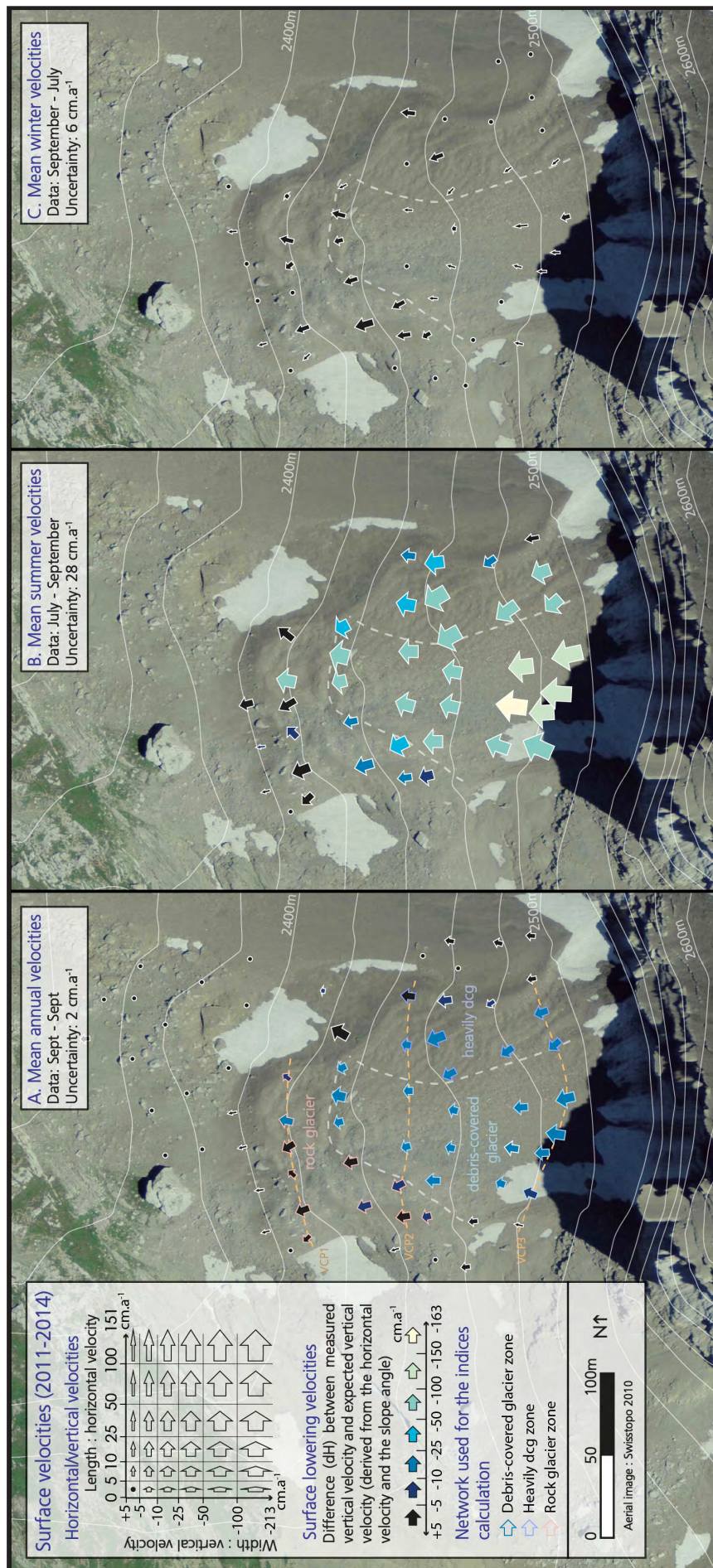


Fig. 3.45. Mean annual, summer and winter surface velocities measured between July 2011 and September 2015 in Entre la Reille. The horizontal velocity cross profiles (VCP) of the Fig. 3.50 are represented in the left image. The white dashed line shows the spatial limits between the three main zones defined in this system.

In contrast to the blocks located in the lower slope, all the blocks monitored in this SDCGSAPE moved during the last years (Fig. 3.45). Between September 2011 and 2015, maximum horizontal and vertical movements reached respectively 135 cm (34 cm.a⁻¹) and -176 cm (-44 cm.a⁻¹). These maximum values were on the same block, located at the top of the upslope depression. At annual timescale (Fig. 3.45A), most of the blocks moved slower than |25| cm.a⁻¹. The upper half of Entre la Reille was the most active zone and the lower half showed mostly horizontal displacements. Only slow sub-horizontal movements were measured in the rock glacier front. Surface lowering were fastest in the upper central zone but did not exceeded 25 cm.a⁻¹. Conversely, the frontal and lateral margin of the system had significantly lower surface lowering values (< 10 cm.a⁻¹). Slow movements were measured in the talus slopes at the West and East of Entre la Reille whereas the footslope and the lower former moraine were inactive. To highlight the dominant dynamic at the four-year scale, we computed the downslope movement/surface lowering (M_d/dH) index (Fig. 3.46). Except the negative values obtained in the central zone that showed the domination of surface lowering here, the values were largely positive in Entre la Reille and illustrated the prevalence of downslope movement. These values were especially high in the rock glacier zone.

Surface velocities considerably accelerated in summer (Fig. 3.45B) and maximum horizontal and vertical values reached respectively 151 cm.a⁻¹ and -213 cm.a⁻¹ in the top of the upper depression. The central upper zone of Entre la Reille was the most active and surface velocities decreased noticeably toward the lateral and distal margins (< |50| cm.a⁻¹). Surface lowering was especially rapid in the upper central zone (> 50 cm.a⁻¹) whereas it was close to zero in the rock glacier front. During winter, surface velocities strongly decreased (< |25| cm.a⁻¹; Fig. 3.45C). Mostly slow sub-horizontal movements occurred during these periods and maximum values were measured in the rock glacier zone. Vertical movements were also mainly observed in this zone. Surface lowering was close to zero during these mostly snow-covered periods.

Three measurement campaigns were carried out during the summer 2014 and permitted the investigation of the surface velocities in early and late summer (Fig. 3.47). This period was especially cool and rainy in the region (Fig. 3.48). As a consequence, if the summer 2014 surface velocities showed generally the same patterns than other summers (Fig. 3.45B & 3.47A), the measured values were then slower (Fig. 3.48). It illustrates thus the strong control of the air temperature

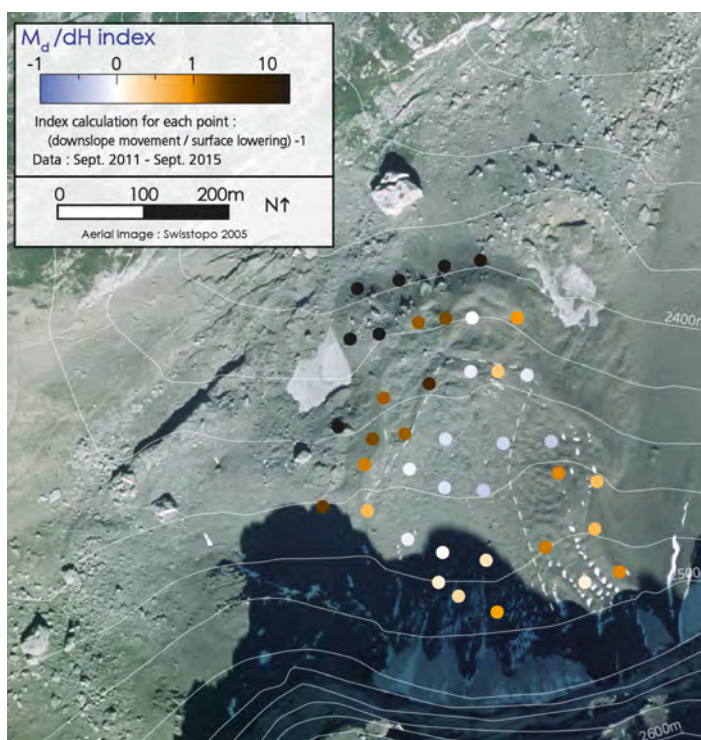


Fig. 3.46. Downslope movement/Surface lowering index computed with the 4-year surface velocities measured in Entre la Reille.

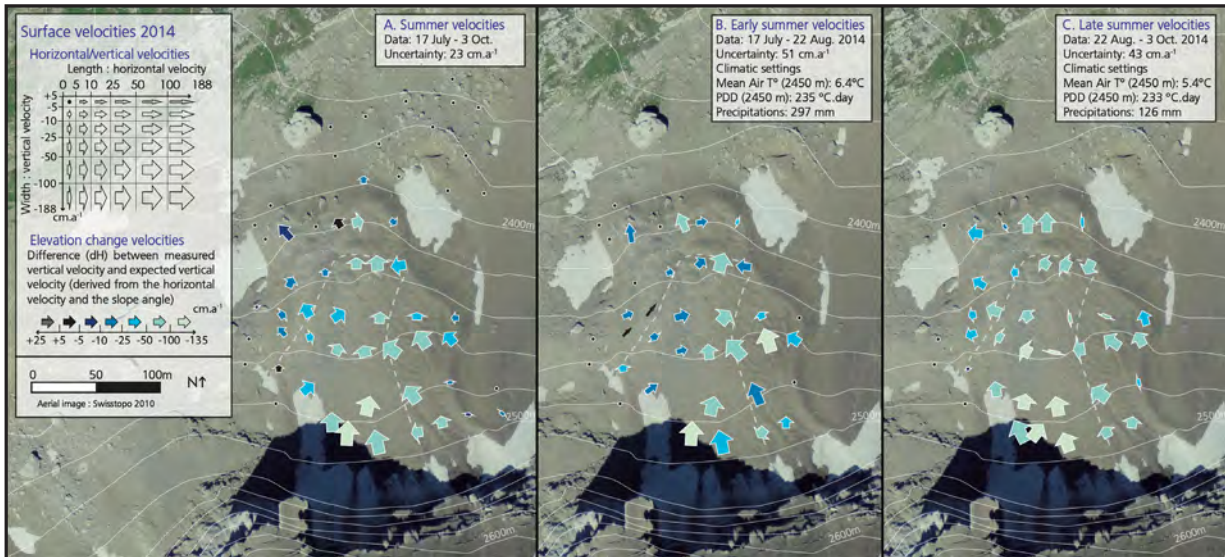


Fig. 3.47. Summer, early-summer and late-summer surface velocities measured in 2014 in Entre la Reille. The climatic settings are derived from the extrapolated air temperature at 2450 m.a.s.l and precipitation at le Moléson weather station (see caption of Tab. 3.3 for details).

Les Diablerets Region

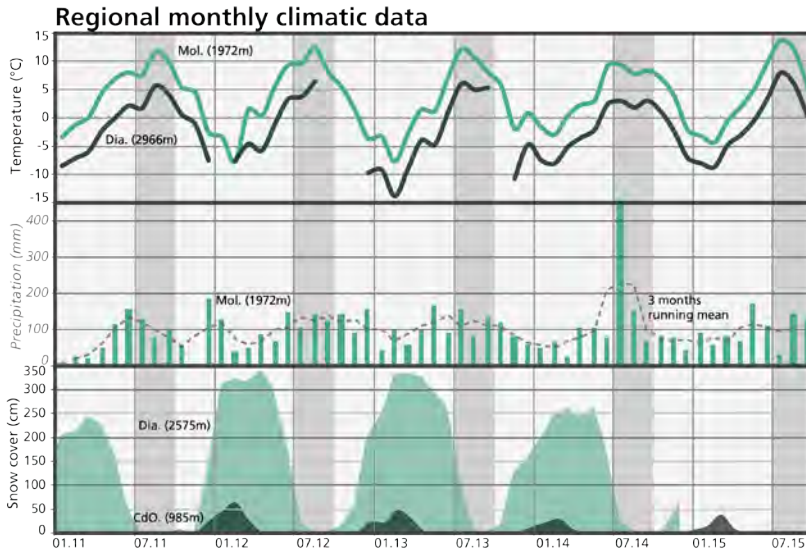
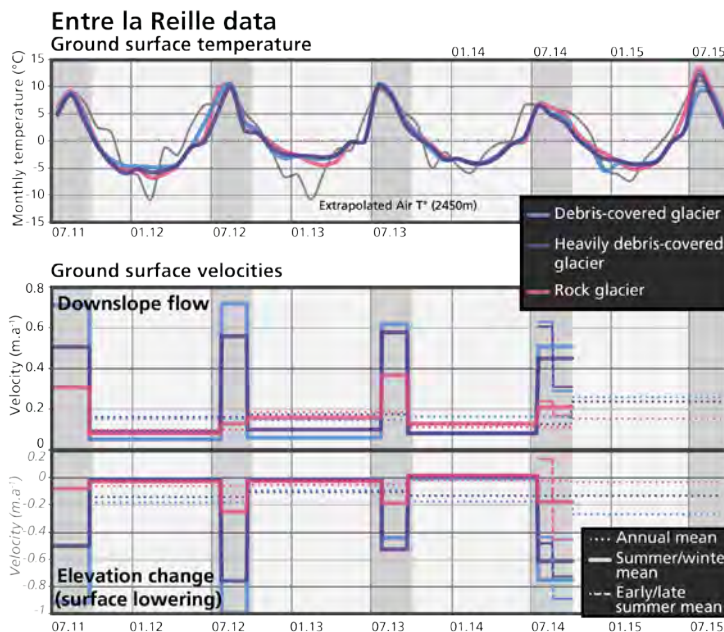


Fig. 3.48. Annual, seasonal and early/late-summer mean downslope flow and surface lowering velocities measured in the three main zones of Entre la Reille between July 2011 and September 2015. The blocks used for this mean calculation are presented in the Fig. 3.45. Monthly means of ground surface temperatures and regional climatic data are represented above. The used weather stations were presented previously (data © MeteoSwiss). The snow height at the IMIS station of les Diablerets was available between 2011 and 2014 (© SLF).



on the summer dynamic of this system. Early summer was slightly warmer and more than two times wetter than late summer (inset of Fig. 3.47B and C). During the first period, the eastern half of Entre la Reille was the most active and mainly strong horizontal movements were measured. Conversely, horizontal velocities generally decreased in late summer (mostly < 50 cm.a⁻¹) but vertical and surface lowering increased in the whole system.

As explained in the section 2.2.2.3, we defined three main zones in Entre la Reille according to homogeneous surface morphology, internal structure characteristics and dynamical behaviours: debris-covered glacier zone (DCG), heavily debris-covered glacier zone (HDCG) and rock glacier zone (RG; Fig. 3.45A). Mean surface velocities values were then computed for each zone to analyse in detail their dynamical behaviour. Annual, seasonal and infra-seasonal (summer 2014) variations of downslope movements and surface lowering are represented with local climatic and ground parameters in the Fig. 3.48 and several dynamical indexes are synthetized in the Fig. 3.49.

At each timescale, the largest variations of velocities occurred in the DCG zone. Here, surface velocities accelerated in summer, in the year 2015 and in early summer for downslope movement and late summer for surface lowering. The marked summer dominant dynamic of the DCG zone showed the strong control of warm air temperature and precipitation during the snow-free period. Conversely, this zone is the less active in winter (< |6| cm.a⁻¹), when the ground is efficiently insulated from the atmosphere by the snow cover. The M_v/dH index is close to zero (Fig. 3.49), showing the same magnitude of downslope movement and surface lowering. To investigate the drivers of the temporal variations of velocities in this zone, we compared the variations of annual and summer mean velocities over the 4 years with those of several climatic and ground parameters

Dynamical indexes		Debris-covered glacier	Heavily debris-covered glacier	Rock glacier	Legend
Intensity of dynamics	Annual velocity				
	Summer velocity				
	Winter velocity				
Temporality of dynamics	Annual and seasonal variability of velocity				Standard deviation of annual / of seasonal velocities
	Proportion of summer activity on annual activity				Horizontal movement (%)
	Proportion of early summer activity on summer activity				Vertical movement (%) Surface lowering (%)
Main dynamics	Downslope movement vs. surface lowering				M_v/dH index (downslope movement / surface lowering) -1 to 10

Fig. 3.49. Mean dynamical index computed in the three main zones of Entre la Reille between 2011 and 2015

Source	Parameters	Coefficient of determination (R ²) of mean zonal surface velocities																		
		Year 2012 to 2015						Summer 2011 to 2014												
		Downslope movement		Surface lowering		R ² means		Downdipole movement		Surface lowering		R ² means								
DCG	HDCG	RG	RG	All	DM	SL	DCG	HDCG	RG	RG	All	DM	SL	DCG	HDCG	RG				
Climatic parameters	Mean annual air temp. (MAAT)	0.55	0.33	0.14	0.99	0.45	0.10	0.43	0.34	0.51	0.77	0.39	0.12	0.10	0.30					
	MAAT yr-1	0.02	0.18	0.03	0.02	0.03	0.58	0.14	0.08	0.21	0.02	0.02	0.10	0.30						
	Winter Temp. (Oct-June)	0.33	0.11	0.18	0.85	0.46	0.26	0.37	0.21	0.52	0.59	0.28	0.22	0.22						
	Autumn Temp. (Oct-Dec)	0.56	0.45	0.16	0.90	0.46	0.00	0.42	0.39	0.45	0.73	0.45	0.08							
	Summer Temp. (July-Sept)	0.53	0.80	0.10	0.16	0.01	0.07	0.28	0.48	0.08	0.34	0.40	0.08	0.56	0.90	0.12	0.03	0.00	0.04	
	Summer Temp. yr-1	0.89	0.93	0.02	0.60	0.03	0.01	0.41	0.62	0.21	0.74	0.48	0.02	0.14	0.73	0.47	0.38	0.11	0.01	0.31
	Ground freezing index	0.22	0.03	0.11	0.63	0.29	0.48	0.29	0.12	0.47	0.43	0.16	0.30	0.14	0.73	0.47	0.38	0.11	0.01	0.31
	Annual Positive degree day (PDD)	0.46	0.57	0.05	0.49	0.21	0.12	0.32	0.36	0.27	0.48	0.39	0.08	0.94	0.28	0.08	0.42	0.10	0.01	0.30
	Annual PDD yr-1	0.69	0.39	0.01	0.73	0.05	0.57	0.41	0.36	0.45	0.71	0.22	0.29							
	Summer PDD	0.19	0.46	0.06	0.01	0.01	0.32	0.18	0.24	0.12	0.10	0.24	0.19	0.56	0.89	0.13	0.03	0.00	0.03	0.27
	Summer PDD yr-1	0.89	0.94	0.03	0.58	0.02	0.01	0.41	0.62	0.20	0.74	0.48	0.02							
	Annual precipitations (P)	0.49	0.53	0.10	0.64	0.32	0.06	0.36	0.37	0.34	0.57	0.43	0.08	0.59	0.00	0.01	0.41	0.08	0.41	0.25
Winter P (Oct-June)	0.03	0.02	0.35	0.43	0.49	0.26	0.26	0.13	0.39	0.23	0.26	0.31	0.03	0.50	0.08	0.57	0.02	0.42	0.27	
Autumn P (Oct-Dec)	0.39	0.17	0.23	0.93	0.55	0.13	0.40	0.26	0.54	0.66	0.36	0.18								
Summer P (July-Sept)	0.21	0.47	0.02	0.04	0.00	0.35	0.18	0.23	0.13	0.12	0.23	0.18	0.83	0.48	0.13	0.02	0.05	0.04	0.26	
Mean snow cover thickness (Nov-April)	0.39	0.20	0.30	0.16	0.11	0.91	0.35	0.30	0.39	0.28	0.15	0.61	0.02	0.49	0.16	0.01	0.57	0.92	0.36	
Cum. autumn snowfalls (Oct-Dec)	0.51	0.29	0.27	0.25	0.07	0.85	0.37	0.36	0.39	0.38	0.18	0.56								
Cum. winter snowfalls (Oct-June)	0.39	0.13	0.05	0.75	0.23	0.50	0.34	0.19	0.49	0.57	0.18	0.28	0.04	0.44	0.00	0.40	0.12	0.64	0.27	
Mean GST	0.07	0.17	0.86	0.63	0.89	0.35	0.49	0.37	0.62	0.35	0.53	0.61								
Summer GST	0.10	0.78	0.07	0.00	0.06	0.01	0.17	0.32	0.02	0.05	0.42	0.04	0.39	0.94	0.01	0.05	0.00	0.16	0.26	
Summer GST yr-1	0.73	0.78	0.00	0.66	0.05	0.01	0.37	0.50	0.24	0.69	0.42	0.01								
Winter equilibrium temp.	0.07			0.59						0.33										

Tab. 3.5. Coefficient of determination (R²) computed comparing variations of annual (2012 to 2015) and summer (2011 to 2014) downslope movement and surface lowering velocities with climatic and ground parameters in the three main zones of Entre la Reille. In the climatic parameters, “yr⁻¹” means that we used the data of the previous year to investigate if the climate signal induces delayed dynamical responses. Temp., P, and GST refer respectively to air temperature, precipitation and ground surface temperature. Annual, autumn, winter and summer periods correspond respectively to October to September, October to December, October to June and July to September. The yellow values are those discussed in the text. The R² > 0.5 are indicated in bold.

ters (Tab. 3.5). We computed then the coefficient of determination (R^2). The following relations appeared the most interesting (in yellow in the Tab. 3.5): annual surface lowering is positively correlated with MAAT (R^2 : 0.99), autumn temperature (R^2 : 0.90) and autumn precipitation (R^2 : 0.93); downslope movement in summer is positively correlated with annual positive degree day (R^2 : 0.94) and negatively with summer precipitations (R^2 : 0.83); surface lowering in summer is positively correlated with the MAAT (R^2 : 0.93). The large number of $R^2 > 0.50$ shows the strong relation that exists between the dynamical behaviour of this zone and climatic variations. The control of air temperature on surface dynamics is especially evidenced.

HDCG zone showed relatively the same dynamical behaviour than DCG zone but the amplitude of temporal variations of velocities was smaller and the measured velocities were generally slower (Fig. 3.48 and Fig. 3.49). Consequently, the velocities values were more stable over years and seasons. Here again, most of annual activity occurred in summer and the same distribution of early/late summer activity was found compared to DCG zone (Fig. 3.49). Mean M_d/dH index is 0.5, indicating that downslope movements were 1.5 times faster than surface lowering. As also observed in the DCG zone (Tab. 3.5), annual downslope movement is negatively correlated with the air temperature (R^2 : 0.93) and degree day (R^2 : 0.94) of the precedent summer. Conversely, this movement is positively correlated with summer temperature (R^2 : 0.80). Annual surface lowering is negatively correlated with mean ground surface temperature (R^2 : 0.89). Finally, downslope movement in summer is positively correlated with summer air temperature (R^2 : 0.90), PDD (R^2 : 0.89) and GST (R^2 : 0.94). R^2 are generally lower in this zone compared to the DCG. It shows that the climatic control on the dynamics of this zone is less obvious, probably because of the thickening of the debris cover and the decrease of the ice concentration.

Compared with these two zones, RG zone showed a different dynamical behaviour (Fig. 3.48 and Fig. 3.49). Temporal variations of velocities between years, seasons and early/late summer were significantly smaller and this zone was generally less active. Surface velocities generally also increased during summers but proportionally, respectively 70% and 50% of the annual horizontal and vertical movements occurred in winter. In contrast, 88% of annual surface lowering was measured during summer. In early summer, positive elevation change was observed and surface lowering appeared only in late summer. The high mean M_d/dH value illustrated the strong domination of downslope movement here. Annual variation of downslope movement is positively correlated with GST (R^2 : 0.89; Tab. 3.5). Annual and summer surface lowering are positively correlated with the mean winter snow cover thickness (R^2 : 0.91; R^2 : 0.92) and the sum of autumn snowfalls (R^2 : 0.85) for the first. In comparison with the DCG zone, the low number of $R^2 > 0.50$ points out that the relation between the dynamical behaviour of this zone and climatic parameters is more complex.

Finally, we investigated the motion mechanism (see also 2.2.2.3) with velocity cross profiles (Fig. 3.50). No indisputable tabular or parabolic shape is observable on these profiles, showing the possible occurrence of both basal sliding and internal deformation. An *en masse* movement of 10 $\text{cm}\cdot\text{a}^{-1}$ and 20 $\text{cm}\cdot\text{a}^{-1}$ could be active below the debris-covered glacier zone (respectively below

Fig. 3.50. Velocity cross profiles obtained from the 4-year surface horizontal velocities measured in Entre la Reille. See Fig. 3.45A for the location of the VCP.

VCP2 and VCP3) whereas movements in the other zones showed rather a parabolic aspect.

3.4.2.5. LiDAR data

Two high-resolutions DEMs of Entre la Reille were produced from terrestrial laser scans in Aug. 2013 and Sept. 2014 (Capt, 2015; Fig. 3.51). The comparison of DEMs and hillshades allowed to compute elevation changes and horizontal velocities. Unfortunately, the snow was still present in the upper West part of Entre la Reille and prevented the analysis of this sector. Some topographical shading (e.g. behind ridges or in concave zones) also limited the data collection. The results obtained at this 13 months period showed high consistency with those measured with the dGPS (3.4.2.4; Capt, 2015) and the relatively good spatial coverage of LiDAR data allowed to highlight the existence of very local dynamics.

Elevation changes are mainly characterised by surface lowering (Fig. 3.51A). Large zones of Entre la Reille were affected by at least a -10 cm.a^{-1} loss during the 13 investigated months. The less

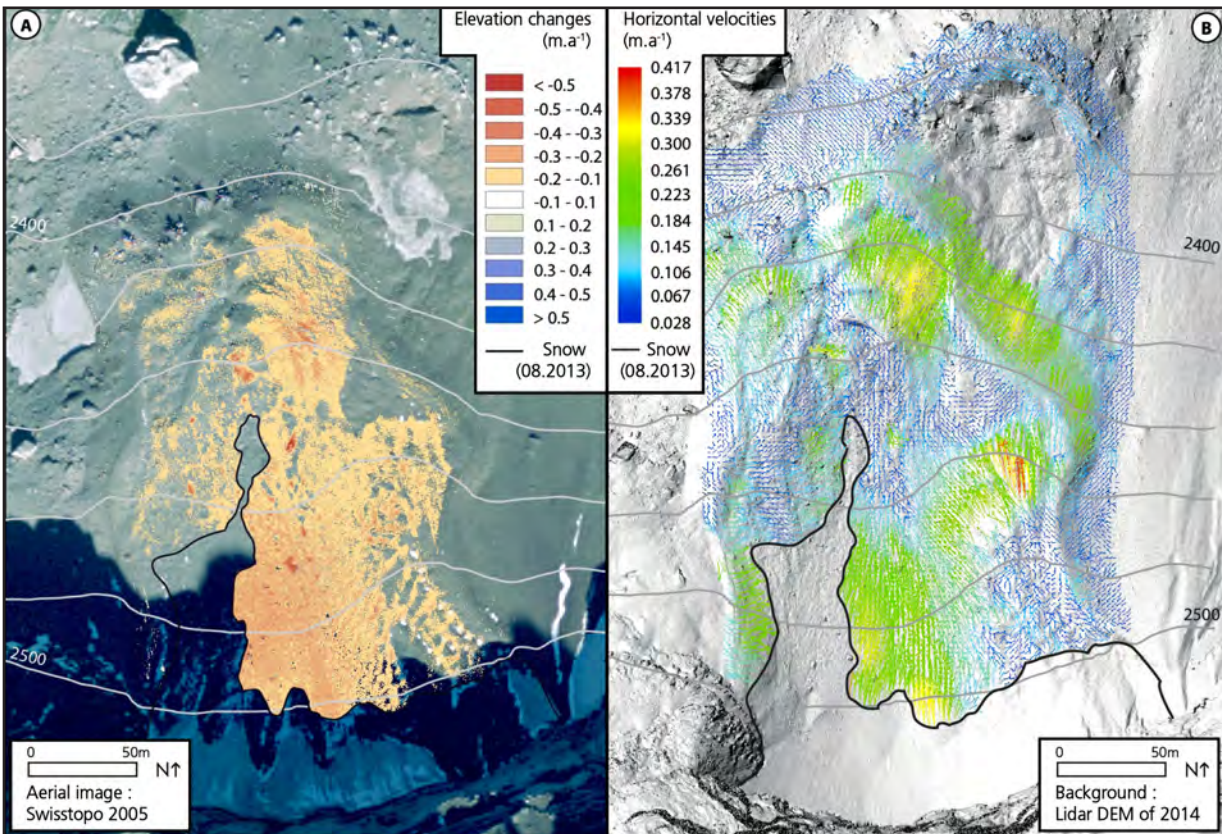
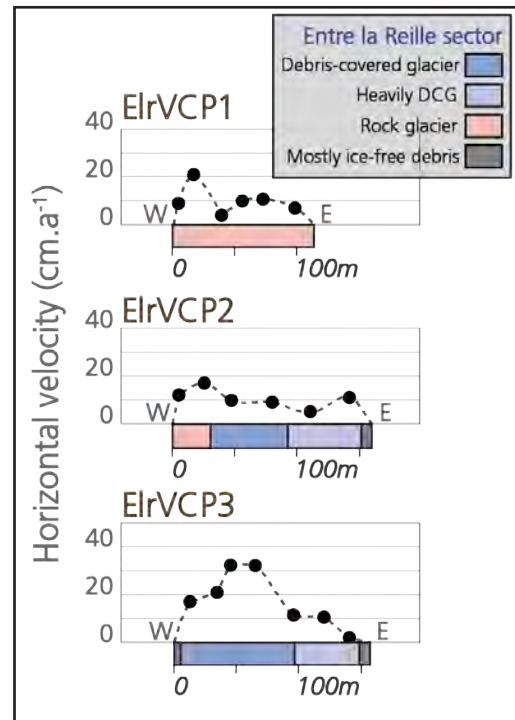


Fig. 3.51. Elevations changes and horizontal velocities obtained comparing the LiDAR-derived DEMs of 13.08.2013 and 22.09.2014. These data were produced by M. Capt (see details in Capt, 2015).

active zone was the West part of the rock glacier. Conversely, surface lowering exceeded 20 cm.a^{-1} in three zones: the upper central concave zone, the central part of the East convex zone and the eastern roots of the rock glacier. Maximum horizontal velocities ($> 20 \text{ cm.a}^{-1}$) were also measured in these three zones (Fig. 3.51B). The velocity reached 40 cm.a^{-1} locally in the eastern convex zone. The movements detected were very homogeneous on the upper concave zone and on the eastern rock glacier roots. Relatively fast horizontal velocities ($> 15 \text{ cm.a}^{-1}$) were also observed in the upper left moraine, in the western part of the rock glacier, around the central gully and in the eastern moraine/rock glacier front. The very patchy distribution of surface velocities is more marked than the one revealed by elevation changes and spatially limited zones of high velocities contrast with lowly active zones ($< 10 \text{ cm.a}^{-1}$).

3.4.3. Synthesis

Results obtained on ground electrical resistivities and surface velocities are gathered in Fig. 3.52A. They show the **spatial heterogeneity of ground characteristics and dynamics in this SD-CGSAPE**. The zones having the highest surface velocities appeared roughly the same over time and correspond to the sectors where the highest ground electrical resistivities ($> 150 \text{ k}\Omega\text{m}$) were measured: the upper West depression, a zone localised in the lower half of the convex East zone, and the transition between the central zone and the roots of the eastern part of the rock glacier. Conversely, the sectors displaying lower resistivities were generally less dynamic at decadal, (multi-) annual and seasonal timescales.

According to these results, we defined the main current components of the Entre la Reille system (Fig. 3.52B) and proposed an interpretation of the internal structure (Fig. 3.53B). Compared to the spatial organisation proposed in the dGPS results analysis (3.4.2.4), the same components are recognised. However, the photogrammetrical and LiDAR data allowed to refine the spatial boundaries and to split the debris-covered glacier zone and the rock glacier in two distinct entities (respectively 1 and 3, and 4 and 5 in the Fig. 3.52B).

3.4.3.1. The glacier of Entre la Reille

The presence of **several fresh moraines** (A to C in Fig. 3.52C) illustrates recent glacier position in Entre la Reille. In contrast, the lower ridge (E in Fig. 3.52C) is probably inherited from the late-Pleistocene or early-Holocene period (Ivy-Ochs et al., 2009), as evidenced by the presence of pioneer vegetation and a large thermokarstic depression in its inner flank, the relatively low ground electrical resistivity values ($< 30 \text{ k}\Omega\text{m}$) and the absence of noticeable surface dynamics. This ridge could be a former rock glacier front but, according to the large inner thermokarstic depression and absence of former surface compression patterns (ridges and furrows), we considered this ridge rather as a frontal moraine ridge. It likely illustrates the cold climatic conditions that occurred during the Pleistocene-Holocene transition period, where glaciers and rock glaciers extended beyond the neoglacial positions in the Alps (Ivy-Ochs et al., 2009). The C ridges include the sharp lateral moraines and were very likely deposited during the LIA maximum (1850 in the

Fig. 3.52. A. Synthesis of the results obtained on the surface velocity and ground electrical resistivity in Entre la Reille. **B.** Interpretation of the system components and of the main local superficial landforms. The green dashed line corresponds to the longitudinal profile presented in the Fig 3.53. **C.** Interpretation of the superficial ridges.

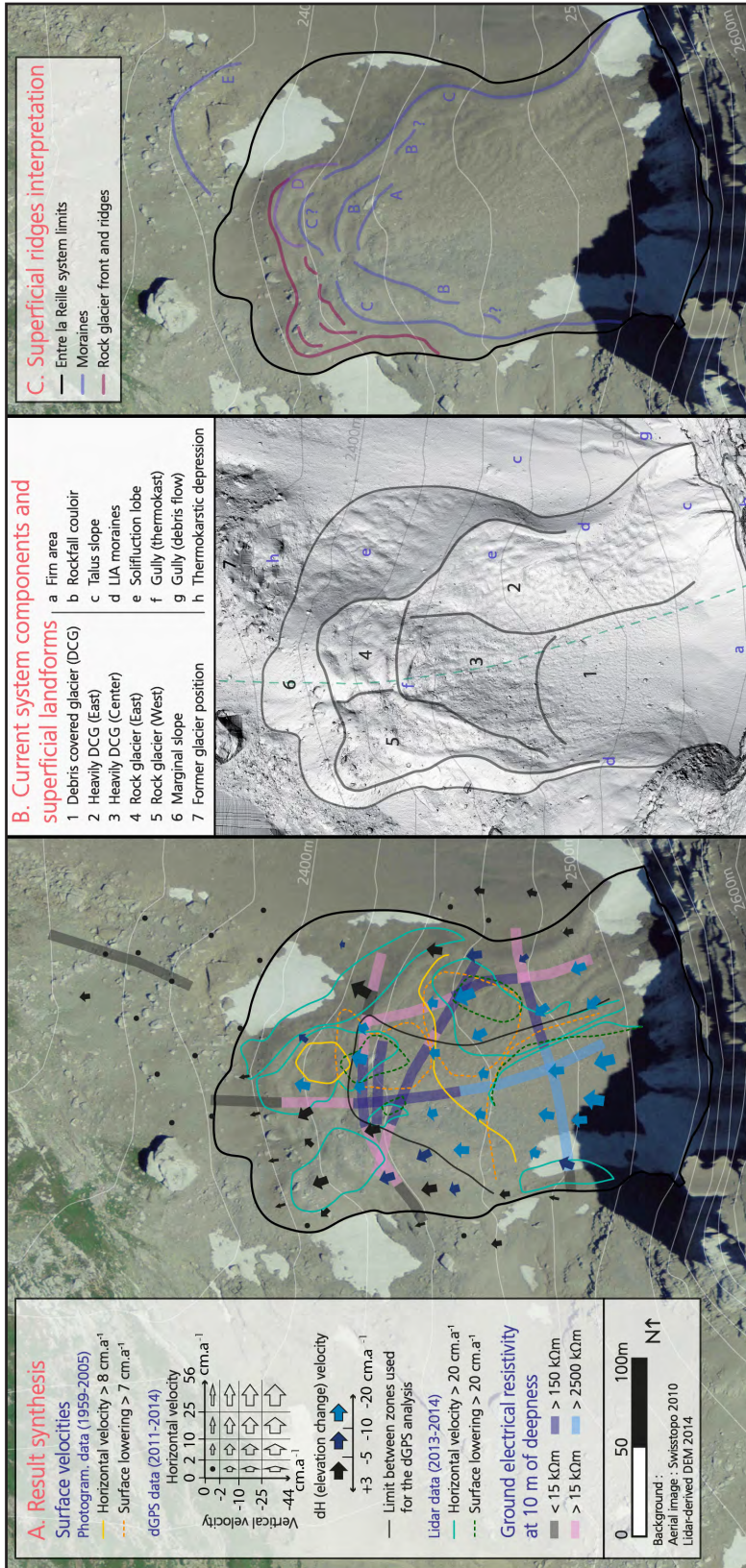
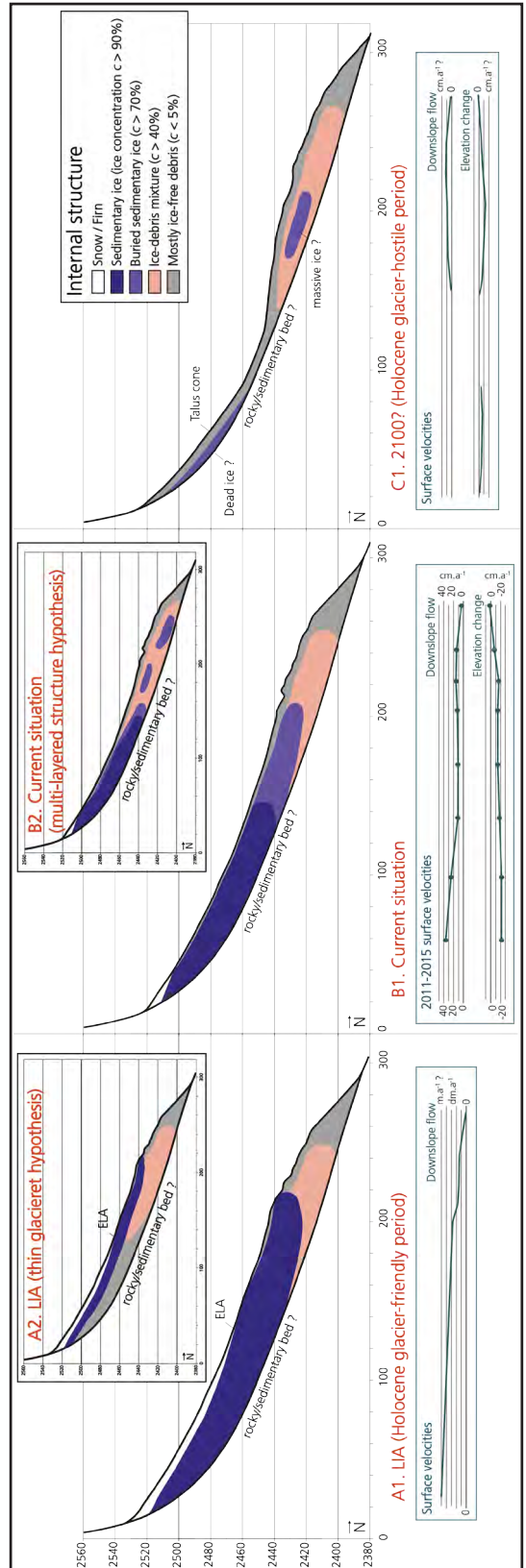


Fig. 3.53. Schematic longitudinal profiles of the internal structure and surface velocities in Entre la Reille system during the LIA maximum, today and in 2100. The ELA position on the A1 situation is only indicative. The tomogram ELR_1 in 2011 (Fig.3.41) and in 2012 (Fig.3.42) serves respectively as basis for the current situation B1 and B2. According to Holocene climate history, the transition from the situation A to C probably occurred cyclically several times over the last millennia.



region; Schoeneich, 1998). The frontal position during this stage is uncertain and the glacier terminus could also be situated at the B or D ridges. The D ridges could also correspond to a rock glacier ridge or a push moraine. According to the probable continuity with the lateral moraines, we propose to **delimit the LIA maximum position at the C ridges. The current zones 1, 2 and 3 merged then in a 0.028 km² glacier** (Fig. 3.52B and C). The mean ice thickness was probably below 10 m, according to the empirical relationship proposed by Chen and Ohmura (1990). Nevertheless, real past and present glacier thicknesses remain unknown in Entre la Reille. The ERT data do not allow clarifying precisely this point because the very resistive glacier ice layer hampers the penetration of the electric current at depth (Hilbich et al., 2009). In this way, Entre la Reille glacier could have either the shape of a lens or a thin sheet during the LIA (Fig. 3.53A1 and A2). The second hypothesis relies on discussion with W. Haeberli, who suggested that only very thin ice patches developed in these environments during the Holocene glacier-friendly conditions. According to this hypothesis, the ice bodies that compose currently Entre la Reille are probably thinner than those represented in the Fig. 3.53B. It is also not sure that large surface of glacier ice outcropped during the LIA. Indeed, large part of the glacier (i.e. the accumulation area) was potentially covered by snow in this **avalanche-fed glacier**. The drainage ratio (e.g. Hughes, 2009) is 1.5, meaning that snow accumulation can be enhanced 2.5 times by snow redistribution in this glacier (Fig. 3.54). Moreover, because of the presence of the 300m very steep backwalls, **the ablation area was probably already partially covered by a debris layer**. The rockfall couloir that dominates the East accumulation area likely also increased the debris coverage on this side of the glacier.

3.4.3.2. Holocene glacier-permafrost interactions

During the LIA, the glacier overrode, pushed and deformed pre-existent sediment accumulation as rockfall deposits or a rock glacier. Indeed, the sediment production was probably high locally over the Holocene and both ground surface temperature measurements (3.4.2.1) and models of permafrost distribution (BAFU, 2005; Lambiel et al., 2009; Boeckli et al., 2012) reveal that cold ground conditions allow the long-term preservation of ground ice in Entre la Reille. Therefore, before and/or between the Holocene glacial occupations, talus-derived rock glacier could form here. As hypothesised for the future evolution (Fig. 3.53C), **glacier-derived rock glacier can also subsist during the Holocene glacier-hostile periods**. Glacier advances over the last millennia mobilised thus former sediments and progressively disconnected the rock glacier from the backwall foot. Without evident origin (slope, central flowline?), the LIA glacier advance mostly deformed the eastern part of the rock glacier whereas the western part probably remained intact (Fig. 3.52C).

3.4.3.3. Recent evolution and current internal structure

Air temperature significantly warmed after the LIA, inducing a general glacier retreat and thinning. The A and B moraines (Fig. 3.52C) could be associated with the small positive mass balance periods observed in the western Alps during the 1880-1890s and the 1910-1920s (e.g. Huss et al., 2010;

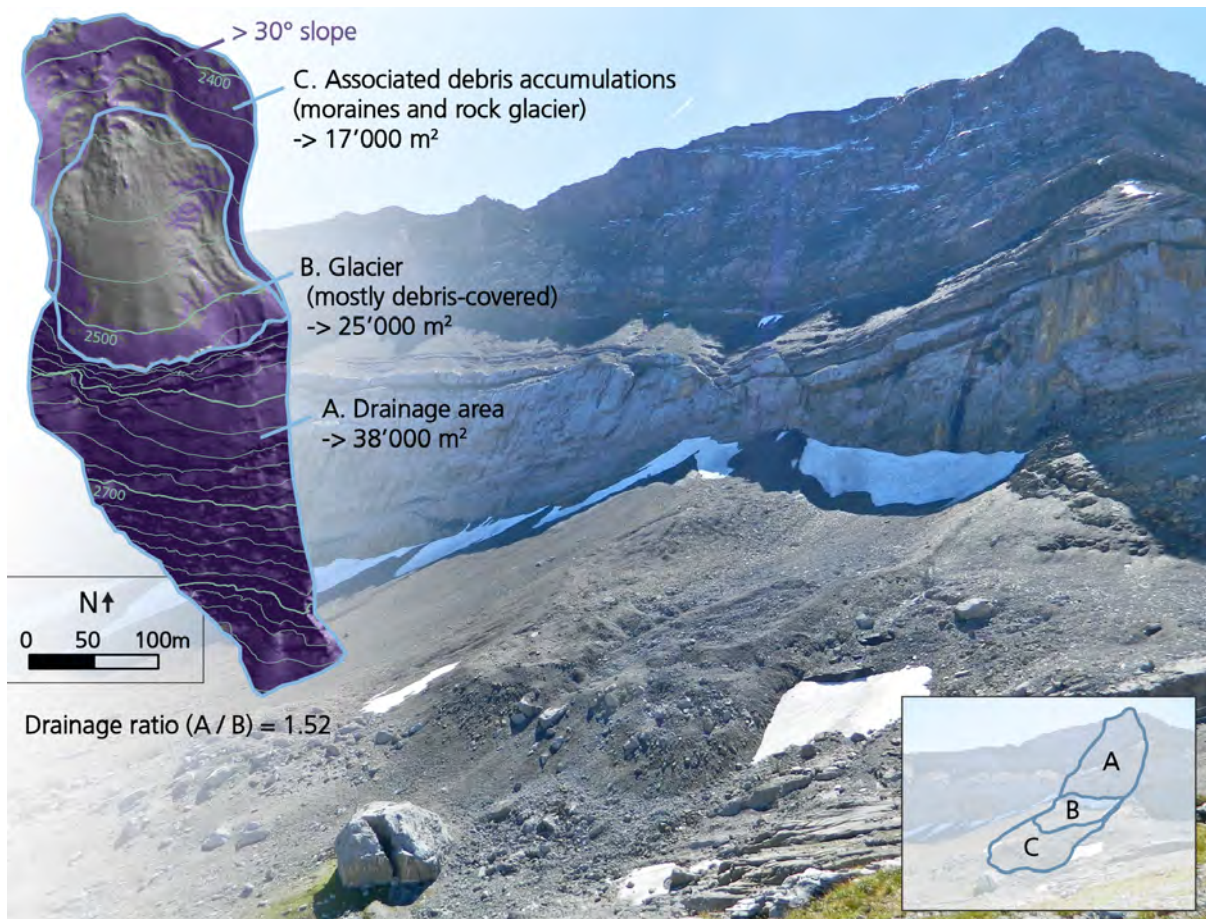


Fig. 3.54. Map and 2014 photographs of the ELR system. The drainage area was defined and measured on ArcGIS. The slope was also derived in ArcGIS from the SwissAlti3d DEM (© Swisstopo).

Deline et al., 2012). Entre la Reille glacier was never mapped over the 20th century and no surface ice was observed in aerial images since the 1950s. Hence, **the glacier was probably rapidly buried under the debris after the LIA** and the slow surface dynamics observed between 1959 and 2005 illustrate that it became **a poorly active remnant ice mass since at least 60 years** (Fig. 3.44).

Today, 5 main sectors contain ground ice in Entre la Reille. **The upper debris-covered zone** (1 in Fig. 3.52B) contrasts in term of internal structure and dynamic with the two heavily debris-covered glacier zones (2 and 3). Indeed, the upper depression is almost mainly composed of buried sedimentary ice. The superficial debris layer is mostly thinner than 50 cm and ice was observed with excavation during field surveys. Because of these characteristics, this zone was **the most active at each timescale of analysis** and strong acceleration of surface velocities was measured in summer. **The dynamical behaviour illustrates the control exerted by air temperature on downslope motion and surface lowering here** (Tab. 3.5). The acceleration of downward motion in early summer, the homogeneous results obtained with the LiDAR data and the shape of VCP could show the occurrence of both basal sliding and internal deformation. This zone is directly related with the upslope firn area and small amount of sedimentary ice could still be forming. **The ice concentration and the debris-cover thickness increase toward the East and the North** according to ERT results (2 and 3 in Fig. 3.52B). The relatively high debris concentration in both

zone is related to the melt of sedimentary ice since the end of the LIA. However, this concentration is also explained by the presence of a very active rockfall couloir above the eastern heavily DCG zone. These zones showed generally slowest flow and surface lowering velocities than the zone 1. **Climatic sensitivity is thus limited** by the thickening of the debris cover and the ice content decrease. In the eastern convex zone, maximum velocities appeared where the highest ground resistivity were measured and where the slope angle is the steepest ($> 30^\circ$). The domination of fine marl debris in this whole zone, often water-saturated in summer as observed during field surveys, also induce the occurrence of superficial solifluction movements, as evidenced by the morphology (Fig. 3.52). The central heavily DCG zone prolongs the DCG zone and is mainly concave. The internal structure here is uncertain and massive ice can be either continuous or patchy, according to the 2011-2012 ERT results (Fig. 3.53B1 and B2). Downslope movements are slow and M_d/dH index (Fig. 3.46) highlights a **dominating downwasting dynamic. In the distal part of the system, the superficial debris thickness reaches several meters and the ice content further decreases as show by the ERT results in the rock glacier.** Dynamically, it can be divided into two zones (4 and 5 in Fig. 3.52B). According to the presence of moraines and ERT results, the eastern side was probably strongly perturbed by the LIA glacier advance. Sedimentary ice could have been integrated in this zone (Fig. 3.53B2) that showed the fastest velocities in the rock glacier and especially marked surface lowering. Conversely, the western part was probably less affected by recent glacier advance and showed mostly homogeneous downward movements over the investigated periods. Surface lowering at annual timescale is close to zero, indicating **the very low ice melt** here. Slow elevation gain was even measured in winter. This is probably due to the fact that the compressive stress increase induced by the rock glacier motion is not offset by the ice melt during the snow covered period.

Entre la Reille SDCGSAPE is thus characterised by components showing heterogeneous internal structure and surface dynamics. Ground ice is still present in the whole system and even if generally slow surface velocities were measured ($< 50 \text{ cm.a}^{-1}$), **all the system remains active.** Surface velocities in the glacier zone were very likely faster during the LIA. The results obtained between 1959 and 2005 showed very slow downward motion and surface lowering velocities. The consistent results of dGPS and LiDAR surveys illustrate thus a general acceleration of surface velocities. This questions the precision of the photogrammetric data that maybe underestimated real changes. Otherwise, the 1959-2005 period includes the 1960s to mid-1980s period when the colder and wetter climate induced a larger accumulation of snow on Entre la Reille. This possibly reduced the motion and downwasting velocities as they appeared strongly driven by air temperature during the snow-free period. **The recent acceleration of surface velocities could thus be due to the increase of air and ground temperature and the lengthening of the snow-free period.**

3.4.3.4. A particular glacier system

The current internal structure of Entre la Reille is related to the complex Holocene climate history. The climatic oscillations, at least during the last millennia (Ackert, 1998; Maisch et al., 2003; Ivy-

Ochs et al., 2009; Matthews et al., 2014), induced thus **the succession of periods favourable for the snow/ice or debris accumulation in Entre la Reille** (Reynard et al., 1999). Hence, the situations A and C (Fig. 3.53) illustrate the two opposed extreme situation that have cyclically succeeded in Entre la Reille. In this context, the current situation highlights the transition from the situation A to C, especially in relation to the noticeable warming of atmosphere since the end of the LIA. However, large amount of ground ice is still present in this system and inherited from the last glacier-friendly period. Thereby, Entre la Reille SDCGSAPE appear as **a more resilient water store compared to local glaciers that have strongly shrunk since the LIA and are rapidly disappearing** (e.g. Scex Rouge, Prapio and Tsanfleuron Glaciers; e.g. Fischer M et al., 2014, 2015 and 2016). **The conjugate effect of four parameters on this remnant glacier explain this situation:** (1) the limitation of ice melt by the several decimetre thick debris cover, (2) the cold permafrost conditions that allow the long-term conservation of ground ice, (3) the shadow effect induced by the 300m backwalls that limits direct solar radiation and thus ice melt and (4) the enhanced accumulation of snow by avalanches (Fig. 3.54). Constant and slow ice melt should continue in the next decades in Entre la Reille according to climatic forecasting. Because of differential melt velocity, ground ice will probably disappear faster in the glacier zones than in the slowly flowing rock glacier (Fig. 3.53C).

3.5. Tsarmine

3.5.1. Site description

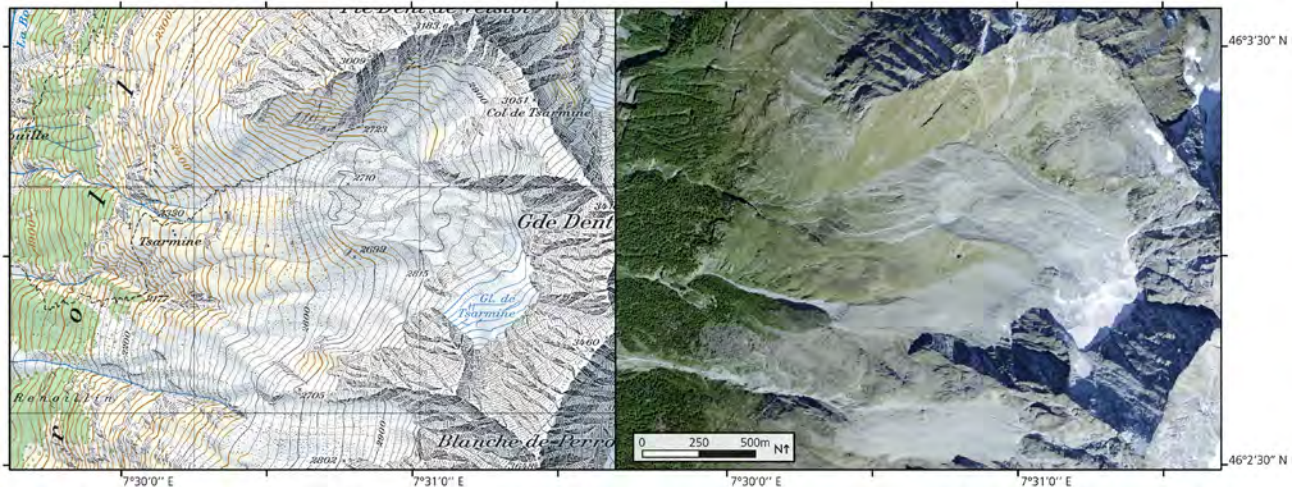
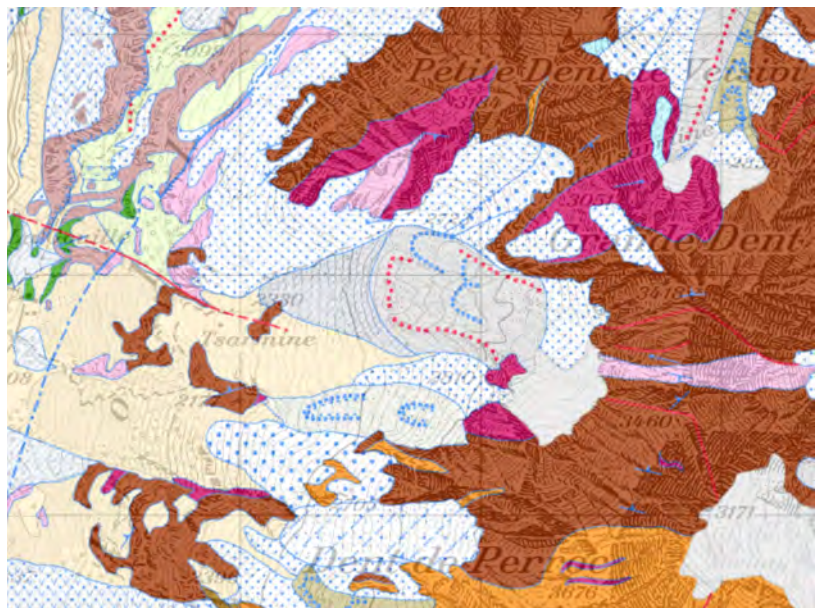


Fig. 3.55. Map (CN25, leave 1327, 2001) and aerial photograph (SWISSIMAGE Level 2, 2010) of Tsarmine (© Swisstopo).

The Tsarmine glacier system was already presented in the sections 2.2.2.2 and 2.3.2.2. This site is developed in a cirque oriented W-NW, located in the east side of the Arolla valley (Fig. 3.55). Bedrock is homogeneously composed by granitic gneiss, orthogneiss and granodiorite of the Dent Blanche Nappe (Fig. 3.56). Weathering produces very large debris in these fractured metamorphic rocks. The sediments observed during the field surveys thus usually exceeded the size of 1 m within the Tsarmine system and superficial porosity was important (e.g. Fig. 3.57). Finer material was nevertheless also observed in the LIA moraines, in the slope of the gullied moraine dam and in the rock glacier front.

Climatic conditions are especially characterised by the local dryness, typical of such intra-alpine region. The glacial domain is thereby restricted in the highest environments and numerous rock glaciers developed above 2500 m a.s.l. (Lambiel et al., 2016). The occurrence of permafrost conditions in Tsarmine is highlighted by the presence of a rock glacier in the northern part of the glacier margin (Fig. 3.57). A rock avalanche of $\sim 80\,000\text{ m}^3$ (R.

Fig. 3.56. Extract of the leaf 1327 (Evolène) of the 1: 25'000 Swiss geological Atlas. The bright colours correspond to the Dent Blanche unit rocks (granitic gneiss, orthogneiss, metagranodiorite, metadiorite). The Tsarmine debris-free glacier zone is roughly represented in light grey and the other grey surface corresponds to the Holocene moraines (ridges in dotted red and blue line) and rock glacier (ridges in double dotted blue line). The white surfaces are recent rockfalls and rock avalanche deposits and the light ochre are Pleistocene moraine deposits. The map and the detailed legend are available on map. portailgeologique.ch.



Mayoraz, personal communication) was triggered in the Grande Dent de Veisivi, the 2 September 2015, after a very hot summer (Fig. 3.58). The observation of water runoff in all the scarp few days after the event, although the period was climatically dry, evidenced the melt of interstitial ice that followed the rock avalanche and therefore, the occurrence of permafrost conditions in the glacier backwalls. The presence of an ice apron, stick on the steep North face of the Dent de Perroc until the 1980s also illustrated permafrost conditions (Delaloye, 2008).



Fig. 3.57. Side view of Tsarmine in August 2013 and some surface features (photographs by A. Dumas and JB Bosson)



Fig. 3.58. Photographs taken during and after the Grande Dent de Veisivi rock avalanche that occurred the 2 September 2015 (photographs by C. Gabbud and B. Maître)

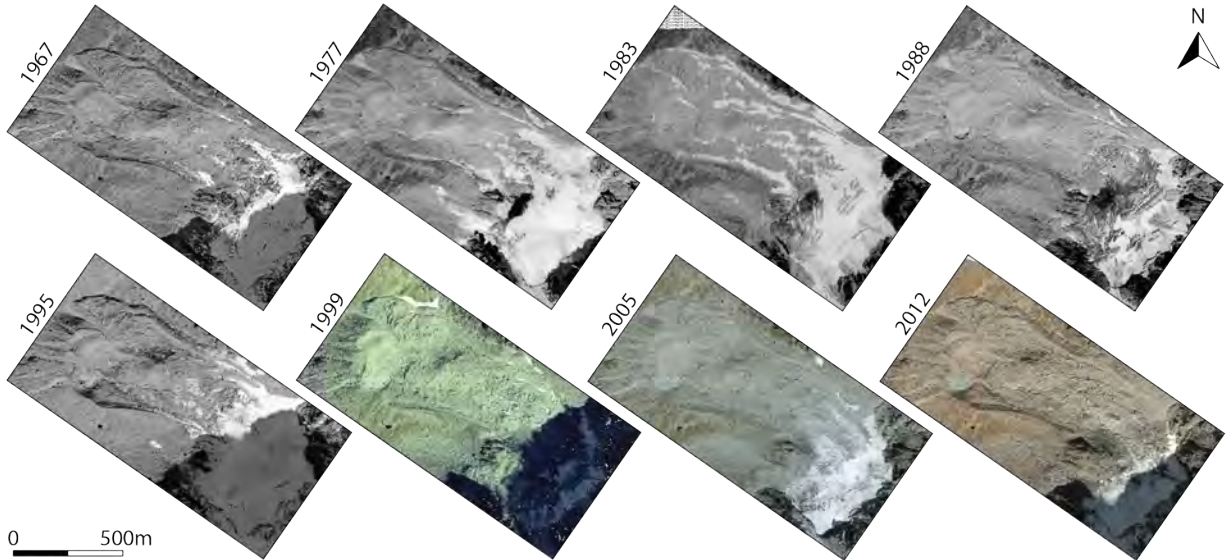


Fig. 3.59. Aerial images of Tsarmine over the last decades (© Swisstopo, available on map.lubis.admin.ch, except © Flotron AG for the 2012 photograph). The photographs were taken between mid-August and early October (see Tab. 2.6 for details on each image). Reproduced from Capt, 2015.

The regional climate evolution was showed in the Fig. 2.21. From the mid-1950s to the 1980s, air temperatures were generally slightly colder than the 1961-1990 climatic norm and allowed the accumulation of large amount of snow in the upper third of Tsarmine (Fig. 3.59). Despite the humidity of the 1980s to mid-2000s period, the rapid increase of air temperature up to more than 1°C above the climatic norm induced the strong limitation of the snow accumulation in Tsarmine and the debris-cover extended upglacier. Except the lake development since the 1980s in the south margin, no significant surface changes can be observed on photographs in the lower half of Tsarmine at decadal timescale (Fig. 3.59).

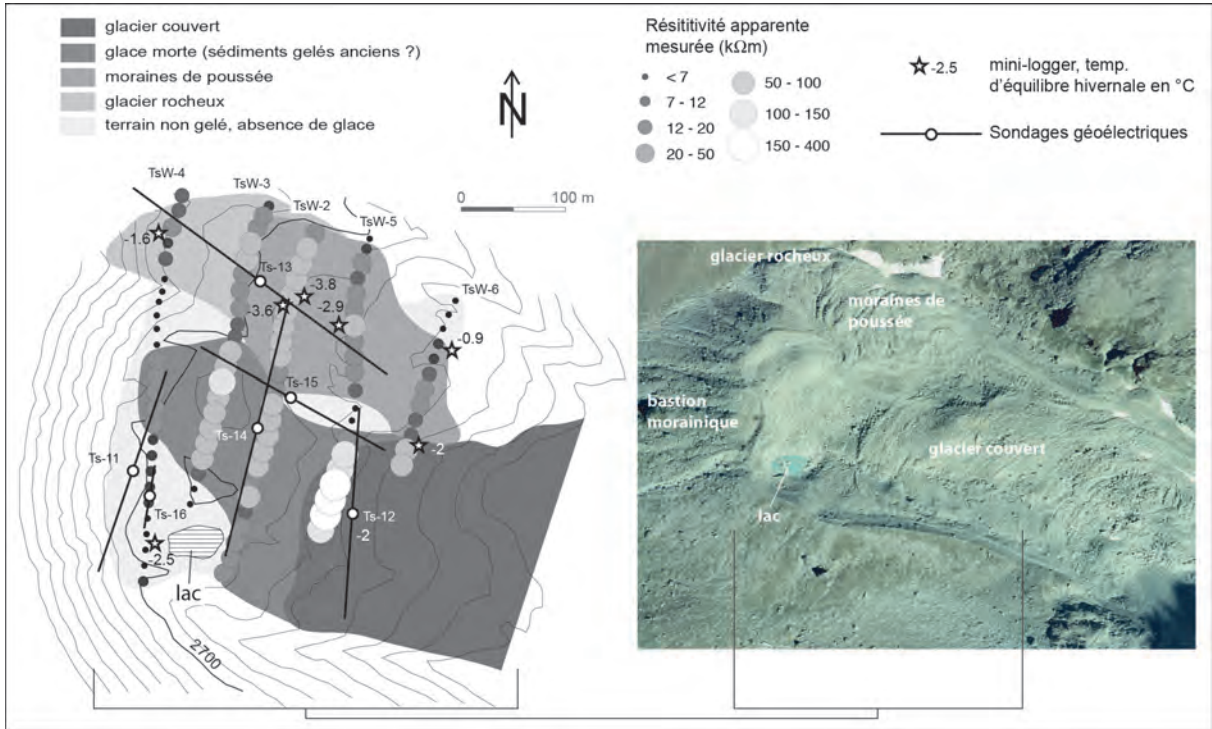


Fig. 3.60. Geoelectrical results and inferred internal structure of the Tsarmine distal zone. The aerial photograph was taken in 2005 (© Swisstopo) Reproduced from Capt (2015) who adapted the figure of Lambiel et al. (2004).

In contrast with the previous SDCGSAPE studied in this chapter, Tsarmine is a larger system (Tab. 3.1) and a small crevassed debris-free glacier is still present in the upper zone. It is prolonged downslope by a debris-covered zone where glacier ice outcrops locally, especially in ice cliff related to the thermokarstic erosion around the central gully and the lake (e.g. Fig. 3.57). According to 1D geoelectrical data, Lambiel et al. (2004; Fig. 3.60) showed that the distal area of Tsarmine was composed by a debris-covered glacier, dead ice, ice-free debris, push moraines and a rock glacier zones. The push-moraines and the above concave upslope zone above the rock glacier illustrated recent glacier-permafrost interactions.

3.5.2. Results

3.5.2.1. Ground surface temperature measurements

The ground surface temperature was measured each two hours at 18 locations in Tsarmine between September 2011 and 2014 (Fig. 3.61 and Tab. 3.6). The dataset contains many gaps, primarily due to the sensors failures. The thermal indexes computed at each location reveal that the coldest ground conditions occurred in the upper and central part of the glacier system (sensors Tsa_1 to Tsa_9). During the three investigated periods, mean ground surface temperatures were negative and winter equilibrium temperature were colder than -2.5°C in this zone. Furthermore, ground surface received relatively low solar energy here (PDD usually below $400^{\circ}\text{C}\cdot\text{day}$) and large amount of cold can be accumulated in the porous layer (GFI lower than $-650^{\circ}\text{C}\cdot\text{day}$). In contrast, warmer thermal index values were measured in the marginal distal areas of Tsarmine. The concave

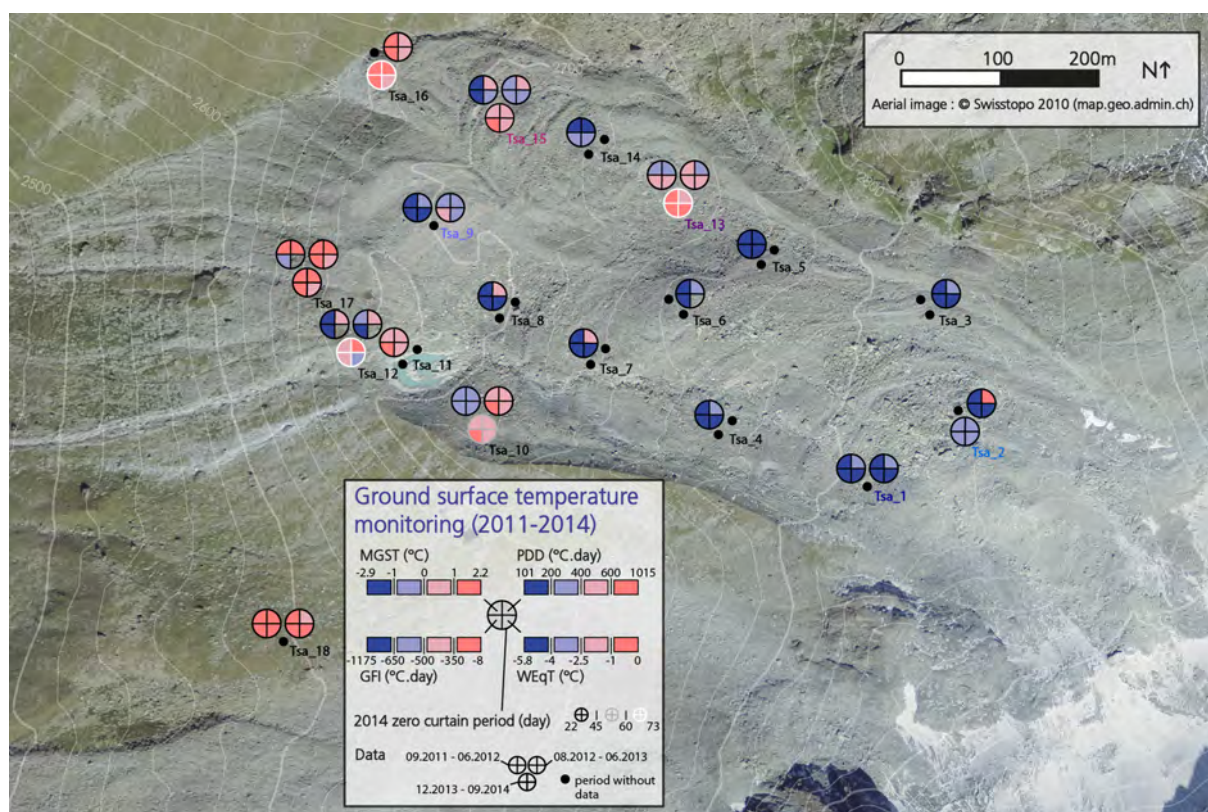


Fig. 3.61. Indices measured with the thermal sensors in Tsarmine. The data are detailed in Tab. 3.6. The dataset comprised many gaps at the 3-year scale and only the three most complete periods between September 2011 and 2014 are presented. PDD, GFI and WEqT correspond respectively to positive degree day, ground freezing index and winter equilibrium temperature.

Thermal sensor	Elevation (m a.s.l.)	Location	Mean ground surface temperature (MGST; °C)				Mean summer GST (°C)	Positive degree day (PDD; °C·day)				Winter equilibrium temperature (Wedt; °C)				Ground freezing Index (GFI; °C·day)				Zero Curtain period (day)
			2012	2013	2014	Mean	2014	2012	2013	2014	Mean	2012	2013	2014	Mean	2012	2013	2014	Mean	2014
Tsa_1	2805	Upper left glacier zone	-2.8	-1.8	-1.8	-2.3		338	307		322	-5	-5.8		-5.4	-1175	-870		-1022	
Tsa_2	2820	Upper right glacier zone		-1.8	-0.8	-1.3	3.1		213	273	243	-5	-5	-3.5	-4.3	-796	-519		-657	30
Tsa_3	2815	Inner side of the upper right LA moraine		-1.1				354				-5.4				-703				
Tsa_4	2780	Central left glacier zone	-1.9					239				-5.2				-818				
Tsa_5	2770	Central right glacier zone	-2.7					101				-4.5				-920				
Tsa_6	2770	Centre of the glacier			-2.1				452							-1120				
Tsa_7	2740	Lower left glacier zone	-1.9					430				-5				-997				
Tsa_8	2705	Glacier terminus	-1.7					433				-5				-586				
Tsa_9	2705	Dead ice zone	-1.4	-0.5		-0.9		249	310		280	-4.2	-3.4		-3.8	-656	-481		-568	
Tsa_10	2720	Inner side of the lower left LA moraine	-0.8	0.3	0.9	0.1	5.6	384	424	485	431	-3.3	-1.6	-1.4	-2.1	-627	-342	-225	-398	49
Tsa_11	2700	Lake area	1					498				-1.2				-203				
Tsa_12	2705	LIA left frontal moraine	-1.1	-0.6	1.4	-0.1	6.1	588	488	655	577			-3.2		-912	-667	-235	-605	60
Tsa_13	2735	Concave rock glacier root	-0.5	0.3	1.3	0.4	4.9	240	341	438	340	-1.9	-1.3	-0.6	-1.3	-380	-242	-62	-228	73
Tsa_14	2720	Upper push moraine zone	-1.6					116				-2.6				-586				
Tsa_15	2705	Lower push moraine zone	-1.1	-0.3	0.7	-0.2	5.5	462	465	471	466	-3.4	-3.9	-2	-3.1	-792	-569	-272	-544	39
Tsa_16	2680	Rock glacier front		1.3	1.9	1.6	6.8		572	694	633	-1.3	-1.6		-1.5	-166	-128		-147	66
Tsa_17	2680	Outer side of the moraine dam	1.6	1.2	2.2	1.6	7.8	1015	669	936	873	-1.8	-2		-1.9	-549	-293	-299	-381	22
Tsa_18	2605	Base of the moraine dam	1.6	2		1.8		599	633		616	-0.8	0		-0.4	-128	-8		-65	
Interpol. Air T _s	2800		-2.6	-3.3	-0.9	-2.3	4.4	465	520	589	525					-1245	-1568	-871	-1228	

Tab. 3.6. Synthesis of the indices computed from the thermal sensor data between September 2011 and 2014. Air temperature at 2800 m. a.s.l. is extrapolated using the daily data of Evolène weather station (1825 m a.s.l.; 46°06'44"N, 7°30'31"E; 7 km distant from the study sites, © MétéoSuisse) with a thermal gradient of 0.61°C/100m, obtained comparing the 4-year daily data of Evolène with those of the Aiguille du Midi weather station (3845 m a.s.l.; 45°52'43"N, 6°53'15"E; 51 km distant from the study sites, © MétéoFrance).

root and the front of the rock glacier, the zone surrounding the lake and the outer side of the moraine dam showed especially warm ground conditions. The topography and especially elevation, aspect, shadow effect can partially explain this spatial distribution of ground surface temperature and the coldest values were measured in the highest and most shadowed zone (Tsa_1, Tsa_2 and Tsa_4). However, the Tsarmine lower half is relatively flat and poorly shadowed by the backwalls. In this way, other factors also control these thermal behaviours, like the presence of ground ice or the surface porosity. The sensors Tsa_10, Tsa_17 and Tsa_18 were placed in a less porous zone, where finer surface material was present. The lower amount of cold air that can be accumulated here could explain the warm measured values. According to the WEqT and to the other thermal indexes, the presence of ground ice was possible close to the surface for the sensors Tsa_1 to Tsa_9. In contrast, the warmest conditions below the rock glacier and other marginal zones pointed out the presence of ground ice at a larger depth or even its absence.

Fig. 3.62 shows GST in the debris-covered, dead ice and rock glacier zones between September 2011 and 2014. The debris-covered glacier (Tsa_1 and Tsa_2) was the coldest zone and especially cold temperature were measured during winter. The rock glacier (Tsa_13 and Tsa_15) was the warmest zone in both winter and summer. The ground temperatures were generally similar to air temperature during the summer snow-free period. As a consequence, the 11-day running mean temperatures exceeded rarely 7°C during the cool summer 2014. The snow layer covered later the ground surface in winter 2011-2012 compared to winters 2012-2013 and 2013-2014. Autumn temperatures exerted thus a stronger influence in 2011-2012 and the larger amount of cold accumulated during this period could explain the lower temperature observed during this winter. Two sensors were placed at respectively 5 and 30 cm of deepness in the location Tsa_7 to investigate

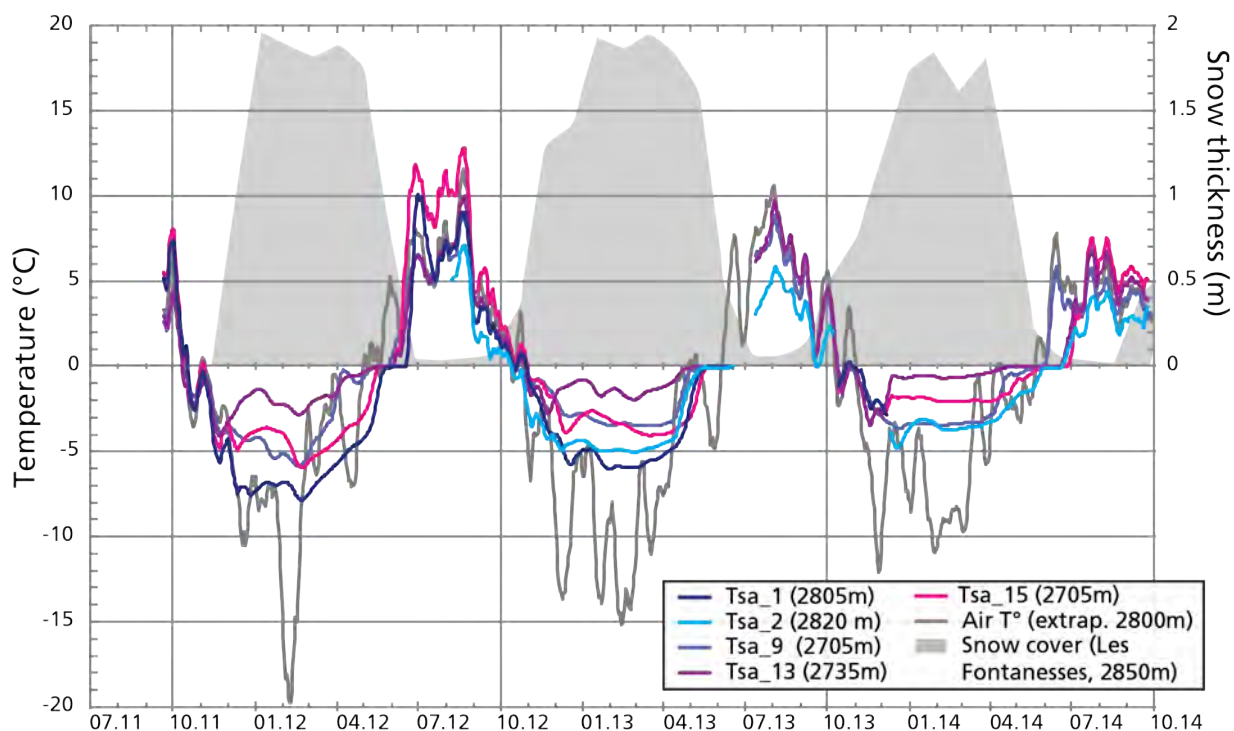


Fig. 3.62. 11-day running means of ground and air temperature in Tsarmine. The position of these thermal sensors is shown on Fig. 3.60. See the caption of the Tab. 3.6 for the description of the extrapolation of air temperature at 2800 m a.s.l. The monthly mean of the snow cover height at les Fontanesses (2850 m a.s.l.; 46°01'43"N, 7°26'45"E; 6 km distant from Tsarmine, © SLF) indicates local variations of snow mantle.

Fig. 3.63. 11-day running means of air and ground temperature at 5 cm and 30 cm of thickness in Tsarmine. Tsa_7 position is shown in Fig. 3.60. See the caption of the Tab. 3.6 and Fig. 3.62 for the description of the air temperature and snow cover thickness.

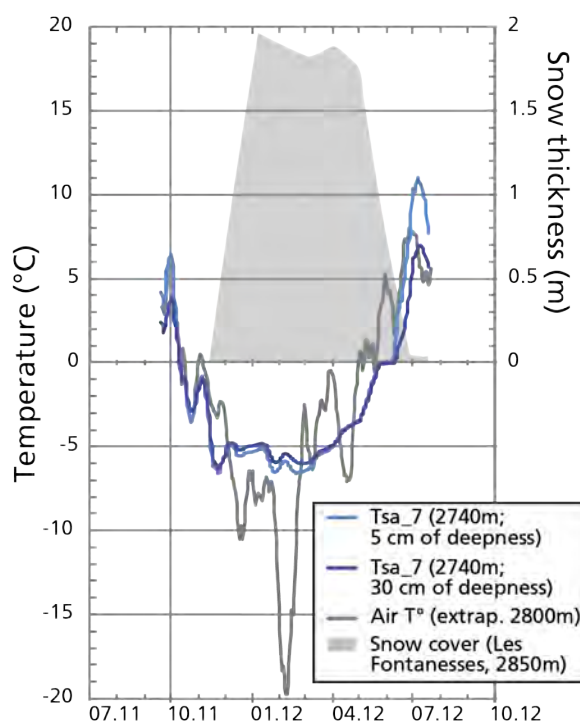
the influence of the debris cover thickness (Fig. 3.63). The deepest sensor showed less temperature variations over the year, illustrating a lower control of air temperature variations. The ground conditions were respectively colder in summer and warmer in winter than near the surface. Up to 4 °C of difference were measured in summer, highlighting the relatively weak thermal conductivity in the debris layer and the trapping of cold air in the ground voids.

3.5.2.2 Electrical resistivity tomography

Two ERT campaigns were carried out in Tsarmine, respectively in mid-August 2013 and 2014. The results were presented and discussed in the publication 2 (see especially section 2.2.2.4 and the Fig. 2.15). A layer of very high resistivities ($> 500 \text{ k}\Omega\text{m}$) was measured few meters below the surface on the central part of Tsarmine and was attributed to the debris-covered glacier. Its end near the lake was clearly evidenced by rapid decrease of ground resistivities ($< 10 \text{ k}\Omega\text{m}$) and corresponded with the strong contrast of resistivity found by Lambiel et al. (2004; Fig. 3.60). This resistive layer ends near 2750 m above the concave zone that dominates the push-moraine and rock glacier area. Ground resistivity mostly ranges between 2 and 80 $\text{k}\Omega\text{m}$ in this depression and increases up to 500 $\text{k}\Omega\text{m}$ in a lens located at 5 m of deepness below the push moraines. The rock glacier front was composed by the relatively homogeneous layer of 15-80 $\text{k}\Omega\text{m}$. Finally, resistivities were larger than 80 $\text{k}\Omega\text{m}$ in the frontal and central depression considered by Lambiel et al. (2004) as a dead ice zone.

3.5.2.3. Ground penetrating radar

A GPR survey was led in March 2015 in collaboration with Mauro Fischer (UniFr). He treated and presented the data in the publication 3 (section 2.3.2.4, see especially the Fig. 2.24, 2.26 and Tab. 2.8). Unfortunately, as this publication focused on the active glacier zone of Tsarmine (debris-free and debris-covered glacier), the GPR data analysis concentrated on this zone and more precisely in the detection of the glacier bed to estimate the ice thickness and volume. Consequently, the data on the distal zones of Tsarmine (the rock glacier and the dead ice zone) remained untapped. Moreover, a deeper analysis of the $\sim 5 \text{ km}$ -long radargrams collected could provide very interesting information on the internal structure of this system, as the presence of englacial crevasses and conduits, the debris cover thickness, the distribution of ice-rich and debris-rich layers or the thermal regime of the glacier in winter.



The results presented in the publication 3 showed that in 2015, Tsarmine was a $4.05 \pm 0.4 \times 10^6$ m³ cirque glacier that had a mean thickness of 15 m. The glacier limits evidenced by the GPR data were very consistent with those of the highly resistive layer observed on the ERT data. Hence, the distal part of the glacier tongue was confined in the left-hand side and the push-moraines and rock glacier areas were disconnected from the glacier. The Tsarmine glacier can be divided in two main parts, separated by a thin ice layer that probably cover a bedrock convexity around 2850 m a.s.l. (Fig. 2.24 and Fig. 2.26). The upper trough was filled by a 20 m thick, crevassed bare ice and firn layer whereas the debris-covered tongue exceeded 30 m of thickness in its center.

3.5.2.4. Photogrammetry and image analysis at decadal timescale

Thanks to the numerous high-quality DEMs produced by N. Micheletti with archival digital photogrammetry in the right-hand side of the Arolla valley (Micheletti et al., 2015a and 2015b), it was possible to produce a comprehensive analysis of the Tsarmine glacier behavior since 1967. M. Capt made most of this analysis (Capt, 2015) which was completed with the GPR data and some data on local glaciers, and presented in the publication 3 (chapter 2.3).

Elevation changes over the last decades were mainly related to snow and ice accumulation and melt. These changes were primarily controlled by the climatic variations and in particular by summer air temperature. As a consequence, the glacier had a positive mass balance between 1967 and 1983 before being affected by a negative mass balance up to 2012 (Fig. 2.22 and Fig. 2.27). However, contrasting with the recent acceleration of loss rate observed in neighboring glaciers, the negative mass balance of Tsarmine stabilized around -0.3 m w.e. a⁻¹ since the 2000s. This illustrated the increase of the control of very local factors on this glacier after the rapid melt of the snow-ice accumulated in the 1960s-1980s period. Indeed, the influence of the debris-cover, permafrost conditions and surrounding relief upon shadow effect and snow redistribution limits the ice melt in Tsarmine and reduces the coupling of this glacier with the regional climate. Moreover, because of the mass transfer and the limitation of ablation by the debris-cover and permafrost conditions in the glacier tongue, most of surface lowering occurred in the debris-free upper half of the system (Fig. 2.22 and Fig. 2.28). This situation was also specific in comparison with other local larger glaciers and a mass gain up to 10 m was even observed at the 45-year timescale in the center of the glacier tongue. Despite the occurrence of these negative feedbacks that slow down the shrinking dynamic, Tsarmine glacier lost around 2×10^6 m³ between 1967 and 2012, a third of its initial volume. In the distal zone of the glacier, up to 20 m of surface lowering was observed in the dead ice and lake area (Fig. 2.22). The gullying of the moraine dam by debris flow were also visible. Finally, an elevation loss lower than 5 m was displayed in the rock glacier rooting zone whereas null to slight elevation gain appeared in its frontal zone.

Horizontal velocities were investigated over the last decades comparing orthorectified aerial images and tracking large boulders (Fig. 2.23 and Fig. 2.25). Maximum velocities (> 3 m) were observed in the debris-cover glacier tongue while no data allowed to assess the movements in the steep upper debris-free part. The homogeneity of the glacier tongue displacement and the rapid decrease of

velocities in the glacier lateral margins indicated the likely occurrence of a several decimetres to meters en masse movement (Fig 2.23 and Fig 3.64). The downward motion was thus probably partly due to basal sliding, which would indicate the presence of water and temperate thermal conditions at the glacier base. According to the block tracking, the glacier flow progressively decreased toward the terminus and over time (Fig. 2.25). Nevertheless, a wave of maximum velocity progressively migrated and attenuated downglacier. Slow ($< 30 \text{ cm.a}^{-1}$) to null movements were detected in the southern glacier margin. The ice melt, especially due to the lake development, induced backward movements around the lake. The dead ice zone seemed to re-activate during the 1999-2005 period. The rock glacier was always active and its flow was faster than 10 cm.a^{-1} since 1967. The increase of velocities in its centre flowline could indicate the prevalence of internal deformation here. The rooting zone of the rock glacier accelerated between 1999 and 2005 and velocities exceeded then 50 cm.a^{-1} .

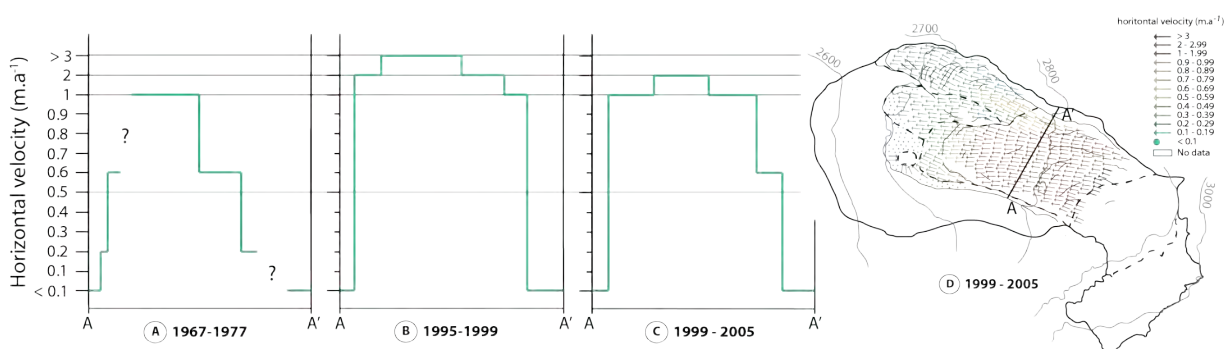


Fig. 3.64. Decadal evolution of a horizontal velocity cross profile located in the lower part of the Tsarmine glacier tongue. Adapted from Capt, 2015

3.5.2.5. dGPS

The position of 84 blocks was measured up to height times with a dGPS between 2011 and 2014 in Tsarmine. Some of the results were already presented in the publication 2 (see especially the section 2.2.2.4 and associated figures). At the 3-year timescale, the velocities were relatively homogeneous in the central zone of Tsarmine, which corresponds to half of the measured blocks: most of horizontal velocities were $> 50 \text{ cm.a}^{-1}$ towards the W-NW, most of vertical and surface lowering velocities were respectively > -25 and 10 cm.a^{-1} (Fig 3.65A). The maximum velocities in the glacier system were measured here, reaching respectively 116, -102 and 50 cm.a^{-1} in horizontal, vertical and surface lowering components, near the central gully. Surface velocities strongly decreased in the distal zone of Tsarmine. The rock glacier zone was mainly affected by a slow subhorizontal flow (horizontal velocities $< 35 \text{ cm.a}^{-1}$ and surface lowering $< 25 \text{ cm.a}^{-1}$) whereas the zone defined by Lambiel et al. (2004) as a dead ice zone showed mostly downwasting dynamic (vertical and surface lowering velocities $> |25| \text{ cm.a}^{-1}$). Contrasting with these active zones, the neighbouring lake and the outer side of the moraine dam had very slow to null surface velocities. Comparing the downslope movement to surface lowering at this timescale (Fig. 2.16b), the first dynamic largely dominated in Tsarmine and its magnitude usually exceeded twice times the one of surface lowering (M_d/dH value > 1). The prevalence of downslope movement was especially marked in the central glacier and rock glacier zones. Conversely, surface lowering dominated in the dead ice zone.

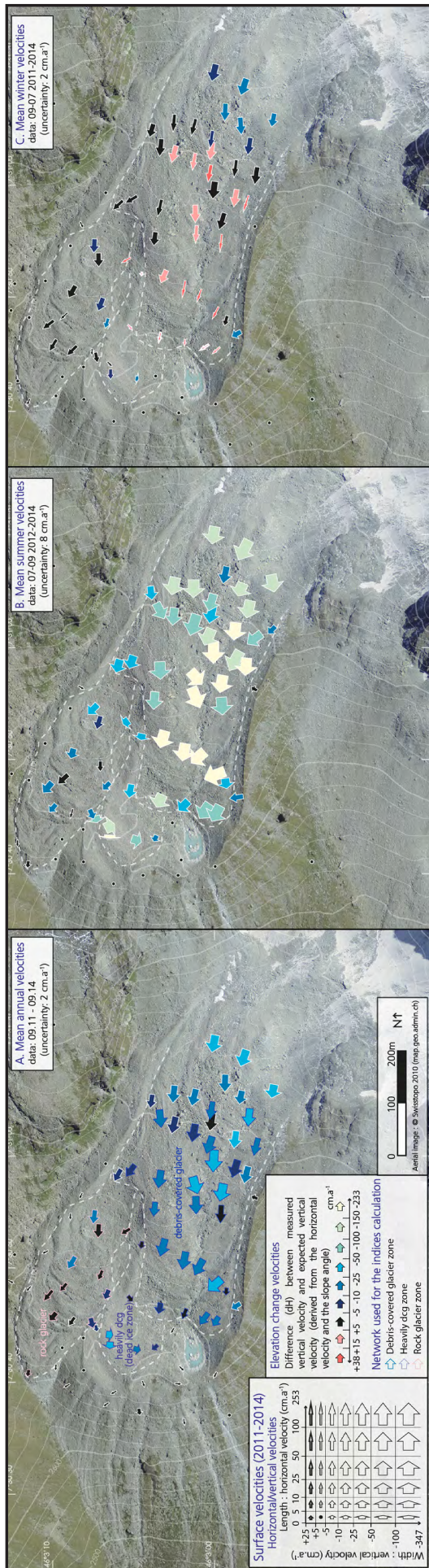


Fig. 3.65. Mean annual, summer and winter surface velocities measured between September 2011 and 2014 in Tsarimine. The white dashed lines show the spatial limits between the main zones defined in this system.

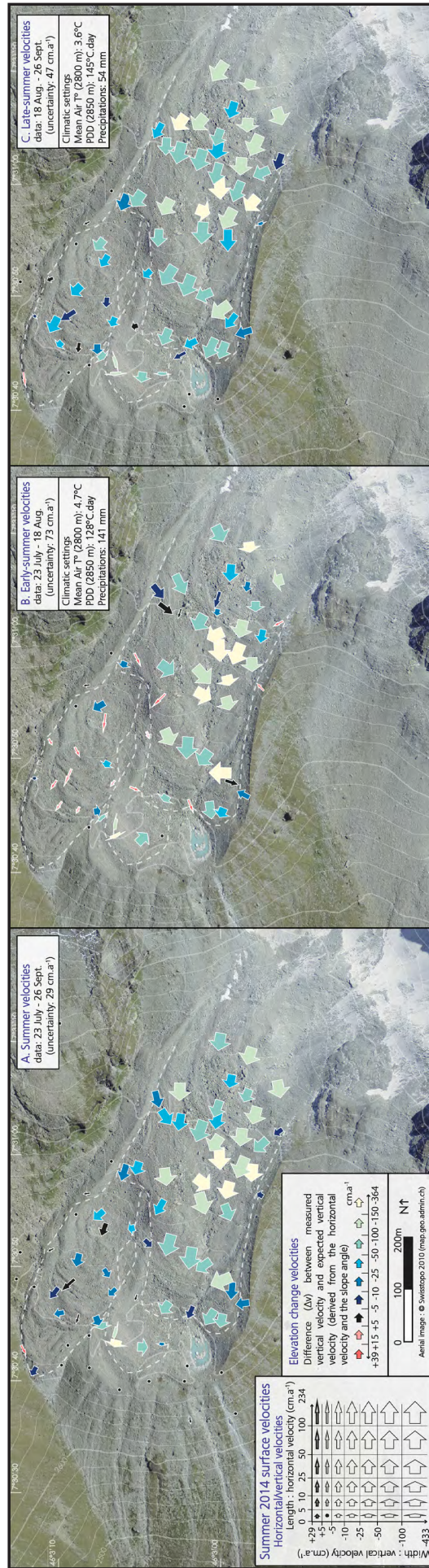


Fig. 3.66. Summer, early-summer and late-summer surface velocities measured in 2014 in Tsarimine. The climatic settings are derived from the extrapolated air temperature at 2800 m.a.s.l and precipitation at Evolène weather station (see caption of Tab 3.6 for details).

The mean summer and winter velocities measured between 2011 and 2014 are displayed in the Fig 3.65B and C. Clearly distinct dynamical regime appeared at seasonal timescale. During summer, that roughly corresponded to the snow-free period, surface velocities strongly increased, especially in the debris-covered glacier and the dead ice zones. Horizontal flow was around 100 cm.a^{-1} and surface lowering velocities were usually faster than 50 cm.a^{-1} . Maximum values were then respectively 253, -347 and 233 cm.a^{-1} for horizontal, vertical and surface lowering velocities, here again around the central gully. The rock glacier showed mainly an acceleration of vertical and surface lowering velocities, which commonly exceeded respectively $|25|$ and $|10| \text{ cm.a}^{-1}$. During winter, horizontal velocities generally decreased for all the points except on the rock glacier where similar to slightly higher velocities were measured compared to summer. The most striking change concerns vertical velocities and elevation variation in the debris-covered glacier zone. Vertical velocities were positive or slightly negative for many points. Consequently, except the surface lowering observed in the upper glacier zone (5 to 25 cm.a^{-1}), surface elevation was either stable or presented a gain up to 38 cm.a^{-1} during this period. Emergence velocity was especially high around the central gully. Nevertheless, due to the rapid surface lowering observed in summer, this winter emergence dynamic only contributed to limit the surface lowering velocities that dominated at annual timescale (Fig 3.65).

Three measurement campaigns were carried out during the summer 2014 to investigate early and late-summer dynamics (Fig 3.66). The mean surface velocities during this summer were roughly similar to the 3-year summer means but vertical and surface lowering velocities generally slightly decreased (Fig 3.66A and (Fig 3.65B)). According to climatic data, early summer was somewhat warmer than late summer although the PDD was greater in the longer late summer period (Fig 3.66B and C). Precipitations were third time larger in early summer. During this period, surface velocities were maximum ($> |100| \text{ cm.a}^{-1}$) in the centre of the glacier, around the gully zone. The upper zone and the glacier terminus were less active. Mostly horizontal movements and emergence velocities, respectively faster than 25 and 5 cm.a^{-1} , were observed in the rock glacier zone. In late summer, all the movements on the glacier zone became more homogeneous as the velocities decreased in its centre and increased in the upper and frontal parts. Vertical velocities were negative and surface lowering was then observed in the rock glacier zone.

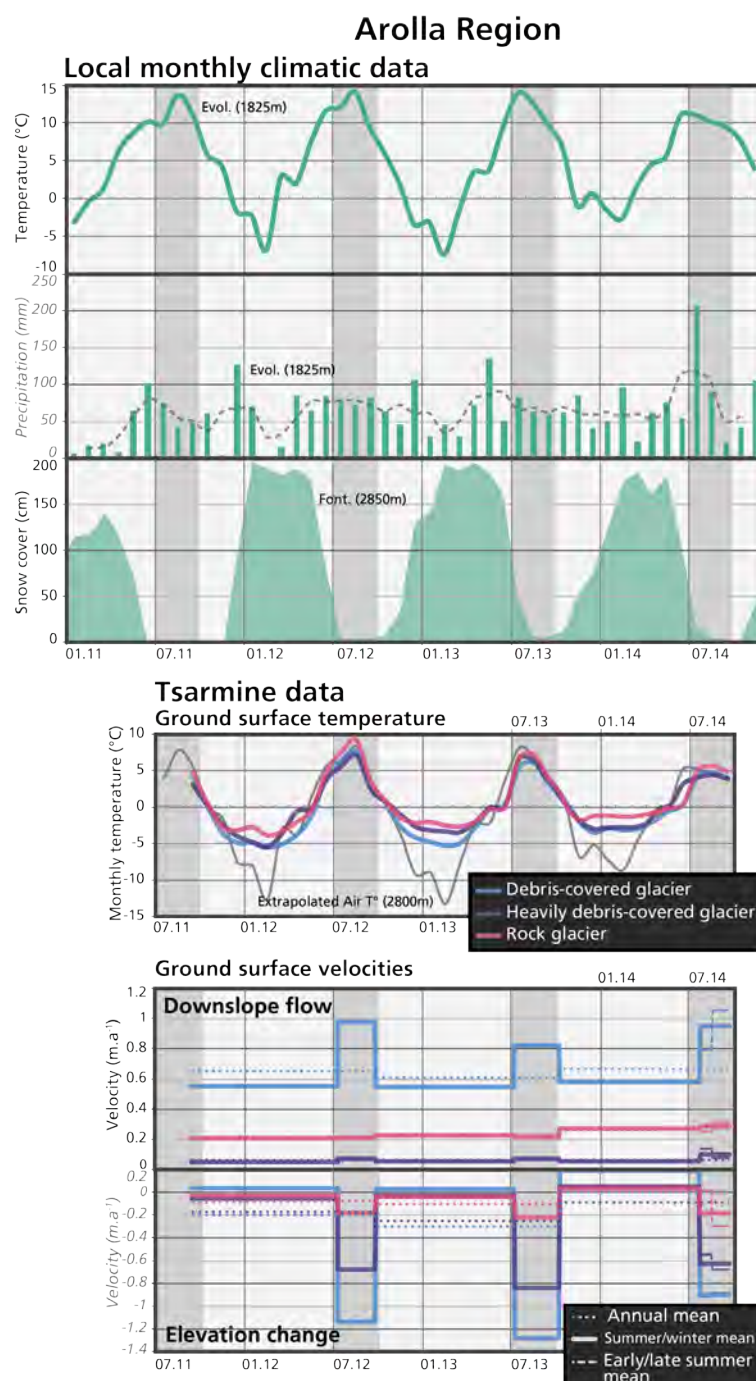
As explained in the section 2.2.2.3, we divided Tsarminé in five main homogeneous zones according to surface characteristics, ground electrical resistivities and surface dynamics (Fig. 2.16b). We used the blocks whose position was the most often measured (Fig. 3.65) to compute zonal dynamical indices (Fig. 3.67 and Fig. 3.68). We concentrated this analysis on the debris-covered glacier, the heavily debris-covered glacier (also referred to as the dead ice zone) and the rock glacier zone because no data were available in the debris-free glacier zone and the weak activity of ice-free debris.

At both annual and seasonal timescales, the fastest velocities were measured in the debris-cover glacier zone. Horizontal movement and downslope flow prevailed here over time, although vertical movement and surface lowering had the fastest velocities in summer (Fig. 3.67 and Fig. 3.68). It explains the relatively high mean M_g/dH index value obtained in this zone (2.53 ; Fig. 3.70). Where-

as vertical velocity and surface lowering exceeded 100 cm.a^{-1} during summer, vertical velocity became slight in winter and a mean surface gain of 9 cm.a^{-1} was observed. While annual surface velocities were relatively stable between 2011 and 2013, the downslope flow of the debris-covered glacier slightly accelerated during the year 2013-2014 (especially during winter) and surface lowering became null (Fig. 3.67). These changes could be attributed to two processes. First, the warmer air and ground surface temperature measured in winter could explain the acceleration of downslope flow. As a consequence, it could have somewhat increased the compressive stress in the glacier tongue and, therefore, contributed to accelerate the emergence velocity that reached 20 cm.a^{-1} . In addition, the early development of the snow cover in autumn 2013 and the cold air temperature of summer 2014 could have limited the ice melt and hence the surface lowering and the offset of the emergence velocity along this year.

The debris-covered glacier zone showed the strongest acceleration of velocities during the snow free period and the largest inter-annual and inter-seasonal variation of velocities, highlighting its sensitivity to climatic variations (Fig. 3.68). Because the July-August 2014 were unusually cool and wet, the dynamical behaviour observed between summer and winter and between early and late summer was maybe not the most representative of the typical behaviour of this zone. Along the year, most of downslope movements occurred in winter while downslope movement accelerated in the second half of the summer at the summer scale. All the surface lowering occurred in summer and in particular during the late summer where the largest PDD were measured.

Fig. 3.67. Annual, seasonal and early/late-summer mean downslope flow and surface lowering velocities measured in the three main zones containing ground ice in Tsarmino between September 2011 and 2014. Monthly means of ground surface temperatures and regional climatic data are represented above. The weather stations used were presented in the previous figures.



The heavily debris-covered glacier showed roughly the same dynamical behaviour than the debris-covered glacier but velocities were slower and no significant emergence velocities was measured during winter (Fig. 3.67 and Fig. 3.68). This zone was mainly active vertically and horizontal movements were weak ($< 10 \text{ cm.a}^{-1}$). It explains the negative M_v/dH index value obtained. Compared to the upper debris-covered glacier, inter-annual and seasonal variations of velocities were smaller and the dynamics were slightly better balanced between winter and summer and early and late summer.

The rock glacier showed clearly a different dynamic regime in comparison with the glacier zones (Fig. 3.67 and Fig. 3.68). Mean horizontal velocities were constant at annual and seasonal timescale (23 cm.a^{-1}) and the downslope movements only slowly accelerated in 2013-2014. This stability illustrated the limited influence of short term climatic variations on the rock glacier creep. Annual vertical velocities and surface lowering were respectively 2 and 5 times slower than horizontal velocities, explaining the high M_v/dH value obtained in this zone (4.47). These velocities strongly accelerated during the snow free period and slowed during winter. In summer, most of movements and especially all of the surface lowering occurred in late summer in this zone.

The 3-year horizontal velocities of three transect were presented in the Fig. 2.18. The velocity cross-profile (VCP) shared cubic and parabolic characteristics in the central debris-covered glacier zone. This probably points out the occurrence of both basal sliding and internal deformation. The summer acceleration of velocities and the observation of water circulation during summer also supported the hypothesis of basal slip occurrence. Conversely, downward velocities remained high

Dynamical indexes		Debris-covered glacier	Heavily debris-covered glacier of low activity	Rock glacier	Legend
Intensity of dynamics	Annual velocity				
	Summer velocity				
	Winter velocity				
Temporality of dynamics	Annual and seasonal variability of velocity				
	Proportion of summer activity on annual activity				
	Proportion of early summer activity on summer activity				
Main dynamics	Downslope movement vs. surface lowering				

Fig. 3.68. Mean dynamical index computed in the three main zones associating ice and debris in Tsarmino between September 2011 and 2014

during winter ($> 50 \text{ cm.a}^{-1}$) when basal sliding usually becomes ineffective under glaciers, which seems to indicate the influence of internal deformation in the glacier whose thickness reaches 30 m here. The VCP located lower on the glacier tongue was more cubic and showed the probable prevalence of basal sliding. In both VCP, peaks of maximum velocity were observed around the gully area. It highlights the influence of water circulation on the glacier dynamic. Finally, the VCP in the rock glacier were rather parabolic and could show the domination of internal deformation.

3.5.2.6. Webcam pictures analysis

A webcam was installed in Tsarminé in summer 2012 on the left LIA moraine to study the dynamic of the glacier front and lake zones (location in Fig. 3.57). Many technical issues occurred (GSM modem connection, webcam rotation, etc.) and thus many gaps exist within the dataset. Several movies were created with the exploitable images and we posted two of them online: the August 2012 to October 2013 period (one picture each 10 days; <http://www.vidtunez.com/watch?v=20b-ZoiSte1E&feature=youtu.be&lang=en-us>) and the July to October 2015 period (one picture each 10 days; <http://www.vidtunez.com/watch?v=2UJpgaYz59s&lang=en-us>). Surface movements are more visible on the summer 2015 movie. This summer was the second warmest in Switzerland since 1864 after the 2003 heatwave (MeteoSwiss, 2016). Air temperature exceeded then of 2°C the 1981-2010 climatic norm in the region of Tsarminé and probably induced a surface velocities speed-up. The Fig. 3.69 synthetizes the dynamics observed by comparing the 5 July and 28 September photographs. The entire debris-covered glacier surface showed downward movement and surface lowering. The magnitude of both processes reached at least few decimetres. In addition, two other processes induced localised multi-metric movements in the glacier: the thermokarstic gullying in the glacier centre and the ice cliff backwasting above the lake. The summer circulation of water in the central gully provoked rapid ice melt and block collapse were observed each summer in this zone. Above the lake, an ice outcrop appeared in the summer 2014 but the ice cliff retreat was relatively slow during this cool and wet summer. This process was very rapid in 2015 and we estimated that the retreat was around 10 m, illustrating the rapid ice melt of bare ice during this very warm summer. No changes were observed in the LIA moraine slope (in the foreground) and North of the lake, illustrating the likely absence of ground ice here. The marginal heavily



Fig. 3.69. Webcam images at the beginning and the end of summer 2015. The zones where dynamics were observed by comparing these two images are delineated on the right image.

debris-covered glacier zone (or dead ice zone, D in the Fig. 3.69) was dynamically decoupled with the upper glacier tongue and only surface lowering was evidenced here. Downslope movements and surface lowering were also observed in the rock glacier zone (above the zones A and D of the Fig. 3.69) but surface changes were smaller compared to the glacier zones and thus hard to clearly delineate. The lower summer magnitude of processes here (see the photogrammetric and dGPS results above) and the position of this zone at 300 m from the webcam complicated the surface change analysis. Finally, the erosion pattern, due to the rock avalanche event of the 3 September 2015 (Fig. 3.58) can be observed in the background. Similar summer surface changes in the glacier zone can be observed in the 2012-2013 movie but the processes magnitude was lower. The comparison of winter images did not reveal noticeable changes, indicating the lower activity of Tsarmine during the snow-covered period.

The webcam photographs were taken at an hourly frequency, which allowed to study the hydrological regime of the proglacial lake (e.g. Fig. 3.70). At annual timescale, three main periods can be defined. Between November and April, water is very likely absent or frozen below the thick snow cover. Water appear on the snow-ice surface during the melt season, in May or June. The rise of the water level is rapid and the lake completely reforms in one day. The water level rise has two origins during the melt season. Intense rainfall events induce relatively direct water elevation, indicating the rapid water transfer in the glacier basin and the strong control of large rainfalls on

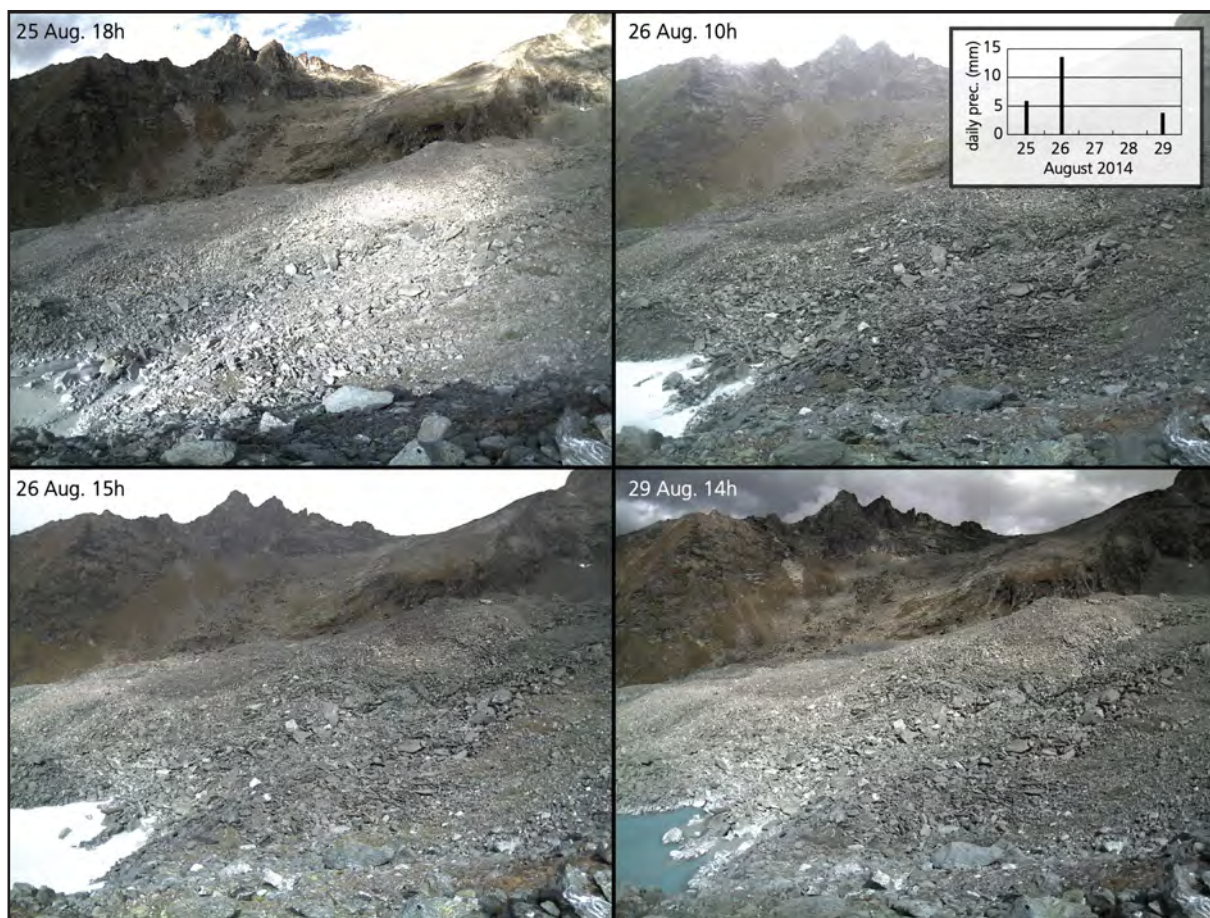


Fig. 3.70. Webcam images in late August 2014, showing the rapid lake level rise in relation with the 25-26 August rainfall events. In contrast, the lake level lowering was slow. The inset gives the daily height of precipitation measured at Evolène weather station (1825 m a.s.l.; 46°06'44"N, 7°30'31"E; 7 km distant from the study sites, © MeteoSwiss).

the lake level (Fig. 3.70). In contrast, the water level also rises after a warm and sunny period but this process always takes at least several hours (the lake level usually rises mainly during the night). The transfer of water in the glacier, therefore, delay the consequences of the water productions by upslope snow and/or ice melt and thus the control of air temperature. Contrasting with these relatively rapid rises of the lake level due to the climatic control, the water level lowering lasts always at least several days, showing the slow water percolation in the porous morainic bed. No water runoffs exist at the moraine dam surface, illustrating the percolation of water through the moraine deposits. Nevertheless, several springs appear around 2400 m a.s.l. below the moraine dam and could be partly related to the resurgence of the lake water. Depending on air temperature and precipitations, the lake is usually temporarily refrozen and covered by snow between May and October. From a general point of view, two main periods can be defined during the melt season. The winter snow mantle melt and the warm temperature of early summer maintain large water supply upslope snow and/or ice melt. Consequently, the lake level remains generally high in this period. Except after intense rainfalls, the level then largely reduces and stay low until the development of the snow layer in October or November.

3.5.3. Synthesis

The internal structure, the morphogenesis and the current evolution of Tsarmine were already presented and discussed in the publications 2 and 3 (respectively sections 2.2 and 2.3). We only summarize these topics here and add complementary elements. Numerous results on the thermal conditions, internal structure and surface dynamics were obtained in Tsarmine. Some of the most relevant are synthetized in the Fig. 3.71. All the results show a very large consistency and different components of this system can be defined and characterised (Fig. 3.72A). For instance, the current limit of the debris-covered glacier evidenced by GPR investigation corresponded to large contrasts of ground resistivity and to specific dynamical regime observed in the dGPS data and webcam images.

3.5.3.1. The Tsarmine glacier

The area of the Tsarmine glacier was 0.25 km² in 2015 (Fig. 3.72). Only **40% of the glacier surface was debris-free**, almost exclusively in the upper slope. Here avalanches accumulate large amount of snow, forming steep and crevassed cones. The current drainage/avalanche ratio (e.g. Hughes, 2009) was 1.84 in 2015 (Fig. 3.72C). **Snow redistribution processes** can thus theoretically nearly triple the amount of precipitation in the Tsarmine glacier. However, despite this snow surplus and the limitation of direct solar radiation by **shadow effect** in this north facing topographical niche, the **surface lowering exceeded 10 m in the upper half between 1967 and 2012 (Fig. 3.72A).** We attribute mainly this elevation loss to snow and ice melts and secondarily to ice flow. Indeed, over the past few decades, elevation changes in **this zone appeared strongly controlled by air temperature variations**, especially during summer: mass gains were observed when cool summer conditions induced shorter and less intense ablation periods before the early 1980s, while rapid surface lowering occurred when summer and annual temperature

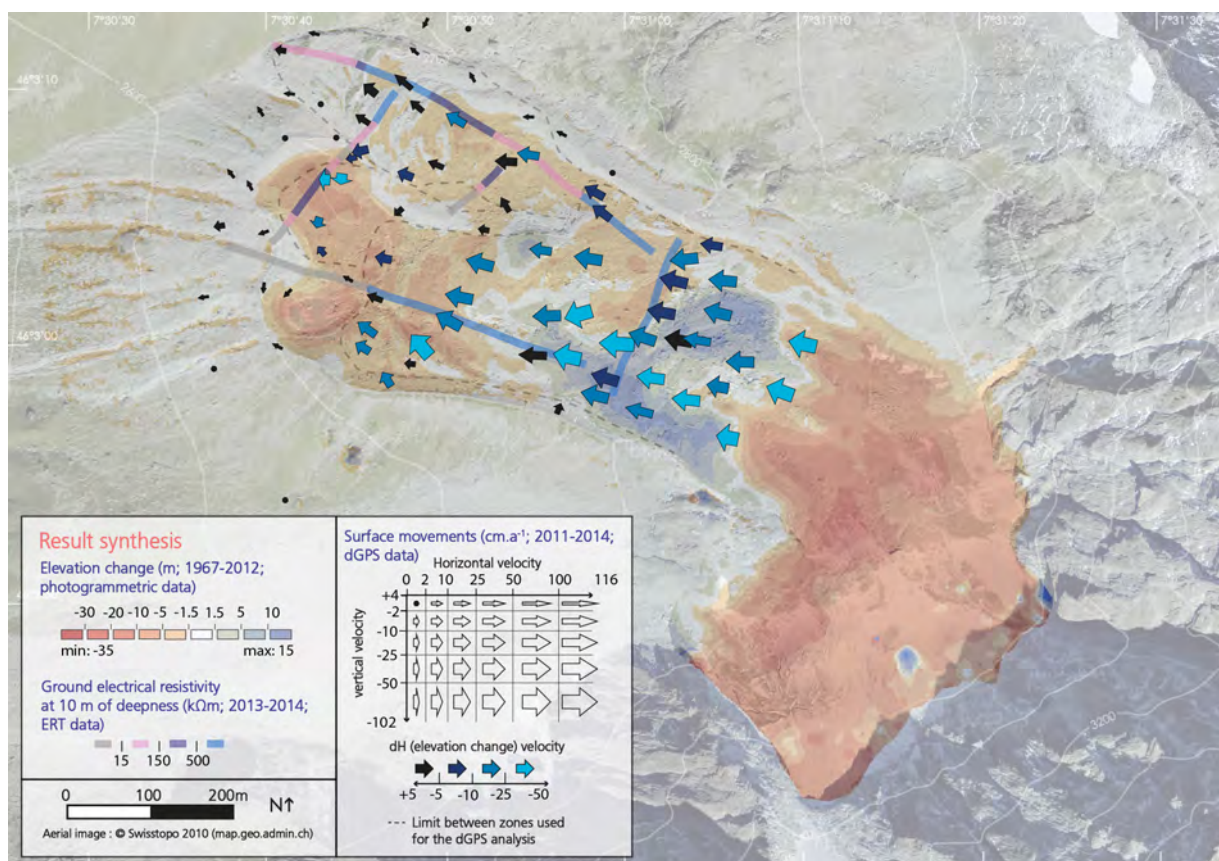


Fig. 3.71. Synthesis of photogrammetric, ERT and dGPS results obtained in Tsarminé

increased subsequently (publication 3, section 2.3). The **debris-cover concentration increased over the past decades here**, in relation with three processes. Firstly, ablation induces the emergence of englacial debris. Moreover, the debris input increased recently with the shrinking of the ice apron that covered the North face of the Blanche de Perroc until the 1980s (Delaloye, 2008; Fig. 3.72B) and with the permafrost degradation induced by the rise of air temperature. In this way, the frequency of rockfall events or rock avalanches like the one that occurred in September 2015 (Fig. 3.58) should increase with the warming forecasted in next decades.

The large debris supply in the glacier system is nevertheless not new and the glacier tongue is fully covered by a decimetric to metric debris mantle. The **lopsided size of the Holocene moraine dam** also illustrates the intense production of sediment in the backwalls over the last millennia. At decadal timescale, the **debris-covered glacier tongue showed smaller surface lowering** in comparison with the upslope debris-free part and an **elevation gain** was even observed in the central zone (Fig. 3.71). The presence of a thick, porous and weakly thermally conductive debris cover (e.g. Fig. 3.63) limited ice ablation and the recent thermal conditions were the most favourable for ground ice preservation here (section 3.5.2.1). The central uplift, observed at decadal timescale was likely enhanced by this insulation effect but was mainly related to the **migration of the ice mass accumulated in the 1960s-1970s period** and associated compressive stress increase (publication 3, section 2.3). Interestingly, a slight uplift that reached few decimetres was also recently measured during winter in the central zone (Fig. 3.65). This uplift could be related to the **emergence velocities** measured in ablation zones of glaciers (Cuffey and Paterson, 2010)

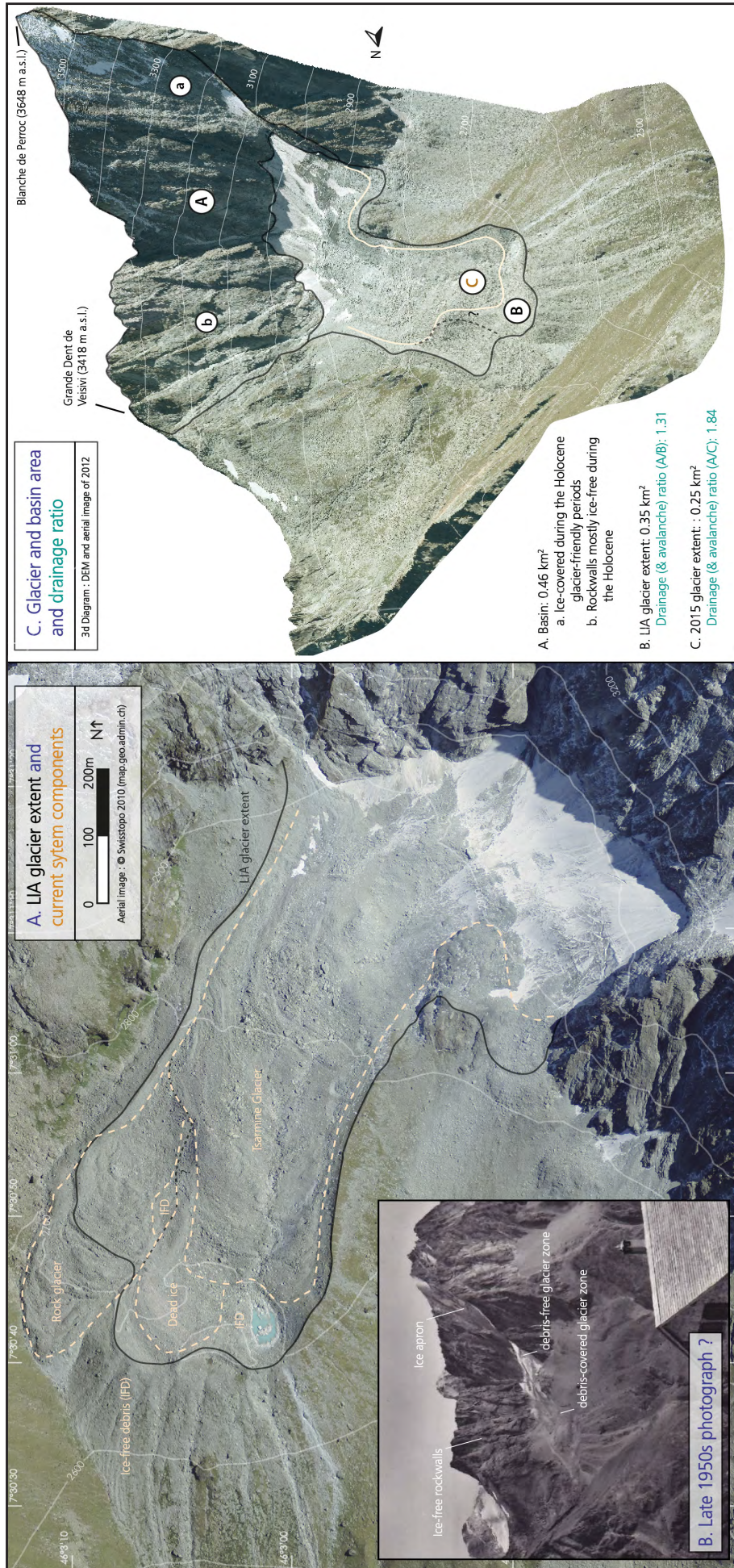


Fig. 3.72. **A.** LIA glacier extent and current system components in Tsaarmine. **B.** Photographs of the Tsaarmine glacier system taken from the Aiguille-Rouges Cabane, probably in the late 1950s (source: delcampe.ch). **C.** 3d sketch of the Tsaarmine glacier system, including its whole topographical basin. The LIA and 2015 drainage ratio were computed considering the whole basin and without taking into account the potential presence of ice apron. The 3d sketch was initially prepared by M. Capt.

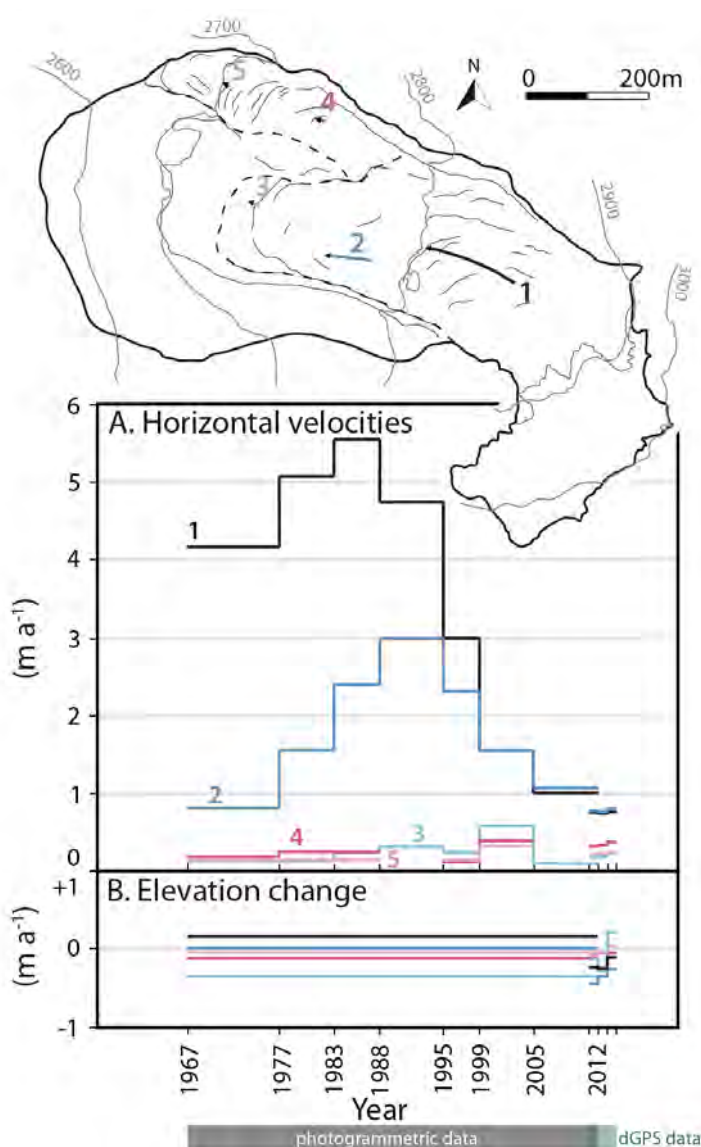
and/or the **compressive stress** due to the $> 50 \text{ cm.a}^{-1}$ downward movements measured here in winter. Nevertheless, this seasonal uplift only contributed to limit the surface lowering that became dominant at annual timescale in the glacier tongue since the 2000s (Fig. 2.22; 3.67 and 3.71). The downward movements had larger magnitude than surface lowering in the glacier but **the flow strongly slowed down since the 1990s in the central zone** (blocks 1 & 2 on Fig. 3.73). Despite the probable occurrence of both basal sliding and internal deformation, it would point out the progressive transition of this glacier **toward a stagnant downwasting mode**. The glacier thus slowly thins under the debris cover (mean surface lowering was $\sim 20 \text{ cm.a}^{-1}$) whereas the outcropping ice rapidly melts (Fig. 3.69 and 3.71). As observed in many other debris-covered glaciers (e.g. Zhang et al., 2011; Pellicciotti et al., 2015), ice cliff backwasting becomes thereby the fastest ablation process. It highlights that without the presence of an extensive debris cover, the strongly unfavourable climatic conditions would induce rapid glacier vanishing in ablation area nowadays. Due to the limitation of the glacier melt by the debris cover, cold climatic conditions in this permafrost environments and shadow effect, as well as to the snow accumulation increase by redistribution processes, the **decadal behaviour of the Tsarmino glacier showed temporal and spatial specificity in comparison with larger local glaciers** (publication 3, section 2.3).

According to the ice thickness and to the current differential dynamic that are occurring in the glacier, the future disconnection between the upslope sheltered accumulation area and the distal heavily debris-covered tongue is possible (Fig. 2.29). The flattening of the central zone could generate the formation of supraglacial ponds, which are very common on debris-covered glacier and accelerate the ice melt (e.g. Benn et al., 2012).

3.5.3.2. Recent glacier history and glacier-permafrost interactions

The existence of **fresh moraines and push-moraines** eases the reconstruction of the LIA extent of Tsarmino glacier (Fig. 3.72). Without considering

Fig. 3.73. Horizontal and elevation change velocities derived from the photogrammetric and the dGPS data between 1967 and 2012 in 5 locations in the glacier and rock glaciers zones in Tsarmino. The basis of this figure was prepared by M. Capt.



the presence of ice aprons on the backwalls, the Tsarmine glacier area was then $\sim 0.35 \text{ km}^2$. Whereas the position of the glacier was clear in the south frontal zone, the presence of steep slopes around the large depression that is currently dominating the push moraine zone (also referred to as the rock glacier rooting zone previously) and the current confinement of the glacier terminus in the south zone question the LIA situation in the North frontal zone.

A sediment accumulation seems now separate the glacier-dead ice zones from the northern rock glacier complex (black dotted line in Fig. 3.72A and C). Two hypothesis can explain the formation of this sediment accumulation and the current spatial organisation of the Tsarmine system components. We think that both are related to the **differential situation that have existed over the Holocene in the accumulation area of the system**. The large zone situated below the 600 m high north face of the Blanche de Perroc is the main accumulation area of the Tsarmine glacier. It receives especially large amount of snow due to avalanching. The backwall were very likely ice-covered during the Holocene glacier-friendly periods and whereas the snow/ice supply was the largest here, debris supply was relatively limited. Consequently, most of the ice of the Tsarmine glacier originates from this zone, which explains that **the LIA and current terminus are located in the left hand side of the system**. In contrast, less ice was accumulated in the footslope located below the Grande Dent de Veisivi. The rockwall area and height are smaller and the west aspect is less favourable for snow accumulation. Moreover, the rockwalls were probably largely ice-free during the Holocene (Fig. 3.72B) and large amount of debris was produced here. The right hand side of the Tsarmine glacier has thus **a higher debris concentration** than the central and left zone. The reduction of ground resistivities toward the North in the Tsa-C ERT profile could highlights such higher concentration (Fig. 2.15). The first hypothesis explaining the current situation in Tsarmine relies on the consideration of a continuous large and thick glacier tongue that occupied all the glacier margins in the LIA (zone B; Fig. 3.72C). A late-LIA or post-LIA (1850? 1890s? 1920s?) positive mass balance period could have thus induced a minor **glacier advance that was confined in the south margin**. Due to the high debris concentration in the right glacier side, a moraine accumulation could have formed, disconnecting the rock glacier complex from the glacier zone. In the second hypothesis, this moraine already existed before the LIA glacier advance, due to the differential ice and debris supply in accumulation area at Holocene timescale. It confined the LIA glacier tongue in the southern distal zone and only a thin ice layer overflowed this moraine and induced the push moraines in the rock glacier root. Another case of a likely Holocene moraine overflow during the LIA can be observed for example in the close Moiry glacier (Fig. 3.74).

At Holocene timescale, a large debris-concentration and also probably a reduced glacier dynamic and water circulations allowed the development of **a rock glacier** in the northern distal zone. In contrast, no similar landform exists in the southern margin, where Holocene glacier dynamic and ice concentration were higher. Many researches showed that temperate glacier and water circulation hampered the preservation of ground ice and thus the formation of rock glaciers in glacier margins (e.g. Kneisel, 2003; Delaloye, 2004). It is thus also probable that the current situation in Tsarmine illustrate this **thermal and hydrological control**. The likely occurrence of basal sliding

in the glacier tongue and the water circulation observed in the southern margin during summer (e.g. Fig. 3.70) indicated relatively warm ground thermal conditions that were unfavourable for ground ice preservation. In this way, this zone showed rapid surface lowering over the last decades and ice has largely disappeared around the lake (Fig. 3.71). The dead ice zone was dynamically disconnected from the upper glacier tongue and experienced mainly stagnant surface lowering in the last years. Conversely, no water runoff were observed or heard on the rock glacier zone, that seems mainly affected by a slow creep, relatively constant over decades (Fig. 3.73) or seasons (Fig. 3.68). Surface lowering was close to zero in this zone ($\sim 5 \text{ cm}\cdot\text{a}^{-1}$ on average between 2011 and 2014) and pointed out that permafrost conditions limit the ice ablation below the several meter thick debris layer. Nevertheless, at decadal and annual timescale, surface lowering was observed in the concave root (Fig. 3.71). The melt of glacier ice is disconnecting the rock glacier from upslope glacier in this zone. The presence of a resistive body below the push moraines indicates that **glacier ice was probably integrated in the flowing ice-debris mixture during the LIA**. Conversely, the ground ice located in the frontal zone is related to older glacier-permafrost interactions.

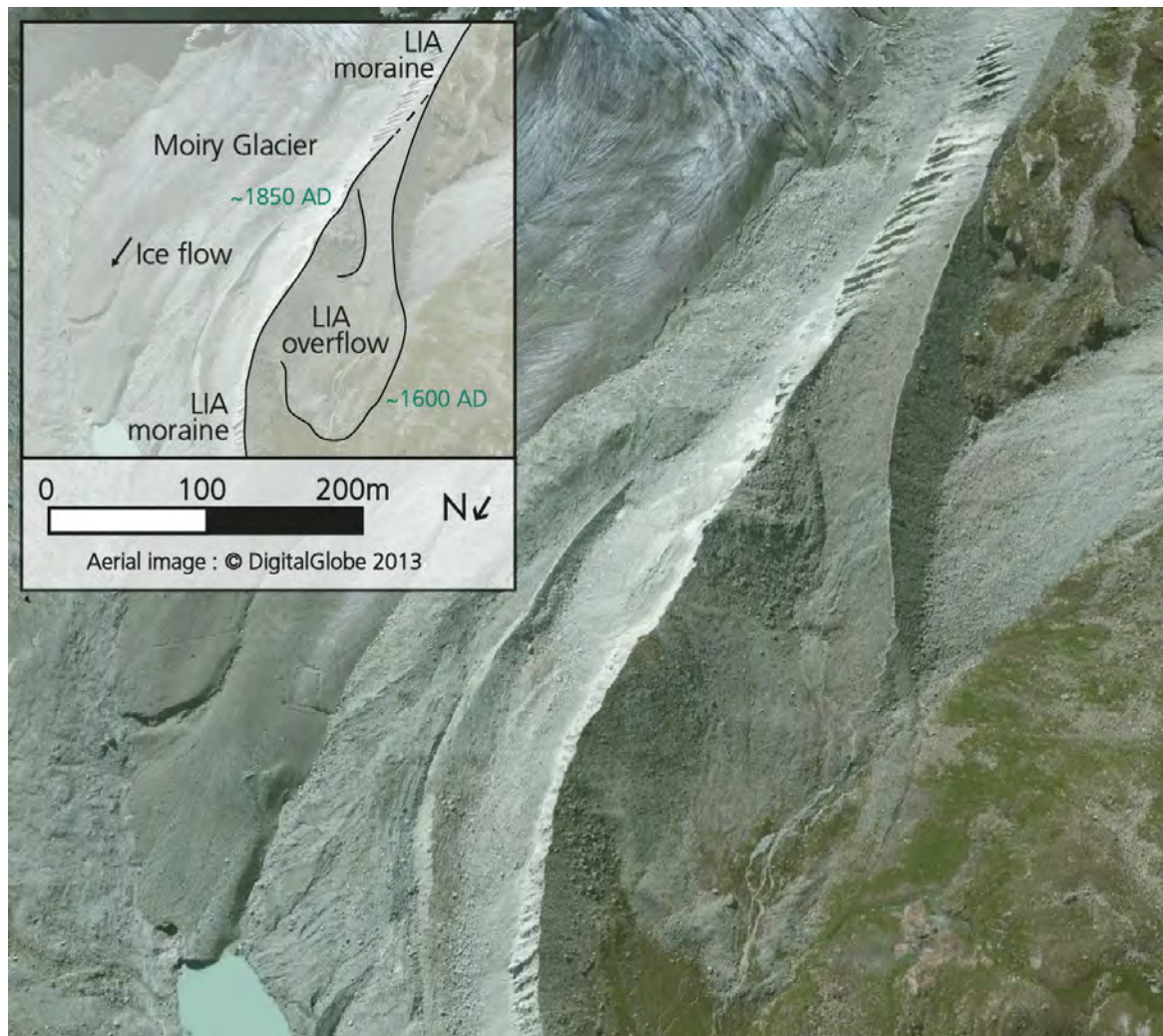


Fig. 3.74. 3d sketch of the left LIA moraine of the Moiry Glacier ($46^{\circ}05'40''\text{N}$, $7^{\circ}35''\text{E}$; 7 km distant from Tsarmine). This historic Holocene moraine was likely locally overflowed ($\sim 2500 \text{ m. a.s.l.}$) by the glacier during the LIA maximum. Despite this coverage by a small glacier lobe that built a morainic arc, the main lateral moraine remained preserved. C. Lambiel (personal communication) proposed an alternative explanation: the two moraines could correspond to two LIA episodes which age is given in green (© Plans software, Apple).

3.6. Chaltwasser

3.6.1. Site description

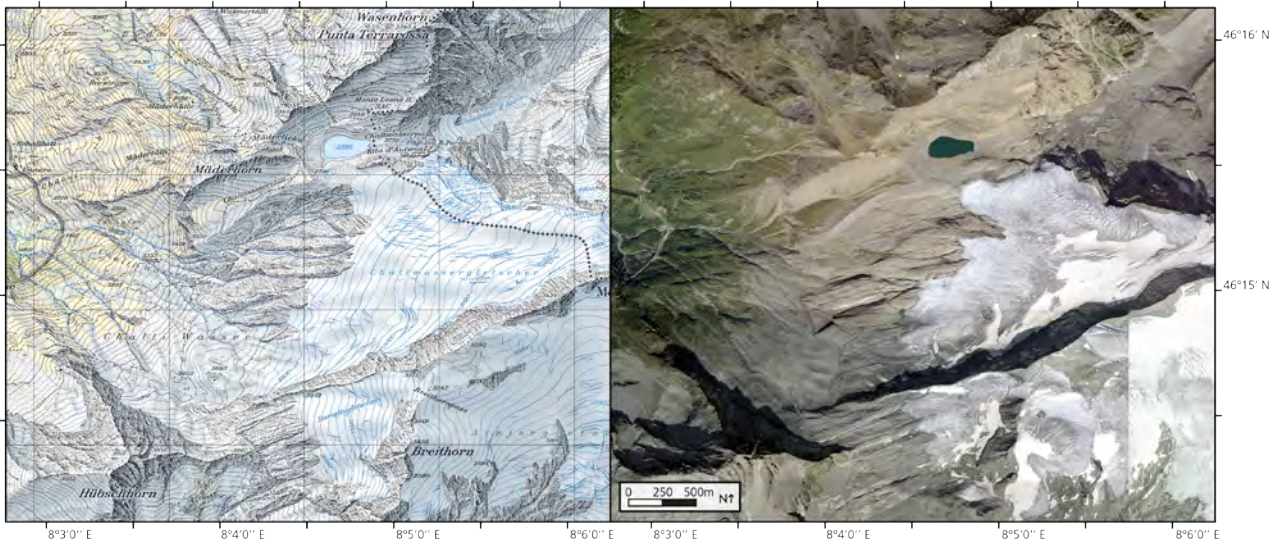


Fig. 3.75. Map (CN25, leave 1289 & 1309, 2005) and aerial photograph (SWISSIMAGE Level 2, 2010) of the Chaltwasser glacier system (© Swisstopo)

Some of the data presented in this section originate from the master thesis of S. D'Aujourd'hui (2013). Detailed presentation, analysis and complementary data, especially on local geomorphology and torrential activity can be found in this work. Only the main results obtained on the internal structure and surface dynamics are summarized and synthesized here. In particular, we retreated the ERT data that we collected with S. D'Aujourd'hui during field investigation. We also show the dGPS monitoring results obtained from the data that we collected in 2013 and 2015 in

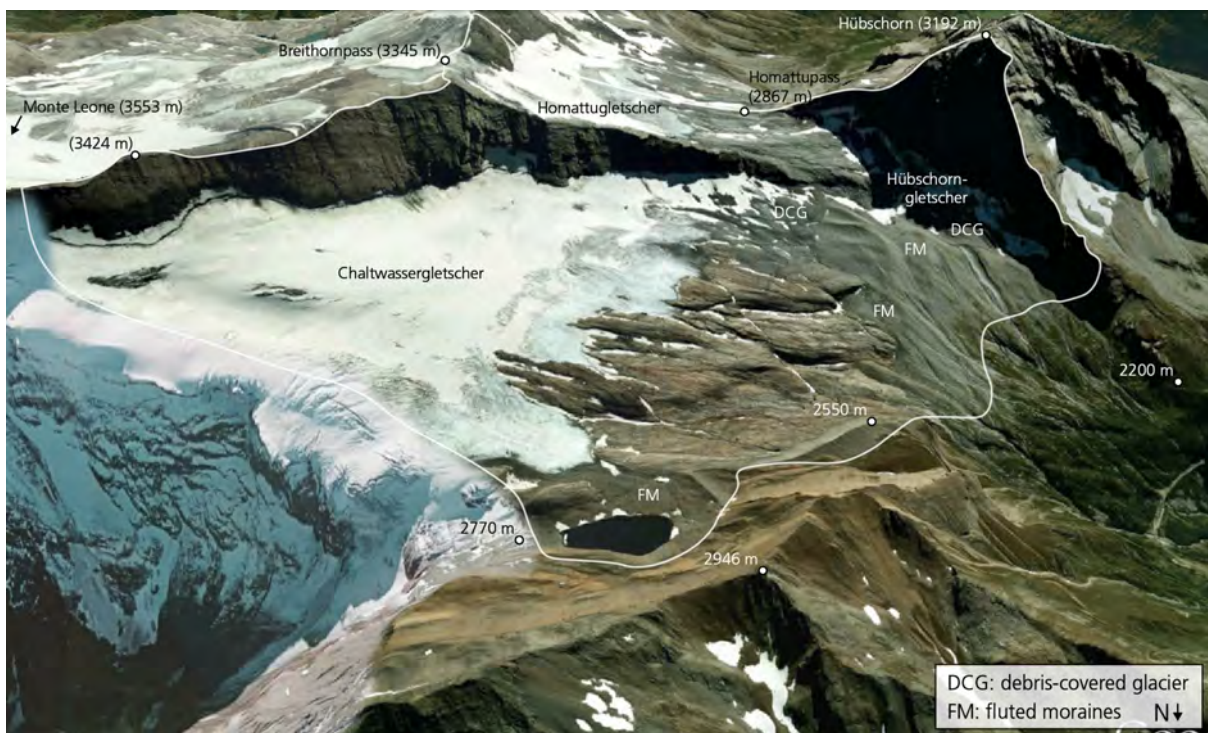


Fig. 3.76. Google Earth view of the Chaltwasser glacier system. Some landforms composing this system are indicated. The aerial image was taken on October 30, 2009 (© Nasa Image and Google Earth).

addition to those of 2012. Finally, we present rapidly the photogrammetric results produced by S. D'Aujourd'hui by comparing the DEMS created from aerial images of 1967 and 2005.

The Chaltwasser glacier system is located in the East of the canton of Valais, near the Simplon Pass (Fig. 3.1). This system was the largest of the investigated sites (4.4 km²). It extends between 2320 and 3424 m a.s.l. in a West facing plateau (Tab. 3.1; Fig. 3.75 and 3.76). The bedrock is mainly composed by gneiss, calc-schist and flysch (Bearth, 1972; Burri et al., 1993). All the south of the system and the main summits (Monte Léone, Breithorn and Hübschorn) are dominated by the gneiss of the Monte Léone nappe. Conversely, the base of the rockwalls, the glacier bed and recently deglaciated areas are composed by the calc-schist and flysch of the Sion-Courmayeur geological zone. Whereas local temperatures and their variations over the last decades are comparable to those observed in the central and western Valais (e.g. Tab. 3.1; Fig. 2.21), the precipitations are higher in the Simplon region than in Tsarminie or the Petit Combin region because of the local influence of the southern atmospheric perturbations (D'Aujourd'hui, 2013).

Due to the post LIA fragmentation of the former Chaltwasser glacier, this system is currently composed by three disconnected glaciers: the Chaltwassergletscher, the Homattugletscher and the Hübschorngletscher (Fig. 3.76). The two first are transection glaciers, whose surface are largely debris free. In consequence, the areas recently deglaciated by these glaciers are composed by large zones of abraded bedrocks and relatively few sediments were deposited. In contrast, the



Fig. 3.77. Picture of the Hübschorn debris-covered glacier taken on September 25, 2015. A permanent snowfield occupies the top slope. An ice cliff is visible in the foreground.

Hübschorngletscher is a very small valley floor glacier located below a 500 m high rockwall that produces large amount of debris. This glacier is thus covered by coarse debris and few ice outcrops are observable (Fig. 3.77). Large sediment stores are nevertheless present in some of the frontal glacier zone and several debris flows originated from these deposits in the last decades (D'Aujo-urd'hui, 2013). Most of this system is located within the permafrost belt, according to permafrost distribution models (BAFU, 2005; Boeckli et al., 2012).

3.6.2. Results and synthesis

3.6.2.1. Electrical resistivity tomography

Ground surface resistivities in the sedimentary margin were investigated below two long profiles in September 2012 (Fig. 3.78). The transversal profile (CW-1) displayed a homogeneous ~ 40 m thick conductive layer ($2 < r < 10 \text{ k}\Omega\text{m}$) in the former frontal moraine accumulations. The same layer was detected in the 10-20 first meters below the surface in the 480 lower meters of the longitudinal profile (CW-2 and CW-3). A 10 to 50 $\text{k}\Omega\text{m}$ layer was present at depth in the lower part of the CW-2 and CW-3 profile. Finally, the resistivity strongly increased ($>80 \text{ k}\Omega\text{m}$) in the top of the CW-3 profile, below the ridge and bulge formed during the late 1970s - early 1990s glacier recurrence observed on aerial images (3 in Fig. 3.79B & C). Resistivities exceeded 1000 $\text{k}\Omega\text{m}$ here at 5 to 10 m of depth.

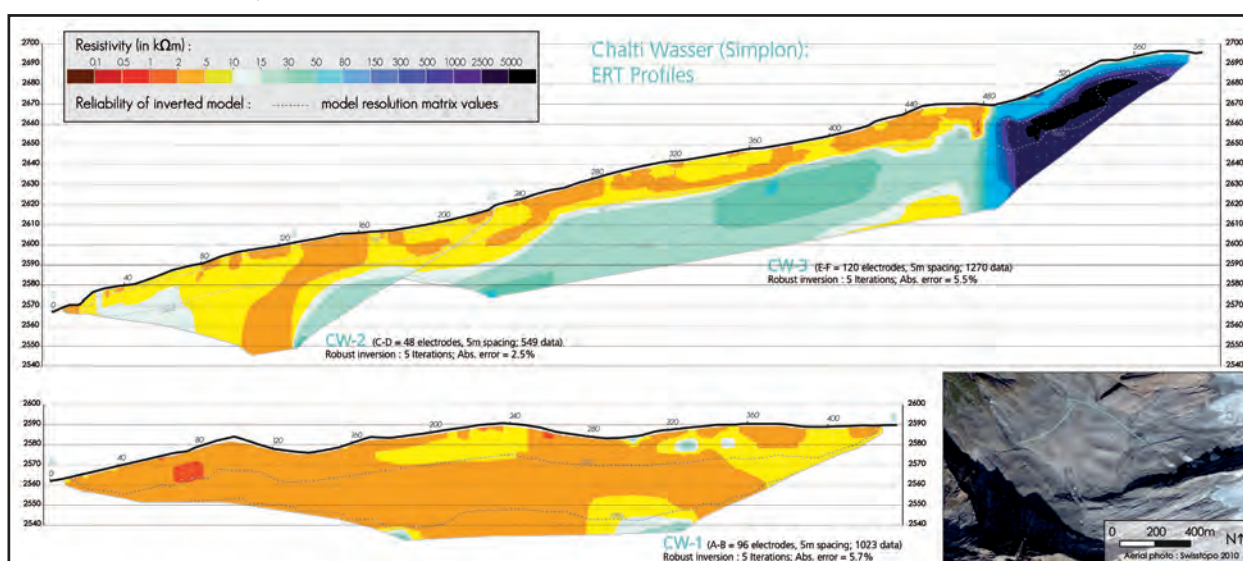


Fig. 3.78. Electrical resistivity tomograms measured in the lower part of the Chaltwasser glacier system on September 6 and 7 2012

3.6.2.2. Photogrammetry

The comparison of the 1967 and 2005 DEMs provided valuable information on the dynamics that recently occurred in the distal part of the Chaltwasser system (Fig. 3.79). As observed on aerial photographs (available on map.lubis.admin.ch), the Chaltwassergletscher and the Homattugletscher terminus were relatively stable from the late 1950s to the late 1970s. Both glaciers advanced then until the early 1990s whereas a rapid retreat was observed in the subsequent years. The consequence of these mass balance variations induced differential elevation changes in the Chalt-

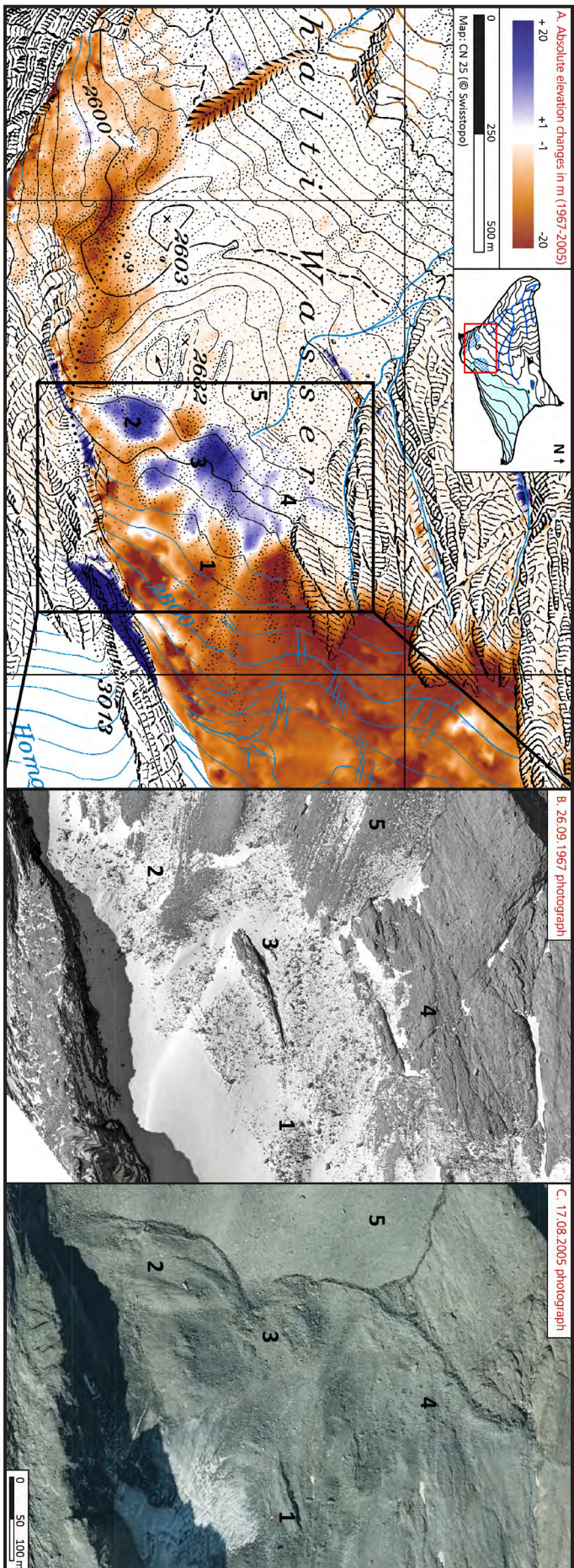


Fig. 3.79. A. Elevation changes extracted from the comparison of DEMs derived from archival aerial photogrammetry. The theoretical 3d precision of both DEMs was around 1 m (D'Ajujurd'hui, 2013). The dark blue zone at the NW of the 2013 elevation point is very likely a DEM creation artefact in this steep rockwall area. **B.** and **C.** show the 1967 and 2005 photographs in the Chaltwasser glacier frontal zone (@Swisstopo). Modified from D'Ajujurd'hui (2013).

wasser glacier. The frontal zone mainly uplifted between 1967 and 2005 due to the accumulation of moraines (4 on Fig. 3.79) and debris-covered ice (2 & 3 on Fig. 3.79). Conversely, the rest of the lower glacier zone had a generalised surface loss that reached 20 m at maximum (1 on Fig. 3.79). The lower ice-free debris did not show noticeable activity (5 on Fig. 3.79). Except variations of the snow cover, few changes were observed on the Hübischornngletscher surface on aerial images. Elevation changes revealed a downwasting at decadal timescale and only the central glacier area remained stable (lower-left of Fig. 3.79). However, this lowering was mainly < 10 m and, thereby, less intense than in the Chaltwasser glacier surface. Finally, the moraine erosion related to the September 1993 debris flow event is clearly visible below the Hübischorn glacier front.

3.6.2.3. dGPS

The position of 50 blocks was measured up to 5 times in the lower part of the system between July 2012 and September 2015 (Fig. 3.80). It allowed investigating the current dynamics and helped to assess the distribution of ground ice. Hence, as revealed by the fast surface movements, the terminus of the Chaltwassergletscher was still located below the debris deposited during the 1970s-1990s glacier advance. However, the weak variation of terminus position, the heterogeneous directions of the movements and the fact that surface lowering values were greater than downslope movements indicated the domination of a stagnant downwasting mode in the glacier front. For most of the blocks, surface lowering was faster than 25 cm.a⁻¹ at annual timescale (117 cm.a⁻¹ at maximum; Fig. 3.80A) and accelerated up to few meters per year in summer (Fig. 3.80B). This illustrates the rapid melt of the ice in this zone, especially during the snow-free period. Generally, slower surface velocities were measured on the Hübischorn debris-covered glacier. Most of the movements were < |60| cm.a⁻¹ at annual timescale. Surface velocities also accelerated beyond |100| cm.a⁻¹ during summer. Contrasting with the Chaltwasser glacier tongue, downslope movements were largest than surface lowering here (Fig. 3.80C). Finally, the absence of noticeable movements for all the blocks located downside and between these debris-covered glacier tongues highlighted the very likely generalised absence of ground ice close to the surface.

3.6.2.4. Results interpretation and synthesis

According to the different results obtained, aerial images from the last decades and field observations, we propose a reconstitution of the recent glacial history in the SW part of the Chaltwasser system (Fig. 3.81). The frontal position of the LIA glacier complex was somewhat hard to define precisely. Indeed, the likely multi-lobed terminus was situated between 2300 and 2400 m a.s.l. in a slope which is mostly steeper than 20°. **The frontal moraine deposits were thus strongly reworked by fluvio-glacial and torrential dynamics after the LIA.** The 1890s-1920s frontal position was probably situated between 2500 and 2600 m a.s.l., where large sediment stores are accumulated. The abundance of fine material, the smooth surface and the presence of many **fluted moraines** (Fig. 3.76) illustrate **the overriding of these accumulations during the LIA and the following decades by a temperate-based glacier.** Two SW facing steep slopes (> 35°) are present in the centre of the moraine deposits (1 et 2 on Fig. 3.81; respectively 40 m and

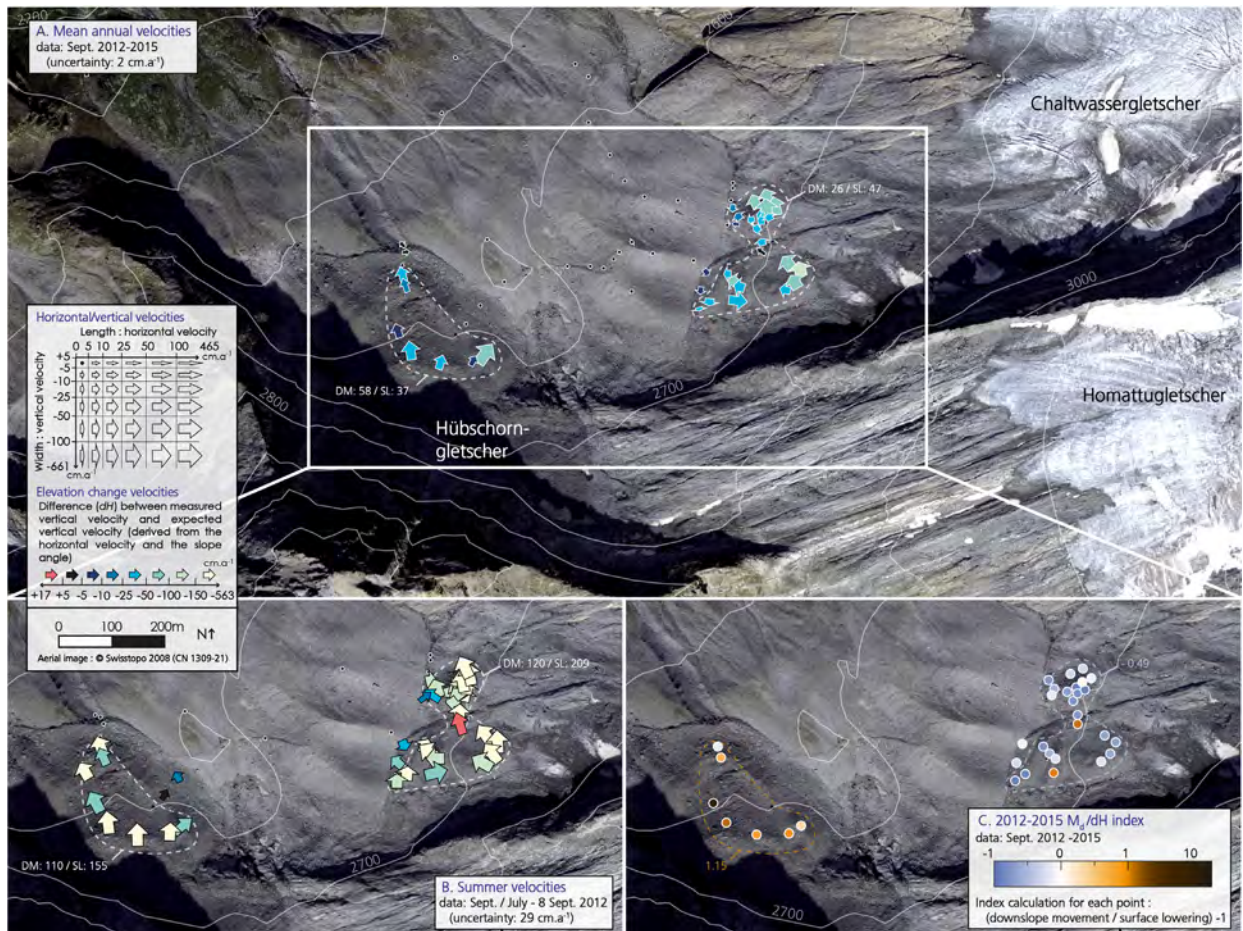


Fig. 3.80. A. and B. Respectively mean 2012-2015 and summer 2012 surface velocities measured in the Chaltwasser system. C. M_d/dH index computed from the 3-year surface velocities. Zonal means of downslope movements (M_d), surface lowering (dH) and M_d/dH index are indicated in each map.

50 m high). We consider these two landforms as **medial subglacial deposits**, resulting from the distinct flow of the Chaltwasser and Homattu glaciers during the LIA and following decades. The two steep slopes could be due to the flow of the Homattu glacier along these subglacial debris accumulations. They also illustrated the different debris supply on these two coalescent ice masses. Indeed, the Holocene erosion of the ice-free backwall induced large accumulation of debris in the SW part of the Chaltwasser glacier (1 et 2 on Fig. 3.81). Currently, this area is thus the main debris-covered zone of the Chaltwasser glacier. Conversely, the Homattu ice mainly originated from the Breithornpass area (Fig. 3.76). This ice mass was thereby not dominated by rockwalls and had a low debris-concentration. The confluence of these debris-rich and debris-poor glaciers could thus explain the current situation: few debris were deposited by the Homattu glacier in the SW whereas the Chaltwasser glacier deposited and overridden its former moraines in the NE, dammed in the SW by the adjacent Homattu glacier. Another hypothesis could be the evacuations of former Chaltwasser deposits by the Homattu glacier during the LIA and 1890s and/or 1920s periods whereas the Chaltwasser glacier overridden these accumulations (former moraines or rock glacier), as illustrated by the presence of fluted moraines at their surface. Today, except the potential presence of dead ice between the Hübhorn and Chaltwasser glaciers (Fig. 3.81; see surface lowering that occurred here between 1964 and 2005 in Fig. 3.79A), **the frontal large accumulations of debris seem mostly ice-free**. Subglacial or postglacial water circulations,

especially indicated by the fluted moraines, probably hindered the preservation of ground ice. According to the resistive layer detected in the ERT profiles (Fig. 3.78) and field observations, this ice-free debris layer reaches locally **several tens of meters**. Finally, we attribute the basal resistive layer present in the lower part of the CW-2 and CW-3 profiles to bedrock. Indeed, it outcropped at 20 m in the NE of the profile and the lower limit of this layer corresponded to a topographic step. This layer could also illustrate the presence of an old covered rock glaciers or coarse moraine deposits (C. Lambiel, personal communication) but we think that these possibilities are less probable.

The **three glaciers associated in the Chaltwasser glacier complex probably disconnected during the strongly negative mass balance period that occurred in the 1940s** (e.g. Huss et al., 2009; Fig. 3.81). **Because of their distinct characteristics, the glaciers behaved in a contrasted way subsequently.** On one hand, the **Chaltwasser and Homattu glaciers** are two transection glaciers which are poorly shaded and snow-supplied by the surrounding relief (e.g. the drainage (and avalanche) ratio are smaller than 0.2; Fig. 3.81). As a consequence, the **mass balance variations** of these glaciers in the last decades seemed strongly **related to climatic and especially air temperature variations** and thereby, were relatively similar to the glacier responses at regional scale (e.g. Huss et al., 2012 & 2015). The glaciers advanced up to the early 1990s because of the transfer downglacier of the mass accumulated in the 1960s-1970s periods. However, the atmospheric warming that started in the 1980s induced unfavourable conditions and the **shrinking of both glaciers** (Fig. 3.79A). According to Fischer M et al. (2015), the 1980-2010 averaged geodetic mass balance of these glaciers ranged between -0.4 and -0.6 m w.e. a⁻¹ (the Hübischorn glacier was not considered by this study, probably in relation to its very small size and its almost complete burying under the debris). The accumulation of fine debris and dust on the ablation area (Fig. 3.81) probably also accelerated the ice melt (e.g. Gabbi et al., 2015). The

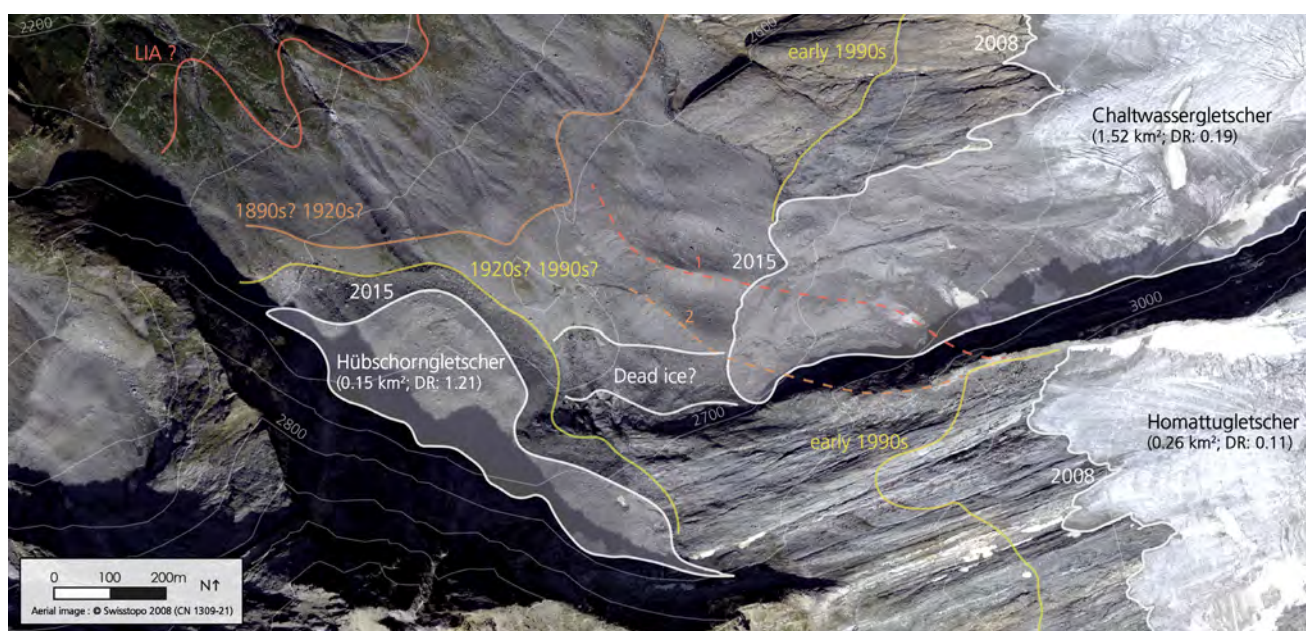


Fig. 3.81. Reconstructions of recent glacier extents in the SW of the Chaltwasser glacier system. The solid lines correspond to glacier extents and the two dashed lines illustrate past ice fluxes limits between the Chaltwasser and Homattu glaciers. The current area and drainage (and avalanche) ratio are indicated for each glacier in the brackets. We only considered the Homattu glacier part that flows in the Chaltwasser basin. As the 2008 aerial image was used as background, the Chaltwasser and Homattu glaciers limits in debris-free surface correspond to this year.

rapid ice melt observed in the debris-covered tongue of Chaltwasser glacier (Fig. 3.81) illustrates that, even below a metric insulating layer, present conditions are largely unfavourable for ice preservation in these glaciers. On the other hand, few surface variations and a smaller decadal downwasting was observed in the **Hübschorn glacier** (Fig. 3.79A). The frontal position of this glacier showed no clear variation since the 1950s. We attribute this **particular behaviour** to the **strong influence of topography on this weakly active ice mass**. The presence of an extensive thick debris cover, the shadow and the snow redistribution (drainage (and avalanche) ratio is 1.21; Fig. 3.81) induced by the backwall noticeably limit the climatic control on this glacier. Ground ice will thus probably melt slower in this area, more favourable than the two other west-facing glacier surfaces. This **heavily debris-covered glacier** could even **transform into a rock glacier** if ground ice preservation and deformation will pursue in the next decades. However, **surface lowering appeared relatively rapid** over the last years (mostly $> 25 \text{ cm.a}^{-1}$; Fig. 3.80) and highlighted the efficiency of ice melt here.

3.7 Le Petit Combin

3.7.1 Site description

To complete the results obtained in SDCGSAPE and investigate another situation in a relatively large system (4.3 km²), we present and interpret rapidly the results obtained by R. Darbellay (2015) in the Petit Combin system. We collaborated in the data processing (ERT results) and general interpretation of results in this master thesis. Detailed presentation, analysis and complementary data can be found in this work. Here, we only summarize and synthesize the results obtained on the internal structure and decadal dynamics and complete them with our field observations and comparison with the decadal behaviour of other glaciers of the region.

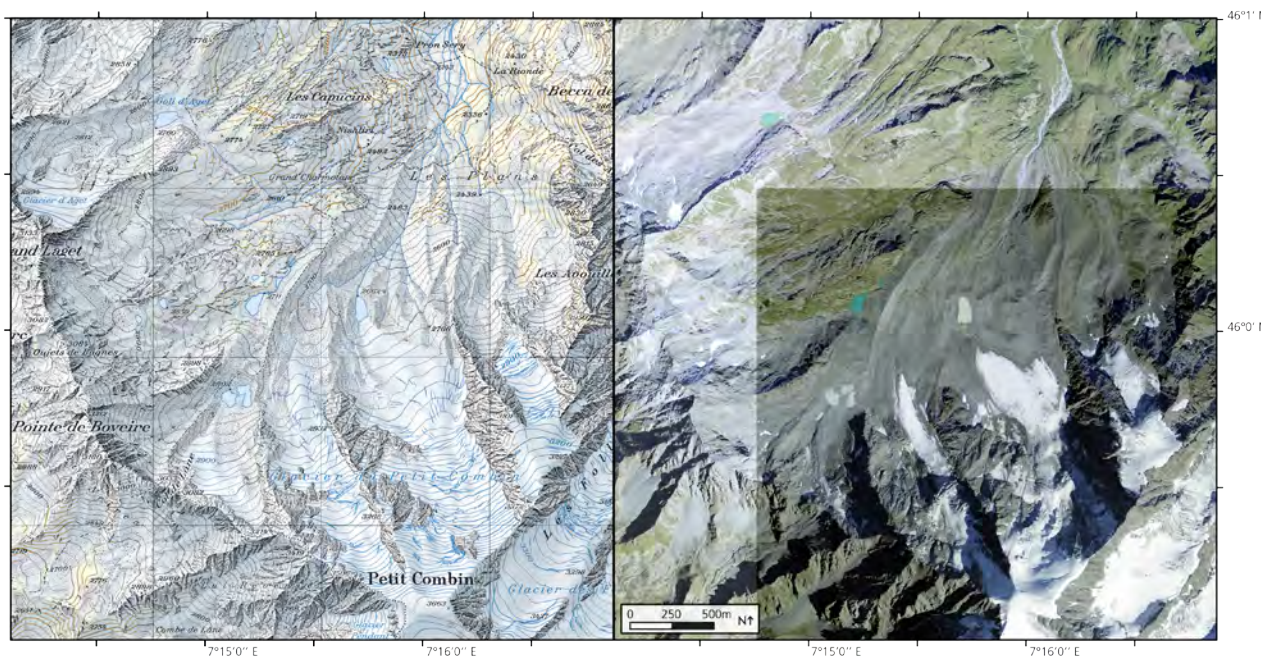


Fig. 3.82. Map (CN25, leave 1345 & 1346, 2001) and aerial photograph (SWISSIMAGE Level 2, 2010) of le Petit Combin glacier system (© Swisstopo)

The Petit Combin glacier system is located in the SW of Switzerland, in the Bagnes valley (Fig. 3.1). It extends between 2330 and 3663 m a.s.l. in a North facing slope originating from the Petit Combin (Tab. 3.1; Fig. 3.82). Local lithology is homogeneous and composed by albitic gneiss and prasinite of the Mont-Fort nappe (Burri et al., 1998). Darbellay (2015) presented detailed regional climatic information. The decadal variations of air temperatures were similar that those observed in the Valais central (Fig. 2.21): after a period some tens of degrees Celsius colder than the 1961-1990 climatic norm between the 1960s and 1970s, air temperatures rapidly warmed since the early 1980s to exceed to more than 1.5°C the climatic norm. Annual precipitations slightly increased since the 1980s.

The Petit Combin glacier complex is currently composed by disconnecting hanging glaciers and associated partly debris-covered tongues (Fig. 3.83). However, signs of recent glacier occupation on backwalls and fresh Holocene moraines show that until recent decades, the Petit Combin glacier formed a large ice complex above 2650 m a.s.l.. The slope angle strongly decreases below the 500 m high steep backwalls. Debris-covered tongues, whose distal limits are hidden by surface

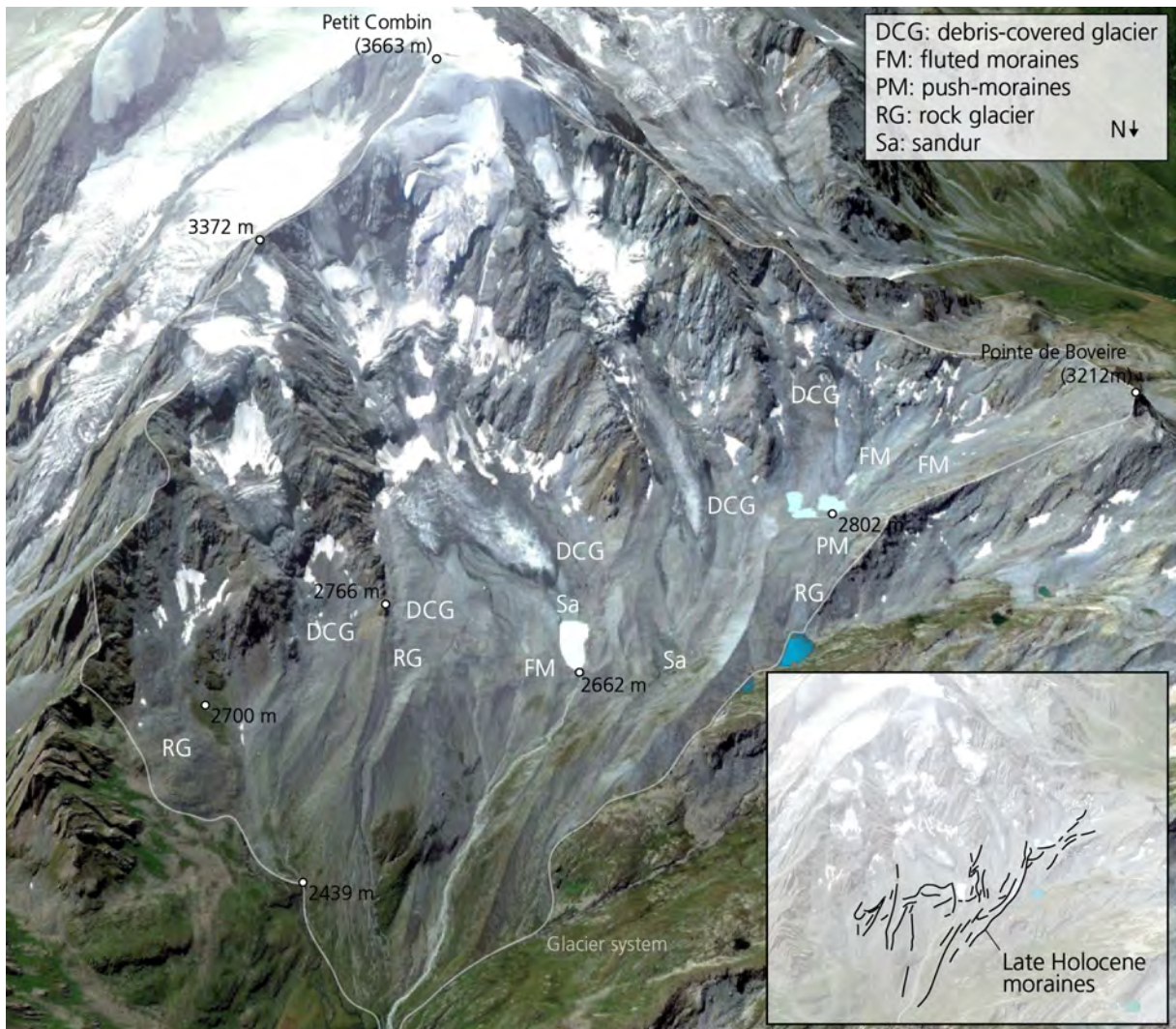


Fig. 3.83. Google Earth view of the Petit Combin glacier system. Some landforms composing this system are indicated as well as late Holocene moraines (inset). The aerial image was taken on August 18, 2009 (© DigitalGlobe and Google Earth).



Fig. 3.84. Picture of the central zone of the Petit Combin glacier system taken on September 13, 2013. The lake (location near the elevation point 2662 m a.s.l. on Fig. 3.78) is dammed by a recent moraine and a delta is progressing in its upper zone. In its right, the solifluction lobes and the vegetation development illustrate post-glacial dynamics on the moraine. In the bottom-right corner, the sandur show the fluvio-glacial processes induced by the melt water streams originating from the western part of the system.

debris, cover the top of this relatively flat area (Fig. 3.83 and 3.84). Below, very large sediment accumulations and moraine-dammed lakes are presents. The moraine complex is composed by numerous lopsided ridges. Finally, the presence of hanging glaciers and of push moraines and rock glaciers in the sedimentary margins highlights the local occurrence of permafrost conditions in the system. It is also pointed out by permafrost distribution models (BAFU, 2005; Deluigi, 2011; Boeckli et al., 2012).

3.7.2. Results and synthesis

3.7.2.1 Electrical resistivity tomography

The current distribution of ground ice in the proglacial margin was investigated with 8 ERT profiles in September 2014 (Fig. 3.85). The abundance of fine material at the surface allowed to collect very reliable data (see the low absolute error values of each tomogram and the large deepness reached by the 0.05 and 0.005 MRMV thresholds). A relatively homogeneous layer of low resistivity ($1 < r < 10 \text{ k}\Omega\text{m}$) appeared in most of the tomograms. Layers displaying resistivities higher than $10 \text{ k}\Omega\text{m}$ were very localised. In PC 1, the central zone situated downslope the four western lakes was conductive ($< 5 \text{ k}\Omega\text{m}$). In contrast, the resistivities were comprised between 10 and $80 \text{ k}\Omega\text{m}$ below 5 m depth in the push moraine located at the West part of the profile. They reached up to $2500 \text{ k}\Omega\text{m}$ in the South-East depression connected to the western debris-covered glacier tongue. PC2 crossed an active rock glacier. Resistivities between 10 and $50 \text{ k}\Omega\text{m}$ were measured below 6 m of superficial conductive material. Finally, a 20 m thick layer with resistivities $> 30 \text{ k}\Omega\text{m}$ appeared in the lower NE end of the central debris-covered glacier zone (PC 6).

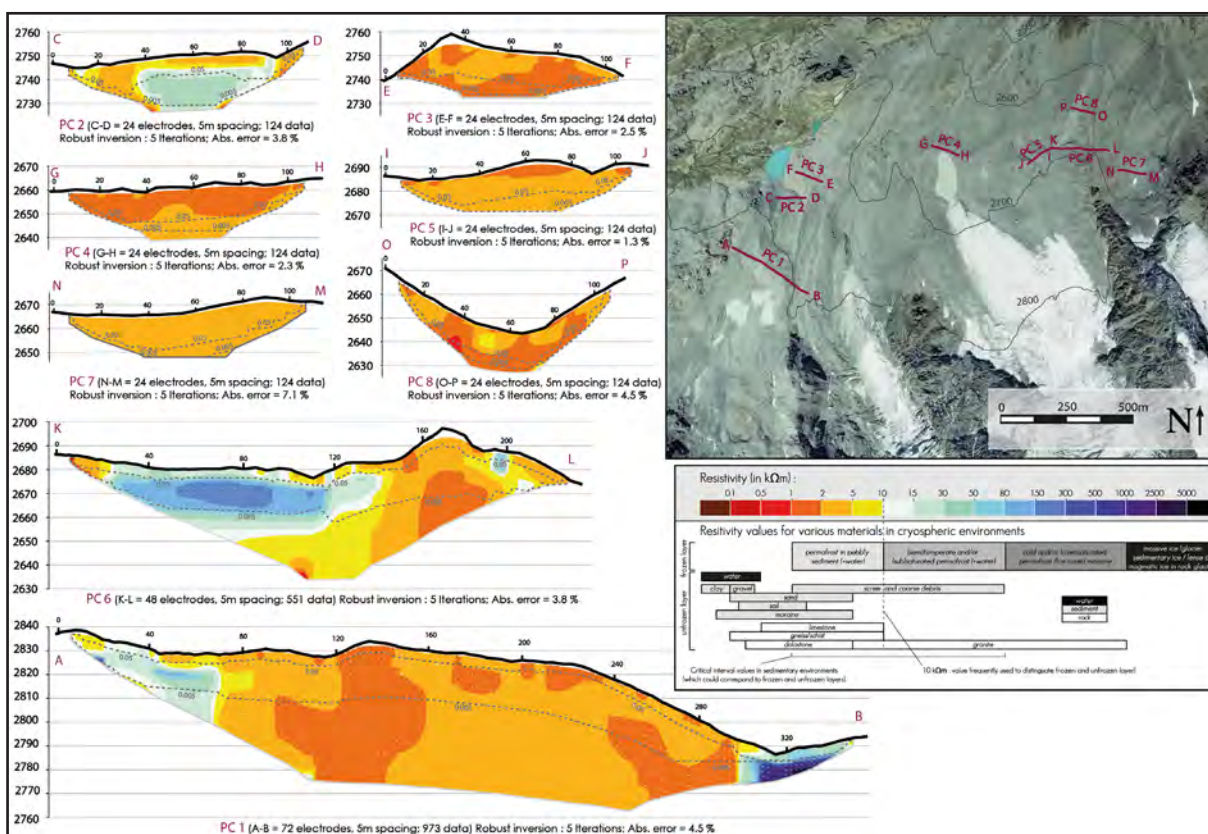


Fig. 3.85. Electrical resistivity tomograms measured in the Petit Combin glacier system on September 2 and 3, 2014. Reproduced from Darbellay (2015).

3.7.2.2. Photogrammetry and image analysis at decadal timescale

Elevation changes and surface horizontal velocities were investigated at decadal timescale by comparing orthorectified aerial images of 1964, 1983, 1999 and 2005 (Fig. 3.86 and 3.87). During the 1964 to 1983 period, cold air temperature allowed the accumulation of large amount of snow in the Petit Combin glacier. It induced a positive mass balance of ~ 0.19 m w.e. a^{-1} and the overall volume gain reached 4.7×10^6 m^3 (Fig. 3.86A). Elevation gains were observed on almost the entire glacier surface and maximum rises (up to 20 m) occurred in the three advancing main glacier

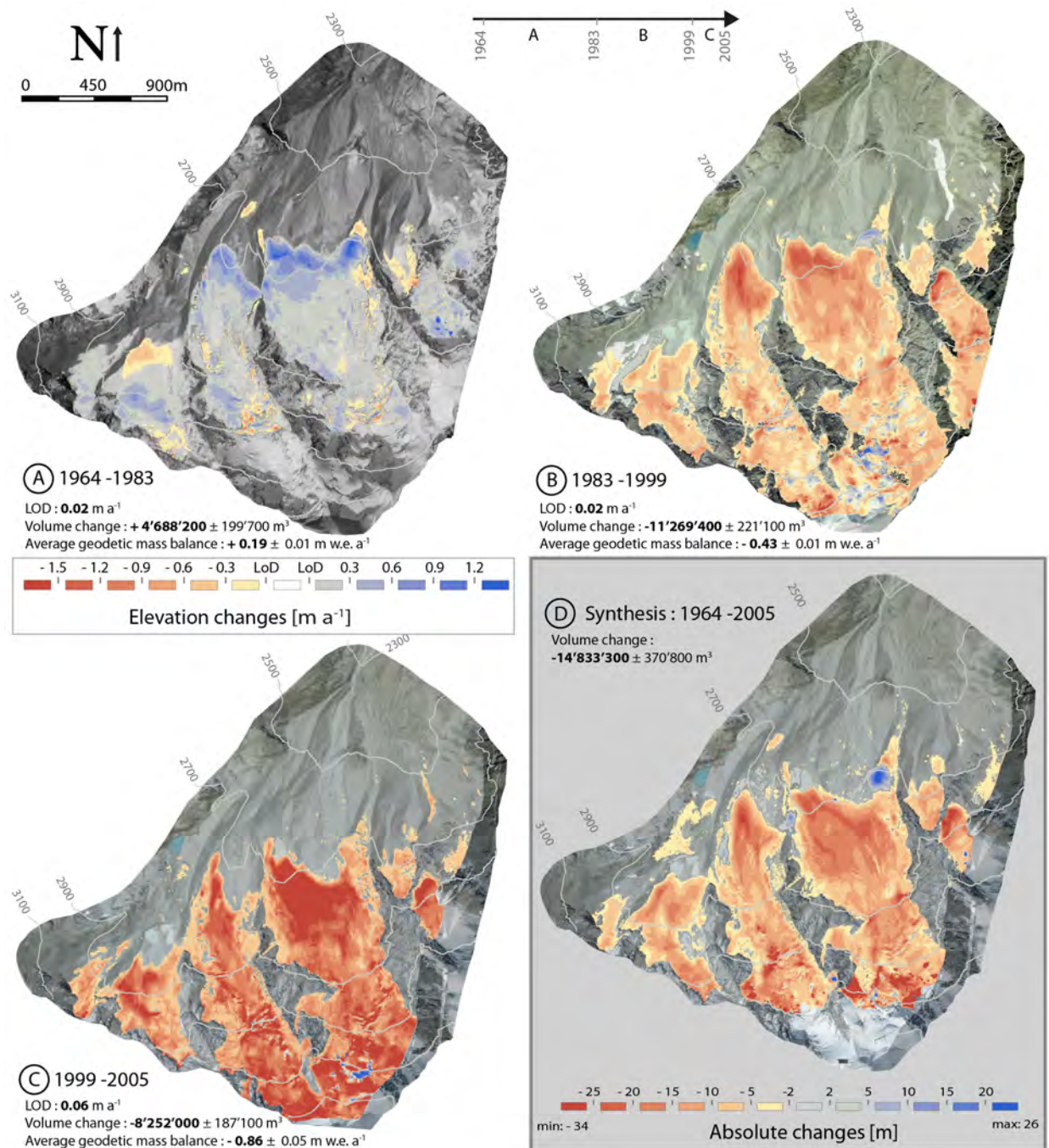


Fig. 3.86. Elevation changes extracted from the comparison of DEMs derived from archival aerial photogrammetry. We computed the average geodetic mass balance according to the methodology presented in the section 2.3.2.3 (Paper 3). These values have to be considered as rough estimations because the photogrammetric results can contain uncertainties in the upper steep zone (see Micheletti et al. 2015b; Darbellay, 2015) and the glacier area was approximated. However, their consistency with regional and alpine-scale values (Fig. 3.89) indicates that these averaged geodetic mass balances provide very realistic orders of magnitude. Adapted from Darbellay (2015).

tongues. Whereas the lower fourth of the glacier surface was partly debris-covered in 1964, the glacier was mainly debris-free in 1983. Its surface was then also more concave and crevassed. During this period, surface lowering affected only limited areas in the lower zone and can be related to ice avalanches in the upper serac zones. The periods 1983-1999 and 1999-2005 largely contrasted with this first positive period and surface lowering became generalised (Fig. 3.86B-C). Cumulated losses were respectively -11.3 and $-8.3 \times 10^6 \text{ m}^3$, corresponding to mass balances of ~ -0.43 and $-0.86 \text{ m w.e. a}^{-1}$. During these periods, the glacier tongues retreated and became covered by a thin and discontinuous debris layer. Except elevation gains in the eastern part of the main glacier tongue and in the serac zones, surface lowering was observed on the entire glacier surface. This process intensified between 1999 and 2005, and its magnitude exceeded 1.5 m.a^{-1} on most of the glacier. At the 41-year timescale (Fig. 3.86D), elevation loss largely dominated in the Petit Combin glacier system. The volume loss was $-15 \times 10^6 \text{ m}^3$, which corresponds to up to 30 m of lowering in some zones. The upper steep glacier zones and the lower tongues were particularly affected. Conversely, a very localised zone gained $> 20 \text{ m}$ in the eastern part of the main glacier tongue and few meters of rise was observed in the western rock glacier front and in moraines. Whereas the loss was mainly related to ice and snow melt, gains could be related to debris deposition, ice formation and increase of compressive stress related to ice flow.

The horizontal surface velocities were measured by the tracking of large boulders visible on aerial images (Fig. 3.87). Between 1999 and 2005, the fastest velocities ($> 1 \text{ m.a}^{-1}$) were detected in all the eastern part of the main tongue. Except one block located at its root, the rock glacier located at the East of the system had horizontal velocities slower than 1 m.a^{-1} . Four active zones were evidenced between 1964 and 2005 in the western margin of the system (Fig. 3.87: map and velocity evolution inset): the upper debris covered zone had the fastest velocities and accelerated progressively to up to 1 m.a^{-1} until 2005. The push-moraines zone flowed slowly towards the four lakes and velocities decreased here over time. The distal zone of the push-moraines had a regular 0.4 m.a^{-1} flow whereas the rock glacier tongue was mostly active in the frontal zone and accelerated to 0.4 m.a^{-1} in the 2000s.

3.7.2.3. Results interpretation and synthesis

Considering the moraine ridges and the erosion patterns in recently deglaciated rockwalls, **the LIA area of the Petit Combin glacier complex was $\sim 3.95 \text{ km}^2$ (Fig. 3.88). Most of the backwalls were ice-covered** and were comprised in the accumulation area. The drainage (and avalanche) ratio was thus close to zero for this glacier. Nevertheless, because of the steepness of most of the upper half of the system ($> 45^\circ$), the **redistribution of snow/ice** from hanging glaciers, ice aprons or the small ice-free rockwalls by avalanching probably always played an active role in the accumulation processes of this glacier. Contrasting with the glacier tongue stereotype, **the glacier front was composed by six distinct lobes during the LIA**. This situation is due to the **distinctive accumulation basin**. Moreover, Holocene glacier fluctuations in high relief environments contributed to built lopsided sediment stores when the sediment transfer toward hydrosystem was inefficient (e.g. Benn et al., 2003). Glaciers thus successively advanced in **large sediment store that canalised and sometime separated the ice flow**. Multilobate glacier ter-

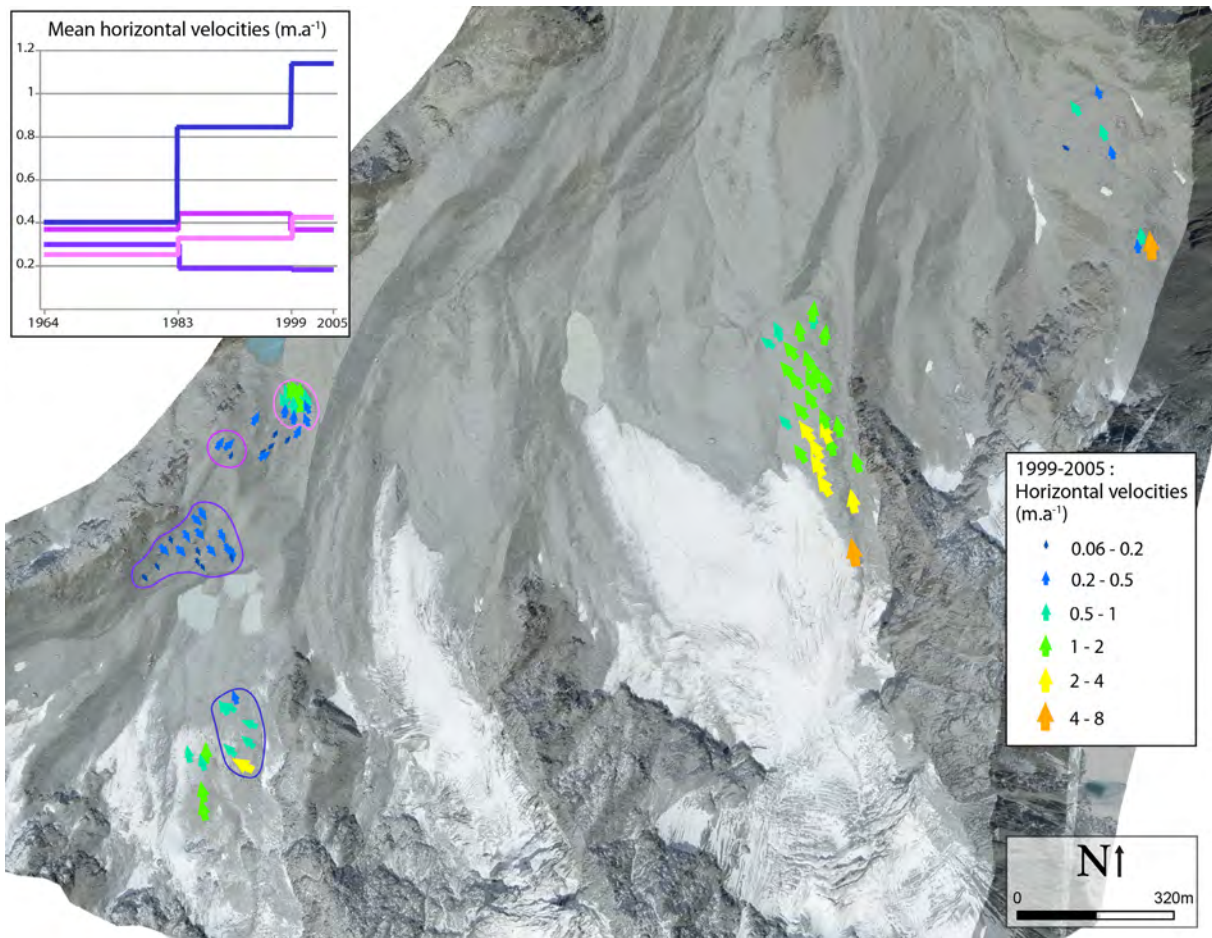


Fig. 3.87. Horizontal velocities derived from feature tracking on the orthorectified aerial images. Modified from Darbellay (2015; background aerial image; © Swisstopo 2005).

minus are thereby very common in Holocene debris-covered glacier systems, as the Petit Combin (Iturrizaga, 2013).

The increase of air temperature induced a **general glacier shrinking since the LIA (Fig. 3.88)**. **Both terminus retreat and outcropping of the upper rockwalls occurred due to the glacier thinning.** It induced the **progressive disintegration of the glacier complex**. Considering all the upper extent of sedimentary ice, **the current glacier surface is ~ 1.93 km², corresponding to 49% of the LIA area.** **The drainage (and avalanche) ratio increased to 0.32 in relation with backwalls deglaciation.** It illustrates that snow redistribution processes enhance the accumulation at the backwalls feet, where many avalanche cones are present. The high and steep surrounding relief also contributes to limit the snow and ice melt. Indeed, the mostly north-facing rockwalls influence the surface energy balance because their **shadows reduce direct solar radiation on glacier surface**. Moreover, due to the erosion of the backwalls, **the glacier tongues are now partly or fully debris-covered**. Comparing the 1999-2005 surface lowering rates in debris-covered and debris-free areas of the two main glacier tongues, Darbellay (2015) showed that this rate was reduced by 40 to 50 % in the areas covered by a continuous and decimetres thick debris layer. This range is slightly higher than the 30 to 40 % of lowering reduction typically measured in debris-covered glaciers (e.g. Takeuchi et al., 2000; Nicholson and Benn, 2006; Kellerer-Pirklbauer et al., 2008; Brock et al., 2010). It shows that the debris mantle in the Petit

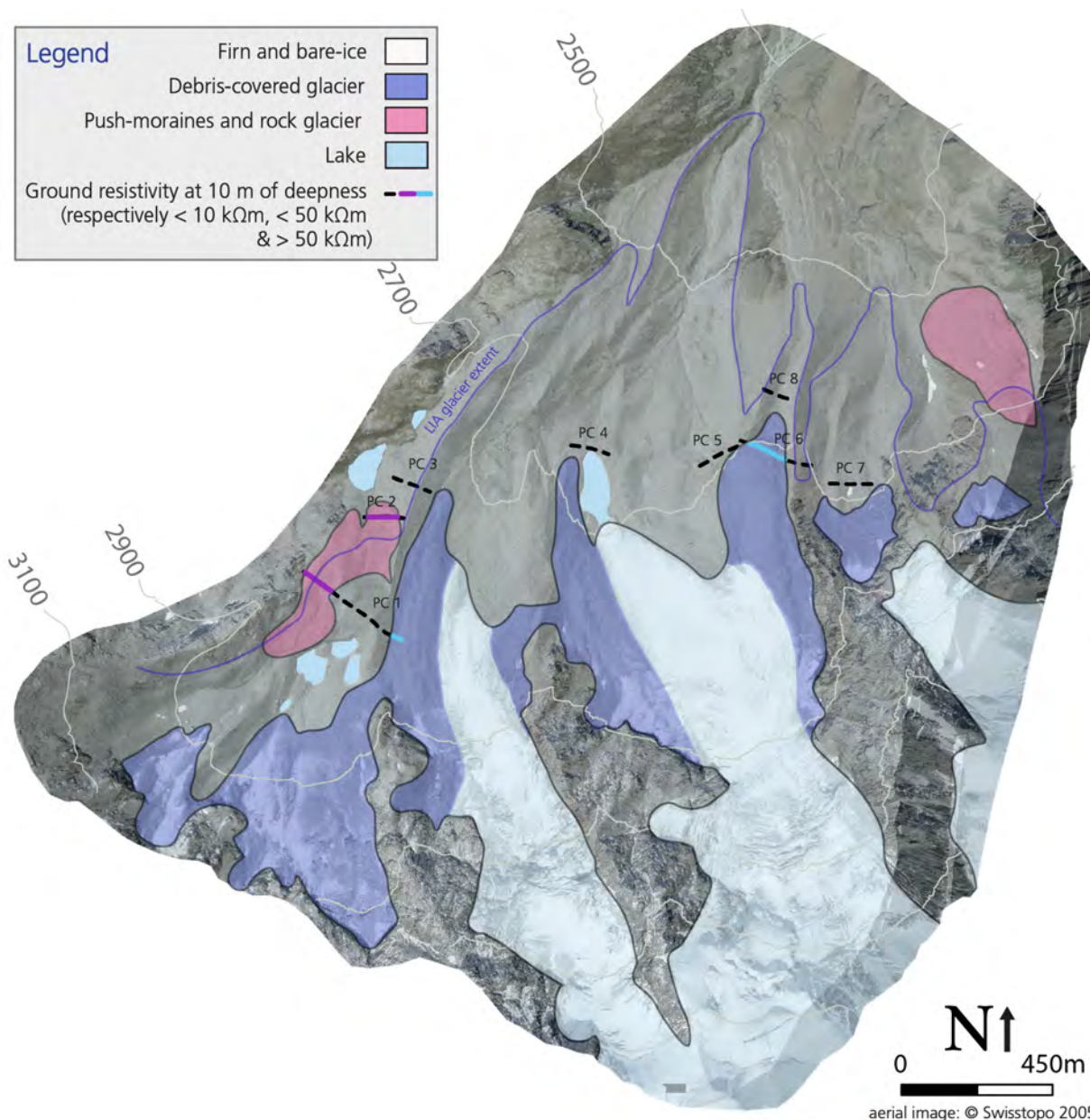


Fig. 3.88. Current ground ice distribution and LIA glacier extent in the Petit Combin glacier system. Modified from Darbellay (2015).

Combin glacier insulates relatively efficiently the ice from the warming atmosphere. Nevertheless, in 1964, 1983 and 1995, most of the glacier tongues were ice-free or covered by a thin and discontinuous debris layer. Studies have shown that such layer can increase the ablation rate and thus the climate sensitivity of glaciers (e.g. Zhang et al., 2011). **The decadal mass balance variations of the Petit Combin glacier fit well with regional glaciers** and alpine-scale situations and losses accelerated since the 1980s (Fig. 3.89). It highlights the **strong control of climate and particularly of air temperature on this glacier**. The atypical temporal and spatial behaviour observed in Tarmine glacier (sections 2.3 and 3.5) did not appear in the Petit Combin at the glacier-scale. Although the controls of topography, debris cover and permafrost conditions could have recently increased on this glacier that became smaller, debris-covered and more sensitive to snow redistribution processes, their influence on its behaviour remained minor in the last decades.

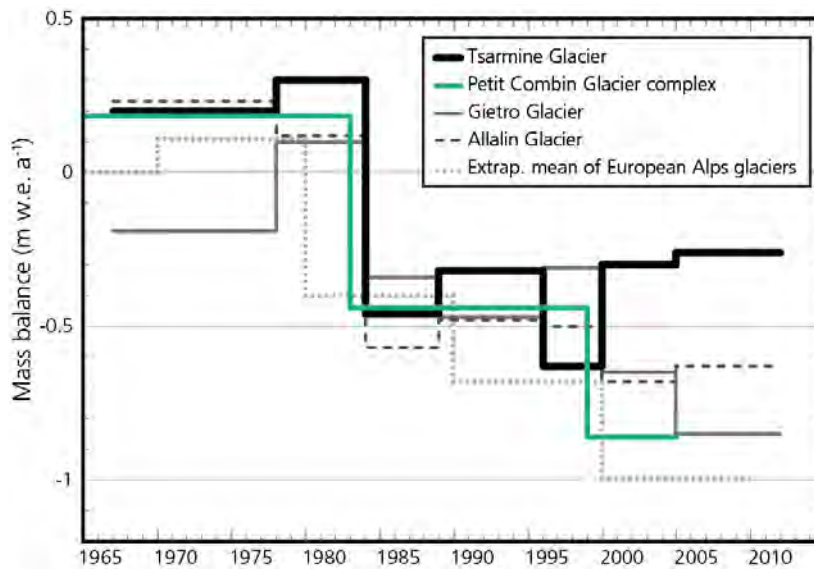


Fig. 3.89. Average geodetic mass balance of the Petit Combin Glacier, of Tsarmin Glacier (section 2.3; Capt et al., 2016), average glaciological mass balance of Gietro and Allalin glaciers (location on Figure 2.20a, Huss et al. 2015) and extrapolated decadal mean of the glaciers of the European Alps (Huss, 2012). The values obtained for the Petit Combin have to be considered as rough estimations (see caption of the Fig. 3.86).

According to the weak to null surface movements detected in the past decades (Fig. 3.86 and 3.87), the low resistivity values (Fig. 3.85), the presence of lakes and surface runoffs, and the development of pioneer vegetation, **ground ice seems currently absent in most of the sedimentary margin of the Petit Combin system** (Fig. 3.88). This situation is probably related to the generalised **temperate thermal conditions at the base of the former glacier**. Indeed, the presence of some fluted moraines indicates past water circulations at the glacier sedimentary bed (Fig. 3.83). Studies have showed that such basal conditions are unfavourable for ground ice preservation (e.g. Kneisel, 2003; Delaloye, 2004). Moreover, **large amount of water was produced** during the post LIA glacier retreat and can also contributed to hinder the ground ice conservation in the distal zones. A particular situation was observed in the eastern part of the main tongue: whereas surface lowering was generalised since the 1980s, this zone uplifted (Fig. 3.86). We mainly attribute this process to the influence of the debris. Indeed, the rockwalls that dominates this glacier zone was one of the only upper ice-free zone in 1964. The debris supply within the crevasses and on the glacier surface was thus important here in comparison to the rest of the system. Ice was thus efficiently insulated from atmosphere and also probably contain a noticeable concentration of debris. The thickness of the supraglacial layer could even be similar to those of the permafrost active layer. As also observed in the centre of Tsarmin at decadal timescale (sections 2.3 and 3.5), **the migration of the mass accumulated in the 1960s-1980s period and associated compressive stress increase induced an uplift in this heavily debris-covered glacier zone**. This mass transfer generating the bulldozing of older glacier ice and/or debris. A steep fine-grained front, that have **a typical rock glacier front** morphology, **appeared in the 1980s** (Fig. 3.90). The formation of this front illustrates the advance of an ice-debris mixture in stagnant moraine deposits. If ground ice preservation and the movements detected here continues (PC6 in Fig. 3.85, and Fig. 3.87), **this zone could pursue its transformation into a rock glacier and develop viscous morphology**. Shroder et al. (2000) and Monnier and Kinnard (2015) documented a similar formation of rock glacier fronts and thus the transition from a heavily debris-covered glaciers toward rock glaciers in the last decade. Two others glacier-permafrost interactions were observed at the western and eastern margins of this system.



Fig. 3.90. Picture of the rock glacier front that formed recently in the eastern side of the main glacier tongue (© Darbellay, 2014)

These two zones can be considered as Holocene push-moraines – rock glacier system. During the positive mass balance periods (as the LIA), the deformation of these zones by the glacier advances generated push moraines. However, the distal ice-debris mixtures were not or poorly affected by these deformations and by glacial meltwaters circulations. In the negative mass balance periods, the differential ablation dynamic induced the disconnection with the upper glacier. Sedimentary ice could have been integrated in the flowing ice-debris mixture. According to climatic oscillations, positive and negative mass balance periods succeeded during the last millennia and contributed to shape these landforms. Their development is restricted to the areas where glacier dynamics and associated water circulation were relatively weak and allowed the long term preservation and deformation of ground ice.

4. Main outcomes and discussion



I | Les Rognes and Griez glacier systems (© P. Deline, 08.2012)

4.1. Introduction

In this chapter, we synthesize the results obtained in the study sites, and discuss them regarding the existing literature. The main outcomes presented in the publications and study sites chapters (respectively part 2 and 3) are gathered in the [Tab. 4.1](#) and [4.2](#).

According to the results, the investigated sites have both common and particular characteristics. For example, except the Chaltwasser system (see discussion below), the same components and spatial organisation have been observed. Current dynamics appeared strongly controlled by the concentration of ice and its deepness in debris-covered areas. The same main active processes were observed in each site. However, their magnitude varied in each individual system, as they are controlled by the geometry of the dynamical zone and very local topographical and environmental parameters. Moreover, some of the investigated sites still contain an active glacier that have both accumulation and ablation areas whereas only buried, poorly active, remnant glaciers are present in other sites. These results as well as main common and particular characteristics are discussed below. We first detail and discuss the current internal structure and dynamics observed (section 4.2). A model of genesis and evolution of glacier systems in high relief and permafrost environments (section 4.3) is proposed thereafter.

Article (topic and study site)	Main outcomes
1. Rognes and Pierre Ronde glaciers and associated geomorphic systems (section 2.1)	<ul style="list-style-type: none"> Both study sites are active geomorphic systems but, because of the topography and the weak magnitude of processes, they are poorly connected with downslope systems. Large amount of debris were accumulated during the Holocene, especially where the backwalls were mostly ice-free during this period. The concentration of ground ice is different in les Rognes and Pierre Ronde. This is mainly due to the influence of topography (elevation, & aspect), the supraglacial debris cover and past water circulations. The front of les Rognes illustrates the continuum that exists between glacial and periglacial morphodynamics.
2. Internal structure and current dynamics in les Rognes, Entre la Reille and Tsarmine (section 2.2)	<ul style="list-style-type: none"> Five components, with different internal structure, were present in all the study sites: firm and bare-ice glaciers, debris covered glaciers, heavily debris-covered glaciers of low activity, rock glaciers and ice free debris. Contrasted responses to short-term climatic variations were observed in these components, mainly in relation with variations of superficial debris layer thickness, and of the concentration of ice, debris and water. Debris-covered glaciers are particularly active in summer and experience both downslope movement and surface lowering, whereas rock glaciers have mostly a constant and slow creep. Glacier-permafrost interactions were observed in the system margin where the debris concentration increases. Les Rognes and Entre la Reille are inherited weakly active glaciers whereas Tsarmine is still an active glacier.
3. Decadal evolution of the Tsarmine Glacier (section 2.3)	<ul style="list-style-type: none"> Both negative and positive elevation changes were observed in the Tsarmine glacier over the last decades. They were especially related to accumulation and ablation of snow/ice in relation with the climatic variations, mass transfer and to the influence of the debris cover. Particular spatial (inversion of ablation gradient) and temporal (mass balance divergence since the 2000s) behaviour occurred in Tsarmine compared to other local glaciers. They are due to the influence of the debris-cover, permafrost conditions and topography upon snow/ice accumulation and ablation. Tsarmine becomes a poorly active buried ice masse and less sensitive to climatic variations. It could slip in two entities in future decades. The mean glacier thickness is 15 m and the glacier volume is $4 \times 10^6 \text{ m}^3$. A third of its initial volume ($4 \times 10^6 \text{ m}^3$) melted between 1967 and 2012 corresponding to a mass balance of $-0.15 \text{ m w.e. a}^{-1}$.

Tab. 4.1. Main outcomes presented in the three articles

4.2. Current internal structure and dynamics

4.2.1. System components, organisation and size

The [Fig. 4.1](#) synthesises the internal structure of each investigated system. Snow, ice, water, sediment and bedrock are observed at their surface. Except the Chaltwasser complex (see discussion below), they are assemblages of three main components, whose internal structure and current dynamics are presented and discussed in the section 4.2.2: (1) a glacier (a flowing body of sedimentary ice that could be covered by snow and/or debris), (2) one or several push moraines-rock

Study site	Main outcomes
Rognes and Pierre Ronde (section 3.2)	<ul style="list-style-type: none"> • Large part of Les Rognes system still contains ground ice whereas Pierre Ronde is mostly ice-free. As a consequence, larger surface dynamics (downslope flow and surface lowering) were observed in les Rognes. Surface lowering was especially rapid in the upper debris-covered glacier of les Rognes (> 50 cm.a⁻¹). This sector was mainly active in summer and especially in early summer. The contrasted situation encountered in the two study sites is mainly related to topography (elevation and aspect), past water circulations and the influence of the debris cover in the distal part. • The front of les Rognes illustrates the continuum that exists between glacial and periglacial morphodynamics.
Les Fours (section 3.3)	<ul style="list-style-type: none"> • Presence of very small inherited glaciers in a fully debris covered slope. • Despite the extended local presence of ground ice, slow surface velocities were measured (< 30 cm.a⁻¹). • The local distribution of glaciers and rock glaciers is mainly related to topography; the presence of small shaded cirques where avalanches accumulated large amount of snow allowed the glaciers development while active rock glaciers developed in steeper areas.
Entre la Reille (section 3.4)	<ul style="list-style-type: none"> • Very small inherited glacier associated with a distal rock glacier. All the glacier and rock glacier zones still contain ground ice and are active. • A strong acceleration of surface velocities occurs in summer. Air temperature appear as the major climatic control. • Surface activity can be very localised according to the Lidar results. • The distal rock glacier illustrates the continuum between glacial and periglacial morphodynamics.
Tsarmine (section 3.5)	<ul style="list-style-type: none"> • Small cirque debris-covered glacier system with a restricted upslope accumulation area. • The glacier tongue had a downslope movement faster than 50 cm.a⁻¹. In addition to internal deformation, basal sliding very likely occurs in relation with hydrological forcing during the melt season. Emergence velocity was measured in winter in the debris covered glacier tongue but elevation changes were negative at annual timescale (10-50 cm.a⁻¹), illustrating the ice melt below the debris. • Ice cliff backwasting occurs very locally. This process induces rapid ice melt compared to downwasting. • Tsarmine glacier becomes a poorly active buried ice masse • Recent glacier-permafrost interactions occurred in the rock glacier roots and glacier ice has probably been integrated in the flowing ice-debris mixture.
Chaltwasser (section 3.6)	<ul style="list-style-type: none"> • Existence of three small glaciers related to the disintegration of the Chaltwasser glacier complex. • The mass variations of the two mostly bare-ice glaciers (Chaltwasser and Homattu glaciers) appeared strongly controlled by air temperature variations over the last decades. These ice masses will probably largely melt in the next decades. The stagnant Chaltwasser terminus is covered by a meter thick debris layer. The several decimetres of annual surface lowering indicated rapid ice melt here. • The Hubschorn glacier is a buried ice mass. Its lifespan seems longer because avalanching strongly increases the snow accumulation and because shadow effect and the extensive debris mantle limit the ice melt. • The Holocene moraines deposits are largely ice free, especially in relation with subglacial and postglacial water circulations.
Petit Combin (section 3.7)	<ul style="list-style-type: none"> • Existence of several disconnecting glaciers related to the disintegration of the Petit Combin glacier complex. • The decadal glacier elevation changes were strongly controlled by regional climate and especially air temperature. Snow redistribution, shadow effect, the presence of a debris cover and permafrost conditions only secondarily influenced the decadal mass changes at the glacier scale. • Recent glacier retreat was fast and the debris cover extended on the glacier tongues. • Marginal push-moraines – rock glaciers illustrate the Holocene glacier-permafrost interactions. An heavily debris-cover glacier zone might be transforming into a rock glacier • The large Holocene moraines deposits are mostly ice free, especially in relation with subglacial and postglacial water circulations.

Tab. 4.2. Main outcomes obtained in the study sites

glacier complexes (creeping ice-debris mixtures having a viscous morphology) and (3) mostly ice-free and poorly active debris accumulations. The glacier occupies the upper and central position whereas ice-free debris and rock glaciers are present in the lower margins. The same three main components and spatial organisation are found in similar systems elsewhere in the world (e.g. Reynard et al., 2003; Ribolini et al., 2010; Monnier et al., 2014; Dusik et al., 2015).

4.2.1.1. Complex associations of ice, debris and water

The studied systems have several particularities that differentiate them from other glacier systems: debris layers cover large part of the glacier surfaces, large amount (lopsided compared to the glacier size) of sediments is accumulated in the margins and, as a consequence of permafrost conditions, active rock glaciers have formed in some of the margins. Moreover, bedrock outcrops in former ablation areas are very rare, except in the centre of the Chaltwasser system. Maisch et al., (1999) and Zemp et al. (2005) showed that the domination of basal erosion or sediment deposition in ablation areas depends on the sediment balance in the glacier catchment (the ratio between debris input from the rockwalls and the debris evacuation by the meltwater streams). As found in most of small swiss glaciers (Maisch et al., 1999), the absence of efficient debris

evacuation by glacial and fluvio-glacial processes explains the development of sedimentary beds below the glaciers over the last millennia. As a consequence, no basal glacial erosion was active in the lower zones of these systems where debris were accumulated. The latter originate mainly from the erosion of the ice-free surrounding relief and secondarily from basal erosion in the accumulation areas. This situation is usually encountered in cirque and valley glacier systems in high relief environments where glaciers accumulated large sediments amount at their bases and margins (e.g. Kirkbride, 2000; Benn et al., 2003; Iturrizaga, 2013). Even if estimations of sediment volume were proposed in les Rognes and Pierre Ronde (section 2.1; Tab. 2.2), quantification of the sediment stores in each system remains a challenging task that requires data on bedrock topography and debris concentration in the ice bodies. Nevertheless, debris accumulations often reach several tens of meters of thickness. Individual sediment stores in these systems are thus likely ranging between 10^5 of m^3 for the smallest sites (Entre la Reille and les Fours) and 10^7 of m^3 in Petit Combin system. Same orders of magnitude have been proposed in the few studies that, to our knowledge, investigated the sediment volume in similar landsystems (e.g. Barsch and Jakob, 1998; Otto et al., 2009; Gärtner-Roer and Nyenhuis, 2010).

Current ice distribution differs in the study sites (Fig. 4.1). Surface or ground ice is still largely present in some systems (les Rognes, les Fours, Entre la Reille, Tsarmine) and its spatial distribution remains close to the LIA extent. Nevertheless, the domination of concave topography between perched historic moraine accumulations indicates a significant ice volume decrease since the LIA. In Pierre Ronde, the Petit Combin and Chaltwasser systems, ice has already disappeared in more than the half of the initial surface, illustrating a fast ice decay after the LIA, especially in the lowest zones. The heterogeneous ice distribution observed in the study sites highlights their different responses to climate forcing. Ice melt rate strongly varies between sites and within individual system, depending especially on the debris-cover thickness, shadow effect, snow redistribution, englacial debris concentration and water circulations. The study sites illustrate thus different stages of glacier systems evolution in the current deglaciation context. Similar contrasted situations showing both large preservation and absence of ice are reported for glacier systems in permafrost environments (e.g. Kneisel, 2003; Ribolini et al., 2010; Monnier et al., 2014; Janke et al., 2015). Even if the Chaltwasser and the Petit Combin systems showed severe retreats, an accumulation area is still present and cryogenesis remain active in these sites, as in Tsarmine. In contrast, the other sites have very restricted or null accumulation areas and are, thereby, inherited ice masses.

Circulation of water was observed (or at least heard) during the summer field investigations in all the study sites. Nevertheless, meltwater streams are only present at the surface of the two largest sites (Petit Combin and Chaltwasser, Fig. 4.1) during the melt season. Few data were collected on the water circulations in the small studied sites but they seemed to support the findings of Pourrier et al. (2014). Water transfer appears fast and concentrated in the debris-covered glacier zones according to the lake level variation in Tsarmine and observations in supraglacial gullies. Water circulation seems conversely underground, slow and diffuse in the marginal ice-free debris and ice-debris mixtures. As a consequence, no surface runoffs were observed and water circulation was rarely heard in these sectors. Some seasonal springs are present tens to hundreds

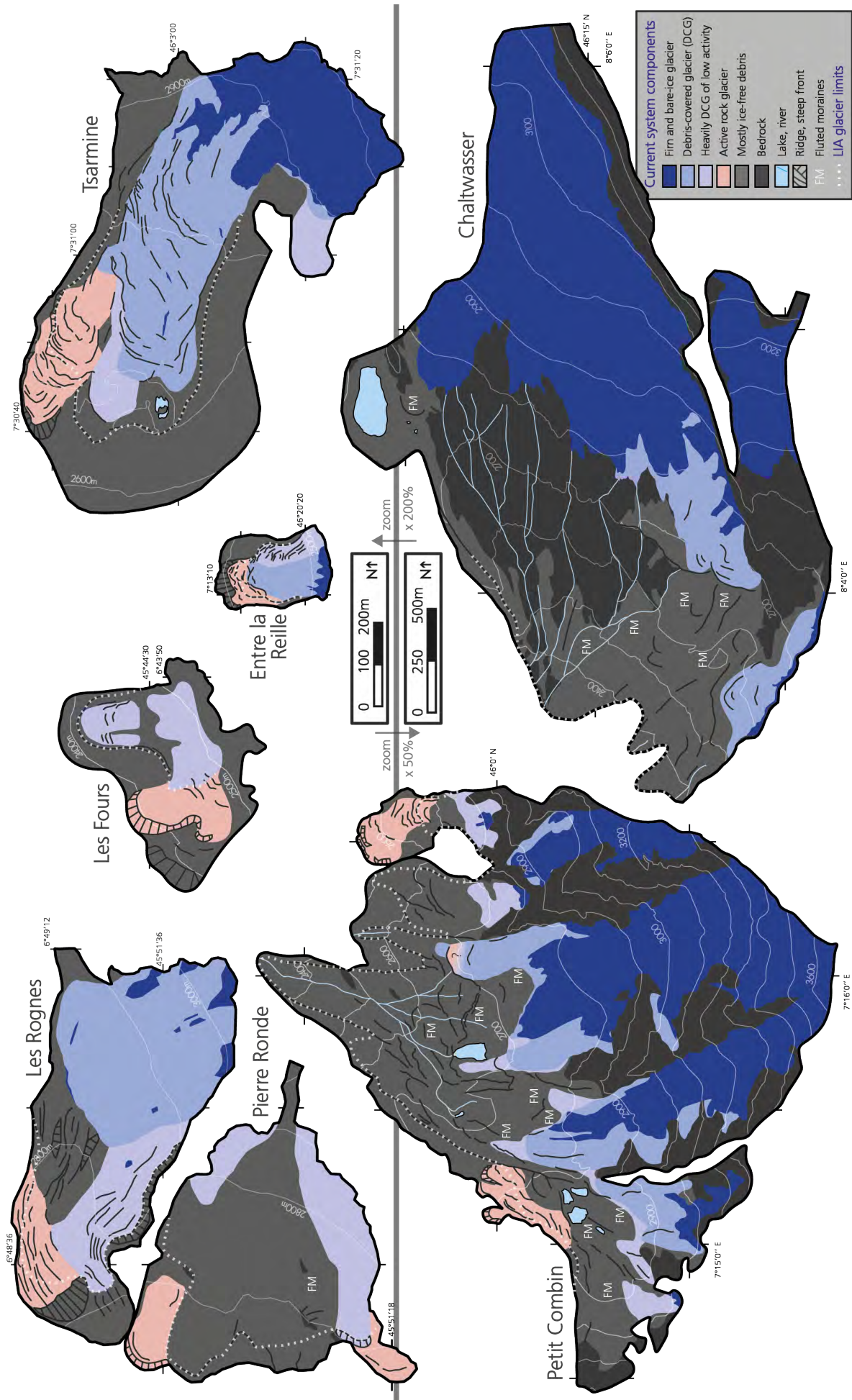


Fig. 4.1. Synthesis of the internal structure in the seven studied systems. The scale is two times larger for the Petit Combin and Chaltwasser systems.

meters below the margins of the systems. Despite the fact that supraglacial and proglacial lakes are common in debris-covered glacier systems in permafrost environments (e.g. Kääb et al., 1997; Ribolini et al., 2007; Monnier et al., 2014), proglacial moraine-dammed lakes were only present in the sedimentary margins of Tsarmine and the Petit Combin system. Most of the area of the studied glaciers were steeper than 15° (Tab. 4.3), which probably explained the absence of supraglacial ponds.

4.2.1.2. Definition and size of SDCGSAPE

The objects of study of this thesis are the SDCGSAPE. These glacier systems were defined in the first chapter of this contribution (1.2.4). However, the Petit Combin and Chaltwasser systems does not completely fit with the definition proposed: only a minor area of the current surface of these glaciers is covered by debris (Fig. 4.1) and the area of glaciers is > 1 km², exceeding some thresholds used in the literature to define small glaciers. In addition, the Chaltwasser glacier system is also different from the other study sites because except the western and northern moraines accumulations, the sediment store is relatively limited. Most of the surfaces of the Chaltwasser and Homattu glaciers are debris-free and abraded bedrock is exposed in areas where they recently retreated. The relatively low accumulation of debris in this system, especially in comparison with the very large accumulation deposited in the margins of the Petit Combin system, which has the same area, is mainly due to the limited area and elevation range of local rockwalls. Indeed, except the 500 m high Hübschorn North face, the glaciers backwalls have relatively restricted size and height (< 300 m). Moreover, according to historic maps, photographs and observation of fresh patterns of glacier abrasion, ice aprons largely covered backwalls during the Holocene cold oscillation, as the LIA. The production of debris was thus relatively limited at the system scale, whereas it was high in the Petit Combin and induced the development of large moraine deposits that confined the glacier. In addition, as explained in the section 3.6.2, the LIA glacier terminus was located between 2300 and 2400 m a.s.l. in a slope steeper than 25°. Hence, frontal deposits were reworked by fluvio-glacial and torrential processes, explaining the limited sediments accumulated in this area. The sediments evacuation from this site, even partial, contrasts thus with the situation observed in the other systems. Except rare mobilisations of debris during extreme hydrological events in Pierre Ronde, Tsarmine, and the Petit Combin systems (indicated by the presence of gullies in the distal parts), these systems are strongly decoupled from downslope geomorphic systems. Large amounts of sediments were, therefore, trapped within them over the last millennia. Finally, the thermal conditions at the LIA glacier front also differentiate the Chaltwasser system from the smallest studied systems. According to permafrost distribution models (BAFU, 2005; Boeckli et al., 2012), the occurrence of permafrost conditions seems unlikely in this zone, which is below the local limit of the periglacial belt. Therefore, even if a large amount of debris had accumulated here during the Holocene, the development of a rock glacier would have been very unlikely. Contrasting with the others study sites, the Chaltwasser system shows thus how differences in debris concentration and permafrost conditions can induce the formation of distinct type of glacier system. The influence of these controls (especially debris input/output and permafrost conditions) will be developed in section on the glacier system evolution model (section 4.3).

According to the definition proposed earlier, the LIA glacier complexes of Chaltwasser and the Petit Combin were not SDCGSAPE. Indeed, they were large assemblages of mostly bare ice glaciers. However, the Holocene push moraines and rock glaciers present in the western and eastern margins of the Petit Combin system show that two components of this glacier complex, respectively the Boveire-Lâne and the Avouillons glaciers, were SDCGSAPE. Moreover, because of the recent glacier shrinking and extent of supraglacial debris cover, several glacier tongues of the Chaltwasser and Petit Combin systems have become heavily debris-covered and a rock glacier front even appeared recently in the eastern part of the main Petit Combin glacier tongue (3.7.2). These parts of glacier complexes can be considered as SDCGSAPE. According to the results obtained, they have the same general internal structure characteristics and current dynamics than the small investigated systems. This illustrates how the number of SDCGSAPE increases during negative mass balance context, with the fragmentation of glacier complexes in high relief and permafrost environments.

As mentioned in the state of knowledge section (1.2.1.2), the classification of glaciers as very-small, small, medium or large glaciers according to surface area thresholds remains an open and delicate question in glaciology. Les Rognes, Pierre Ronde, les Fours, Entre la Reille and Tsarmine are smaller than 0.5 km² and can be classified as very small glaciers (e.g. [Huss and Fischer, 2016](#)). We consider this order of magnitude as interesting in high relief environments because it allows to distinguish the weakly active cirque or valley glaciers where surrounding relief can strongly in-

	Glacier type	Current area (km ²); % of LIA extent	Aspect	Elevation range (m a.s.l.)	Mean glacier thickness (m)	Mean slope along central flowline (°)	Ice volume (m ³)	Water equivalent (m ³)	Accumulation area	Maximum backwall height (m)	Drainage area (in km ²)	Drainage ratio	Main control
Les Rognes	Buried remnant of a cirque glacier	0.15 (37)	N	2800-3100	14 ^a	32	2'500'000 ^b	2'250'000 ^c	No	100	0.04	0.28 ^d	(CC→) TC
Pierre-Ronde	Buried remnants of a cirque glacier	0.07 (20)	NW	2720-2930	11 ^a	46	850'000 ^b	770'000 ^c	No	200	0.11	- ^d	(CC→) TC
Les Fours	Buried remnants of a glaciere	0.03 (~ 60?)	N	2420-2530	8 ^a	22	310'000 ^b	280'000 ^c	No	100	0.08	- ^d	TC
Entre la Reille	Buried remnant of a glaciere	0.03 (90)	N	2430-2550	8 ^a	31	220'000 ^b	198'000 ^c	Very restricted	300	0.04	1.52	TC
Tsarmine	Debris-covered cirque glacier	0.25 (71)	NW	2715-3070	15	21	4'050'000 ± 400'000	3'645'000 ± 360'000	Yes	600	0.46	1.84	CC → TC
Chaltwasser	Mostly debris-free transection glacier	1.52	NW	2670-3270	33 ^a	15	58'000'000 ^b	52'200'000 ^c	Yes	300	0.29	0.19	CC
Hübschorn	Buried remnant of a cirque glacier	0.15	NE	2560-2820	14 ^a	37	2'500'000 ^b	2'250'000 ^c	Very restricted	500	0.18	1.21	(CC→) TC
Petit Combin	Complex of cirque and hanging glaciers	1.93 (49)	N	2660-3660	36 ^a	30	81'000'000 ^b	73'000'000 ^c	Yes	500	0.63	0.32	CC

Tab. 4.3. Main current characteristics of the studied glaciers. In the third column, the ratios of LIA extent are not given for the Chaltwasser and Hübschorn glaciers because they originate from the disintegration of a glacier complex. Except for the Tsarmine Glacier where GPR data were collected, ^a & ^b provide order of magnitude of mean glacier thickness and glacier volume using the scaling exponential relationships proposed respectively by [Chen and Ohmura \(1990: mean glacier thickness = 28.5 x area \(in km²\)^{0.357}\)](#) and [Bahr et al. \(1997: mean glacier thickness = 0.033 x area \(in km²\)^{1.36}\)](#). Nevertheless, these values have to be considered with caution. Indeed, very small glaciers have usually a large thickness to length ratio because of their lens shape ([Kuhn, 1995; Tab 1.1. and Fig. 1.26](#)) and each individual glacier geometry is particular. Thus, these scaling relations often under- or over-estimate the geometrical parameters of very small glaciers ([M. Fischer, personal communication](#)). ^c The water equivalent is simply the conversion of the ice volume using the density of ice factor 0.9 (i.e. 0.9 kg m⁻³: e.g. [Azócar and Brenning, 2010; Cuffey and Paterson, 2010](#)). ^d The drainage ratio of les Rognes is only a theoretical value because this glacier has no more significant accumulation area. This ratio is senseless for the remnant buried glaciers in les Fours and Pierre Ronde. Main control of recent glaciers evolution is also indicated. Obviously, the climatic control (CC) influences the current evolution of all glaciers. Nevertheless, topographical control (TC) and especially the influence of shading, snow/ice redistribution and accumulation of debris on the glacier surface can strongly limit the influence of the climatic variations. Past (in bracket) and present dominant control are illustrated with an arrow.

fluence the mass balance and dynamic from the larger and more active glaciers where the relative influence of topography decreases. However, it is important to bear in mind that these size-classes are only open orders of magnitude (see section 1.2.1.2). The same main processes affect all the glaciers, regardless their size, but orders of magnitude in processes intensity differ as a function of the glacier area and thickness. The threshold between small and medium glaciers, and thus the maximum area of SDGCSAPE, is less clear (1, 5, 10 km²? e.g. Pfeffer et al., 2014; Huss and Hock, 2015). Systems having the same components (debris-free and debris-covered glacier zones and marginal rock glaciers) and dynamics as the SDGCSAPE studied can reach an area of several km² in the periglacial environments of very arid regions on Earth (e.g. Ackert, 1998; Owen and England, 1998; Humlum, 2000; Bolch and Gorbunov, 2014; Monnier et al., 2011 & 2014; Janke et al., 2015). Nevertheless, to our knowledge, this kind of system very rarely exceed an area of 10 km². In mountainous environments, two processes could explain this system size limitation. Firstly, the tongues of the largest glaciers usually extend beyond permafrost environments (e.g. Pfeffer et al., 2014), which hampers the development of rock glaciers. Secondly, the largest glaciers often have a temperate thermal regime and large water circulations that limit the preservation of ground ice, even in permafrost environments. We suggest thereby 10 km² as a maximum area limit for SDGCSAPE but this threshold remains open and requires in-depth consideration in the future.

4.2.2. Main components and associated dynamics

4.2.2.1. Glaciers

Internal structure and morphology

- Sedimentary ice masses were observed and/or evidenced by geophysical surveys in all the studied systems (Fig. 4.1). No direct data were nevertheless collected on the Pierre Ronde remnants of glacier but small ice outcrops were visible on photographs taken in the last decades. Some of the physical characteristics of the studied glaciers are gathered in the Tab. 4.3 and our interpretation of their internal structure is synthetized in the Fig. 2.19.
- According to direct observations, ERT and GPR results, as well as results collected in similar landforms (Shean et al., 2007; Ribolini et al., 2010; Monnier et al., 2014; Janke et al., 2015), glaciers are essentially composed of sedimentary ice and have a low debris concentration. The ice thickness ranges from meters to tens of meters. The estimated ice volumes and water equivalent ($10^5 - 10^7$ m³; Tab. 4.3) are tiny compared to the volume accumulated in large glaciers (e.g. Huss and Hock, 2015). However, they are substantial water reservoirs at very local scale (Rangecroft et al., 2015; Huss and Fischer, 2016), and among the main local water sources in the weakly glacierized catchments as the ones of Entre la Reille, les Fours or Chaltwasser.
- Glacier ice can outcrop or being covered by snow or debris. A typical frontal and lateral increase of the debris-cover thickness and englacial debris-concentration was deduced from the marginal decrease of ground resistivities (e.g. Benn et al., 2003; Kirkbride and Deline, 2013). The supraglacial layer is mainly constituted by coarse and angular debris that show the passive

transfer of rockfall deposits on the glacier surface (e.g. [Clark et al., 1994](#)). The debris mantle thickness reached several meters downglacier, where ice outcrops became very rare. The marginal increase of debris concentration is especially due to the presence of debris-rich layers in these zones affected by compressive stress (e.g. [Kuhn, 1995](#); [Fukui et al., 2008](#); [Kirkbride and Deline, 2013](#); [Seppi et al., 2015](#)). As accumulation zones shrank over the last decades and the debris input increased in high relief environments ([Kirkbride and Deline, 2013](#); [Carturan et al., 2013b](#); [Deline et al., 2015](#)), large portion of the studied glaciers are now debris-covered. Pierre Ronde, les Rognes, les Fours, Entre la Reille and the Hübschorn can even be considered as buried glaciers because no or very limited upper debris-free areas exist ([Janke et al., 2015](#)). The non-representation of Les Fours, Pierre Ronde and Entre la Reille glaciers in historical maps and the few ice outcrops observed at their surface in old photographs indicates that these very small glaciers were probably always largely hidden under snow and debris layers. The dynamics of these thin ice masses were also likely too weak to induce the development of large crevasses at their surfaces (e.g. [Etzelmüller and Hagen, 2005](#)), which also prevents their identifications.

- Snowfields, avalanches cones, crevassed and non-crevassed ice surfaces, discontinuous and continuous debris covers, longitudinal and transversal ridges, solifluction lobes (in the eastern convex zone in Entre la Reille), thermokarstic outcrops of buried ice and surface meltwater streams are the main features that occupy the surfaces of the glaciers. These features were also described in the glacier zones in similar systems (e.g. [Monnier et al., 2011](#); [Janke et al., 2015](#); [Monnier and Kinnard, 2015](#)). The surfaces were generally concaves and situated below the LIA deposits or freshly abraded bedrock. In the very small and buried systems (Pierre Ronde, les Rognes, les Fours, Entre la Reille), the upper debris-slope homogeneity illustrated the progressive transformation of these remnants of ice in talus slopes (e.g. [Gomez et al., 2003](#)).

Dynamics

- Two main dynamics were observed at the surface of the studied glaciers from decadal to seasonal timescales: downward flow and surface lowering. Our interpretation of occurring dynamics is synthetized in the [Fig. 2.19](#).
- According to the dynamical data collected by dGPS, Lidar or photogrammetry, a gravity-driven flow (ranging from m.a^{-1} in the largest sites to cm.a^{-1} in les Fours) was active in all the studied glacier zones. These sedimentary ice masses were not static and hence, can be considered as glaciers from a dynamical point of view (e.g. [WGMS, 2008](#); [Dobhal, 2011](#); [Serrano et al., 2011](#)). However, some of them were very weakly active and can be considered genetically as inherited dead ice bodies. Indeed, no sedimentary ice was forming in relation with the vanishing of accumulation areas ([Fig. 4.1](#)). Deformation of saturated basal sediments can occur in the studied environments (e.g. [Waller, 2001](#); [Krainer and Mostler, 2006](#); [Serrano et al., 2011](#)). However, no data on the bed characteristics and dynamics were collected and we mainly attributed the downward flow to internal deformation and basal sliding (section 2.2.2.5). The recording of surface movements during both snow-covered and snow-free periods indicated that all the glaciers

were affected by internal deformation. The intensity of this process depends strongly on glacier thickness (Cuffey and Paterson, 2010). It partly explains why the thickest glaciers (Tab. 4.3) had the fastest surface velocities. In contrast, the thin glaciers in les Fours and Entre la Reille had slow deformation. The strong accelerations of downward motion in summer, the relatively cubic shape of the velocities cross profiles as well as the observation of water circulations evidenced the very likely occurrence of hydrological forcing during the melt season. The concentration of water at the glacier bed induced an en masse sliding (e.g. Anderson et al., 2004; Copland et al., 2009). This process is very common in glaciers and can also occur in permafrost environments (e.g. Rippin et al., 2005; Bingham et al., 2006). It indicates that at least the base of the sliding glacier zone is temperate (Mayer et al., 2006; Bingham et al., 2008). Nevertheless, because of the presence of hanging glaciers in the Petit Combin system and the influence of permafrost conditions on glacier thermal regime (Etzelmüller and Hagen, 2005), the studied glaciers are very likely polythermal. Furthermore, the very slow surface flow measured in les Fours seems to indicate that basal sliding is inactive or weakly active in this buried remnant glacier. The dGPS monitoring carried out at seasonal timescale in the three main study sites (les Rognes, Entre la Reille and Tsarmine) showed that glacier motion was primarily controlled by air temperature. High air temperature induces the production of meltwater that can accelerate the flow when it reaches the glacier base. In addition, the high air temperature can also contribute to increase the temperature of ice and thus its deformation rate. Conversely, the relation of glacier motion with precipitations during the melt season appeared more complex and secondary. At decadal timescale, a decrease of downward flow was observed in Tsarmine glacier. This dynamic is very common in the current climatic context because of both the driving stress limitation by ice mass thinning and the decrease of mass turnover (e.g. Paul et al., 2007). It affects particularly heavily debris-covered glaciers because the debris mantle can reverse the ablation gradient, which induces flattening of the glacier surface (Benn et al., 2012; Carrivick et al., 2015; Rowan et al., 2015). In addition, glacier flow can be obstructed by the sediments accumulations present in the frontal zones of these systems (e.g. Shroder et al., 2000; Kirkbride and Deline, 2013).

- Surface lowering largely dominated from decadal to seasonal timescales. If this dynamic can be secondarily related to local extensive flow, we mainly attribute its occurrence to ice melt. Indeed, surface velocities and landforms indicated the general domination of compressive stress. As in the majority of glaciers (e.g. Haeberli et al., 2013; Huss et al., 2015), surface lowering appeared strongly controlled by air temperatures during the melt season. The latter became very unfavourable for glaciers in the northwestern Alps since the 1980s and generated strong glacier shrinking (e.g. Deline et al., 2012; Fischer M et al., 2015). As a consequence, the debris-free glacier terminus retreated from tens to hundreds of meters in the Petit Combin and Chaltwasser systems, as observed in aerial images and in photogrammetry results. However, the very small investigated glaciers showed very weak areas decrease. Except in Pierre Ronde, sedimentary ice is still largely present in these systems. This situation often characterises heavily debris-covered glaciers, due to the efficient limitation of ablation rate by the decimetre to meter thick debris mantle in the distal area (e.g. Scherler et al., 2011; Haeberli et al., 2013; Carrivick et al., 2015). This type of glaciers responds then rather to atmospheric warming by a stationary

thinning than by an active retreat. The thermal data collected showed how summer ground temperatures were efficiently limited under a few decimetres thick debris layer (e.g. [Fig. 3.12](#) & [3.63](#)). Nevertheless, the lowering rates measured with the dGPS between 2011 and 2014 ranged between few decimetres to meters per year. This highlights that despite ablation rate limitation by the debris cover, local climatic conditions were strongly unfavourable for glaciers. Compared to the primary control of air temperature during the melt season, the dGPS monitoring in the three main sites showed the complex influence of the snow cover and rainfall on surface lowering. Two distinct behaviours appeared in the study sites: surface lowering decreased in les Rognes and Entre la Reille in summer 2013 compared to summers 2012 and 2014 ([Fig. 3.16](#) & [3.48](#)) while it increased in Tsarmine during the summer 2013 ([Fig. 3.67](#)). This process was probably related to the slow melt of the snow mantle in les Rognes and Entre la Reille in 2013, which limited the ablation during the early summer period. Despite the similar presence of a large snow cover in early summer, the surface lowering increased in Tsarmine during this summer. In contrast with the two other sites, both mean air temperature and cumulative positive degree days were larger over the summer 2013 in Tsarmine, highlighting the likely predominance of these variables on surface lowering in this glacier. The extremely rapid ice cliff backwasting (around 10 m during the hot summer 2015), thermokarstic erosion in the central gully and the rapid lowering of the upper debris-free zone since the 1980s in Tsarmine, or the presence of ice caves in les Rognes were also clear signs of this glacier-hostile context. Localised uplift was observed in the last decades in Tsarmine, Petit Combin and Chaltwasser glaciers. We attributed this dynamic to the downward transfer of the mass accumulated during the 1960s-1970s positive mass balance period (e.g. [Huss, 2012](#)) and the associated increase of compressive stress. The migration of a mass gain downglacier is rarely observed in debris-free systems and was explained here by the preservation of this mass under the debris cover. [Thomson et al. \(2000\)](#) observed a similar dynamic on the Miage debris-covered glacier. Nevertheless, surface lowering dominated in recent years, even in the zones where surfaces uplifted over the last decades. At seasonal timescale, only a slow emergence velocity was measured in winter in the ablation zone of Tsarmine, due to ice transfer and associated compressive stress (e.g. [Kellerer-Pirklbauer et al., 2008](#); [Purdie et al., 2010](#)). However, downwasting dominated at annual timescale in this glacier.

- Heavily debris-covered glacier zones of low activity were observed in almost all the systems ([Fig. 4.1](#)). These zones seemed dynamically detached from the neighbouring glaciers zones. According to ERT results, the englacial debris concentration and superficial layer thickness increased in these zones. Two different dynamics were encountered here. In the front of Tsarmine (and also probably in the Petit Combin, Les Fours and Pierre Ronde), horizontal movements were limited and surface lowering was relatively rapid ($\text{dcm}\cdot\text{a}^{-1}$), especially during summer. Water circulations were heard in this zone, which can be considered as downwasting dead ice (e.g. [Schomacker., 2008](#)). In contrast, the SW part of les Rognes (and also maybe the eastern side of Entre la Reille) had more balanced lowering and flow dynamics and developed surface deformation patterns. According to [Evans \(2013\)](#), these patterns could indicate a cold thermal regime of the ice. Moreover, no signs of water runoff were observed or heard. This zone could illustrate therefore the transition from glacier dynamics to a very slow periglacial creep. We discuss this transition in the next section.

- According to their current and past characteristics, the studied glaciers can be divided into three different types (Tab. 4.3). A first distinctive criterion allows to oppose the glaciers that always been very small (les Rognes, Pierre Ronde, les Fours, Entre la Reille, Tsarmine) from those that recently became small as a consequence of large glaciers shrinking and/or fragmentation (Chaltwasser, Hübischorn and Petit Combin; e.g. Scotti et al., 2014; Huss and Fischer, 2016). A second criterion separates the glaciers whose extent and dynamical behaviour are mainly controlled by climatic conditions (climatically-controlled glaciers: CC in Tab. 4.3 and illustrated by the situation A in the Fig. 4.2) from those where the occurrence of negative feedbacks such as avalanching, shading or insulation by debris cover limits the climatic control and explains the extent and behaviour (topographically-controlled glaciers: TC in Tab. 4.3 and situation B and C, i.e. below the climatic ELA, in the Fig. 4.2). Entre la Reille and les Fours are two typical examples of such glaciological anomaly related to the influence of negative feedbacks (e.g. Kuhn, 1995; Grunewald and Scheithauer, 2010; Carturan et al., 2013a). These very small glaciers developed in topographical niches hundred meters below the regional climatic ELA. In the changing climate context, both positive feedbacks (acceleration of ice melt by accumulation of impurities on firn and bare ice glaciers, shortening of the snow-covered period, bedrock outcropping, water circulations and lake development, cavity development, etc.; see e.g. Paul et al., 2007) and negative feedbacks (limitation of ice vanishing by shading, avalanching, extent and thickening of debris cover, ice cooling in permafrost environments due to the diminution of snow insulation, etc.; see e.g. DeBeer and Sharp, 2009; Kirkbride and Deline, 2013; Scotti et al., 2014; Huss and Fischer, 2016) can occur and make more complicated the glacier responses to climatic forcing. Effects of positive

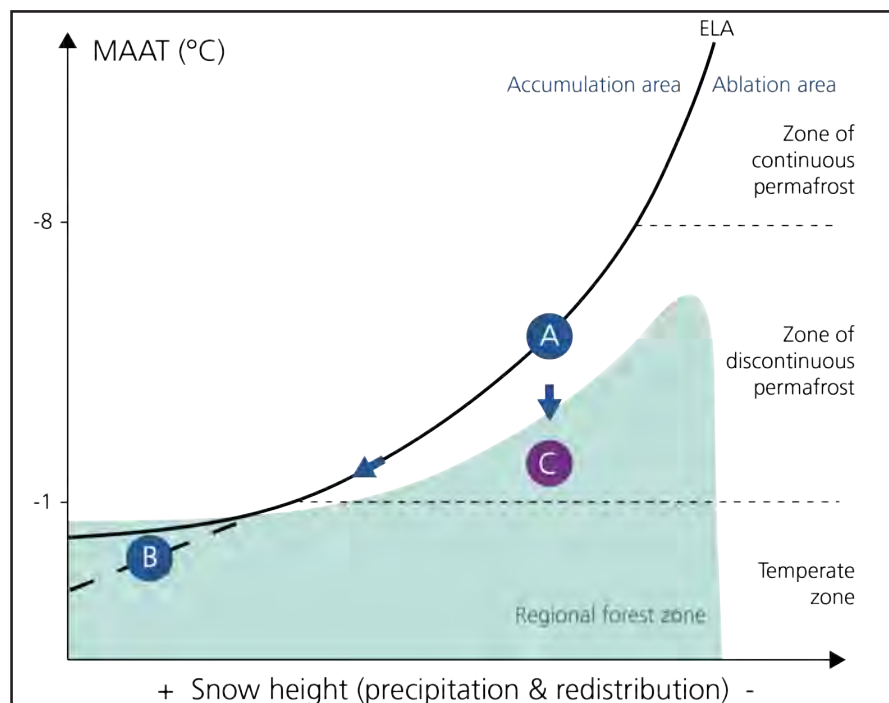


Fig. 4.2. Scheme of equilibrium line altitude (ELA) variation according to mean annual air temperature (MAAT) and snow height. The A to B and A to C transitions illustrate how the influence of avalanching, shading (A to B) or debris cover (A to C) on ice accumulation and ablation rates can influence the evolution of an individual glacier. The colour change in the A to C transition indicates how periglacial dynamics can succeed to glacial dynamics in the debris-covered glacier to rock glacier continuum that possibly occur under permafrost conditions. These transitions are discussed in the section 4.2.2.1. Modified from Haerberli et al. (2013). The modification of this reference figure has been proposed by Mauro Fischer during our rewarding discussions on very small glacier systems.

feedbacks seem to dominate in large and/or debris-free glaciers (e.g. DeBeer and Sharp, 2009; Haeberli et al., 2013; Thibert et al., 2013; López-Moreno et al., 2015). Conversely, the confinement of ice masses in topographical niches generally limits the shrinking of very small glaciers in high relief environments by increasing the relative influence of snow redistribution processes and shadow effect (e.g. Carturan et al., 2013a; Capt et al., 2016; A to B in Fig. 4.2). For instance, the drainage ratio and thereby the potential of snow redistribution theoretically increase as the glacier surface and cover on the surrounding relief decrease. In addition, the development of thick debris covers allows the preservation of glacier ice in ablation areas, especially in periglacial environments where its thickness can reach the one of active layer of permafrost (Lilleøren et al., 2013; Capt et al., 2016, illustrated by the transition from A to C in the Fig. 4.2). Several studies showed thereby the decrease of the regional climate control on some very small glaciers in deglaciation context (e.g. López-Moreno et al., 2006; Scotti et al., 2014; Carrivick et al., 2015). This dynamic was observed in les Rognes, Pierre Ronde, Tsarmine or the Hübshorn glaciers, that became mainly inherited, sheltered ice masses (CC to TC in Tab. 4.3). Current extent of these glaciers are thus anomalies at regional scale, as they are completely or largely located below the rising climatic ELA. Nonetheless, the surface lowering rates measured at their surfaces indicates that the occurrence of negative feedbacks only slowdown the effect of atmospheric warming. Imbalance between these preserved ice masses and climatic settings is important and continuous glacier shrinking is expected in the next decades even if the climatic conditions stabilize (e.g. Juvet et al., 2010; Carturan et al., 2013b; López-Moreno et al., 2015).

4.2.2.2. Push moraines – rock glacier complexes

Internal structure and morphology

- Except in the Chaltwasser system, viscous landforms indicating recent glacier-permafrost interactions were observed in the margins of each system (Fig. 4.1). Their surfaces showed the typical morphology of push moraines – rock glaciers complexes (Berthling, 2011; Monnier et al., 2011): below or beside a concave former or active debris-covered glacier zone, a coarse sediment surface presents succession of ridges and furrows and is bounded by a steep front of fine sediments. According to the height of the fronts, these landforms were generally 10 to 30 m thick, which is a usual range for local rock glaciers (e.g. Otto et al., 2009). In comparison with the glacier zones, these zones were more convex and not bounded by sharp moraine crest. No ice outcrops or indices of water circulations were observed during field investigations or with aerial images. The winter snow layer melted earlier during the spring or summer from these zones than in neighbouring ablation areas of glaciers.
- Ground electrical resistivity mainly ranged between 15 and 80 kΩm below several meters of more conductive material. However, lenticular structures, having a resistivity higher than 1000 kΩm, were also detected in the rock glacier rooting zones of Tsarmine and les Fours. Analogous results were obtained in other push mmoraines – rock glacier complexes (Reynard et al., 2003; Kneisel and Käab, 2007; Ribolini et al., 2010). An idealised interpretation of the internal structure

of these zones is proposed in the Fig. 2.19. Resistivity values and contrasts illustrate the possible coexistence of ice-cemented sediments and ice-core lenses below the several meters thick unfrozen active layer. The studied rock glaciers did not present the generalised ice-cored structured observed in some other rock glaciers associated with debris-covered glaciers (e.g. Potter et al., 1998; Burger et al., 1999). The ice concentration is difficult to evaluate with the sole ERT results. If massive ice composed the spatially restricted highly resistive lenses, ice concentration in the cemented debris has been estimated to 40-60% of the total volume, according to the data existing in similar active glacial rock glaciers (Hausmann et al., 2007 & 2012; Janke et al., 2015).

Dynamics

- A downward flow (dcm.a^{-1}) and a slow surface lowering (cm.a^{-1}) were measured in the push moraines – rock glacier complexes during the last years. Both dynamics are common in rock glaciers in the current climatic context (e.g. Haeberli et al., 2006; Janke et al., 2013). Our interpretation of occurring dynamics is synthetized in the Fig. 2.19. The two dynamics were recorded in both summer and winter seasons and their velocities were maximum during late summer. This illustrated the influence of air temperature and the delay induced by the several meter-thick active layer in the transmission of the air temperature signal (e.g. Delaloye et al., 2008 & 2010). The lower surface dynamics measured here in comparison with the glacier areas show also that the climatic signal is attenuated during its transfer in the thick active layer limiting the climatic-sensitivity of ice-debris mixtures (Kääb et al., 2007a).
- The downward flow was mainly attributed to internal deformation of the ice-debris mixture. Indeed, the acceleration of horizontal velocities was weak during the melt season, no evidence of water circulations was observed and the velocity cross profiles were mainly parabolic. The occurrence of sliding along internal shear planes or saturated sedimentary beds (as detected in other rock glaciers e.g. Arenson et al., 2002; Krainer and Mostler, 2006) seemed therefore ineffective or secondary on downward motion. The predominance of internal deformation and secondary to null influence of other motion mechanisms probably explain the lower horizontal velocity measured in the rock glaciers, compared to the glacier zones (e.g. two times slower on average in Tsarmine, les Rognes and Entre la Reille; Fig. 2.17). Moreover, decrease of ice concentration toward the rock glacier margins commonly increases the internal friction, which contributes to limit the downward motion (e.g. Haeberli, 2000).
- Surface lowering indicated that a slow melt was active below the active layer. However, its low intensity, especially compared to the magnitude of this dynamic in the glacier sectors at decadal to seasonal timescales, shows that the thick coarse sediment mantle has a thickness close to the permafrost active layer and efficiently insulates ground ice from air temperatures (e.g. Lilleøren et al., 2013; Monnier and Kinnard, 2015). According to the occurrence of permafrost conditions, the current formation of magmatic ice by the freezing of water at depth appears possible in these coarse sediment accumulations (e.g. (Kneisel, 2003; Reynard et al., 2003; Ribolini et al., 2010). However, we did not found indices that allow inferring the occurrence of this process.

Moreover, domination of surface lowering over the last decades seems to indicate the null to weak magnitude of this process.

- The preservation and flow of ground ice in the margins of SDCGSAPE illustrate therefore the glacier-permafrost continuum that has occurred locally over the last millennia (Ackert, 1998; Berthling, 2011). The numerous push moraines observed at the transition zones between the mainly concave glaciers and convex rock glaciers indicates the recent deformation of marginal frozen debris by glacier advances. However, the frontal part of the rock glaciers did not present such patterns of recent bulldozing or signs of glacier overriding. The distal rock glacier parts are mainly composed of ice-cemented debris according to ERT results. If these active landforms could have been developed over a large part of the Holocene, we rather attribute their formations to the neoglacial period as proposed by many authors (Ackert, 1998; Humum, 2000; Guglielmin et al., 2004; Ribolini et al., 2007). Indeed, climatic conditions became more favourable for glacier development over the last 3 to 4 millennia (e.g. Ivy-Ochs et al., 2009; Kirkbride and Winkler, 2012). During that period, repeated glacier advances, whose magnitude was comparable or lower than the LIA, accumulated large debris accumulations in the margins of SDCGSAPE, generating the current morphology (e.g. Matthews et al., 2014). It is possible that former frozen sediments were deformed at the beginning of the Neoglacial period. It is also possible that the rock glaciers developed from heavily debris-covered glaciers or moraine deposits. Sedimentary ice and magmatic ice could thus coexist in these landforms (Kneisel, 2003; Kneisel and Käab, 2007; Ribolini et al., 2010). The detection of very resistive lenses in the rock glacier roots in Tsarminé or les Fours shows the likely integration of heavily debris-covered sedimentary ice in the distal flowing mixture. Slow ice melt and the integration of debris within massive ice during the flow can explain the transition in time from ice-cored structure toward ice-cemented structure in the distal zone (Clark et al., 1994). Finally, the differential ablation as well as the flow can disconnect rock glaciers from upslope vanishing glaciers in negative mass balance periods. As discussed by other authors (e.g. Ackert, 1998; Berthling, 2011), we think that the rock glaciers illustrate the complex recent Holocene history: glaciers successively deformed and sometimes overrode flowing ice-debris mixtures in positive mass balance periods and abandoned ground ice within them in negative mass balance periods, allowing the formation of push-moraines – rock glacier complexes in the margins of SDCGSAPE. In contrast with this long-term history, appearance in the last decades of a steep fine-grained front in the terminus of a heavily debris-covered tongue in the Petit Combin system could indicate the formation of a new rock glacier (3.7.2; Fig. 3.90). Shroder et al. (2000) and Monnier and Kinnard, (2015) reported similar cases but this situation seems relatively rare around the world. However, it shows that some heavily debris-covered glaciers can evolve rapidly into rock glaciers. The changes of dynamics responsible of this transition are discussed in the section 4.2.3.

4.2.2.3. Ice free debris accumulations

Large accumulations of mostly ice-free debris were observed in marginal zones (Fig. 4.1). The thickness of these accumulations can reach several tens of meters. Both fine and coarse, as well

as angular and rounded debris were observed at their surface. However, these accumulations generally contrasted with the coarse sediment surface of debris-covered glaciers and rock glaciers by the abundance of fine materials and the smooth topography. Pioneer vegetation and fluted moraines were also encountered exclusively at their surfaces within the systems. The ground resistivity ranged mainly from 1 to 10 k Ω m, which is typical of ice-free moraine deposits (Hauck and Kneisel, 2008).

Whereas rock glaciers mainly occupy lateral margins and were in contact with relatively weakly active glacier parts, ice-free debris accumulations are present in Holocene moraine deposits and in the recently deglaciated central areas. Glacial thermal regime and associated water circulations appear as the main controls explaining the distribution of ground ice in the sedimentary margins of SDCGSAPE (Kneisel, 2003; Delaloye, 2004; Evans, 2013). On one hand, ground ice was preserved in the coarse debris sectors, weakly impacted by glacier fluctuations and associated water fluxes (i.e. lateral margins of active glaciers as the Petit Combin or Tsarmine or frontal zones of poorly active glaciers as Entre la Reille or les Rognes). Cold and weakly active glacier zones are common in permafrost environments (e.g. Etzelmüller and Hagen, 2005; Gilbert et al., 2012) and allow the preservation of ground ice (e.g. Bolch and Gorbunov, 2014; Dusik et al., 2015). On the other hand, the presence of fluted moraines, fine rounded material and some clues of water circulations show that ground ice rapidly melted in contact with temperate glaciers. Moreover, large amount of water is produced during the glacier retreat and contribute to the warming of the ground. This control could explain that no preserved ice was found in the front of the largest glaciers, where dynamics and production of water were the highest. In contrast, the weak activity of very small glaciers and associated low water production, as at Entre la Reille, did not hinder the preservation of ground ice at their front. The sediments size can also have an influence on ground ice preservation: ice is rarely found below fine material (e.g. Dusik et al., 2015), whereas the accumulation of cold air between coarse debris fosters ground ice preservation (Gruber and Haeberli, 2009; Bolch and Gorbunov, 2014).

Low to null surface dynamics were detected in ice-free debris accumulations. Studies in recently deglaciated areas showed that activity quickly decreased after the glacier retreat with the development of pioneer vegetation (e.g. Geilhausen et al., 2012; Carrivick et al., 2013). The rare movements observed during the dGPS monitoring are probably related to superficial reworking due to avalanching and solifluction. At decadal timescale, parts of moraine accumulations in Tsarmine, Chatlwasser, Petit Combin and Pierre Ronde systems were mobilised and gullied by debris flows.

4.3. Genesis and evolution model of glacier systems in high relief environments

4.3.1. Debris concentration – ice preservation model and genetic sequence

4.3.1.1. Continuum in high relief and permafrost environments and associated glacialic landforms

Reflections on the genesis and evolution of glacier systems in high relief environments (and thus on SDCGSAPE) are proposed in this last section. They are based on the results obtained in this study and on the literature review. They are in line with the previous works that investigated the controls influencing the genesis and evolution of glaciers in high relief environments (e.g. [Benn et al., 2003](#); [Whalley, 2009](#); see the section 1.2.2.3). A model explaining the distribution of glacier systems and their components is proposed ([Fig. 4.3](#)). It relies on the variations in time and space of (1) debris cover thickness and englacial debris concentration, and (2) ice preservation potential in ablation area. This second variable is in part the consequence of the first variable but other controls, as the permafrost conditions or the water circulation, influence the ice preservation potential in ablation area ([Fig. 4.3](#)). In addition, some genetic sequences that can be encountered in high relief glacial environments are detailed ([Fig. 4.4](#)). In the following, these two diagrams are presented and discussed with example from the study sites. Examples from la Gurráz-Turia systems ([Fig. 4.5](#)) are also proposed additionally. We especially discussed the nature and origin of the landforms that compose these systems with Marie Gardent, when she was inventorying the glaciers in the French Alps. La Gurráz-Turia systems provide useful examples of how, at very local scale,

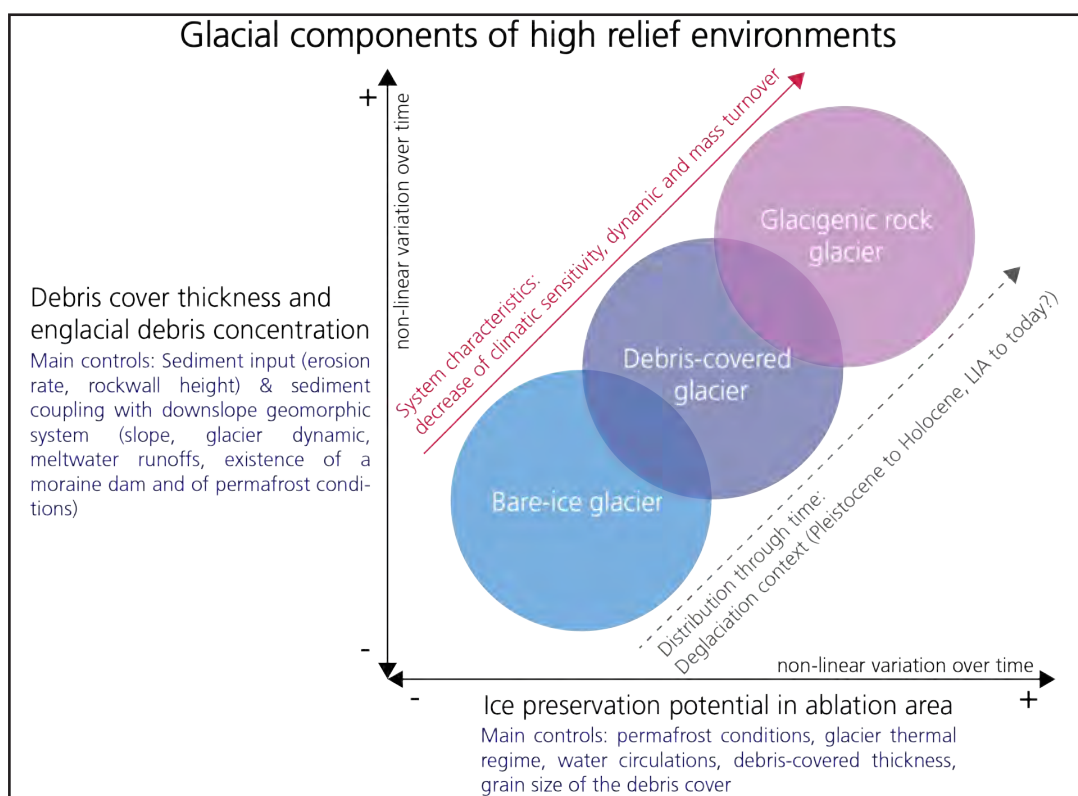


Fig. 4.3. Scheme indicating the influence of variations of debris concentration and ice preservation potential on the glacier system development. The main controls of both parameters are indicated below in blue.

variations in ice and debris concentration and ice preservation potential induce the formation of different glacial and non-glacial landforms in high relief and permafrost environments.

The two end members of the proposed model are bare ice glaciers and glacigenic rock glaciers. Debris-covered glaciers are positioned in between. Bare ice glacier is the most common type of glacier in the world (e.g. Pfeffer et al., 2014). Conversely, debris-covered glaciers and glacigenic rock glaciers only develop from bare ice glaciers, respectively in high relief environments and in high relief and permafrost environments, when some factors increase the debris concentration in the glacier system and the ice preservation potential in the ablation area (Fig. 4.3 and 4.4). In positive or balanced mass balance period, every glacier system has an upslope firn and bare ice zone (i.e. accumulation area). According to glacier system characteristics, the ablation area can be either composed by a bare ice and/or debris-covered glacier zone, and/or a glacigenic rock glacier. In a negative mass balance period, the full burying of the glacier by the debris can occur in high relief environments during the final stage of deglaciation (Gomez et al., 2003; Janke et al., 2015; Bosson and Lambiel, 2016). Hence, the whole system can become a debris-covered glacier or a glacigenic rock glacier. In the proposed model (Fig. 4.3 and 4.4), it is important to keep in mind that bare ice glacier, debris-covered glacier and glacigenic rock glacier can correspond to the whole system (e.g. the Homattu glacier in the Chaltwasser system are only bare ice glaciers) or be a component of the system (e.g. Tsarmine glacier has a bare ice and debris-covered glacier zones, as well as a marginal glacigenic rock glacier).

The model and associated genetic sequences proposed here focus on glacier systems and glaciogenic landforms. However, glaciers (and SDCGSAPE) are only a component (i.e. the glacial component) of the wider and complex morphodynamical continuum that exists in high relief and cold environments (e.g. Shakesby et al., 1987; Kirkbride, 1989; Whalley, 2009; Fig. 1.46). The use of the concept of *continuum* is in line here with the sense discussed by Kirkbride (1989). In essence, all the components of a continuum are related by at least one common characteristic. According to variations in time and space of this characteristic, the continuum components can evolve toward the others. Following Kirkbride (1989), the glacial, periglacial and azonal depositional landforms developed in high relief and permafrost environments can be regarded as a continuous spectrum, related to the variations of ice and debris supplies over time and space. This continuum is the consequence of the interaction, the coexistence and the succession of processes, that allow the existence of an infinity of transitional features between the landform stereotypes present in these environments (e.g. bare ice glaciers, debris-covered glaciers, rock glaciers, talus slopes). The two end members of this continuum are ice-free debris accumulations (e.g. talus slopes, moraine deposits) and debris-free snow/ice accumulations (e.g. snow patches, glaciers). At any time, each landform is thus a consequence of specific ice and debris supplies and evolution pathway (or genetic sequence). However, due to the permanent change of these supplies at the geological time-scale, this continuum of landform is dynamic and evolve in a non-linear way. Supply variations can produce *progressive* landform evolution (e.g. Fig. 4.3 and 4.4). For instance, bare ice glacier can transform over time into a debris-covered glacier which in turn evolves as a glacigenic rock glacier as proposed in the northern margin of Tsarmine or in Entre la Reille. Bare ice glacier can also

Genetic sequence of glacier systems in high relief environments

Examples in this contribution	Location and context of morphogenesis	Occurrence of permafrost conditions	Genetic sequence Steady state (ideal?) landform Main Genetic process(es)	current responses to climatic change	imprint in deglaciated landscape
1 Most of Chaltwasser glacier, Homattu glacier (section 3.6), Guraz glacier (Fig. 4.5)	Basic sequence of glacier formation in all mountainous and polar regions	Not necessary	<p>Snow accumulation (cryogenesis) → Bare-ice glacier (ice content >95%) → Debris-covered glacier (ice content >90%)</p> <p>↑ water release ↑ sediment release</p>	<p>Relatively rapid and simple responses with:</p> <ul style="list-style-type: none"> - ice melt-out (rate depends on topo-climatic conditions as shadow effect, distribution of snow by wind and avalanches, meltwater evacuation, etc.) with normal ablation gradient (ablation increasing toward the tongue) - general deceleration of the flow (reduction of driving stress due to glacier shrinking and limitation of mass turnover) 	<p>Abraded rocky bed and/or thin sedimentary bed, null to small marginal moraine accumulations, possible fluvio-glacial outwash plain/fan.</p>
2 Most of Petit Combin glacier (section 3.7), South part of Tsarime crique glaciers and weak slope angle and/or in a negative mass balance context	Common sequence in glacier systems (or part of glacier system) with major sediment input (e.g. valley floor and cirque glaciers) and weak slope angle and/or in a negative mass balance context	Not necessary	<p>↑ Accumulation of debris on the ablation area surface with the emergence of englacial sediment load (due to ice melt and/or ascending ice flux) and/or with supraglacial supply (rockfalls, rock avalanches, etc.)</p> <p>↑ Debris-covered glacier (ice content >90%) → Bare-ice glacier (ice content >95%) → Firn</p> <p>↑ weak water release ↑ extremely weak sediment release</p>	<p>Delayed and attenuated responses with:</p> <ul style="list-style-type: none"> - ice melt-out (rate depends on topo-climatic conditions as shadow effect, distribution of snow by wind and avalanches, meltwater evacuation, thickness of debris cover) with normal to reversed ablation gradient (ablation rate can decrease toward the tongue due to the increase of the debris cover thickness); the response to climate signal is rather expresses with vertical (downwashing) than horizontal (length of glacier system) variations - deceleration of the flow (reduction of driving stress due to glacier shrinking, limitation of mass turnover and surface gradient reduction) 	<p>Sedimentary bed with hummocky patterns, massive marginal moraine accumulations (development of a moraine dam when coupling between glacier system and hydrosystem is inefficient), possible fluvio-glacial outwash plain/fan with efficient coupling between glacier system and hydrosystem.</p>
3 North part of Tsarime (section 3.5), Entre la Heille (section 3.4), distal zone of les Rognes (section 3.2), Guraz rock glacier (Fig. 4.5)	Sequence occurring in permafrost environments in glacier systems (or part of glacier system) with very-weak sediment evacuation, a slope angle allowing the creep of the ice-debris mixture and/or in a negative mass balance context. Development in the distal/marginal part where ice is preserved under a thicker debris cover.	Necessary	<p>↑ Thickening of the debris cover in the distal zone due to a large debris supply or ice melt. When this layer become several meters thick (corresponding to the active layer permafrost), it insulates the ice from atmosphere and prevents its melt. It also limits the influence of hydrological forcing on ice-debris motion which becomes mainly due to internal deformation</p> <p>↑ Debris-covered glacier (ice content >90%) → Bare-ice glacier (ice content >95%) → Glaciogenic rock glacier (ice content >90%)</p> <p>↑ extremely weak water release ↑ extremely weak sediment release</p>	<p>Slow and complex responses with:</p> <ul style="list-style-type: none"> - slow ice melt-out (rate depends on topo-climatic conditions, meltwater evacuation, thickness of debris cover) - possible acceleration of the flow (augmentation of ice plasticity with the increase of ice temperature, augmentation of water content) or deceleration of the flow (reduction of driving stress due to thinning and flattening) - the creep of the ice-debris mixtures leads to the formation of a steep front and superficial expressions of compressive-extensives fluxes (ridges and furrows) 	<p>Sedimentary bed with thermokarst, ridges and furrows patterns and large marginal sediment accumulations.</p>
4 Distal zones of the northern part of Tsarime (section 3.5), Entre la Heille (section 3.4), northern front of les Rognes (section 3.2), Guraz rock glacier (Fig. 4.5)	Sequence occurring in permafrost environments in ice-cored rock glacier (or part of ice-cored progressive melt of the sedimentary ice body and possible the integration of magmatic ice	Necessary	<p>↑ Melting of a part of the sedimentary ice and/or integration of magmatic ice in the creeping ice-debris mixture</p> <p>↑ Debris-covered glacier (ice content >90%) → Bare-ice glacier (ice content >95%) → Glaciogenic rock glacier (ice content >90%)</p> <p>↑ extremely weak water release ↑ extremely weak sediment release</p>	<p>Slow and complex responses with:</p> <ul style="list-style-type: none"> - slow ice melt-out (rate depends on topo-climatic conditions, meltwater evacuation, thickness of debris cover) - possible acceleration of the flow (augmentation of ice plasticity with the increase of ice temperature, augmentation of water content) or deceleration of the flow (reduction of driving stress due to thinning and flattening) - the creep of the ice-debris mixtures leads to the formation of a steep front and superficial expressions of compressive-extensives fluxes (ridges and furrows) 	<p>Sedimentary bed with thermokarst, ridges and furrows patterns and large marginal sediment accumulations.</p>

Fig. 4.4. Scheme illustrating the type of glacier systems and their associated genetic sequence that can develop in high relief environments.

transform into a debris-covered glacier and then into a talus slope at the backwall foot as in the Pierre Ronde or les Rognes (see 2.1.2.5; Gomez et al., 2003). At the same time, changes in the ice and debris supplies can *reset* the landform evolution process and induce new evolution pathway. Taking the example of the possible progressive evolution of bare ice glacier into a debris-covered glacier and a glacigenic rock glacier (Fig. 4.3 and 4.4), which mainly occurs in debris-rich marginal zones of the glacier systems or with the increase of the debris concentration in a negative mass balance period, a positive mass balance period can induce the readvance of a large bare ice glacier on a former debris-covered glacier and glacigenic rock glacier and, thereby, their partial or complete disappearing or reworking. Hence, such glacier advance can be considered in some way as a return to initial condition of this system. According to the constant variations of climatic conditions over the Late Pleistocene and Holocene period (e.g. Fig. 1.36), landforms evolved continuously and non-linearly over the last millennia. During the recent Neoglacial period, glacier systems have thus experienced complex and *cyclic* morphogenetic dynamics, with successions of progressive landforms evolutions and system resets. In this context, the global warming initiated after the LIA induced a general decrease in ice supply and increase in debris supply, favouring the transition from glacial morphodynamics toward periglacial and azonal morphodynamics in high relief and permafrost environments.

The model proposed focuses on the glacigenic components that contain ice, namely bare ice glacier, debris-covered glacier and glacigenic rock glacier (Fig. 4.3 and 4.4). However, ice-free glacigenic landforms (e.g. moraine deposits) or non-glacigenic landforms (e.g. talus slopes, fluvial fans, *periglacial* rock glaciers) can be present in SDCGSAPE (see especially the sections 1.2.2.2 and 1.2.3) and by extension in all the glacier systems located in high relief and permafrost environments. These landforms will not be directly considered here although the relation that can exist between periglacial rock glaciers and SDCGSAPE is discussed in the following.

4.3.1.2. Bare ice glacier

Bare ice glacier develops when the sediment input is relatively low in the system and/or when the sediment evacuation toward downslope geomorphic system is efficient (Fig. 4.3 and 4.4). The absence of large surrounding relief or its coverage by the glacier strongly limit the debris concentration in glacier system (e.g. as for the Chaltwasser glacier, the Homattu glacier in the section 3.6 and Fig. 4.1 or the Gurraz glacier in Fig. 4.5). Moreover, erosion rate varies noticeably as a function of lithology and climate. Consequently, bare ice glacier can even be the predominant type of glacier in high relief environments where the weathering is low (e.g. in the Scandinavian peninsula, Benn et al., 2003). In addition, an efficient coupling between glacier system and hydrosystem in sediment transfer also limits the debris concentration in the system. Large glacier dynamics and meltwater productions as well as an important slope angle at the glacier terminus foster the sediment evacuation beyond the glacier system. These characteristics were encountered at the terminus of the Chaltwasser glacier (section 3.6) and Gurraz glacier (Fig. 4.5) during the LIA, explaining the limited amount of frontal deposits.

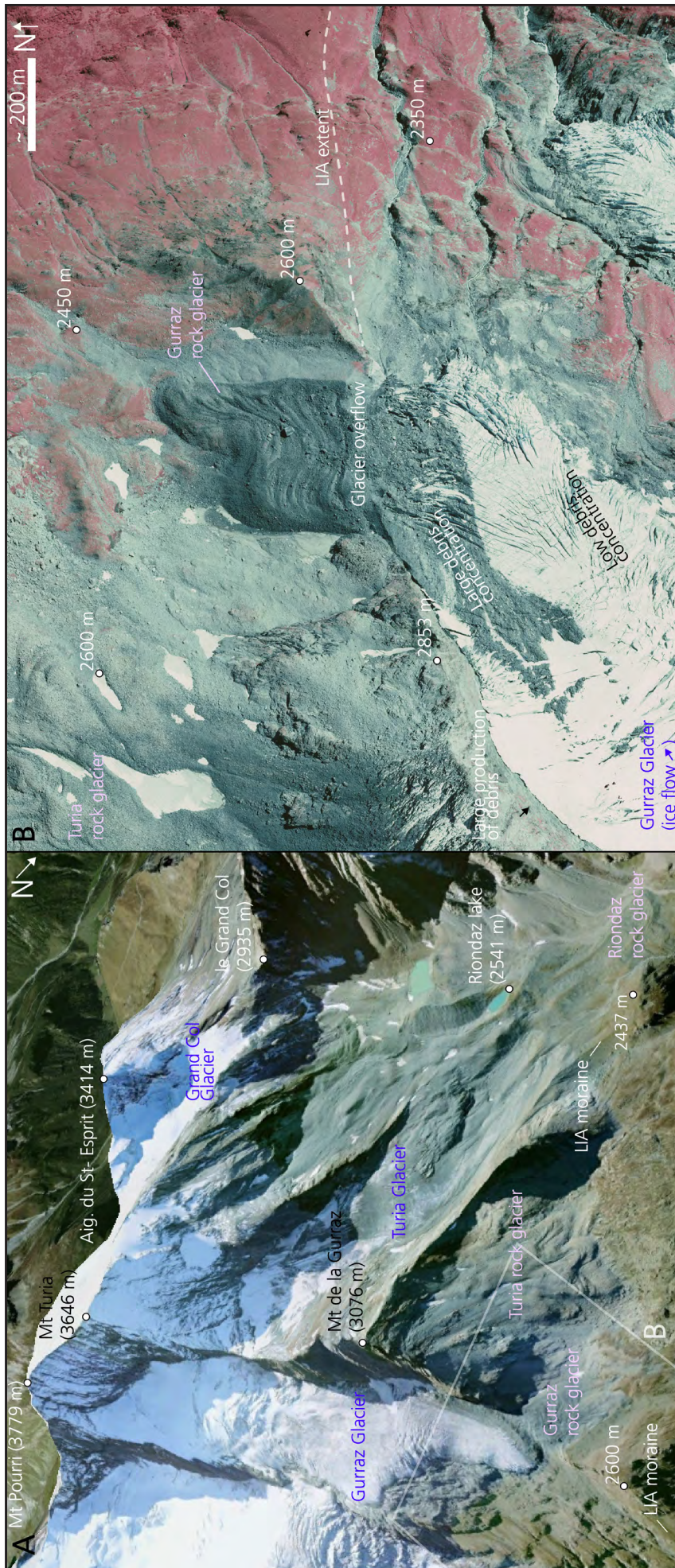


Fig. 4.5. 3d view of the Gurráz and Turia systems located in the French Alps (45°33' N, 6°52' E; © Google Earth 2016). In the right, infrared photograph of 1982 centred on the Gurráz rock glacier (© IGN: IGNF_PVA_1-0_1982-08-22_C3330-0034_1982_IFN73_IRC_1185). The red evidences the vegetation.

The englacial debris concentration is usually very low in bare ice glaciers (an idealised internal structure is proposed in the Fig. 2.19). They are strongly sensitive to climatic variations and the ice preservation potential is weak in the ablation areas (Fig. 4.3). Both mass change and glacier motion velocities are theoretically the largest on bare ice glaciers. Indeed, hydro-climatic forcing is not filtered at their surface by a debris layer, which induces rapid and intense dynamical responses (e.g. Thomson et al., 2000; Herman et al., 2015; Capt et al., 2016). Whereas crevasses are rare or absent at the surface of debris-covered glaciers and glacigenic rock glaciers, their common presence in bare ice glaciers illustrates their larger dynamic. In the current climatic context, a rapid ice melt and a general deceleration of glacier dynamics is usually observed in bare ice glaciers (e.g. Paul et al., 2007; Fig. 4.4).

4.3.1.3. Debris-covered glacier

The development of a debris cover and the increase of debris concentration in debris-covered glaciers can be due to a larger sediment supply from the surrounding relief and/or to an ineffective coupling with downslope geomorphic system (Fig. 4.3 and 4.4). Hence, debris-covered glaciers usually extent in relatively flat cirque or valley floor, below high rockwalls. The development of a debris cover in the ablation area of a glacier can be due to both direct deposition of debris and to the emergence of the englacial load in relation to ice melt and emergence fluxes (e.g. Kirkbride and Deline, 2013). As developed by several authors (e.g. Kirkbride, 2000; Shroder et al., 2000; Hambrey et al., 2008; Iturrizaga, 2013), the current morphology of debris-covered glacier systems is often related to the Holocene climatic fluctuations and to the occurrence of feedbacks that further limited the sediment evacuation from the system. Indeed, the progressive accumulation of large sediment stores at the bed and around the debris-covered glacier limited the slope gradient and glacier dynamics. Thus, as in all the studied sites except the Chaltwasser system (Fig. 4.1), debris-covered glaciers are usually confined within their recent Holocene deposits and sediments evacuation from the low dynamic glacier tongue was efficiently inhibited by the sedimentary dam. As showed in other geomorphic systems (e.g. Church and Slaymaker, 1989), debris-covered glaciers have become thus progressively imprisoned in their history, along the last Holocene glacier fluctuations. Moreover, water production is also perturbed and limited by the presence of the debris cover (e.g. Mattson, 2000), which also limits the efficiency of the sediment evacuation.

Except the presence of a supraglacial debris cover and the possible higher englacial concentration of debris, studies on the internal structure of debris-covered glaciers do not reveal specific characteristics in comparison with bare ice glaciers (e.g. Shean et al., 2007; Monnier et al., 2014; Janke et al., 2015; Fig. 2.19). Beyond a few centimetre threshold, the thickening of the weakly thermally conductive debris cover efficiently insulates the ice from atmosphere (e.g. Nicholson and Benn, 2006; Evatt et al., 2015). It significantly contributes to limit the ice melt and thereby, increase the ice preservation potential in ablation area (Fig. 4.3). Consequently, debris-covered glaciers can extent lower and have smaller accumulation area ratio than bare ice glaciers because larger energy is required to melt the ice (C situation in Fig. 4.2). Because of the presence of the superficial insulating layer, the climatic sensitivity and the dynamics decrease in debris-covered

glaciers (Scherler et al., 2011; Capt et al., 2016). However, hydro-climatic forcing still controls the dynamics of these glaciers and their dynamical responses seems only attenuated and delayed in comparison with bare ice glaciers (e.g. Bosson and Lambiel, 2016). Therefore, the same general dynamics than in bare ice glaciers, namely ice melt and flow deceleration, are currently occurring in debris-covered glaciers (Fig. 4.4). However, the debris cover limit the velocity of glacier shrinking. In addition, the attenuation and possible reversal of the mass balance gradient by the thickening of the debris cover downglacier can induce a flattening that enhance the flow decrease of the glacier tongue (e.g. Benn et al., 2012; Rowan et al., 2015; Capt et al., 2016).

4.3.1.4. Glacigenic rock glacier

Glacigenic rock glaciers can develop in the heavily debris-covered margins of glaciers located in high relief and permafrost environments (e.g. Bosson and Lambiel, 2016; Fig. 4.1; 4.3 and 4.4). Compared to the two previous glacier zones, the debris cover thickness and englacial debris concentration are usually larger here (internal structure is idealised in Fig. 2.19). This situation is mainly due to the progressive melt of ground ice during the creep of these ice-debris mixtures (Clark et al., 1994). The slow surface lowering (typically some cm per year) observed at the surface of each studied rock glacier likely illustrates this slow process of ablation. The magnitude of this process could even be sometimes higher than the measured surface lowering because of the offset induced by the compressive stress in some of these zones. Indeed, alternation of ridges and furrows at the surfaces indicates the domination of compressive stress in most of the rock glacier areas. Hence, the downward flow can generate a slow thickening of the compressed ice-debris mixture and thus a surface uplift. In this way, elevation gains were observed in the Tsarmine rock glacier at seasonal scale, respectively during winter and early summer, when the melt process is weakly active and does not compensate the uplift related to the downward movement (Fig. 3.66 and 3.67). The progressive melt of ground ice over time probably explains the transition from localised ice-cored structures toward ice-cemented structures (Fig. 4.4). In addition to this ablation process, the growth of the debris concentration in the rock glacier roots can be related to the increase of the foliation angle of the englacial debris-rich bands due to the compressive stress in constrained glacier margins (Kirkbride and Deline, 2013) or to rotational slip of the very small ice lenses (Kuhn, 1995).

The development of glacigenic rock glaciers is possible during both glacier-friendly and glacier-hostile climatic conditions. Indeed, they develop with the preservation of glacier ice in the debris-rich margins of glacier systems and the creep of the ice-debris mixtures. Regardless the variations of climatic conditions, the existence of these debris-rich glacier margins is common in high relief and permafrost environments because of the high debris supply from the surrounding relief and weak coupling between glaciers and hydrosystem in sediment transfer (Benn et al., 2003). Glacigenic rock glacier can thus form in these margins in positive or balanced mass balance conditions. Additionally, the relative sediment concentration in the glacier margins usually also increases during negative mass balance periods because of the ice melt and the enhancement of the debris supply by the deglaciation and permafrost degradation in the backwalls. The possible

recent formation of a glacigenic rock glacier in an area occupied by the Petit Combin LIA glacier (Fig. 3.90 and 4.1; see 3.7.2.3) could indicate the transition from glacial to periglacial dynamics here in the current negative mass balance period.

As mentioned above for some debris-covered glacier systems, the occurrence of some feedbacks along the Holocene development of glacigenic rock glaciers (i.e. the damming effect and the reduction of the slope gradient induced by the sediment accumulation, the ice-cementation of the sediment accumulation) strongly limit the efficiency of sediment evacuation from these landforms. Their decoupling with downslope geomorphic systems is thus usually total (e.g. Humlum, 2000; Otto et al., 2009; Azócar and Brenning, 2010). In this way, considering their role in sediment transfer systems, most of rock glaciers are slowly creeping sedimentary sinks, imprisoned in their history.

The transition from debris-covered glaciers to glacigenic rock glaciers and the continuum between glacial and periglacial morphodynamics only occur under permafrost conditions (Owen and England, 1998; Berthling, 2011; Monnier and Kinnard, 2015). Indeed, debris-covered glaciers extending in temperate environments do not present the morphological characteristics of rock glaciers (i.e. advancing steep front of fine material, ridges and furrows). At the same time, the development of glacigenic rock glaciers does not affect all the debris-covered glaciers located in permafrost environments and the combination of some factors seems required. The superficial debris layer thickness has to be close to the active layer of permafrost (1). It strongly increases the ice preservation potential, especially when the debris cover thickness is larger than the active layer of permafrost (Harris and Murton, 2005; Lilleøren et al., 2013). In comparison, glacier ice melts even below several meters of debris in temperate environments, which probably prevents the development of rock glaciers. Moreover, glacigenic rock glaciers seem to develop solely in weakly active glacier margins, where meltwater circulations are limited (2). Indeed, large glacier dynamics and associated water circulations noticeably limit the ice preservation potential. Some authors even propose that a cold thermal regime is required to allow the long-term preservation of ground ice in the glacier system margins and the development of landforms related to glacier-permafrost interactions (3?; e.g. Kneisel, 2003; Delaloye, 2004; Bolch and Gorbunov, 2014; Matthews et al., 2014; Dusik and al., 2015). Rock glaciers and push moraines could thus solely be present in former or current cold glacier zones. However, to our knowledge, no in situ thermal data allow to support this proposition and the complex thermal regime of glacier in permafrost environments remain poorly known (e.g. Gilbert et al., 2012; Huss and Fischer, 2016). Nevertheless, contrasting with neighbouring debris-covered glaciers, no water circulations and noticeable influence of hydrological forcing during the melt season were observed in the studied glacigenic rock glaciers (e.g. Bosson and Lambiel, 2016). It could support the idea of a cold thermal regime in these ice-debris mixtures. In addition, the grain size could also be a development control for glacigenic rock glaciers (4?). Indeed, ice preservation potential is greater below mantle of coarse sediments because of the negative thermal anomaly related to the trapping of cold air in the void. Finally, the slope angle has to be high enough to allow the creep of the ice-debris mixture (5).

The increase of ice preservation potential by the factors discussed above is only the basic condition for the formation of glacigenic rock glaciers. Specific dynamics are then required to induce the morphological transformation of debris-covered glaciers into rock glaciers. Even if basal or internal sliding, or speed-up events due to hydro-climatical forcing can be observed in rock glaciers (e.g. [Haeberli et al., 2006](#); [Perruchoud and Delaloye, 2007](#); [Delaloye et al., 2008](#) and [2010](#)), the results obtained in the studied glacigenic rock glaciers suggest the limited influence of these processes, contrasting especially with the observation made in the neighbouring debris-covered glaciers (e.g. [Bosson and Lambiel, 2016](#)). Glacigenic rock glaciers motion seemed mainly due to a slow and relatively constant internal deformation (cm to dcm per year). The increase of debris-cover thickness and englacial debris concentration in rock glaciers limit thus the influence of short term hydro-climatical forcing and reduce or even deactivate the process of *en masse* slip. [Pourrier et al. \(2014\)](#) showed for instance how water circulations become rare and diffuse in glacigenic rock glaciers in comparison with the rapid and concentrated fluxes observed in bare ice and debris-covered glaciers. Moreover, the larger englacial debris concentration probably also increases the internal friction and limits the flow of glacigenic rock glaciers (e.g. [Hausmann et al., 2012](#)). A dynamical contrast appeared thus between the glacigenic rock glaciers and debris-covered glaciers. The slow deformation of the weakly climatically sensitive rock glaciers generates a viscous morphology that is not observed at the debris-covered glacier surfaces ([Owen and England, 1998](#); [Monnier and Kinnard, 2015](#); [Bosson and Lambiel, 2016](#)). Moreover, the ice melt rates are largely lower in these zones. It allows the long term development of these creeping landforms, even in glacier-hostile context as the current period. Conversely, debris-covered glaciers are strongly sensitive to short-term hydro-climatical forcing. As a consequence, a marked seasonal rhythm characterises ice flow and melt. The occurrence of *en masse* seasonal movements could prevent the formation of a viscous morphology. Finally, whereas the front of active glacigenic rock glaciers advances continuously, debris-covered glacier terminus is often weakly active and recent glaciers fluctuations were confined within static Holocene moraines. In comparison with neighbouring glacier zones, mass turnover is very limited in glacigenic rock glaciers, which can be considered as active, inherited and efficiently sheltered ice masses. Some authors proposed that glacigenic rock glacier systems can even have a balanced mass balance with a very restricted upslope firn area ([Clark et al., 1994](#); [Ackert, 1998](#)). In negative mass balance conditions, differential ablation and flow can lead to their disconnection with their glacial rooting zones ([Lilleøren et al., 2013](#); [Seppi et al., 2015](#); [Bosson and Lambiel, 2016](#)).

The case of la Gurraz glacier system supports the proposed model ([Fig. 4.3](#) and [4.4](#)) by showing how some variations of debris cover thickness, englacial debris concentration and ice preservation potential induce the development of different landforms ([Fig. 4.5](#)). A small glacigenic rock glacier develops from a restricted glacier overflow ([Fig. 4.5b](#)). This landform is now disconnected from the vanishing glacier and perched above northern moraine deposits. Whereas la Gurraz glacier is essentially bare ice, steep and highly active (as evidenced by the numerous crevasses), the debris concentration increased locally due to the intense weathering of the Mont de la Gurraz. When the ice level was high enough, the Gurraz glacier overflowed in this zone of high debris concentration and weak glacial dynamic. The occurrence of permafrost conditions and the slope angle allowed

the long term development of a glacigenic rock glacier here. In the current climatic context, the rock glacier still appears active and ice seems efficiently preserved below the sedimentary mantle. In contrast, comparison of recent aerial photographs and historical sources show a rapid shrinking of the Gurráz glacier (Gardent, 2014 and personal observations).

This section focalises on glacigenic rock glaciers and on the morphodynamical continuum that can exist between bare ice glaciers, debris-covered glaciers and rock glaciers. Nevertheless, as other non-glacigenic landforms, *periglacial* rock glaciers can form in glacier systems located in high relief and permafrost environments. Indeed, these landforms may develop anywhere where permafrost conditions allow the formation of magmatic ice in sediment accumulations and where the slope angle is sufficient to induce the creep of the ice-debris mixture (e.g. Haeberli et al., 2006; Berthling, 2011). Strictly periglacial rock glaciers, that do not require the presence of glacier ice for their formation can thus theoretically develop in any moraine accumulations subject to permafrost conditions (these landforms may be referred to as *debris rock glaciers* or *moraine-derived rock glaciers* in the literature). Moreover, according to the complex variations of ice and debris supplies over the Holocene, glacial (bare-ice glaciers, and/or debris-covered glaciers and/or glacigenic rock glaciers) and non-glacial landforms (talus slopes and/or periglacial rock glaciers) can have succeeded to each other over the last millennia in some high relief and permafrost environments. The deformation of former periglacial rock glaciers during glacier advances or their preservation in the glacier margins unaffected by the glacier advances is thus possible. The push moraines complexes present in most of the studied sites and the common extent of rock glacier areas beyond the LIA glacier limits (Fig. 4.1) could thus highlight this complex Holocene history and the interaction and coexistence of glacial and periglacial landforms. However, the internal structure between the glaciers and rock glaciers zones often appeared as a continuum and the distinction of strictly periglacial landforms from glacial landforms was complicate. Heavily debris-covered glaciers, glacigenic rock glaciers and periglacial rock glaciers could therefore be complexly nested together in the studied glacier margins. In addition, the ice-cemented structure developed over time by the flowing glacigenic rock glaciers also complicates their differentiation from periglacial rock glaciers. For instance, it is hard to know the origin of the frontal zone of the rock glacier in Tsarmine. Indeed, the moderate resistivities measured (10-150 kΩm) and its development from marginal moraines could illustrate both periglacial or glacigenic origin. Although the distinction between ice from a sedimentary and magmatic origin may be very challenging within rock glaciers (Haeberli et al., 2006), sound study of their internal structure could allow to better understand the origin of the present landforms and recent Holocene morphodynamics.

4.3.2 Paradoxical effects of atmospheric warming

Paradoxical effects of atmospheric warming can be observed in some glacier systems located in high relief environments. Whereas, in negative mass balance periods, the bare ice glaciers *rapidly* vanish and paraglacial-temperate morphodynamics progressively replace the glacial morphodynamics (e.g. Ballantyne, 2002; Evans, 2013), the increase of the debris concentration limits the climatic sensitivity of some glaciers in high relief environments and, therefore, extends their

lifespan (Fig. 4.3). The efficiency of this dynamic is further enhanced under permafrost conditions, where the cold air temperature, the long snow-covered period and the morphodynamical continuum between bare ice, debris-covered glaciers and glacial rock glaciers can increase the ice preservation potential.

This paradoxical effect of climatic evolution toward glacier-hostile conditions can be observed at different timescale (schematically represented by the grey line of the distribution through time in the Fig. 4.3; Knight and Harrison, 2014). The strong increase of air temperature since the Last Glacial Maximum (LGM, c. 30 000 - 20 000 BP) noticeably reduced the glaciers area and thickness in high relief environments. For instance, relatively small ice caps, valley and cirque glaciers developed during the Holocene in the European Alps, while the relief was largely covered by ice sheets and ice streams during the LGM. The debris concentration in glacier systems was thus low during the LGM and increased significantly during the Holocene, with the deglaciation of large portion of relief surrounding the glacier systems. The relative influence of avalanching and shadow effect on glacier mass balance also increased as the glacier size decreased in high relief environments. Thereby, whereas the large alpine ice sheets were very likely highly sensitive to climatic variations during the Pleistocene, some of the small Holocene glacier systems became less sensitive to climate and had a larger ice preservation potential. Brazier et al. (1998) and Benn et al. (2003) proposed analogous conclusions from the analysis of relict and active landforms in New-Zealand. This paradoxical effect can also be observed at a smaller timescale, as for example in the current deglaciation period that follows the LIA. Indeed, climate changes since 1850 induced a noticeable glacier retreat and thinning. It also led to an increase of the debris concentration and of the influence of surrounding relief in some glacier systems (e.g. Kirkbride and Deline, 2013; Scotti et al., 2014; Carrivick et al., 2015; Bosson and Lambiel, 2016; Capt et al., 2016). Ice preservation potential increased thus sometimes as a consequence of the decrease of climatic sensitivity. The extent of the debris cover was observed in all high relief regions and transitions from debris-covered glaciers into glacial rock glaciers could even occur at this short timescale (as observed in the centre of the Petit Combin system (section 3.7)? see also Shroder et al., 2000; Monnier and Kinnard, 2015). The cooling of glacier ice in negative mass balance period in permafrost environments is also a paradoxical process that can limit the climatic sensitivity of glaciers (Baelum and Benn, 2011; Gilbert et al., 2012; Huss and Fischer, 2016). Bosson et al. (2015) suggested that this process could induce an increase of glacier-permafrost interactions and partly explain the development of rock glaciers during a phase of atmospheric warming. Nevertheless, empirical data on thermal conditions and on englacial and subglacial processes are required to clarify this assumption and improve the knowledge of glacier-permafrost interactions.

Therefore, as the climatic conditions become unfavourable for glaciers, the ice preservation potential can paradoxically increase in some glacier systems located in high relief and permafrost environments (Fig. 4.3 and 4.4). However, this effect only slows the generalised glacier decline dynamic and, to some extent, climatic conditions become too unfavourable for glaciers existence. Evidenced in an increasing number of studies (e.g., Paul et al., 2007; Scotti et al., 2014; Huss and Fischer, 2016), complex and non linear processes can thereby characterise the responses of glaciers

to an atmospheric warming and both accelerate or slow the consequence of the climatic forcing. These complex processes required further investigations, to better understand changes in glacial environments, and their transition toward periglacial, paraglacial and/or temperate environments (Berthling, 2011; Knight and Harrison, 2014; Huss and Hock, 2015).

5. Conclusion and outlooks



J | Les Rognes, Pierre Ronde and the Bionnassay glaciers basin (© T. Ferber, 10.2014)

5.1. General synthesis

This contribution gathers and synthesizes five years of research on **small debris-covered glacier systems located in alpine permafrost environments** (SDCGSAPE). A **review of the scattered existing literature** (section 1.2) and the **collection of a large dataset** allowed to improve the knowledge on these complex systems and to **set the foundation of their comprehensive analysis**. In particular, this contribution **defines these systems**, identifies the **main components**, highlights the main characteristics of their **internal structure** and of their **dynamics** and proposes an **evolution model of glacier systems in high relief and permafrost environments**.

The data were collected in a multi-sites, multi-methods and multi-temporal study, carried out in the northwestern Alps (parts 2 and 3). The **current internal structure** of these systems was mainly investigated with **electrical resistivity tomography**. The consistency of the results obtained with those of other methods and field observations shows the relevance of this geophysical method for characterising the internal structure of the sedimentary environments and especially for ground ice detection and mapping. Ground surface thermal conditions and **surface dynamics** were monitored between 2011 and 2014 with thermal sensors and **dGPS measurements**. Additional GPR, Lidar, and photogrammetric data were collected in enriching collaboration with PhD colleagues (Mauro Fischer and Natan Micheletti) and master students (Maxime Capt, Simone d'Aujourd'hui and Robin Darbellay). The photogrammetric data and the analysis of historical maps and photographs allowed to investigate the evolution of these systems in recent decades. Three articles were published in international scientific journals during this study (part 2) but numerous unpublished results were also obtained and presented in this contribution (part 3). Finally, a synthesis of the current internal structure and occurring dynamics and reflections on the genesis of these systems and their main evolution controls are proposed (part 4).

SDCGSAPE are dynamical systems where a small glacier is associated with large and possibly frozen sediment accumulations. The glacier occupies the top central slopes whereas sediments stores accumulate in the lower margins. Without considering the Chaltwasser and Petit Combin glaciers, which are larger and mainly climatically-controlled glaciers, **the very small glaciers investigated still contain an important amount of ice ($10^5 - 10^6 \text{ m}^3$)**. Compared to the situations of neighbouring debris-free glaciers, **their presence at relatively low elevations and their geometry are anomalies** in the current unfavourable climatic context. The decadal behaviours of these glaciers also contrast with glacier responses at regional scale. **They illustrate the partial limitation of climatic control by the increase of accumulation rate by avalanching and the decrease of ablation rate by shading and thermal insulation by the debris cover.** The cold air temperatures and the ~ 9 month-long snow-covered periods in these **permafrost environments probably also contribute to limit the glacier shrinking**. Over the last decades, the debris cover extension upglacier and a decrease in glacier dynamics were observed. **These glaciers become stagnant, buried inherited remnants of sedimentary ice, mainly affected by downwasting dynamics.** Nevertheless, **glaciers remain the most dynamical components of SDCGSAPE**. Both surface lowering and glacier flow were measured, typically reaching several

decimetres per year. They were mainly attributed respectively to ice melt and internal deformation as well as basal sliding. The strong acceleration surface velocities in summer highlighted the **fundamental control of air temperature and probably of water circulations during the snow-free period.**

The ice concentration generally decreases toward the margins and both ice-free debris and ice-debris mixtures were observed. Their spatial distribution appears strongly controlled by former glacier dynamics and associated water circulations. Indeed, the frontal zones affected by the strongest glacier motion, sub-glacial and post-glacial water circulations are largely ice-free. The presence of fine rounded sediments and fluted moraines illustrate the recent influence of glacier dynamics in these zones. Ice-free debris thickness could reach several tens of meters. Surface velocities are low (null to $< 10 \text{ cm.a}^{-1}$) and pioneer vegetation develops locally. Conversely, **large amount of ground ice** was detected in the margins where recent glacier dynamics and water circulations were limited. The thickness of the coarse superficial layer reaches several meters. The very slow surface lowering here (typically few centimetres per year) points out the low ice melt and hence, the fact that the debris cover thickness is close to the active layer of the permafrost. The **efficient sheltering of ground ice below this thick layer allowed its long-term preservation** and surface morphology in these zones illustrates **Holocene glacier-permafrost interactions**. Rooting zones are mainly concave and occupied by a debris-covered glacier or ice free debris. The concavity evidences recent ice melt in these zones and the **ongoing disconnection between upslope glacier and these ice-debris mixtures. Push moraines** can be present below these concave zones, as a result of past glacier advance in these frozen debris. Lenses of very high electrical resistivities ($> 500 \text{ k}\Omega\text{m}$) were measured inside some push moraines. They indicate the recent **abandon and integration of glacier ice in the marginal ice debris mixture**. Finally, the frontal zone has a typical **rock glacier morphology** with a succession of ridges and furrows and a marginal steep front. Moderate to high ground resistivities values indicated ice-cemented structures. A **slow and constant flow** (few decimetres per year) was measured at the surface of these push moraines – rock glacier complex. These landforms illustrate thus the **continuum** that can exist **between heavily debris-covered glaciers and rock glaciers in debris-rich permafrost environments**. The long-term preservation and flow of ground ice, weakly sensitive to climatic variations, allows the transition from glacial to periglacial morphodynamics.

The current internal structure and associated dynamics in SDCGSAPE reflect, therefore, the **complex Holocene morphodynamics in permafrost environments. According to variations of climatic parameters (mainly air temperatures and secondarily precipitations), glacial, periglacial and azonal morphodynamics interacted or succeeded one another in these debris-rich environments**. The relative concentration of ice and debris varied consequently over the last millennia. Except rare hydrological events (debris flows and water pocket outburst flows), **no processes efficiently evacuate the sediments toward downslope geomorphic systems**. Despite the activity occurring within the systems, **SDCGSAPE acted thus mainly as sediment sinks during the Holocene**: Pleistocene and Holocene glaciers shaped **gentle bed topography**

that limited the magnitude of processes and allowed the noticeable accumulations of snow, ice and debris. **Lopsided marginal sediment stores** that enclosed the systems were especially accumulated during the Holocene by fluctuating glaciers and creeping rock glaciers. In comparison with other glaciers and cold regions systems, the particularities of SDCGSAPE relies thereby on the enhanced input of snow, ice and debris, the limited output of debris and the possible occurrence of permafrost conditions in all the system.

Ongoing climate changes strongly affect these cryospheric systems. The shrinking of the ice masses was observed in each system, illustrating the **current transition from glacial to periglacial and azonal morphodynamics**. **System's energy and ice content decrease** in this warming context. In contrast, the **sediment input intensifies** in relation with the deglaciation and the permafrost degradation in the surrounding relief. Few rock avalanches and many high frequency-low magnitude rockfall events were thus observed during the field surveys. **From decadal to seasonal timescales, dynamics appear strongly related to the concentration and depth of ground ice.** The decrease of ice concentration and water circulations, and the increase of superficial debris layer limit locally the climatic sensitivity and allow **the long-term preservation of ground ice in these permafrost environments**. The large amount of inherited buried ice masses present in these systems, especially in the weakly climatically-coupled rock glaciers, could become **important water resources in high relief regions while a worldwide and rapid deglaciation is forecasted in the 21st century.**

5.2. Research perspectives

This contribution attempted to set the basis of a comprehensive scientific framework on SDCGSAPE. However, several research topics still have to be explored to complete and deepen the existing knowledge. The study of these systems showed their active and somewhat atypical responses to ongoing climatic changes. In a period where glaciers become smaller, confined in permafrost environments and have larger debris concentration, the study of SDCGSAPE allows to anticipate some of the future glacial responses in high mountain environments. Glacial, periglacial and azonal morphodynamics occur and sometimes interact in these large stores of sediment and preserved water reservoirs. Multidisciplinary studies, going beyond the classical research frontiers in cryospheric sciences, are thus required (Haerberli, 2005; Berthling et al., 2013; Knight and Harrison, 2014). We identified the following research perspectives but others could probably be added on these fascinating systems:

- *Development of knowledge on internal structure:* Investigations have to enhance the knowledge on the **internal structure** of these systems and **to quantify the amount of ice, debris and water that they contain**. Many questions remain especially open on the **ice** present in these systems: How to differentiate sedimentary ice from magmatic ice? Why the concentration of these types of ice could have varied in time and space in these systems and what are precisely the formation mechanism involved? What is the age of ice? Does cryogenesis

occur currently in these systems? What is the thermal regime of the ice bodies and how does it respond to ongoing climatic changes? The **water** component and associated hydrological network also deserve further studies to answer the following questions: In which network does water circulate and what is the time of transfer? Does water percolation in the distal zone contribute to evacuate the finest sediments? Finally, the amount and origin of **debris** should be more deeply investigated: How did the debris concentration vary in time and space during the Holocene? What are the Holocene and current rates of basal erosion and rockwall retreat? In situ measurements and especially the drilling of **boreholes** (e.g. [Arenson et al., 2003](#); [Gilbert et al., 2012](#); [Huss and Fischer, 2016](#)) and the combined use of **geophysical methods** such as ERT, GPR, seismic refraction or gravimetry (e.g. [Hubbard and Glasser, 2005](#); [Hausmann et al., 2007 & 2012](#); [Hauck and Kneisel., 2008](#)) would allow to collect elements of answer to most of these questions.

- *Development of knowledge on current dynamics:* Field and remote measurements have to be pursued and intensified **to monitor the responses of SDCGSAPE to current climatic changes**. The **identification of occurring processes, their quantification** (order of magnitudes, spatial and temporal variations, interactions, etc.) as well as **their understanding** (controls, triggers, etc.) still deserve sound investigations. It would allow to compare the behaviour of the different components of these systems together and with similar landforms around the world. Among others, answers to these following still need to be completed: in which measure does avalanching, shading, the presence of a debris cover, water circulation, or permafrost conditions influence accumulation and ablation rates in these systems? How water and debris influence their motion mechanism? Does a distinct dynamical behaviour between rock glaciers and heavily debris-covered glaciers (especially in the type and/or magnitude of processes responsible of motion mechanism) clearly exist? How evolve the ice melt rate and how long the ice will subsist in these? SDCGSAPE could also be sources of **geohazard** (e.g. debris flows, glacial lakes outburst floods, landslides, rockfalls) that deserve specific studies. The stability of ice-free accumulations and ice-debris mixtures should be thoroughly analysed. Technological progresses especially in **monitoring tools** as terrestrial laser scanners (e.g. [Kummert and Delaloye, 2015](#); [Fischer M. et al., 2016](#)), permanent dGPS beacon (e.g. [Shepherd et al., 2009](#); [Bartholomew et al., 2010](#)) or permanent camera (e.g. [Messerli and Grinsted, 2015](#)) open promising perspectives to capture in detail the dynamics occurring at the surface of SDCGSAPE. In this way, the accurate, rapid and secure zonal analysis allowed by remote sensing tools will progressively replace the punctual, time-consuming and sometimes dangerous (e.g. exposition to rockfall hazards) field measurements, as the dGPS surveys, and allow to collect fuller datasets. Comparison of DEMs at decadal to seasonal timescales also showed their large potential to shed light on the dynamics occurring in cold regions (e.g. [Kummert and Delaloye, 2015](#); [Micheletti et al., 2015b](#); [Capt et al., 2016](#); [Fischer M. et al., 2016](#)).
- *Integration in inventories and mapping:* As stated in the introduction, these complex glaciers remain weakly considered in regional and global **inventories and mapping**, especially because a continuum exists at the surface between firn, bare ice glacier, debris-covered glacier

and rock glacier. The intensification of empirical measurements presented above will improve the knowledge on these complex systems and the use of consensual inventory criteria. It will facilitate their integration in these ambitious and substantial works. Interesting perspectives are also open by the global intensification of high-resolution aerial image acquisitions and the availability of some of these images on free software as *GoogleEarth* or *Plans*. Moreover, the development of remote sensing methods allowed significant progress in the detection of debris-covered ice (e.g. Fischer M. et al., 2014; Robson et al., 2015). Finally, the presence of **similar systems on the surface of Mars** open fascinating research perspectives (e.g. Hubbard et al., 2014). Their inventory and their comparison with terrestrial analogous could contribute to fundamental scientific findings concerning the surface characteristics and evolution of this planet.

- *Integration in evolution models*: Recent progresses in **modelling** improved the knowledge on glaciers and rock glaciers and allowed to **anticipate their future evolution** (e.g. Kääb et al., 2007; Kanan and Rajagopal, 2013; Huss and Hock, 2015; Shea et al., 2015). However, the occurrence of very local complex positive and negative feedbacks, as well as non-linear processes are barely considered in models (e.g. Knight and Harrison, 2014; Pellicciotti et al., 2015). Encouraging attempts were recently made to integrate this complexity into models (e.g. Rowan et al., 2015; Huss and Fischer, 2016). Nevertheless, efforts have to be pursued to take into account topics as the influence on ice masses motion and volume change of debris concentration and superficial layer thickness, thermal regime, water circulations or changing permafrost conditions. The consideration of the interactions between heavily-debris covered glaciers and rock glaciers also remains, to our knowledge, an unexplored modelling topic. As all the components of the cryosphere, SDCGSAPE are severely impacted by the climatic changes and models could allow to better anticipate the evolution of these ice and debris accumulations.

References

- Ackert, R. P. (1998). A rock glacier/debris-covered glacier system at Galena Creek, Absaroka Mountains, Wyoming. *Geografiska Annaler: Series A, Physical Geography*, 80(3-4), 267-276.
- Anderson, R. S., Anderson, S. P., MacGregor, K. R., Waddington, E. D., O'Neel, S., Riihimaki, C. A., & Loso, M. G. (2004). Strong feedbacks between hydrology and sliding of a small alpine glacier. *Journal of Geophysical Research: Earth Surface*, 109(F3).
- Arendt, A., Walsh, J., & Harrison, W. (2009). Changes of Glaciers and Climate in Northwestern North America during the Late Twentieth Century. *J. Clim.*, 22: 4117-4134.
- Arenson, L., Hoelzle, M., & Springman, S. (2002). Borehole deformation measurements and internal structure of some rock glaciers in Switzerland. *Permafrost and Periglacial Processes*, 13(2), 117-135.
- Avian, M., Kellerer-Pirklbauer, A., & Bauer, A. (2009). LiDAR for monitoring mass movements in permafrost environments at the cirque Hinteres Langtal, Austria, between 2000 and 2008. *Natural Hazards and Earth System Sciences* 9: 1087-1094.
- Azócar, G., & Brenning, A. (2010). Hydrological and geomorphological significance of rock glaciers in the dry Andes, Chile (27-33 S). *Permafrost and Periglacial Processes*, 21(1), 42-53.
- Badoux, H., & Gabus, J. (1991). *Les Diablerets, Atlas géologique de la Suisse au 1/25 000*, 88. Swisstopo: Wabern.
- Bælum, K., & Benn, D. (2011). Thermal structure and drainage system of a small valley glacier (Tellbreen, Svalbard), investigated by ground penetrating radar. *The Cryosphere*, 5(1), 139-149.
- BAFU (2005). *Hinweiskarte der potentiellen Permafrostverbreitung in der Schweiz*, Swiss Federal Office for the Environment: Bern.
- Bahr, D. B. (1997). Global distributions of glacier properties: a stochastic scaling paradigm. *Water Resources Research*, 33, 1669-1679.
- Bahr, D. B., & Radic, V. (2012). Significant contribution to total mass from very small glaciers. *The Cryosphere*, 6(4), 763-770.
- Ballantyne, C. K. (2002). Paraglacial geomorphology. *Quaternary Science Reviews*, 21(18), 1935-2017.
- Ballantyne, C. K., Schnabel, C., & Xu, S. (2009). Exposure dating and reinterpretation of coarse debris accumulations ('rock glaciers') in the Cairngorm Mountains, Scotland. *Journal of Quaternary Science*, 24(1), 19-31.
- Baroni, C., & Orombelli, G. (1996). The alpine "Iceman" and Holocene climatic change. *Quaternary Research*, 46(1), 78-83.
- Barsch, D. (1996). *Rockglaciers: indicators for the present and former geocology in high mountain environments (Vol. 16)*. Springer Science & Business Media.
- Barsch, D. & Jakob M. (1998). Mass transport by active rockglaciers in the Khumbu Himalaya. *Geomorphology*, 26, 215-222.
- Bartholomew, I., Nienow, P., Mair, D., Hubbard, A., King, M. A., & Sole, A. (2010). Seasonal evolution of subglacial drainage and acceleration in a Greenland outlet glacier. *Nature Geoscience*, 3(6), 408-411.
- Bauder, A., Fischer, M., Funk, M., Huss, M., & Kappenberger, G. (2015). *The Swiss Glaciers; 2009/2010 and 2010/2011*. Glaciological Report No. 131/132. Cryospheric Commission (EKK).
- Bearth, P. (1972). *Simplon, Atlas géologique de la Suisse au 1/25 000*, 61. Swisstopo: Wabern.
- Begert, M., Schlegel, T., & Kirchhofer, W. (2005). Homogeneous temperature and precipitation series of Switzerland from 1864 to 2000. *Int. J. Climatol.*, 25(1): 65-80.
- Benn, D. I. (1994). Fluted moraine formation and till genesis below a temperate valley glacier: Slettmarkbreen, Jotunheimen, southern Norway. *Sedimentology*, 41(2), 279-292.
- Benn, D. I., Kirkbride, M. P., Owen, L. A., & Brazier, V. (2003). *Glaciated valley landsystems*. *Glacial Landsystems*. Arnold, London, 372-406.
- Benn, D., & Evans, D. J. (2010). *Glaciers and glaciation (éd. Second Edition)*. Routledge.
- Benn, D., Bolch, T., Hands, K., Gulle, J., Luckman, A., Nicholson, L. I.,... & Wiseman, S. (2012). Response of debris-covered glaciers in the Mount Everest region to recent warming, and implications for outburst flood hazards. *Earth-Science Reviews*, 114(1), 156-174.
- Bennett, M. R. (2011). Ice-Marginal Processes. Dans *Encyclopedia of Snow, Ice and Glaciers* (pp. 623-625). Springer.

- Berger, J., Krainer, K., & Mostler, W. (2004). Dynamics of an active rock glacier (Ötztal Alps, Austria) Alps, Austria). *Quaternary Research*, 62(3), 233-242.
- Berthling, I. (2011). Beyond confusion: Rock glaciers as cryo-conditioned landforms. *Geomorphology*, 131(3), 98-106.
- Berthling, I., & Etzelmüller, B. (2011). The concept of cryo-conditioning in landscape evolution. *Quaternary Research*, 75(2), 378-384.
- Berthling, I., Schomacker, A., & Benediktsson, Í. Ö. (2013). The glacial and periglacial research frontier: where from here. *Treatise on Geomorphology*, Shroder J, Jr (ed). Academic Press: San Diego, 479-499.
- Berthier, E., Vincent, C., Magnusson, E., Gunnlaugsson, A. T., Pitte, P., Le Meur, E., Masioka, S. M., Ruiz, L., Pálsson, F., Belart, J. M. C., Wagnon, Patrick (2014). Glacier topography and elevation changes derived from Pleiades sub-meter stereo images. *The Cryosphere*, 8 (6), 3275-2291.
- Bingham, R. G., Nienow, P. W., & Sharp, M. J. (2003). Intra-annual and intra-seasonal flow dynamics of a High Arctic polythermal valley glacier. *Annals of Glaciology*, 37(1), 181-188.
- Bingham, R. G., Nienow, P. W., Sharp, M. J., & Copland, L. (2006). Hydrology and dynamics of a polythermal (mostly cold) High Arctic glacier. *Earth Surface Processes and Landforms*, 31(12), 1463-1479.
- Bingham, R. G., Hubbard, A. L., Nienow, P. W., & Sharp, M. J. (2008). An investigation into the mechanisms controlling seasonal speedup events at a High Arctic glacier. *Journal of Geophysical Research: Earth Surface* (2003--2012), 113(F2).
- Bockheim, J., Vieira, G., Ramos, M., López-Martínez, J., Serrano, E., Guglielmin, M., ... & Nieuwendam, A. (2013). Climate warming and permafrost dynamics in the Antarctic Peninsula region. *Global and Planetary Change*, 100, 215-223.
- Bodin, X., Schoeneich, P., Lhotellier, R., Gruber, S., Deline, P., Ravelin, L., & Monnier, S. (2008). Towards a first assessment of the permafrost distribution in the French Alps. In 6th Swiss Geoscience Meeting 2008, Lugano, 175-176.
- Boeckli, L., Brenning, A., Gruber, S., & Noetzi, J. (2012). Permafrost distribution in the European Alps: calculation and elevation of an index map and summary statistics. *The Cryosphere*. 6, 807-820. doi:10.5194/tc-6-807-2012.
- Bolch, T. (2011). Debris. Dans *Encyclopedia of Snow, Ice and Glaciers* (pp. 176-178). Springer.
- Bolch, T. & Gorbunov, A.P. (2014). Characteristics and Origin of Rock Glaciers in Northern Tien Shan (Kazakhstan/Kyrgyzstan). *Permafrost and Periglacial Processes*, 25, 320-332.
- Bonani, G. (1992). Altersbestimmung von Milligrammproben der Ötztaler Gletscherleiche mit der Beschleunigermassenspektrometrie-Methode (AMS). na.
- Bonani, G., Ivy, S. D., Hajdas, I., Niklaus, T. R., Suter, M., & others. (1994). AMS 14C age determinations of tissue, bone and grass samples from the Otztal ice man. *Radiocarbon*, 36(2), 247-250.
- Bosson, J.B. (2010). Contribution à l'étude du patrimoine géomorphologique de la Réserve Naturelle des Contamines Montjoie et démarches de géovalorisation. Master thesis, University of Lausanne.
- Bosson, J.B. (2012). Les glaciers enterrés du vallon des Jovet. *Nature et Patrimoine en Pays de Savoie* 38: 16-23.
- Bosson, J.B. (2013). Etude de la répartition de la glace dans le sol et de la dynamique actuelle du secteur des Rebanets Chassots (Contamines-Montjoie, Massif du Mont-Blanc). Résultats obtenus lors de l'été 2013. Unpublished, University of Lausanne.
- Bosson, J.B. (2014). Etude de la répartition de la glace dans le sol et de la dynamique actuelle du secteur des Rebanets Chassots (Contamines-Montjoie, Massif du Mont-Blanc). Résultats obtenus lors de l'été 2014. Unpublished, University of Lausanne.
- Bosson, J.B., Deline, P., Bodin, X., Schoeneich, P., Baron, L., Gardent, M., & Lambiel, C. (2015). The influence of ground ice distribution on geomorphic dynamics since the Little Ice Age in pro-glacial areas of two cirque glacier systems. *Earth Surf. Proc. Land.*, 40, 666-680.
- Bosson, J.B., & Lambiel, C; (2016). Internal structure and current evolution of small debris-covered glacier systems located in alpine permafrost environments. *Front in Earth-Science.*, 4 :39.
- Bouët, M. (1985). *Climat et météorologie de la Suisse romande*. Payot: Lausanne.
- Boulton, G. (1996). Theory of glacial erosion, transport and deposition as a consequence of subglacial sediment deformation. *Journal of Glaciology*, 42(140), 43-62.
- Bozhinskiy, A., Krass, M., & Popovnin, V. (1986). Role of debris cover in the thermal physics of glaciers. *Journal of Glaciology*, 32(111), 255-266.

- Brazier, V., Kirkbride, M. P., & Owens, I. F. (1998). The relationship between climate and rock glacier distribution in the Ben Ohau Range, New Zealand. *Geografiska Annaler: Series A, Physical Geography*, 80(3-4), 193-207.
- Bret, J. (2011). Reconstitution des fluctuations glaciaires sur les bassins versant d'Armançette et de Tré la Tête depuis le dernier maximum du Petit Age Glaciaire (1820-2008). Master thesis, Université de Savoie.
- Brock, B. W., Mihalcea, C., Kirkbride, M. P., Diolaiuti, G., Cutler, M. E., & Smiraglia, C. (2010). Meteorology and surface energy fluxes in the 2005--2007 ablation seasons at the Miage debris-covered glacier, Mont Blanc Massif, Italian Alps. *Journal of Geophysical Research: Atmospheres* (1984--2012), 115(D9).
- Brown, J., Harper, J., & Humphrey, N. (2010). Cirque glacier sensitivity to 21st century warming: Sperry Glacier, Rocky Mountains, USA. *Global and Planetary Change*, 74(2), 91-98.
- Burger, K., Degenhardt, J., & Giardino, J. (1999). Engineering geomorphology of rock glaciers. *Geomorphology*, 31(1), 93-132.
- Burn, C. R. & Smith, C. A. S. (1988). Observations of the « thermal offset » in near-surface mean annual ground temperatures at several sites near Mayo, Yukon Territory, Canada. *Arctic*, 41(2), 99-104.
- Burri, M., Frank, E., Jeanbourquin, J., Labhart, T., Liszky M. & Streckeisen A. (1993). Brig, Atlas géologique de la Suisse au 1/25 000, 93. Swisstopo: Wabern.
- Burri, M., Allimann, M., Chessex, R., Dal Piaz, G. V., Delle Valle, G., Du Bois, L., Gouffon, Y., Guermani, A., Hagen, T., Krummenacher D., & Looser, M.-O. (1998). Chanrion-Mt-Vélan, Atlas géologique de la Suisse au 1/25 000, 101. Swisstopo: Wabern.
- Capt, M. (2015). Evolution des petits systèmes glaciaires situés dans le domaine périglaciaire alpin à différentes échelles temporelles: les cas de Tsarmine (Arolla, Valais) et Entre la Reille (Diablerets, Vaud). Master thesis, University of Lausanne.
- Capt, M., Bosson, J.B., Fischer, M., Micheletti, N., & Lambiel, C. (2016). Decadal evolution of a small heavily debris-covered glacier located in Alpine permafrost environment. *J. Glaciol*, 62(233), 535-551.
- Carrivick, J.L., Geilhausen, M., Warburton, J., Dickson, N.E., Carver, S.J., Evans, A.J., & Brown, L.E. (2013). Contemporary geomorphological activity throughout the proglacial area of an alpine catchment. *Geomorphology*, 188, 83-95.
- Carrivick, J.L., Berry, K., Geilhausen, M., James, W.H.M., Williams, C., Brown, L.E., Rippin, D.M., & Carver, S.J. (2015). Decadal-scale changes of the Ödenwinkelkees, Central Austria, suggest increasing control of topography and evolution towards steady state. *Geog. Ann. A*, 97, 543-562.
- Carturan, L., Cazorzi, F., & Fontana, G. D. (2012). Distributed mass-balance modelling on two neighbouring glaciers in Ortles-Cevedale, Italy, from 2004 to 2009. *Journal of Glaciology*, 58(209), 467-486.
- Carturan, L., Baldassi, G. A., Bondesan, A., Calligaro, S., Carton, A., Cazorzi, F., ... & Moro, D. (2013a). Current behaviour and dynamics of the lowermost Italian glacier (Montasio Occidentale, Julian Alps). *Geografiska Annaler: Series A, Physical Geography*, 95(1), 79-96.
- Carturan, L., Filippi, R., Seppi, R., Gabrielli, P., Notarnicola, C., Bertoldi, L., Paul, P., Rastner, P., Cazorzi, F., Dinale, R., & Dalla Fontana, G. (2013b). Area and volume loss of the glaciers in the Ortles-Cevedale group (Eastern Italian Alps): controls and imbalance of the remaining glaciers. *Cryosphere*, 7, 1339-1359.
- Chandler, J.H., Lane, S.N., & Walstra, J. (2007). Quantifying landform change. In Fryer, J., Mitchell, H., & Chandler, J.H. eds. *Applications of 3D Measurement from Images*. Dunbeath, Whittles Publishing, 139-170
- Chen, J. & Ohmura, A. (1990). Estimation of alpine glacier water resources and their change since the 1870s. *International Association of Hydrological Sciences Publications*, 193, 127-135.
- Chiarle, M., Iannotti, S., Mortara, G., & Deline, P. (2007). Recent debris flow occurrences associated with glaciers in the Alps. *Global and Planetary Change*, 56(1), 123-136.
- Chueca, J., Julian, A., & Lopez-Moreno, J. I. (2007). Recent evolution (1981--2005) of the Maladeta glaciers, Pyrenees, Spain: extent and volume losses and their relation with climatic and topographic factors. *Journal of glaciology*, 53(183), 547-557.
- Church, M. & Slaymaker, O. (1989). Disequilibrium of Holocene sediment yield in glaciated British Columbia. *Nature*, 337, 452-454.
- Clark, D. H., Clark, M. M., & Gillespie, A. R. (1994). Debris-covered glaciers in the Sierra Nevada, California, and their implications for snowline reconstructions. *Quaternary Research*, 41(2), 139-153.
- Clark, D. H., Steig, E. J., Potter Jr, N., & Gillespie, A. R. (1998). Genetic variability of rock glaciers. *Geografiska Annaler: Series A, Physical Geography*, 80(3-4), 175-182.

- Cogley, J.G., Hock, R., Rasmussen, L.A., Arendt, A.A., Bauder, A., Braithwaite, R.J., Jansson, P., Kaser, G., Möller, M., Nicholson, L., & Zemp, M. (2011). Glossary of Glacier Mass Balance and Related Terms. IHP-VII Technical Documents in Hydrology 86, IACS Contribution 2. Paris: UNESCO-IHP.
- Collins, M., Knutti, R., & 12 others. (2013). Long-term Climate Change: Projections, Commitments and Irreversibility. In Stocker TF, and 9 others eds. *Climate Change 2013: The Physical Science Basis. Contribution of Working Group I to the Fifth Assessment Report of the Intergovernmental Panel on Climate Change*, Cambridge University Press: Cambridge; 1029–1136.
- Colucci, R. R., & Guglielmin, M. (2014). Precipitation--temperature changes and evolution of a small glacier in the southeastern European Alps during the last 90 years. *International Journal of Climatology*.
- Copland, L., Pope, S., Bishop, M. P., Shroder, J. F., Clendon, P., Bush, A.,... & Owen, L. A. (2009). Glacier velocities across the central Karakoram. *Annals of Glaciology*, 50(52), 41-49.
- Cossart, E., & Fort, M. (2008). Sediment release and storage in early deglaciated areas: Towards an application of the exhaustion model from the case of Massif des Ecrins (French Alps) since the Little Ice Age. *Norsk Geografisk Tidsskrift-Norwegian Journal of Geography*, 62(2), 115-131.
- Cuffey, K. M., & Paterson, W. S. (2010). *The physics of glaciers*. Academic Press.
- D'Agata, C., & Zanutta, A. (2007). Reconstruction of the recent changes of a debris-covered glacier (Brenva Glacier, Mont Blanc Massif, Italy) using indirect sources: methods, results and validation. *Global and Planetary Change*, 56(1), 57-68.
- Darbellay, R. (2015). Structure interne et évolution récente des systèmes des systèmes glaciaires alpins situés à l'intérieur du domaine périglaciaire : le cas du Petit Combin (Bagnes, Valais). Master thesis, University of Lausanne.
- Davies, M. C., Hamza, O., & Harris, C. (2001). The effect of rise in mean annual temperature on the stability of rock slopes containing ice-filled discontinuities. *Permafrost and Periglacial Processes*, 12(1), 137-144.
- D'Aujourd'hui, S. (2013). Etude de la dynamique sédimentaire d'un bassin versant torrentiel de haute montagne. Le cas des Chalti Wasser, Simplon (Vs). Master thesis, University of Lausanne.
- DeBeer, C. M., & Sharp, M. J. (2009). Topographic influences on recent changes of very small glaciers in the Monashee Mountains, British Columbia, Canada. *Journal of Glaciology*, 55(192), 691-700.
- Delaloye, R. (2004). Contribution à l'étude du pergélisol de montagne en zone marginale. Ph.D. dissertation, Université de Fribourg.
- Delaloye, R. (2008). Parois glaciaires...parois rocheuses: l'évolution séculaire des grandes faces alpines. In Rothenbühler, C. eds. *Klimaveränderungen auf der Spur. Studien des Europäischen Tourismus Instituts an der Academia Engiadina* 5, 93-104.
- Delaloye, R., Perruchoud, E., Avian, M., Kaufmann, V., Bodin, X., Hausmann, H., ... & Lambiel, C. (2008). Recent interannual variations of rock glacier creep in the European Alps. *Proceedings of the 9th International Conference on Permafrost, Fairbanks, Alaska*, 29, pp. 343-348.
- Delaloye, R., Lambiel, C., & Gärtner-Roer, I. (2010). Overview of rock glacier kinematics research in the Swiss Alps. *Geogr. Helv*, 65, 135-145.
- Deline, P. (1999). Les variations holocènes récentes du glacier du Miage (Val Veny, Val d'Aoste)[Late holocene fluctuations of the Miage glacier (Val Veny, Valley of Aosta)]. *Quaternaire*, 10(1), 5-13.
- Deline, P. (2005). Change in surface debris cover on Mont Blanc massif glaciers after the 'Little Ice Age' termination. *The Holocene*, 15(2), 302-309.
- Deline, P., Gardent, M., Magnin, F., & Ravanel, L. (2012). The morphodynamics of the Mont Blanc massif in a changing cryosphere: a comprehensive review. *Geografiska Annaler: Series A, Physical Geography*, 94(2), 265-283.
- Deline, P., Gruber, S., Delaloye, R., Fischer, L., Geertsema, M., Giardino, M., ... & McColl, S. (2015). Ice Loss and Slope Stability in High-Mountain Regions. *Snow and Ice-related Hazards, Risks and Disasters*. Elsevier pp. 521e562.
- Deluigi, N. (2012). Modélisation de la répartition du pergélisol alpin à l'aide de l'apprentissage automatique. Master thesis, University of Lausanne.
- Deluigi, N., & Lambiel, C. (2012). PERMAL: a machine learning approach for alpine permafrost distribution modeling. *Jahrestag. Schweiz. Geomorphol. Ges*, 4, 47-62.
- Demuth, M.N. (2011). LIDAR in Glaciology. in *Encyclopedia of Snow, Ice and Glaciers* (pp. 713-722). Springer.
- Dikau, R. (2004). Equilibrium Slope. Dans *Encyclopedia of Geomorphology*, Goudie AS (ed). Routledge.

- Diolaiuti, G.A., Bocchiola, D., Vigiasindi, M., D'Agata, C., & Smiraglia, C. (2012). The 1975-2005 glacier changes in Aosta Valley (Italy) and the relations with climate evolution. *Prog. Phys. Geog.*, 36(6), 764-785.
- Dobhal, D. (2011). Dead ice. Dans *Encyclopedia of Snow, Ice and Glaciers* (pp. 176-176). Springer.
- Dobhal, D. (2011). Glacier. *Encyclopedia of Snow, Ice and Glaciers*, 127-127.
- Dobhal, D., Mehta, M., & Srivastava, D. (2013). Influence of debris cover on terminus retreat and mass changes of Chorabari Glacier, Garhwal region, central Himalaya, India. *Journal of Glaciology*, 59(217), 961-971.
- Dusik, J.-M., Leopold, M., Heckmann, T., Haas, F., Hilger, L., Morche, D., ... & Becht, M. (2015). Influence of glacier advance on the development of the multipart Riffeltal rock glacier, Central Austrian Alps. *Earth Surface Processes and Landforms*.
- Emmer, A., Loarte, E. C., Klimeš, J., & Vilimek, V. (2015). Recent evolution and degradation of the bent Jatunraju glacier (Cordillera Blanca, Peru). *Geomorphology*, 228, 345-355.
- Etzelmüller, B. B., Berthling, I., & Sollid, J. L. (2003). Aspects and concepts on the geomorphological significance of Holocene permafrost in southern Norway. *Geomorphology*, 52(1), 87-104.
- Etzelmüller, B., & Hagen, J. O. (2005). Glacier-permafrost interaction in Arctic and alpine mountain environments with examples from southern Norway and Svalbard. *Geological Society, London, Special Publications*, 242(1), 11-27.
- Evans, D. (2003). Ice-marginal terrestrial landsystems: active temperate glacier margins. *Glacial Landsystems*. Arnold, London, 12-43.
- Evans, D. (2013). Geomorphology and retreating glacier. *Treatise on Geomorphology*, Shroder J, Jr (ed). Academic Press: San Diego, 8, 460-478.
- Evatt, G.W., Abrahams I.D., Heil, M., Mayer, C., Kingslake, J., Mitchell, S.L., Fowler, A.C. & Clark, C.D. (2015). Glacial melt under a porous debris layer. *J. Glaciol.*, 61(229), 825–836.
- Fatland, D. R., Lingle, C. S., & Truffer, M. (2003). A surface motion survey of black rapids glacier, alaska, usa. *Annals of Glaciology*, 36(1), 29-36.
- Field, C., Barros, V., Dokken, D., Mach, K., Mastrandrea, M., Bilir, T., ... & others. (2014). IPCC, 2014: Climate Change 2014: Impacts, Adaptation, and Vulnerability. Part A: Global and Sectoral Aspects. Contribution of Working Group II to the Fifth Assessment Report of the Intergovernmental Panel on Climate Change. IPCC, 2014: Climate Change 2014: Impacts, Adaptation, and Vulnerability. Part A: Global and Sectoral Aspects. Contribution of Working Group II to the Fifth Assessment Report of the Intergovernmental Panel on Climate Change. Cambridge University Press, Cambridge, United Kingdom and New York, NY, USA.
- Fischer, A. (2009). Calculation of glacier volume from sparse ice-thickness data, applied to Schaufelferner, Austria. *J. Glaciol.*, 55(191), 453–460.
- Fischer, A., & Kuhn, M. (2013). Ground-penetrating radar measurements of 64 Austrian glaciers between 1995 and 2010. *Ann. Glaciol.*, 54(64), 179–188.
- Fischer, A., Seiser, B., Stocker Waldhuber, M., Mitterer, C., & Abermann, J. (2015). Tracing glacier changes in Austria from the Little Ice Age to the present using a lidar-based high-resolution glacier inventory in Austria. *The Cryosphere*, 9(2), 753-766.
- Fischer, M., Huss, M., Barboux, C., & Hoelzle, M. (2014). The new Swiss Glacier Inventory SGI2010: relevance of using high-resolution source data in areas dominated by very small glaciers. *Arctic, Antarctic, and Alpine Research*, 46(4), 933-945.
- Fischer, M., Huss, M., & Hoelzle, M. (2015). Surface elevation and mass changes of all Swiss glaciers 1980–2010. *Cryosphere*, 9, 525-540
- Fischer, M., Huss, M., Kummert, M. & Hoelzle, M. (2016) Use of an ultra-long-range terrestrial laser scanner to monitor the mass balance of very small glaciers in the Swiss Alps. *The Cryosphere Discuss.*, doi:10.5194/tc-2016-46.
- Fitzsimons, S., & Lorrain, R. (2014). Subglacial Processes. Dans *Encyclopedia of Snow, Ice and Glaciers* (pp. 1101-1105). Springer.
- Florentine, C., Skidmore, M., Speece, M., Link, C., Shaw, C.A. (2014). Geophysical analysis of transverse ridges and internal structure at Lone Peak Rock Glacier, Big Sky, Montana, USA. *J. Glaciol.*, 60(221), 453–462.
- Fountain, A. G., Jacobel, R. W., Schlichting, R., & Jansson, P. (2005). Fractures as the main pathways of water flow in temperate glaciers. *Nature*, 433(7026), 618-621.
- Frauenfelder, R., Haeberli, W., & Hoelzle, M. (2003). Rockglacier occurrence and related terrain parameters in a study area of the Eastern Swiss Alps. *Proceedings 8th International Conference on Permafrost*. Swets and Zeitlinger, Lisse, (pp.

- 253-258).
- Frey, P. A. (1988). *E. Viollet-le-Duc et le massif du Mont-Blanc, 1868-1879*. Payot: Lausanne.
- Fu, P., & Harbor, J. (2011). Glacial erosion. Dans *Encyclopedia of Snow, Ice and Glaciers* (pp. 332-341). Springer.
- Fukui, K., Sone, T., Strelin, J. A., Torielli, C. A., Mori, J., & Fujii, Y. (2008). Dynamics and GPR stratigraphy of a polar rock glacier on James Ross Island, Antarctic Peninsula. *Journal of Glaciology*, 54(186), 445-451.
- Gabbi, J., Huss, M., Bauder, A., Cao, F., & Schwikowski, M. (2015). The impact of Saharan dust and black carbon on albedo and long-term mass balance of an Alpine glacier. *The Cryosphere*, 9(4), 1385-1400.
- Gardent, M. (2014). *Inventaire et retrait des glaciers dans les alpes françaises depuis la fin du Petit Age Glaciaire*. Ph.D. dissertation, Grenoble.
- Gardner, A.S., Moholdt, G., Cogley, J.G., Wouters, B., Arendt, A.A., Wahr, J., Berthier, E., Hock, R., Pfeffer, W.T., Kaser, G., Kigtenberg, S.R.M., Bolch, T., Sharp, M.J., Hagen, J.O., Van den Broeke, M.R., & Paul, F. (2013). A reconciled estimate of glacier contributions to sea level rise: 2003 to 2009. *Science*, 340(6134), 852-857.
- GärtnerRoer, I., & Nyenhuis, M. (2010). Volume estimation, kinematics and sediment transfer rates of active rockglaciers in the Turtmann Valley, Switzerland. Dans *Landform-Structure, Evolution, Process Control* (pp. 185-198). Springer.
- Geilhausen, M., Otto, J.-C., & Schrott, L. (2012). Spatial distribution of sediment storage types in two glacier landsystems (Pasterze & Obersulzbachkees, Hohe Tauern, Austria). *Journal of Maps*, 8(3), 242-259.
- Gilbert, A., Vincent, C., Wagnon, P., Thibert, E., & Rabatel, A. (2012). The influence of snow cover thickness on the thermal regime of Tête Rousse Glacier (Mont Blanc range, 3200 m asl): Consequences for outburst flood hazards and glacier response to climate change. *Journal of Geophysical Research: Earth Surface* (2003--2012), 117(F4).
- Glen, J. W. (1955). The creep of polycrystalline ice. *Proceedings of the Royal Society of London A: Mathematical, Physical and Engineering Sciences*, 228, pp. 519-538.
- Godon, C., Mugnier, J.-L., Fallourd, R., Paquette, J.-L., Pohl, A., & Buoncristiani, J.-F. (2013). The Bossons glacier protects Europe's summit from erosion. *Earth and Planetary Science Letters*, 375, 135-147.
- Gomez, A., Palacios, D., Luengo, E., Tanarro, L.M., Schulte, L., & Ramos, M. (2003). Talus instability in a recent deglaciation area and its relationship to buried ice and snow cover evolution (Picacho des Veleta, Sierra Nevada, Spain). *Geografiska Annaler* 85 A(2): 165-182.
- Grosjean, M., Suter, P. J., Trachsel, M., & Wanner, H. (2007). Ice-borne prehistoric finds in the Swiss Alps reflect Holocene glacier fluctuations. *Journal of Quaternary Science*, 22(3), 203-207.
- Gruber, S., & Haeberli, W. (2009). Mountain permafrost. Dans *Permafrost Soils* (pp. 33-44). Springer.
- Grunewald, K., & Scheithauer, J. (2010). Europe's southernmost glaciers: response and adaptation to climate change. *Journal of Glaciology*, 56(195), 129-142.
- Gudmundsson, G., Bassi, A., Vonmoos, M., Bauder, A., Fischer, U., & Funk, M. (2000). High-resolution measurements of spatial and temporal variations in surface velocities of Unteraargletscher, Bernese Alps, Switzerland. *Annals of Glaciology*, 31(1), 63-68.
- Guglielmin, M., Camusso, M., Polesello, S., & Valsecchi, S. (2004). An old relict glacier body preserved in permafrost environment: the Foscagno rock glacier ice core (Upper Valtellina, Italian Central Alps). *Arctic, Antarctic, and Alpine Research*, 36(1), 108-116.
- Haeberli, W. (1973). Die Basis-Temperatur der winterlichen Schneedecke als möglicher Indikator für die Verbreitung von Permafrost in den Alpen. *Zeitschrift für Gletscherkunde und Glazialgeologie*, 9, 221-227.
- Haeberli, W. (1979). Holocene push-moraines in alpine permafrost. *Geografiska Annaler. Series A. Physical Geography*, 43-48.
- Haeberli, W. (1985). Creep of mountain permafrost: internal structure and flow of alpine rock glaciers. *Mitteilungen der Versuchsanstalt für Wasserbau, Hydrologie und Glaziologie an der ETH Zurich*, 77, 5-142.
- Haeberli, W. (1985). Global land-ice monitoring: present status and future perspectives. United States Department of Energy, Glaciers, Ice Sheets, and Sea level: Effect of a CO₂-Induced Climatic Change. Report DOE/EV 60235-1. National Academy Press, Seattle, WA, 216-231.
- Haeberli, W. (1995). Glacier fluctuations and climate change detection: operational elements of a worldwide monitoring strategy. World Meteorological Organization.
- Haeberli, W. (2000). Modern research perspectives relating to permafrost creep and rock glaciers: a discussion. *Permafrost and Periglacial Processes*, 11(4), 290-293.

- Haeberli, W. (2005). Investigating glacier-permafrost relationships in high-mountain areas: historical background, selected examples and research needs. *Geological Society, London, Special Publications*, 242(1), 29-37.
- Haeberli, W., Hallet, B., Arenson, L., Elconin, R., Humlum, O., Kääh, A., ... & Mühl, D. V. (2006). Permafrost creep and rock glacier dynamics. *Permafrost and periglacial processes*, 17(3), 189-214.
- Haeberli, W., Huggel, C., Paul, F., & Zemp, M. (2013). Glacial responses to climate change. *Treatise on Geomorphology*, Shroder JF (chief ed.), James LA, Harend CP, Clague JJ (eds). Academic Press: San Diego, CA, 152-175.
- Hagg, W., Mayer, C., Lambrecht, A., & Helm, A. (2008). Sub-debris melt rates on southern Inylchek Glacier, central Tian Shan. *Geografiska Annaler: Series A, Physical Geography*, 90(1), 55-63.
- Hambrey, M. J., & Glasser, N. F. (2011). Sediment Entrainment, Transport, and Deposition. Dans *Encyclopedia of Snow, Ice and Glaciers* (pp. 984-1003). Springer.
- Hambrey, M. J., Quincey, D. J., Glasser, N. F., Reynolds, J. M., Richardson, S. J., & Clemmens, S. (2008). Sedimentological, geomorphological and dynamic context of debris-mantled glaciers, Mount Everest (Sagarmatha) region, Nepal. *Quaternary Science Reviews*, 27(25), 2361-2389.
- Hamilton, S. J., & Whalley, W. B. (1995). Rock glacier nomenclature: A re-assessment. *Geomorphology*, 14(1), 73-80.
- Harris, C. (2004). Permafrost. Dans *Encyclopedia of Geomorphology*, Goudie AS (ed). Routledge.
- Harris, C., & Murton, J. B. (2005). Interactions between glaciers and permafrost: an introduction. *Geological Society, London, Special Publications*, 242(1), 1-9.
- Hauck, C., Vonder Mühl, D., Maurer, H. (2003). Using DC resistivity tomography to detect and characterize mountain permafrost. *Geophysical Prospecting* 51, 273-284.
- Hauck, C., & Kneisel, C. (2008). *Applied geophysics in periglacial environments*. Cambridge: Cambridge University Press.
- Hausmann, H., Krainer, K., Brückl, E., & Mostler, W. (2007). Internal structure and ice content of Reichenkar rock glacier (Stubai Alps, Austria) assessed by geophysical investigations. *Permafrost and Periglacial Processes*, 18(4), 351-367.
- Herman, F., Beyssac, O., Brughelli, M., Lane, S. N., Leprince, S., Adatte, T., ... & Cox, S. C. (2015). Erosion by an Alpine glacier. *Science*, 350(6257), 193-195.
- Hilbich, C., Marescot, L., Hauck, C., Loke, M.H., & Mäusbacher, R. (2009). Applicability of Electrical Resistivity Tomography Monitoring to Coarse Blocky and Ice-rich Permafrost Landforms. *Permafrost and Periglacial Processes* 20: 269-284.
- Hodgkins, R. (1997). Glacier hydrology in Svalbard, Norwegian high arctic. *Quaternary Science Reviews*, 16(9), 957-973.
- Hodkinson, I. D., Coulson, S. J., & Webb, N. R. (2003). Community assembly along proglacial chronosequences in the high Arctic: vegetation and soil development in north-west Svalbard. *Journal of Ecology*, 91(4), 651-663.
- Hodkinson, I. D., Coulson, S. J., & Webb, N. R. (2004). Invertebrate community assembly along proglacial chronosequences in the high Arctic. *Journal of Animal Ecology*, 73(3), 556-568.
- Hoffman, M. J., Fountain, A. G., & Achuff, J. M. (2007). 20th-century variations in area of cirque glaciers and glacierets, Rocky Mountain National Park, Rocky Mountains, Colorado, USA. *Annals of Glaciology*, 46(1), 349-354.
- Holzhauser, H., Magny, M., & Zumbühl, H. J. (2005). Glacier and lake-level variations in west-central Europe over the last 3500 years. *The Holocene*, 15(6), 789-801.
- Hubbard, B., & Glasser, N.F. (2005). *Field Techniques in Glaciology and Glacial Geomorphology: Ice Radar*, Chichester: Wiley, 148-178
- Hubbard, B., Souness, C., & Brough, S. (2014). Glacier-like forms on Mars. *The Cryosphere*, 8(6), 2047-2061.
- Huggel, C., Clague, J. J., & Korup, O. (2012). Is climate change responsible for changing landslide activity in high mountains? *Earth Surface Processes and Landforms*, 37(1), 77-91.
- Hughes, P. D. (2009). Twenty-first century glaciers and climate in the Prokletije Mountains, Albania. *Arctic, Antarctic, and Alpine Research*, 41(4), 455-459.
- Humlum, O. (1988). Rock glacier appearance level and rock glacier initiation line altitude: a methodological approach to the study of rock glaciers. *Arctic and Alpine Research*, 160-178.
- Humlum, O. (2000). The geomorphic significance of rock glaciers: estimates of rock glacier debris volumes and headwall recession rates in West Greenland. *Geomorphology*, 35(1), 41-67.
- Huss, M., Funk, M., & Ohmura, A. (2009). Strong Alpine glacier melt in the 1940s due to enhanced solar radiation. *Geophysical Research Letters* 36.

- Huss, M. (2010). Mass balance of Pizolgletscher. *Geographica Helvetica*, 65(2), 80-91.
- Huss, M., Hock, R., Bauder, A., & Funk, M. (2010). 100-year mass changes in the Swiss Alps linked to the Atlantic Multidecadal Oscillation. *Geophysical Research Letters* 37.
- Huss, M. (2012). Extrapolating glacier mass balance to the mountain-range scale: the European Alps 1900--2100. *The Cryosphere*, 6(4), 713-727.
- Huss, M. (2013). Density assumptions for converting geodetic glacier volume change to mass change. *The Cryosphere*, 7, 877-887.
- Huss, M., Dhulst, L., & Bauder, A. (2015). New long-term mass balance series for the Swiss Alps. *J. Glaciol.*, 61(227).
- Huss, M., & Hock, R. (2015). A new model for global glacier change and sea-level rise. *Frontiers in Earth Science*, 3, 54.
- Huss, M., & Fischer, M. (2016). Sensitivity of Very Small Glaciers in the Swiss Alps to Future Climate Change. *Frontiers in Earth Science*, 4, 34.
- IPCC (2014) Climate Change 2014: Synthesis Report. Contribution of Working Groups I, II and III to the Fifth Assessment Report of the Intergovernmental Panel on Climate Change, eds: Core Writing Team, R.K. Pachauri and L.A. Meyer. IPCC, Geneva, Switzerland
- Iribarren Anaconda, P., Mackintosh, A., & Norton, K. P. (2015). Hazardous processes and events from glacier and permafrost areas: lessons from the Chilean and Argentinean Andes. *Earth Surface Processes and Landforms*, 40(1), 2-21.
- Irvine-Fynn, T., Moorman, B., Williams, J., & Walter, F. (2006). Seasonal changes in ground-penetrating radar signature observed at a polythermal glacier, Bylot Island, Canada. *Earth Surface Processes and Landforms*, 31(7), 892-909.
- Iturrizaga, L. (2013). Bent glacier tongues: A new look at Lliboutry's model of the evolution of the crooked Jatunraju Glacier (Parón Valley, Cordillera Blanca, Perú). *Geomorphology*, 198, 147-162.
- Ivy-Ochs, S., Kerschner, H., Maisch, M., Christl, M., Kubik, P. W., & Schlüchter, C. (2009). Latest Pleistocene and Holocene glacier variations in the European Alps. *Quaternary Science Reviews*, 28(21), 2137-2149.
- Janke, J. R., & Frauenfelder, R. (2008). The relationship between rock glacier and contributing area parameters in the Front Range of Colorado. *Journal of Quaternary Science*, 23(2), 153-163.
- Janke, J. R., Regmi, N., Giardino, J., & Vitek, J. (2013). Rock glaciers. Dans *Treatise in Geomorphology* (pp. 238-273). Elsevier.
- Janke, J. R., Bellisario, A. C., & Ferrando, F. A. (2015). Classification of debris-covered glaciers and rock glaciers in the Andes of central Chile. *Geomorphology*, 241, 98-121.
- Joerin, U. E., Stocker, T. F., & Schlüchter, C. (2006). Multicentury glacier fluctuations in the Swiss Alps during the Holocene. *The Holocene*, 16(5), 697-704.
- Joerin, U., Nicolussi, K., Fischer, A., Stocker, T., & Schlüchter, C. (2008). Holocene optimum events inferred from subglacial sediments at Tschierwa Glacier, Eastern Swiss Alps. *Quaternary Science Reviews*, 27(3), 337-350.
- Jóhannesson, T., Raymond, C., & Waddington, E. (1989). Time-scale for adjustment of glaciers to changes in mass balance. *Journal of Glaciology*, 35(121), 355-369.
- Jomelli, V., Favier, V., Rabatel, A., Brunstein, D., Hoffmann, G., & Francou, B. (2009). Fluctuations of glaciers in the tropical Andes over the last millennium and palaeoclimatic implications: A review. *Palaeogeography, Palaeoclimatology, Palaeoecology*, 281(3), 269-282.
- Jouvet, G., Huss, M., Funk, M., & Blatter, H. (2011). Modelling the retreat of Grosser Aletschgletscher, Switzerland, in a changing climate. *Journal of Glaciology*, 57(206), 1033-1045.
- Kääb, A., Haeberli, W., & Gudmundsson, G.H. (1997). Analysing the Creep of Mountain Permafrost using High Precision Aerial Photogrammetry: 25 Years of Monitoring Gruben Rock Glacier, Swiss Alps Permafrost Periglac. *Process*. 8, 409-426.
- Kääb, A., Reynolds, J.M., & Haeberli, W. (2005). Glacier and permafrost hazards in high mountains. In *Global change and mountain regions – a state of knowledge overview*, in Huber, U.M., Bugmann, H.K.M., & Reasoner, M.A. (eds). Springer: 225-234.
- Kääb, A., Chiarle, M., Raup, B. & Schneider C. (2007) Climate change impacts on mountain glaciers and permafrost. *Global and Planetary Change*, 56, vii-ix.
- Kääb, A. (2011). Natural Hazards Associated with Glaciers and Permafrost. Dans *Encyclopedia of Snow, Ice and Glaciers* (pp. 763-775). Springer.
- Kannan, K., & Rajagopal, K.R. (2013). A model for the flow of rock glaciers. *International Journal of Non-Linear Mechanics*, 48, 59-64.

- Kappas, M. (2011). Aerial Photogrammetry for Glacial Monitoring. in *Encyclopedia of Snow, Ice and Glaciers* (pp. 4-15). Springer.
- Kellerer-Pirklbauer, A., Lieb, G. K., Avian, M., & Gspurning, J. (2008). The response of partially debris-covered valley glaciers to climate change: the example of the Pasterze Glacier (Austria) in the period 1964 to 2006. *Geografiska Annaler. Series A, Physical Geography*, 269-285.
- King, L., Gorbunov, A. P., & Evin, M. (1992). Prospecting and mapping of mountain permafrost and associated phenomena. *Permafrost and Periglacial Processes*, 3(2), 73-81.
- Kirkbride, M. P. (1989). About the concepts of *continuum* and *age*. *Boreas*, 87-99.
- Kirkbride, M. P. (1995). Ice flow vectors on the debris-mantled Tasman Glacier, 1957-1986. *Geografiska Annaler. Series A. Physical Geography*, 147-157.
- Kirkbride, M. P., & Warren, C. R. (1999). Tasman Glacier, New Zealand: 20th-century thinning and predicted calving retreat. *Global and Planetary Change*, 22(1), 11-28.
- Kirkbride, M. P. (2000). Ice-marginal geomorphology and Holocene expansion of debris-covered Tasman Glacier, New Zealand. *IAHS PUBLICATION*, 211-218.
- Kirkbride, M. P. (2011). Debris-covered glaciers. Dans *Encyclopedia of Snow, Ice and Glaciers* (pp. 180-182). Springer.
- Kirkbride, M. P., & Winkler, S. (2012). Correlation of Late Quaternary moraines: impact of climate variability, glacier response, and chronological resolution. *Quaternary Science Reviews*, 46, 1-29.
- Kirkbride, M. P., & Deline, P. (2013). The formation of supraglacial debris covers by primary dispersal from transverse englacial debris bands. *Earth Surface Processes and Landforms*, 38(15), 1779-1792.
- Kneisel, C. (1999). Permafrost in Gletschervorfeldern. Eine vergleichende Untersuchung in den Ostschweizer Alpen und Nordschweden, PhD Thesis. *Trierer Geographischen Studien 22*: Trier.
- Kneisel, C. (2003). Permafrost in recently deglaciated glacier forefields-measurements and observations in the eastern Swiss Alps and northern Sweden. *Zeitschrift für Geomorphologie, NF*, 289-305.
- Kneisel, C., & Kääh, A. (2007). Mountain permafrost dynamics within a recently exposed glacier forefield inferred by a combined geomorphological, geophysical and photogrammetrical approach. *Earth Surface Processes and Landforms*, 32(12), 1797-1810.
- Knight, P. G. (2011). Glaciology. *Encyclopedia of Snow, Ice and Glaciers*, 440-443.
- Knight, J., & Harrison, S. (2014). Mountain glacial and paraglacial environments under global climate change: lessons from the past, future directions and policy implications. *Geografiska Annaler: Series A, Physical Geography*, 96(3), 245-264.
- Krainer, K., & Mostler, W. (2006). Flow velocities of active rock glaciers in the Austrian Alps. *Geografiska Annaler. Series A. Physical Geography*, 267-280.
- Krainer, K., & Ribis, M. (2012). A rock glacier inventory of the Tyrolean Alps (Austria). *Austrian journal of earth sciences*, 105(2), 32-47.
- Krainer, K., Mussner, L., Behm, M., & Hausmann, H. (2012). Multi-disciplinary investigation of an active rock glacier in the Sella Group (Dolomites; Northern Italy). *Austrian Journal of Earth Sciences*, 105(2), 48-62.
- Krysiecki, J.M., Garcia, S., Schoeneich, P., Echelard, T., Bodin, X., & Evans, A. (In prep). D'un possible surge à la fin du 19^{ème} siècle aux dynamiques actuelles: essai d'évaluation des vitesses moyennes de surface du glacier rocheux du Dérochoir sur 115 ans via la présence d'un chemin muletier.
- Kuhn, M. (1995). The mass balance of very small glaciers. *Zeitschrift für Gletscherkunde und Glazialgeologie*, 31(1), 171-179.
- Kumar, R. (2011). Glacieret. Dans *Encyclopedia of Snow, Ice and Glaciers* (pp. 738-739). Springer.
- Kummert, M. & Delaloye, R. (2015). Quantifying sediment transfer between the front of an active alpine rock glacier and a torrential gully. In: *Geomorphometry for Geosciences*, Jasiewicz J., Zwolinski Zb., Mitasova H., Hengl T. (eds), 2015. Adam Mickiewicz University in Poznan - Institute of Geoecology and Geoinformation, International Society for Geomorphometry, Poznan
- Lambiel, C., & Delaloye, R. (2004). Contribution of Real-time Kinematic GPS in the Study of Creeping Mountain Permafrost: Examples from the Western Swiss Alps. *Permafrost and Periglacial Processes* 15: 229-241. DOI: 10.1002/ppp.496.
- Lambiel, C., Reynard, E., Cheseaux, G., & Lugon, R. (2004). Distribution du pergélisol dans un versant instable, le cas de Tsarmine (Arolla, Evolène, Vs). *Bull. Murithienne*, 122, 89-102.

- Lambiel, C. (2006). Le pergélisol dans les terrains sédimentaires à forte déclivité: distribution, régime thermique et instabilités. UNIL-Faculté des géosciences et de l'environnement-Institut de géographie.
- Lambiel, C., Bardou, E., Delaloye, R., Schuetz, P., & Schoeneich, P. (2009). Extension spatiale du pergélisol dans les Alpes vaudoises : implication pour la dynamique sédimentaire locale. *Bull. Soc. vaudoise sci. nat.* 91(4), 407-424.
- Lambiel, C., Delaloye, R., & Gärtner-Roer, I. (2011). Creep. Dans *Encyclopedia of Snow, Ice and Glaciers* (pp. 163-165). Springer.
- Lambrecht, A., Mayer, C., Hagg, W., Popovnin, V., Rezepkin, A., Lomidze, N., & Svanadze, D. (2011). A comparison of glacier melt on debris-covered glaciers in the northern and southern Caucasus. *Cryosphere*, 525-538.
- Lane, S.N., Westaway, R.M., & Hicks, D.M. (2003). Estimation of erosion and deposition volumes in a large, gravel-bed, braided river using synoptic remote sensing. *Earth Surf. Proc. Land.*, 28(3), 249-271.
- Leemann, A., & Niessen, F. (1994). Holocene glacial activity and climatic variations in the Swiss Alps: reconstructing a continuous record from proglacial lake sediments. *The Holocene*, 4(3), 259-268.
- Lilleøren, K. S., Etzelmüller, B. B., Gärtner-Roer, I., Kääh, A., Westermann, S., & Gudmundsson, A. (2013). The Distribution, Thermal Characteristics and Dynamics of Permafrost in Tröllaskagi, Northern Iceland, as Inferred from the Distribution of Rock Glaciers and Ice-Cored Moraines. *Permafrost and Periglacial Processes*, 24(4), 322-335.
- López-Moreno, J. I., Noguès-Bravo, D.-B. D., Chueca-Cia, J. J., & Julian-Andrés, A. (2006). Glacier development and topographic context. *Earth Surface Processes and Landforms*, 31(12), 1585-1594.
- López-Moreno, J., Noguès-Bravo, D., Chueca-Cia, J.J., & Julian-Andrés, A. (2006). Change of topographic control on the extent of cirque glaciers since the Little Ice Age. *Geophysical research letters*, 33(24), L24505.
- López-Moreno, J.I., Revuelto, J., Rico, I., Chueca-Cía, J., Julián-Andrés, A., Serreta, A., ... & García-Ruiz, J.M. (2015). Accelerate wastage of the Monte Perdido Glacier in the Spanish Pyrenees during recent stationary climatic conditions. *Cryosphere Disc.*, 9, 5021-5051.
- Lukas, S. (2011). Ice-cored moraines. Dans *Encyclopedia of Snow, Ice and Glaciers* (pp. 616-619). Springer.
- Magnin, F. (2015). Distribution et caractérisation du permafrost des parois du massif du Mont Blanc. Une approche combinant monitoring, modélisation et géophysique. Université de Savoie, thèse de doctorat.
- Maisch, M., Haeblerli, W., Hoelzle, M., & Wenzel, J. (1999). Occurrence of rocky and sedimentary glacier beds in the Swiss Alps as estimated from glacier-inventory data. *Annals of Glaciology*, 28(1), 231-235.
- Maisch, M., Wipf, A., Denneler, B., Battaglia, J., & Benz, C. (1999). Die Gletscher der Schweizer Alpen: Gletscherhochstand 1850. Aktuelle Vergletscherung, Gletscherschwund, Szenarien (2. ed.). vdf, Hochschulverlag an der ETH, Zurich.
- Maisch, M., Haeblerli, W., Frauenfelder, R., Kääh, A., & Rothenbühler, C. (2003). Lateglacial and Holocene evolution of glaciers and permafrost in the Val Muragl, Upper Engadine, Swiss Alps. *Proceedings of the 8th International Conference on Permafrost*, 2, pp. 717-722.
- Marescot, L. (2006). Introduction à l'imagerie électrique du sous-sol. *Bulletin de la Société vaudoise des Sciences naturelles*. 90, 23-40.
- Matthews, J. A., Winkler, S., & Wilson, P. (2014). Age and origin of ice-cored moraines in Jotunheimen and Breheimen, southern Norway: insights from Schmidt-hammer exposure-age dating. *Geografiska Annaler: Series A, Physical Geography*, 96(4), 531-548.
- Mattson, L. E., JS, G., & GJ, Y. (1993). Ablation on debris covered glaciers: an example from the Rakhiot Glacier, Panjab, Himalaya. *IAHS publication*, 218, 289-296.
- Mattson, L. E. (2000). The influence of a debris cover on the mid-summer discharge of Dome Glacier, Canadian Rocky Mountains. *IAHS PUBLICATION*, 25-34.
- Mayer, C., Lambrecht, A., Belo, M., Smiraglia, C., & Diolaiuti, G. (2006). Glaciological characteristics of the ablation zone of Baltoro glacier, Karakoram, Pakistan. *Annals of Glaciology*, 43(1), 123-131.
- Meigs, A., Krugh, W.C., Davis, K., & Bank, G. (2006). Ultra-rapid landscape response and sediment yield following glacier retreat, Icy Bay, southern Alaska. *Geomorphology* 78: 207-221.
- Menessier, G., Rosset, F., Bellière, J., Dhellemmes, R., Oulianoff, N., Antoine, P., Carme, F., Franchi, S., & Stella, A. (1976). St-Gervais-les-Bains, Carte Géologique de la France à 1/50 000 703. BRGM : Orléans.
- Mercier, D. (2011). La géomorphologie paraglaciale: changements climatiques, fonte des glaciers et crises érosives associées. Editions universitaires européennes.
- Messerli, A. & Grinsted A. (2015). Image GeoRectification And Feature Tracking toolbox: ImGRAFT, *Geosci. Instrum. Method.*

- MétéoSuisse (2016). Bulletin climatologique année 2015. Genève
- Micheletti, N., Lambiel, C., & Lane, S.N. (2015a). Investigating decadal scale geomorphic dynamics in an Alpine mountain setting. *J. Geophys. Res.* 120(10), 2155-2175.
- Micheletti, N., Lane, S.N., & Chandler, J.H. (2015b). Application of archival aerial photogrammetry to quantify climate forcing of alpine landscapes. *Photogram. Rec.*
- Mihalcea, C., Mayer, C., Diolaiuti, G., D'agata, C., Smiraglia, C., Lambrecht, A., ... & Tartari, G. (2008). Spatial distribution of debris thickness and melting from remote-sensing and meteorological data, at debris-covered Baltoro glacier, Karakoram, Pakistan. *Annals of glaciology*, 48(1), 49-57.
- Monnier, S., Camerlynck, C., Rejiba, F., Kinnard, C., Feuillet, T., & Dhemaied, A. (2011). Structure and genesis of the Thabor rock glacier (Northern French Alps) determined from morphological and ground-penetrating radar surveys. *Geomorphology*, 134(3), 269-279.
- Monnier, S., Camerlynck, C., Rejiba, F., Kinnard, C., & Galibert, P.-Y. (2013). Evidencing a large body of ice in a rock glacier, Vanoise Massif, Northern French Alps. *Geografiska Annaler: Series A, Physical Geography*, 95(2), 109-123.
- Monnier, S., Kinnard, C., Surazakov, A., & Bossy, W. (2014). Geomorphology, internal structure, and successive development of a glacier foreland in the semiarid Chilean Andes (Cerro Tapado, upper Elqui Valley, 30° 08' S., 69° 55' W.). *Geomorphology*, 207, 126-140.
- Monnier, S., & Kinnard, C. (2015). Reconsidering the glacier to rock glacier transformation problem: New insights from the central Andes of Chile. *Geomorphology*, 238, 47-55.
- Moorman, B. J. (2005). Glacier-permafrost hydrological interconnectivity: Stagnation Glacier, Bylot Island, Canada. *Cryospheric systems: glaciers and permafrost*, 242, 63-74.
- Müller, F., Caflish, T., & Müller, G. (1976). *Firn und Eis des Schweizer Alpen: Glescherinventar, No. 57*, Geographisches Institut der ETH Zürich: Zürich.
- Nakawo, M., & Rana, B. (1999). Estimate of ablation rate of glacier ice under a supraglacial debris layer. *Geografiska Annaler: Series A, Physical Geography*, 81(4), 695-701.
- Nakawo, M., Fountain, A., & Raymond, C. (2000). Debris-covered glaciers.
- Nicholson, L., & Benn, D. I. (2006). Calculating ice melt beneath a debris layer using meteorological data. *Journal of Glaciology*, 52(178), 463-470.
- Nicholson, L., Marín, J., Lopez, D., Rabatel, A., Bown, F., & Rivera, A. (2010). Glacier inventory of the upper Huasco valley, Norte Chico, Chile: glacier characteristics, glacier change and comparison with central Chile. *Annals of Glaciology*, 50(53), 111-118.
- Nicolussi, K., & Patzelt, G. (2000). Discovery of early Holocene wood and peat on the forefield of the Pasterze Glacier, Eastern Alps, Austria. *The Holocene*, 10(2), 191-199.
- Nicolussi, K., & Patzelt, G. (2000). Untersuchungen zur holozanen Gletscherentwicklung von Pasterze und Gepatschferner (Ostalpen). Mit 41 Abbildungen. *Zeitschrift für Gletscherkunde und Glazialgeologie*, 36, 1-88.
- Nicolussi, K., Kaufmann, M., Patzelt, G., Thurner, A., & others. (2005). Holocene tree-line variability in the Kauner Valley, Central Eastern Alps, indicated by dendrochronological analysis of living trees and subfossil logs. *Vegetation History and Archaeobotany*, 14(3), 221-234.
- Nobes, D.C. (2011). Ground Penetrating Radar Measurements Over Glaciers. in *Encyclopedia of Snow, Ice and Glaciers* (pp. 490-504). Springer.
- Nussbaumer, S.U., & Zumbühl, H.J. (2012). The Little Ice Age history of the Glacier des Bossons (Mont Blanc massif, France): a new high-resolution glacier length curve based on historical documents. *Climatic Change* 111(2): 301-334.
- Otto, J.-C., Schrott, L., Jaboyedoff, M., & Dikau, R. (2009). Quantifying sediment storage in a high alpine valley (Turtmanntal, Switzerland). *Earth Surface Processes and Landforms*, 34(13), 1726-1742.
- Otto, J.-C., Keuschnig, M., Goetz, J., Marbach, M., & Schrott, L. (2012). Detection of mountain permafrost by combining high resolution surface and subsurface information: an example from the Glatzbach catchment, Austrian Alps. *Geografiska Annaler: Series A, Physical Geography*, 94(1), 43-57.
- Owen, L. A., & England, J. (1998). Observations on rock glaciers in the Himalayas and Karakoram Mountains of northern Pakistan and India. *Geomorphology*, 26(1), 199-213.

- Owens, P.N., & Slaymaker, O. (2004). An introduction to mountain geomorphology. In *Mountain Geomorphology*, Owens PN, Slaymaker O (eds). Arnold: 3-29.
- Owens, P., & Slaymaker, O. (2014). *Mountain geomorphology*. Routledge.
- Paasche, Ø. (2011). Cirque glaciers. In Singh VP, Singh P and Haritashya UK eds. *Encyclopedia of snow, ice and glaciers*. Dordrecht: Springer.
- Parolo, B., Della, P., Pan, R. K., Ghosh, R., Huberman, B. A., Kaski, K., & Fortunato, S. (2015). Attention decay in science. Available at SSRN 2575225.
- Paul, F., Kääb, A., & Haeberli, W. (2007). Recent glacier changes in the Alps observed by satellite: Consequences for future monitoring strategies. *Global and Planetary Change*, 56(1), 111-122.
- Pellicciotti, F., Stephan, C., E, M., Herreid, S., Immerzeel, W., & Bolch, T. (2015). Mass-balance changes of the debris-covered glaciers in the Langtang Himal, Nepal, from 1974 to 1999. *Journal of Glaciology*, 61, 373-386.
- Perruchoud, E., & Delaloye, R. (2007). Short-term changes in surface velocities on the Beccs-de-Bosson rock glacier (western Swiss Alps). *Grazer Schriften der Geographie und Raumforschung Band 43*.
- Pettersson, R., Jansson, P., & Holmlund, P. (2003). Cold surface layer thinning on Storglaciären, Sweden, observed by repeated ground penetrating radar surveys. *Journal of Geophysical Research: Earth Surface (2003--2012)*, 108(F1).
- Pfeffer, W. T., Arendt, A. A., Bliss, A., Bolch, T., Cogley, J. G., Gardner, A. S., ... & others. (2014). The Randolph Glacier Inventory: a globally complete inventory of glaciers. *Journal of Glaciology*, 60(221), 537-552.
- Potter, N. (1972). Ice-cored rock glacier, Galena Creek, northern Absaroka Mountains, Wyoming. *Geological Society of America Bulletin*, 83(10), 3025-3058.
- Potter, N., Steig, E., Clark, D., Speece, M., Clark, G. t., & Updike, A. B. (1998). Galena Creek rock glacier revisited: new observations on an old controversy. *Geografiska Annaler. Series A. Physical Geography*, 251-265.
- Pourrier, J., Jourde, H., Kinnard, C., Gascoin, S., & Monnier, S. (2014). Glacier meltwater flow paths and storage in a geomorphologically complex glacial foreland: The case of the Tapado glacier, dry Andes of Chile (30° S). *Journal of Hydrology*, 519, 1068-1083.
- Purdie, H.L., Brook, M.S. & Fuller, I.C. (2008). Seasonal Variation in Ablation and Surface Velocity on a Temperate Maritime Glacier: Fox Glacier, New Zealand. *Arctic, Antarctic, and Alpine Research*, 40(1), 140-147.
- Radić, V., Bliss, A., Beedlow, A.C., Hock, R., Miles, E., & Cogley, J.G. (2014). Regional and global projections of twenty-first century glacier mass changes in response to climate scenarios from global climate models. *Climate Dyn.*, 42(1-2), 37-58.
- Ramirez, E., Francou, B., Ribstein, P., Descloitres, M., Guerin, R., Mendoza, J., ... & Jordan, E. (2001). Small glaciers disappearing in the tropical Andes: a case-study in Bolivia: Glaciar Chacaltaya (16 S). *Journal of Glaciology*, 47(157), 187-194.
- Rangecroft, S., Harrison, S., & Anderson, K. (2015). Rock glaciers as water stores in the Bolivian Andes: an assessment of their hydrological importance. *Arctic, Antarctic, and Alpine Research*, 47(1), 89-98.
- Ravanel, L., & Deline, P. (2008). La face ouest des Drus (massif du Mont-Blanc): évolution de l'instabilité d'une paroi rocheuse dans la haute montagne alpine depuis la fin du petit âge glaciaire. *Gomorphologie*, 4, 261272.
- Ravanel, L., & Lambiel, C. (2012). Evolution récente de la moraine des Gentianes (2894 m, Valais, Suisse): un cas de réajustement paraglacière? *Environnements périglaciaires(18-19)*, 8p.
- Reynard, E., Delaloye, R., & Lambiel, C. (1999). Prospection géoélectrique du pergélisol alpin dans le massif des Diablerets (VD) et au Mont Gelé (Nendaz, Vs). *Bull. Murithienne*. 117, 89-103.
- Reynard, E., Lambiel, C., Delaloye, R., Devaud, G., Baron, L., Chapellier, D., ... & Monnet, R. (2003). Glacier/permafrost relationships in forefields of small glaciers (Swiss Alps). *Proceedings 8th International Conference on Permafrost, Zurich, Switzerland, 2*, pp. 947-952.
- Ribolini, A., Chelli, A., Guglielmin, M., & Pappalardo, M. (2007). Relationships between glacier and rock glacier in the Maritime Alps, Schiantala Valley, Italy. *Quaternary Research*, 68(3), 353-363.
- Ribolini, A., Guglielmin, M., Fabre, D., Bodin, X., Marchisio, M., Sartini, S., ... & Schoeneich, P. (2010). The internal structure of rock glaciers and recently deglaciated slopes as revealed by geoelectrical tomography: insights on permafrost and recent glacial evolution in the Central and Western Alps (Italy--France). *Quaternary Science Reviews*, 29(3), 507-521.
- Rignot, E., Hallet, B., & Fountain, A. (2002). Rock glacier surface motion in Beacon Valley, Antarctica, from synthetic-aperture radar interferometry. *Geophysical Research Letters*, 29(12), 48-1.

- Rippin, D., Willis, I., Arnold, N., Hodson, A., & Brinkhaus, M. (2005). Spatial and temporal variations in surface velocity and basal drag across the tongue of the polythermal glacier midre Lovenbreen, Svalbard. *Journal of Glaciology*, 51(175), 588-600.
- Robson, B.A., Nuth, C., Dahl, S.O., Hölbling D., Strozzi T., Nielsen P.R. (2015). Automated classification of debris-covered glaciers combining optical, SAR and topographic data in an object-based environment, *Remote Sensing of Environment*, 170, 372-387.
- Rödder, T., Braun, L., & Mayer, C. (2008). Accumulation rates and snow redistribution processes at the Ice chapel, Berchtesgaden Alps. *Z. Gletscherkunde Glazialgeol*, 42(2), 3-20.
- Roer, I., Haeberli, W., Avian, M., Kaufmann, V., Delaloye, R., Lambiel, C., & Kääh, A. (2008). Observations and considerations on destabilizing active rock glaciers in the European Alps. *Ninth International Conference on Permafrost*, 2, pp. 1505-1510.
- Rowan, A.V., Egholm, D.L., Quincey, D.J., & Glasser, N.F. (2015). Modelling the feedbacks between mass balance, ice flow and debris transport to predict the response to climate change of debris-covered glaciers in the Himalaya. *Earth and Planetary Science Letters*, 430, 427-438.
- Sanders, J. W., Cuffey, K. M., Moore, J. R., MacGregor, K. R., & Kavanaugh, J. L. (2012). Periglacial weathering and headwall erosion in cirque glacier bergschrunds. *Geology*, 40(9), 779-782.
- Scapozza, C., Lambiel, C., Baron, L., Marescot, L., & Reynard, E. (2011). Internal structure and permafrost distribution in two alpine periglacial talus slopes, Valais, Swiss Alps. *Geomorphology*, 132(3), 208-221.
- Scapozza, C. (2012). Stratigraphie, morphodynamique, paléoenvironnements des terrains sédimentaires meubles à forte déclivité du domaine périglaciaire alpin, PhD Thesis. *Geovisions 40: Institut de géographie et durabilité, Université de Lausanne*.
- Scherler, D., Bookhagen, B., & Strecker, M. R. (2011). Spatially variable response of Himalayan glaciers to climate change affected by debris cover. *Nature geoscience*, 4(3), 156-159.
- Schmidt, S., & Nüsser, M. (2009). Fluctuations of Raikot Glacier during the past 70 years: A case study from the Nanga Parbat massif, northern Pakistan. *Journal of Glaciology*, 55(194), 949-959.
- Schoeneich, P. (1998). Le retrait glaciaire dans les vallées des Ormonts, de l'Orgrin et de l'Étivaz (Préalpes vaudoises). Thèse de doctorat. Lausanne: Institut de Géographie, Université de Lausanne, Travaux et recherches n°14.
- Schomacker, A. & Kjær, K.H. (2007). Origin and de-icing of multiple generations of ice-cored moraines at Bruarjökull, Iceland. *Boreas*. 36, 411-425.
- Schomacker, A. (2008). What controls dead-ice melting under different climate conditions? A discussion. *Earth-Science Reviews*, 90(3), 103-113.
- Schomacker, A. (2011). Moraine. Dans *Encyclopedia of Snow, Ice and Glaciers* (pp. 747-756). Springer.
- Scotti, R., Brardinoni, F., & Crosta, G. B. (2014). Post-LIA glacier changes along a latitudinal transect in the Central Italian Alps. *The Cryosphere*, 8(6), 2235-2252.
- Seppi, R., Zanoner, T., Carton, A., Bondesan, A., Francese, R., Carturan, L., ... & Ninfo, A. (2015). Current transition from glacial to periglacial processes in the Dolomites (South-Eastern Alps). *Geomorphology*, 228, 71-86.
- Serrano, E., & López-Martínez, J. (2000). Rock glaciers in the South Shetland Islands, Western Antarctica. *Geomorphology* 35 (1-2): 145-162.
- Serrano, E., Gonzalez-Trueba, J. J., Sanjose, J. J., & Del Rio, L. M. (2011). Ice patch origin, evolution and dynamics in a temperate high mountain environment: the Jou Negro, Picos de Europa (NW Spain). *Geografiska Annaler: Series A, Physical Geography*, 93(2), 57-70.
- Shakesby, R. A., Dawson A. G. & Matthews J. A. (1987). Rock glaciers, protalus ramparts and related phenomena, Rondane, Norway : a continuum of large-scale talus-derived landforms. *Boreas*, 305-317.
- Shakesby, R. A. (1997). Pronival (protalus) ramparts: a review of forms, processes, diagnostic criteria and palaeoenvironmental implications. *Progress in Physical Geography*, 21(3), 394-418.
- Shea, J. M., Immerzeel, W. W., Wagnon, P., Vincent, C., & Bajracharya, S. (2015). Modelling glacier change in the Everest region, Nepal Himalaya. *The Cryosphere*, 9(3), 1105-1128.
- Shean, D. E., Head, J. W., & Marchant, D. R. (2007). Shallow seismic surveys and ice thickness estimates of the Mullins Valley debris-covered glacier, McMurdo Dry Valleys, Antarctica. *Antarctic Science*, 19(04), 485-496.
- Shepherd, A., Hubbard, A., Nienow, P., King, M., Mc Millan, M. & Joughin, I. (2009). Greenland ice sheet motion coupled with

- daily melting in late summer. *Geophysical Research Letters*, 36(L01501).
- Shroder, J. F., Bishop, M. P., Copland, L., & Sloan, V. F. (2000). Debris-covered Glaciers and Rock Glaciers in the Nanga Parbat Himalaya, Pakistan. *Geografiska Annaler: Series A, Physical Geography*, 82(1), 17-31.
- Shukla, A., Arora, M., & Gupta, R. (2010). Synergistic approach for mapping debris-covered glaciers using optical--thermal remote sensing data with inputs from geomorphometric parameters. *Remote Sensing of Environment*, 114(7), 1378-1387.
- Shur, Y., Jorgenson, M. T., & Kanevskiy, M. (2011). Permafrost. Dans *Encyclopedia of Snow, Ice and Glaciers* (pp. 841-848). Springer.
- Six, D., & Vincent, C. (2014). Sensitivity of mass balance and equilibrium-line altitude to climate change in the French Alps. *Journal of Glaciology*, 60(223), 867-878.
- Slaymaker, O. (2004). Equifinality. Dans *Encyclopedia of Geomorphology*, Goudie AS (ed). Routledge.
- Slaymaker, O. (2011). Criteria to distinguish between periglacial, proglacial and paraglacial environments. *Quaestiones Geographicae*, 30(1), 85-94.
- Slaymaker, O., & Owens, P. (2004). *Mountain geomorphology*. Mountain geomorphology. Arnold Publication.
- Small, R.J. (1983). Lateral moraines of glacier de Tsijiore Nouve: Form, Development, and Implications. *J. Glaciol.*, 29(102), 250-259.
- Sold, L., Huss, M., Hoelzle, M., Anderegggen, H., Joerg, P.C., & Zemp, M. (2013). Methodological approaches to infer end-of-winter snow distribution on alpine glaciers. *J. Glaciol.*, 59(218), 1047-1059.
- Stocker, T., Qin, D., Plattner, G., Tignor, M., Allen, S., Boschung, J., ... & Midgley, B. (2013). IPCC, 2013: climate change 2013: the physical science basis. Contribution of working group I to the fifth assessment report of the intergovernmental panel on climate change.
- Stokes, C., Popovnin, V., Aleynikov, A., Gurney, S., & Shahgedanova, M. (2007). Recent glacier retreat in the Caucasus Mountains, Russia, and associated increase in supraglacial debris cover and supra-/proglacial lake development. *Annals of Glaciology*, 46(1), 195-203.
- Stummer, P., Maurer, H., & Green, A.G. (2004). Experimental design: Electrical resistivity data sets that provide optimum subsurface information. *Geophysics* 69(1): 120-139.
- Summerfield, M. A. (1991). *Global Geomorphology: an introduction to the Study of Landforms*. Pearson Prentice Hall, Harlow, England.
- Takeuchi, N., Kohshima, S., Yoshimura, Y., Seko, K., and Fujita, K., (2010). Characteristics of cryoconite holes on a Himalayan glacier, Yala Glacier Central Nepal. *Bulletin of Glaciological Research*, 17, 51-59
- Thibert, E., Eckert, N., & Vincent, C. (2013). Climatic drivers of seasonal glacier mass balances: an analysis of 6 decades at Glacier de Sarnes (French Alps). *The Cryosphere*, 7(1), 47-66.
- Thomson, M., Kirkbride, M., & Brock, B. (2000). Twentieth century surface elevation change of the Miage Glacier, Italian Alps. *IAHS PUBLICATION*, 219-226.
- Vacher, P., Dumoulin, S., Morestin, F., & Mguil-Touchal, S. (1999). Bidimensional strain measurement using digital images. *Proc. of the Inst. of Mechanical Engineers*, 213 (8), 811-817.
- Van Everdingen, R. O. (1998). Multi-language glossary of permafrost and related ground-ice terms in Chinese, English, French, German, Icelandic, Italian, Norwegian, Polish, Romanian, Russian, Spanish, and Swedish. International Permafrost Association, Terminology Working Group.
- Vaughan, D. G., Comiso, J. C., Allison, I., Carrasco, J., Kaser, G., Kwok, R., ... & others. (2013). Observations: cryosphere. *Climate change*, 317-382.
- Vincent, C., Garambois, S., Thibert, E., Lefèbvre, E., Le Meur, E., & Six, D. (2010). Origin of the outburst flood from Glacier de Tête Rousse in 1892 (Mont Blanc area, France). *Journal of Glaciology* 56(198): 688-698.
- Vincent, C., Desclotres, M.S., Garambois, S., Legchenko, A., Guyard, H., & Gilbert, A. (2012). Detection of a subglacial lake in Glacier de Tête Rouse (Mont Blanc area, France). *Journal of Glaciology* 58(211): 866-878.
- Vincent, C., Thibert, E., Gagliardini, O., Legchenko, A., Gilbert, A., Garambois, S., Condom, T., Baltassat, J.M., Girard, J.F. (2015). Mechanisms of subglacial cavity filling in Glacier de Tête Rousse, French Alps. *Journal of Glaciology* 61(228): 609-623.
- Waller, R. (2001). The influence of basal processes on the dynamic behaviour of cold-based glaciers. *Quaternary International*,

86(1), 117-128.

- Waller, R. I., & Tuckwell, G. W. (2005). Glacier-permafrost interactions and glaciotectonic landform generation at the margin of the Leverett Glacier, West Greenland. *Geological Society, London, Special Publications*, 242(1), 39-50.
- Walstra, J., Chandler, J.H., Dixon, N., & Dijkstra, T.A. (2004). Extracting landslide movements from historical aerial photographs. In Lacerda W, Erlich M, Fontoura SAB and Sayao, ASF eds. *Landslides: Evaluation and Stabilization*. London, Taylor & Francis, 843-850
- Wanner, H., Solomina, O., Grosjean, M., Ritz, S. P., & Jetel, M. (2011). Structure and origin of Holocene cold events. *Quaternary Science Reviews*, 30(21), 3109-3123.
- Wayne, W. J. (1981). Ice segregation as an origin for lenses of non-glacial ice in. *Journal of Glaciology*, 27, 506-510.
- WGMS. (2008). *Global Glacier Changes: Facts and Figures*. (R. I. Zemp M, Éd.) UNEP and World Glacier Monitoring Service: Zurich.
- Whalley, W. B. (2009). On the interpretation of discrete debris accumulations associated with glaciers with special reference to the British Isles. *Geological Society, London, Special Publications*, 320(1), 85-102.
- Whalley, W. B., & Martin, H. E. (1992). Rock glaciers: II models and mechanisms. *Progress in Physical Geography*, 16(2), 127-186.
- Whalley, W. B., & Palmer, C. F. (1998). A glacial interpretation for the origin and formation of the Marinets Rock Glacier, Alpes Maritimes, France. *Geografiska Annaler: Series A, Physical Geography*, 80(3-4), 221-236.
- Whalley, W. B., & Azizi, F. (2003). Rock glaciers and protalus landforms: Analogous forms and ice sources on Earth and Mars. *Journal of Geophysical Research: Planets (1991--2012)*, 108(E4).
- Winkler, S., & Matthews, J. A. (2010). Observations on terminal moraine-ridge formation during recent advances of southern Norwegian glaciers. *Geomorphology*, 116(1), 87-106.
- Zemp, M., Kääb, A., Hoelzle, M. & Haeberli, W. (2005). GIS-based modelling of glacial sediment balance. *Z. Geomorph. N.F.*, 138, 113-129.
- Zemp, M., Frey, H., Gärtner-Roer, I., Nussbaumer, S. U., Hoelzle, M., Paul, F., ... & others. (2015). Historically unprecedented global glacier decline in the early 21st century. *Journal of Glaciology*, 61(228), 745-762.
- Zhang, Y., Fujita, K., Liu, S., Liu, Q., & Nuimura, T. (2011). Distribution of debris thickness and its effect on ice melt at Hailuoguo glacier, southeastern Tibetan Plateau, using in situ surveys and ASTER imagery. *Journal of Glaciology*, 57(206), 1147-1157.

List of personal publications and participations to conferences

Academic works

- Bosson, J.B. (2010). Contribution à l'étude du patrimoine géomorphologique de la Réserve Naturelle des Contamines Montjoie et démarches de géovalorisation. Master thesis, University of Lausanne.
- Bosson, J.B. (2016). Internal structure, dynamics and genesis of small debris-covered glacier systems located in alpine permafrost environments. PhD thesis, University of Lausanne.

Publications in peer-reviewed journals

- Bosson, J.B. (2012). Les glaciers enterrés du vallon des Jovet. *Nature et Patrimoine en Pays de Savoie* 38: 16-23.
- Bosson, J.B., & Reynard, E. (2012). Geomorphological heritage, conservation and promotion in high-alpine protected areas. *eco. mont.*, 4(1), 13-22 (DOI: 10.1553/eco.mont-4-1s13).
- Bosson, J.B., Deline, P., Bodin, X., Schoeneich, P., Baron, L., Gardent, M., & Lambiel, C. (2015). The influence of ground ice distribution on geomorphic dynamics since the Little Ice Age in pro-glacial areas of two cirque glacier systems. *Earth Surface Processes and Landforms.*, 40, 666-680 (DOI: 10.1002/esp.3666).
- Bosson, J.B., & Lambiel, C. (2016). Internal structure and current evolution of small debris-covered glacier systems located in alpine permafrost environments. *Frontiers in Earth-Science (Cryospheric Sciences)*, 4:39 (DOI: 10.3389/feart.2016.00039).
- Capt, M., Bosson, J.B., Fischer, M., Micheletti, N., & Lambiel, C. (2016). Decadal evolution of a small heavily debris-covered glacier located in Alpine permafrost environment. *J. Glaciol.*, 62(233), 535-551 (DOI: 10.1017/jog.2016.56).

Participations to scientific conferences

- Bosson, J.B. & Lambiel, C. (2011). Poster: Thesis project: Contemporary glacial and periglacial dynamics in high mountains glacier forefields. Swiss Society of Geomorphology Meeting. St-Niklaus.
- Bosson, J.B. & Reynard, E. (2011). Presentation: Importance of geomorphological analysis for geomorphological heritage promotion in protected areas: the case of Contamines-Montjoie Natural Reserve (Mont-Blanc Massif, France). International Symposium on Geosite Management. Le Bourget-du-Lac.
- Bosson, J.B., Lambiel, C., Utz, S., Kummert, M., & Grangier, L. (2012). Poster: Internal structure and evolution of a small debris-covered glaciers (Entre la Reille, les Diablerets, Switzerland). European Geoscience Union. Wien.
- Bosson, J.B., Lambiel, C., Utz, S., Regamey, B., & Deluigi, N. (2012). Poster: Current evolution of some high mountain debris-covered glaciers systems in Western Alps: Entre la Reille (Switzerland) & les Rognes (France). Swiss Geosciences Meeting. Bern.
- Bosson, J.B., Lambiel, C., Utz, S., Baron, L., Deline, P., Bodin, X., Schoeneich, P., Gardent, M., (2013). Presentation: Ground ice distribution and geomorphological dynamics in high mountain sedimentary environments (les Rognes, France). Alpine Glaciology Meeting. Grenoble.
- Bosson, J.B., Deline, P., Bodin, X., Schoeneich, P., Baron, L., Gardent, M., & Lambiel, C. (2013). Presentation & Poster: Ground ice distribution in a high mountain sedimentary environment and its influence on sediment fluxes and local hazards (les Rognes, France). IAG conference on Geomorphology. Paris.
- Bosson, J.B., Capt, M., Nendaz, T., & Lambiel, C. (2013). Presentation: The relation between internal structure and geomorphic dynamics in high mountain small glacier systems (les Rognes & Pierre Ronde, France). Swiss Geosciences Meeting. Lausanne.
- Bosson, J.B. & Lambiel, C. (2014). Presentation: Current evolution of small alpine debris-covered glaciers in permafrost environments (les Rognes, France). European Geoscience Union. Wien.
- Bosson, J.B. & Lambiel, C. (2014). Presentation: Current changes in small glaciers systems in Alpine permafrost environments. European Conference on Permafrost. Evora.
- Bosson, J.B., Capt, M., Micheletti, N. & Lambiel, C. (2014). Poster: Last decades evolution of glacier systems in Alpine permafrost environments (Entre la Reille and Tsarmine, Switzerland). European Conference on Permafrost. Evora.
- Bosson, J.B. & Lambiel, C. (2014). Presentation: Current evolution of small glacier systems in alpine permafrost environments in relation with their internal structure. Swiss Geosciences Meeting. Fribourg.
- Bosson, J.B., Capt, M., & Lambiel, C. (2014). Presentation: Decadal to seasonal evolution of small debris-covered glaciers in permafrost environments in relation to their internal structure and climatic factors. European Geoscience Union. Wien.
- Bosson, J.B., Capt, M., Fischer, M., Micheletti, N., Lane, S.N. & Lambiel, C. (2015). Poster: Internal structure, dynamics and genesis of a small heavily debris-covered glaciers system (Tsarmine, Switzerland). Swiss Geosciences Meeting. Basel.

